Status of the Pacific Hake (whiting) stock in U.S. and Canadian waters in 2025

Joint Technical Committee of the Pacific Hake/Whiting Agreement
Between the Governments of the United States and Canada

February 25th, 2025

This document reports the collaborative efforts of the official U.S. and Canadian members of the Joint Technical Committee, and others that contributed significantly.

Authors of this document are (all authors contribute extensively so the order rotates annually):

Kelli F. Johnson[1,2]
Andrew M. Edwards[3]
Aaron M. Berger[4]
Chris J. Grandin[3]
Chantel R. Wetzel[1]

[1] *Northwest Fisheries Science Center, National Marine Fisheries Service, National Oceanic and Atmospheric Administration, U.S. Department of Commerce, 2725 Montlake Blvd. East, Seattle, WA 98112-2097, USA*

[2] *Office of Science and Technology, National Marine Fisheries Service, National Oceanic and Atmospheric Administration, U.S. Department of Commerce, 7600 Sand Point Way Northeast, Seattle, WA 98115, USA*

[3] *Pacific Biological Station, Fisheries and Oceans Canada, 3190 Hammond Bay Road, Nanaimo, B.C. V9T 6N7, Canada*

[4] *Northwest Fisheries Science Center, National Marine Fisheries Service, National Oceanic and Atmospheric Administration, U.S. Department of Commerce, 2032 SE OSU Dr. Bldg. 955, Newport, OR 97365-5275, USA*

This document should be cited as follows:

Johnson, K.F., A.M. Edwards, A.M. Berger, C.J. Grandin, and C.R. Wetzel. 2025. Status of the Pacific Hake (whiting) stock in U.S. and Canadian waters in 2025. Prepared by the Joint Technical Committee of the U.S. and Canada Pacific Hake/Whiting Agreement, National Marine Fisheries Service and Fisheries and Oceans Canada. 286 p.

TABLE OF CONTENTS

Appendices

ONE-PAGE SUMMARY

- The stock assessment model for 2025 has the same population dynamics structure as the 2024 model, except for recruitment deviations in the terminal two years and projection years being fixed at zero. The model is fit to an acoustic survey index of biomass, annual commercial catch data, and age-composition data from the survey and commercial fisheries. Unlike last year's assessment, the model was not fit to the relative index of age-1 fish.

- Data for 2024 were included for each data set and minor changes to pre-2024 data were made as necessary. Similar to last year's assessment, a model-based approach was used for the input weight-at-age matrix and time-varying temperature-dependent maturity, both of which inform fecundity.

- Coast-wide catch in 2024 was 170,850 t (t represents tonnes), 48% below the average over the most recent 10 years (325,582 t), out of a total allowable catch (TAC), adjusted for carryovers, of 555,000 t. The U.S. caught 166,923 t (40.7% of their quota) and Canada caught 3,928 t (2.7% of their quota).

- The median estimate of the 2025 relative spawning biomass (female spawning biomass at the start of 2025 divided by that at unfished equilibrium, B_0) is 67% but it is highly uncertain (with 95% credible interval from 29% to 157%). After declining from 2018–2022, the median relative spawning biomass increased from 2022–2025, due to the estimated above average, but uncertain, size of the 2020 and 2021 cohorts entering maturity.

- The median estimate of female spawning biomass at the start of 2025 is 1,223,070 t (with 95% credible interval from 521,117 to 3,028,177 t). This is a slight increase from this assessment's estimate for the 2024 female spawning biomass of 1,189,495 t (with 95% credible interval from 530,297 to 2,899,665 t).

- The estimated probability that female spawning biomass at the start of 2025 is below the $B_{40\%}$ (40% of B_0) reference point is 11.1%, and the probability that the relative fishing intensity exceeded 1 in 2024 is 4.8%. The joint probability of both these occurring is 1.9%.

- Based on the default harvest rule, the estimated median catch limit for 2025 is 560,742 t (with 95% credible interval from 203,161 to 1,605,930 t).

- Projections were conducted across a wide-range of catch levels. Projections setting the 2025 and 2026 catches equal to the 2024 coast-wide TAC of 555,000 t show the estimated median relative spawning biomass decreasing from 67% in 2025 to 49% in 2026 and then to 33% in 2027, with a 63% chance of the female spawning biomass falling below $B_{40\%}$ in 2027. With realized catches of 400,000 t in 2025 and 2026, it was estimated that the stock will reach approximately $B_{40\%}$ at the start of 2027, given the current assumption of average recruitment from 2023 onward.

- Despite estimates of a current stock status likely above $B_{40\%}$, the recent lack of survey abundance and fishery catch in Canada suggests a population structure not conducive to achieving harvest quotas in northern fisheries over recent years.

EXECUTIVE SUMMARY

Stock

This assessment reports the status of the coastal Pacific Hake (or Pacific whiting, *Merluccius productus*) stock off the west coast of the United States (U.S.) and Canada at the start of 2025. This stock exhibits seasonal migratory behavior, ranging from offshore and generally southern waters during the winter spawning season to coastal areas between northern California and northern British Columbia during the spring, summer, and fall when the fishery is conducted. The stock tends to move farther to the north during the summer in years with warmer water compared to years with colder waters. Older Pacific Hake tend to migrate farther north than younger Pacific Hake in all years, with catches in Canadian waters typically consisting of fish greater than four years old. Separate, and much smaller, populations of Pacific Hake occurring in the major inlets of the Northeast Pacific Ocean, including the Strait of Georgia, Puget Sound, and the Gulf of California, are not included in this analysis.

Catches

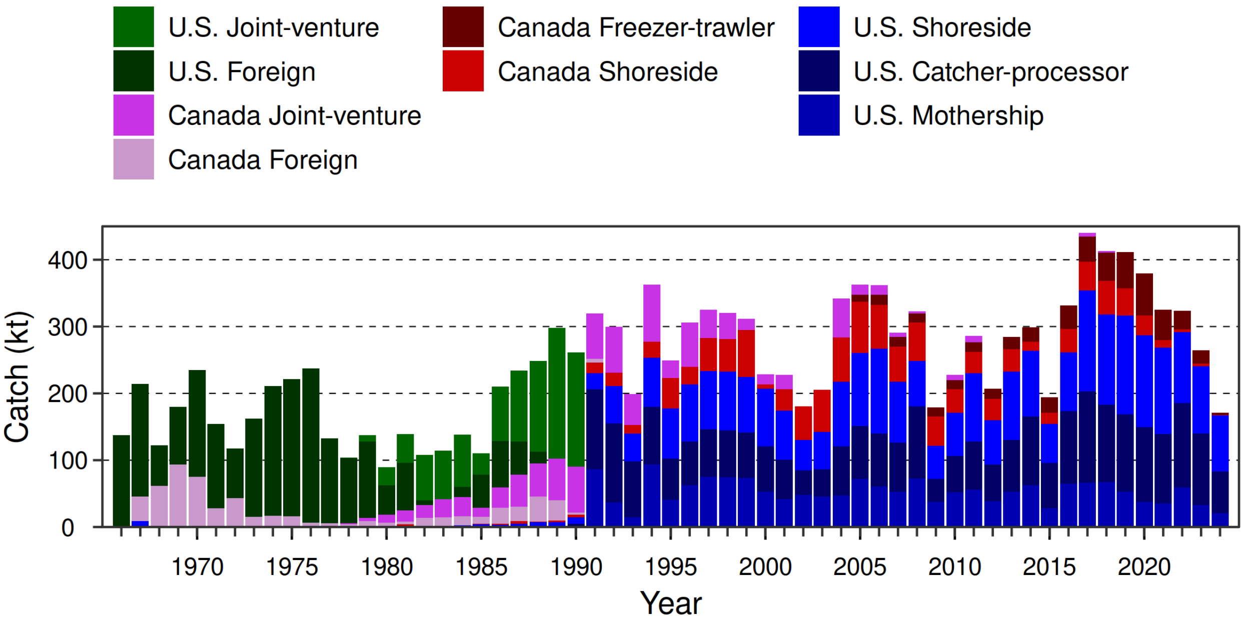

Figure a. Total Pacific Hake catch used in the assessment by sector, 1966–2024. U.S. tribal catches are included in the sectors where they are represented.

Coast-wide fishery landings of Pacific Hake averaged 242,034 t from 1966 to 2024, with a low of 89,930 t in 1980 and a peak of 440,563 t in 2017 (Figure a). Prior to 1966, total removals were negligible compared to the modern fishery. Over the early period (1966–1990) most removals were from foreign or joint-venture fisheries. Across the time series, annual catch in U.S. waters averaged 185,684 t (76.7% of the total catch), while catch from Canadian waters averaged 56,350 t. Over the last 10 years, 2015–2024 (Table a), the average coast-wide catch was 325,582 t with U.S. and Canadian catches averaging 266,013 t and 59,569 t, respectively. Since 2017, the coast-wide catch has been declining annually through 2024 to 170,850 t out of a total allowable catch (TAC, adjusted for carryovers) of 555,000 t. Attainment in the U.S. was 40.7% of its quota and in Canada it was 2.7% in 2024.

Table a. Total Pacific Hake catch used in the assessment by sector for the most recent ten years. U.S. tribal catches are included in the sectors where they are represented.

Year	U.S. Mother-ship	U.S. Catcher-processor	U.S. Shore-side	U.S. Research	U.S. Total	Canada Joint-venture	Canada Shore-side	Canada Freezer-trawler	Canada Total	Total
2015	27,665	68,484	58,011	0	154,160	0	16,775	22,909	39,684	193,844
2016	65,036	108,786	87,762	745	262,328	0	35,012	34,731	69,743	332,071
2017	66,428	136,960	150,454	0	353,842	5,608	43,427	37,686	86,721	440,563
2018	67,121	116,073	134,633	0	317,827	2,724	50,747	41,942	95,413	413,240
2019	52,646	116,146	147,830	0	316,622	0	40,794	54,218	95,013	411,635
2020	37,978	111,147	137,568	95	286,788	0	30,085	62,404	92,489	379,277
2021	35,208	104,030	129,204	917	269,359	0	11,269	45,807	57,076	326,435
2022	59,516	126,247	105,934	0	291,697	0	3,868	27,803	31,671	323,368
2023	33,074	107,117	100,397	0	240,588	0	3,657	20,296	23,952	264,540
2024	20,942	61,914	84,067	0	166,923	0	1,185	2,742	3,928	170,850

In this document, the terms catch and landings are used interchangeably. Estimates of discard within the target fishery are included but discarding of Pacific Hake in non-target fisheries is not. Discard from all fisheries, including those that do not target Pacific Hake, is estimated to be less than 1% of landings in recent years. The catches in 2024 declined below the long-term average catch (242,034 t), continuing the pattern of declining catches over recent years (especially in Canada). Landings between 2001 and 2008 were predominantly comprised of fish from the very large 1999 year class, with a cumulative removal (through 2024) from that cohort of 2.14 Mt [1 Mt = 1 million metric tonnes]. Through 2024, the cumulative catches of the 2010, 2014, and 2016 year classes were estimated at 2.58 Mt, 1.80 Mt, and 1.15 Mt, respectively. In the 2024 catch, the 2021 cohort was the largest (37%), followed by the 2020 cohort (17%), and then the 2016 cohort (10%).

Data and assessment

This Joint Technical Committee (JTC) assessment depends on fishery landings (1966–2024), an acoustic survey biomass index of age-2+ fish (Figure b) and age compositions (1995–2023), fishery age compositions (1975–2024), maturity-at-age data, and weight-at-age data (1975–2024). In 2011, the survey biomass index of age-2+ fish was the lowest in the time series and was followed by the index increasing in 2012, 2013, and again in 2015 before decreasing to near the time series average in 2017. The survey (Figure b) shows a decline from 2019 (the fourth highest of the series) to 2023 (the third lowest of the series). Age-composition data from the aggregated fisheries and the acoustic survey provide data that facilitates estimating relative cohort strength, i.e., strong and weak cohorts. No survey data are used to inform the size of the 2022–2024 year classes.

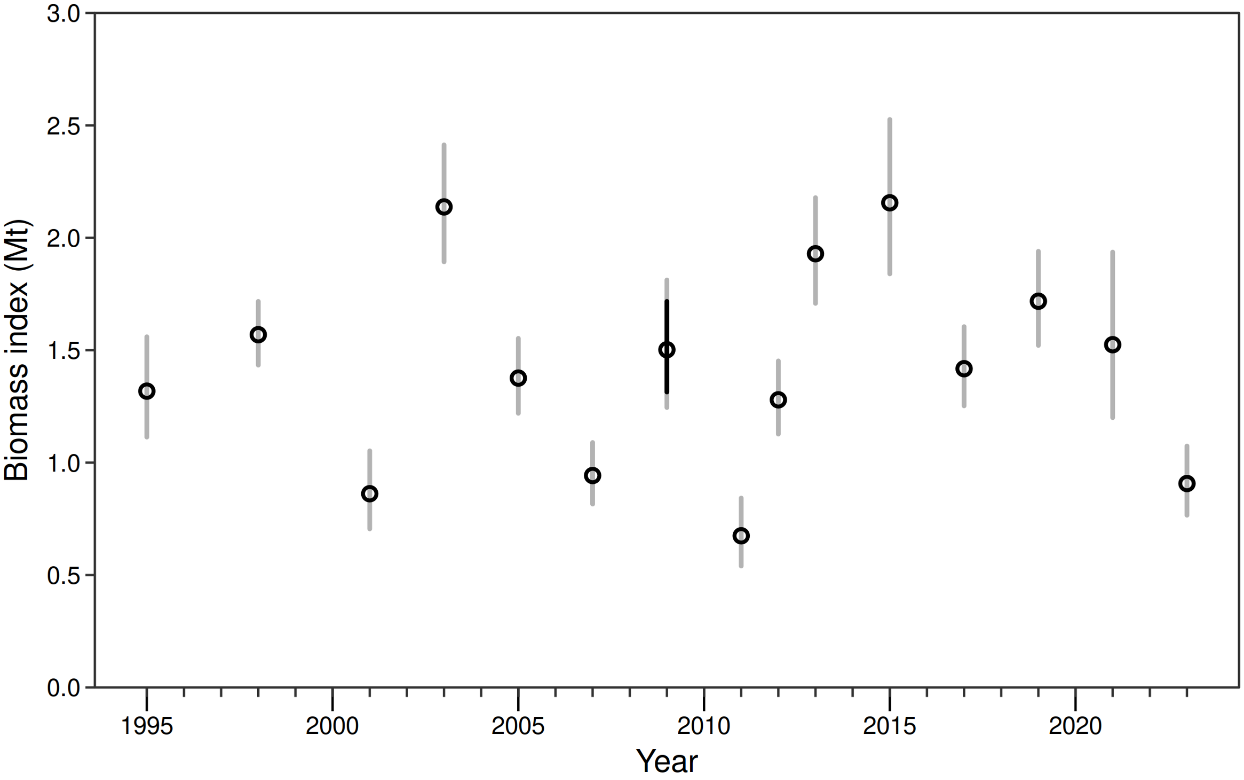

Figure b. Acoustic survey biomass index of age-2+ fish (Mt). Approximate 95% confidence intervals are based on sampling variability (intervals without the additional squid/Pacific Hake apportionment uncertainty included in 2009, black line).

The assessment uses a Bayesian estimation approach, sensitivity analyses, and retrospective investigations to evaluate the potential consequences of parameter uncertainty, alternative structural models, and historical performance of the assessment model, respectively. The Bayesian approach combines prior knowledge about natural mortality, stock–recruitment steepness (e.g., a parameter for stock productivity), and several other parameters, with likelihoods for the acoustic survey biomass index, acoustic survey age-composition data, and fishery age-composition data. Integrating the joint posterior distribution over model parameters provides probabilistic inferences about uncertain model parameters and forecasts derived from those parameters; this is done via Markov chain Monte Carlo sampling using the efficient No-U-Turn Sampler (NUTS). Sensitivity analyses are used to identify alternative model assumptions that may also be consistent with the data. All models, including bridging, sensitivity, and retrospective models, use a Bayesian framework for estimation. Retrospective analyses identify possible poor performance of the assessment model with respect to future predictions. Past assessments have conducted closed-loop simulations that provide insights into how alternative combinations of survey frequency, assessment model selectivity assumptions, changes in the distribution or Pacific Hake, and harvest control rules affect expected management outcomes given repeated application of these procedures over the long term. The results of past (and ongoing) closed-loop simulations help inform decisions made for this assessment.

This 2025 assessment is again configured using Stock Synthesis. The same general population dynamics structure as the base assessment model from 2024 was used except for terminal recruitment and forecast recruitment deviations (so from 2023 onwards), which were fixed at zero in this assessment. Updates to data in this assessment include incorporating fishery catch and age-composition data from 2024, weight-at-age data for 2024, maturity-at-age data for 2023, and minor changes to pre-2024 data. The model-based approaches used to develop the input weight-at-age matrix and time-varying temperature-dependent maturity were retained from last year's assessment to inform fecundity.

The relative index of age-1 fish from the survey was not used to fit this assessment model because it was found to have a strong influence on estimates of recruitment even for cohorts that had several years of data, and because it lacks time-specific measurements of uncertainty. Thus, the only data point that can directly inform the size of the 2023 cohort is from age-1 observations in the commercial fishery in 2024. Given the unique seasonal fishing conditions during the year and that this fishery-dependent data point can be overly influential on the estimated 2023 recruitment, estimated recruitment in 2023 was based solely on the stock–recruitment relationship, with no estimated recruitment deviations (i.e., deviations fixed at zero, giving average recruitment). By necessity, this was also done for 2024 and the projection years. This differs to previous assessment models, for which recruitments at the end of the time series included a random component (extra variability around the stock-recruitment relationship).

This assessment continues to use (since 2014) time-varying (rather than constant) selectivity to maintain flexibility within the fishery dynamics given variability in Pacific Hake distribution patterns. The Dirichlet-multinomial estimation approach to weighting composition data was retained, and a sensitivity to an alternative data-weighting approach was investigated. Time-varying fecundity, which was introduced in 2019, was retained and improved upon with time-varying estimates of maturity in 2024. Assumptions for the forecast period for weight at age, maturity at age, and selectivity continue to be based on conditions during the last five years, as done since the 2020 assessment.

Stock biomass

Results from the base model indicate that since the 1960s, Pacific Hake female spawning biomass has ranged from well below to above unfished equilibrium (Figures c and d). Model estimates suggest that it was below the unfished equilibrium in the 1960s, at the start of the assessment period, due to lower than average recruitment.

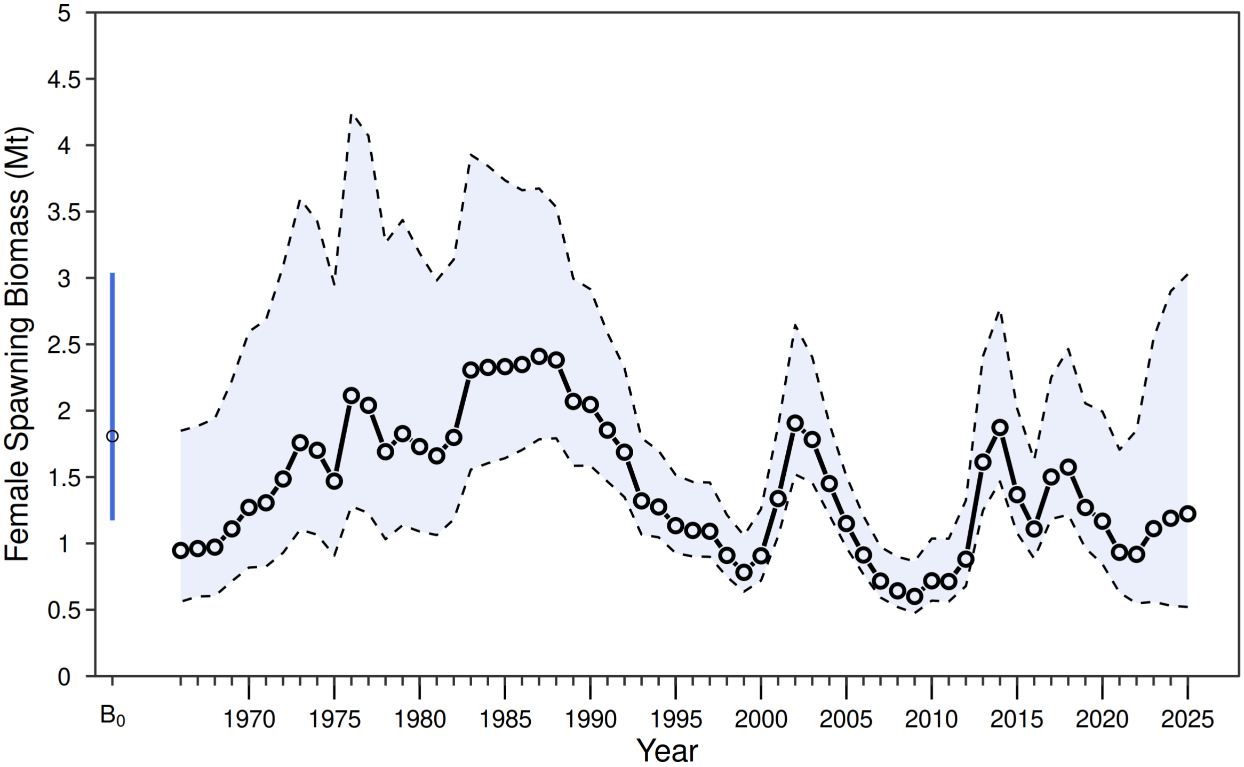

Figure c. Median (solid line) of the posterior distribution for beginning of the year female spawning biomass (B_t in year t; Mt) through 2025 with 95% posterior credibility intervals (shaded area). The left-most circle with a 95% posterior credibility interval is the estimated unfished equilibrium biomass, B_0.

The stock is estimated to have increased rapidly and was above unfished equilibrium in the mid-1970s and mid-1980s (after two large recruitment events in the early 1980s). It then declined steadily to a low in 1999. This was followed by a brief increase to a peak in 2002 as the very large 1999 year class matured. The 1999 year class largely supported the fishery for several years due to relatively small recruitment events between 2000 and 2007. With the aging 1999 year class, median female spawning biomass declined throughout the late 2000s, reaching a time-series low of 0.601 Mt in 2009. Median female spawning biomass is estimated to have peaked again in 2014 due to a very large 2010 year class and an above-average 2008 year class. The subsequent decline from 2014 to 2016 is primarily from the 2010 year class surpassing the age at which the gains in weight from growth are greater than the losses in weight from mortality (growth-mortality transition). The 2014 year class is estimated to be large, though not as large as the 1999 and 2010 year classes, resulting in increasing biomass through 2018. The estimated biomass declined from 2018 to 2022 due to the 2014 and 2016 year classes moving through the growth-mortality transition during a period of high catches. The increase in female spawning biomass from 2022–2025 is due to the above-average 2020 and 2021 cohorts entering maturity and the recent declining trend in catch.

The median estimate of the 2025 relative spawning biomass (spawning biomass at the start of 2025 divided by that at unfished equilibrium, B_0) is 67%. However, the uncertainty is large, with a 95% posterior credibility interval from 29% to 157% (Table b), partly due to remaining unknowns about the size of the potentially large 2021 cohort because it has only been observed once by the acoustic survey.

The median estimate of the 2025 female spawning biomass is 1.223 (with a 95% posterior credibility interval from 0.521 to 3.028) Mt. The current estimate of the 2024 female spawning biomass is 1.189 (0.530–2.900) Mt, giving a much narrower range of uncertainty compared to the estimate from the 2024 assessment of 1.885 (0.853–4.828) Mt. The median is reduced from last year's assessment due to the reduction in the estimate of the 2022 year class with updated data, the aforementioned fixed zero recruitment deviation for the 2023 recruitment, and removal of the age-1 index from the model (which in particularly reduced estimates of several recent year classes).

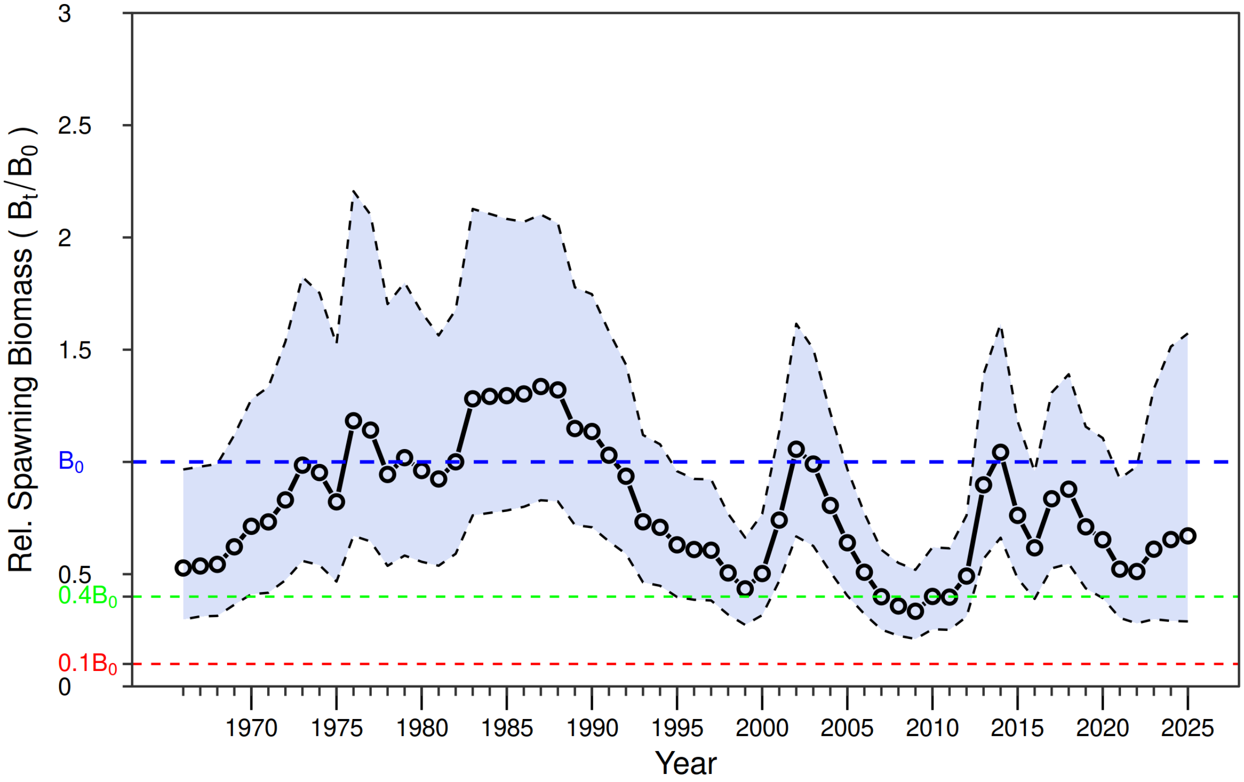

Figure d. Median (solid line) of the posterior distribution for relative spawning biomass (B_t/B_0) through 2025 with 95% posterior credibility intervals (shaded area). Dashed horizontal lines show 10%, 40%, and 100% of the unfished equilibrium (B_0).

Table b. Recent trends in estimated beginning of the year female spawning biomass (SB; kt) and SB relative to estimated SB at unfished equilibrium (Rel. SB; %).

Year	SB 2.5th percentile	SB Median	SB 97.5th percentile	Rel. SB 2.5th percentile	Rel. SB Median	Rel. SB 97.5th percentile
2016	885.9	1,108.8	1,628.2	39.0%	61.7%	95.6%
2017	1,184.1	1,500.6	2,251.5	52.6%	83.6%	130.9%
2018	1,215.9	1,574.8	2,464.8	54.6%	87.9%	139.1%
2019	964.4	1,270.7	2,054.8	43.7%	71.1%	115.7%
2020	844.7	1,167.3	1,993.4	39.3%	65.4%	110.6%
2021	629.5	932.8	1,705.9	30.5%	52.2%	92.5%
2022	548.1	917.7	1,852.1	28.1%	51.2%	98.0%
2023	559.9	1,111.3	2,547.9	29.9%	61.1%	132.6%
2024	530.3	1,189.5	2,899.7	29.2%	65.4%	151.4%
2025	521.1	1,223.1	3,028.2	28.9%	67.1%	157.3%

Recruitment

Pacific Hake have low to moderate recruitment (relative to the long-term average) with occasional large year classes (Table c and Figure e). Very large year classes in 1980, 1984, and 1999 supported much of the commercial catch from the 1980s to the mid-2000s. From 2000 to 2007, estimated recruitment was at some of the lowest values in the time series but this was followed by an above average 2008 year class and a very strong 2010 year class. Above average year classes have occurred since then in 2014, 2016, 2020 and 2021 (median recruitment above the mean of all median recruitments), which have been sustaining the fishery over the last decade, with below average year classes for all other years from 2011–2022.

Table c. Estimates of recent recruitment (millions of age-0 fish) and recruitment deviations, where deviations below (above) zero indicate recruitment below (above) that estimated from the stock–recruitment relationship.

Year	Recruit-ment 2.5th percentile	Recruit-ment Median	Recruit-ment 97.5th percentile	Rec. Deviations 2.5th percentile	Rec. Deviations Median	Rec. Deviations 97.5th percentile
2015	7.7	31.3	107.4	-4.696	-3.370	-2.173
2016	3,453.0	4,996.9	8,892.3	1.265	1.753	2.222
2017	769.5	1,317.7	2,700.2	-0.217	0.388	0.984
2018	34.3	160.2	517.0	-3.255	-1.745	-0.670
2019	37.3	186.1	685.2	-3.106	-1.563	-0.429
2020	1,594.9	3,401.6	9,144.2	0.576	1.348	2.169
2021	2,890.0	7,055.4	19,306.6	1.293	2.099	2.966
2022	14.1	130.8	1,011.6	-4.042	-1.893	0.031
2023	474.0	878.8	1,850.0	–	–	–
2024	475.6	882.3	1,873.5	–	–	–

The addition of 2024 data for this assessment do not significantly change the general pattern of recruitment estimated in recent assessments. However, estimates of absolute recent recruitments are all reduced from the previous assessment due to new data, updated assumptions about recent recruitments and, in particular, removal of the age-1 index. The estimate of 2020 recruitment is above average, whereas in the previous two assessments it was highly uncertain but thought to be possibly very large. The 2021 recruitment is estimated to be potentially large with a median of 7.1 billion fish based on several years of fishery data and the 2023 survey. The 2022 cohort was observed by the age-1 index in 2023 and fit to in the 2024 assessment, which suggested it is average to below average in size; however, with the removal of the age-1 index in this year's assessment the 2022 cohort is now estimated to be very small, based on fishery age data. There are also no survey data available to inform the estimates of the 2023–2024 year class sizes, for which recruitment deviations were set to zero. The general notion remains that recent Pacific Hake recruitment is highly uncertain, and estimates for recent years (based on limited data) can change substantially as new data refines estimates. Retrospective analyses of year class strength for young fish have shown the estimates of recent recruitment to be unreliable prior to at least a modelled age of 3 (observed as age-2 fish the previous year)

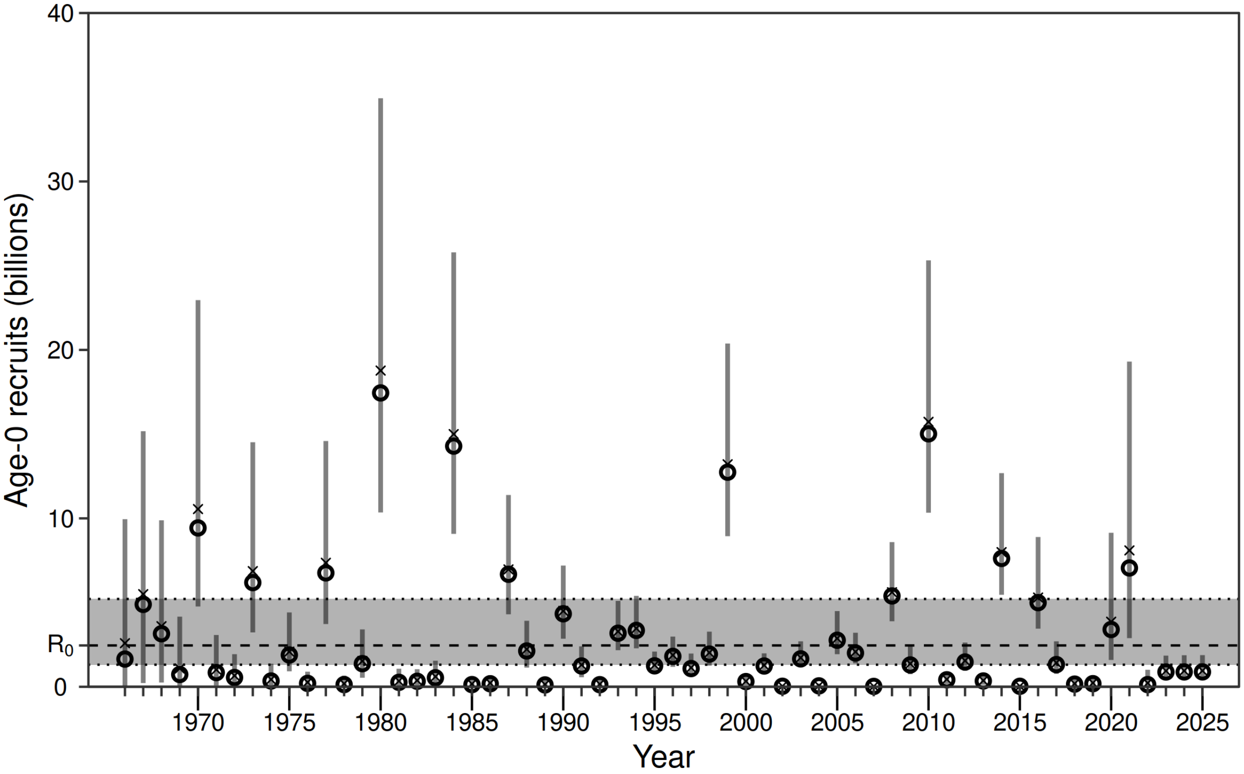

Figure e. Medians (solid circles) and means (X) of the posterior distribution for recruitment (billions of age-0 fish) with 95% posterior credibility intervals (vertical lines). The median of the posterior distribution for mean unfished equilibrium recruitment (R_0) is shown as the horizontal dashed line with the 95% posterior credibility interval shaded between the dotted lines.

without a survey in the most recent year and a modelled age of 2 with a survey, giving further motivation for fixing recruitment deviations to 0 for 2023 this year.

Default harvest policy

The default $F_{40\%}$–40:10 harvest policy prescribes the maximum rate of fishing mortality to equal $F_{\text{SPR}=40\%}$. This rate gives a spawning potential ratio (SPR) of 40%, meaning that the female spawning biomass per recruit with $F_{\text{SPR}=40\%}$ is 40% of that without fishing. If female spawning biomass is below $B_{40\%}$ (40% of B_0), the policy reduces the TAC linearly until it equals zero at $B_{10\%}$ (10% of B_0). Relative fishing intensity for fishing rate F is (1 - SPR(F))/(1 - $\text{SPR}_{40\%}$), where $\text{SPR}_{40\%}$ is an SPR of 40%; it is reported here interchangeably as a proportion or a percentage. A relative fishing intensity above 1.0 means fishing at a rate above $F_{\text{SPR}=40\%}$.

Exploitation status

The median estimated relative fishing intensity on the stock is below the management level of 1.0 for all years (see Table d for recent years and Figure f). Over the last five years, it was the highest in 2019 at 86.6%, dropped in 2020 to 68.9%, increased through 2021

Table d. Recent estimates of relative fishing intensity, (1 - SPR)/(1 - $\mathrm{SPR}_{40\%}$), and exploitation fraction (catch divided by age-2+ biomass).

Year	Rel. Fishing Intensity 2.5^{th} percentile	Rel. Fishing Intensity Median	Rel. Fishing Intensity 97.5^{th} percentile	Exploit. Fraction 2.5^{th} percentile	Exploit. Fraction Median	Exploit. Fraction 97.5^{th} percentile
2015	0.293	0.481	0.686	0.048	0.071	0.090
2016	0.544	0.795	1.028	0.070	0.104	0.132
2017	0.570	0.845	1.170	0.094	0.140	0.178
2018	0.509	0.778	1.067	0.072	0.113	0.147
2019	0.581	0.866	1.121	0.084	0.137	0.182
2020	0.438	0.689	0.926	0.092	0.158	0.219
2021	0.437	0.708	0.966	0.096	0.175	0.260
2022	0.434	0.739	1.051	0.074	0.151	0.258
2023	0.355	0.662	0.996	0.039	0.092	0.185
2024	0.344	0.666	1.078	0.024	0.060	0.135

and 2022 to 70.8% and 73.9% respectively, then dropped in 2023 to 66.2% and in 2024 was 66.6% (Table d and Figure f). Although there is a considerable amount of imprecision around these estimates due to uncertainty in recruitment and spawning biomass, the 95% posterior credibility interval of relative fishing intensity was below 1.0 from 2013–2015 and again in 2020, 2021, and 2023 (Figure f).

The median exploitation fraction (catch divided by biomass of fish of age-2 and above) peaked in 2006 and 2008 (Figure g). The median exploitation fraction has decreased from a recent high in 2021 of 0.18 to 0.06 in 2024, which is the lowest over the past 10 years (Table d and Figure g).

Management performance

Over the last decade (2015–2024), the mean coast-wide utilization rate (proportion of catch target removed) has been 59.6% and catches have been below coast-wide targets (Table e). From 2020 to 2024, the mean utilization rates differed between the U.S. (61.1%) and Canada (36.6%). While Canada's rate was higher than the U.S.'s in 2020, it has dropped considerably over the past few years to historic lows. The utilization rate for the coast-wide fishery this year was the lowest of the previous decade (30.8%) due, in part, to difficulties locating aggregations of fish during the spring and throughout the year in northern areas. The usual 73.88% and 26.12% allocation of coast-wide TAC, as specified in the Joint U.S.-Canada Agreement for Pacific Hake, was implemented for the 2024 fishery. Total landings last exceeded the coast-wide quota in 2002 when utilization was 112%.

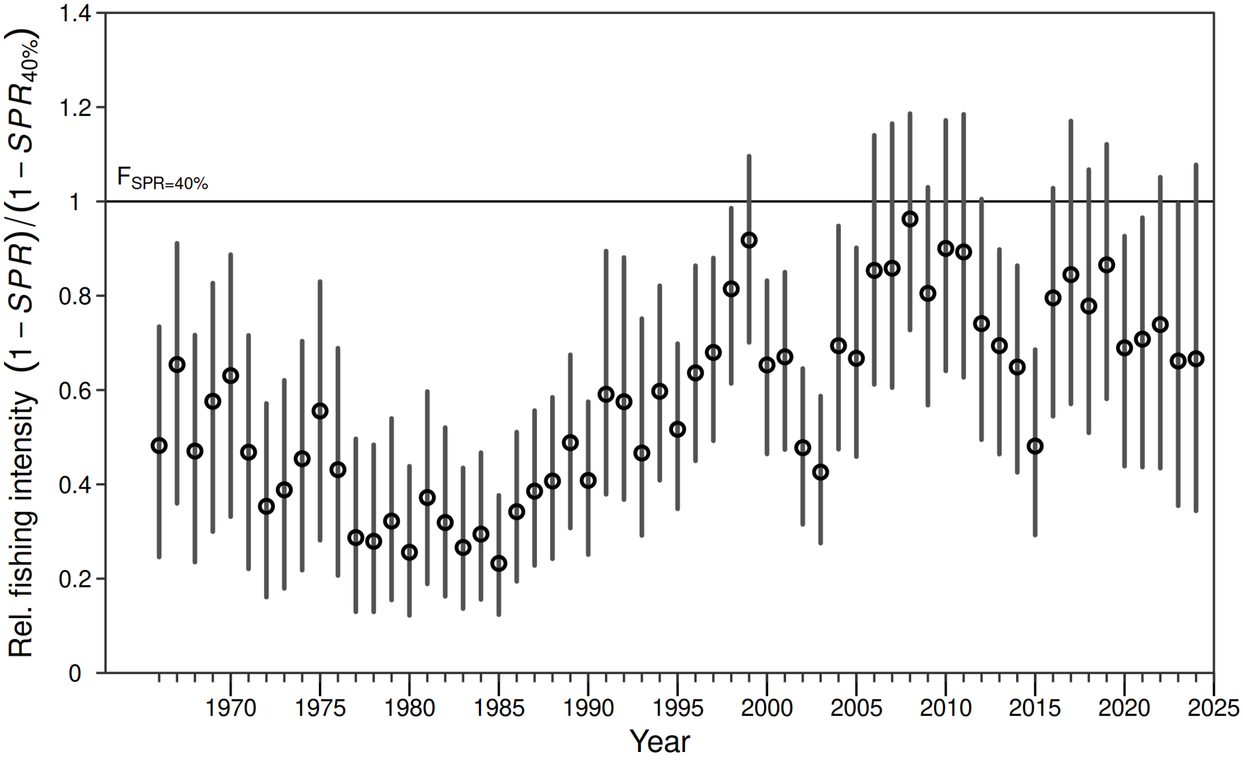

Figure f. Trend in median relative fishing intensity (relative to the $F_{\text{SPR}=40\%}$ management level) through 2024 with 95% posterior credibility intervals. The $F_{\text{SPR}=40\%}$ management level defined in the Joint U.S.-Canada Agreement for Pacific Hake is shown as a horizontal line at 1.0.

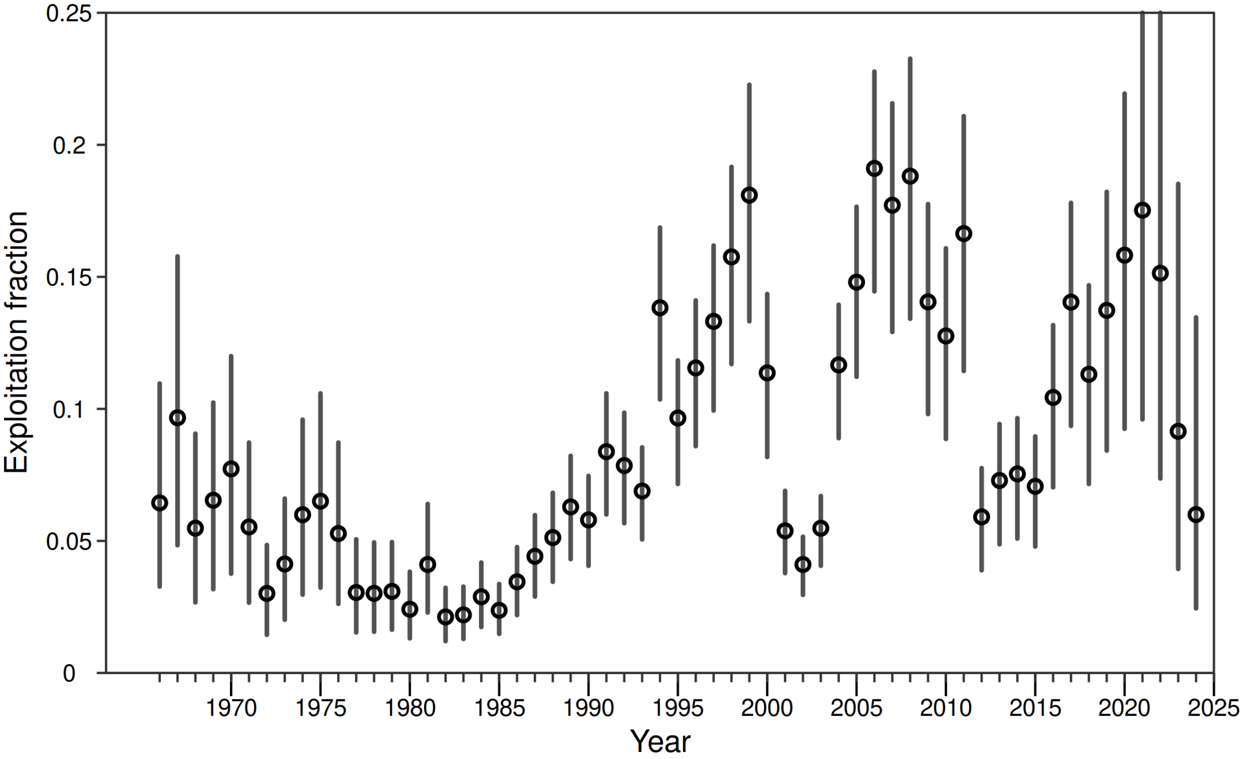

Figure g. Trend in median exploitation fraction (catch divided by age-2+ biomass) through 2024 with 95% posterior credibility intervals.

Table e. Recent trends in Pacific Hake landings and management decisions. Catch targets in 2020 and 2021 were specified unilaterally. All landings and catch targets are given in tonnes.

Year	U.S. landings	Canada landings	Total landings	U.S. prop. of total catch	Canada prop. of total catch	U.S. catch target	Canada catch target	Total catch target	U.S. prop. of catch target removed	Canada prop. of catch target removed	Total prop. of catch target removed
2015	154,160	39,684	193,844	79.5%	20.5%	325,072	114,928	440,000	47.4%	34.5%	44.1%
2016	262,328	69,743	332,071	79.0%	21.0%	367,553	129,947	497,500	71.4%	53.7%	66.7%
2017	353,842	86,721	440,563	80.3%	19.7%	441,433	156,067	597,500	80.2%	55.6%	73.7%
2018	317,827	95,413	413,240	76.9%	23.1%	441,433	156,067	597,500	72.0%	61.1%	69.2%
2019	316,622	95,013	411,635	76.9%	23.1%	441,433	156,067	597,500	71.7%	60.9%	68.9%
2020	286,788	92,489	379,277	75.6%	24.4%	424,810	104,480	529,290	67.5%	88.5%	71.7%
2021	269,359	57,076	326,435	82.5%	17.5%	369,400	104,480	473,880	72.9%	54.6%	68.9%
2022	291,697	31,671	323,368	90.2%	9.8%	402,646	142,354	545,000	72.4%	22.2%	59.3%
2023	240,588	23,952	264,540	90.9%	9.1%	461,750	163,250	625,000	52.1%	14.7%	42.3%
2024	166,923	3,928	170,850	97.7%	2.3%	410,034	144,966	555,000	40.7%	2.7%	30.8%

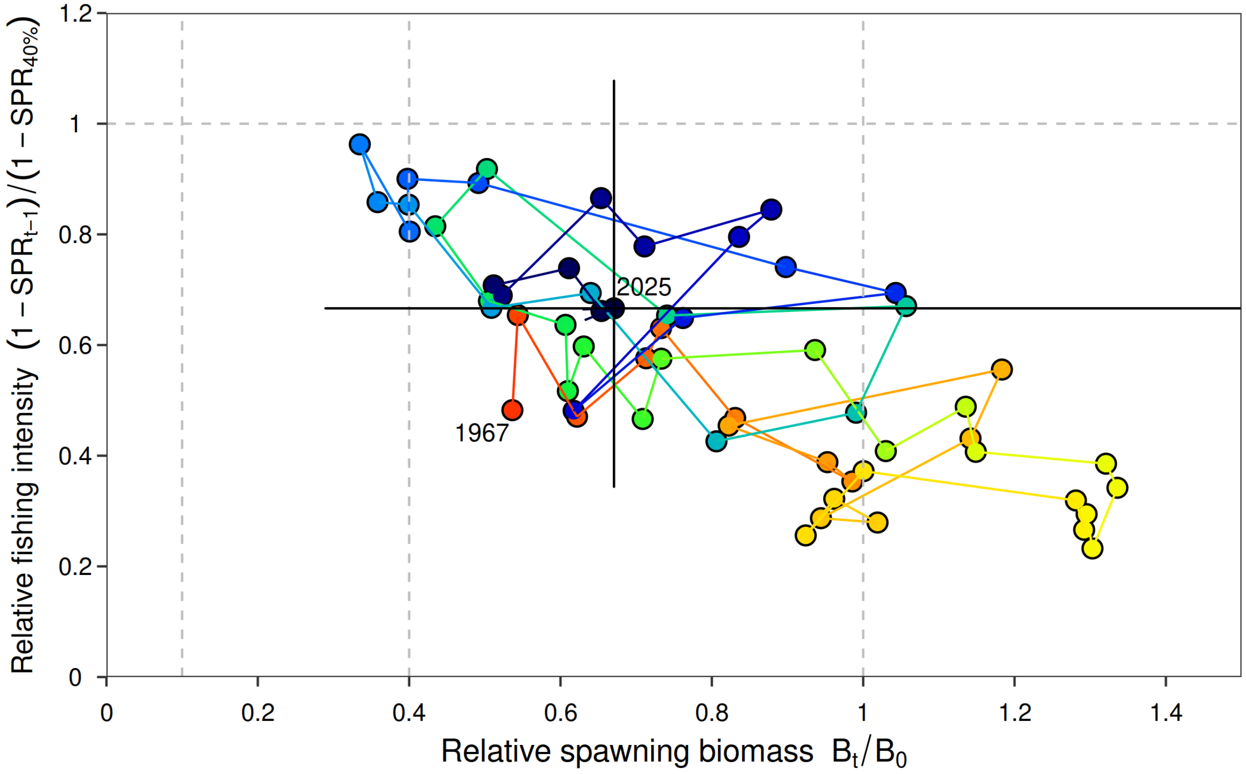

Figure h. Estimated historical path of median relative spawning biomass in year t and corresponding median relative fishing intensity in year $t-1$. Labels show the time series start and end years; labels correspond to year t (i.e., year of the relative spawning biomass). Gray bars span the 95% credibility intervals for 2025 relative spawning biomass (horizontal) and 2024 relative fishing intensity (vertical).

The median relative spawning biomass was above the $B_{40\%}$ reference level in all years except 2007–2009 and 2011 (Figures d and h), and the median relative fishing intensity has always been below 1.0 (Figure h). Relative spawning biomass increased from the lows in 2007–2012 with above average recruitment in 2008, 2010, 2014, 2016, 2020, and 2021. Correspondingly, median relative fishing intensity has remained below 1, and total catch has been declining since the time series high in 2017. While there is large uncertainty in the 2024 estimates of relative fishing intensity and relative spawning biomass, the model estimates a 1.9% joint probability of being both above the target relative fishing intensity ($F_{\text{SPR}=40\%}$) in 2024 and below the relative spawning biomass level of $B_{40\%}$ at the start of 2025.

Reference points

The term 'reference points' is used throughout this document to describe common conceptual summary metrics (Table f). The Agreement specifically identifies $F_{\text{SPR}=40\%}$ as the default harvest rate and $B_{40\%}$ as a point where the 40:10 TAC adjustment is triggered (see the Glossary in Appendix C). The medians of sustainable yields and biomass reference points are lower that those reported in the 2024 assessment, due to the absolute scale of the biomass being lower (due to updated data and changes in model assumptions). The probability that female spawning biomass at the beginning of 2025 is below $B_{40\%}$ is $\text{P}(B_{2025} < B_{40\%}) = 11.1\%$, and of being below $B_{25\%}$ is $\text{P}(B_{2025} < B_{25\%}) = 1.3\%$. The probability that the relative fishing intensity was above the $F_{\text{SPR}=40\%}$ level of 1.0 at the end of 2024 is 4.8%.

Table f. Summary of median and 95% credibility intervals of equilibrium conceptual reference points for the base assessment model. Equilibrium reference points were computed using 1975–2024 averages for mean weight-at-age and baseline selectivity-at-age (1966–1990; prior to time-varying deviations). Dashes (–) indicate values that are static at one value and do not have a credible interval associated with them.

Quantity	2.5%	Median	97.5%
Unfished female spawning biomass (B_0, kt)	1,173	1,808	3,038
Unfished recruitment (R_0, millions)	1,312	2,456	5,215
Reference points (equilibrium) based on $F_{SPR=40\%}$			
Female spawning biomass at $F_{\text{SPR}=40\%}$ ($B_{\text{SPR}=40\%}$, kt)	381	642	1,090
SPR at $F_{\text{SPR}=40\%}$	–	40%	–
Exploitation fraction corresponding to $F_{\text{SPR}=40\%}$	16.3%	19.1%	22.2%
Yield associated with $F_{\text{SPR}=40\%}$ (kt)	164	296	558
Reference points (equilibrium) based on $B_{40\%}$ (40% of B_0)			
Female spawning biomass ($B_{40\%}$, kt)	469	723	1,215
SPR at $B_{40\%}$	40.7%	43.5%	51.6%
Exploitation fraction resulting in $B_{40\%}$	12.5%	16.7%	20.3%
Yield at $B_{40\%}$ (kt)	163	288	545
Reference points (equilibrium) based on estimated MSY			
Female spawning biomass (B_{MSY}, kt)	281	459	859
SPR at MSY	23.1%	29.3%	46.4%
Exploitation fraction corresponding to SPR at MSY	15.1%	27.4%	36.8%
MSY (kt)	171	313	602

Unresolved problems and major uncertainties

Measures of uncertainty in the base model underestimate the total uncertainty in the current stock status and projections because they do not account for possible alternative structural models for hake population dynamics and fishery processes (e.g., selectivity) and the scientific basis for prior probability distributions. To address such structural uncertainties, sensitivity analyses were performed to investigate a range of alternative assumptions and present the key ones in the main document.

The Pacific Hake stock displays high recruitment variability relative to other West Coast groundfish stocks, resulting in large and rapid biomass changes. This leads to a dynamic fishery that potentially targets strong cohorts and results in time-varying fishery selectivity. This volatility results in a high level of uncertainty in estimates of current stock status and stock projections because, with limited data to estimate incoming recruitment, the cohorts are fished before the assessment can accurately determine how big they are (i.e., cohort strength is typically not well known until it is observed by the fishery and survey, typically at a minimum age of three). Further, the impact of interactions among variance parameters that govern variability in fishery selectivity and recruitment parameters through time, as well as those used in relative data weighting, are not well understood. If variance parameters were estimated as random effects, such interactions could propagate uncertainty beyond what is presented in this assessment.

While the removal of both the age-1 index and recent recruitment deviations in this assessment reduced uncertainty around recent spawning stock biomass estimates, it also results in a significant underestimate of uncertainty during the forecast period. The model estimates the 2020 and 2021 cohorts as above average in size, and while their absolute size remains highly uncertain, the uncertainty is less than in last year's assessment (which is only partly due to 2024 data). This reduced uncertainty propagates directly into current and forecasted estimates of female spawning biomass. The 2023 acoustic survey provided additional information on the size of the 2020 year-class (as well as informed the 2021 year class). Collectively, these lessened uncertainty around estimates of female spawning biomass, as did the changes in model assumptions. However, information on the size of the 2023 year class from the 2024 fishery was considered suspect given the unique fishing conditions during the year and so, as mentioned earlier, recruitment deviations from 2023 onwards were set to zero. This does not allow very large (or very small) random recruitments to occur and propagate through the projections as these cohorts mature. Thus, while this results in calculated uncertainty for projections being less than for previous assessments, the true uncertainty is underestimated because median recruitment is assumed rather than allowing a broad distribution. This assumption was deemed preferable this year to allowing potentially large recruitments that can inflate the forecast biomass yet are based on limited or no data and so may not materialise in practice.

Forecast decision tables

The catch limit for 2025 based on the default $F_{40\%}$–40:10 harvest policy has a median of 560,742 t with a wide range of uncertainty, the 95% credibility interval being 203,161–1,605,930 t.

Decision tables give the projected population status (relative spawning biomass) and fishing intensity relative to the target under different catch alternatives for the base model (Tables g and h). The tables are organized to show the projected outcome for each potential catch level and year (row) across the quantiles (columns) of the posterior distribution. Tables show results for up to three years (only two years in subsequent assessments following JMC advice) of future catch levels based on subsequent estimates of stock status and fishing intensity. Figure i shows the projected relative spawning biomass for several of the catch alternatives. Population dynamics and governing parameters assumed during the forecast period include selectivity, weight-at-age and fecundity-at-age averaged over the five most recent years (2020–2024), and constant values for all other parameters.

A relative fishing intensity of 1 should indicate fishing at the $F_{\text{SPR}=40\%}$ default harvest rate catch target. But, the projected median relative fishing intensity can be slightly different than the target because the $F_{\text{SPR}=40\%}$ default harvest-rate catch limit is calculated using baseline selectivity-at-age (1966–1990; prior to time-varying deviations), whereas the forecasted catches use selectivity averaged over the last five years. Recent changes in selectivity will thus be reflected in the determination of fishing relative to the default harvest policy. For example, fishing at the $F_{\text{SPR}=40\%}$ default harvest-rate catch limit (scenario k: default HR) in 2024 results in a median relative fishing intensity of 0.96 (Table h).

Management metrics that were identified as important to the Joint Management Committee and the Advisory Panel in 2012 are presented for 2026 and 2027 projections (Tables i and j; Figures j and k). These metrics summarize the probability of various outcomes from the base model given each potential management action. Although not linear, probabilities can be interpolated from these results with reasonable accuracy for intermediate catch values in 2025 (Table i and Figure j). However, interpolation is not appropriate for the default harvest rule scenario in 2026 because it is conditional on the 2025 catch.

Table g. Forecast quantiles of Pacific Hake relative spawning biomass at the beginning of the year. Catch alternatives are defined by letters a-k and are a constant value across all forecasted years unless otherwise defined in the first column. Acronyms are defined in the glossary (Appendix C).

Catch alternative			Biomass at start of year	Relative spawning biomass		
	Catch year	Catch (t)		5%	50%	95%
			Start of 2025	0.33	0.67	1.36
a:	2025	0	Start of 2026	0.34	0.64	1.23
	2026	0	Start of 2027	0.34	0.60	1.09
	2027	0	Start of 2028	0.34	0.56	0.97
b:	2025	150,000	Start of 2026	0.30	0.60	1.19
	2026	150,000	Start of 2027	0.27	0.53	1.01
	2027	150,000	Start of 2028	0.25	0.46	0.86
c:	2025	200,000	Start of 2026	0.29	0.58	1.18
	2026	200,000	Start of 2027	0.25	0.50	0.99

Continued on next page ...

... *Continued from previous page*

Catch alternative			Biomass at	Relative spawning biomass		
	Catch year	Catch (t)	start of year	5%	50%	95%
	2027	200,000	Start of 2028	0.21	0.43	0.83
d:	2025	250,000	Start of 2026	0.28	0.57	1.16
	2026	250,000	Start of 2027	0.22	0.48	0.96
	2027	250,000	Start of 2028	0.17	0.40	0.79
e:	2025	300,000	Start of 2026	0.27	0.56	1.15
	2026	300,000	Start of 2027	0.20	0.45	0.94
	2027	300,000	Start of 2028	0.14	0.36	0.76
f:	2025	350,000	Start of 2026	0.25	0.54	1.13
	2026	350,000	Start of 2027	0.17	0.43	0.91
	2027	350,000	Start of 2028	0.11	0.33	0.73
g:	2025	400,000	Start of 2026	0.24	0.53	1.12
	2026	400,000	Start of 2027	0.15	0.41	0.89
	2027	400,000	Start of 2028	0.09	0.30	0.70
h:	2025	450,000	Start of 2026	0.23	0.52	1.11
	2026	450,000	Start of 2027	0.13	0.38	0.87
	2027	450,000	Start of 2028	0.09	0.27	0.67
i:	2025	500,000	Start of 2026	0.21	0.50	1.09
	2026	500,000	Start of 2027	0.12	0.36	0.84
	2027	500,000	Start of 2028	0.08	0.23	0.64
j:	2025	555,000	Start of 2026	0.20	0.49	1.08
2024 TAC	2026	555,000	Start of 2027	0.11	0.33	0.81
	2027	555,000	Start of 2028	0.08	0.20	0.60
k:	2025	560,742	Start of 2026	0.20	0.49	1.07
Default HR	2026	463,364	Start of 2027	0.12	0.35	0.84
($F_{\text{SPR}=40\%}$–40:10)	2027	406,150	Start of 2028	0.08	0.25	0.65

Table h. Forecast quantiles of Pacific Hake relative fishing intensity (1 - SPR)/(1 - $\text{SPR}_{40\%}$), expressed as a proportion. Catch alternatives are defined by letters a-k and are a constant value across all forecasted years unless otherwise defined in the first column. Acronyms are defined in the glossary (Appendix C).

Catch alternative			**Relative fishing intensity**		
	Catch year	**Catch (t)**	**5%**	**50%**	**95%**
a:	2025	0	0.00	0.00	0.00
	2026	0	0.00	0.00	0.00
	2027	0	0.00	0.00	0.00
b:	2025	150,000	0.25	0.47	0.77
	2026	150,000	0.24	0.46	0.77
	2027	150,000	0.22	0.45	0.77
c:	2025	200,000	0.31	0.57	0.88
	2026	200,000	0.30	0.56	0.90
	2027	200,000	0.29	0.56	0.93
d:	2025	250,000	0.37	0.65	0.97
	2026	250,000	0.36	0.65	1.01
	2027	250,000	0.35	0.66	1.07
e:	2025	300,000	0.42	0.72	1.04
	2026	300,000	0.42	0.73	1.11
	2027	300,000	0.41	0.76	1.20
f:	2025	350,000	0.47	0.78	1.09
	2026	350,000	0.47	0.80	1.19
	2027	350,000	0.47	0.84	1.28
g:	2025	400,000	0.51	0.83	1.14
	2026	400,000	0.52	0.87	1.25
	2027	400,000	0.52	0.92	1.32
h:	2025	450,000	0.55	0.87	1.19
	2026	450,000	0.56	0.93	1.29
	2027	450,000	0.57	1.00	1.34
i:	2025	500,000	0.59	0.91	1.22
	2026	500,000	0.61	0.98	1.32
	2027	500,000	0.62	1.07	1.35
j:	2025	555,000	0.63	0.96	1.26
2024 TAC	2026	555,000	0.65	1.03	1.34
	2027	555,000	0.67	1.15	1.36
k:	2025	560,742	0.63	0.96	1.26
Default HR	2026	463,364	0.59	0.96	1.32
($F_{\text{SPR}=40\%}$–40:10)	2027	406,150	0.55	0.99	1.34

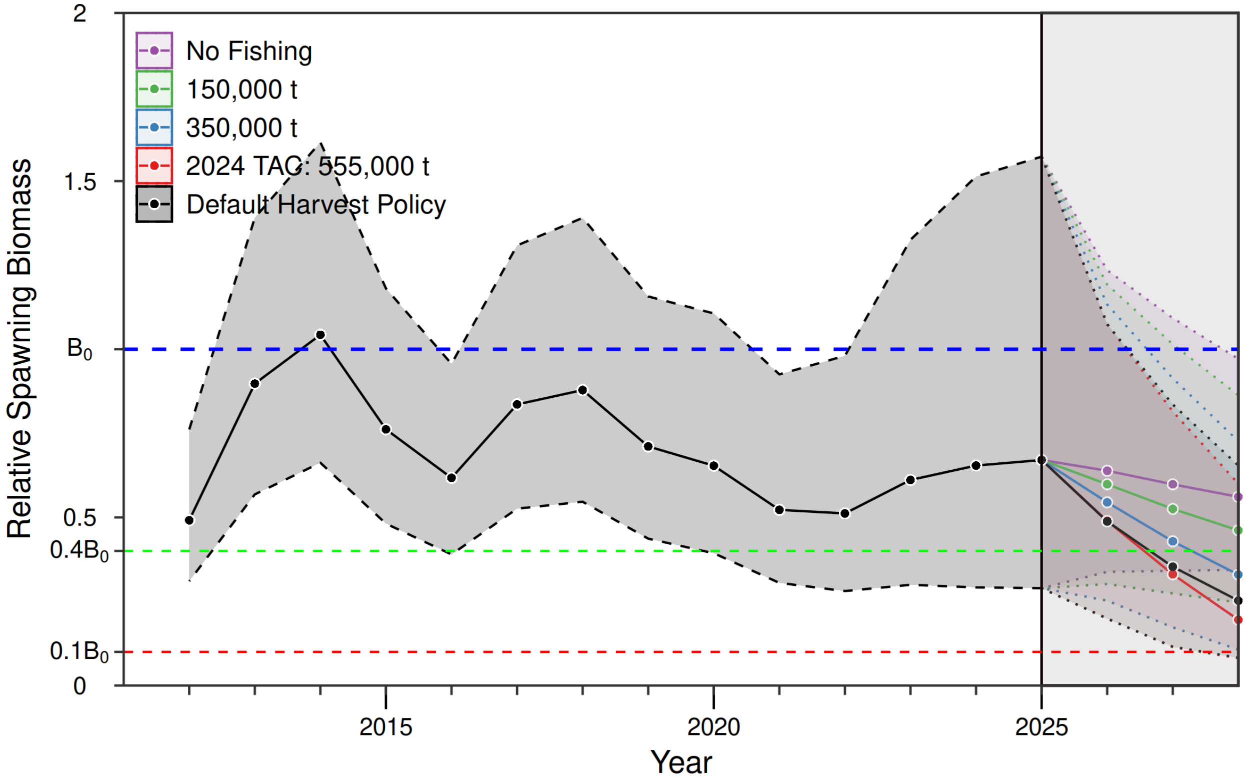

Figure i. Median and 95% posterior credibility intervals of estimated relative spawning biomass to the start of 2025 from the base model and projections to the start of 2028 for several catch alternatives, which are defined in Table g.

With zero catch for the next two years and median recruitment from 2023 onward, the biomass has a 89% probability of decreasing from 2025 to 2026 (Table i and Figure j) and a 93% probability of decreasing from 2026 to 2027 (Table j and Figure k).

For all explored catches, the maximum probability of female spawning biomass at the start of 2026 dropping below $B_{10\%}$ is 0.1% and of dropping below $B_{40\%}$ is 34.4% (Table i and Figure j). With realized catches of 400,000 t in 2025 and 2026, it is estimated that the stock will reach approximately $B_{40\%}$ at the start of 2027, given the current assumption of average recruitment from 2023 onward. As the above average 2014 and 2016 cohorts continue to age, total biomass of these cohorts even without fishing mortality is expected to decrease as losses from mortality outweigh increases from growth. The estimated above-average 2021 cohort will continue to play a large role in determining female spawning biomass during the forecast years presented here.

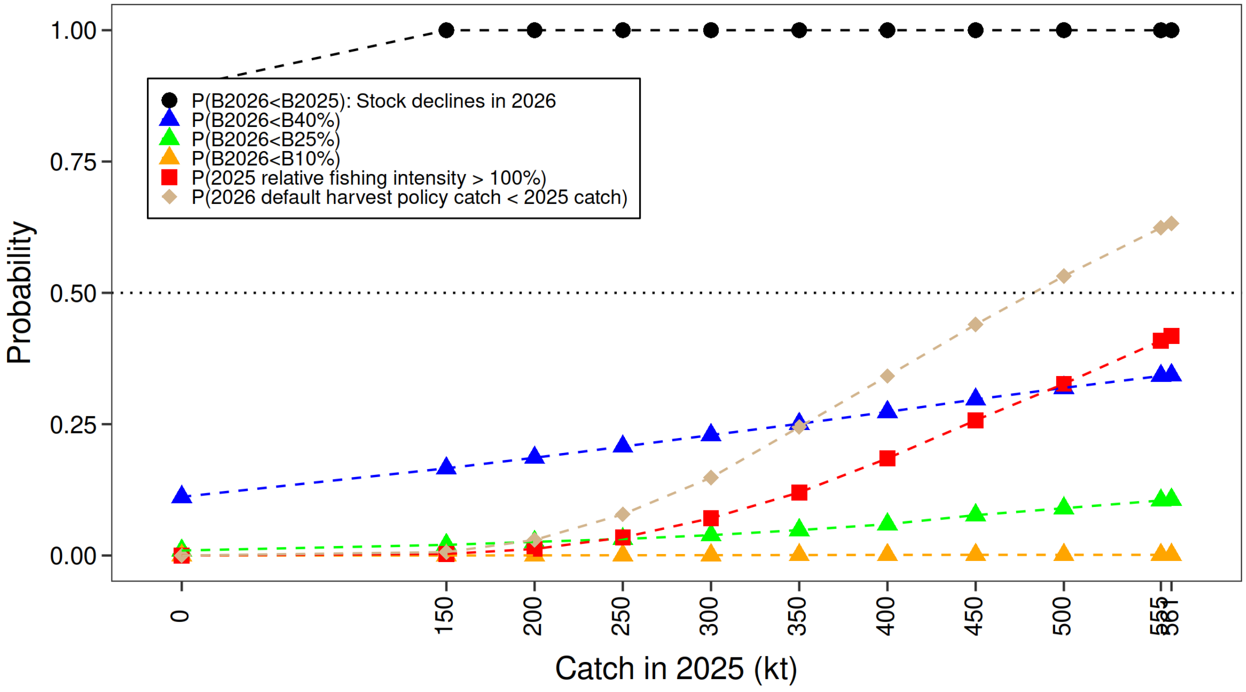

Figure j. Graphical representation of the probabilities related to spawning biomass, relative fishing intensity, and the 2026 default harvest policy catch for alternative 2025 catch options (explained in Table g) as listed in Table i. The symbols indicate points that were computed directly from model output and lines interpolate between the points.

Table i. Probabilities related to spawning biomass, relative fishing intensity, and the 2026 default harvest policy catch for alternative 2025 catch options (catch options are explained in Table g).

	Catch (t) in 2025	$B_{2026} < B_{2025}$	$B_{2026} < B_{40\%}$	$B_{2026} < B_{25\%}$	$B_{2026} < B_{10\%}$	**2025 Fishing intensity > 100%**	**2026 Default HR catch < 2025 catch**
a:	0	0.89	0.11	0.01	0.00	0.00	0.00
b:	150,000	1.00	0.17	0.02	0.00	0.00	0.01
c:	200,000	1.00	0.19	0.03	0.00	0.01	0.03
d:	250,000	1.00	0.21	0.03	0.00	0.03	0.08
e:	300,000	1.00	0.23	0.04	0.00	0.07	0.15
f:	350,000	1.00	0.25	0.05	0.00	0.12	0.24
g:	400,000	1.00	0.27	0.06	0.00	0.18	0.34
h:	450,000	1.00	0.30	0.08	0.00	0.26	0.44
i:	500,000	1.00	0.32	0.09	0.00	0.33	0.53
j:	555,000	1.00	0.34	0.10	0.00	0.41	0.62
k:	560,742	1.00	0.34	0.11	0.00	0.42	0.63

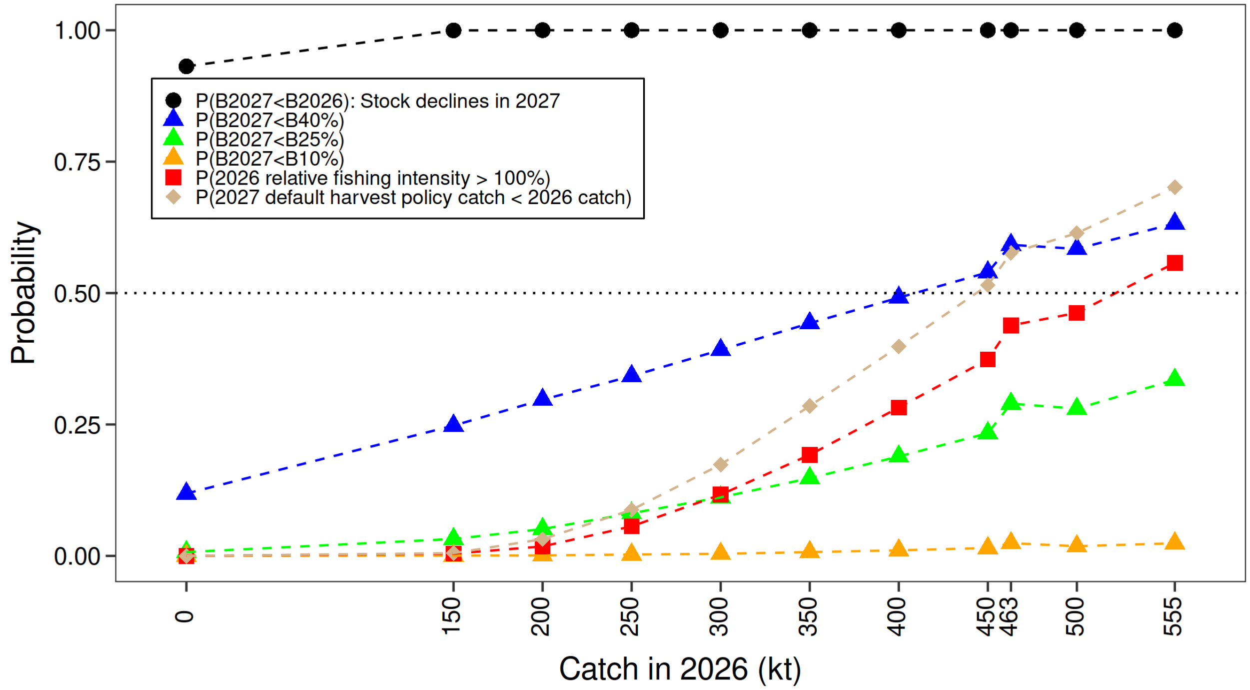

Figure k. Graphical representation of the probabilities related to spawning biomass, relative fishing intensity, and the 2027 default harvest policy catch for alternative 2026 catch options (including associated 2025 catch; catch options explained in Table g) as listed in Table j. The symbols indicate points that were computed directly from model output and lines interpolate between the points.

Table j. Probabilities related to spawning biomass, relative fishing intensity, and the 2027 default harvest policy catch for alternative 2026 catch options, given the 2025 catch level shown in Table i (catch options are explained in Table g).

	Catch (t) in 2026	$\mathbf{B_{2027} < B_{2026}}$	$\mathbf{B_{2027} < B_{40\%}}$	$\mathbf{B_{2027} < B_{25\%}}$	$\mathbf{B_{2027} < B_{10\%}}$	**2026 Fishing intensity > 100%**	**2027 Default HR catch < 2026 catch**
a:	0	0.93	0.12	0.01	0.00	0.00	0.00
b:	150,000	1.00	0.25	0.03	0.00	0.00	0.01
c:	200,000	1.00	0.30	0.05	0.00	0.02	0.03
d:	250,000	1.00	0.34	0.08	0.00	0.06	0.09
e:	300,000	1.00	0.39	0.11	0.00	0.12	0.17
f:	350,000	1.00	0.44	0.15	0.01	0.19	0.29
g:	400,000	1.00	0.49	0.19	0.01	0.28	0.40
h:	450,000	1.00	0.54	0.23	0.01	0.37	0.52
i:	500,000	1.00	0.58	0.28	0.02	0.46	0.61
j:	555,000	1.00	0.63	0.34	0.02	0.56	0.70
k:	463,364	1.00	0.59	0.29	0.02	0.44	0.58

Research and data needs

There are many research projects and data collections that could improve the stock assessment for Pacific Hake and lead to improved biological understanding and decision-making. The following is a list of needs (new and ongoing) that the JTC has identified as having a high probability of improving the overall quality and robustness of the stock assessment. Only the top three are shown in the executive summary.

1. Continue to conduct research to evaluate ways to improve recent, current, and future estimates of recruitment for use in stock assessment. This could include the development of time series of recruitment indices, time series of informative environmental or ecosystem variables, and models that have predictive skill (e.g., Vestfals et al. 2023). Explorations should also consider options for incorporating information on recruitment into the assessment model and the management framework for Pacific Hake. For example, time series could be included in the stock assessment as a standalone data source (similar to the acoustic indices) or improvements could be made to the modeling framework such that these environmental time series could impact the stock–recruitment relationship directly. Results from such work should be connected to or in cooperation with ongoing research related to recruitment variability as discussed in Section 3.3. Related, there is a need to streamline and broaden the availability of products from oceanographic models (e.g., Regional Ocean Modeling System) so they are available across international boundaries and updated on a recurring basis, thereby allowing for their use as informative links in operational stock assessments. A successful example of this has been the annual production of Pacific Hake distribution forecasts that depend on 6–9 month forecasts of subsurface (i.e., 100 m depth) temperature from J-SCOPE. The continued collection of annual histological samples across ages, and the associated resources to complete the histological laboratory work, is needed to inform time-varying maturity in the assessment model. Furthermore, the existing management strategy evaluation framework should be used, or further developed, to examine how information on recruitment can inform robust management decisions.

2. Conduct research on current and future index of abundance data sets or species distribution models that provide new age-based (e.g., recruitment or population-wide) or spatial population structure and distribution information to the stock assessment. In particular, continue to explore the utility of eDNA-based spatiotemporal biomass indices of population abundance. Develop species distribution models for Pacific Hake that utilize ecosystem information as drivers of observations across spatiotemporal domains. Investigate alternative ways to utilize survey age-composition information in the assessment model. Develop estimates of uncertainty for the relative age-1 index and test performance for furture use. Broaden the scope of uncertainty considered in the age-2+ index and adjust for changes arising from the U.S. Integrated Survey Initiative. Bootstrapping of the acoustic survey time series, or related methods, could help incorporate uncertainty related to the target-strength relationship, subjective scoring of echograms, thresholding methods, and methods used to estimate the species mixes for interpreting the acoustic backscatter into the variance calculations. Research should be communicated with those involved in

developing the U.S. West Coast Integrated Survey Initiative. The management strategy evaluation framework should be used, or further developed, to examine how changes in survey methods can be used to inform robust management decisions.

3. Continue to develop value-added scientific products to complement the stock assessment for management decision-making. In particular, work with regional partners to develop risk tables or other annual workflows that provides key metrics, indicators, or other summaries of general ecosystem conditions relevant to the coast-wide population of Pacific Hake. It would be advantageous to include indicators that are potentially associated with Pacific Hake biology and ecology (e.g., recruitment, distribution, predation, prey, and communities). Such information can broaden the context within which a single species stock assessment is interpreted, be used to support model development, refine uncertain assessment conclusions (e.g., productivity), and provide other non-assessment indicators of the system's state to management.

1 INTRODUCTION

The Joint U.S.-Canada Agreement for Pacific Hake (called the Agreement) was signed in 2003, went into force in 2008, and was implemented in 2010. The committees defined by the Agreement were first formed in 2011, and 2012 was the first year for which the process defined by the Agreement was followed. This is the fourteenth annual stock assessment conducted under the Agreement process.

Under the Agreement, Pacific Hake (*Merluccius productus*, also referred to as Pacific whiting) stock assessments are to be prepared by the Joint Technical Committee (JTC) comprised of both U.S. and Canadian scientists and reviewed by the Scientific Review Group (SRG) that consists of representatives from both nations. Additionally, the Agreement calls for both of these bodies to include scientists nominated by an Advisory Panel (AP) of fishery stakeholders.

The primary data sources for this assessment include an acoustic survey, annual fishery catch, mean weight-at-age data, maturity-at-age data, as well as survey and fishery age-composition data. The assessment depends primarily upon an index of biomass from the acoustic survey for information on the scale of the current population. Age-composition data provide additional information allowing the model to resolve strong and weak cohorts. The catch is an important source of information regarding changes in abundance and places a lower bound on the available population biomass in each year.

This assessment is fully Bayesian, with the base model incorporating prior information on several key parameters (including informative priors on natural mortality, M, and steepness of the stock–recruitment relationship, h) and integrating over parameter uncertainty to provide results that can be probabilistically interpreted. From a range of alternate models investigated by the JTC, a subset of sensitivity analyses are also reported to provide a broad qualitative comparison of structural uncertainty with respect to the base model (Section 3.8). The model is implemented using version 3.30.23.1 of the Stock Synthesis software (Methot, Jr. and Wetzel 2013). The 2025 base model is structurally similar to last year's model, except the 2025 base model does not include estimates of annual recruitment deviations in the final two years of the model (i.e., 2023 and 2024) and the age-1 index has been excluded. All model runs reported in this document are performed in a Bayesian context. Responses to 2024 SRG requests are in Section 3.3 and a Glossary of terms appears in Appendix C.

1.1 Stock structure and life history

Pacific Hake is a semi-pelagic, schooling species distributed along the west coast of North America, generally ranging in latitude from 25° to 55° North Latitude (N. Lat.); Figure 1. It is among 18 species of Pacific Hake from four genera (being the majority of the family *Merluccidae*), which are found in both hemispheres of the Atlantic and Pacific Oceans (Alheit and Pitcher 1995; Lloris et al. 2005). The coastal population of Pacific Hake is currently the most abundant groundfish population in the California Current system. Smaller populations of this species occur in the major inlets of the Northeast Pacific Ocean, including the Strait of Georgia, the Puget Sound, and the Gulf of California. Each of these smaller populations are genetically distinct from the coastal population (Vrooman and Paloma 1977; Iwamoto et al. 2004; King et al. 2012; García-De León et al. 2018; Longo et al. 2024). The coastal population is also distinguished from the inshore populations by larger size at age and seasonal migratory behavior and from fish off the west coast of Baja California by smaller size at age and later spawning (Zamora-García et al. 2020).

The coastal population of Pacific Hake typically ranges from the waters off southern California to northern British Columbia and rarely into southern Alaska, with the northern boundary related to fluctuations in annual migration (Hamel et al. 2015) depending, in part, on water temperature (Malick et al. 2020a, 2020b). In spring, adult Pacific Hake migrate onshore and northward to feed along the continental shelf and slope from Northern California to Vancouver Island. In summer, Pacific Hake often form extensive mid-water aggregations in association with the continental shelf break, with the highest densities located over bottom depths of 200–300 m (Dorn and Methot 1991, 1992).

Older Pacific Hake exhibit the greatest northern migration each season, with two- and three-year old fish rarely being observed in Canadian waters north of Southern Vancouver Island. During El Niño events (warm ocean conditions such as in 1998 and 2016), a larger proportion of the population migrates into Canadian waters (Figure 2), due to temperature effects (Malick et al. 2020a) and possibly intensified northward transport during the period of active migration (Dorn 1995; Agostini et al. 2006). In contrast, La Niña conditions (colder water, such as in 2001, 2011, and 2021) result in a southward shift in the distribution of Pacific Hake, with a much smaller proportion of the population found in Canadian waters compared to during El Niño years, a trend evident from the acoustic surveys (Figure 2). In general, warmer than average thermal habitat conditions for mature Pacific Hake lead to relatively higher biomass further north and relatively lower biomass around the U.S.–Canadian border, while cooler than average conditions lead to relatively higher biomass of immature Pacific Hake generally spread evenly across their distribution (Malick et al. 2020a). The distribution of age-1 fish also changes between years (Figure 3).

1.2 Ecosystem considerations

Pacific Hake are important to ecosystem dynamics in the Eastern Pacific Ocean due to their relatively large total biomass and potentially large role as both prey and predator (Hicks et al. 2013). Ongoing research investigating abiotic (i.e., environmental conditions) and biotic (e.g., maturity and diet) drivers of the distribution, recruitment, growth, and survival of Pacific Hake could provide insight into how the population is linked with broader ecosystem considerations. For example, Turley and Rykaczewski (2019) found decreased survival of larval Pacific Hake as storm events increased, contrary to many other species in the Southern California Current Ecosystem. An analysis of drivers of recruitment across the maternal preconditioning, egg, and larval phases of Pacific Hake recruitment indicated recruitment is associated with eddy kinetic energy, the location of the North Pacific Current bifurcation, and upwelling during maternal preconditioning, as well as with northward long-shore transport and the number of days between storm events during larval stages (Vestfals et al. 2023). Phillips et al. (2022) suggest temperature dynamically influences the co-occurrence of Pacific Hake and krill (i.e., euphausiids; *Euphausiacea*), which can influence annual Pacific Hake growth and recruitment as the availability of key prey species shifts. Temperature was also found to impact the co-occurrence of Pacific Hake and Shortbelly Rockfish (*Sebastes jordani*, Sebastidae) during the 2014–2016 marine heatwave (Free et al. 2023). An index of abundance for Humboldt Squid (*Dosidicus gigas*) suggests that the abundance of Pacific Hake decreases with increasing squid abundance (Stewart et al. 2014; Taylor et al. 2015). Many additional research topics relevant to Pacific Hake distribution, recruitment, and growth patterns in relation to oceanographic conditions have been investigated (Ressler et al. 2007; Hamel et al. 2015; Malick et al. 2020a, 2020b) and provide a foundation for further research on these topics.

Motivated by such research, focusing on Vestfals et al. (2023) in particular, we include a new Pacific Hake-specific ecosystem summary in Appendix H. We collate time series of relevant ecosystem processes that are believed to influence Pacific Hake recruitment. These include prey/competitors (Pacific Herring, *Clupea pallasii*, off Vancouver Island) and predators (age-1 Pacific Hake), basin-scale oceanography, and local calculations of sea-surface temperature, alongshore transport, sea-surface height, mixed layer depths, and the strength of poleward undercurrent. These are calculated for specific areas and time periods corresponding to different life-history stages of Pacific Hake (Vestfals et al. 2023). While not comprehensive or definitive, this is a start to including such Pacific Hake-relevant ecosystem information in the annual stock assessment.

Recent oceanographic trends and large-scale ecosystem conditions, as summarized in the National Oceanic and Atmospheric Administration's (NOAA) annual California Current Ecosystem Status Reports (Leising et al. in prep, for 2024) provide insight into potential drivers of Pacific Hake population dynamics and fleet operations. Periods of high productivity are often marked by strong winter and spring upwelling which brings nutrients to coastal waters, cooler temperatures, an energy-rich copepod community, and high productivity of krill, a key food source for Pacific Hake (Buckley and Livingston 1997; Harvey et al. 2021).

During 2024 (Leising et al. in prep), basin-scale climate patterns suggest below average to average conditions in the California Current Ecosystem (CCE). A strong El Niño in 2023-24 resulted in warm temperatures during winter and spring and delayed upwelling. The responses of lower trophic level communities to these conditions were typical of those observed during previous El Niño events. For example, the biomass of lipid-rich northern copepods and adult krill were below average in the northern region of the CCE in winter and spring. However, the El Niño conditions dissipated quickly and the ecosystem transitioned to cooler and more productive conditions following a strong spring upwelling. The northern copepods and krill recovered to near average abundances in summer and fall, and the forage community throughout the CCE was relatively diverse and productive. Observations of forage communities in the central and southern regions of the CCE indicate that the abundances of larval and juvenile Pacific Hake in these regions are above average and have been increasing over the past five years. At the same time, consumption of Pacific Hake by Bluefin Tuna and Swordfish has been well above average in recent years (2022-23) and the spawning stock biomass of these predators has been increasing over this same period as well. See Appendix H for more details and a 'risk table' documenting ecosystem and climate factors potentially affecting Pacific Hake stock productivity and uncertainty.

Using empirical weight-at-age data in the model allows for time-varying growth without needing a mechanistic relationship or environmental data, which facilitates an 'Ecosystem Approach to Fisheries Management' (a priority for Department of Fisheries and Oceans [DFO] and NOAA; see Section 2.4.1). Furthermore, the year-specific maturity-at-age specifically includes a temperature effect from a spatiotemporal model (Section 2.4.2). Related ongoing research should provide more insights into the specific mechanisms affecting changes in growth and fecundity, which will enable further condition-specific prediction capabilities (e.g., assumptions of growth, or weight at age, and fecundity during forecast years). It is hypothesized that temporal changes in weight-at-age data may be due to ecosystem effects such as prey availability, predator abundance, and ocean temperature (Chittaro et al. 2022).

1.3 Management of Pacific Hake

Since the implementation of the Magnuson–Stevens Fishery Conservation and Management Act in the U.S. and the declaration of a 200-mile fishery-conservation zone in the U.S. and Canada in the late 1970s, annual quotas (or catch targets) have been used to limit the catch of Pacific Hake in both countries' zones. Scientists from both countries historically collaborated through the Technical Subcommittee of the Canada–U.S. Groundfish Committee (TSC), and there were informal agreements on the adoption of annual fishing policies. During the 1990s, however, disagreements between the U.S. and Canada on the allotment of the catch limits between U.S. and Canadian fisheries led to quota overruns; the 1991–1992 national quotas summed to 128% of the coast-wide limit, while the 1993–1999 combined quotas were an average of 112% of the limit. The Agreement establishes U.S. and Canadian shares of the coast-wide total allowable catch (TAC) at 73.88% and 26.12%, respectively, and this distribution has largely been adhered to since 2005. A bilateral agreement on the coast-wide TAC could not be reached in 2020 and 2021; so, catch targets were set unilaterally during these years for the first time since the inception of the Agreement. Catch allocations as specified in the Agreement have since been applied.

Since 1999, an upper limit on catch has been calculated using an $F_{\text{SPR}=40\%}$ default harvest rate with a 40:10 adjustment. This decreases the catch linearly from the catch at a relative spawning biomass of 40% to zero catch at a relative spawning biomass values of 10% or less (called the default harvest policy in the Agreement); relative spawning biomass is the female spawning biomass divided by that at unfished equilibrium. Further considerations have almost always resulted in catch targets being set lower than the recommended catch limit. Total catch has not exceeded the coast-wide quota since 2002, and harvest rates are likely to have never exceeded the $F_{\text{SPR}=40\%}$ target.

1.3.1 Management of Pacific Hake in the United States

In the U.S. zone, participants in the directed fishery are required to use pelagic trawls with a codend mesh of at least 7.5 cm. Regulations have also restricted the area and season of fishing to reduce the bycatch of Chinook Salmon (*Oncorhynchus tshawytscha*), depleted rockfish populations, and other species as related to their specific harvest specifications. The current allocation agreement, effective since 1997, divides the U.S. harvest into tribal (17.5%) and non-tribal (82.5%, including a small amount set aside for research) components. Starting in 1996, the Makah Tribe has conducted a fishery with the tribal allocation in its usual and accustomed fishing area. The non-tribal harvest allocation is divided among catcher-processors (34%), motherships (24%), and shoreside vessels (42%). Since 2011, the non-tribal U.S. fishery has been fully rationalized with allocations in the form of Individual Fishing Quotas (IFQs) to the shoreside sector and group shares to cooperatives in the at-sea mothership (MS) and catcher-processor (CP) sectors. The At-Sea Hake Observer Program (A-SHOP) has been monitoring fishing vessel activity since 1975, originally monitoring foreign and joint-venture vessels. All domestic vessels have full observer coverage since 1991, including the 2020 and 2021 fishing seasons, despite the COVID-19 pandemic.

Shortly after the 1997 allocation agreement was approved by the Pacific Marine Fisheries Commission, fishing companies owning catcher-processor vessels with U.S. West Coast groundfish permits established the Pacific whiting Conservation Cooperative (PWCC). The primary role of the PWCC is to distribute the catcher-processor allocation among its members to achieve greater efficiency and product quality, as well as promoting reductions in waste and bycatch rates relative to the former 'derby' fishery in which all vessels competed for a fleet-wide quota. The mothership fleet has also formed a cooperative where bycatch allocations are pooled and shared among the vessels. The individual cooperatives have internal systems of in-season monitoring and spatial closures to avoid and reduce bycatch of salmon and rockfish.

1.3.2 Management of Pacific Hake in Canada

Canadian groundfish managers distribute their portion of the coast-wide TAC as quota to individual license holders. In 2024, Canadian Pacific Hake fishermen were allocated a TAC of 144,966 t, which did not include any carryover quota. Canadian priority lies with the domestic fishery. However, when there is determined to be an excess of fish for which there is not enough domestic processing capacity, fisheries managers give consideration to a Joint-Venture fishery in which foreign processor vessels are allowed to accept codends from Canadian catcher vessels while at sea. The last year there was Joint-Venture quota allocation was in 2018.

In 2024, all Canadian Pacific Hake trips were subject to 100% observer coverage by electronic monitoring for both the shoreside component of the domestic fishery and the freezer-trawler component. There is no in-person observer program for the Canadian Pacific Hake fisheries.

Retention of all catch, with the exception of prohibited species, was mandatory. The retention of groundfish other than Sablefish, Mackerel, Walleye Pollock, and Pacific Halibut on dedicated Pacific Hake trips using electronic monitoring was not allowed to exceed 10% of the landed catch weight. The bycatch allowance for Walleye Pollock was 30% of the total landed weight.

1.4 Fisheries

The fishery for the coastal population of Pacific Hake occurs along the coasts of Northern California, Oregon, Washington, and British Columbia primarily during May–November. The fishery is conducted with mid-water trawls and has met the Marine Stewardship Council (MSC) Fisheries Standard to be certified as meeting sustainable fishing benchmarks since 2009. Foreign fleets dominated the fishery until 1991, when domestic fleets began taking the majority of the catch. Catches were occasionally greater than 200,000 t prior to 1986, and since then, they have been greater than 200,000 t for all except five years.

In 2021, the Pacific Hake fishery was Canada's largest commercial wild fishery (species with the largest catch), representing 10% of Canada's total landings of all species (www.dfo-mpo.gc.ca). Over CAD $19 million in wages was estimated to have been paid to employees of the processing industry in British Columbia in 2021, with an exported value of greater than CAD $60 million in product to Ukraine (greater than CAD $25 million), China, South Africa, Lithuania, and other countries (Fisheries and Oceans Canada 2023).

In the United States, over USD $89.2 million in labor costs is estimated to have been paid to employees in 2022 (www.noaa.gov). This includes wages paid to: crew and captains fishing on catcher vessels that deliver shoreside and at-sea to motherships, workers in shore-based processing facilities, crew, captains, and workers on catcher-processor vessels, and workers on mothership vessels. The exported value of Pacific Hake was USD $172 million in 2022, including to Netherlands, Lithuania and Spain, which make up about 58% of the total (www.noaa.gov). The total economic impact of the Pacific Hake fishery on the U.S. West Coast in 2022 was USD $295 million in income and 4,324 jobs (Steiner et al. 2024).

The Joint Management Committee (JMC) determined an adjusted (for carryovers) coastwide TAC of 555,000 t for 2024. The U.S. catch target was set at 410,034 t and the Canadian catch target at 144,966 t. A brief review of the 2024 fishery is presented here by country (Tables 1–3 and Figure 4). Additional information is available in annual U.S. and Canada Advisory Panel reports (Appendices E and D).

1.4.1 Fisheries for Pacific Hake in the United States

In 2024, the U.S. specified catch target (i.e., adjusted for carryovers) of 410,034 t was further divided among the research, tribal, catcher-processor, mothership, and shoreside sectors. After the tribal allocation of 17.5% (71,756 t) and a 750 t allocation for research catch and bycatch in non-groundfish fisheries, the 2024 non-tribal U.S. catch limit of 337,528 t was allocated to the catcher-processor (34%), mothership (24%), and shoreside (42%) commercial sectors. Reallocation of 45,000 t of tribal quota to non-tribal sectors on

September 26 resulted in final quotas for the catcher-processor, mothership, and shoreside sectors of 130,060 t, 91,807 t, and 160,662 t, respectively.

Prior to 2015, the shoreside sector was allowed to fish starting June 15 north of 42° N. Lat. (the Oregon–California border) and April 1 between 40° 30′ N. Lat. and 42° N. Lat., whereas the at-sea sectors were allowed to fish starting May 15. Between 2015–2022, the shoreside sector was allowed to fish north of 40° 30′ N. Lat. starting May 15 and south of 40° 30′ N. Lat. starting April 15, although only 5% of the shoreside allocation was released for this early period. Since 2023, all sectors have been allowed to fish starting May 1. Regulations do not allow at-sea processing or night fishing (midnight to one hour after official sunrise) south of 42° N. Lat. at any time during the year.

In 2024, the total catch of Pacific Hake in U.S. waters was ranked 34th over all years (Table 1) and the U.S. utilization rate (40.7%) was the lowest it has ever been (see Appendix E for more details). The catcher-processor, mothership, and shoreside sectors caught 47.6%, 22.8%, and 52.3% of their final reallocated quotas, respectively. Tribal landings, which are included in the shoreside sector totals were 0 t (zeros may not reflect actual catch if less than three vessels were fishing; see appendix E for further details). The median fishing depth for the at-sea sectors was slightly deeper than the last few years (Figure 5). The shoreside sector had the largest monthly catches during July, August, and September. While, the at-sea sectors had the largest monthly catches during May, September, and October.

In both U.S. at-sea sectors, age-3 and age-4 fish associated with the 2021 and 2020 year classes were common ages caught. Both ages were seen last year in appreciable numbers as age-2 and age-3 fish. The reported proportions at age summarize sampling efforts on 192 catcher-processor hauls and 51 mothership hauls (Table 4). For the catcher-processor sector, the four most abundant age classes (by numbers) seen in 2024 were age-3 (39.0%), age-4 (18.9%), age-1 (11.8%), and age-8 (8.8%); Table 5. For the mothership sector, the four most abundant age classes for 2024 were age-3 (59.8%), age-2 (11.9%), age-4 (10.1%), and age-1 (7.5%) (Table 6).

Age-samples from 59 shoreside trips in 2024 showed similar age compositions in the catch compared to the at-sea sectors, though not nearly as many smaller (age-2 and age-1) fish and more age-8 and age-10 fish from the 2016 and 2014 year classes. The four most abundant age classes with the highest occurrence in 2024 were age-3 (28.6%), age-4 (17.9%), age-8 (12.9%), and age-10 (10.2%) (Table 7). Age-compositions from the at-sea and shoreside sectors during this last year were less similar than they were the previous year.

1.4.2 Fisheries for Pacific Hake in Canada

The 2024 Canadian Pacific Hake domestic fishery removed 3,928 t from Canadian waters (Table 2), which was 2.7% of the Canadian TAC of 144,966 t. For the third year in a row, the attainment for Canada was much lower than usual, due to the fishing vessels having a difficult time finding fish in Canadian waters (see Appendix D and the last two years' assessments, Berger et al. (2023) and Grandin et al. (2024), for more details).

The shoreside vessels, which land fresh round product onshore, landed 1,185 t in 2024, the lowest on record since 1990, and less than half of the 2023 landings of 3,657 t. The freezer trawlers, which freeze headed and gutted product while at sea, landed 2,742 t. This was the lowest amount the freezer trawlers have landed since 2013, despite doubling the number of vessels since then.

Fishing started in early April and ended in November. The general view of the Canadian fleet is that abundance in Canadian waters remained below normal levels in 2024, including the normally-abundant areas outside of Southwest Vancouver Island. Reports of difficulties finding fish in 2024 led to most vessels not leaving the dock, therefore amplifying the effect of low catches. The fish caught in Canada appeared to be mostly from four age classes (see below), with very few smaller fish (less than 500 grams) caught.

The most abundant year classes in the Canadian shoreside catch in 2024 (by numbers; Table 8) were age-8 (30.8%), age-7 (18.0%), age-10 (15.9%), and age-14 (11.7%). The most abundant year classes in the Canadian freezer-trawler catch (by numbers; Table 9) were age-8 (29.9%), age-10 (18.9%), age-7 (14.9%), and age-9 (12.9%).

2 DATA

Fishery-dependent and fishery-independent data used in this assessment (Figure 7) include the following sources:

- Total catch from all U.S. and Canadian fisheries that targeted Pacific Hake from 1966 to 2024 (Tables 1–3).
- Fishery age compositions aggregated by year and country-specific sector for the last ten years are available (Tables 5–9) to investigate region-specific trends; age compositions aggregated by year, composed of data from the U.S. fishery (1975–2024) and the Canadian fishery (1988–2024), are used to fit the model (Table 10 and Figure 8).
- An age-2+ biomass index and age compositions from the Joint U.S. and Canadian Integrated Acoustic and Trawl Survey (1995, 1998, 2001, 2003, 2005, 2007, 2009, 2011, 2012, 2013, 2015, 2017, 2019, 2021, 2023; Tables 11, 12, and 13; Figures 8 and 9).
- The relative age-1 index (billions of age-1 fish) derived from the Joint U.S. and Canadian Integrated Acoustic and Trawl Survey was used in a sensitivity model exploration in this assessment (Table 32; Figure 46).
- An age-1+ relative biomass index for Pacific Hake based on environmental DNA was used in a sensitivity model exploration in this assessment. The index covers the years 2019, 2021, and 2023. A full explanation of the data and index can be found in Appendix G.

The following biological relationships, derived from external analysis of auxiliary data, were input as fixed values in the assessment model:

- Ageing-error matrices based on cross-read and double-blind-read otoliths.

- Annual proportions of female Pacific Hake at each age that are mature (Section 2.4.2) from histological analyses of ovary samples (Table 14; Figure 10).
- Weight-at-age from fishery and survey catches (1975–2024; Figures 11–14).
- Derived fecundity-at-age as the product of year-specific weight-at-age multiplied by year-specific maturity-at-age (Figures 10 and 13).

Additional data sources not used in this assessment are discussed in Section 2.3.

2.1 Fishery-dependent data

2.1.1 Total catch

The catch of Pacific Hake for 1966–2024 is summarized by country-specific sectors (Tables 1–3) and modeled as annual coast-wide catches. Catches in U.S. waters prior to 1978 are available only by year from Bailey et al. (1982) and historical assessment documents. Canadian catches prior to 1989 are also unavailable in disaggregated form. U.S. shoreside landings are from the Pacific Fishery Information Network (PacFIN) database. Foreign and Joint-Venture catches for 1981–1990 and U.S. domestic at-sea catches for 1991–2024 are calculated from the Alaska Fisheries Science Center's North Pacific Groundfish and Halibut Observer (NORPAC) database, which also stores A-SHOP data. Canadian Joint-Venture catches from 1989 are from the Groundfish Biological (GFBio) database. Canadian shoreside landings are from the Groundfish Catch (GFCatch) database for 1989–1995, the Pacific Harvest Trawl (PacHarvTrawl) database for 1996–March 31, 2007, and the Fisheries Operations System (FOS) database for April 2007–present.

Minor updates to catches used in previous assessments were made based on the best available information extracted from the aforementioned databases. Tribal catches were available in PacFIN for the U.S. tribal fishery at the time the data were extracted and were cross-checked with numbers based on information provided by the Makah Tribe. The Makah Tribe is also working on providing historical catches such that shoreside catches can be summarized separately from tribal catches since the onset of the fishery.

Historically, the fishery for Pacific Hake has been well covered by observers with slight differences in coverage by sector. Currently, U.S. shoreside vessels carry observers and are required to retain all catch and bycatch for sampling by plant observers. Vessels participating in the U.S. at-sea sectors are also required to have observers on board and have since 1990. U.S. foreign and Joint-Venture vessels had varying levels of coverage from 1975–1990 ranging from 21–100% coverage. Canadian Joint-Venture and Canadian freezer-trawler vessels were monitored by at-sea observers from 1996–2019. In 2020 and 2021 there were no observers on Canadian freezer trawlers due to staffing issues and in 2022 the decision was made to stop providing observers on board all Canadian vessels. Early in 2022 a sampling plan designed by Canadian managers, scientists, and the sampling contractor, Archipelago Marine Research Ltd. (AMR), was put into place to ensure the ongoing sampling of Pacific Hake on Canadian vessels (see Section 2.1.2). Canadian trawl catches are monitored autonomously at sea by cameras onboard vessels. Catch is recorded by dockside samplers within the Groundfish Trawl Dockside Monitoring Program using total catch weights provided by processing plants. Discards are negligible relative to the total fishery catch for all sectors.

2.1.2 Fishery biological data

Biological information from the U.S. at-sea sectors was extracted from the NORPAC database. This included sex, length, weight, and age information from the foreign and Joint-Venture fisheries from 1975–1990 and from the domestic at-sea fishery since 1990. Observers collected data by selecting fish randomly from each haul. The number of otoliths collected per haul has varied over time but is currently three fish every third haul.

Since 1991, biological samples from the U.S. shoreside sector have been sampled by port samplers located where there are substantial landings of Pacific Hake, primarily Eureka, Newport, Astoria, and Westport. Port samplers took one sample per offload (or trip) consisting of 100 randomly selected fish for individual length and weight. From those 100 fish, typically 20 fish were randomly subsampled for otolith extraction.

When there were observers (1996–2019) aboard Canadian freezer trawlers, they collected 50 otoliths and 300 lengths per sample, sampling once per day during trips that on average lasted seven days. Since 2022, freezer-trawler employees have collected fish for sampling from two tows per trip and delivered them to the dock as frozen specimens where they are eventually sampled for length, weight, sex, and otoliths. Each delivery consists of approximately 100 fish, 50 fish from one tow and 50 fish from another tow, where each tow is bagged separately. Due to unforeseen circumstances while at sea, some trips did not deliver any bags and some only delivered one bag.

For electronically observed Canadian shoreside trips, port samplers obtained biological data from the landed catch. For each sampled trip, approximately 50 ages and 300 lengths were sampled from the catch. Observed domestic haul-level information is aggregated to the trip level to be consistent with the unobserved trips that were sampled in ports.

In years when there was a Canadian Joint-Venture fishery, length samples were collected every second day of fishing operations and otoliths were collected once per week. Length and age samples were taken randomly from a given codend. The sample weight from which biological information was collected was inferred from length–weight relationships.

The sampling unit for shoreside samples is the trip, while the haul is the primary unit for the at-sea samples (Table 4). There is no least common denominator for aggregating at-sea and shoreside samples because detailed haul-level information is not recorded for shoreside trips and hauls sampled in the at-sea sectors cannot be aggregated to a comparable trip level. As a result, initial sample sizes are simply the summed hauls and trips for fishery biological data.

Biological data were analyzed based on the sampling protocols used to collect them and expanded to estimate the corresponding statistic from the entire landed catch by fishery and year when sampling occurred. A description of the analytical steps for expanding the age compositions can be found in earlier stock assessment documents (Hicks et al. 2013; Taylor et al. 2014).

The aggregate fishery age-composition data (1975–2024) confirm the well-known pattern of large cohorts born in 1973, 1977, 1980, 1984, 1987, 1999, 2008, 2010, 2014, and 2016, and suggests large cohorts for 2020 and 2021 (Table 10 and Figure 8). Recent age-composition data still easily track the 2010 cohort, as well as the large cohorts born since then. Currently, the 2021 cohort is the largest observed cohort in the U.S. at-sea sectors (Tables 5–6), and shoreside sector (Table 7), and the 2016 cohort is the largest observed cohort in both Canadian fleets (Tables 8–9). Age-1 fish were observed by the fishery this year (Table 10) in the U.S. For the combined data in 2024, the 2021 cohort was the largest (37%), followed by the 2020 cohort (17%), and then the 2016 cohort (10%). For the combined data in 2023, the 2021 cohort was the largest (36%), followed by the 2020 cohort (25%), and then the 2016 cohort (13%).

We caution that proportion-at-age data contain information about the relative numbers-at-age, which can be affected by changing recruitment, selectivity, or fishing mortality, making these data difficult to interpret on their own. For example, the above-average 2005 and 2006 year classes declined in proportion in the 2011 fishery samples but persisted in small proportions for years in the fishery catch. Their reductions in 2011 were due to mortality and the overwhelming size of the more recent large cohorts. The assessment model is fit to these data to estimate the absolute sizes of incoming cohorts, which become more precise after they have been observed over several years.

Both the weight- (Figure 14; Section 2.4.1) and length-at-age information suggest that growth of Pacific Hake has fluctuated markedly over time (see Figure 7 in Stewart et al. 2011). This is particularly evident in the frequency of larger fish ($>$ 55 cm) before 1990 and a shift towards larger fish starting again in the 2000s.

2.2 Fishery-independent data

2.2.1 Acoustic survey

The Joint U.S. and Canadian Integrated Acoustic and Trawl Survey (Stewart et al. 2011) has been the primary fishery-independent tool used to assess the distribution, abundance, and biology of coastal age-2+ Pacific Hake along the west coasts of the U.S. and Canada. The acoustic surveys performed in 1995, 1998, 2001, 2003, 2005, 2007, 2009, 2011, 2012, 2013, 2015, 2017, 2019, 2021, and 2023 were used in this assessment (Table 12). The acoustic survey samples transects that represent all waters off the coasts of the U.S. and Canada thought to contain all portions of the age-2+ Pacific Hake stock. Observations of age-0 and age-1 Pacific Hake are excluded from the age-2+ index due to largely different schooling behavior relative to older Pacific Hake, concerns about their catchability by the trawl gear, and differences in expected location during the summer months when the survey takes place. Observations of age-1 Pacific Hake are recorded during the survey, and additional analyses, described below, are conducted to develop a relative age-1 index that is excluded from the base model this year in the final bridging step (see Section 3.4.1 and Appendix B).

The 2023 survey covered U.S. and Canadian waters from Point Conception to north of Haida Gwaii using 116 transects (Figure 2). In the U.S., transects were mostly separated by 10 nautical miles; six transects were dropped to account for available ship days at sea.

In Canada, transects were separated by 10 nautical miles along Vancouver Island and then 20 nautical miles further north. The NOAA Ship Bell M. Shimada and the Canadian Coast Guard's Sir John Franklin worked collaboratively to complete the full extent of the survey in 2023.

Distributions of the backscatter of Pacific Hake plotted for each acoustic survey since 1995 illustrate the variable spatial patterns across time of age-2+ fish (Figure 2). This variability is due in part to changes in the composition of the age-2+ population because older Pacific Hake tend to migrate farther north and partially due to environmental and/or climatic factors. The 1998 acoustic survey is notable because it shows an extreme northward distribution that is thought to be related to the strong 1997–1998 El Niño. In contrast, the distribution of Pacific Hake during the 2001 acoustic survey was compressed into the lower latitudes off the coast of Oregon and Northern California following the strong La Niña event in 2000. In 2003, 2005, and 2007 the distribution of Pacific Hake did not show an unusual coast-wide pattern despite 2003 and 2007 being characterized as El Niño years. In 2011, 2012, and 2013 the majority of the biomass distribution of Pacific Hake was again found in U.S. waters, which is more likely due to age composition than the environment because 2013 had some warmer than average sea-surface temperatures. In 2015, sea-surface temperatures were warmer again, resulting in a northern shift in the overall distribution. The distribution of Pacific Hake in 2017 was more uniform across latitudes than observed in 2015, which is likely a result of having large proportions of both the 2010 and 2014 cohorts (Figure 2). Weak El Niño conditions in 2019 decreased in their prevalence starting in March of that year, leading to neutral conditions by July. Consequently, during the 2019 survey Pacific Hake were found on all survey transects from just north of Morro Bay, California to the northern end of Vancouver Island, with the greatest offshore extent found off of Cape Mendocino, California. During the 2021 survey, the majority of Pacific Hake were found in U.S. waters, congruent with the continuation of La Niña conditions in the California Current from 2020 to 2021. Despite the switch to El Niño conditions in April of 2023, very few fish were seen in Canadian waters during the 2023 survey. Ongoing research is looking into relationships between environmental conditions and Pacific Hake distribution and recruitment that will help to inform the mechanisms behind observations (Malick et al. 2020b; Phillips et al. 2023).

During the acoustic surveys, mid-water trawls are made opportunistically to determine the species composition of the observed acoustic sign and to obtain the Pacific Hake length data necessary to scale the acoustic backscatter into biomass (see Table 12 for the number of trawls in each survey year). Biological samples collected from these trawls are post-stratified, based on similarity in size composition, and the composite length frequency is used to characterize the size distribution of Pacific Hake along each transect and to predict the expected backscattering cross section for Pacific Hake based on the fish-size target-strength (TS) relationship. Any potential biases that might be caused by factors such as alternative TS relationships are partially accounted for in catchability. But, variability in the estimated survey biomass due to uncertainty in TS is not explicitly accounted for in the assessment.

Data from the acoustic survey are analyzed using kriging, which accounts for spatial correlation, to provide an estimate of total biomass as well as an estimate of the year-specific sampling variability due to patchiness of schools of Pacific Hake and irregular transects (Petitgas 1993; Rivoirard et al. 2000; Mello and Rose 2005; Simmonds and MacLennan 2006). Advantages to the kriging approach are discussed in the 2013 stock assessment (Hicks et al. 2013).

For the 2016 assessment (Grandin et al. 2016), the data from all surveys since 1998 were reanalyzed using consistent assumptions, an updated version of the EchoPro software, and a common input-file structure because some previously generated files had spurious off-transect zeros because of how the data were exported. The same analytical procedure was carried out during the reanalysis of 1995 survey data (Berger et al. 2017) and during the preparation of survey data collected since 2017. The assumptions are as follows:

- fixed minimum ($k_{min} = 3$) and maximum ($k_{min} = 10$) number of points used to calculate the value in a cell;
- search radius is three times the length scale that is estimated from the variogram; and
- biomass decays with distance from the end of the transect when extrapolating biomass beyond the western end of a transect, which was refined and supported by the SRG starting with the 2016 assessment (Grandin et al. 2016).

Starting in 2021, the EK 60 echosounders were replaced with EK 80 echosounders, and thus, survey estimates from years using the new echosounders are scaled by a factor of 1.06 to convert the EK 80 to EK 60 acoustic data. The survey team will eventually be converting all pre-2021 EK 60 data to an equivalent EK 80 format. Thus, a full time series of consistently analyzed survey biomass (Table 12 and Figure 9) and age compositions (Table 11 and Figure 8) since 1995 are used to fit the stock assessment model. These data contain many sources of variability (see Stewart et al. 2011) but results from research done in 2010 and 2014 on their representativeness show that trawl sampling and post-stratification is only a small source of variability. Specifically, repeated trawls at different depths and spatial locations on the same aggregation of Pacific Hake were similar and analyses regarding the method used to stratify the data led to similar overall conclusions.

Estimated age-2+ biomass in the survey increased steadily over the four surveys conducted in 2011–2013 and 2015 (Table 12 and Figure 9). It decreased in 2017 to 1.42 Mt, then increased to 1.72 Mt in 2019, and has since decreased to 0.91 Mt in 2023. The 2023 survey age composition was made up of 50.58%, 24.66%, 8.09%, 5.38%, and 2.92% from the 2021, 2020, 2016, 2014, and 2017 year classes, respectively. Note that the estimate of biomass does not include age-0 or age-1 fish and the age compositions used to estimate selectivity of the survey also exclude age-0 and age-1 fish (Table 11). Estimates of country-specific age-2+ biomass are also provided (Table 13).

The separate relative age-1 index (numbers of fish) was excluded from the base model this year as described in the bridging models (see Section 3.4.1). This is similar to the 2013–2021 assessments (Hicks et al. 2013; Johnson et al. 2021), where the relative age-1 index was only explored as a sensitivity model. The index was included in the base model from 2022–2024. For the sensitivity model, the relative index of age-1 fish was estimated similarly to previous years, including the use of a 1.06 scaling factor to account for differences between the EK 60 and EK 80 echosounders Similar to what is done for the age-2+ index. The index indicates relative changes between years, not absolute values, and confirms the large year classes in 2008, 2010, 2014, and 2016, and suggests large cohorts for 2020 and 2022 (Table 12 and Figure 3).

Incorporating the relative age-1 index can result in estimates of recruitment strength that are informed on average one year earlier than models without the index (e.g., Figures 54 and G.1 in Johnson et al. 2021). The suite of sensitivity models related to the relative age-1 index explored over the past decade indicate that its use typically informs recruitment such that the direction of cohort strength (i.e., weak, strong, or neutral) remains unchanged in subsequent assessments even after being informed by more data. The utility of an informed recruitment signal was deemed far greater than an uninformed recruitment assumption. The Joint U.S. and Canadian Integrated Acoustic and Trawl Survey team supports exploring its use in the stock assessment and is committed to continually evaluating and refining approaches to improve the estimates and related uncertainty. This year the age-1 index was excluded from the base model in the final bridging step (see Section 3.4.1 for more details).

2.3 Other data not used in this assessment

Some data sources were not included in the base model but have been explored or were included in previous stock assessments. Data sources not discussed here have either been discussed at past Pacific Hake assessment review meetings or are discussed in more detail in the 2013 stock assessment document (Hicks et al. 2013). These primarily include those listed below.

- Fishery and survey length compositions.
- Fishery and survey conditional age-at-length compositions.
- Calculation of a reliable fishery catch-per-unit-effort (CPUE) metric is particularly problematic for Pacific Hake, and it has never been used as an index for the assessment of this stock (see Hicks et al. 2013 for more details).
- Biomass indices and age compositions from the following years of the Joint U.S. and Canadian Integrated Acoustic and Trawl Survey: 1977, 1980, 1983, 1986, 1989, and 1992.
- Bottom trawl surveys in the U.S. and Canada (various years and spatial coverage from 1977–2024).
- Northwest Fisheries Science Center/Southwest Fisheries Science Center/PWCC coast-wide juvenile Pacific Hake and rockfish surveys (2001–2024). However, the JTC is analyzing the age-0 Pacific Hake data from these surveys in collaboration with researchers from the Southwest Fisheries Science Center and Australia, to investigate potential for developing an early indication of potential cohort strength.
- California Cooperative Oceanic Fisheries Investigations (CalCOFI) larval Pacific Hake production index, 1951–2006. The data source was previously explored and

rejected as a potential index of Pacific Hake female spawning biomass. However, the JTC are exploring new avenues to utilize CalCOFI data based on recently developed methods (related to previous bullet).

- Bycatch of Pacific Hake in the trawl fishery for Pink Shrimp off the coast of Oregon (2004, 2005, 2007, and 2008).
- Historical biological samples collected in Canada prior to 1990 but currently not available in electronic form.
- Historical biological samples collected in the U.S. prior to 1975 but currently not available in electronic form or too incomplete to allow for their analysis with methods consistent with more current sampling programs.
- Northwest Fisheries Science Center winter 2016 and 2017 acoustic research surveys of spawning Pacific Hake.

2.4 Externally analyzed data

2.4.1 Weight-at-age

A matrix of empirically derived population weight-at-age data by year (Figures 11–14) is used in the current assessment model to translate numbers at age to biomass at age. Annual weight-at-age data was modelled from biological samples pooled from all fisheries and most surveys for the years 1965 to 2024 (Figures 11–14). Samples from near-shore areas, such as the Puget Sound, were not included. The earliest samples come from the U.S. shoreside vessels that date back to 1965. With the effort to reconstruct all historical data, some additional historical samples were found within the U.S. databases for this assessment, such as these early shoreside samples. Additional effort is ongoing to ensure that all samples taken during the acoustic survey research trips are also available. Past investigations into calculating weight-at-age data for the fishery and survey independently showed little impact on model results, and thus, a single matrix is used for all fleets and beginning and middle-of-the-year population weight-at-age.

A generalized linear mixed model (GLMM) with a lognormal distribution has been used to model weight-at-age data external to the assessment since the 2024 assessment, with weight relating to a smoothed effect of age between ages zero and fifteen; random effects for cohort and year; and fixed effects for sex. The model is similar to models investigated for Walleye Pollock off Alaska, where models with correlations between age, cohort, and year were found to best fit the data (Cheng et al. 2023). Weights from fish ages 15 and above for each year were pooled, and thus, ages 15–20 are assumed to have the same weight-at-age. Estimated parameters from this model were used to predict weight for ages zero to fifteen from 1975 to 2024 for each sex. The means of annual, age-specific estimates across both sexes were used for input into the assessment model. The number of samples (Figure 12) is generally proportional to the amount of catch.

The biomass at the start of a given year is based on the weight-at-age from the same mid-year, when the majority of samples are available (Figure 11). Prior to 1975, weight-at-age input to Stock Synthesis is assumed to be equal to the mean of all available years for each respective age (1975-2024) (Figure 11). Forecast weight-at-age data are based on age-specific means from the most recent five years (2020–2024), consistent with forecast selectivity (Figure 11).

The use of empirical weight-at-age data is a convenient method to capture the variability in both the weight-at-length relationship within and among years as well as the variability in length-at-age data, without requiring parametric models to represent growth relationships. Previous attempts to explicitly model year- and cohort-specific growth were not successful for Pacific Hake and have not been revisited since Stewart et al. (2011). The empirical weight-at-age method requires the assumption that observed values are not biased by strong selectivity at length or weight and that the spatial and temporal patterns of the data sources provide a representative view of the underlying population. Simulations show that, in general, using empirical weight-at-age data when many observations are available results in more accurate estimates of spawning biomass than modeling growth (Kuriyama et al. 2016).

2.4.2 Maturity and fecundity

Maturity-at-age has always been modelled external to the assessment but up through the the 2023 assessment (Berger et al. 2023) the maturity ogive was time-invariant. Starting with the 2024 assessment (Appendix G in Grandin et al. 2024), annual age-based maturity ogives (Figure 10) were developed using the same data, i.e., histological estimates of functional maturity (Table 14), but fit with a spatiotemporal GLMM (Head et al. 2025). These data include samples collected north of Point Conception (34° $44'$ N. Lat.) and south of the U.S./Canada border from the acoustic survey, winter and summer acoustic research trips, U.S. catcher-processor vessels by A-SHOP observers, and the U.S. West Coast Groundfish Bottom Trawl Survey since 2009. Southern samples have been excluded from maturity analyses since 2018 (Edwards et al. 2018) because they are thought to mature at earlier ages and smaller sizes. Canadian samples (n = 73) were excluded from the spatiotemporal model because their of their lack of spatiotemporal resolution. These Canadian samples could be included in future analyses after all of the Canadian samples are analyzed and/or more Canadian samples are collected and analyzed.

The probability of being functionally mature was estimated using the inverse logit of the effects of a spatial field, spatially varying coefficients for the quadratic function of age to account for the potential for skip spawning in older individuals, a smooth effect of calendar day modeled with penalized (P-spline) regression (Eilers and Marx 1996), a linear offset for fishery-dependent samples, and year effects as a quadratic function of modeled subsurface (130.67 m) temperature indices in the domain of the West Coast Groundfish Bottom Trawl Survey (Lellouche et al. 2021). The model is

$$E[\mathbf{y}] = g^{-1}\left(\mathbf{X}\boldsymbol{\beta} + \mathbf{Z}\mathbf{b} + \boldsymbol{\omega}_s + \mathbf{x}_{age} * \boldsymbol{\zeta}_{s,age} + \mathbf{x}_{age^2} * \boldsymbol{\zeta}_{s,age^2}\right), \tag{1}$$

where $g^{-1}()$ represents the inverse-logit function, $\mathbf{X}$ represents the design matrix of fixed effects with estimated parameters $\boldsymbol{\beta}$ that include the quadratic effects of temperature, the P-spline is represented with random effect design matrix $\mathbf{Z}$ and corresponding coefficients $\mathbf{b}$,

$\boldsymbol{\omega}_s$ represents a constant spatial field shared across years, and $\boldsymbol{\zeta}_{s,age}$ and $\boldsymbol{\zeta}_{s,age^2}$ represent spatially varying coefficient effects of age. The stochastic partial differential equation approximation to Gaussian Random Fields (Lindgren et al. 2011) was used to approximate the spatial field with a series of estimated random effects. The mesh representing the spatial field used a cutoff distance of 50 km. The temperature covariate has the potential to add mechanistic relationships to the modeling and reduce uncertainty in years where no or few samples are collected.

Biomass-weighted averages of temperature were created using estimates of the spatial distribution of Pacific Hake from West Coast Groundfish Bottom Trawl Survey catch-per-unit-effort data. These estimates were modeled using the same spatial-GLMM approach as was used for the maturity model with a smooth effect of calendar day via a P-spline, a time varying intercept modeled with a random walk, a spatial field, and spatiotemporal variation modeled as a first-order autoregressive process. A Tweedie distribution (Shono 2008) was used to model the catches given their skewed nature. Predictions were made to spatial cells from the GLORYS12v1 re-analysis that were in the spatial domain of the West Coast Groundfish Bottom Trawl Survey on July 1 (middle of the survey). These predictions were then used to create a weighted average of temperature across space.

Maturity-at-age was estimated to be higher in fishery-dependent samples, medium-aged fish, and in summer months. Spatial patterning was similar across ages. The estimated marginal effect of temperature indicated a concave relationship between temperature and functional maturity. Temperatures in 2018 and 2020 were near the peak of this relationship, while most years were cooler. Temperatures in 2016 and 2019 were high above the threshold corresponding to the peak of the temperature–maturity relationship, and maturity-at-age was estimated to decline in these years.

Annual maturity-at-age predictions were made since 2009 using estimated coefficients for non-A-SHOP samples and day 278 (i.e., October 5th). Projections were also made forward in time to 2024 using available temperature indices. This forward projection was needed because maturity information was not sampled in 2022 and data from 2024 have yet to be analyzed. The same biomass estimates used to create biomass-weighted temperatures were applied to the estimates of probabilities of being mature in logit space. Estimate of the spatial variance was higher than the estimate of the spatiotemporal variance for the biomass estimates suggesting that differences in locations are more prominent than differences in locations between years. That is, Pacific Hake have a patchy distribution but those patches appear in largely the same locations year after year. The center of gravity of the distribution was furthest to the north in years that corresponded to high temperatures and subsequent decreases in maturity. The total weighted average maturity for each age–year combination was converted to normal space with an inverse-logit transformation.

Time-varying fecundity-at-age (Figure 13) was calculated by using year-specific weight-at-age estimates multiplied by year-specific maturity-at-age (Berger et al. 2019) estimates. The methods used to estimate early (before 2009) and projection period weight at age were also used to estimate maturity for these time periods. Additionally, samples from age-15+ fish were pooled for both the maturity and weight-at-age estimation due to limited sample sizes. Consequently, the age 15+ estimates were applied to ages 15–20 in the population dynamics model (Figure 10).

Some fish at almost every age were found to be functionally immature based on histological criteria. Older, functionally immature fish are a combination of 'skip spawners' that will not be spawning in the upcoming year and senescent fish that appear to no longer have viable ovaries. Results from ongoing research investigating the impacts of functionally immature individuals on estimates of female spawning biomass could help refine the fraction of fish mature at each age.

Tissue samples have been collected from many of the same fish from which ovaries were sampled. In the future, these tissue samples may help determine whether the fish south of 34° 44′ N. Lat. are from the same population as the rest of the coastal population via genetic analyses.

2.4.3 Ageing error

The large inventory of Pacific Hake age determinations includes many duplicate reads of the same otolith, either by more than one laboratory or by more than one age reader within a laboratory. Recent west coast groundfish and Pacific Hake assessments have utilized the cross- and double-read approach to generate an ageing-error matrix describing the imprecision and bias in the observation process as a function of fish age. New data and analyses were used in the 2009 assessment to address an additional process influencing the ageing of Pacific Hake, namely cohort-specific ageing error related to the relative strength of a year-class. This process reflects a tendency for uncertain age determinations to be assigned to predominant year classes. The result is that the presence of strong year classes is inflated in the age data while neighboring year classes are under-represented relative to what would be observed if ageing error was consistent with age across cohorts.

To account for these observation errors in the model, year-specific ageing-error matrices (defined via vectors of standard deviations of observed age at true age) are applied, where the standard deviations of strong year classes are reduced by a constant proportion. For the 2009 and 2010 assessments, this proportion was determined empirically by comparing double-read error rates for strong year classes with rates for other year classes. In 2010, a blind double-read study was conducted using otoliths collected across the years 2003–2009. One read was conducted by a reader who was aware of the year of collection, and therefore of the age of the strong year classes in each sample, while the other read was performed by a reader without knowledge of the year of collection, and therefore with little or no information to indicate which ages would be more prevalent. The results were analyzed via an optimization routine to estimate both ageing error and cohort effect. The resultant ageing error was similar to the ageing error derived from the 2008 analysis. Since 2011, cohort-specific ageing error has been used to reduce the ageing-error standard deviation by a factor of 0.55 for the following largest cohorts: 1980, 1984, 1999, 2010, and 2014. In the 2014 base model (Taylor et al. 2014), the 2008 cohort was also included in this set but subsequent estimates show this year class to not be as strong as previously thought, and thus, cohort-specific ageing error has not been included for the 2008 cohort since 2015. Also, cohort-specific ageing error does not include the reduction in ageing error for age-1 fish under the assumption that they never represent a large enough proportion of the samples to cause measurement error related to the cohort-effect.

Additional exchanges of otoliths between ageing labs within the U.S. and Canada are in process but were not completed in time for this assessment. The additional across-lab double reads will be informative for updating the ageing-error matrix. Unfortunately, increased protocols for moving samples across the border have led to delays.

2.5 Estimated parameters and prior probability distributions

Several prior distributions (Table 15) are used to fit the model. The priors that are assumed to be informative are discussed below.

2.5.1 Natural mortality

Since the 2011 assessment, a combination of the informative prior for natural mortality used in previous Canadian assessments and results from analyses using Hoenig's method (Hoenig 1983) support the use of a lognormal distribution with a median of 0.20 and a standard deviation (in log space) of 0.10. Sensitivity to this prior has been evaluated extensively in many previous assessments of Pacific Hake (see Hicks et al. (2013) for a discussion of the historical treatment of natural mortality and its prior) and is repeated here (see Section 3.8), including increasing the prior standard deviation and using an alternative prior distribution based on a life history meta-analysis (Hamel 2015; Hamel and Cope 2022). The Hamel–Cope prior used a lognormal prior distribution with a median of 0.22 (based on a maximum age of 25) and a standard deviation (in log space) of 0.31. Alternative prior distributions for natural mortality typically have a significant impact on the model results. But in the absence of new information on natural mortality there has been little option to update the prior.

2.5.2 Steepness

The prior for the steepness parameter of the stock–recruitment relationship is based on the median (0.79) and the 20th (0.67) and 80th (0.87) percentiles from the meta-analysis of the family Gadidae (Myers et al. 1999) and has been used in U.S. assessments since 2007. This prior has a beta distribution with parameters 9.76 and 2.80, which translate to a mean of 0.777 and a log-standard deviation of 0.113. Sensitivities to the variance on the prior on steepness were evaluated in the 2012 and 2013 assessments (Stewart et al. 2012; Hicks et al. 2013). Sensitivities to the mean of the prior are explored in this assessment (see Section 3.8).

2.5.3 Variability on fishery selectivity deviations

Time-varying selectivity was introduced in the 2014 assessment (Taylor et al. 2014) and is modeled using annual deviations since 1991 applied to the selectivity-at-age parameters for the fishery. A normal distribution with a fixed standard deviation ($\Phi = 1.4$; see Edwards et al. (2018) for justification) is used as a penalty function to keep deviations from straying far from zero. Selectivity for age-0 fish is fixed at 0.0 and parameters for ages that are estimated represent the change in selectivity from the next youngest age. Beyond the age of 6, age-specific parameters are fixed at zero giving constant selectivity beyond the last estimated value. The condition that maximum selectivity equals 1.0 results in one fewer degrees of freedom than the number of estimated parameters. Further testing of alternative methods for parameterizing time-varying selectivity (e.g., Xu et al. 2019) should be investigated in conjunction with the estimation of additional time-varying parameters.

2.5.4 Age-composition likelihood

Since 2018, the assessment has used the linear formulation of the Dirichlet-multinomial (D-M) likelihood (Thorson et al. 2017) to fit the age-composition data. Estimated parameters θ_{fish} and θ_{surv} serve to automatically adjust the weight given to the fishery- and the survey-composition data, respectively. As of 2021, Stock Synthesis includes the constant of integration in the likelihood calculation for the D-M model such that likelihoods are comparable across weighting methods.

Integration of weighting the composition data within the assessment increases the efficiency of the assessment process, removes the subjective choice of how many iterations are required, and ensures that the results of model sensitivities, retrospective analyses, and likelihood profiles are automatically tuned, rather than having the age compositions be given the same weight as the base model. Note that the following description holds for both the survey data and the fishery data, with θ equal to θ_{surv} or θ_{fish}, respectively.

The likelihood function for the linear parameterization of the D-M likelihood (see Equation 10 of Thorson et al. (2017)) is

$$\mathrm{L}(\boldsymbol{\pi}, \theta | \tilde{\boldsymbol{\pi}}, n) = \frac{\Gamma(n+1)}{\prod_{a=1}^{A_{\text{max}}} \Gamma(n\tilde{\pi}_a + 1)} \frac{\Gamma(\theta n)}{\Gamma(n + \theta n)} \prod_{a=1}^{A_{\text{max}}} \frac{\Gamma(n\tilde{\pi}_a + \theta n \pi_a)}{\Gamma(\theta n \pi_a)}, \tag{2}$$

where $\tilde{\pi}_a$ is the observed proportion at age a, π_a is the corresponding expected proportion at age a estimated by the model, $\tilde{\boldsymbol{\pi}}$ and $\boldsymbol{\pi}$ designate the vectors of these proportions, A_{max} is the maximum age in the model, and n is the input sample size. The parameter θ is defined as a linear scaling parameter such that θn is the variance-inflation parameter of the D-M distribution. The linear parameterization has been shown to be superior over the saturation parameterization in simulation testing (Fisch et al. 2022), and thus, corroborates our decision to continue to use it even though the saturation parameterization is available in Stock Synthesis.

The effective sample size (n_{eff}) associated with this likelihood is given by

$$n_{\text{eff}} = \frac{1}{1+\theta} + \frac{n\theta}{1+\theta}. \tag{3}$$

The input sample sizes used in this assessment, which are based on the number of trips and/or hauls, are large enough that the first term is insignificant compared to the second term. Consequently, $\theta/(1+\theta)$ can be compared to the sample size multipliers used in the McAllister–Ianelli (M-I) data-weighting method (McAllister and Ianelli 1997) that was used for assessments prior to 2018 (Table 16) and as a sensitivity here (see Section 3.8). In short, the M-I method involves iteratively adjusting multipliers of the input sample sizes passed to the multinomial likelihoods until they are roughly equal to the harmonic mean of the effective sample sizes. The effective sample size is dependent on how well the model expectation matches the observed values. Typically, this process involves no more than four to five iterations.

A uniform prior between -5 and 20 for $\log\theta_{\text{fish}}$ and $\log\theta_{\text{surv}}$ tends to lead to inefficient sampling of $\log\theta_{\text{surv}}$ because many samples occur in a part of the parameter space where the effective sample size multiplier, $\theta_{\text{surv}}/(1+\theta_{\text{surv}})$, is between 0.99 and 1.0 (Berger et al. 2019). In that area, the input sample sizes given the uniform prior have full weight and the likelihood surface is almost completely flat with respect to $\log\theta_{\text{surv}}$. The current prior on $\log\theta_{\text{surv}}$ can be associated with an approximately uniform prior of the weight $\theta_{\text{surv}}/(1+\theta_{\text{surv}})$, where the parameters of the normal distribution were back-calculated from a uniform distribution with the bounds of 0 and 1 (Grandin et al. 2020). The normal prior for both $\log\theta_{\text{fish}}$ and $\log\theta_{\text{surv}}$ has a mean of 0 and a standard deviation of 1.813.

Composition data can also be weighted using the Francis method (T2.6 in Table 2 of Francis 2011), which is based on variability in the observed ages by year. This method, like the M-I method, is iterative, where the sample sizes are adjusted such that the fit of the expected mean age should be within the estimated uncertainty at a rate that is consistent with the variability expected given the effective sample sizes. The Francis method is known to be sensitive to outliers and prone to convergence issues when selectivity varies with time. As a result, the Francis method was not included as a sensitivity.

3 ASSESSMENT

3.1 Modeling history

In spite of the relatively short history of fishing, Pacific Hake have surely been subject to a larger number of stock assessments than any other marine species off the west coast of the U.S. and Canada. These assessments have included a large variety of age-structured models. Initially, a cohort analysis tuned to fishery CPUE was used (Francis et al. 1982). Later, the cohort analysis was tuned to National Marine Fisheries Service (NMFS) triennial acoustic survey estimates of absolute biomass-at-age (Hollowed et al. 1988). Since 1989, Stock Synthesis models (or base versions of it) fit to fishery catch-at-age data and acoustic survey estimates of population biomass and age composition have been the primary assessment method.

While the general form of the age-structured assessment has remained similar since 1991, modeling procedures have been modified in a variety of ways. There have been alternative data choices, post-data collection processing routines, data-weighting schemes, structural assumptions for the stock assessment model, MCMC sampling algorithms, and control rules (Table 16). Analysts are constantly trying to improve the caliber and relevance of the assessment by responding to new scientific developments related to statistics and biological dynamics, policy requirements, and different or new insights brought up during the peer review process to ensure a robust stock assessment.

Data processing, filtering, and weighting choices have been modified several times since the first assessment. For example, modifications to the target-strength relationship used to scale acoustic data changed in 1997 (Dorn and Saunders 1997), and kriging was implemented to account for the spatial correlation in the acoustic data in 2010 (Stewart and Hamel 2010). While survey data have been the key index for biomass since 1988, surveys that have been used have varied considerably. The Alaska Fisheries Science Center/Northwest Fisheries Science Center West Coast Triennial Shelf Survey was used from 1988 before being discarded from the 2009 assessment (Hamel and Stewart 2009). Acoustic surveys from the years prior to 1995 were used for assessments in the early 1990s, but Stewart et al. (2011) reviewed these early surveys and deemed that sampling was insufficient to be comparable with more recent data. Several recruitment indices have been considered but ultimately none were identified as adding appreciable contribution to model results (Helser et al. 2002; Helser et al. 2005; Stewart and Hamel 2010), except for the fishery-independent acoustic-based relative age-1 index that was included in the base model in the 2022-2024 assessments and removed in the final bridging step this year. The process for generating fecundity-at-age from the combination of weight-at-age and maturity data changed in 2019 from using time-invariant to year-specific weight-at-age values. In 2024, time-varying maturity ogives were also added to the calculation of fecundity-at-age (see Section 2.4.2 for details). Even where data have been consistently used, the weighting of these data in the statistical likelihood has changed through the use of various emphasis factors (e.g., Dorn 1994; Dorn et al. 1999), a multinomial sample size on age compositions (e.g., Dorn et al. 1999; Helser et al. 2002; Helser et al. 2005; Stewart et al. 2011), internal estimations of effective sample size using the Dirichlet-multinomial distribution (Edwards et al. 2018), and assumptions regarding year-specific survey variance. Since 2021, a more computationally efficient Bayesian MCMC sampler [No-U-Turn Sampler; NUTS; Hoffman and Gelman (2014)] was used to estimate posterior distributions (Monnahan and Kristensen 2018; Monnahan et al. 2019), a change from previous assessments that used the random walk Metropolis Hastings (rwMH) sampler (details described in Johnson et al. 2021). The list of changes discussed above is for illustrative purposes only and represents a small fraction of the different choices analysts have made and that reviewers have requested.

The structure of the assessment models has perhaps had the largest number of changes. In terms of spatial models, analysts have considered spatially explicit forms (Dorn 1994, 1997), spatially implicit forms (Helser et al. 2006), and single-area models (Stewart et al. 2012). Predicted recruitment has been modeled by sampling historical recruitment (e.g., Dorn 1994; Helser et al. 2005), using a stock–recruitment relationship parameterized using maximum sustainable yield (MSY) and the fishing mortality rate estimated to produce the MSY [F_{MSY}; Martell (2010)], and using several alternative steepness priors (Stewart et al. 2012; Hicks et al. 2013). Selectivity has also been modeled in several ways, invariant (Stewart et al. 2012; Hicks et al. 2013), time-varying with (Helser et al. 2002) and without

(Dorn 1994; Dorn and Saunders 1997; Stewart et al. 2012; Hicks et al. 2013) a random walk, alternative levels of allowable deviation through time (Hicks et al. 2013; Berger et al. 2017), age-based (Dorn 1994; Dorn and Saunders 1997; Stewart et al. 2012; Hicks et al. 2013), and length-based (Helser and Martell 2007).

Several harvest control rules have been explored for providing catch limits from stock assessment output. Pacific Hake stock assessments have presented decision makers with constant F, variable F, and the following hybrid control rules: $F_{\mathrm{SPR}=35\%}$, $F_{\mathrm{SPR}=40\%}$, $F_{40\%}$–40:10, $F_{\mathrm{SPR}=45\%}$, $F_{45\%}$–40:10, and $F_{\mathrm{SPR}=50\%}$ (e.g., Dorn 1996; Hicks et al. 2013). Changes to policies such as the United States' National Standards Guidelines in 2002 and the $F_{40\%}$–40:10 harvest control rule in the Agreement (Appendix C) have required specific changes to control rules.

In addition to the examples given above and changes documented in stock assessments, there have been many more investigations conducted at review panel meetings. Starting in 2013, the addition of the MSE (Hicks et al. 2013; Jacobsen et al. 2021) facilitated investigating changes to the modeling procedure in terms of pre-specified objectives that aim for a sustainable coast-wide fishery.

3.2 Description of base model

The 2025 base model has the same general population dynamics structure as the 2024 assessment's base model. The statistical-catch-at-age model assumes that the Pacific Hake population is a single coast-wide stock subject to one aggregated fleet with combined male and female population dynamics. Stock Synthesis (Methot, Jr. and Wetzel 2013) version 3.30.23.1 was the modeling platform used. The largest changes between the 2024 and 2025 stock assessments are the addition of another year of fishery data, a change in the estimation of recruitment from 2023 onwards, and the exclusion of the age-1 index of relative numbers of age-1 fish from the acoustic survey. Given the unique seasonal fishing conditions during the year, the fishery age composition of age-1 fish in 2024 was considered potentially suspect as a standalone observation (i.e., without the addition of survey information). Therefore, recruitment in 2023 was based on the stock–recruitment relationship (no additional recruitment deviate estimate). In addition, no recruitment deviations were estimated for 2024 onwards (including the forecast years) because no information is available to inform the estimates. The age-1 index (Section 2.2.1) was excluded from the base model because it was found to be strongly influencing recruitment estimates even for cohorts that had several years of data (see Section 3.4.1), and it does not have an externally calculated measure of uncertainty.

The 2025 base model includes a time series (1995 to 2023) of acoustic age-2+ biomass estimates. Maturity is assumed to be time-invariant prior to 2009, and time-varying, with the integration of annual maturity ogives informed by sea temperature at depth, since 2009 (see Section 2.4.2). Fecundity-at-age is time-varying as defined by annual weight-at-age multiplied by annual maturity ogives (1975–2024; additionally see Section 2.4.1). The D-M likelihood approach (Thorson et al. 2017) is used to estimate the weights associated with age-composition data, rather than iteratively tuning the sample size multiplier as in 2017 and earlier assessments (see Section 2.5.4). Time-varying fishery selectivity is retained in the 2025 base model with the magnitude of the allowable deviations unchanged from the 2024 base model (see Section 2.5.3). The general parameterization of selectivity was retained, although additional parameters were required to estimate an additional year of deviations. The selectivity of the acoustic survey is assumed to be time invariant. Selectivity curves were modeled as non-parametric functions estimating age-specific values for each age beginning at age two for the index of age-2+ biomass and age one for the fishery until a maximum age of 6, after which all ages are assumed to have the same selectivity.

Prior probability distributions are used for a select few parameters and fixed values are used for several parameters. For the base model, the instantaneous rate of time-invariant natural mortality (M) is estimated with a lognormal prior having a median of 0.20 and a standard deviation (in log-space) of 0.1 (see Section 2.5.1). The stock–recruitment relationship is a Beverton–Holt parameterization, with the log of the mean unexploited recruitment ($\log R_0$) freely estimated. This assessment uses the same beta-distributed prior for stock–recruitment steepness (h), based on Myers et al. (1999), that has been applied since 2011 (Stewart et al. 2011). Year-specific recruitment deviations were estimated from 1966–2022. The standard deviation, σ_r, of recruitment variability serves as a recruitment deviation constraint and is fixed at 1.4 in this assessment. This value is based on consistency with the observed variability in the time series of recruitment deviation estimates and is the same as assumed in assessments from 2013 to 2024 (Table 16). Catchabilities associated with the biomass index (q_b), and with the relative age-1 index (q_1) bridging model, were calculated analytically as per Ludwig and Walters (1981) for each sample of posterior parameters, resulting in a distribution of catchability for each.

Statistical likelihood functions used for data fitting are typical of many stock assessments. The biomass index was fit via a lognormal likelihood function, using the observed (and extra 2009) sampling variability, estimated via kriging, as year-specific weightings. When included, the relative age-1 index was specified as having a Student's t-distribution for its error structure with the number of degrees of freedom equal to one less than the number of available data points, and its selectivity was set to one for age one and zero for all other ages. An additional constant and additive standard deviation on the log-scale component is included for the biomass index (and the relative age-1 index when included), which was freely estimated to accommodate unaccounted-for sources of process and observation error. A D-M likelihood was applied to age-composition data, with input sample sizes equal to the sum of the number of trips and hauls sampled across all fishing fleets or the number of trawl sets in the research surveys (see Section 2.5.4).

Model results and statistical inference were based on 8,000 MCMC samples (using the `adnuts` R package; Monnahan and Kristensen (2018)) compiled across 8 chains, each with a 250 sample burn in period, to describe posterior distributions for model parameters and derived quantities. The number of samples used for bridging models, sensitivity models, and retrospective models was also 8,000. Medians (50% quantiles) are reported together with the bounds of 95% credibility intervals calculated as the 2.5% quantile and the 97.5% quantile of posterior distributions from the MCMC samples, to give equal-tailed intervals. A full explanation of the NUTS algorithm and the `adnuts` package, including an analysis with the Pacific Hake stock can be found in Monnahan et al. (2019).

3.3 Response to 2024 Scientific Review Group (SRG) review

The Scientific Review Group (SRG) meeting was held from February 6–9th, 2024, at the Vancouver Island Conference Centre, Nanaimo, BC.

The following are the 'SRG Recommendations and Conclusions for the Stock Assessment' from the 2024 SRG report and the associated responses from the JTC:

1. **The SRG recommends continuing sensitivities for steepness, natural mortality , σ_R, excluding the age-1 index, alternative standard deviations for time-varying selectivity, and down-weighting fishery age-composition data.**

Response – The incorporation of these sensitivities have been included per our standard workflow. Due to the removal of the age-1 index in the base model this year, the relevant sensitivity model was to include the age-1 index.

2. **The SRG recommends that the JTC explore alternative ways of estimating natural mortality (M) to update the current approach in the model, which is based on methods from more than a decade ago, and particularly consider options which have age-based M.**

Response – Pacific Hake have several natural predators, including themselves, particularly on younger ages. Recently, Trzcinski et al. (2024) identified Pacific Hake as the largest mean proportion of the diet of harbor seals. Additionally, the abundance of harbor seals is near carrying capacity in Canadian waters and has been since the late 1990s. Stock Synthesis allows for the inclusion of a predator index to estimate predation mortality in addition to baseline natural mortality. Data for predation mortality can be absolute numbers of dead fish due to the predator, an index of predator effort, and predation composition (age or length) data. A predation index based on estimated abundance of harbor seals could be added to the assessment model, but this has not been explored.

A potential, better path forward is to use Dynamic Structural Equation Modeling (DSEM) to include indices for multiple predators and allow for two-way interactions between them and M. This capability is not, and will not be, available within Stock Synthesis but is possible using models written in Template Model Builder. A proof of concept has been implemented at the Alaska Fisheries Science Center and discussions are ongoing to implement this in the Fisheries Integrated Modeling System (FIMS). Thus, for the 2025 assessment a simple version of FIMS will be fit, where the simple version does not have the capacity to estimate ageing error or facilitate DSEMs. A more complex FIMS model will be presented to the SRG in 2026.

In 2023 the JTC unsuccessfully estimated age-specific M using Stock Synthesis, where it was seen as an unsuccessful exercise because estimates of M increased with age due to a lack of data to inform the estimates. Second, the JTC explored the use of Lorenzen M but this is not possible in Stock Synthesis without simultaneously estimating growth. Thus, the JTC sees using estimates of age-specific M from the Climate- Enhanced, Age-based model with Temperature-specific Trophic Linkages and Energetics (CEATTLE) model as a way forward (Holsman et al. 2016). Output from CEATTLE includes time series of estimates of baseline M and estimates of M at age for ages 0–1, 2, 3, 4, 5, and 6^+, where the M at-age estimates are strictly natural mortality due to cannibalism. Two sensitivities were run for this assessment, one where baseline mortality at age was fixed and one where it was estimated. Results are presented in Section 3.8.

3. **The SRG encourages an analysis of catch and biomass distribution for Canada and US that examines latitudinal shifts in fishing over time, and tries to predict factors influencing these shifts.**

Response – The JTC is collaborating with lead analyst Owen Liu (NWFSC) who is building species distribution models for Pacific Hake. This work will include incorporating environmental factors across the full transboundary range of Pacific Hake and will evaluate prediction skill for developing short-term forecasts. Results from this work are expected to be presented at the 2026 SRG meeting.

The JTC is also investigating patterns of hake in the U.S. West Coast Bottom Trawl Survey in California waters where fishery data is limited. Data sharing agreements between countries are concurrently being developed so that the JTC can explore coast-wide fishing location information to better understand spatial fleet dynamics over time. The JTC will also be investigating spatial fishing effort, catch, and revenue over time using data summary tools (e.g., Pacific Fishing Effort Mapping Project) that are currently under development (but available for beta explorations).

4. **Pacific Hake dynamics are highly variable even without fishing mortality. The SRG applauds the efforts of the JTC to estimate dynamic reference points, and encourages efforts by the MSE Technical Team to include dynamic reference points in the MSE process.**

Response – There has been limited time (thus far) to evaluate dynamic reference points using the MSE. The MSE technical team lost the dedicated MSE post-doc earlier this year, and the previous MSE coordinator at the NWFSC, Kristin Marshall, has moved to a new position. The JTC is attempting to balance their available research time in 2025 with requests such as this one with others (e.g., request 11). The JTC has included dynamic reference point figures and summary metrics in this stock assessment.

5. **The SRG recommends continued work to collect ovary samples, with a focus on fecundity and functional maturity, as well as continued annual maturity analysis.**

Response – The estimates of maturity have been updated with recent data for this assessment. The selection of the best day of the year to predict maturity to remains an area for further discussion. The JTC has researched the internal assumptions of Stock Synthesis to help inform the best day of the year, but no investigation can make up for the lack of data during the winter spawning season. Additional work is being put forward to implement a research effort with Oregon State University and the University of Washington to investigate broader assumptions about Pacific Hake fecundity.

6. **On three occasions since 2009 (2011–12, 2016–17, 2023), stock assessments have predicted a rapid increase in biomass similar to that seen in the 2024 assessment, where this rapid increase was not visible in subsequent assessments. The SRG recommends investigating what factors might be causing these shifts in biomass estimates and projections.**

Response – This comment seems to arise from Figure 63 showing summaries of historical assessment estimates of spawning biomass. Uncertainty is not fully considered in this figure because it is only shown for the most recent assessment (i.e., only point estimates are shown for historical estimates). In particular, with median estimates presented:

- *from 2010–11 (presumably, not 2011–12) the subsequent assessments greatly reduce the absolute size of the stock, but still show an increase, likely due to the change in data included in 2012 (e.g., addition of 2011 survey biomass estimate).*
- *from 2016–17 and 2023 the increases are actually larger in later assessments, not smaller. For example, 2016–17 increase from each assessment is:*
    - *2017 base model: increase of 136,000 t*
    - *2018 base model: increase of 194,000 t*
    - *2024 base model: increase of 423,000 t;*
- *the 2022–2023 (presumably) increase from each assessment is:*
    - *2023 base model: increase of 486,000 t*
    - *2024 base model: increase of 549,000 t.*

An age-0 recruitment index could help, and the JTC plans to continue analyses of age-0 Pacific Hake data presented at previous SRG meetings when time allows.

7. **The SRG encourages the JTC to consider methods to determine the maximum input sample size for the age compositions (e.g., Stewart and Hamel 2014, Hulson et al. 2023).**

Response – The JTC agrees that determining input sample sizes is important for fishery and survey age compositions, which then provides the basis from which model-based re-weighting is done. The JTC has considered alternative methods and has determined additional research is needed to inform the calculation of input sample size for both fishery and survey ages. Fishery input sample sizes are calculated using a mixture of either the number of hauls or trips, when haul information is not available (e.g., shoreside), and further work is needed to determine the effective sample sizes at the haul and trip level and how to calculate a fleet-wide input sample size. Survey age compositions represent age structure associated with the acoustic survey as viewed through an estimated selectivity curve for the acoustic-trawl sampling net. Yet, selectivity for ages two and older with acoustics is theoretically at or near one. Additionally, if the survey moves to using a new net, changing selectivity, the effective sample size could vary requiring consideration on how to model the survey. The JTC did not investigate this issue for this year's assessment but supports the prioritization of this research for future assessments.

Instead, the JTC has conducted a sensitivity analyses using input sample sizes following the Stewart and Hamel (2014) approach. The results of that sensitivity are included in Section 3.8.

8. **The SRG has previously noted that σ_R is an influential parameter, and encourages further work by the JTC. The SRG supports continuing efforts to explore new recruitment parameterizations, including treating recruitment deviations as random effects, to better estimate σ_R.**

Response – Future improvements in the stock assessment software used to assess Pacific Hake (e.g., ability to use random effects in the modeling framework) will allow for fruitful work on this. The Fisheries Integrated Modeling System (FIMS) will replace Stock Synthesis in the coming years and will have random effects capabilities. The Pacific Hake assessment is a primary test case for

FIMS, and further versions of the Pacific Hake assessment in FIMS are expected at forthcoming SRG meetings.

Other frameworks (e.g., Woods Hole Assessment Model, or WHAM, and bespoke models) can already use random effects. The JTC has completed initial explorations using WHAM and concluded random effect structures will be beneficial for modeling Pacific Hake.

The JTC is also following pertinent research aimed at advancing related novel methods (e.g., dynamic structural equation models) for incorporating time-variation into stock assessment models (occurring at the Alaska Fisheries Science Center and University of Washington) and approaches for operational assessment use, including the estimation of σ_R.

9. **The SRG noted that the age-1 index did not include a value for 2001 because it was zero. Although this decision had negligible influence on the results because the estimate for 2000 recruitment was close to zero, the SRG noted that Stock Synthesis uses a lognormal likelihood which does not handle zero values. Given that future zero values are expected to have a bigger influence on the results in the short-term, the SRG recommends that the JTC explore likelihood forms that can fit to very low index values from the age-1 survey (e.g., robust likelihood). The SRG acknowledges that implementing new likelihoods will require changes to the Stock Synthesis platform.**

Response – Researchers at the Alaska Fisheries Science Center have the same problem and have yet to find a solution. The JTC will not be investigating this in the near future nor will Stock Synthesis be altered to accommodate a future solution. However, the JTC will continue to monitor new research on this front as new assessment platforms are developed.

10. **The SRG recommends that the JMC review the decision tables and reconsider required harvest scenarios to reduce the number of similar and overlapping Scenarios.**

Response – The JTC helped initiate discussions on decision table structure at a 6 December 2024 JMC meeting. Refinements of the number of catch scenarios were discussed and a JMC recommendation was put forth. The JTC followed those recommendations for the decision tables used in this assessment. This included a reduction in the total number of catch scenarios.

11. **The SRG noted that alternative structures of the assessment model have not been comprehensively examined since 2011 (e.g., multiple fleets and/or spatial model), and were informed that limited staffing and availability of the JTC inhibits these time-consuming analyses. The SRG recommends examining structural assumptions of the stock assessment as time allows. More complex structural assumptions may utilize the data more thoroughly, explain different trends across areas and/or fleets, and estimate stock status more accurately, but simpler models may be more appropriate for determination of the TAC. The MSE can be used to determine best performing assessment models for management.**

Response – The JTC plans to evaluate the multitude of changes in the assessment process itself (e.g., data availability, assumptions, etc.) that would be needed to develop alternative model structures and share future plans at the 2025 SRG meeting. This includes the development of a research *plan, including complimentary or standalone analyses, alternative model structures to explore, and simulation analyses to evaluate and compare alternative models (e.g., using one or more tools, such as MSE).*

The JTC explored the ability to disaggregate data across the entire historical time series. There are no issues with catch data, because those data are already disaggregated by fleet across the time series. Similarly, biological data are already disaggregated from 2007 to present. However, the ability to disaggregate pre-2007 biological is not immediately straightforward given new data pulls for these historical data are not typically conducted. Differences resulting from new data pulls need to be thoroughly investigated.

Other steps the JTC plans to take in the future include evaluating alternative data and model assumptions that arise for validity given proposed new model structures; evaluating variance and bias trade-offs associated with new parameterizations (e.g., doubling the number of time-varying selectivity parameters when doubling the number of fleets); comparing alternative spatially-implicit assessment approaches (e.g., time-varying selectivity versus area-varying selectivity, or both); and developing states of nature scenarios to test model structure robustness in an MSE framework.

Additionally, model complexity in the spatial domain needs to be addressed relative to other structural assumptions in the assessment model. Other assumptions may have a higher propensity to be influential and be more sensitive to model results. These may include data weighting, improving estimates of natural mortality via predator time series, multiple fleets instead of a single aggregated fleet, and using fleet-specific weight-at-age data instead of aggregated weight-at-age (the JTC has looked at this before, but it hasn't been revisited in over a decade).

Changes to the structure of the assessment model may not be the most immediate need for understanding changes in hake distribution. Some of the other (higher priority) SRG requests noted above will help with understanding fundamental mechanisms, which can help to formulate hypotheses to inform relevant model structures. These include spatial CPUE modeling, investigating hake distribution changes in bottom trawl surveys, correlating hake distribution changes with California Current Integrated Ecosystem Assessment results, and Pacific Hake distribution modeling research informed by environmental data.

3.4 Modeling results

3.4.1 Changes from 2024

A set of 'bridging' models was constructed to evaluate the component-specific effects of the steps to change from the 2024 base model to the 2025 base model. The steps are as follows:

- Update to the latest version of Stock Synthesis, version 3.30.23.1, to follow current best practices;
- Incrementally update catch, maturity-at-age/weight-at-age/fecundity-at-age, and fishery age-composition data from years previous to 2024 (in that order);
- Incrementally add 2024 catch, maturity-at-age/weight-at-age/fecundity-at-age, and fishery age-composition data (in that order);

- Turn off estimation of the 2023 and 2024 recruitment deviations (i.e., recruitment comes from the stock–recruitment relationship) due to limited data to inform the estimation of 2023 year class strength in the absence of survey data. Similarly, no recruitment deviations were estimated during the forecast period; and
- Exclude the age-1 index.

Stock Synthesis version 3.30.23.1 includes a number of changes since the version used by Grandin et al. (2024). However, none of the changes were specifically relevant to this assessment, and thus, the software update had no effect on assessment results (Figure 15).

The update of pre-2024 data occurs because databases are continually updated; this yielded minor adjustments to the data. For example, samples that were recently aged but not available for the 2024 assessment were included. Updates to pre-2024 data were small enough that they had little impact on the model results.

The addition of the 2024 catch, modelled weight-at-age estimates, and fishery age compositions extends the model to the start of 2025. Historical recruitment estimates and the stock trajectory were relatively unchanged through 2023 (except for changes in recruitment due to adding fishery age compositions), but female spawning biomass increased in the final year of the model due to the estimate of above-average recruitment in 2023 (Figure 16). With the lack of a survey in 2024, the 2023 recruitment deviation is being informed solely by age-1 observations in the 2024 fishery age-composition data.

The penultimate step in this year's bridging led to turning off the estimation of the 2023 and 2024 recruitment deviations (i.e., recruitment without deviation from the stock–recruitment relationship, Figure 16). Given the unique seasonal fishing conditions during the year, the 2023 estimate of recruitment was considered potentially suspect without the addition of survey information. This change led to decreased estimates of female spawning biomass at the start of 2025 relative to the previous model bridging steps. The next assessment will include data from the 2025 survey that will provide an age-2+ index with age compositions providing additional information on the 2023 year-class strength. Given this survey information, the 2026 assessment will explore estimating recruitment deviations for 2023 and beyond.

The final bridging step was to exclude the age-1 index from the base model. Exluding the age-1 index considerably shifted the female spawning biomass trajectory downwards from 2015 onwards, with the largest changes coming since 2022 (Figure 16). Recruitment deviations in 2018 and 2022 were reduced considerably, while all others since 2019 were slightly reduced. The fit to the acoustic survey index in 2023 was improved, but the fit in 2021 was lessened.

The decision to exclude the age-1 index occurred through discussions and supporting analyses at the 2025 Scientific Review Group meeting (see Appendix B for additional details). In summary, the performance of the age-1 index over recent years was called into question given that it was found to be strongly influencing recruitment estimates even for cohorts that had several years of data (going back to 2015). In addition, the age-1 index does not have an externally calculated measure of uncertainty, including any measure of year to year differences in the quality of the index. Analyses conducted during the review week identified the 2019 and 2023 index points as having a particularly high impact on model results. The model considerably underfit these data points such that the age-1 index was suggesting larger recruitment in 2018 and 2022 than all other data sources in the assessment. Further analyses into the performance of the age-1 index and the quantification of yearly uncertainty measures will provide the means to potentially include this index once again in future assessments.

3.4.2 Assessment model results

Model Fit

Stationarity of the posterior distribution for model parameters was assessed via a suite of standard single-chain and multi-chain diagnostic tests via graphical summaries and interactive web applications (ShinySTAN; Appendix A). All estimated parameters showed good mixing during sampling, no evidence for lack of convergence, and acceptable autocorrelation (results for some key parameters are shown in Figures A.1–A.4). Correlation-corrected effective sample sizes were sufficient to summarize the posterior distributions and neither the Geweke nor the Heidelberger and Welch statistics for these parameters exceeded critical values more frequently than expected via random chance (Figure A.5). The Gelman-Rubin multi-chain diagnostic test, which compares within-chain variance to among-chain variance, further indicated that convergence was adequately achieved (examined via `ShinySTAN`). Correlations among key parameters were generally low, with the exception of M and $\log R_0$ (Figure A.6). Estimates of recruitment in 2014 and 2016 were correlated with the derived quantity of catch from the default harvest rule in 2025, as to be expected given the dependencies among these quantities (Figure A.6). An examination of deviations in recruitment (log-scale differences between estimated and expected recruitment values) from recent years (Figures A.6 and A.7) indicates the highest correlation (0.93) was between the 2014 and 2016 recruitment deviations. This is the same as in the last assessment despite the fact that each cohort has been observed for an additional year.

Regarding the D-M parameter θ_{fish}, the estimate (median and 95% credible interval) for $\log \theta_{\text{fish}}$ was -0.643 (-0.829 to -0.445), giving an effective sample size multiplier $\theta_{\text{fish}}/(1+\theta_{\text{fish}})$ of 0.345 (0.304–0.391). The related log of the survey age-composition parameter θ_{surv}, i.e., $\log \theta_{\text{surv}}$, was 2.729 (1.481–4.925), and the resulting effective sample size multiplier $\theta_{\text{surv}}/(1+\theta_{\text{surv}})$ of 0.939 (0.815–0.993).

The base model fit to the acoustic survey biomass index (Figure 17) remains similar to the 2024 base model, except the fit to the 2023 survey biomass is slightly improved. The low 2023 survey biomass pulls down the last few years of estimated biomass, such that the fit to the 2019 data point is very good compared to the 2023 assessment when it was overestimated. The 2021 fit remains underestimated but within the range of the input standard deviation. The median of the posterior distribution for the analytically-derived catchability associated with the acoustic survey biomass index (q_b) was 0.894 (Figure 18).

The 2023 biomass index is the third lowest in the series (Table 12), and is below the model estimate, similar to the 2001 index that has always been below model estimates (Berger et al. 2023). While no direct cause for the 2001 index anomaly is known, the survey did begin earlier that year than all other surveys between 1995 and 2009 (Table 12), which may explain some portion of the anomaly, along with age structure. For 2023, the survey timing is not anomalous. The estimated biomass increase from 2023 to 2024 is driven by the addition of 2023 survey age-composition data (Figure 15).

The relatively stable estimated biomass from 2013–2019 is unchanged from the previous assessment. The underestimation of the 2009 and 2023 biomass estimates are larger than the underestimation of any other year. The uncertainty of the 2009 value (both modeled and actual) is high because of the presence of large numbers of Humboldt Squid during the survey. Humboldt Squid have similar target strength to hake which could introduce bias in the biomass estimate for that year, which also likely influenced the population dynamics of Pacific Hake through predation in that year. Future data will reduce the large uncertainty in the 2023 biomass estimate, which may reduce the underestimation.

Differences between the median posterior density estimates from the fit to the survey index are likely due to slight differences in what the fishery composition data and survey composition data, when considered independently, would otherwise suggest as population trends. Additionally, the population has undergone recent high, but declining, catch levels and produced a couple of above-average cohorts that are now mature.

Fits to the age-composition data continue to show close correspondence to the dominant and small cohorts observed in the data when the data give a consistent signal (Figures 19 and 20). The fit to commercial age-composition data is particularly good as a result of the large sample sizes and time-varying selectivity parameterization. In the 2024 fishery, the 2021 cohort was the largest (37%), followed by the 2020 cohort (17%), and then the 2016 cohort (10%). Age compositions from the 2023 acoustic survey suggest a similar age structure for older fish.

The 2020 cohort is well fit by the acoustic survey (Figure 20). Combined, the 2015–2024 fishery age-composition data and the 2017–2023 acoustic survey age-composition data suggest that 2014 was a strong recruitment year, and the model was able to adequately fit these observations (Figure 20). The 2016 cohort, which has been observed three times by the survey, still appears to be smaller than the 2014 cohort.

The 2023 survey was the first to sample the 2021 cohort, suggesting that it was a large contingent of the population (50.6% of the 2023 survey catch). The 2020 cohort, which has now been observed by the acoustic survey, is expected to be above average in size. Residual patterns to the fishery and survey age data do not show patterns that would indicate systematic bias in model predictions (Figure 21).

The median estimates for numbers, biomass, exploitation rate, and catch (in numbers and in biomass) for each age class in each year are given in Tables 17–21. For the major cohorts, the resulting estimated age-specific catch, natural mortality, and surviving biomasses are given in Table 22. For example, at age-4 the catch weight of the 2016 cohort was slightly more than that of the 2014 cohort, and the resulting surviving biomass of the 2016 cohort was approximately one-third of the surviving biomass of the 2014 cohort.

Posterior distributions for both steepness and natural mortality are influenced by priors (Figures 22–23). The posterior for steepness is only slightly updated by the data, as expected given the low level of information available to inform steepness as found in previous hake assessments. The posterior of natural mortality, on the other hand, is shifted to the right of the prior distribution and the prior may be constraining the posterior distribution from shifting further. Broadening the prior distribution by increasing the prior standard deviation for the natural mortality parameter is examined in sensitivity runs (see Section 3.8). Other parameters showed updating from diffuse priors to posterior distributions, including $\log \theta_{\text{fish}}$ and $\log \theta_{\text{surv}}$ (as outlined in Section 2.5.4).

The 2025 base model specified the same level of variation (standard deviation of $\Phi = 1.4$) associated with time-varying fishery selectivity as the 2024 base model, effectively allowing the model flexibility (i.e., a lower penalty on the overall likelihood) to fit to data that suggests high variability among years for each age. This level of variation led to results that remained consistent with the 2023 acoustic survey age-composition data (but not the biomass index) and gave reasonable fits to the fishery age-composition data, given that there is considerable uncertainty associated with spatial changes in fish availability (due to movement) and recent variability in oceanographic conditions. Estimated selectivity deviations for age-3 and age-4 fish are larger from 2010 to 2012 than in subsequent years until 2020 when the deviation for age-4 was large again (Figures 24 and 25). The median selectivity peaks at age-4 in 2010, 2012 and 2020 and at age-3 in 2011 suggesting targeting (or generally higher availability) of the younger cohorts in those years. This pattern is consistent with the 2008 cohort appearing strong in the fishery age compositions initially, but decreasing in prominence from 2013 onward (Figure 19). Fishery selectivity on age-2 fish was at its highest in 2016. Fishery selectivity for 2024 was higher than average for age-1 fish followed by a relatively flat pattern from age-2 to age-5 before increasing at older ages (Figure 25). Even though the survey selectivity is time invariant, the posterior shows a broad band of uncertainty between ages 2 and 5 (Figure 26). The decline in survey selectivity between ages 3 and 4 may be an artifact of the interaction between large cohorts and the biennial timing of recent surveys, with the 2010, 2014, 2016, and 2020 cohorts occurring in the survey at ages 3 and/or 5 but not age 4. Fishery selectivity is likewise very uncertain (Figures 25 and 26), but in spite of this uncertainty, changes in year-to-year patterns in the estimates are still evident, particularly for age-2, age-3, and age-4 fish, though these patterns might also reflect time-varying mortality processes.

Stock biomass

The base stock assessment model indicates that, since the 1960s, Pacific Hake female spawning biomass has ranged from well below to above unfished equilibrium (Figures 27 and 28 and Tables 23 and 24). The model estimates that it was below the unfished equilibrium in the 1960s, at the start of the assessment period, due to lower than average recruitment. The stock is estimated to have increased rapidly and was above unfished equilibrium in the mid-1970s and mid-1980s (after two large recruitments in the early 1980s). It then declined steadily to a low in 1999. This was followed by a brief increase to a peak in 2003 as the very large 1999 year class matured. The 1999 year class largely supported the fishery for several years due to relatively small recruitments between 2000 and 2007. With the aging 1999 year class, median female spawning biomass declined throughout the late 2000s, reaching a time-series low of 0.601 million t in 2009. The assessment model estimates that median female spawning biomass then peaked again in 2014 due to a very large 2010 year class and an above-average 2008 year class. The subsequent decline from 2014 to 2016 is primarily from the 2010 year class surpassing the age at which gains in weight from growth are greater than the loss in weight from mortality (growth-mortality transition). The 2014 year class is estimated to be large, though not as large as the 1999 and 2010 year classes, resulting in increasing biomass through 2018. The estimated biomass declined from 2018 to 2021 due to the 2014 and 2016 year classes moving through the growth-mortality transition during a period of high catches. The increase in female spawning biomass from 2022 through 2025 is due to the above-average 2020 and 2021 cohorts entering maturity and the recent declining trend in catch.

The median estimate of the 2025 relative spawning biomass (spawning biomass at the start of 2025 divided by that at unfished equilibrium, B_0) is 67%. However, the uncertainty is large, with a 95% posterior credibility interval from 29% to 157% (Tables 23 and 24), partly due to remaining unknowns about the size of the potentially large 2021 cohort because the acoustic survey has only provided one year of information about it during the 2023 survey. Even when used, the biennial age-1 index does not provide additional information for odd year cohorts like this one.

The median estimate of the 2025 female spawning biomass is 1.223 million t (with a 95% posterior credibility interval from 0.521 to 3.028 million t). The current estimate of the 2024 female spawning biomass is 1.189 (0.530–2.900) million t, giving a narrower range of uncertainty compared to the estimate from the 2024 assessment of 1.885 (0.853–4.828) million t. The current median is reduced from last year, partly due to the influence of the age-2+ biomass index pulling down the estimated biomass for recent years, the reduction in the estimate of the 2022 year class with updated data, the removal of the age-1 index, and the setting of the 2023 year class using only the stock-recruitment relationship (i.e., no estimated recruitment deviate; Figure 15).

Recruitment

The new data for this assessment do not significantly change the general pattern of recruitment estimated in recent assessments. However, estimates of absolute recruitment for the most recent years can change with new data and updated assumptions about recent recruitments. In particular, the 2023 and 2024 year classes were set based solely on the stock–recruitment relationship for this assessment, such that no recruitment deviations were estimated for these years (as well as none for forecast years). The only information on the size of the 2023 cohort (age-1 fish in 2024) in this assessment comes from the age composition of fishery catches. The catch of age-1 fish was particularly high in 2024, potentially due to the unique seasonal fishing conditions during the year (see Appendix E) and the relative loss of older age classes in the population. Thus, this data point was considered suspect as a standalone observation (i.e., without the addition of survey information). By restricting 2023 recruitment to the stock–recruitment relationship, the assessment model was not allowed to predict a very high 2023 year class based solely on the age-1 catch in the fishery. Another year of data, particularly for the age-2+ acoustic–trawl survey in 2025 will provide additional information on the size of the 2023 year class.

The 2021 recruitment is estimated to be well above average (though highly uncertain), with the absolute size being similar to the 2014 year class (current estimate is 7.055, with a 95% credible interval of 2.9–19.3 billion fish). Last year's assessment also indicated a large 2021 year class, so the addition of 2024 data did not appreciably change this estimate. The 95% credible interval in the 2024 assessment was 4.09–29.50 billion fish, reduced and narrowed in the current assessment to 2.9–19.3 billion fish. The median has changed by -31% (-3.1 billion fish). The general notion remains that recent recruitment is highly uncertain, and estimates for recent years (based on limited data) can change with more data.

The median estimate of 2020 recruitment continues to be estimated as above average, though has declined slightly compared to the median estimate from last year's assessment (3.4 billion fish compared to 4.7 billion fish, respectively). The addition of 2024 fishery data had little affect reducing the uncertainty associated with the size of this cohort (95% interval: 1.6–9.1 billion fish compared to last year's model with 2.1–12.7 billion fish).

In general, Pacific Hake have low average recruitment (relative to the long-term average) with occasional large year classes (Figures 29 and 30, Tables 23 and 24). Very large year classes in 1980, 1984, and 1999 supported much of the commercial catch from the 1980s to the mid-2000s. From 2000 to 2007, estimated recruitment was at some of the lowest values in the time series, but this was followed by an above average 2008 year class and a very strong 2010 year class. Above average year classes have occurred since then in 2014, 2016 and 2021, which have been sustaining the fishery over the last decade (Figure 19). The current assessment estimates a strong 2014 year class (Figure 31) comprising 50% of the 2016 catch, 38% of the 2017 catch, 28% of the 2018 catch, 33% of the 2019 catch, 31% of the 2020 catch, 25% of the 2021 catch, 15% of the 2022 catch, 8% of the 2023 catch, and 8% of the 2024 catch. The strong 2016 cohort comprises 26% of the 2018 catch, 21% of the 2019 catch, 36% of the 2020 catch, 34% of the 2021 catch, 23% of the 2022 catch, 13% of the 2023 catch, and 10% of the 2024 catch. The strong 2021 cohort comprises 36% of the 2023 catch, and 37% of the 2024 catch.

The large size of the 2014, 2016, and 2021 cohorts is informed by observations from several years of fishery data and the acoustic survey. For all other years from 2011 to 2022, the model currently estimates small year classes (median recruitment below the mean of all median recruitments), except for 2020 as previously mentioned. The 2022 cohort was observed in recent years by the fishery. To date, this information suggests that it is well below average (Figure 29). It will be observed as part of the age-2+ survey index for the first time in 2025. There is no information in the data to estimate the sizes of the 2024 and 2025 year classes. Retrospective analyses of year class strength for young fish have shown the estimates of recent recruitment to be unreliable prior to at least model age-3 (observed at age-2 the previous year) without a survey in the most recent year and age-2 with a survey.

From Figure 29 it looks as though the 2014 recruitment could be as large as the 2010 recruitment. However, the assessment model estimates a 0% chance that this could be the case. The overlapping of the credible intervals in Figure 29 is because large MCMC estimates of 2010 recruitment are associated with large estimates of 2014 recruitment (presumably with large estimates of R_0). By scaling all recruitments by the 2010 recruitment, Figure 32 provides an intuitive way to compare recruitment across years (see Edwards et al. 2022 for motivation and methods). It shows that only the 1980 recruitment is probably larger than 2010 (median relative value > 1), and the 1984 recruitment has a small chance of being as large as 2010. Whereas Figure 29 suggests that 1967, 1973, 1977, 1999, 2014, and 2021 could also possibly be larger than in 2010, giving an over-optimistic impression of how often we can expect cohorts the size of the 2010 cohort to occur. The 2021 cohort is still very uncertain but has a small chance of exceeding the 2010 cohort (Figure 32). Figure 32 shows how the 2010 cohort is the largest in the last 30 years, and that such large cohorts are rarer than is inferred from Figure 29.

The estimated recruitments with uncertainty for each year and the overall stock–recruitment relationship are provided in Figure 33. Extremely large variability about the expectation and about the joint uncertainty of individual recruitment and female spawning biomass pairs are evident. High and low recruitments have been produced throughout the range of observed female spawning biomass (Figure 33). The standard deviation of the time series of median recruitment deviation estimates for the years 1970–2023, which are informed by the age compositions is 1.74.

Exploitation status

The median estimated relative fishing intensity on the stock is below 1.0 for all years (Figure 34 and Tables 23 and 24). It was closest to 1.0 in 1999 and 2008, but catch in 2008 did not exceed the catch limit that was specified, based on the best available science and harvest control rules in place at the time; however, catch did exceed the catch limit in 1999 (Table 3). Exploitation fraction (catch divided by biomass of fish of age-2 and above) has shown relatively similar patterns (Figure 35 and Tables 23 and 24). Although displaying similar patterns, the exploitation fraction does not necessarily correspond to fishing intensity because fishing intensity more directly accounts for the age-structure of both the population and the catch. Median relative fishing intensity is estimated to have declined from 90.0% in 2010 to 48.1% in 2015, and then leveled off around 80% from 2016 to 2019. It then declined to around 70% from 2020 to 2022 before declining further to 66.6% in 2024. The median exploitation fraction has increased from a recent low of 0.06 in 2012 to 0.18 in 2021. It has since declined rapidly to 0.06 in 2024. Although there is a considerable amount of imprecision around these recent estimates due to uncertainty in recruitment and spawning biomass, the 95% posterior credibility interval of relative fishing intensity was below 100% from 2013–2015 and again from 2020–2021 (Figure 34).

Management performance

Over the last decade (2015–2024), the mean coast-wide utilization rate (i.e., proportion of catch target removed) has been 59.6% and catches have been below coast-wide targets (Table 3). From 2020 to 2024, the mean utilization rates differed between the U.S. (61.1%) and Canada (36.6%). While Canada's rate was higher than the U.S.'s in 2020, it has dropped considerably over the past few years to historic lows. The utilization rate for the coast-wide fishery this year was the lowest of the previous decade (30.8%) due, in part, to difficulties locating aggregations of fish during the Spring and throughout the year in northern areas. Prior to 2024, the previous low was in 2015 at 44.1% coast-wide attainment. Before 2015, the under-utilization in the U.S. was mostly a result of unrealized catch in the tribal apportionment, while reports from stakeholders in Canada suggested that Pacific Hake were less aggregated in Canada and availability had declined. In 2016, the utilization rate increased but remained below pre-2015 levels, despite the total 2016 catch being one of the highest of the preceding years. This is in large part due to increasing catch targets as biomass continues to increase. While the total utilization rate between 2017–2021 was relatively steady, it decreased to 42.3% in 2023 and to 30.8% in 2024. This is due to the utilization rate in Canada steadily declining since 2020 to the time-series low in 2024, and also a fall in the U.S. utilization rate to 40.7% in 2024. Country-specific quotas (or catch targets) in 2020 and 2021 were specified unilaterally, due to the lack of an agreement on coast-wide 2020 and 2021 TACs. The usual 73.88% and 26.12% allocation of coast-wide TAC, as specified in the Joint U.S.-Canada Agreement for Pacific Hake, was once again implemented since 2022. Total landings last exceeded the coast-wide quota in 2002 when utilization was 112%.

As noted above, the median relative fishing intensity was below 100% (i.e. median fishing intensity below $F_{\text{SPR}=40\%}$) for all years. The median relative spawning biomass was above 40% (the $B_{40\%}$ reference point) in all years except 2007–2009 and 2011 (Table 23 and Figure 28). These are also shown on a phase plot of the joint history of relative spawning biomass and relative fishing intensity (Figure 36). Relative spawning biomass increased from the lows in 2007–2011 with above average recruitment in 2008, 2010, 2014, 2016, and 2021. Correspondingly, median relative fishing intensity has remained below 100%, and total catch has been declining since the time series high in 2017. While there is large uncertainty in the 2024 estimates of relative fishing intensity and relative spawning biomass, the model estimates a 1.9% joint probability of being both above the $F_{\text{SPR}=40\%}$ fishing intensity in 2024 and below the $B_{40\%}$ spawning biomass level at the start of 2025.

3.5 Model uncertainty

The base assessment model integrates over the substantial uncertainty associated with several important model parameters including: biomass index catchability (q b) and observation errors, the magnitude of the stock (via the R_0 parameter for equilibrium recruitment), productivity of the stock (via the steepness parameter, h, of the stock–recruitment relationship), the rate of natural mortality (M), annual selectivity for key ages, recruitment deviations, and survey and fishery data weights (via the D-M parameters θ_{fish} and θ_{surv}).

The medians of the key parameters from the posterior distribution changed somewhat compared to those in last year's base model (Table 25). Parameter differences were largely due to the removal of the age-1 index this year, but also from other data and structural changes (see Section 3.4.1). For derived management quantities, the largest change was a reduction in the estimated relative spawning biomass at the start of 2024 from 98.7% in last year's model to 65.4% this year as a result of removing the age-1 index and associated changes to recruitment estimates (e.g., reduced estimate of the 2018 and 2022 year classes).

The Pacific Hake stock displays a very high degree of recruitment variability, perhaps the largest of any west coast groundfish stock, resulting in large and rapid biomass changes. This volatility, coupled with a dynamic fishery that potentially targets strong cohorts (resulting in time-varying selectivity) will in most circumstances continue to result in highly uncertain estimates of current stock status and even less-certain projections of the stock trajectory. This is particularly true for female spawning biomass estimates in 2025 and throughout the current forecast period, because there is considerable uncertainty associated with the absolute size of the, now mostly mature, 2020 and 2021 year classes that propagates into forecasts. Although the 2023 acoustic survey helped to refine these estimates and reduce uncertainty, further observations of these year classes will improve estimates. The removal of recruitment deviation estimates from 2023 onward through the forecast period led to an underestimation of uncertainty during the forecast period.

Uncertainty measures in the base model underestimate the total uncertainty in the current stock status and projections, because they do not account for alternative structural models for hake population dynamics and fishery processes (e.g., recruitment, selectivity, or spatial fleet or population structure), the effects of alternative data-weighting choices, survey catchability, and the scientific basis for prior probability distributions. To address structural uncertainties, the JTC investigated a range of alternative models, and we present the key sensitivity analyses along with other informative sensitivity analyses using full MCMC results (Section 3.8).

The JTC continues to be committed to advancing MSE analyses, by coordinating research with the Pacific Hake MSE Working Group and other scientists in the region engaged in similar research. Incorporating feedback from the Working Group and stakeholders will ensure that operating models will be able to provide insight into the important questions defined by interested parties. Specifically, the development of MSE tools will evaluate major sources of uncertainty relating to data, model structure and the harvest policy for this fishery, and will compare potential methods to address them. In the coming years, this will include a host of research evaluations (see Section 3.3 and Section 3.12), including evaluating the utility of incorporating environmentally-driven age-0 recruitment indices into the stock assessment.

3.6 Reference points

The term 'reference points' is used throughout this document to describe common conceptual summary metrics. The Agreement specifically identifies $F_{\text{SPR}=40\%}$ as the default harvest rate and $B_{40\%}$ as a point where the 40:10 TAC adjustment is triggered (see the Glossary in Appendix C).

We report estimates of the base reference points (e.g., $F_{\text{SPR}=40\%}$, $B_{40\%}$, B_{MSY}, and MSY) with posterior credibility intervals in Table 26. The median of the female spawning biomass at $F_{\text{SPR}=40\%}$ (namely the median of $B_{\text{SPR}=40\%}$) and the median yield at $F_{\text{SPR}=40\%}$ have declined slightly from the estimates in the 2024 assessment (Table 25).

As part of the DFO Sustainable Fisheries Framework, Fisheries and Oceans Canada (2009) defined a limit reference point as being a biomass below which serious harm is believed to be occurring to the stock, and an upper stock reference point above which the stock is considered to be healthy. These would equate to the Agreement reference points of $B_{10\%}$ and $B_{40\%}$ (the female spawning biomass being 10% and 40%, respectively, of the unfished equilibrium female spawning biomass). The probabilities of the female spawning biomass at the start of 2025 being above each of these points are $\mathrm{P}(B_{2025} > B_{10\%}) = 100\%$ and $\mathrm{P}(B_{2025} > B_{40\%}) = 88.9\%$ such that the stock is estimated to be in the 'healthy zone' (above the upper stock reference point of $B_{40\%}$). This probability is slightly lower than in last year's assessment, where the equivalent calculation was $\mathrm{P}(B_{2024} > B_{40\%}) = 98.1\%$. Note that a probability of '100%' (or '0%') is based on the MCMC results, and is not meant to imply that something definitely occurs (or definitely does not occur).

With respect to DFO's provisional limit reference point of $0.4B_{\mathrm{MSY}}$ and provisional upper stock reference point of $0.8B_{\mathrm{MSY}}$, the probabilities are $\mathrm{P}(B_{2025} > 0.4B_{\mathrm{MSY}}) = 100.0\%$ and $\mathrm{P}(B_{2025} > 0.8B_{\mathrm{MSY}}) = 99.4\%$ such that the stock is estimated to be in the provisional 'healthy zone'. For completeness, we note that $\mathrm{P}(B_{2025} > B_{\mathrm{MSY}}) = 98.1\%$.

Reference levels of stock status that are used by the U.S. Pacific Fisheries Management Council (PFMC) for Pacific Hake include $B_{40\%}$ and a Minimum Stock Size Threshold (MSST) of $B_{25\%}$. For 2025, the estimated posterior median relative spawning biomass is 67%, such that the female spawning biomass is well above $B_{40\%}$ and $B_{25\%}$. The probability that female spawning biomass at the beginning of 2025 is above $B_{40\%}$ is $\mathrm{P}(B_{2025} > B_{40\%}) = 88.9\%$ (as noted above), and of being above $B_{25\%}$ is $\mathrm{P}(B_{2025} > B_{25\%}) = 98.7\%$.

3.7 Model projections

The catch limit for 2025 based on the default $F_{40\%}$–40:10 harvest policy has a median of 560,742 t and a wide range of uncertainty (Figure 37), with the 95% credibility interval being 203,161–1,605,930 t.

Decision tables give projected population status (relative spawning biomass and relative fishing intensity) under different catch alternatives for the base model (Tables 27 and 28). The tables are organized such that the projected outcome for each potential catch level and year (each row) can be evaluated across the quantiles (columns) of the posterior distribution. Table 27 shows projected relative spawning biomass outcomes, and Table 28 shows projected fishing intensity outcomes relative to $F_{\mathrm{SPR}=40\%}$.

Population dynamics and governing parameters assumed during the forecast period include posterior recruitments taken from the stock-recruitment curve; selectivity, weight-at-age and maturity (and thus fecundity) averaged over the five most recent years (2020–2024); and all estimated parameters constant (at their estimates for each particular MCMC sample).

Relative fishing intensity exceeding 1 (or 100% when shown as a percentage) indicates fishing in excess of the $F_{\mathrm{SPR}=40\%}$ default harvest rate limit. It is possible for values in forecast years to exceed this slightly because the $F_{\mathrm{SPR}=40\%}$ default harvest-rate catch limit is calculated using baseline selectivity-at-age (1966–1990; prior to time-varying deviations), whereas the forecasted catches under the default harvest-rate are removed using selectivity averaged over the last five years. Recent changes in selectivity could be reflected in the projection of slight over- or under-fishing relative to the desired $F_{\mathrm{SPR}=40\%}$ rate.

Key management metrics are presented for 2026 and 2027 projections (Tables 29–30 and Figures 41–42). These metrics summarize the probability of various outcomes from the base model given each potential management action. Although not linear, probabilities can be interpolated from this table for intermediate catch values in 2025 (Table 29 and Figure 41). However, interpolation may not be applicable for all catches in 2026 because they are conditional on catch levels from the previous year or years.

Figure 40 shows the projected relative spawning biomass trajectory through 2028 for several of these management actions. With zero catch for the next two years, the biomass has a 89% probability of decreasing from 2025 to 2026 (Table 29 and Figure 41) and a 93% probability of decreasing from 2026 to 2027 (Table 30 and Figure 42).

The probability of the female spawning biomass decreasing from 2025 to 2026 is greater or equal to 100% for all catch levels examined other than zero (Table 29 and Figure 41). For all explored catches, the maximum probability of the female spawning biomass dropping below $B_{10\%}$ at the start of 2026 is 0.1% and at the start of 2027 is 2.4% (Tables 29–30 and Figures 41–42). The similar maximum probability of dropping below $B_{40\%}$ at the start of 2026 is 34.4% and at the start of 2027 is 63.2%. The model estimates that in two years time the stock will be at $B_{40\%}$ with a catch of 250,000 t in 2026 and 2027, given the current assumption of median recruitment from 2023 onward.

It should be noted that forecasted biomass is not only influenced by catch levels. As the above average 2014 and 2016 cohorts continue to age, total biomass of these cohorts even without fishing mortality will continue to decrease (Tables 18 and 22) as losses from mortality outweigh increases from growth. The above-average 2021 cohort entered this growth-mortality transition period around 2024 (Tables 18 and 22). The 2021 cohort will play a large role in determining female spawning biomass during the forecast years presented here. Similarly, the application of no recruitment deviations from 2023 onwards also plays a major role in forecasted female spawning biomass levels. The below-average 2015, 2018, and 2019 cohorts will contribute much less to forecasted spawning biomass than the larger cohorts.

The age composition (in numbers) of the catch in 2025 is projected to be (using MCMC medians) 51% age-4 fish from the 2021 cohort, 21% age-5 fish from the 2020 cohort, 6% age-9 fish from the 2016 cohort, and 4% age-11 fish from the 2014 cohort (Figure 43). However, those estimates are highly uncertain with the 95% credibility interval for the age-4 fraction spanning 32%–69%.

Due to the higher average weight of older fish compared to younger fish, the median expected proportion of the 2025 catch by weight is 48% for the age-4 2021 cohort (compared to 51% by numbers) and 6% for the large age-11 2014 cohort (compared to 4% by numbers; Figure 43).

With respect to the DFO reference points, with the largest 2025 catch of 560,742 t given in Table 29, at the start of 2026 the stock is expected to be above the critical zone with a probability of $\mathrm{P}(B_{2026} > B_{10\%}) = 100\%$ and in the healthy zone with a probability of $\mathrm{P}(B_{2026} > B_{40\%}) = 66\%$. With respect to the DFO provisional reference points (based on B_{MSY}), the stock is expected to be above the provisional critical zone with a probability of $\mathrm{P}(B_{2026} > 0.4B_{\mathrm{MSY}}) = 100\%$, in the healthy zone with a probability of $\mathrm{P}(B_{2026} > 0.8B_{\mathrm{MSY}}) = 94\%$, and above B_{MSY} with a probability of $\mathrm{P}(B_{2026} > B_{\mathrm{MSY}}) = 88\%$ for this catch.

With respect to PFMC stock size reference points, a level of 2025 catch consistent with the Agreement default harvest control rule (560,742 t) has a 34% estimated probability of resulting in the biomass going below $B_{40\%}$ at the start of 2026 (and 11% probability of going below $B_{25\%}$; Table 29).

3.8 Sensitivity analyses

Sensitivity analyses were conducted to investigate influence of data inputs and structural uncertainty of the base model by investigating how changes to the model affected the estimated values and derived quantities. All sensitivity analyses compared MCMC posteriors with the same number of posterior samples as the base model. Several key underlying structural model assumptions were identified that have persisted across many previous hake assessments, and thus warrant revisiting annually as a set of reference sensitivity examinations to new base models. Many additional sensitivity runs were conducted while developing and testing the 2025 base model. Here we focus on the main sensitivities, relative to the base model, which are as follows:

1. Consideration of higher standard deviations on the prior distribution for natural mortality;
2. Consideration of an alternative prior distribution (mean and standard deviation) for natural mortality based on the Hamel (2015) and Hamel and Cope (2022) life-history meta-analytic method;
3. Consideration of an alternative prior distribution and a fixed value for steepness, to change the resiliency of the stock;
4. Consideration of higher and lower variation about the stock–recruitment relationship (σ_r);
5. Addition of the relative age-1 index as a data source;
6. Down weighting the fishery age-composition data;
7. Consideration of alternative standard deviations for time-varying selectivity;
8. Addition of a relative index of abundance based on environmental-DNA;
9. Using the middle of the year to predict maturity-at-age data; and
10. Assuming M is specific to ages 0–1, 2, 3, 4, 5, and 6^+.

Most of the sensitivities resulted in a similar trajectory of the population dynamics as the base model (Tables 31–33 and Figures 44–62), with the largest deviations occurring in the sensitivities related to natural mortality. All sensitivity models matched the base model in terms of trends from the start of the model to approximately 2020, e.g., increases in female spawning biomass in the early- to mid-2010s driven by the 2010, 2014, and 2016 cohorts, followed by a period of general decline during a period of high catches. Some of the models differed from the base model in their trajectories of recent trends and unfished levels. All sensitivity models, except when age-specific natural mortality was fixed, indicate that 2025 median estimate of relative spawning biomass is above $B_{40\%}$.

As previously mentioned, the overall scale of the population was impacted by various alternative assumptions, and the uncertainty about size of the recent cohorts was more variable across sensitivity analyses than earlier cohorts that have been observed for more years.

The standard deviation of the prior distribution on natural mortality was increased from the base model value of 0.1 to 0.2, 0.3, and 0.31. Note that the median of the prior was also changed for the latter sensitivity due to the use of the Hamel and Cope (2022) prior. Estimates of natural mortality were higher than the base model for each of these changes to the prior. The medians of the MCMC osteriors for natural mortality increased from 0.233 to 0.286, 0.307, and 0.309, respectively. The 95% credibility intervals also increased, with the largest differences in the upper end rather than the lower end of the intervals. The credible interval for the base model was 0.194–0.280, and for the sensitivity runs were 0.221–0.347, 0.236–0.362 , and 0.242–0.362, respectively, (Table 31). In addition to increased estimates of natural mortality, results from these sensitivity models also showed increases in the overall scale of the population, the estimated stock status relative to B_0 prior to 1990, and the uncertainty in female spawning biomass on both absolute and relative scales. They also led to roughly a halving of the estimated relative fishing intensity in 2024 and roughly a doubling of equilibrium yield at $B_{\text{SPR=40\%}}$ (Table 31 and Figures 44 and 45).

The mean of the prior distribution on steepness was decreased from 0.777 to 0.5 and, separately, steepness was fixed at 1.0. The decrease in the mean of the prior resulted in a decrease in the median estimate of steepness from 0.812 (0.564–0.958) to 0.538 (0.353–0.764; Table 31). However, neither sensitivity analysis had a large impact on the overall model results (Figures 44 and 45), because Pacific Hake female spawning biomass has remained above levels where changes in steepness would appreciably influence the stock–recruitment relationship (Figure 33).

The fixed value for σ_r was changed from 1.40 to alternative low (1.00) and high (1.60) states. Both sensitivities led to results that were similar to the base model and higher calculated standard deviation of recruitment deviations (from the main period) than the fixed value used in the analysis, i.e., when σ_r was 1.00 the calculated value was 1.59 and when σ_r was 1.60 the calculated value was 1.95. For the base model, the calculated standard deviation of the recruitment deviations was intermediate with a median of 1.83. These calculated standard deviations should match the input if the vectors of deviations were from the 'population' of values rather than just a sample. A systematic bias larger than the input value indicates that the standard deviation of recruitment deviations is accounting for more variability than just variability in recruitment. The high σ_r model led to a larger difference between the female spawning biomass at unfished equilibrium and the female spawning biomass at the initial year of the model than the low σ_r model (Figure 44). Similar to previous assessments, estimates of unfished equilibrium recruitment are sensitive to σ_r, whereas absolute estimates of female spawning biomass are relatively insensitive. The method that Methot and Taylor (2011) proposed to tune σ_r was developed in the context of maximum likelihood estimation and not Bayesian inference, where the latter potentially allows for estimating σ_r using random effects, and thus, this proposed method is not used here to tune the fixed input value.

The sensitivity of the base model to the addition of the relative age-1 index provides a method to evaluate how the information about juvenile fish is propagated through the model. Estimates of female spawning biomass throughout most of the time series are similar between models with and without the relative age-1 index, which starts in 1995, but start to noticeably diverge in 2017 (Table 31, Figures 46 and 47). The 2025 estimates of relative spawning biomass are 67.1% for the base model (95% credible interval of 28.9–157.3%) and 86.3% for the model where the relative age-1 index is included (95% credible interval of 38.9–196.3%). This difference is due to the relative age-1 index providing additional information on recruitment for cohorts associated with recent age-1 indices (i.e., 2020 and 2022 cohorts detected in the 2021 and 2023 age-1 indices). In particular, the sensitivity with the relative age-1 index indicates slightly larger 2020 and 2021 year classes than the base model without the relative age-1 index (Figure 48). Similarly, recruitment in 2022 is estimated to be somewhat larger for the model with the relative age-1 index than the base model, though both median recruitment deviations are negative. Adding the relative age-1 index led to changes in fit to the age-2+ survey biomass index. Both models underestimate the 2021 age-2+ index (the base model more so), and both overestimate the 2023 age-2+ (the base model less so; Figure 49). The inclusion of the age-1 index leads to higher estimates of female spawning biomass in recent years compared to the base model.

The base model includes a Dirichlet-multinomial likelihood component that includes two estimated parameters to automatically weight the fishery and survey age compositions. The base model was compared to a model that down weighted the fishery age compositions relative to the survey age compositions. This down weighting was based on the McAllister–Ianelli method, which requires manual iterative adjustments to the input sample sizes using a derived multiplier. The McAllister–Ianelli method, which was used in assessments prior to 2018 (Table 16), attempts to make the arithmetic mean of the input sample size approximately equal to the harmonic mean of the effective sample size. Here, this was accomplished with weighting factors of 0.14 and 0.46 (ratio of 0.30) for fishery and survey age compositions, respectively. These weighting factors are not specific to this year's base model because an iterative process is not possible when using Bayesian inference, rather they are values calculated from previous maximum likelihood estimates. The median estimate from the Dirichlet-multinomial method used in the base model was 0.345 and 0.939, respectively (ratio of 0.37). Down weighting fishery composition data led to minor changes in relative spawning biomass, recruitment estimates, and increased uncertainty in estimates of early recruitment deviations compared to the base model (Figures 47 and 48). The majority of these changes were realized in the 1980s but estimates of female spawning biomass in the most recent years were also different between these two models. In particular, estimates of female spawning biomass in the most recent four years indicated less recovery of the population when fishery-age composition data were down weighted.

A biomass-based index of Pacific Hake relative abundance has been developed using environmental DNA (see Appendix G) that covers the years 2019, 2021, and 2023. The index was specified as having a Student's t-distribution for the error structure (similar to the sensitivity with the relative age-1 index) with 2 degrees of freedom given that there are

3 data points in the time series. An additional constant and additive standard deviation on the log-scale to accommodate unaccounted-for sources of process and observation error was determined unneccessary. The index is representative of all fish age-1 and older, with a median estimate of catchability of 0.148. Catchability is not as intuitive as for the other indices as it scales copies of DNA per microliter to biomass. The eDNA index declined from 2019 to 2023, though more steeply between 2019 to 2021 than between 2021 and 2023 (see Figure G.16). The eDNA index is fit well in the model (Figure 50), somewhat at the cost of reduced fits to the age-composition data. While the inclusion of the eDNA index did not significantly alter most key parameters and management quantities (Table 32), it did lead to reductions in estimates of female spawning biomass from 2021 onward, similar to when fishery age-composition data are down weighted (Figure 46). The eDNA index was included here as an initial exploration and proof-of-concept. Further explorations are needed, such as integrating eDNA data with acoustic data outside the assessment model to produce more accurate and robust survey estimates, before it should be used for management advice. The construction of a longer time series, through continued eDNA sampling, will be advantageous for understanding Pacific Hake population dynamics and the biological communities that interact with Pacific Hake.

Changing the day of year that maturity was predicted to from 278 to 182 led to decreases in estimates of female spawning biomass for the majority of the time series except for the terminal year. Estimates of unfished spawning biomass were also lower for this model (Table 32, Figure 46), and thus estimates of relative biomass are similar between this sensitivity and the base model (Figure 47).

The degree of flexibility of annual variation in the fishery selectivity was tested using three alternative values of standard deviations (Φ) (Figures 52–56). The consideration of alternative Φ values is discussed earlier in Section 2.5.3. Changing Φ, which controls the flexibility in time-varying selectivity, from the base model value of $\Phi = 1.40$ to 0.21, 0.70, and 2.10 did not appreciably influence the estimates, or precision, associated with recruitment in 2014 or 2016 but it did impact more recent estimates of recruitment (Figure 54). Changes in estimates of recruitment did not linearly scale with the changes in Φ and patterns were not consistent across years. For example, in 2011 higher Φ values led to higher estimates of recruitment but for the 2021 estimate of recruitment a Phi of 0.70 led to the lowest estimate (Figure 55). The higher estimates of recruitment for $\Phi = 0.21$ led to a large increase in female spawning biomass in recent years compared to the base model due to the pattern in recruitment estimates. Estimates of terminal female spawning biomass decrease as Φ changes from 0.21 to 2.1 to 1.4 to 0.7. (Figure 52). When $\Phi = 0.21$, the fit to the most recent age-2+ survey biomass index was the worst of the three investigated models (Figure 56).

Cannibalistic mortality at age since 1993 was estimated using CEATTLE (Holsman et al. 2016) and input into the assessment as fixed values. These annual deviations were available for six groups of fish, age-1 fish and younger, age-2 fish, age-3 fish, age-4 fish, age-5 fish, and fish ages six and older. The annual deviations were used the following sensitivities related to specifying natural mortality at age rather than time-invariant and age-invariant natural mortality, like what is in the base model. The first sensitivity estimated baseline mortality for each age group, while the second sensitivity fixed baseline mortality at 0.13

for all groups based on the estimate of baseline mortality from CEATTLE. Given the time-varying age-specific deviations, mortality was, on average, more than 20 times larger for age-1 fish than any other age. Age-2 fish also experienced more cannibalism than older fish in most years but estimates of cannibalism were higher for age-3 than age-2 fish in some years (Figure 62). Cannibalism for fish age six and above was zero in all years. The annual age-specific deviations were estimated by fitting CEATTLE to diet data up to 2019. More recent diet data exists but it has yet to be analyzed and included in the regional database for its use in CEATTLE. Age-0 and age-1 fish were found in over 7,000 stomachs of the 17,000 Pacific Hake stomachs analyzed. Additionally, CEATTLE is informed by temperature at 130 m depth from GLORYS output at the same spatial footprint of the acoustic survey. More details about fitting data on Pacific Hake to CEATTLE can be found in Wassermann et al. (2025).

Estimates of spawning biomass and other derived quantities were quite similar when baseline natural mortality was estimated (Figures 57–61), with the largest differences seen in the mid-1980s and in the terminal years where the deviations are the highest (Figure 62). Notably, estimates of spawning biomass decreased to near target levels when baseline natural mortality was fixed at 0.13 for all ages. The uncertainty in almost all estimated quantities decreased when baseline mortality was fixed. Estimates of recruitment deviations were smaller for the initial period and larger for the main period, though the differences were relatively small, when age-specific natural mortality was not estimated compared to the other two models (Figure 60).

3.9 Retrospective analyses

Retrospective analyses were performed by iteratively removing the terminal year data used to fit the model until ten years of data were removed Table 34. Retrospective analyses are informative for identifying consistent under- and over-estimation of estimates, particularly for spawning biomass and recruitment deviations.

As more information is gained regarding large cohorts, the estimated strength of the cohort tends to decrease (Figures 63 and 64). In this assessment, the previous trend was true for both large (positive) and small (negative) recruitment deviations, where all cohorts except the 2016 and 2018 cohorts were estimated to be smaller with time. For cohorts that have positive recruitment deviations, such as the 2014 cohort, the uncertainty is narrower around the median due to a higher sampling rate over the years than the cohorts with negative recruitments such as the 2015 cohort.

The retrospective plots in this year's assessment look slightly different than those from previous assessments; recruitment deviations for the last two years of the time series plus the assessment year are fixed at zero.

The latest data confirm that 2020 is not likely to be an extremely large cohort (Figures 63 and 64). The 2021 cohort at age-3 had a lower median than the 2020 cohort at age-3 but did not decrease as much as the 2020 cohort at age 4. Confirming cohort strengths for even-numbered recruitment years takes longer than for odd-numbered recruitment years because the survey does not include them in the age-2+ survey until they are of age three.

Almost all estimates of recruitment deviations, positive or negative, stabilize by the age of six (Figure 65).

The stability of the recruitment estimates seen in Figure 63 is also evident in the absolute estimates of uncertainty for each cohort. Uncertainty in biomass for cohorts from 2014–2023 has been substantially reduced in the 2025 base model compared to removing 1–5 years of data (Figure 66, upper and lower panels).

Overall, there is little retrospective change to the relative spawning biomass trajectory up to the mid-2010s, and most retrospective change occurs in the final 5 years of the retrospective model (upper panel of Figure 66). The most change in spawning biomass occurs when two years of data are removed because of changes in the estimate of absolute recruitment in 2020 to a much larger recruitment event compared to the base model. The large positive recruitment event is not present in the three-year peel of data when the terminal-year estimates are again informed by both fishery and survey data. Except for the previously explained changes, there is very little retrospective bias, with only slight year-specific positive bias in female spawning biomass, some minor adjustments to recruitment deviates, and a slight negative trend in B_0 as the retrospective year increases.

3.10 Comparison with past assessments

A comparison of the base models, approved for management, used in each year since 1991 indicates that the variability between model results, especially early on in the estimated time series, is larger than the estimated uncertainty reported from the current base model (Figure 67). There have been substantial differences in the structural assumptions of the models and, thus, results submitted each year. Prior to 2004, catchability was fixed at 1.0. This assumption was investigated between 2004 and 2007, leading to variability in model results because of the use of several different, but fixed, values of catchability. Since 2008, catchability has been freely estimated by the model ($q_b = 0.89$). The fixing of survey catchability had the effect of driving the estimate of initial biomass upward, which in turn scaled the entire biomass trajectory up, leading to higher estimates of relative spawning biomass than in more recent assessments. The median estimates of female spawning biomass for 2016 and 2017 have remained similar to the previous assessment, being somewhat lower than in the 2016 and 2017 assessments. In addition to more information about the 2014 and 2016 cohorts, the 2018 assessment model also included a change in the data weighting method, an update to maturity and fecundity, and a change to selectivity parameterization (Table 16). From 2022 to 2024, the relative age-1 index was used to inform cohort size at an early age. The age-1 index was removed in the 2025 assessment. While there was a significant change from this assessment to the previous one (see Section 3.4.1), the uncertainty interval associated with the 2025 assessment brackets the majority of the historical estimates.

The level of uncertainty associated with each assessment's estimate of that year's current female spawning biomass (i.e., that used to convey current stock status and inform management advice) changes from assessment to assessment given updates in data and Pacific Hake population structure and dynamics. Uncertainty around the absolute amount of 2025 female spawning biomass is similar to the final-year estimates from previous assessments, with both absolute interquartile range and the relative amount of dispersion (or variability relative to the stock size; similar to a coefficient of variation) consistent with previous assessments (Figure 68).

3.11 Performance of past projections

Without rigorous simulation experiments it can be difficult to operationally assess the accuracy of projections in stock assessments because the truth is never known with 100% certainty. For Pacific Hake, hindsight comparisons have been conducted since 2021 (Johnson et al. 2021) to evaluate performance of projections provided in decision tables (such as Tables 29 and 30) of past assessments relative to updated assessments. Overall, results indicate that assessment model projections give a relatively good idea of general projected trends and status.

As an example, the 2019 assessment (Berger et al. 2019) gave the estimated probability of the female spawning biomass declining in the subsequent year, i.e., $\mathrm{P}(B_{2020} < B_{2019})$, for several possible catches in 2019, such as 0 t, 180,000 t, 350,000 t, 410,000 t etc. Now that we 'know' the catch in 2019 was 411,635 t, we can select the 410,000 t row (close enough to 411,635 t) in the table from the 2019 assessment to give that assessment's $\mathrm{P}(B_{2020}<B_{2019})$ = 61%; Figure 69. We can also calculate this probability from the current assessment model (being the most up-to-date picture we have of stock dynamics) which implicitly includes the 411,635 t catch from 2019, giving $\mathrm{P}(B_{2020} < B_{2019}) = 99\%$; Figure 69. We extracted similar probabilities from past assessment documents going back to 2012 and calculate analogous probabilities, $\mathrm{P}(B_{\mathrm{t}+1} < B_{\mathrm{t}})$, from the current base model [Figure 69; see Edwards et al. (2022) for full methods].

Each assessment correctly predicted whether the stock would most likely increase or decrease the following year, except for 2017 and 2023 (Figure 69). Estimates from previous assessments are almost always closer to 50% than those from the current base model (Figure 69), because the current assessment model has more information and thus provides a more definitive probability (closer to 0% or to 100%) than year t's assessment model. It is desirable that the probabilities from the assessment documents are not too definitive (too close to 0% or to 100%), because they are admitting a wide range of uncertainty given unknown recent recruitments.

The 2017 and 2023 assessments 'incorrectly' projected that the stock would likely decline the following year (given the catch that subsequently occurred), because the current assessment model estimates a likely increase (Figure 69). For the 2017 (Berger et al. 2017) assessment the biomass trend was projected to be relatively flat the following year, so even slight changes in biomass could influence the binomial outcome of an 'increase' or 'decrease' in biomass, despite the overall change in biomass not being very substantial. The 2023 assessment (Berger et al. 2023) had minimal information on the 2021 cohort and predicted the biomass would probably decline in 2024 with any non-zero 2023 catch. However, the current assessment estimates that the 2021 cohort was potentially large, which further highlights how impactful a realized large deviation from average recruitment (rather than assuming average recruitment) can be on forecasted outcomes. Similarly, the 2012 assessment had no information on the very large 2010 recruitment, and so also over-estimated the probability of decline the following year (Figure 69). A range of catch alternatives are shown for the current assessment because realized 2025 catches are not yet known (Figure 69), and all (including no catch) suggest the stock will decline from 2025 to 2026.

A similar approach was used to calculate the probability of the biomass falling below $B_{40\%}$ in the subsequent year, i.e., $\mathrm{P}(B_{\mathrm{t+1}} < B_{40\%})$; Figure 70. The 2012 assessment was the only one that gave a >50% chance of the biomass falling below $B_{40\%}$ in the subsequent year, but later data determined that the 2010 year class was substantial and so in hindsight the probability of going below $B_{40\%}$ was 0% (based on the current assessment). From the 2016 assessment onwards, the estimated $\mathrm{P}(B_{\mathrm{t+1}} < B_{40\%})$ probabilities rose, until falling due to the incoming above-average 2020 cohort and lower catches (Figure 70). The same probabilities calculated from the current base model similarly rose, but all remained lower than the previous assessments' calculations, until being above since 2022 onwards. The current assessment estimates a probability of 11–12% that the biomass was below $B_{40\%}$ in each of 2023–2025, above the respective probabilities of 8%, 3%, and 1% estimated in the 2022–2024 assessments.

3.12 Research and data needs

There are many research projects and data collections that could improve the stock assessment for Pacific Hake and lead to improved biological understanding and decision-making. The following is a list of needs (new and ongoing) that the JTC has identified as having a high probability of improving the overall quality and robustness of the stock assessment. Only the top three are shown in the executive summary.

1. Continue to conduct research to evaluate ways to improve recent, current, and future estimates of recruitment for use in stock assessment. This could include the development of time series of recruitment indices, time series of informative environmental or ecosystem variables, and models that have predictive skill (e.g., Vestfals et al. 2023). Explorations should also consider options for incorporating information on recruitment into the assessment model and the management framework for Pacific Hake. For example, time series could be included in the stock assessment as a standalone data source (similar to the acoustic indices) or improvements could be made to the modeling framework such that these environmental time series could impact the stock–recruitment relationship directly. Results from such work should be connected to or in cooperation with ongoing research related to recruitment variability as discussed in Section 3.3. Related, there is a need to streamline and broaden the availability of products from oceanographic models (e.g., Regional Ocean Modeling System) so they are available across international boundaries and updated on a recurring basis, thereby allowing for their use as informative links in operational stock assessments. A successful example of this has been the annual production of Pacific Hake distribution forecasts that depend on 6–9 month forecasts of subsurface (i.e., 100 m depth) temperature from J-SCOPE. The continued collection of annual histological samples across ages, and the associated resources to complete the histological laboratory work, is needed to inform time-varying maturity in the assessment model. Furthermore, the existing management strategy evaluation framework should be used, or further developed, to examine how information on recruitment can inform robust management decisions.

2. Conduct research on current and future index of abundance data sets or species distribution models that provide new age-based (e.g., recruitment or population-wide) or spatial population structure and distribution information to the stock assessment. In particular, continue to explore the utility of eDNA-based spatiotemporal biomass indices of population abundance. Develop species distribution models for Pacific Hake that utilize ecosystem information as drivers of observations across spatiotemporal domains. Investigate alternative ways to utilize survey age-composition information in the assessment model. Develop estimates of uncertainty for the relative age-1 index and test performance for furture use. Broaden the scope of uncertainty considered in the age-2+ index and adjust for changes arising from the U.S. Integrated Survey Initiative. Bootstrapping of the acoustic survey time series, or related methods, could help incorporate uncertainty related to the target-strength relationship, subjective scoring of echograms, thresholding methods, and methods used to estimate the species mixes for interpreting the acoustic backscatter into the variance calculations. Research should be communicated with those involved in

developing the U.S. West Coast Integrated Survey Initiative. The management strategy evaluation framework should be used, or further developed, to examine how changes in survey methods can be used to inform robust management decisions.

3. Continue to develop value-added scientific products to complement the stock assessment for management decision-making. In particular, work with regional partners to develop risk tables or other annual workflows that provides key metrics, indicators, or other summaries of general ecosystem conditions relevant to the coast-wide population of Pacific Hake. It would be advantageous to include indicators that are potentially associated with Pacific Hake biology and ecology (e.g., recruitment, distribution, predation, prey, and communities). Such information can broaden the context within which a single species stock assessment is interpreted, be used to support model development, refine uncertain assessment conclusions (e.g., productivity), and provide other non-assessment indicators of the system's state to management.

4. Explore the operational use of environmental DNA data for characterizing aspects of Pacific Hake population dynamics (in addition to use as a relative abundance index as highlighted under need #2 above), such as changes in species (and community) distribution or density and the incorporation of these data into the assessment. Recent research demonstrated that environmental DNA provides similar information as the acoustic survey at scales relevant to management, i.e., coast-wide and not just sample-to-sample comparisons (Shelton et al. 2022). Continued regular collections of water samples for eDNA extraction and analysis will be imperative to expand on the currently available three year (2019, 2021, and 2023) time-series to inform medium to long-term trends in abundance.

5. Use, build, and expand upon the existing management strategy evaluation framework to evaluate major sources of uncertainty relating to data, model structure, and the harvest policy for this fishery (as needed) and compare potential methods to address them. In particular, utilize and adapt the management strategy evaluation framework to address new and ongoing stock assessment research and data needs through the Pacific Hake Management Strategy Evaluation Working Group, including relevant requests by the Scientific Review Group (see Section 3.3). For example, research investigating links between Pacific Hake biomass, spatial distribution, growth, recruitment, and natural mortality, and how these biological processes vary with ocean conditions and ecosystem variables such as temperature, transport, and prey availability could inform models used in the MSE. Ongoing investigations have the potential to improve the scenarios considered in future work on the MSE framework and the basic understanding of drivers of Pacific Hake population dynamics and availability to fisheries and surveys.

6. Explore alternative spatial model structures and associated parameterizations for Pacific Hake through the use of simulation analyses. In particular, explore the tradeoffs between the current assessment (panmictic, or single area, and single fleet model that uses time-varying selectivity to account for spatiotemporal variability in fish availability) and alternative spatial configurations. These could include the

use of multiple fleets (e.g., an areas-as-fleets model) in a single area, or the use of multiple areas that track fish through explicit movement estimation or implicitly through spatiotemporal changes in survival. The statistical advantages of random effect estimation for these spatial models will likely be required.

7. Continue to develop Fourier-Transform Near-Infrared Spectroscopy (FT-NIRS) methods of fish age determination. Ongoing studies have shown that Pacific Hake is a species that will benefit from the efficiencies gained with machine-assisted fish ageing, potentially leading to an increase in the number of ages available for the assessment each year. To date, neural-network models that have been conditioned with traditional (human-read) otoliths have shown good agreement to FT-NIRS read otoliths.
8. Complete the ongoing inter-laboratory otolith exchange and use the results to update estimates of ageing error used in the stock assessment. This would include updated information about ageing imprecision, the effects of large cohorts, and comparisons between ageing methods such as break and burn, surface reads, and Fourier-Transform Near Infrared Spectroscopy. The last inter-laboratory comparison was done in 2010 ('CARE' exchanges). Related, streamlining procedures that ease the exchange of biological materials (e.g., otoliths) across international borders would increase the efficiency at which research products can be produced.
9. Improve stock assessment forecasts through research that identifies linkages between Pacific Hake biology and ecosystem, oceanographic, or climate variables across the population domain. In particular, explore possible relationships with recruitment, growth, fecundity (including weight-at-age and maturity), and population density to improve biomass forecasting capabilities for Pacific Hake.
10. Explore alternative approaches and related assumptions for parameterizing time-varying fishery selectivity in the assessment. Simulations that evaluate methods for including multiple variance structures, including interactions, tradeoffs, and related assumptions, across multiple processes (e.g., selectivity, recruitment, data weighting) in integrated stock assessment models would be particularly beneficial.
11. Explore the potential to use acoustic data collected from commercial fishing vessels to study Pacific Hake distributions, schooling patterns, and other questions of interest. This could be similar to the 'acoustic vessels of opportunity' program on fishing vessels targeting Pollock in Alaska (Stienessen et al. 2019).

4 ACKNOWLEDGMENTS

We thank the authors of previous assessments whose work remains an influential part of this assessment. We are grateful for the hard work of the U.S. and Canadian acoustics teams, including (in alphabetical order) Alicia Billings, Julia Clemons, Steve Deblois, Stéphane Gauthier, Elizabeth Phillips, John Pohl, Chelsea Stanley, Rebecca Thomas, and Amanda Vitale, as well as the crews of the NOAA ship *Bell Shimada*, the Canadian Coast Guard Ship *CCGS Sir John Franklin*, and the fishing vessel *Nordic Pearl*. We thank the following individuals who contributed technical assistance, analysis tools, data, or comments to this and/or previous assessments: Scott Buchanan, Dezhang Chu, Chelsea Cooke, Cassandra Donavan, Mark Freeman, Marie Guldin, Jamie Hale, Owen Hamel, Jim Hastie, Melissa Head, Jason Jannot, William Jasper, Tyler Johnson, Brian Langseth, Jerry Leonard, Kristin Marshall, Rick Methot, Patrick McDonald, Cole Monnahan, Andrea Odell, Kiva Oken, Elizabeth Phillips, Chelsea Rothkop, Ole Shelton, Erin Steiner, Brad Stenberg, Ian Taylor (who once again gave insightful comments on a draft version), Jim Thorson, Vanessa Tuttle, Audrey Ty, Eric Ward, and contributions by many others that are too numerous to list here. We also thank the attendees at the official JTC meeting who provided valuable insight into the 2024 commercial fisheries in Canada and the U.S., as well as additional perspective on the acoustic survey and Pacific Hake related research. We appreciate the input from the AP (particularly for providing Appendices D and E) and other industry representatives as well as the JMC members. We would also like to thank the U.S. mothership sector for providing access to their data in such a timely manner and Vanessa Tuttle, Stephanie Johnson, Erin Steiner, Kayleigh Somers, Kate Richerson, Owen Hamel, and Kristin Marshall for conversations and actions that facilitated the exchange.

We thank all the members of the Scientific Review Group for their thoughtful review and smoothly run SRG meeting, including co-chairs Owen Hamel and Steven Schut, panel members Trevor Branch, Jaclyn Cleary, Allan Hicks, Sam Johnson, and AP advisors Shannon Mann and Lori Steele.

Finally, we are very thankful for the Treaty coordinator, Colin Sayre, for handling logistics related to Treaty communications and meetings.

We thank the Stock Synthesis, the `r4ss` R package, and the `adnuts` R package development teams for continually improving stock assessment tools used in this assessment. Calculations and figures from Stock Synthesis output were performed using R version 4.4.2 (2024-10-31). Many R (R Core Team 2023) packages were used to produce this document (in particular `bookdown`, `rmarkdown`, `knitr`, and `adnuts`)

Having all of the code under `git` version control has greatly increased the collaboration between authors. It has been in use since the 2016 assessment (Grandin et al. 2016) and has ensured delivery of the assessment document each year within a contracted time frame.

5 REFERENCES

Agostini, V.N., Francis, R.C., Hollowed, A.B., Pierce, S.D., Wilson, C., and Hendrix, A.N. 2006. The relationship between Pacific hake (*Merluccius productus*) distribution and poleward subsurface flow in the California Current System. Canadian Journal of Fisheries and Aquatic Sciences 63: 2648–2659.

Alheit, J., and Pitcher, T.J. (*Editors*). 1995. Hake: Biology, fisheries and markets. Springer, Netherlands.

Bailey, K.M., Francis, R.C., and Stevens, P.R. 1982. The life history and fishery of Pacific whiting, *Merluccius productus*. CalCOFI Reports XXIII: 81–98.

Berger, A.M., Edwards, A.M., Grandin, C.J., and Johnson, K.F. 2019. Status of the Pacific Hake (whiting) stock in U.S. and Canadian waters in 2019. Joint Technical Committee of the Pacific Hake/Whiting Agreement Between the Governments of the United States; Canada.

Berger, A.M., Grandin, C.J., Johnson, K.F., and Edwards, A.M. 2023. Status of the Pacific Hake (whiting) stock in U.S. and Canadian waters in 2023. Joint Technical Committee of the Pacific Hake/Whiting Agreement Between the Governments of the United States; Canada.

Berger, A.M., Grandin, C.J., Taylor, I.G., Edwards, A.M., and Cox, S. 2017. Status of the Pacific Hake (whiting) stock in U.S. and Canadian waters in 2017. Joint Technical Committee of the Pacific Hake/Whiting Agreement Between the Governments of the United States; Canada.

Bizzarro, J.J., Dewitt, L., Wells, B.K., Curtis, K.A., Santora, J.A., and Field, J.C. 2023. A multi-predator trophic database for the California Current Large Marine Ecosystem. Scientific Data 10: 496.

Buckley, T.W., and Livingston, P.A. 1997. Geographic variation in the diet of Pacific hake, with a note on cannibalism. CalCOFI Reports XXXVIII: 53–62.

Cheng, M.L.H., Thorson, J.T., Ianelli, J.N., and Cunningham, C.J. 2023. Unlocking the triad of age, year, and cohort effects for stock assessment: Demonstration of a computationally efficient and reproducible framework using weight-at-age. Fisheries Research 266: 106755.

Chittaro, P., Grandin, C., Pacunski, R., and Zabel, R. 2022. Five decades of change in somatic growth of Pacific hake from Puget Sound and Strait of Georgia. PeerJ 10: e13577.

Cleary, J.S., Hawkshaw, S., Grinnell, M.H., and Grandin, C. 2019. Status of B.C. Pacific Herring (*Clupea pallasii*) in 2017 and forecasts for 2018. Fisheries and Oceans Canada. Canadian Science Advisory Secretariat Science Advisory Report 2018/028: v + 285 p.

DFO. 2024. Stock status update with application of management procedures for Pacific Herring (*Clupea pallasii*) in British Columbia: status in 2023 and forecast for 2024. Fisheries and Oceans Canada. Canadian Science Advisory Secretariat Science Advisory Report 2024/001: 65 p.

Di Lorenzo, E., Schneider, N., Cobb, K.M., Franks, P.J.S., Chhak, K., Miller, A.J., McWilliams, J.C., Bograd, S.J., Arango, H., Curchitser, E., Powell, T.M., and Rivière, P. 2008. North Pacific Gyre Oscillation links ocean climate and ecosystem change. Geophysical Research Letters 35: L08607.

Dorn, M.W. 1994. Status of the coastal Pacific whiting resource in 1994. U.S. Dep. Commer., NOAA Tech. Memo.

Dorn, M.W. 1995. The effects of age composition and oceanographic conditions on the annual migration of Pacific whiting, *Merluccius productus*. CalCOFI Reports XXXVI: 97–105.

Dorn, M.W. 1996. Status of the coastal Pacific whiting resource in 1996. *In* Appendix Volume I: Status of the Pacific Coast Groundfish Fishery through 1996 and recommended acceptable biological catches in 1997: Stock assessment and fishery evaluation. Pacific Fisheries Management Council, Portland, OR. pp. A1–A77.

Dorn, M.W. 1997. Mesoscale fishing patterns of factory trawlers in the Pacific hake (*Merluccius productus*) fishery. CalCOFI Reports XXXVIII: 77–89.

Dorn, M.W., and Methot, R.D. 1991. Status of the coastal Pacific whiting resource in 1991. *In* Appendix: Status of the Pacific Coast Groundfish Fishery through 1991 and recommended biological catches for 1992: Stock assessment and fishery evaluation. Pacific Fishery Management Council, Portland, OR.

Dorn, M.W., and Methot, R.D. 1992. Status of the coastal Pacific whiting resource in 1992.

Dorn, M.W., and Saunders, M.W. 1997. Status of the coastal Pacific whiting stock in U.S. And Canada in 1997. *In* Appendix: Status of the Pacific Coast Groundfish Fishery through 1997 and recommended biological catches for 1998: Stock assessment and fishery evaluation. Pacific Fishery Management Council, Portland, OR. pp. 1–84.

Dorn, M.W., Saunders, M.W., Wilson, C.D., Guttormsen, M.A., Cooke, K., Kieser, R., and Wilkins, M.E. 1999. Status of the coastal Pacific hake/whiting stock in U.S. And Canada in 1998.

Edwards, A.M., Berger, A.M., Grandin, C.J., and Johnson, K.F. 2022. Status of the Pacific Hake (whiting) stock in U.S. and Canadian waters in 2022. Joint Technical Committee of the Pacific Hake/Whiting Agreement Between the Governments of the United States; Canada.

Edwards, A.M., Tai, T.C., Watson, J., Peña, M.A., Hilborn, A., Hannah, C.G., Rooper, C.N., Flynn, K.L., and Oldford, G.L. 2024. pacea: An R package of Pacific ecosystem information to help facilitate an ecosystem approach to fisheries management. DOI: 10.5281/zenodo.13840804.

Edwards, A.M., Taylor, I.G., Grandin, C.J., and Berger, A.M. 2018. Status of the Pacific Hake (whiting) stock in U.S. and Canadian waters in 2018. Joint Technical Committee of the Pacific Hake/Whiting Agreement Between the Governments of the United States; Canada.

Eilers, P.H.C., and Marx, B.D. 1996. Flexible smoothing with b-splines and penalties. Statistical Science 11: 89–121.

Fisch, N., Ahrens, R., Shertzer, K., and Camp, E. 2022. An empirical comparison of alternative likelihood formulations for composition data, with application to cobia and Pacific hake. Canadian Journal of Fisheries and Aquatic Sciences 79: 1745–1764.

Fisheries and Oceans Canada. 2009. A fishery decision-making framework incorporating the precautionary approach.

Fisheries and Oceans Canada. 2023. DFO Groundfish Pacific Region 2023/2024 Integrated Fisheries Management Plan, version 3.1. 23-2236.337: 367 p.

Francis, R.C., Swartzman, G.L., Getz, W.M., Haar, R., and Rose, K. 1982. A management analysis of the Pacific whiting fishery. U.S. Dep. Commer., NOAA Tech. Memo. NWAFC Processed Report 82-06.

Francis, R.I.C.C. 2011. Data weighting in statistical fisheries stock assessment models. Canadian Journal of Fisheries and Aquatic Sciences 68: 1124–1138.

Free, C.M., Anderson, S.C., Hellmers, E.A., Muhling, B.A., Navarro, M.O., Richerson, K., Rogers, L.A., Satterthwaite, W.H., Thompson, A.R., Burt, J.M., Gaines, S.D., Marshall, K.N., White, J.W., and Bellquist, L.F. 2023. Impact of the 2014–2016 marine heatwave on US and Canada West Coast fisheries: Surprises and lessons from key case studies. Fish and Fisheries 24: 652–674.

García-De León, F.J., Galván-Tirado, C., Sánchez Velasco, L., Silva-Segundo, C.A., Hernández-Guzmán, R., de los Angeles Barriga-Sosa, I., Díaz Jaimes, P., Canino, M., and Cruz-Hernández, P. 2018. Role of oceanography in shaping the genetic structure in the North Pacific hake *Merluccius productus*. PLOS ONE 13(3): e0194646.

Grandin, C.J., Hicks, A.C., Berger, A.M., Edwards, A.M., Taylor, N., Taylor, I.G., and Cox, S. 2016. Status of the Pacific Hake (whiting) stock in U.S. and Canadian waters in 2016. Joint Technical Committee of the Pacific Hake/Whiting Agreement Between the Governments of the United States; Canada.

Grandin, C.J., Johnson, K.F., Edwards, A.M., and Berger, A.M. 2020. Status of the Pacific Hake (whiting) stock in U.S. and Canadian waters in 2020. Joint Technical Committee of the Pacific Hake/Whiting Agreement Between the Governments of the United States; Canada.

Grandin, C.J., Johnson, K.F., Edwards, A.M., and Berger, A.M. 2024. Status of the Pacific Hake (whiting) stock in U.S. and Canadian waters in 2024. Joint Technical Committee of the Pacific Hake/Whiting Agreement Between the Governments of the United States; Canada.

Hamel, O.S. 2015. A method for calculating a meta-analytical prior for the natural mortality rate using multiple life history correlates. ICES Journal of Marine Science 72(1): 62–69.

Hamel, O.S., and Cope, J.M. 2022. Development and considerations for application of a longevity-based prior for the natural mortality rate. Fisheries Research 256: 106477.

Hamel, O.S., Ressler, P.H., Thomas, R.E., Waldeck, D.A., Hicks, A.C., Holmes, J.A., and Fleischer, G.W. 2015. Biology, fisheries, assessment and management of Pacific hake (*Merluccius productus*). *In* Hakes: Biology and exploitation. *Edited by* H. Arancibia. John Wiley & Sons, Ltd. pp. 234–262.

Hamel, O.S., and Stewart, I.J. 2009. Stock assessment of Pacific Hake, *Merluccius productus*, (a.k.a. Whiting) in U.S. And Canadian waters in 2009. Pacific Fishery Management Council, Portland, OR.

Harvey, C.J., Garfield, N., Williams, G.D., and Tolimieri, N. 2021. Ecosystem status report of the California Current for 2020–21: A summary of ecosystem indicators compiled by the California Current Integrated Ecosystem Assessment Team (CCIEA). U.S. Dept. Comm., NOAA Tech. Memo. NMFS-NWFSC-170.

Head, M.A., Billings, A.A., Tuttle, V.J., Johnson, K.F., Berger, A.M., and Happel, S.A. 2025. Decade-scale spatio-temporal variability in maturity of Pacific hake, *Merluccius productus*, along the US West Coast. Environmental Biology of Fishes.

Helser, T.E., Dorn, M.W., Saunders, M.W., Wilson, C.D., Guttormsen, M.A., Cooke, K., and Wilkins, M.E. 2002. Stock assessment of Pacific whiting in U.S. And Canadian waters in 2001.

Helser, T.E., Fleischer, G.W., Martell, S., and Taylor, N. 2005. Stock assessment of Pacific hake (whiting) in U.S. And Canadian waters in 2004.

Helser, T.E., and Martell, S. 2007. Stock assessment of Pacific hake (whiting) in U.S. And Canadian waters in 2007. U.S.-Canada Pacific Hake Joint Technical Committee (JTC).

Helser, T.E., Stewart, I.J., Fleischer, G.W., and Martell, S. 2006. Stock assessment of Pacific hake (whiting) in U.S. And Canadian waters in 2006.

Hicks, A.C., Taylor, N., Grandin, C., Taylor, I.G., and Cox, S. 2013. Status of the Pacific hake (whiting) stock in U.S. and Canadian waters in 2013. International Joint Technical Committee for Pacific Hake.

Hoenig, J.M. 1983. Empirical use of longevity data to estimate mortality rates. Fishery Bulletin 82(4): 898–903.

Hoffman, M.D., and Gelman, A. 2014. The No-U-Turn Sampler: Adaptively setting path lengths in Hamiltonian Monte Carlo. Journal of Machine Learning Research 15: 1593–1623.

Hollowed, A.B., Adlerstein, S., Francis, R.C., and Saunders, M. 1988. Status of the Pacific whiting resource in 1987 and recommendations for management in 1988.

Holsman, K.K., Ianelli, J., Aydin, K., Punt, A.E., and Moffitt, E.A. 2016. A comparison of fisheries biological reference points estimated from temperature-specific multi-species and single-species climate-enhanced stock assessment models. Deep-Sea Research Part II: Topical Studies in Oceanography 134: 360–378.

Iwamoto, E., Ford, M.J., and Gustafson, R.G. 2004. Genetic population structure of Pacific hake, *Merluccius productus*, in the Pacific Northwest. Environmental Biology of Fishes 69: 187–199.

Jacobsen, N.S., Marshall, K.N., Berger, A.M., Grandin, C.J., and Taylor, I.G. 2021. Management strategy evaluation of Pacific Hake: Exploring the robustness of the current harvest policy to spatial stock structure, shift in fishery selectivity, and climate-driven distribution shifts. U.S. Dept. Comm., NOAA Tech. Memo. NMFS-NWFSC-168.

Johnson, K.F., Edwards, A.M., Berger, A.M., and Grandin, C.J. 2021. Status of the Pacific Hake (whiting) stock in U.S. and Canadian waters in 2021. Joint Technical Committee of the Pacific Hake/Whiting Agreement Between the Governments of the United States; Canada.

King, J.R., McFarlane, G.A., Jones, S.R.M., Gilmore, S.R., and Abbott, C.L. 2012. Stock delineation of migratory and resident Pacific hake in Canadian waters. Fisheries Research 114: 19–30.

Kuriyama, P.T., Ono, K., Hurtado-Ferro, F., Hicks, A.C., Taylor, I.G., Licandeo, R.R., Johnson, K.F., Anderson, S.C., Monnahan, C.C., Rudd, M.B., Stawitz, C.C., and Valero, J.L. 2016. An empirical weight-at-age approach reduces estimation bias compared to modeling parametric growth in integrated, statistical stock assessment models when growth is time varying. Fisheries Research 180: 119–127.

Lellouche, J.-M., Greiner, E., Bourdallé-Badie, R., Garric, G., Melet, A., Drévillon, M., Bricaud, C., Hamon, M., Galloudec, O.L., Regnier, C., Candela, T., Testut, C.-E., Gasparin, F., Ruggiero, G., Benkiran, M., Drillet, Y., and Traon, P.-Y.L. 2021. The Copernicus global 1/12° oceanic and sea ice GLORYS12 reanalysis. Frontiers in Earth Science 9: 2296–6463.

Lindgren, F., Rue, H., and Lindström, J. 2011. An explicit link between Gaussian fields and Gaussian Markov random fields: The stochastic partial differential equation approach. Journal of the Royal Statistical Society Series B: Statistical Methodology 73(4): 423–498.

Lloris, D., Matallanas, J., and Oliver, P. 2005. Hakes of the world (family Merlucciidae). An annotated and illustrated catalogue of hake species known to date. FAO Species Catalogue for Fishery Purposes, Rome.

Longo, G.C., Head, M.A., Parker-Stetter, S.L., Taylor, I.G., Tuttle, V.J., Billings, A.A., Gauthier, S., McClure, M.M., and Nichols, K.M. 2024. Population genomics of coastal Pacific Hake. North American Journal of Fisheries Management 44: 222–234.

Ludwig, D., and Walters, C.J. 1981. Measurement errors and uncertainty in parameter estimates for stock and recruitment. Canadian Journal of Fisheries and Aquatic Sciences 38(6): 711–720.

Malick, M.J., Cox, S.P., Mueter, F.J., Dorner, B., and Peterman, R.M. 2017. Effects of the North Pacific Current on the productivity of 163 Pacific salmon stocks. Fisheries Oceanography 26: 268–281.

Malick, M.J., Hunsicker, M.E., Haltuch, M.A., Parker-Stetter, S.L., Berger, A.M., and Marshall, K.N. 2020a. Relationships between temperature and Pacific hake distribution vary across latitude and life-history stage. Marine Ecology Progress Series 639: 185–197.

Malick, M.J., Siedlecki, S.A., Norton, E.L., Kaplan, I.C., Haltuch, M.A., Hunsicker, M.E., Parker-Stetter, S.L., Marshall, K.N., Berger, A.M., Hermann, A.J., Bond, N.A., and Gauthier, S. 2020b. Environmentally driven seasonal forecasts of Pacific hake distribution. Frontiers in Marine Science 7: 578490.

Mantua, N.J., Hare, S. R., Zhang, Y., Wallace, J.M., and Francis, R.C. 1997. A Pacific interdecadal climate oscillation with impacts on salmon production. Bulletin of the American Meteorological Society 7: 1069–1079.

Martell, S. 2010. Assessment and management advice for Pacific hake in U.S. And Canadian waters in 2010.

McAllister, M.K., and Ianelli, J.N. 1997. Bayesian stock assessment using catch-age data and the sampling-importance resampling algorithm. Canadian Journal of Fisheries and Aquatic Sciences 54(2): 284–300.

McClure, M.M., Haltuch, M.A., Willis-Norton, E., Huff, D.D., Hazen, E.L., Crozier, L.G., Jacox, M.G., Nelson, M.W., Andrews, K.S., Barnett, L.A.K., Berger, A.M., Beyer, S., Bizzarro, J., Boughton, D., Cope, J.M., Carr, M., Dewar, H., Dick, E., Dorval, E., Dunham, J., Gertseva, V., Greene, C.M., Gustafson, R.G., Hamel, O.S., Harvey, C.J., Henderson, M.J., Jordan, C.E., Kaplan, I.C., Lindley, S.T., Mantua, N.J., Matson, S.E., Monk, M.H., Moyle, P., Nicol, C., Pohl, J., Rykaczewski, R.R., Samhouri, J.F., Sogard, S., Tolimieri, N., Wallace, J., Wetzel, C., and Bograd, S.J. 2023. Vulnerability to climate change of managed stocks in the California Current large marine ecosystem. Frontiers in Marine Science 10: 1103767.

Mello, L.G.S., and Rose, G.A. 2005. Using geostatistics to quantify seasonal distribution and aggregation patterns of fishes: An example of Atlantic cod (*Gadus morhua*). Canadian Journal of Fisheries and Aquatic Sciences 62(3): 659–670.

Methot, Jr., R.D., and Wetzel, C.R. 2013. Stock synthesis: A biological and statistical framework for fish stock assessment and fishery management. Fisheries Research 142: 86–99.

Methot, R.D., and Taylor, I.G. 2011. Adjusting for bias due to variability of estimated recruitments in fishery assessment models. Canadian Journal of Fisheries and Aquatic Sciences 68(10): 1744–1760.

Monnahan, C.C., Branch, T.A., Thorson, J.T., Stewart, I.J., and Szuwalski, C.S. 2019. Overcoming long Bayesian run times in integrated fisheries stock assessments. ICES Journal of Marine Science 76: 1477–1488.

Monnahan, C.C., and Kristensen, K. 2018. No-U-turn sampling for fast Bayesian inference in ADMB and TMB: Introducing the adnuts and tmbstan R packages. PLOS ONE 13(5): e0197954.

Myers, R.A., Bowen, K.G., and Barrowman, N.J. 1999. Maximum reproductive rate of fish at low population sizes. Canadian Journal of Fisheries and Aquatic Sciences 56(12): 2404–2419.

Petitgas, P. 1993. Geostatistics for fish stock assessments: A review and an acoustic application. ICES Journal of Marine Science 50: 285–298.

Phillips, E.M., Chu, D., Gauthier, S., Parker-Stetter, S.L., Shelton, A.O., and Thomas, R.E. 2022. Spatiotemporal variability of euphausiids in the California Current Ecosystem: Insights from a recently developed time series. ICES Journal of Marine Science 79: 1312–1326.

Phillips, E.M., Malick, M.J., Gauthier, S., Haltuch, M.A., Hunsicker, M.E., Parker-Stetter, S.L., and Thomas, R.E. 2023. The influence of temperature on Pacific hake co-occurrence with euphausiids in the California Current Ecosystem. Fisheries Oceanography 32(3): 267–279.

R Core Team. 2023. R: A language and environment for statistical computing. R Foundation for Statistical Computing, Vienna, Austria.

Ressler, P.H., Holmes, J.A., Fleischer, G.W., Thomas, R.E., and Cooke, K.C. 2007. Pacific hake, *Merluccius productus*, autecology: A timely review. Marine Fisheries Review 69(1-4): 1–24.

Rivoirard, J., Simmonds, J., Foote, K.G., Fernandes, P., and Bez, N. 2000. Geostatistics for estimating fish abundance. Blackwell Science, Osney Mead, Oxford.

Shelton, A.O., Ramón-Laca, A., Wells, A., Clemons, J., Chu, D., Feist, B.E., Kelly, R.P., Parker-Stetter, S.L., Thomas, R., Nichols, K.M., and Park, L. 2022. Environmental DNA provides quantitative estimates of Pacific hake abundance and distribution in the open ocean. Proceedings of the Royal Society B 289: 20212613.

Shono, H. 2008. Application of the Tweedie distribution to zero-catch data in CPUE analysis. Fisheries Research (1–2, 93): 154–162.

Simmonds, J., and MacLennan, D.N. 2006. Fisheries acoustics: Theory and practice, 2nd edition. Wiley-Blackwell, Oxford, UK.

Steiner, E., Philips, A., and Chen, A. 2024. Economic status of the pacific hake fishery. U.S. Dept. Comm., NOAA Tech. Memo. NMFS-NWFSC-197.

Stewart, I.J., Forrest, R.E., Grandin, C., Hamel, O.S., Hicks, A.C., Martell, S.J.D., and Taylor, I.G. 2011. Status of the Pacific Hake (Whiting) stock in U.S. and Canadian waters in 2011. Joint U.S.; Canada Hake Technical Working Group.

Stewart, I.J., Forrest, R.E., Taylor, N., Grandin, C., and Hicks, A.C. 2012. Status of the Pacific hake (whiting) stock in U.S. and Canadian Waters in 2012. International Joint Technical Committee for Pacific hake.

Stewart, I.J., and Hamel, O.S. 2010. Stock Assessment of Pacific Hake, *Merluccius productus*, (a.k.a. Whiting) in U.S. and Canadian Waters in 2010. Pacific Fisheries Management Council, Portland, OR.

Stewart, I.J., Hicks, A.C., Taylor, I.G., Thorson, J.T., Wetzel, C., and Kupschus, S. 2013. A comparison of stock assessment uncertainty estimates using maximum likelihood and Bayesian methods implemented with the same model framework. Fisheries Research 142: 37–46.

Stewart, J.S., Hazen, E., Bograd, S.J., Byrnes, J.E.K., Foley, D.G., Gilly, W.F., Robison, B.H., and Field, J.C. 2014. Combined climate- and prey-mediated range expansion of Humboldt squid (*Dosidicus gigas*), a large marine predator in the California Current System. Global Change Biology 20(6): 1832–1843.

Stienessen, S.C., Honkalehto, T., Lauffenburger, N.E., Ressler, P.H., and Lauth, R.R. 2019. Acoustic Vessel-of-Opportunity (AVO) index for midwater Bering Sea walleye pollock, 2016–2017. U.S. Dept. Comm., NOAA Tech. Memo. AFSC Processed Rep. 2019-01, Seattle, WA.

Taylor, I.G., Grandin, C., Hicks, A.C., Taylor, N., and Cox, S. 2015. Status of the Pacific Hake (whiting) stock in U.S. and Canadian waters in 2015. Joint Technical Committee of the Pacific Hake/Whiting Agreement Between the Governments of the United States; Canada.

Taylor, N., Hicks, A.C., Taylor, I.G., Grandin, C., and Cox, S. 2014. Status of the Pacific Hake (whiting) stock in U.S. and Canadian waters in 2014 with a management strategy evaluation. International Joint Technical Committee for Pacific Hake.

Thorson, J.T., Johnson, K.F., Methot, R.D., and Taylor, I.G. 2017. Model-based estimates of effective sample size in stock assessment models using the Dirichlet-multinomial distribution. Fisheries Research 192: 84–93.

Turley, B.D., and Rykaczewski, R.R. 2019. Influence of wind events on larval fish mortality rates in the southern California Current Ecosystem. Canadian Journal of Fisheries and Aquatic Sciences 76(12): 2418–2432.

Vestfals, C.D., Marshall, K.N., Tolimieri, N., Hunsicker, M.E., Berger, A.M., Taylor, I.G., Jacox, M.G., and Turley, B.D. 2023. Stage-specific drivers of Pacific hake (*Merluccius productus*) recruitment in the California Current Ecosystem. Fisheries Oceanography 32(4): 352–389.

Vrooman, A.M., and Paloma, P.A. 1977. Dwarf hake off the coast of Baja California, Mexico. CalCOFI Reports XXIV: 67–72.

Wassermann, S.N., Adams, G.D., Haltuch, M.A., Kaplan, I.C., Marshall, K.N., and Punt, A.E. 2025. Even low levels of cannibalism can bias population estimates for Pacific hake. ICES Journal of Marine Science 82: fsae064.

Wippel, B., Dufault, A.M., Marshall, K., and Kaplan, I.C. 2017. Data from: *A Synthesis of Diets and Trophic Overlap of Marine Species in the California Current*. Hague, NL: Data Archiving and Networked Services.

Xu, H., Thorson, J.T., Methot, R.D., and Taylor, I.G. 2019. A new semi-parametric method for autocorrelated age- and time-varying selectivity in age-structured assessment models. Canadian Journal of Fisheries and Aquatic Sciences 76(2): 268–285.

Zamora-García, O.G., Márquez-Farías, J.F., Stavrinaky-Suárez, A., Díaz-Avalos, C., Zamora-García, N., and Lara-Mendoza, R.E. 2020. Catch rate, length, and sex ratio of Pacific hake (*Merluccius productus*) in the northern Gulf of California. Fishery Bulletin 118(4): 365–379.

6 TABLES

Table 1. Annual catches of Pacific Hake (t) in U.S. waters by fleet, 1966–2024. Tribal catches are included in the fleet totals. Research catch includes landed catch associated with research-related activities. Catch associated with surveys and discarded bycatch in fisheries not targeting hake is not currently included in the table or model.

Year	Foreign	Joint-venture	Mother-ship	Catcher-processor	Shore-side	Research	Total
1966	137,000	0	0	0	0	0	137,000
1967	168,700	0	0	0	8,960	0	177,660
1968	60,660	0	0	0	160	0	60,820
1969	86,190	0	0	0	90	0	86,280
1970	159,510	0	0	0	70	0	159,580
1971	126,490	0	0	0	1,430	0	127,920
1972	74,090	0	0	0	40	0	74,130
1973	147,440	0	0	0	70	0	147,510
1974	194,110	0	0	0	0	0	194,110
1975	205,650	0	0	0	0	0	205,650
1976	231,330	0	0	0	220	0	231,550
1977	127,010	0	0	0	490	0	127,500
1978	96,827	860	0	0	690	0	98,377
1979	114,910	8,830	0	0	940	0	124,680
1980	44,023	27,537	0	0	790	0	72,350
1981	70,365	43,557	0	0	838	0	114,760
1982	7,089	67,465	0	0	1,023	0	75,577
1983	0	72,100	0	0	1,051	0	73,151
1984	14,772	78,889	0	0	2,721	0	96,382
1985	49,853	31,692	0	0	3,894	0	85,439
1986	69,861	81,640	0	0	3,432	0	154,932
1987	49,656	105,997	0	0	4,795	0	160,448
1988	18,041	135,781	0	0	6,867	0	160,690
1989	0	195,636	0	0	7,414	0	203,049
1990	0	170,972	0	4,537	9,632	0	185,142
1991	0	0	86,408	119,411	23,970	0	229,789
1992	0	0	36,721	117,981	56,127	0	210,829
1993	0	0	14,558	83,466	42,108	0	140,132
1994	0	0	93,610	86,251	73,616	0	253,477
1995	0	0	40,805	61,357	74,962	0	177,124
1996	0	0	62,098	65,933	85,128	0	213,159
1997	0	0	75,128	70,832	87,416	0	233,376
1998	0	0	74,686	70,377	87,856	0	232,920
1999	0	0	73,440	67,655	83,470	0	224,565
2000	0	0	53,110	67,805	85,854	0	206,770
2001	0	0	41,901	58,628	73,412	0	173,940
2002	0	0	48,404	36,342	45,708	0	130,453
2003	0	0	45,396	41,214	55,335	0	141,945
2004	0	0	47,561	73,176	96,503	0	217,240
2005	0	0	72,178	78,890	109,052	0	260,120
2006	0	0	60,926	78,864	127,165	0	266,955
2007	0	0	52,977	73,263	91,441	0	217,682
2008	0	0	72,440	108,195	67,760	0	248,395
2009	0	0	37,550	34,800	49,222	0	121,573
2010	0	0	52,022	54,291	64,653	0	170,967
2011	0	0	56,394	71,678	102,146	1,042	231,261
2012	0	0	38,512	55,264	65,920	448	160,145
2013	0	0	52,470	77,950	102,141	1,018	233,578
2014	0	0	62,102	103,203	98,640	197	264,141
2015	0	0	27,665	68,484	58,011	0	154,160
2016	0	0	65,036	108,786	87,762	745	262,328
2017	0	0	66,428	136,960	150,454	0	353,842
2018	0	0	67,121	116,073	134,633	0	317,827
2019	0	0	52,646	116,146	147,830	0	316,622

Continued on next page ...

... Continued from previous page

Year	Foreign	Joint-venture	Mother-ship	Catcher-processor	Shore-side	Research	Total
2020	0	0	37,978	111,147	137,568	95	286,788
2021	0	0	35,208	104,030	129,204	917	269,359
2022	0	0	59,516	126,247	105,934	0	291,697
2023	0	0	33,074	107,117	100,397	0	240,588
2024	0	0	20,942	61,914	84,067	0	166,923

Table 2. Annual catches of Pacific Hake (t) in Canadian waters by fleet, 1966–2024.

Year	Foreign	Joint-venture	Shore-side	Freezer-trawler	Total
1966	700	0	0	0	700
1967	36,710	0	0	0	36,710
1968	61,360	0	0	0	61,360
1969	93,850	0	0	0	93,850
1970	75,010	0	0	0	75,010
1971	26,700	0	0	0	26,700
1972	43,410	0	0	0	43,410
1973	15,130	0	0	0	15,130
1974	17,150	0	0	0	17,150
1975	15,700	0	0	0	15,700
1976	5,970	0	0	0	5,970
1977	5,190	0	0	0	5,190
1978	3,450	1,810	0	0	5,260
1979	7,900	4,230	300	0	12,430
1980	5,270	12,210	100	0	17,580
1981	3,920	17,160	3,280	0	24,360
1982	12,480	19,680	0	0	32,160
1983	13,120	27,660	0	0	40,780
1984	13,200	28,910	0	0	42,110
1985	10,530	13,240	1,190	0	24,960
1986	23,740	30,140	1,770	0	55,650
1987	21,450	48,080	4,170	0	73,700
1988	38,080	49,240	830	0	88,150
1989	29,750	62,718	2,562	0	95,029
1990	3,810	68,314	4,021	0	76,144
1991	5,610	68,133	16,174	0	89,917
1992	0	68,779	20,043	0	88,822
1993	0	46,422	12,352	0	58,773
1994	0	85,154	23,776	0	108,930
1995	0	26,191	46,181	0	72,372
1996	0	66,779	26,360	0	93,139
1997	0	42,544	49,227	0	91,771
1998	0	39,728	48,074	0	87,802
1999	0	17,201	70,121	0	87,322
2000	0	15,625	6,382	0	22,007
2001	0	21,650	31,935	0	53,585
2002	0	0	50,244	0	50,244
2003	0	0	63,217	0	63,217
2004	0	58,892	66,175	0	125,067
2005	0	15,695	77,335	9,985	103,014

Continued on next page ...

... Continued from previous page

Year	**Foreign**	**Joint-venture**	**Shore-side**	**Freezer-trawler**	**Total**
2006	0	14,319	65,289	15,136	94,744
2007	0	6,780	52,649	14,121	73,550
2008	0	3,592	57,795	13,214	74,602
2009	0	0	44,130	13,223	57,353
2010	0	8,081	35,362	13,573	57,016
2011	0	9,717	31,760	14,596	56,073
2012	0	0	32,147	14,912	47,059
2013	0	0	33,665	18,584	52,249
2014	0	0	13,326	21,792	35,118
2015	0	0	16,775	22,909	39,684
2016	0	0	35,012	34,731	69,743
2017	0	5,608	43,427	37,686	86,721
2018	0	2,724	50,747	41,942	95,413
2019	0	0	40,794	54,218	95,013
2020	0	0	30,085	62,404	92,489
2021	0	0	11,269	45,807	57,076
2022	0	0	3,868	27,803	31,671
2023	0	0	3,657	20,296	23,952
2024	0	0	1,185	2,742	3,928

Table 3. Pacific Hake landings and management decisions, 1966–2024. A dash (–) indicates the management decision was either not specified or was unknown to the authors at the time of this assessment.

Year	U.S. landings	Canada landings	Total landings	U.S. prop. of total catch	Canada prop. of total catch	U.S. catch target	Canada catch target	Total catch target	U.S. prop. of catch target removed	Canada prop. of catch target removed	Total prop. of catch target removed
1966	137,000	700	137,700	99.5%	0.5%	–	–	–	–	–	–
1967	177,660	36,710	214,370	82.9%	17.1%	–	–	–	–	–	–
1968	60,820	61,360	122,180	49.8%	50.2%	–	–	–	–	–	–
1969	86,280	93,850	180,130	47.9%	52.1%	–	–	–	–	–	–
1970	159,580	75,010	234,590	68.0%	32.0%	–	–	–	–	–	–
1971	127,920	26,700	154,620	82.7%	17.3%	–	–	–	–	–	–
1972	74,130	43,410	117,540	63.1%	36.9%	–	–	–	–	–	–
1973	147,510	15,130	162,640	90.7%	9.3%	–	–	–	–	–	–
1974	194,110	17,150	211,260	91.9%	8.1%	–	–	–	–	–	–
1975	205,650	15,700	221,350	92.9%	7.1%	–	–	–	–	–	–
1976	231,550	5,970	237,520	97.5%	2.5%	–	–	–	–	–	–
1977	127,500	5,190	132,690	96.1%	3.9%	–	–	–	–	–	–
1978	98,377	5,260	103,637	94.9%	5.1%	130,000	–	–	75.7%	–	–
1979	124,680	12,430	137,110	90.9%	9.1%	198,900	35,000	–	62.7%	35.5%	–
1980	72,350	17,580	89,930	80.5%	19.5%	175,000	35,000	–	41.3%	50.2%	–
1981	114,760	24,360	139,120	82.5%	17.5%	175,000	35,000	–	65.6%	69.6%	–
1982	75,577	32,160	107,737	70.1%	29.9%	175,000	35,000	–	43.2%	91.9%	–
1983	73,151	40,780	113,931	64.2%	35.8%	175,000	45,000	–	41.8%	90.6%	–
1984	96,382	42,110	138,492	69.6%	30.4%	175,000	45,000	270,000	55.1%	93.6%	51.3%
1985	85,439	24,960	110,399	77.4%	22.6%	175,000	50,000	212,000	48.8%	49.9%	52.1%
1986	154,932	55,650	210,582	73.6%	26.4%	295,800	75,000	405,000	52.4%	74.2%	52.0%
1987	160,448	73,700	234,148	68.5%	31.5%	195,000	75,000	264,000	82.3%	98.3%	88.7%
1988	160,690	88,150	248,840	64.6%	35.4%	232,000	98,000	327,000	69.3%	89.9%	76.1%
1989	203,049	95,029	298,079	68.1%	31.9%	225,000	98,000	323,000	90.2%	97.0%	92.3%
1990	185,142	76,144	261,286	70.9%	29.1%	196,000	73,500	245,000	94.5%	103.6%	106.6%
1991	229,789	89,917	319,705	71.9%	28.1%	228,000	98,000	253,000	100.8%	91.8%	126.4%
1992	210,829	88,822	299,650	70.4%	29.6%	208,800	90,000	232,000	101.0%	98.7%	129.2%
1993	140,132	58,773	198,905	70.5%	29.5%	142,000	61,000	178,000	98.7%	96.3%	111.7%
1994	253,477	108,930	362,407	69.9%	30.1%	260,000	110,000	325,000	97.5%	99.0%	111.5%
1995	177,124	72,372	249,495	71.0%	29.0%	178,400	76,500	223,000	99.3%	94.6%	111.9%
1996	213,159	93,139	306,299	69.6%	30.4%	212,000	91,000	265,000	100.5%	102.4%	115.6%

Continued on next page ...

... Continued from previous page

Year	U.S. landings	Canada landings	Total landings	U.S. prop. of total catch	Canada prop. of total catch	U.S. catch target	Canada catch target	Total catch target	U.S. prop. of catch target removed	Canada prop. of catch target removed	Total prop. of catch target removed
1997	233,376	91,771	325,147	71.8%	28.2%	232,000	99,400	290,000	100.6%	92.3%	112.1%
1998	232,920	87,802	320,722	72.6%	27.4%	232,000	80,000	290,000	100.4%	109.8%	110.6%
1999	224,565	87,322	311,887	72.0%	28.0%	232,000	90,300	290,000	96.8%	96.7%	107.5%
2000	206,770	22,007	228,777	90.4%	9.6%	232,000	90,300	290,000	89.1%	24.4%	78.9%
2001	173,940	53,585	227,525	76.4%	23.6%	190,400	81,600	238,000	91.4%	65.7%	95.6%
2002	130,453	50,244	180,697	72.2%	27.8%	129,600	–	162,000	100.7%	–	111.5%
2003	141,945	63,217	205,162	69.2%	30.8%	148,200	–	228,000	95.8%	–	90.0%
2004	217,240	125,067	342,307	63.5%	36.5%	250,000	–	514,441	86.9%	–	66.5%
2005	260,120	103,014	363,135	71.6%	28.4%	269,069	95,128	364,197	96.7%	108.3%	99.7%
2006	266,955	94,744	361,699	73.8%	26.2%	269,545	95,297	364,842	99.0%	99.4%	99.1%
2007	217,682	73,550	291,231	74.7%	25.3%	242,591	85,767	328,358	89.7%	85.8%	88.7%
2008	248,395	74,602	322,997	76.9%	23.1%	269,545	95,297	364,842	92.2%	78.3%	88.5%
2009	121,573	57,353	178,926	67.9%	32.1%	135,939	48,061	184,000	89.4%	119.3%	97.2%
2010	170,967	57,016	227,982	75.0%	25.0%	193,935	68,565	262,500	88.2%	83.2%	86.9%
2011	231,261	56,073	287,334	80.5%	19.5%	290,903	102,848	393,751	79.5%	54.5%	73.0%
2012	160,145	47,059	207,204	77.3%	22.7%	186,036	65,773	251,809	86.1%	71.5%	82.3%
2013	233,578	52,249	285,828	81.7%	18.3%	269,745	95,367	365,112	86.6%	54.8%	78.3%
2014	264,141	35,118	299,259	88.3%	11.7%	316,206	111,794	428,000	83.5%	31.4%	69.9%
2015	154,160	39,684	193,844	79.5%	20.5%	325,072	114,928	440,000	47.4%	34.5%	44.1%
2016	262,328	69,743	332,071	79.0%	21.0%	367,553	129,947	497,500	71.4%	53.7%	66.7%
2017	353,842	86,721	440,563	80.3%	19.7%	441,433	156,067	597,500	80.2%	55.6%	73.7%
2018	317,827	95,413	413,240	76.9%	23.1%	441,433	156,067	597,500	72.0%	61.1%	69.2%
2019	316,622	95,013	411,635	76.9%	23.1%	441,433	156,067	597,500	71.7%	60.9%	68.9%
2020	286,788	92,489	379,277	75.6%	24.4%	424,810	104,480	529,290	67.5%	88.5%	71.7%
2021	269,359	57,076	326,435	82.5%	17.5%	369,400	104,480	473,880	72.9%	54.6%	68.9%
2022	291,697	31,671	323,368	90.2%	9.8%	402,646	142,354	545,000	72.4%	22.2%	59.3%
2023	240,588	23,952	264,540	90.9%	9.1%	461,750	163,250	625,000	52.1%	14.7%	42.3%
2024	166,923	3,928	170,850	97.7%	2.3%	410,034	144,966	555,000	40.7%	2.7%	30.8%

Table 4. Annual summary of U.S. and Canadian fishery sampling included in this stock assessment by fleet, 1975–2024. The majority of values are reported as number of hauls but U.S. shoreside and Canadian Shoreside fleets are reported as the number of trips. A dash (–) indicates there was no sampled catch. The number of fish with otoliths sampled per haul has varied over time but is typically small.

Year	U.S. Foreign (hauls)	U.S. Joint-venture (hauls)	U.S. Mother-ship (hauls)	U.S. Combined Mother-ship Catcher-processor (hauls)	U.S. Catcher-processor (hauls)	U.S. Shore-based (trips)	Canada Foreign (hauls)	Canada Joint-venture (hauls)	Canada Shore-side (trips)	Canada Freezer trawlers (hauls)	U.S. Shore-side (trips)
1975	13	–	–	–	–	–	–	–	–	–	–
1976	142	–	–	–	–	–	–	–	–	–	–
1977	320	–	–	–	–	–	–	–	–	–	–
1978	336	5	–	–	–	–	–	–	–	–	–
1979	99	17	–	–	–	–	–	–	–	–	–
1980	191	30	–	–	–	–	–	–	–	–	–
1981	113	41	–	–	–	–	–	–	–	–	–
1982	52	118	–	–	–	–	–	–	–	–	–
1983	–	117	–	–	–	–	–	–	–	–	–
1984	49	74	–	–	–	–	–	–	–	–	–
1985	37	19	–	–	–	–	–	–	–	–	–
1986	88	32	–	–	–	–	–	–	–	–	–
1987	22	34	–	–	–	–	–	–	–	–	–
1988	39	42	–	–	–	–	–	3	–	–	–
1989	–	77	–	–	–	–	–	3	–	–	–
1990	–	143	–	–	–	15	–	5	–	–	–
1991	–	–	–	116	–	26	–	18	–	–	–
1992	–	–	–	164	–	46	–	33	–	–	–
1993	–	–	–	108	–	36	–	25	3	–	–
1994	–	–	–	143	–	50	–	41	1	–	–
1995	–	–	–	61	–	51	–	35	3	–	–
1996	–	–	–	123	–	35	–	28	1	–	–
1997	–	–	–	127	–	65	–	27	1	–	–
1998	–	–	–	149	–	64	–	21	9	–	–
1999	–	–	–	389	–	80	–	14	26	–	–
2000	–	–	–	413	–	91	–	25	1	–	–
2001	–	–	–	429	–	82	–	28	1	–	–
2002	–	–	–	342	–	71	–	–	36	–	–

Continued on next page ...

... Continued from previous page

Year	U.S. Foreign (hauls)	U.S. Joint-venture (hauls)	U.S. Mother-ship (hauls)	U.S. Combined Mother-ship Catcher-processor (hauls)	U.S. Catcher-processor (hauls)	U.S. Shore-based (trips)	Canada Foreign (hauls)	Canada Joint-venture (hauls)	Canada Shore-side (trips)	Canada Freezer trawlers (hauls)	U.S. Shore-side (trips)
2003	–	–	–	358	–	78	–	–	21	–	–
2004	–	–	–	381	–	72	–	20	28	–	–
2005	–	–	–	499	–	58	–	11	31	14	–
2006	–	–	–	549	–	83	–	21	21	46	–
2007	–	–	–	524	–	68	–	1	7	29	–
2008	–	–	324	–	356	63	–	–	20	31	–
2009	–	–	316	–	278	65	–	–	7	19	–
2010	–	–	443	–	331	–	–	–	2	9	75
2011	–	–	481	–	506	–	–	–	1	4	81
2012	–	–	299	–	332	–	–	–	38	51	76
2013	–	–	409	–	474	–	–	–	4	61	96
2014	–	–	423	–	557	–	–	–	28	28	68
2015	–	–	203	–	431	–	–	–	6	21	84
2016	–	–	502	–	671	–	–	–	19	40	76
2017	–	–	353	–	684	–	–	–	68	76	112
2018	–	–	414	–	569	–	–	–	43	91	92
2019	–	–	307	–	566	–	–	–	33	103	129
2020	–	–	192	–	433	–	–	–	32	–	99
2021	–	–	186	–	409	–	–	–	–	2	124
2022	–	–	299	–	472	–	–	–	22	16	109
2023	–	–	127	–	391	–	–	–	12	14	76
2024	–	–	51	–	192	–	–	–	21	8	59

Table 5. Recent age-proportion data used in the assessment for the U.S. Catcher-Processor fleet. Proportions are calculated from numbers of individuals in each age group. Age 15+ is an accumulator group.

Year	Number of fish	Number of hauls	Age (% of total for each year)														
			1	2	3	4	5	6	7	8	9	10	11	12	13	14	15+
2015	1,263	431	3.49	1.66	7.55	3.45	76.45	3.20	2.16	0.33	0.77	0.52	0.00	0.12	0.12	0.00	0.15
2016	1,995	671	0.40	52.87	2.37	5.57	2.23	31.31	1.56	2.06	0.73	0.20	0.44	0.20	0.00	0.04	0.00
2017	2,026	684	1.75	0.87	50.75	2.36	4.99	3.08	28.79	3.01	2.11	1.17	0.25	0.58	0.17	0.00	0.12
2018	1,670	569	4.58	35.63	1.05	27.44	1.90	2.57	2.83	19.47	2.22	1.05	0.30	0.54	0.15	0.19	0.09
2019	1,685	566	0.00	6.45	26.06	1.43	38.29	1.60	4.00	1.54	17.34	1.20	1.10	0.28	0.14	0.25	0.32
2020	1,281	433	0.00	0.14	9.33	41.91	1.55	29.82	1.72	1.63	1.59	10.41	0.65	1.01	0.07	0.05	0.11
2021	1,206	409	3.88	0.62	2.82	13.37	36.29	1.66	22.87	1.90	1.99	1.64	10.94	1.37	0.43	0.16	0.07
2022	1,269	472	0.89	47.51	1.65	1.90	8.54	19.54	0.74	12.20	1.58	0.74	0.44	2.86	1.08	0.28	0.04
2023	1,277	391	0.69	51.27	24.03	0.78	0.93	3.56	8.87	1.21	4.97	0.59	0.35	0.50	1.91	0.27	0.06
2024	516	192	11.84	3.91	39.03	18.92	1.06	1.38	3.36	8.76	1.46	6.44	1.02	0.99	0.63	0.79	0.41

Table 6. Recent age-proportion data used in the assessment for the U.S. Mothership fleet. Proportions are calculated from numbers of individuals in each age group. Age 15+ is an accumulator group.

Year	Number of fish	Number of hauls	Age (% of total for each year)														
			1	**2**	**3**	**4**	**5**	**6**	**7**	**8**	**9**	**10**	**11**	**12**	**13**	**14**	**15+**
2015	601	203	1.81	0.65	10.41	4.77	71.42	4.00	4.13	1.07	0.63	0.83	0.29	0.00	0.00	0.00	0.00
2016	1,495	502	0.53	59.25	1.45	5.10	2.44	26.82	1.54	1.92	0.38	0.32	0.09	0.15	0.00	0.00	0.00
2017	1,054	353	7.78	0.77	51.20	2.21	3.41	1.28	27.73	1.88	1.96	0.49	0.08	0.81	0.19	0.16	0.06
2018	1,230	414	16.95	25.30	1.18	28.83	1.14	2.28	1.70	16.82	2.47	1.24	0.74	0.32	0.48	0.49	0.05
2019	903	307	0.00	14.98	20.59	0.97	36.30	1.33	4.12	1.53	16.62	1.47	1.04	0.42	0.48	0.14	0.01
2020	568	192	0.00	0.00	8.62	40.11	2.40	28.62	1.49	2.06	2.51	11.89	1.12	0.80	0.39	0.00	0.00
2021	545	186	0.00	0.43	1.78	11.57	37.92	2.18	22.34	1.27	1.98	2.77	13.83	2.40	0.67	0.21	0.67
2022	840	299	1.45	42.64	1.97	2.83	6.91	19.41	1.07	14.51	1.82	0.47	0.52	3.82	1.53	0.43	0.62
2023	448	127	2.28	39.59	33.18	1.15	1.21	5.46	7.49	0.67	5.19	0.70	0.25	0.49	2.06	0.29	0.00
2024	107	51	7.46	11.87	59.81	10.10	0.00	0.00	1.23	3.74	0.00	4.29	0.98	0.00	0.00	0.45	0.07

Table 7. Recent age-proportion data used in the assessment for the U.S. shoreside fleet. Proportions are calculated from numbers of individuals in each age group. Age 15+ is an accumulator group.

Year	Number of fish	Number of trips	Age (% of total for each year)														
			1	2	3	4	5	6	7	8	9	10	11	12	13	14	15+
2015	1,680	84	6.12	1.34	7.42	4.91	67.24	4.05	5.06	0.78	1.05	1.28	0.24	0.17	0.00	0.00	0.32
2016	1,518	76	0.11	65.44	1.41	3.25	1.55	22.03	1.60	2.70	0.72	0.29	0.31	0.26	0.14	0.10	0.08
2017	2,235	112	3.68	0.71	35.37	2.63	3.66	2.50	43.03	2.89	2.12	1.66	0.64	0.53	0.27	0.11	0.20
2018	1,834	92	7.72	27.85	1.75	31.45	1.24	2.40	2.61	19.08	2.65	1.32	0.86	0.49	0.40	0.15	0.05
2019	2,566	129	0.00	15.79	22.48	0.93	32.20	1.86	3.30	1.74	16.71	1.28	1.61	0.90	0.54	0.31	0.37
2020	1,974	99	0.00	0.02	8.34	34.50	1.35	32.07	1.24	2.29	1.57	15.88	1.06	0.88	0.43	0.06	0.32
2021	2,480	124	0.17	0.26	1.97	12.69	34.48	2.73	25.93	1.92	2.80	2.08	11.12	2.27	0.85	0.22	0.50
2022	2,180	109	0.50	15.14	1.46	2.86	11.07	31.21	2.36	18.84	2.40	1.59	1.67	7.63	2.07	0.67	0.51
2023	1,596	76	0.11	17.99	26.23	1.82	3.34	8.43	19.32	2.03	11.38	1.87	0.73	1.22	3.99	0.72	0.82
2024	1,288	59	8.21	1.99	28.57	17.95	1.91	1.98	6.76	12.91	1.59	10.24	0.98	0.95	0.76	3.81	1.41

Table 8. Recent age-proportion data used in the assessment for the Canadian Shoreside fleet. Proportions are calculated from numbers of individuals in each age group. Age 15+ is an accumulator group.

Year	Number of fish	Number of trips	Age (% of total for each year)														
			1	2	3	4	5	6	7	8	9	10	11	12	13	14	15+
2015	296	6	2.73	0.00	1.13	2.60	63.66	8.14	11.35	1.33	5.64	1.85	0.00	0.56	0.00	0.34	0.69
2016	188	19	0.00	4.66	0.81	7.51	3.91	62.24	5.83	7.35	1.54	2.10	0.00	1.22	0.91	0.27	1.65
2017	680	68	6.95	0.34	7.86	1.73	3.01	7.26	48.09	13.20	6.93	1.33	1.26	1.20	0.14	0.15	0.55
2018	466	43	0.50	5.15	1.91	22.50	1.23	4.48	5.93	35.33	12.44	4.43	2.61	1.05	0.96	1.23	0.24
2019	296	33	0.00	13.24	11.41	2.87	30.27	1.90	4.36	2.70	26.37	2.28	3.26	0.83	0.51	0.00	0.00
2020	1,438	32	0.00	0.04	9.59	19.80	1.37	30.16	2.71	3.49	2.56	24.07	2.86	2.11	0.22	0.48	0.54
2022	596	22	0.00	0.00	0.13	1.42	13.76	22.91	6.59	17.47	4.75	4.29	4.52	13.98	5.88	2.41	1.88
2023	413	12	0.00	0.31	5.16	1.37	2.64	17.33	31.55	6.31	13.18	1.35	2.87	3.12	9.43	3.12	2.26
2024	819	21	0.00	0.00	0.04	2.78	1.68	3.46	18.00	30.80	3.11	15.91	2.75	3.38	2.24	11.71	4.14

Table 9. Recent age-proportion data used in the assessment for the Canadian Freezer trawler fleet. Proportions are calculated from numbers of individuals in each age group. Age 15+ is an accumulator group.

Year	Number of fish	Number of hauls	Age (% of total for each year)														
			1	2	3	4	5	6	7	8	9	10	11	12	13	14	15+
2015	215	21	0.00	0.00	4.52	1.88	55.17	12.21	15.70	2.91	2.90	3.27	1.16	0.29	0.00	0.00	0.00
2016	352	40	0.51	4.55	0.77	2.20	9.00	64.31	6.93	6.91	2.00	0.73	0.16	0.70	0.42	0.00	0.79
2017	760	76	0.00	0.60	7.32	2.42	5.52	5.04	50.00	12.24	9.74	2.37	2.49	1.35	0.21	0.19	0.50
2018	1,225	91	0.09	4.74	0.70	17.64	2.48	3.96	5.14	45.58	9.43	5.27	2.37	1.14	0.65	0.56	0.26
2019	901	103	0.04	18.05	15.01	3.65	19.30	2.75	3.93	4.60	23.03	5.34	2.39	1.16	0.39	0.36	0.00
2021	100	2	0.00	0.00	0.00	16.89	24.00	7.11	27.55	2.82	2.82	9.26	5.55	1.18	0.00	2.82	0.00
2022	421	16	0.00	0.00	0.00	0.24	6.20	22.15	8.02	17.76	7.55	4.38	6.08	16.52	7.45	2.87	0.76
2023	369	14	0.00	0.00	0.27	0.40	3.26	15.99	21.59	5.06	19.62	6.11	3.20	7.55	13.89	1.95	1.10
2024	390	8	0.00	0.00	0.17	1.15	3.16	3.00	14.92	29.92	12.95	18.87	2.99	1.61	1.32	6.28	3.67

Table 10. Aggregated fishery age-proportion data used in the base model. Proportions are calculated from numbers of individuals in each age group where the contributions from each fleet are weighted by the catch in that fleet. Sample sizes are sum of hauls and trips from individual fleets (shown in preceding tables) as described in Section 2.1.2. Age 15+ is an accumulator group.

Year	Number of samples	Age (% of total for each year)														
		1	2	3	4	5	6	7	8	9	10	11	12	13	14	15+
1975	13	4.61	33.85	7.43	1.25	25.40	5.55	8.03	10.54	0.95	0.60	0.87	0.45	0.00	0.48	0.00
1976	142	0.09	1.34	14.47	6.74	4.10	24.58	9.77	8.90	12.10	5.43	4.30	4.08	1.07	2.36	0.69
1977	320	0.00	8.45	3.68	27.47	3.59	9.11	22.68	7.60	6.54	4.02	3.55	2.31	0.57	0.31	0.12
1978	341	0.47	1.11	6.51	6.31	26.42	6.09	8.87	21.50	9.78	4.71	4.68	2.34	0.52	0.35	0.34
1979	116	0.00	6.49	10.24	9.38	5.72	17.67	10.26	17.37	12.76	4.18	2.88	0.96	1.65	0.00	0.44
1980	221	0.15	0.54	30.09	1.85	4.49	8.16	11.23	5.01	8.94	11.08	9.46	2.63	3.79	1.52	1.07
1981	154	19.49	4.03	1.40	26.73	3.90	5.55	3.38	14.68	3.77	3.19	10.19	2.31	0.50	0.16	0.72
1982	170	0.00	32.05	3.52	0.49	27.35	1.53	3.68	3.89	11.76	3.27	3.61	7.64	0.24	0.30	0.66
1983	117	0.00	0.00	34.14	4.00	1.82	23.46	5.13	5.65	5.30	9.38	3.91	3.13	2.26	1.13	0.70
1984	123	0.00	0.00	1.39	61.90	3.62	3.85	16.78	2.85	1.51	1.24	3.34	0.92	0.59	1.44	0.56
1985	57	0.92	0.11	0.35	7.24	66.75	8.41	5.61	7.11	2.04	0.53	0.65	0.25	0.00	0.00	0.03
1986	120	0.00	15.34	5.38	0.53	0.76	43.63	6.90	8.15	8.26	2.19	2.82	1.83	3.13	0.46	0.61
1987	56	0.00	0.00	29.58	2.90	0.14	1.01	53.26	0.40	1.25	7.09	0.00	0.74	1.86	1.76	0.00
1988	84	0.00	0.65	0.07	32.28	0.98	1.45	0.66	46.05	1.35	0.84	10.48	0.79	0.05	0.06	4.28
1989	80	0.00	5.62	2.43	0.29	50.21	1.26	0.29	0.08	35.19	1.80	0.40	2.32	0.08	0.00	0.04
1990	163	0.00	5.19	20.56	1.89	0.59	31.35	0.51	0.20	0.04	31.90	0.30	0.07	6.41	0.00	0.99
1991	160	0.00	3.46	20.37	19.63	2.52	0.79	28.26	1.18	0.14	0.18	18.69	0.42	0.00	3.61	0.74
1992	243	0.46	4.24	4.30	13.05	18.59	2.27	1.04	33.93	0.77	0.08	0.34	18.05	0.41	0.04	2.43
1993	172	0.00	1.05	23.24	3.26	12.98	15.67	1.50	0.81	27.42	0.67	0.09	0.12	12.00	0.05	1.13
1994	235	0.00	0.04	2.83	21.39	1.26	12.63	18.69	1.57	0.57	29.91	0.26	0.28	0.02	9.63	0.91
1995	147	0.62	1.28	0.47	6.31	28.97	1.15	8.05	20.27	1.58	0.22	22.42	0.44	0.45	0.04	7.74
1996	186	0.00	18.28	16.24	1.51	7.74	18.14	1.00	4.91	10.98	0.58	0.35	15.72	0.01	0.11	4.44
1997	220	0.00	0.74	29.47	24.95	1.47	7.84	12.49	1.80	3.98	6.67	1.28	0.22	6.08	0.73	2.28
1998	243	0.01	4.78	20.34	20.29	26.60	2.87	5.41	9.31	0.92	1.56	3.90	0.35	0.09	2.94	0.63
1999	509	0.06	10.24	20.36	17.98	20.06	13.20	2.69	3.93	4.01	0.99	1.54	2.14	0.39	0.33	2.07
2000	530	1.00	4.22	10.94	14.29	12.88	21.06	13.12	6.55	4.65	2.51	2.07	2.31	1.29	0.72	2.41
2001	540	0.00	17.34	16.25	14.25	15.69	8.56	12.10	5.99	1.78	2.23	1.81	0.70	1.42	0.69	1.21
2002	449	0.00	0.03	50.64	14.93	9.69	5.72	4.44	6.58	3.55	0.87	0.84	1.04	0.24	0.48	0.95
2003	456	0.00	0.10	1.39	67.79	11.66	3.35	5.01	3.20	3.15	2.12	0.88	0.44	0.54	0.13	0.23
2004	501	0.00	0.02	5.34	6.13	68.29	8.12	2.18	4.13	2.51	1.27	1.07	0.35	0.27	0.16	0.17
2005	613	0.02	0.57	0.46	6.56	5.38	68.72	7.95	2.36	2.91	2.21	1.18	1.09	0.25	0.09	0.25
2006	720	0.33	2.81	10.44	1.67	8.57	4.88	59.04	5.28	1.72	2.38	1.13	1.01	0.43	0.14	0.19

Continued on next page ...

... Continued from previous page

Year	Number of samples	Age (% of total for each year)														
		1	2	3	4	5	6	7	8	9	10	11	12	13	14	15+
2007	629	0.78	11.52	3.81	15.70	1.59	6.89	3.81	43.95	5.08	1.71	2.20	1.66	0.48	0.19	0.64
2008	763	0.77	8.85	30.55	2.24	14.18	1.07	3.77	3.43	28.95	2.67	1.46	0.68	0.56	0.22	0.61
2009	664	0.79	0.62	37.35	30.09	2.75	9.07	0.70	2.00	1.30	12.50	1.49	0.36	0.61	0.17	0.19
2010	860	0.03	25.02	3.32	35.14	23.80	2.33	2.58	0.34	0.46	0.96	4.35	1.09	0.28	0.15	0.15
2011	1,075	2.68	8.70	71.57	2.60	6.06	4.27	1.00	0.81	0.28	0.33	0.07	1.32	0.14	0.08	0.11
2012	796	0.17	40.32	11.58	33.26	2.42	5.35	2.61	1.11	0.66	0.24	0.34	0.34	0.95	0.26	0.39
2013	1,044	0.03	0.54	69.93	5.93	10.54	1.18	3.54	2.04	0.97	1.45	0.28	0.31	0.53	2.25	0.48
2014	1,104	0.00	3.30	3.83	64.85	7.04	12.19	1.68	2.89	1.81	0.68	0.38	0.06	0.19	0.22	0.88
2015	745	3.62	1.10	7.07	3.85	69.56	4.95	5.55	0.94	1.46	1.21	0.24	0.17	0.04	0.03	0.21
2016	1,308	0.32	50.47	1.65	4.68	2.73	32.57	2.31	3.00	0.82	0.44	0.27	0.33	0.14	0.06	0.21
2017	1,293	3.77	0.73	38.48	2.38	4.13	3.10	36.80	4.38	3.08	1.33	0.61	0.72	0.21	0.09	0.20
2018	1,209	7.15	25.61	1.37	27.79	1.52	2.76	3.04	22.51	3.99	1.85	0.96	0.58	0.41	0.36	0.10
2019	1,138	0.01	13.12	21.21	1.61	32.59	1.84	3.78	2.12	18.61	1.90	1.65	0.69	0.40	0.25	0.22
2020	756	0.00	0.06	8.84	36.49	1.55	30.68	1.57	2.14	1.78	14.19	1.08	1.03	0.28	0.09	0.23
2021	721	1.39	0.36	1.96	13.40	33.99	2.92	24.72	1.97	2.43	3.02	10.57	1.82	0.57	0.57	0.30
2022	918	0.82	33.57	1.54	2.25	8.85	23.11	1.81	15.01	2.29	1.21	1.22	5.44	1.92	0.61	0.36
2023	620	0.68	35.74	24.65	1.15	1.89	6.17	12.94	1.64	7.90	1.31	0.63	1.11	3.28	0.53	0.37
2024	331	9.36	4.10	36.54	16.94	1.33	1.49	4.82	10.30	1.45	8.06	1.03	0.85	0.61	2.24	0.88

Table 11. Acoustic age 2+ survey age-proportion data used in the base model. Proportions are calculated from numbers of individuals in each age group. Age 15+ is an accumulator group.

Year	**Number of samples**	**Age (% of total for each year)**														
		1	**2**	**3**	**4**	**5**	**6**	**7**	**8**	**9**	**10**	**11**	**12**	**13**	**14**	**15+**
1995	69	0.00	20.48	3.26	1.06	19.33	1.03	4.03	16.37	1.44	0.72	24.86	0.24	1.67	0.21	5.32
1998	105	0.00	6.83	8.03	17.03	17.25	1.77	11.37	10.79	1.73	4.19	7.60	1.27	0.34	9.74	2.06
2001	57	0.00	50.62	10.95	15.12	7.86	3.64	3.84	2.60	1.30	1.34	0.65	0.68	0.87	0.15	0.39
2003	71	0.00	23.06	1.63	43.40	13.07	2.71	5.14	3.43	1.82	2.44	1.44	0.49	0.43	0.42	0.52
2005	47	0.00	19.07	1.23	5.10	4.78	50.67	6.99	2.50	3.99	2.45	1.71	0.74	0.48	0.14	0.16
2007	69	0.00	28.29	2.16	11.64	1.38	5.01	3.25	38.64	3.92	1.94	1.70	0.83	0.77	0.34	0.12
2009	72	0.00	0.55	29.33	40.21	2.29	8.22	1.25	1.79	1.93	8.32	3.63	1.44	0.28	0.48	0.26
2011	46	0.00	27.62	56.32	3.71	2.64	2.94	0.70	0.78	0.38	0.66	0.97	2.10	0.76	0.31	0.11
2012	94	0.00	62.12	9.78	16.70	2.26	2.92	1.94	1.01	0.50	0.23	0.27	0.66	0.98	0.51	0.12
2013	67	0.00	2.17	74.97	5.63	8.68	0.95	2.20	2.59	0.71	0.35	0.10	0.13	0.36	0.77	0.38
2015	78	0.00	7.45	9.19	4.38	58.98	4.88	7.53	1.69	1.68	1.64	0.95	0.16	0.29	0.24	0.92
2017	58	0.00	0.49	52.73	2.80	3.70	3.31	26.02	4.13	2.91	1.14	0.91	0.87	0.42	0.33	0.25
2019	75	0.00	10.72	27.23	1.51	31.31	2.50	3.18	2.68	16.12	2.28	0.96	0.36	0.38	0.47	0.28
2021	65	0.00	8.03	5.78	14.04	28.24	3.49	20.90	3.06	2.05	1.95	9.92	1.50	0.31	0.22	0.50
2023	64	0.00	50.58	24.66	1.03	1.17	2.92	8.09	0.88	5.38	0.77	0.58	0.67	2.30	0.41	0.56

Table 12. Summary of the acoustic age 2+ surveys from 1995 to 2023.

Year	Start date	End date	Vessels	Age-2+ biomass index (million t)	Sampling CV age-2+	Number of hauls with age samples
1995	1-Jul	1-Sep	Miller Freeman Ricker	1.318	0.086	69
1998	6-Jul	27-Aug	Miller Freeman Ricker	1.569	0.046	105
2001	15-Jun	18-Aug	Miller Freeman Ricker	0.862	0.102	57
2003	29-Jun	1-Sep	Ricker	2.138	0.062	71
2005	20-Jun	19-Aug	Miller Freeman	1.376	0.062	47
2007	20-Jun	21-Aug	Miller Freeman	0.943	0.074	69
2009	30-Jun	7-Sep	Miller Freeman Ricker	1.502	0.096	72
2011	26-Jun	10-Sep	Bell Shimada Ricker	0.675	0.113	46
2012	23-Jun	7-Sep	Bell Shimada Ricker F/V Forum Star	1.279	0.065	94
2013	13-Jun	11-Sep	Bell Shimada Ricker	1.929	0.062	67
2015	15-Jun	14-Sep	Bell Shimada Ricker	2.156	0.081	78
2017	22-Jun	13-Sep	Bell Shimada Nordic Pearl	1.418	0.063	58
2019	13-Jun	15-Sep	Bell Shimada Nordic Pearl	1.718	0.062	75
2021	27-Jun	24-Sep	Bell Shimada Nordic Pearl	1.525	0.122	65
2023	23-Jun	6-Sep	Bell Shimada John Franklin	0.907	0.086	64

Table 13. Summary of the acoustic survey age-2+ biomass attributed to each country.

Year	U.S. Age-2+ biomass (million t)	U.S. sampling CV age-2+	U.S. prop. of biomass	Canada Age-2+ biomass (million t)	Canada sampling CV age-2+	Canada prop. of biomass
1995	1.061	0.084	0.805	0.257	0.271	0.195
1998	0.606	0.093	0.386	0.963	0.047	0.614
2001	0.793	0.088	0.920	0.069	0.777	0.080
2003	1.678	0.063	0.785	0.459	0.174	0.215
2005	0.707	0.096	0.514	0.669	0.076	0.486
2007	0.683	0.085	0.724	0.260	0.149	0.276
2009	1.104	0.106	0.735	0.398	0.210	0.265
2011	0.602	0.104	0.893	0.072	0.607	0.107
2012	1.141	0.059	0.892	0.139	0.342	0.108
2013	1.805	0.054	0.936	0.124	0.568	0.064
2015	1.698	0.085	0.788	0.458	0.214	0.212
2017	1.028	0.073	0.725	0.390	0.126	0.275
2019	1.527	0.054	0.889	0.191	0.334	0.111
2021	1.459	0.103	0.957	0.066	1.641	0.043
2023	0.885	0.071	0.976	0.022	2.113	0.024

Table 14. Number of Pacific Hake ovaries collected for histological analysis and included in the estimates of time-varying maturity.

Year	NWFSC Trawl Survey	U.S. Acoustic Survey/ Research	U.S. At-Sea Hake Observer Program	Total
2009	244	0	0	**244**
2012	64	181	0	**245**
2013	63	186	135	**384**
2014	197	0	196	**393**
2015	216	160	131	**507**
2016	66	131	194	**391**
2017	102	57	177	**336**
2018	109	54	0	**163**
2019	46	59	0	**105**
2020	0	0	0	**0**
2021	0	68	0	**68**
2022	0	0	0	**0**
2023	0	76	0	**76**
Total	**1,107**	**972**	**833**	**2,912**

Table 15. Summary of estimated model parameters and priors in the base model. The beta prior is parameterized with a mean and standard deviation (SD). The lognormal prior is parameterized with the median and SD in log space.

Parameter	Number of parameters	Bounds (low, high)	Prior (Mean, SD) single value = fixed
Stock Dynamics			
Log (R_0)	1	(13, 17)	Uniform
Steepness (h)	1	(0.2, 1)	Beta (0.78, 0.11)
Recruitment variability (σ_r)	–	–	1.4
Log recruitment deviations: 1946–2022	77	(-6, 6)	Lognormal (0.00, σ_r)
Natural mortality (M)	1	(0.05, 0.4)	Lognormal (-1.61, 0.10)
Data Source			
Acoustic Survey			
Additional variance for survey log (SE)	1	(0.05, 1.2)	Uniform
Non-parametric age-based selectivity: ages 3–6	4	(-5, 9)	Uniform
Fishery and Survey			
Selectivity deviations (1991–2024, ages 2–6)	170	(-10, 10)	Normal (0.00, 1.40)
Data Weighting			
Dirichlet-multinomial fishery likelihood, $\log(\theta_{fishery})$	2	(-5, 20)	Normal (0.00, 1.81)
Dirichlet-multinomial survey likelihood, $\log(\theta_{survey})$	2	(-5, 20)	Normal (0.00, 1.81)

Table 16. Annual changes in the modeling framework used to assess Pacific Hake since 2011. Methods used to weight the age-composition data (Comp Method), i.e., McAllister-Ianelli (M-I) and Dirichlet-multinomial (D-M) approaches, are explained in the main text. The Markov chain Monte Carlo column gives the number of Markov chain Monte Carlo samples used to describe model results and produce statistical inference.

Year	Framework	Survey	Comp Method	Num. MCMC samples	Change
2011	SS3 3-20, TINSS	yes	M-I (0.100, 0.890)	999	Increased compatibility of SS and TINSS, except for age-composition likelihood
2012	SS3 3-23b	yes	M-I (0.120, 0.940)	999	One framework for base model; TINSS changed to CCAM
2013	SS3 3-24j	no	M-I (0.120, 0.940)	999	Developed MSE
2014	SS3 3-24s	yes	M-I (0.120, 0.940)	999	Time-varying fishery selectivity
2015	SS3 3-24u	no	M-I (0.120, 0.940)	999	No major changes
2016	SS3 3-24u	yes	M-I (0.110, 0.510)	999	Re-analyzed 1998-2015 acoustic-survey data; Removed 1995 survey data
2017	SS3 3-24u	no	M-I (0.140, 0.410)	999	Added 1995 survey data; Increased allowable selectivity variation to 0.20
2018	SS3 3-30-10-00	yes	D-M (0.450, 0.920)	2,000	Used D-M to weight age compositions; Updated maturity and fecundity; Stopped transforming selectivity parameters
2019	SS3 3-30-10-00	no	D-M (0.363, 0.919)	2,000	Change to time-varying fecundity
2020	SS3 3-30-14-08	yes	D-M (0.364, 0.912)	2,000	Normal prior for D-M parameters; remove sum to zero constraint for recruitment deviations
2021	SS3 3-30-16-03	no	D-M (0.361, 0.911)	8,250	No U-turn MCMC Sampling (adnuts)
2022	SS3 3-30-16-03	yes	D-M (0.363, 0.930)	12,005	Add relative age-1 index
2023	SS3 3-30-20-00	no	D-M (0.348, 0.930)	8,000	No major changes
2024	SS3 3-30-22-00	yes	D-M (0.348, 0.930)	8,000	Time-varying maturity
2025	SS3 3-30-23-01	no	D-M (0.342, 0.940)	8,000	Turn off estimation of late and forecast recruitment deviations; exclude relative age-1 index

Table 17. Estimated numbers-at-age at the beginning of the year from the base model (posterior medians; millions).

Year									Age											
	0	**1**	**2**	**3**	**4**	**5**	**6**	**7**	**8**	**9**	**10**	**11**	**12**	**13**	**14**	**15**	**16**	**17**	**18**	**19**	**20+**
1966	1,647	1,506	942	476	294	188	139	107	87	74	62	49	41	35	29	23	19	15	12	10	33
1967	4,893	1,311	1,195	736	363	220	138	98	75	61	52	44	35	29	25	20	16	13	11	9	41
1968	3,152	3,897	1,037	929	548	261	155	90	64	49	40	34	29	23	19	16	13	11	9	7	40
1969	731	2,505	3,101	811	709	411	194	109	64	45	35	28	24	20	16	13	12	9	8	6	40
1970	9,431	580	1,985	2,416	613	519	297	131	75	44	31	24	19	16	14	11	9	8	6	5	37
1971	845	7,470	460	1,540	1,804	446	370	196	87	50	29	21	16	13	11	9	7	6	5	4	32
1972	552	673	5,912	359	1,178	1,355	330	262	139	62	35	21	15	11	9	8	6	5	4	4	29
1973	6,188	438	535	4,641	278	902	1,030	243	193	102	46	26	15	11	8	7	6	5	4	3	28
1974	345	4,894	348	421	3,577	211	680	752	177	140	74	33	19	11	8	6	5	4	3	3	25
1975	1,888	274	3,874	272	322	2,689	157	484	535	125	100	53	24	14	8	6	4	4	3	2	22
1976	203	1,496	217	3,018	207	240	1,974	110	338	371	88	70	37	17	9	5	4	3	2	2	19
1977	6,762	161	1,185	170	2,325	157	181	1,441	80	246	271	64	51	27	12	7	4	3	2	2	16
1978	132	5,357	128	933	133	1,801	122	137	1,091	60	186	205	48	39	20	9	5	3	2	2	15
1979	1,373	105	4,239	101	728	103	1,390	92	104	827	46	141	155	37	29	15	7	4	2	2	14
1980	17,446	1,090	83	3,331	78	562	79	1,045	69	78	622	34	106	117	27	22	12	5	3	2	12
1981	265	13,826	865	66	2,605	61	435	60	797	53	59	473	26	81	89	21	17	9	4	2	12
1982	327	210	10,941	681	51	1,997	46	323	44	593	39	44	352	19	60	66	15	12	7	3	11
1983	537	260	166	8,615	530	39	1,533	35	243	34	446	29	33	264	15	45	50	12	9	5	12
1984	14,288	428	206	131	6,729	411	30	1,164	26	185	25	339	22	25	201	11	34	38	9	7	14
1985	131	11,301	339	162	103	5,204	317	23	878	20	139	19	255	17	19	151	8	26	28	7	18
1986	181	104	8,948	267	127	80	4,033	241	17	671	15	106	15	195	13	14	116	6	20	22	20
1987	6,680	143	82	7,025	207	98	61	3,004	180	13	500	11	79	11	145	10	11	86	5	15	32
1988	2,128	5,289	114	64	5,415	158	74	45	2,201	132	9	366	8	58	8	106	7	8	63	3	34
1989	113	1,686	4,186	89	50	4,121	119	54	33	1,606	96	7	268	6	42	6	77	5	6	46	29
1990	4,335	89	1,336	3,263	67	37	3,040	84	38	23	1,133	68	5	189	4	30	4	55	4	4	53
1991	1,237	3,429	71	1,045	2,509	51	28	2,200	61	27	17	820	49	3	137	3	22	3	40	3	41
1992	127	985	2,713	52	715	1,859	36	20	1,568	43	20	12	584	35	2	97	2	15	2	28	31
1993	3,181	100	780	2,120	37	504	1,370	25	14	1,088	30	14	8	405	24	2	67	2	11	1	42
1994	3,349	2,518	80	613	1,591	26	360	985	18	10	783	21	10	6	292	18	1	48	1	8	31
1995	1,245	2,654	1,995	62	473	1,127	17	229	626	11	6	496	14	6	4	185	11	1	31	1	25
1996	1,806	989	2,098	1,572	48	360	783	11	151	414	8	4	329	9	4	2	123	7	1	20	17
1997	1,082	1,432	782	1,575	1,150	34	260	493	7	95	260	5	3	207	6	3	2	77	5	0	24
1998	1,943	858	1,133	614	1,104	778	23	164	310	5	60	164	3	2	130	4	2	1	49	3	15
1999	12,740	1,538	680	876	384	753	459	14	102	193	3	37	102	2	1	81	2	1	1	30	11
2000	310	10,091	1,218	494	573	220	475	281	9	62	118	2	23	62	1	1	50	1	1	0	25
2001	1,234	246	7,983	954	362	409	149	301	178	5	39	75	1	14	39	1	0	31	1	0	16
2002	32	977	195	6,266	702	243	273	98	198	117	4	26	49	1	9	26	0	0	21	1	11
2003	1,660	26	774	154	4,836	513	172	194	69	140	83	3	18	35	1	7	18	0	0	15	8

Continued on next page ...

... Continued from previous page

Year	Age																			
	0	1	2	3	4	5	6	7	8	9	10	11	12	13	14	15	16	17	18	19	20+
2004	56	1,313	20	611	120	3,619	369	122	138	49	100	59	2	13	25	0	5	13	0	0	16
2005	2,764	44	1,040	16	453	72	2,503	245	81	91	33	66	39	1	9	16	0	3	9	0	11
2006	2,007	2,189	35	818	12	316	43	1,591	156	51	58	21	42	25	1	5	10	0	2	5	7
2007	23	1,589	1,731	25	579	7	193	26	954	93	31	35	12	25	15	0	3	6	0	1	8
2008	5,394	19	1,256	1,313	16	375	4	112	15	550	54	18	20	7	15	9	0	2	4	0	5
2009	1,297	4,273	15	959	878	10	226	2	60	8	296	29	10	11	4	8	5	0	1	2	3
2010	15,018	1,028	3,380	11	646	595	7	148	2	39	5	194	19	6	7	3	5	3	0	1	3
2011	416	11,883	814	2,570	7	353	362	5	101	1	27	4	132	13	4	5	2	3	2	0	3
2012	1,473	331	9,389	626	1,501	5	239	252	3	70	1	19	2	92	9	3	3	1	2	1	2
2013	347	1,167	262	7,235	453	1,000	3	167	177	2	49	1	13	2	65	6	2	2	1	2	2
2014	7,620	275	926	205	5,330	330	723	2	110	116	2	32	0	9	1	43	4	1	2	1	3
2015	31	6,034	218	718	147	3,902	236	494	1	75	80	1	22	0	6	1	29	3	1	1	2
2016	4,997	25	4,756	170	538	107	2,824	173	362	1	55	58	1	16	0	4	1	21	2	1	2
2017	1,318	3,955	19	3,356	124	380	73	1,960	120	252	1	38	40	1	11	0	3	0	15	1	2
2018	160	1,045	3,099	13	2,351	83	261	47	1,246	76	160	0	24	26	0	7	0	2	0	9	2
2019	186	127	793	2,247	9	1,661	60	170	30	811	50	104	0	16	17	0	5	0	1	0	8
2020	3,402	148	100	552	1,616	6	1,087	37	106	19	504	31	65	0	10	10	0	3	0	1	5
2021	7,055	2,694	117	77	413	1,048	4	683	23	66	12	317	19	41	0	6	6	0	2	0	4
2022	131	5,575	2,126	90	57	279	663	2	422	14	41	7	196	12	25	0	4	4	0	1	2
2023	879	103	4,425	1,524	68	39	186	403	1	256	9	25	4	119	7	15	0	2	2	0	2
2024	882	695	81	3,344	1,099	51	27	117	254	1	162	5	16	3	75	5	10	0	1	2	1
2025	884	698	528	59	2,531	828	37	18	77	168	1	107	3	10	2	50	3	6	0	1	2

Table 18. Estimated total biomass-at-age at the beginning of the year from the base model (posterior medians; kilotonnes).

Year	Age																				
	0	1	2	3	4	5	6	7	8	9	10	11	12	13	14	15	16	17	18	19	20+
1966	31	140	244	188	139	100	80	65	59	56	49	41	37	33	28	25	21	17	13	11	36
1967	92	122	310	290	171	117	79	60	52	46	41	37	31	27	24	22	18	15	12	9	44
1968	59	362	269	367	259	139	89	55	44	37	31	28	26	21	18	18	14	12	10	8	43
1969	14	232	803	320	335	220	111	67	44	34	27	24	22	19	16	15	13	10	8	7	44
1970	177	54	514	953	289	278	170	80	51	33	24	20	18	15	13	12	10	9	7	6	40
1971	16	693	119	607	852	239	212	120	60	37	23	17	14	12	11	10	8	7	6	5	35
1972	10	62	1,531	142	556	725	189	160	95	46	28	17	13	10	9	8	7	6	5	4	32
1973	116	41	139	1,831	131	483	590	148	132	77	36	22	14	10	8	7	6	5	4	3	30
1974	6	454	90	166	1,689	113	390	459	121	105	58	28	17	10	8	7	5	5	4	3	27
1975	25	17	764	69	117	1,250	78	285	372	95	80	46	22	13	7	6	4	4	3	3	22
1976	3	146	55	1,365	94	149	1,465	87	332	421	104	89	52	24	14	9	6	5	4	3	29
1977	155	13	346	70	1,352	87	127	1,218	76	281	341	85	74	41	19	12	7	5	4	3	28
1978	2	550	25	374	59	1,066	64	92	924	56	198	244	62	51	29	14	8	5	3	3	24
1979	25	8	1,318	33	381	57	952	56	85	827	48	173	215	52	44	27	12	7	4	3	24
1980	320	88	17	1,432	28	301	42	689	43	62	584	34	125	150	37	33	17	8	4	3	19
1981	4	1,248	193	20	1,330	24	245	33	579	35	49	464	27	97	117	31	24	13	6	3	17
1982	4	13	2,472	209	17	1,037	18	174	25	421	24	34	331	19	67	87	20	16	9	4	15
1983	7	16	28	3,015	198	15	859	14	148	21	333	19	28	258	15	56	62	15	12	6	15
1984	255	27	37	36	2,944	181	13	723	13	128	17	278	16	22	211	13	40	44	10	8	17
1985	2	1,120	67	49	37	2,874	165	11	677	12	111	15	249	14	20	197	11	34	37	9	23
1986	3	8	2,395	78	45	32	2,298	130	9	545	9	87	12	188	11	16	130	7	22	24	23
1987	119	11	16	2,626	66	36	24	1,665	99	7	385	6	63	8	133	8	9	73	4	12	27
1988	40	490	26	20	2,541	60	30	19	1,422	82	5	312	5	49	7	113	7	8	67	4	37
1989	2	148	1,009	29	17	2,046	45	22	15	1,054	58	4	227	4	35	5	66	4	5	39	24
1990	83	8	335	1,237	27	15	1,653	35	18	12	793	45	3	168	3	28	4	52	3	4	50
1991	25	328	17	404	1,150	24	12	1,282	28	14	9	610	35	2	127	2	16	2	29	2	30
1992	2	101	723	20	331	965	18	9	1,018	22	10	7	463	25	2	101	2	16	2	29	33
1993	56	8	189	735	14	225	643	11	6	653	13	6	4	280	15	1	42	1	7	1	26
1994	69	241	20	248	723	12	187	537	10	5	532	11	5	3	228	14	1	37	1	6	24
1995	24	282	552	24	239	601	9	131	394	7	4	369	8	4	2	166	10	1	28	1	22
1996	34	93	600	642	22	199	430	6	93	274	5	2	252	5	2	2	80	5	0	13	11
1997	22	134	208	696	571	18	155	291	4	65	181	3	2	165	3	2	1	51	3	0	15
1998	35	81	271	229	538	402	12	95	187	3	39	110	2	1	99	2	1	1	29	2	9
1999	220	135	175	315	169	408	248	8	65	125	2	25	72	1	1	67	2	1	1	25	9
2000	7	1,135	391	254	324	144	359	211	7	56	103	1	21	59	1	1	43	1	1	0	22
2001	31	30	2,532	474	227	265	105	245	151	5	37	70	1	14	39	1	0	31	1	0	16
2002	1	122	65	3,031	418	172	188	73	179	107	3	26	49	1	9	28	1	0	23	1	12
2003	40	3	242	70	2,522	310	116	127	52	124	71	2	18	32	0	7	18	0	0	15	8

Continued on next page ...

... Continued from previous page

Year	Age																				
	0	**1**	**2**	**3**	**4**	**5**	**6**	**7**	**8**	**9**	**10**	**11**	**12**	**13**	**14**	**15**	**16**	**17**	**18**	**19**	**20+**
2004	1	144	6	268	60	1,965	218	81	93	37	84	49	1	12	21	0	4	12	0	0	14
2005	49	4	311	7	234	40	1,418	151	58	65	25	58	34	1	8	16	0	3	8	0	10
2006	31	197	10	379	6	188	26	973	109	41	44	17	40	22	1	6	11	0	2	6	7
2007	0	115	407	10	302	4	114	16	609	66	24	26	10	23	13	0	3	6	0	1	7
2008	84	1	285	529	9	249	3	79	11	428	44	16	18	7	15	9	0	2	4	0	6
2009	21	324	3	327	418	6	157	2	46	7	236	25	9	10	4	9	5	0	1	2	3
2010	252	88	765	4	283	344	5	117	1	36	5	174	19	7	7	3	6	3	0	1	3
2011	8	969	189	868	3	171	217	3	87	1	24	3	124	13	5	5	2	4	2	0	3
2012	29	30	2,166	225	618	2	125	163	3	67	1	18	2	90	9	4	4	1	3	2	2
2013	7	121	72	2,738	210	501	2	100	137	2	52	1	15	2	70	8	3	3	1	2	3
2014	165	30	294	94	2,658	190	422	1	81	108	2	40	0	11	1	56	5	2	2	1	3
2015	1	529	54	283	66	1,791	118	250	1	49	62	1	24	0	6	1	33	3	1	1	2
2016	97	2	1,103	61	242	51	1,309	87	194	1	35	46	1	17	0	5	1	24	2	1	3
2017	32	434	6	1,352	60	220	43	1,100	77	166	0	29	38	1	14	0	4	1	19	2	3
2018	3	137	1,035	6	1,243	50	176	32	851	58	120	0	22	27	0	11	0	3	0	14	3
2019	4	12	255	1,011	5	877	34	107	20	531	34	73	0	13	16	0	6	0	2	0	9
2020	77	16	26	278	894	3	625	23	76	14	350	23	49	0	8	11	0	3	0	1	5
2021	136	320	36	32	262	690	2	439	17	54	9	244	16	33	0	6	6	0	2	0	4
2022	2	561	741	45	30	211	489	2	318	12	37	6	170	11	22	0	4	4	0	1	2
2023	22	9	1,185	776	39	22	144	302	1	201	7	22	4	101	6	14	0	2	2	0	2
2024	19	70	24	1,590	615	31	18	79	185	1	126	4	13	2	67	5	10	0	2	2	1
2025	19	71	159	28	1,417	514	25	12	56	128	0	86	3	9	2	52	3	7	0	1	2

Table 19. Estimated exploitation-fraction-at-age (catch-at-age divided by biomass-at-age at the beginning of the year) presented as a percentage for each year from the base model (posterior medians; percentage of age class removed by fishing).

Year											Age										
	0	1	2	3	4	5	6	7	8	9	10	11	12	13	14	15	16	17	18	19	20+
1966	0.00	0.85	5.09	8.13	10.15	10.61	16.12	15.13	13.49	12.32	11.76	11.02	10.26	9.93	9.48	8.46	8.46	8.46	8.46	8.46	8.46
1967	0.00	1.42	8.46	13.40	16.63	17.34	26.10	24.50	21.84	19.95	19.04	17.84	16.61	16.09	15.35	13.70	13.70	13.70	13.70	13.70	13.70
1968	0.00	0.82	4.93	7.86	9.77	10.25	15.64	14.69	13.09	11.96	11.41	10.69	9.96	9.64	9.20	8.21	8.21	8.21	8.21	8.21	8.21
1969	0.00	1.14	6.79	10.79	13.37	14.03	21.25	19.95	17.79	16.24	15.51	14.53	13.53	13.10	12.50	11.15	11.15	11.15	11.15	11.15	11.15
1970	0.00	1.33	7.98	12.68	15.65	16.39	24.73	23.21	20.69	18.90	18.04	16.90	15.74	15.24	14.55	12.98	12.98	12.98	12.98	12.98	12.98
1971	0.00	0.82	4.91	7.82	9.74	10.20	15.62	14.66	13.07	11.94	11.40	10.68	9.94	9.63	9.19	8.20	8.20	8.20	8.20	8.20	8.20
1972	0.00	0.55	3.30	5.29	6.62	6.95	10.71	10.05	8.96	8.18	7.81	7.32	6.81	6.60	6.30	5.62	5.62	5.62	5.62	5.62	5.62
1973	0.00	0.63	3.77	6.03	7.52	7.90	12.11	11.37	10.13	9.25	8.83	8.28	7.71	7.46	7.12	6.35	6.35	6.35	6.35	6.35	6.35
1974	0.00	0.79	4.69	7.48	9.37	9.82	14.93	14.01	12.49	11.41	10.89	10.20	9.50	9.20	8.78	7.83	7.83	7.83	7.83	7.83	7.83
1975	0.00	1.44	7.37	13.99	14.47	13.50	20.45	17.31	14.65	13.41	12.71	11.63	11.01	11.00	10.80	10.10	10.10	10.10	10.10	10.10	10.10
1976	0.00	0.59	3.81	5.21	7.74	6.76	9.25	8.63	6.98	6.06	5.81	5.41	4.90	4.83	4.76	4.37	4.37	4.37	4.37	4.37	4.37
1977	0.00	0.42	1.90	3.28	3.51	4.41	5.68	4.74	4.22	3.50	3.18	3.00	2.76	2.61	2.54	2.34	2.34	2.34	2.34	2.34	2.34
1978	0.00	0.31	2.65	3.22	4.33	3.91	7.20	5.63	4.48	4.10	3.56	3.18	2.97	2.85	2.66	2.41	2.41	2.41	2.41	2.41	2.41
1979	0.00	0.47	2.00	4.60	4.35	4.92	6.53	7.33	5.47	4.47	4.28	3.65	3.23	3.14	2.98	2.59	2.59	2.59	2.59	2.59	2.59
1980	0.00	0.35	2.37	2.71	4.85	3.87	6.45	5.19	5.56	4.25	3.64	3.42	2.90	2.67	2.56	2.26	2.26	2.26	2.26	2.26	2.26
1981	0.00	0.51	3.41	6.13	5.46	8.21	9.62	9.72	7.46	8.20	6.58	5.53	5.15	4.54	4.12	3.70	3.70	3.70	3.70	3.70	3.70
1982	0.00	0.62	2.79	5.02	7.08	5.30	11.73	8.36	8.07	6.36	7.32	5.76	4.80	4.66	4.05	3.44	3.44	3.44	3.44	3.44	3.44
1983	0.00	0.51	3.03	3.62	5.07	6.02	6.64	8.96	6.11	6.04	4.99	5.64	4.40	3.82	3.66	2.97	2.97	2.97	2.97	2.97	2.97
1984	0.00	0.56	3.36	5.36	5.00	5.91	10.32	6.90	8.89	6.21	6.44	5.22	5.85	4.75	4.07	3.64	3.64	3.64	3.64	3.64	3.64
1985	0.00	0.27	2.27	3.60	4.49	3.54	6.16	6.53	4.17	5.51	4.04	4.11	3.30	3.85	3.09	2.47	2.47	2.47	2.47	2.47	2.47
1986	0.00	0.58	2.79	6.24	7.73	8.10	9.37	9.91	10.04	6.57	9.10	6.54	6.60	5.52	6.35	4.76	4.76	4.76	4.76	4.76	4.76
1987	0.00	0.72	4.78	6.11	10.63	11.11	17.12	12.01	12.13	12.59	8.64	11.75	8.37	8.79	7.26	7.80	7.80	7.80	7.80	7.80	7.80
1988	0.00	0.64	4.29	7.65	7.66	11.25	17.25	16.17	10.83	11.22	12.21	8.22	11.08	8.22	8.52	6.57	6.57	6.57	6.57	6.57	6.57
1989	0.00	0.97	5.79	10.29	14.29	12.08	25.87	24.16	21.63	14.86	16.13	17.23	11.50	16.14	11.81	11.44	11.44	11.44	11.44	11.44	11.44
1990	0.00	0.76	4.34	7.01	9.76	11.47	14.17	18.67	16.66	15.29	11.01	11.73	12.42	8.63	11.95	8.17	8.17	8.17	8.17	8.17	8.17
1991	0.00	0.89	11.98	31.02	12.56	13.44	20.32	15.32	19.28	17.64	16.97	11.99	12.67	13.96	9.58	12.38	12.38	12.38	12.38	12.38	12.38
1992	0.00	0.62	3.98	15.50	20.86	11.92	22.42	23.58	16.98	21.91	21.01	19.84	13.90	15.29	16.63	10.65	10.65	10.65	10.65	10.65	10.65
1993	0.00	0.44	2.63	13.79	18.02	18.08	17.30	18.25	18.34	13.54	18.31	17.24	16.13	11.77	12.77	12.97	12.97	12.97	12.97	12.97	12.97
1994	0.00	0.32	2.29	4.66	20.50	20.45	34.19	32.48	32.72	33.71	26.09	34.64	32.31	31.49	22.66	22.97	22.97	22.97	22.97	22.97	22.97
1995	0.00	0.33	1.70	3.74	6.53	20.23	28.05	25.53	23.17	23.93	25.84	19.63	25.83	25.10	24.13	16.22	16.22	16.22	16.22	16.22	16.22
1996	0.00	1.53	15.53	16.43	14.00	11.98	33.21	34.00	29.56	27.51	29.79	31.57	23.77	32.57	31.22	28.04	28.04	28.04	28.04	28.04	28.04
1997	0.00	0.40	2.81	23.24	25.85	18.40	30.72	30.88	30.19	26.92	26.25	27.90	29.31	22.98	31.07	27.81	27.81	27.81	27.81	27.81	27.81
1998	0.00	0.93	8.72	49.36	24.55	43.82	37.11	32.72	31.41	31.50	29.43	28.18	29.68	32.47	25.12	31.72	31.72	31.72	31.72	31.72	31.72
1999	0.00	1.26	27.45	42.85	56.03	33.05	37.76	38.06	32.05	31.55	33.16	30.42	28.86	31.66	34.17	24.69	24.69	24.69	24.69	24.69	24.69
2000	0.00	0.26	3.08	13.27	15.40	19.30	23.71	23.82	22.94	19.81	20.44	21.08	19.17	18.94	20.50	20.66	20.66	20.66	20.66	20.66	20.66
2001	0.00	0.33	2.24	12.89	21.06	21.84	21.64	18.68	17.93	17.70	16.02	16.23	16.59	15.71	15.32	15.48	15.48	15.48	15.48	15.48	15.48
2002	0.00	0.14	1.02	4.64	11.62	13.23	13.44	12.38	10.21	10.05	10.40	9.24	9.28	9.88	9.23	8.40	8.40	8.40	8.40	8.40	8.40
2003	0.00	0.09	0.61	2.51	9.28	13.59	13.60	13.99	12.32	10.42	10.74	10.91	9.61	10.05	10.55	9.21	9.21	9.21	9.21	9.21	9.21
2004	0.00	0.47	4.20	12.83	39.13	20.80	24.15	21.61	21.24	19.16	16.99	17.20	17.31	15.88	16.38	16.07	16.07	16.07	16.07	16.07	16.07
2005	0.00	0.26	1.62	6.23	20.57	32.14	31.08	28.48	24.35	24.53	23.21	20.19	20.26	21.24	19.22	18.51	18.51	18.51	18.51	18.51	18.51
2006	0.00	1.35	15.37	20.25	25.29	34.13	36.00	35.62	31.18	27.33	28.86	26.80	23.11	24.15	24.98	21.11	21.11	21.11	21.11	21.11	21.11

Continued on next page ...

... Continued from previous page

Year	Age																				
	0	1	2	3	4	5	6	7	8	9	10	11	12	13	14	15	16	17	18	19	20+
2007	0.00	1.37	15.94	30.27	30.69	26.09	40.93	40.19	37.99	34.10	31.32	32.47	29.88	26.84	27.67	26.73	26.73	26.73	26.73	26.73	26.73
2008	0.00	2.48	13.99	34.22	22.30	32.13	42.27	40.51	38.00	36.83	34.65	31.24	32.10	30.77	27.26	26.25	26.25	26.25	26.25	26.25	26.25
2009	0.00	0.88	8.89	38.68	27.11	15.37	22.13	21.61	19.78	19.03	19.33	17.85	15.95	17.07	16.14	13.36	13.36	13.36	13.36	13.36	13.36
2010	0.00	0.66	15.58	28.86	63.67	35.64	17.89	15.72	14.67	13.77	13.88	13.84	12.67	11.79	12.45	10.99	10.99	10.99	10.99	10.99	10.99
2011	0.00	1.97	10.55	69.94	33.12	25.92	17.70	14.69	12.33	11.79	11.60	11.48	11.35	10.82	9.93	9.79	9.79	9.79	9.79	9.79	9.79
2012	0.00	1.31	10.15	21.52	34.22	19.11	19.13	15.46	12.25	10.55	10.57	10.21	10.02	10.31	9.70	8.31	8.31	8.31	8.31	8.31	8.31
2013	0.00	0.32	2.71	16.34	15.05	15.77	27.38	24.78	19.12	15.54	14.02	13.80	13.21	13.49	13.70	12.03	12.03	12.03	12.03	12.03	12.03
2014	0.00	0.68	5.92	17.74	13.51	14.73	20.76	19.16	16.56	13.11	11.16	9.89	9.64	9.61	9.69	9.19	9.19	9.19	9.19	9.19	9.19
2015	0.00	2.63	5.67	11.60	13.70	16.65	13.21	13.03	11.49	10.19	8.45	7.06	6.20	6.30	6.20	5.83	5.83	5.83	5.83	5.83	5.83
2016	0.00	7.20	42.64	18.14	21.23	22.13	23.59	21.70	20.45	18.48	17.17	13.98	11.59	10.59	10.61	9.75	9.75	9.75	9.75	9.75	9.75
2017	0.00	7.84	29.21	25.27	24.97	19.83	30.28	31.39	27.57	26.64	25.24	23.02	18.58	16.03	14.46	13.53	13.53	13.53	13.53	13.53	13.53
2018	0.00	26.79	21.92	17.66	17.89	11.33	23.52	23.37	23.14	20.84	21.11	19.63	17.74	14.91	12.70	10.69	10.69	10.69	10.69	10.69	10.69
2019	0.00	3.33	32.91	18.35	21.47	29.42	33.78	30.32	28.78	29.21	27.58	27.42	25.28	23.79	19.73	15.69	15.69	15.69	15.69	15.69	15.69
2020	0.00	0.44	3.29	9.56	28.99	20.29	32.04	29.85	25.59	24.90	26.50	24.56	24.20	23.23	21.58	16.71	16.71	16.71	16.71	16.71	16.71
2021	0.00	1.62	5.71	12.24	20.27	27.44	29.34	30.27	26.94	23.68	24.16	25.24	23.18	23.79	22.53	19.54	19.54	19.54	19.54	19.54	19.54
2022	0.00	0.36	24.13	7.39	17.18	18.12	28.31	28.07	27.67	25.24	23.26	23.29	24.11	23.07	23.35	20.65	20.65	20.65	20.66	20.66	20.66
2023	0.00	2.03	15.43	15.66	7.10	12.90	23.59	24.23	22.95	23.19	22.18	20.06	19.91	21.47	20.26	19.15	19.15	19.15	19.15	19.15	19.15
2024	0.00	34.94	16.85	8.08	7.49	7.31	22.12	21.65	20.06	19.15	18.74	18.22	17.71	17.59	16.36	13.88	13.88	13.88	13.88	13.88	13.88

Table 20. Estimated catch-at-age in numbers for each year from the base model (posterior medians; thousands).

Year	Age																				
	0	1	2	3	4	5	6	7	8	9	10	11	12	13	14	15	16	17	18	19	20+
1966	0	1,112	12,120	15,081	14,077	10,645	12,943	9,986	7,979	6,890	5,729	4,595	3,810	3,305	2,656	2,175	1,741	1,418	1,110	909	3,061
1967	0	1,589	25,220	38,357	28,123	20,247	20,714	14,623	11,259	8,886	7,700	6,403	5,222	4,318	3,689	2,993	2,416	1,979	1,603	1,254	6,010
1968	0	2,833	12,935	28,206	25,134	14,345	13,886	8,022	5,703	4,412	3,496	3,029	2,509	2,042	1,690	1,446	1,170	940	773	628	3,536
1969	0	2,535	55,027	33,851	44,509	30,591	23,456	13,161	7,646	5,458	4,193	3,377	2,881	2,407	1,953	1,611	1,372	1,100	907	738	4,800
1970	0	678	40,677	121,702	44,148	45,174	41,843	18,328	10,357	6,017	4,298	3,295	2,667	2,273	1,896	1,527	1,267	1,083	875	712	5,131
1971	0	5,721	5,719	47,780	84,289	23,694	32,935	17,455	7,632	4,343	2,522	1,800	1,385	1,111	957	796	642	527	453	366	2,807
1972	0	333	50,771	7,368	37,292	51,812	19,718	16,064	8,479	3,719	2,103	1,229	879	672	543	463	384	315	255	219	1,765
1973	0	244	5,169	110,633	9,761	38,390	72,670	16,164	13,278	7,096	3,075	1,754	1,032	728	560	457	386	323	262	214	1,869
1974	0	3,593	4,216	12,414	158,406	10,888	58,406	65,312	14,701	11,964	6,373	2,771	1,581	927	657	503	410	347	293	236	2,108
1975	0	234	56,478	9,689	16,914	169,175	15,801	49,623	55,757	12,460	10,208	5,420	2,357	1,336	793	557	428	349	296	248	2,186
1976	0	862	2,121	71,432	7,302	10,047	136,050	7,420	23,387	26,390	5,871	4,808	2,538	1,121	633	372	265	203	164	139	1,262
1977	0	52	6,610	2,334	47,667	3,871	7,269	58,051	3,171	9,953	11,242	2,522	2,042	1,084	478	270	159	113	86	70	648
1978	0	1,713	672	12,069	2,559	41,844	4,608	5,216	41,790	2,283	7,169	8,093	1,812	1,475	779	343	194	114	81	62	564
1979	0	39	26,424	1,524	16,685	2,792	62,115	4,115	4,636	37,086	2,030	6,365	7,161	1,611	1,314	693	306	172	101	72	603
1980	0	310	392	38,806	1,367	11,702	2,731	35,850	2,370	2,677	21,406	1,168	3,670	4,133	927	757	400	176	99	58	423
1981	0	6,411	6,620	1,219	72,846	2,015	23,660	3,297	43,393	2,866	3,219	25,844	1,404	4,432	4,978	1,127	918	482	213	119	633
1982	0	78	69,741	10,523	1,169	55,183	2,070	14,601	2,037	26,801	1,773	1,996	15,985	873	2,737	3,073	695	567	298	132	520
1983	0	79	859	109,806	10,112	887	57,406	1,289	9,053	1,265	16,575	1,097	1,226	9,887	543	1,696	1,897	429	348	184	446
1984	0	147	1,221	1,900	148,014	10,744	1,284	50,028	1,121	7,880	1,104	14,457	955	1,061	8,582	472	1,467	1,647	376	304	613
1985	0	3,030	1,490	1,766	1,671	102,132	10,215	729	28,328	635	4,458	620	8,174	539	600	4,860	268	833	930	212	563
1986	0	45	66,801	4,822	3,466	2,571	215,306	12,891	922	35,689	801	5,632	781	10,334	681	756	6,139	339	1,048	1,168	1,079
1987	0	78	769	161,100	6,977	3,952	4,009	200,256	12,025	858	33,185	747	5,238	726	9,618	632	703	5,721	314	975	2,104
1988	0	3,154	1,113	1,547	195,387	6,635	5,132	3,097	154,326	9,227	658	25,549	573	4,029	562	7,387	484	540	4,387	241	2,396
1989	0	1,419	58,345	3,005	2,497	247,958	11,425	5,234	3,141	156,602	9,392	672	25,984	584	4,098	567	7,503	494	549	4,464	2,769
1990	0	57	14,610	86,672	2,692	1,747	234,088	6,357	2,935	1,750	87,351	5,239	374	14,484	325	2,283	316	4,198	275	306	4,039
1991	0	2,987	2,001	125,062	145,742	3,050	2,473	197,013	5,338	2,445	1,469	73,623	4,377	312	12,172	273	1,914	265	3,523	230	3,679
1992	0	620	29,060	2,866	69,925	115,613	3,971	2,185	173,576	4,706	2,166	1,287	64,566	3,848	275	10,707	240	1,685	234	3,106	3,451
1993	0	33	4,987	103,196	2,497	41,421	110,892	2,017	1,117	88,673	2,406	1,099	661	33,096	1,974	140	5,469	122	860	118	3,349
1994	0	776	427	11,477	149,995	2,420	63,640	174,050	3,184	1,750	138,808	3,761	1,720	1,035	51,716	3,085	220	8,568	192	1,354	5,471
1995	0	948	9,402	880	15,568	122,292	2,499	33,194	91,190	1,653	912	72,623	1,959	901	543	27,064	1,613	115	4,485	100	3,586
1996	0	1,445	94,511	106,393	2,997	23,614	142,608	2,082	27,418	75,182	1,368	759	59,979	1,623	747	446	22,334	1,334	96	3,701	3,068
1997	0	544	5,893	163,558	148,269	3,118	47,576	89,830	1,302	17,292	47,436	858	472	37,771	1,019	470	283	14,098	842	60	4,274
1998	0	757	23,915	112,880	133,123	175,694	4,239	30,915	58,831	846	11,296	31,021	564	307	24,771	668	305	184	9,213	548	2,848
1999	0	1,725	48,439	136,336	95,539	135,766	93,319	2,847	20,664	39,128	564	7,546	20,633	379	206	16,496	447	204	123	6,134	2,272
2000	0	2,975	12,272	34,121	50,086	27,714	85,075	49,979	1,510	11,042	20,933	305	4,045	11,073	201	111	8,827	239	110	66	4,521
2001	0	95	57,261	61,735	47,897	58,262	22,427	45,788	26,928	819	5,951	11,309	163	2,172	5,968	109	59	4,758	128	59	2,481
2002	0	177	646	141,741	48,897	22,998	25,076	8,935	18,316	10,717	327	2,372	4,527	66	870	2,379	43	24	1,903	52	1,014
2003	0	3	1,495	1,732	234,918	42,298	15,607	17,632	6,243	12,864	7,534	226	1,665	3,173	46	609	1,673	30	17	1,338	753
2004	0	691	243	35,024	23,915	410,803	52,416	17,148	19,530	6,938	14,168	8,334	253	1,826	3,509	51	672	1,848	33	18	2,311
2005	0	11	5,133	404	48,362	12,866	441,084	42,886	14,138	15,927	5,682	11,564	6,819	206	1,506	2,857	42	548	1,511	28	1,914
2006	0	2,700	1,469	77,474	1,571	64,193	9,366	346,843	33,669	11,098	12,517	4,472	9,112	5,362	162	1,184	2,250	33	430	1,189	1,529
2007	0	1,588	65,184	3,151	93,588	1,049	46,548	6,272	231,820	22,528	7,433	8,357	2,981	6,087	3,584	109	791	1,503	22	288	1,819
2008	0	36	40,663	181,254	1,970	80,541	1,279	31,723	4,247	158,200	15,330	5,071	5,705	2,028	4,139	2,443	74	540	1,025	15	1,444
2009	0	2,902	282	126,986	113,985	945	34,732	369	9,152	1,227	45,704	4,430	1,455	1,647	588	1,195	702	21	156	296	422
2010	0	591	120,350	1,162	181,410	123,122	835	18,418	194	4,874	647	24,415	2,343	771	869	310	634	372	11	82	382
2011	0	19,491	20,154	607,200	1,009	44,674	38,420	491	10,677	113	2,818	373	14,107	1,360	446	505	179	370	217	7	271
2012	0	389	220,957	49,398	212,326	413	23,974	25,300	325	7,057	74	1,864	247	9,312	903	295	333	119	244	143	184
2013	0	393	1,950	448,022	32,018	79,621	451	24,803	26,297	335	7,336	77	1,926	255	9,668	935	304	346	123	252	341
2014	0	199	17,708	16,787	359,706	28,282	87,467	244	13,256	13,997	181	3,897	41	1,030	137	5,137	495	163	185	66	317
2015	0	14,208	3,044	33,163	9,130	298,584	15,464	32,737	91	4,963	5,239	67	1,457	15	386	51	1,928	187	61	69	144
2016	0	163	472,307	11,015	51,664	11,551	308,734	18,804	39,425	109	5,970	6,324	81	1,763	19	464	62	2,318	225	74	258
2017	0	34,715	1,618	343,374	15,265	43,982	12,825	345,358	21,062	44,116	122	6,675	7,085	91	1,970	21	521	69	2,598	252	373
2018	0	37,611	228,394	1,109	223,568	5,628	41,175	7,269	196,951	12,020	25,159	69	3,809	4,036	52	1,124	12	297	39	1,483	358

Continued on next page ...

... Continued from previous page

Year	Age																				
	0	1	2	3	4	5	6	7	8	9	10	11	12	13	14	15	16	17	18	19	20+
2019	0	385	84,769	186,702	958	258,924	11,281	32,454	5,738	155,552	9,441	19,846	55	3,002	3,186	41	885	9	234	31	1,455
2020	0	68	836	27,796	260,872	683	199,613	6,744	19,309	3,420	92,844	5,659	11,855	33	1,789	1,899	24	529	6	139	887
2021	0	5,523	2,101	3,989	53,990	190,617	699	132,543	4,473	12,829	2,280	61,659	3,748	7,870	22	1,188	1,261	16	351	4	682
2022	0	2,084	179,492	3,373	5,363	39,187	138,120	463	87,955	2,965	8,510	1,508	40,836	2,487	5,199	14	788	837	11	233	455
2023	0	195	182,844	123,014	2,775	2,887	33,822	73,418	245	46,715	1,572	4,514	796	21,698	1,320	2,766	8	419	444	6	367
2024	0	25,065	4,649	128,892	46,800	2,227	4,131	17,145	37,193	125	23,698	794	2,294	404	11,010	666	1,404	4	213	224	189

Table 21. Estimated catch-at-age in total biomass for each year from the base model (posterior medians; tonnes).

Year	Age																				
	0	1	2	3	4	5	6	7	8	9	10	11	12	13	14	15	16	17	18	19	20+
1966	0	67	2,392	3,808	5,132	4,949	6,446	5,874	5,548	5,232	4,592	4,024	3,525	3,060	2,505	2,194	1,756	1,431	1,120	917	3,088
1967	0	96	4,977	9,685	10,253	9,412	10,316	8,602	7,828	6,747	6,172	5,607	4,831	3,998	3,479	3,019	2,437	1,996	1,617	1,265	6,063
1968	0	172	2,553	7,122	9,164	6,669	6,916	4,719	3,965	3,350	2,802	2,653	2,322	1,891	1,594	1,459	1,180	948	780	634	3,568
1969	0	154	10,860	8,548	16,228	14,221	11,682	7,742	5,316	4,145	3,361	2,957	2,665	2,229	1,842	1,625	1,385	1,109	915	745	4,842
1970	0	41	8,028	30,731	16,096	21,000	20,839	10,781	7,201	4,569	3,445	2,885	2,467	2,104	1,789	1,540	1,278	1,093	883	719	5,176
1971	0	347	1,129	12,065	30,731	11,015	16,403	10,267	5,306	3,298	2,022	1,576	1,282	1,028	903	803	648	532	457	369	2,832
1972	0	20	10,020	1,860	13,596	24,086	9,820	9,449	5,895	2,824	1,686	1,076	814	623	512	467	387	317	257	221	1,781
1973	0	15	1,020	27,936	3,559	17,847	36,192	9,508	9,232	5,388	2,465	1,536	955	674	528	461	390	326	264	215	1,885
1974	0	218	832	3,135	57,754	5,062	29,088	38,419	10,221	9,084	5,108	2,427	1,463	859	619	508	414	350	295	239	2,126
1975	0	14	11,146	2,446	6,167	78,645	7,869	29,190	38,767	9,461	8,182	4,747	2,180	1,237	748	562	432	352	298	251	2,205
1976	0	84	538	32,322	3,324	6,225	100,997	5,904	23,009	29,933	6,937	6,110	3,556	1,594	912	585	417	320	257	219	1,984
1977	0	4	1,928	967	27,707	2,134	5,124	49,058	3,007	11,381	14,139	3,367	2,958	1,661	753	462	272	194	148	120	1,110
1978	0	176	134	4,834	1,145	24,763	2,430	3,520	35,388	2,116	7,644	9,669	2,319	1,966	1,114	540	305	180	128	98	888
1979	0	3	8,217	504	8,730	1,538	42,528	2,512	3,791	37,117	2,121	7,795	9,916	2,293	1,975	1,197	528	297	175	124	1,041
1980	0	25	78	16,679	491	6,273	1,448	23,643	1,459	2,153	20,100	1,167	4,335	5,299	1,239	1,144	605	266	149	88	639
1981	0	579	1,479	369	37,197	811	13,345	1,841	31,538	1,896	2,655	25,353	1,479	5,299	6,549	1,655	1,348	707	312	175	929
1982	0	5	15,758	3,226	382	28,667	797	7,877	1,139	19,024	1,093	1,562	15,019	845	3,050	4,035	912	744	391	173	682
1983	0	5	147	38,432	3,776	332	32,173	536	5,519	779	12,370	724	1,037	9,640	553	2,129	2,381	538	437	230	560
1984	0	9	217	517	64,765	4,727	533	31,063	540	5,434	734	11,861	700	956	9,033	556	1,727	1,939	442	358	722
1985	0	300	293	534	608	56,405	5,331	359	21,850	371	3,553	486	7,968	450	625	6,333	349	1,086	1,212	276	734
1986	0	3	17,877	1,406	1,221	1,028	122,653	6,943	491	29,007	470	4,598	632	9,996	573	848	6,888	380	1,176	1,311	1,211
1987	0	6	151	60,214	2,234	1,441	1,559	111,031	6,599	454	25,570	423	4,167	549	8,824	540	600	4,882	268	832	1,796
1988	0	292	256	485	91,700	2,514	2,081	1,340	99,670	5,753	377	21,737	362	3,429	461	7,868	516	575	4,673	256	2,552
1989	0	124	14,069	986	879	123,142	4,304	2,111	1,415	102,736	5,675	380	22,023	353	3,381	483	6,393	421	468	3,803	2,359
1990	0	5	3,667	32,854	1,092	717	127,288	2,624	1,357	882	61,151	3,441	232	12,928	210	2,153	298	3,959	260	288	3,809
1991	0	286	490	48,275	66,820	1,410	1,086	114,824	2,472	1,238	773	54,818	3,085	200	11,349	197	1,380	191	2,540	166	2,653
1992	0	64	7,749	1,071	32,405	59,983	1,952	1,021	112,671	2,368	1,137	715	51,214	2,774	183	11,081	248	1,744	243	3,215	3,572
1993	0	3	1,210	35,751	954	18,485	52,062	898	495	53,209	1,067	518	333	22,849	1,255	88	3,425	76	538	74	2,097
1994	0	74	106	4,644	68,134	1,142	32,982	94,945	1,724	920	94,269	1,924	943	582	40,428	2,379	170	6,607	148	1,044	4,219
1995	0	101	2,600	347	7,846	65,219	1,301	18,989	57,480	1,008	515	54,022	1,108	524	329	24,365	1,452	104	4,038	90	3,228
1996	0	136	27,033	43,464	1,371	13,030	78,241	1,116	16,901	49,805	837	438	45,986	908	436	290	14,515	867	62	2,405	1,994
1997	0	51	1,567	72,274	73,586	1,633	28,247	53,060	786	11,716	32,954	561	293	29,972	598	308	185	9,244	552	39	2,802
1998	0	71	5,724	42,076	64,859	90,619	2,168	17,934	35,543	510	7,284	20,894	361	180	18,716	400	182	110	5,512	328	1,704
1999	0	152	12,475	48,973	42,028	73,579	50,309	1,523	13,124	25,242	346	5,050	14,554	244	123	13,600	368	168	101	5,057	1,873
2000	0	335	3,941	17,574	28,294	18,072	64,222	37,552	1,178	9,979	18,332	259	3,778	10,464	175	96	7,646	207	95	57	3,915
2001	0	11	18,164	30,664	30,006	37,734	15,755	37,257	22,830	703	5,646	10,593	150	2,102	5,924	107	58	4,671	126	58	2,436
2002	0	22	215	68,567	29,126	16,285	17,250	6,670	16,581	9,859	291	2,374	4,512	61	871	2,619	48	26	2,094	57	1,116
2003	0	0	468	792	122,529	25,605	10,554	11,590	4,662	11,360	6,450	190	1,594	2,905	40	609	1,671	30	17	1,337	752
2004	0	76	71	15,390	12,077	222,988	31,029	11,346	13,148	5,175	11,924	6,927	209	1,644	3,063	45	598	1,645	30	16	2,057
2005	0	1	1,536	178	25,033	7,214	249,798	26,503	10,222	11,429	4,310	10,082	5,925	171	1,379	2,716	40	521	1,437	26	1,820
2006	0	243	417	35,909	841	38,150	5,666	212,043	23,512	8,845	9,444	3,633	8,587	4,835	141	1,221	2,322	34	444	1,227	1,577
2007	0	115	15,321	1,281	48,851	596	27,593	3,787	148,064	16,030	5,759	6,244	2,420	5,504	3,143	99	718	1,364	20	262	1,652
2008	0	3	9,218	72,976	1,079	53,377	868	22,448	3,204	123,150	12,684	4,653	5,096	1,889	4,353	2,668	81	590	1,120	16	1,577
2009	0	220	61	43,322	54,311	577	24,127	262	7,110	991	36,345	3,815	1,402	1,483	559	1,375	808	24	179	341	485
2010	0	50	27,249	409	79,629	71,144	581	14,588	164	4,408	581	21,967	2,304	815	870	352	718	421	13	93	432
2011	0	1,590	4,677	204,985	417	21,672	23,055	355	9,198	102	2,579	345	13,205	1,335	477	548	194	401	235	7	294
2012	0	36	50,976	17,781	87,435	196	12,565	16,411	266	6,710	70	1,830	247	9,058	934	356	402	143	294	173	222
2013	0	41	533	169,524	14,865	39,858	244	14,857	20,409	319	7,766	83	2,164	281	10,475	1,153	375	426	152	311	420
2014	0	22	5,616	7,689	179,367	16,310	51,107	154	9,708	12,952	197	4,781	52	1,299	172	6,782	654	216	244	87	419
2015	0	1,246	750	13,063	4,084	137,059	7,714	16,555	52	3,211	4,087	63	1,549	16	411	58	2,180	211	69	78	163
2016	0	15	109,513	3,934	23,198	5,552	143,082	9,475	21,083	64	3,801	4,946	77	1,820	19	521	69	2,600	252	83	289
2017	0	3,809	468	138,283	7,446	25,423	7,457	193,724	13,448	29,154	85	5,104	6,715	100	2,399	27	677	90	3,380	328	486
2018	0	4,933	76,306	536	118,232	3,398	27,682	4,919	134,582	9,118	18,846	56	3,394	4,279	64	1,661	17	438	58	2,192	529

Continued on next page ...

... *Continued from previous page*

Year	Age																				
	0	1	2	3	4	5	6	7	8	9	10	11	12	13	14	15	16	17	18	19	20+
2019	0	35	27,289	83,955	490	136,603	6,385	20,465	3,812	101,792	6,544	13,837	42	2,412	3,087	50	1,078	11	285	38	1,773
2020	0	7	217	14,005	144,379	406	114,799	4,163	13,902	2,530	64,547	4,245	9,027	26	1,527	2,094	27	583	6	154	978
2021	0	657	652	1,658	34,317	125,444	464	85,218	3,232	10,543	1,837	47,555	3,147	6,440	19	1,183	1,256	16	350	4	680
2022	0	210	62,559	1,682	2,818	29,679	101,772	344	66,318	2,450	7,632	1,351	35,329	2,249	4,645	15	796	845	11	236	460
2023	0	17	48,977	62,623	1,590	1,643	26,058	55,062	194	36,604	1,288	4,089	727	18,368	1,184	2,624	7	398	422	5	348
2024	0	2,531	1,402	61,277	26,201	1,383	2,736	11,604	27,171	96	18,532	638	1,897	337	9,860	702	1,482	4	224	237	200

Table 22. Calculations showing changes in biomass at each age due to natural mortality and fishing for recent strong cohorts. Start Biomass is the biomass at the beginning of the year, Catch Weight is the catch for the cohort for the year, Natural Mortality is the biomass attributed to natural mortality, and Surviving Biomass is what survives to the end of the year. Surviving Biomass does not equal the Start Biomass in the following year because the empirical weights-at-age change between years. Estimated quantities are posterior medians.

Age	Start Biomass (kt)	Catch Weight (kt)	Natural Mortality (kt)	Surviving Biomass (kt)
2021 cohort				
0	135.5	0.0	28.4	107.1
1	560.7	0.2	115.5	445.0
2	1,185.2	49.0	240.5	895.6
3	1,589.6			
2020 cohort				
0	77.4	0.0	16.1	61.3
1	320.3	0.7	66.9	252.8
2	741.1	62.6	147.3	531.3
3	776.0	62.6	154.0	559.3
4	615.2			
2016 cohort				
0	96.9	0.0	20.2	76.7
1	434.0	3.8	90.1	340.0
2	1,035.5	76.3	208.3	750.8
3	1,010.6	84.0	199.9	726.7
4	894.4	144.4	169.8	580.2
5	689.9	125.4	128.0	436.5
6	488.7	101.8	90.2	296.8
7	302.1	55.1	56.8	190.2
8	185.3			
2014 cohort				
0	165.2	0.0	34.4	130.8
1	529.3	1.2	110.9	417.1
2	1,102.7	109.5	215.0	778.2
3	1,351.6	138.3	266.6	946.8
4	1,243.3	118.2	246.4	878.6
5	876.5	136.6	166.6	573.3
6	625.0	114.8	117.4	392.7
7	439.1	85.2	82.6	271.2
8	318.1	66.3	58.8	193.0
9	200.6	36.6	37.4	126.6
10	126.3			
2010 cohort				
0	252.2	0.0	52.6	199.6
1	969.1	1.6	201.8	765.7
2	2,166.0	51.0	445.9	1,669.1
3	2,737.6	169.5	551.3	2,016.7
4	2,657.7	179.4	532.5	1,945.9
5	1,791.3	137.1	357.9	1,296.3
6	1,308.8	143.1	257.3	908.5
7	1,099.6	193.7	207.0	698.9
8	851.4	134.6	162.6	554.2
9	530.7	101.8	99.2	329.7
10	350.3	64.5	65.6	220.1
11	244.2	47.6	45.3	151.3
12	169.7	35.3	31.4	103.0

Continued on next page ...

... Continued from previous page

Age	Start Biomass (kt)	Catch Weight (kt)	Natural Mortality (kt)	Surviving Biomass (kt)
13	100.8	18.4	18.9	63.6
14	67.2			
1999 cohort				
0	220.0	0.0	45.7	174.2
1	1,134.8	0.3	236.7	897.8
2	2,532.3	18.2	526.5	1,987.6
3	3,031.1	68.6	623.4	2,339.2
4	2,522.1	122.5	511.8	1,887.8
5	1,964.7	223.0	383.0	1,358.7
6	1,417.5	249.8	266.7	901.1
7	972.7	212.0	177.5	583.2
8	609.2	148.1	109.8	351.4
9	428.3	123.1	74.5	230.6
10	235.6	36.3	45.1	154.2
11	174.4	22.0	33.6	118.9
12	123.7	13.2	24.2	86.3
13	89.7	9.1	17.7	63.0
14	70.1	10.5	13.5	46.2
15	56.2	6.8	11.0	38.5
16	33.0	2.2	6.6	24.2
17	24.0	2.6	4.7	16.6
18	19.3	3.4	3.7	12.3
19	13.9	2.2	0.5	11.3
20	9.3			

Table 23. Time series of median posterior population estimates from the base model. Relative spawning biomass is spawning biomass relative to the unfished equilibrium (B_0). Total biomass includes females and males of ages 0 and above. Age-2+ biomass includes females and males ages 2 and above. Exploitation fraction is total catch divided by total age-2+ biomass. Relative fishing intensity is (1 - SPR)/(1 - $\text{SPR}_{40\%}$) such that values below 100% represent fishing below $F_{40\%}$. In the last row, dashes (–) indicate quantities requiring 2025 catch which has not taken place yet.

Year	Female spawning biomass (kt)	Relative spawning biomass (%)	Total biomass (kt)	Age-2+ biomass (kt)	Age-0 recruits (millions)	Relative fishing intensity (%)	Exploitation fraction (%)
1966	947	52.7	2,361	2,138	1,647	48.2	6.4
1967	961	53.6	2,483	2,218	4,893	65.4	9.7
1968	972	54.4	2,654	2,228	3,152	47.1	5.5
1969	1,109	62.2	3,016	2,754	731	57.6	6.5
1970	1,271	71.3	3,285	3,036	9,431	63.1	7.7
1971	1,306	73.3	3,510	2,796	845	46.8	5.5
1972	1,485	83.1	3,983	3,902	552	35.3	3.0
1973	1,758	98.6	4,101	3,943	6,188	38.8	4.1
1974	1,702	95.3	3,985	3,525	345	45.4	6.0
1975	1,469	82.2	3,444	3,403	1,888	55.6	6.5
1976	2,114	118.3	4,657	4,499	203	43.1	5.3
1977	2,040	114.2	4,524	4,356	6,762	28.7	3.0
1978	1,691	94.4	3,990	3,438	132	27.9	3.0
1979	1,827	101.9	4,474	4,440	1,373	32.2	3.1
1980	1,729	96.2	4,142	3,728	17,446	25.6	2.4
1981	1,659	92.4	4,658	3,386	265	37.2	4.1

Continued on next page ...

... Continued from previous page

Year	Female spawning biomass (kt)	Relative spawning biomass (%)	Total biomass (kt)	Age-2+ biomass (kt)	Age-0 recruits (millions)	Relative fishing intensity (%)	Exploitation fraction (%)
1982	1,798	100.0	5,096	5,078	327	31.9	2.1
1983	2,306	128.1	5,205	5,180	537	26.6	2.2
1984	2,326	129.2	5,083	4,799	14,288	29.4	2.9
1985	2,332	129.5	5,785	4,656	131	23.2	2.4
1986	2,347	130.3	6,113	6,099	181	34.2	3.5
1987	2,409	133.6	5,436	5,301	6,680	38.6	4.4
1988	2,382	132.1	5,384	4,853	2,128	40.7	5.1
1989	2,070	114.9	4,891	4,739	113	48.8	6.3
1990	2,046	113.6	4,602	4,508	4,335	40.8	5.8
1991	1,853	103.0	4,172	3,815	1,237	59.1	8.4
1992	1,687	93.6	3,916	3,815	127	57.5	7.9
1993	1,320	73.3	2,954	2,888	3,181	46.6	6.9
1994	1,275	70.9	2,931	2,620	3,349	59.7	13.8
1995	1,134	63.1	2,894	2,584	1,245	51.7	9.7
1996	1,098	61.0	2,779	2,652	1,806	63.6	11.6
1997	1,091	60.7	2,600	2,442	1,082	68.0	13.3
1998	910	50.5	2,154	2,036	1,943	81.5	15.8
1999	782	43.5	2,081	1,724	12,740	91.8	18.1
2000	907	50.3	3,158	2,013	310	65.3	11.4
2001	1,338	74.1	4,289	4,228	1,234	67.0	5.4
2002	1,907	105.7	4,523	4,400	32	47.8	4.1
2003	1,783	99.1	3,787	3,744	1,660	42.6	5.5
2004	1,451	80.6	3,080	2,934	56	69.4	11.7
2005	1,150	64.0	2,508	2,454	2,764	66.7	14.8
2006	913	50.9	2,119	1,893	2,007	85.4	19.1
2007	716	39.9	1,761	1,644	23	85.8	17.7
2008	643	35.8	1,803	1,717	5,394	96.3	18.8
2009	601	33.5	1,618	1,273	1,297	80.5	14.1
2010	718	40.1	2,126	1,786	15,017	90.0	12.8
2011	713	39.8	2,702	1,727	416	89.3	16.6
2012	881	49.2	3,565	3,506	1,473	74.1	5.9
2013	1,613	89.8	4,049	3,922	347	69.4	7.3
2014	1,873	104.3	4,168	3,969	7,620	64.9	7.5
2015	1,367	76.2	3,276	2,743	31	48.1	7.1
2016	1,109	61.7	3,282	3,183	4,997	79.5	10.4
2017	1,501	83.6	3,601	3,137	1,318	84.5	14.0
2018	1,575	87.9	3,797	3,654	160	77.8	11.3
2019	1,271	71.1	3,014	2,998	186	86.6	13.7
2020	1,167	65.4	2,496	2,397	3,402	68.9	15.8
2021	933	52.2	2,339	1,863	7,055	70.8	17.5
2022	918	51.2	2,722	2,136	131	73.9	15.1
2023	1,111	61.1	2,929	2,891	879	66.2	9.2
2024	1,189	65.4	2,937	2,849	882	66.6	6.0
2025	1,223	67.1	2,668	2,573	884	–	–

Table 24. Time-series of 95% posterior credibility intervals for the quantities shown in Table 23. In the last row, dashes (–) indicate quantities requiring 2025 catch which has not taken place yet.

Year	Female spawning biomass (kt)	Relative spawning biomass (%)	Total biomass (kt)	Age-2+ biomass (kt)	Age-0 recruits (millions)	Relative fishing intensity (%)	Exploitation fraction (%)
1966	560-1,849	29.8-96.6	1,507-4,634	1,256-4,206	52-9,951	24.6-73.4	3.3-11.0
1967	600-1,884	31.2-97.9	1,608-4,898	1,359-4,431	223-15,174	36.0-91.1	4.8-15.8
1968	604-1,940	31.4-99.1	1,709-5,377	1,348-4,570	255-9,886	23.5-71.7	2.7-9.1
1969	715-2,227	36.4-112.0	1,953-6,202	1,759-5,676	45-4,164	30.0-82.7	3.2-10.2
1970	818-2,595	41.1-127.9	2,096-6,811	1,956-6,239	4,769-22,957	33.2-88.7	3.8-12.0

Continued on next page ...

... Continued from previous page

Year	Female spawning biomass (kt)	Relative spawning biomass (%)	Total biomass (kt)	Age-2+ biomass (kt)	Age-0 recruits (millions)	Relative fishing intensity (%)	Exploitation fraction (%)
1971	826-2,685	41.7-133.4	2,187-7,404	1,772-5,811	73-3,077	22.1-71.6	2.7-8.7
1972	929-3,088	47.3-153.6	2,468-8,353	2,426-8,141	63-1,937	16.1-57.2	1.4-4.8
1973	1,104-3,596	55.9-182.4	2,550-8,470	2,464-8,073	3,231-14,519	17.9-62.1	2.0-6.6
1974	1,065-3,426	54.0-175.3	2,468-8,091	2,202-7,123	37-1,370	21.8-70.4	3.0-9.6
1975	908-2,951	46.7-152.4	2,118-6,961	2,091-6,853	920-4,415	28.1-83.0	3.2-10.6
1976	1,280-4,249	67.1-220.6	2,814-9,385	2,723-9,076	23-898	20.7-68.9	2.6-8.7
1977	1,228-4,070	64.6-210.1	2,722-8,969	2,622-8,642	3,726-14,590	13.0-49.6	1.5-5.1
1978	1,031-3,265	53.7-170.3	2,443-7,741	2,096-6,647	17-660	13.0-48.4	1.6-4.9
1979	1,137-3,436	58.3-179.9	2,786-8,460	2,766-8,371	538-3,408	15.5-54.0	1.6-5.0
1980	1,090-3,187	55.5-166.7	2,606-7,675	2,346-6,870	10,350-34,939	12.2-43.8	1.3-3.8
1981	1,063-2,981	53.8-156.3	3,008-8,368	2,174-6,081	31-1,073	18.9-59.7	2.3-6.4
1982	1,181-3,139	59.1-167.8	3,357-8,974	3,341-8,945	54-1,045	16.2-52.0	1.2-3.2
1983	1,556-3,928	76.2-212.7	3,505-8,882	3,485-8,832	84-1,547	13.6-43.5	1.3-3.3
1984	1,604-3,843	77.3-210.5	3,520-8,440	3,313-7,951	9,078-25,792	15.6-46.7	1.7-4.2
1985	1,642-3,735	78.4-208.3	4,083-9,335	3,279-7,457	18-553	12.4-37.7	1.5-3.4
1986	1,704-3,661	80.0-206.9	4,429-9,639	4,417-9,612	26-687	19.4-51.1	2.2-4.8
1987	1,784-3,674	82.9-210.2	4,016-8,311	3,918-8,094	4,305-11,388	22.8-55.6	2.9-6.0
1988	1,792-3,534	82.4-206.3	4,044-8,018	3,648-7,207	1,141-3,920	24.2-58.5	3.5-6.8
1989	1,585-2,995	71.9-177.8	3,731-7,109	3,626-6,914	17-430	30.7-67.5	4.3-8.2
1990	1,586-2,915	70.9-174.7	3,566-6,573	3,501-6,441	2,856-7,199	25.1-57.5	4.1-7.5
1991	1,466-2,586	64.6-158.0	3,288-5,849	3,019-5,327	567-2,401	37.9-89.5	6.0-10.6
1992	1,349-2,320	59.0-143.3	3,124-5,439	3,041-5,285	17-489	36.8-88.1	5.7-9.9
1993	1,066-1,794	46.4-112.0	2,376-4,032	2,328-3,933	2,173-5,101	29.2-75.1	5.1-8.5
1994	1,046-1,698	44.8-107.9	2,386-3,952	2,149-3,499	2,286-5,399	40.9-82.1	10.4-16.9
1995	927-1,515	39.8-95.9	2,344-3,927	2,108-3,486	759-2,091	34.8-69.8	7.2-11.8
1996	902-1,463	38.6-92.4	2,270-3,758	2,171-3,566	1,185-2,981	45.0-86.4	8.6-14.1
1997	899-1,459	38.3-92.2	2,129-3,498	2,009-3,272	620-1,974	49.2-88.0	9.9-16.2
1998	749-1,215	32.0-76.9	1,760-2,914	1,674-2,742	1,255-3,275	61.4-98.6	11.7-19.2
1999	637-1,059	27.4-66.3	1,663-2,895	1,400-2,342	8,941-20,378	70.1-109.6	13.3-22.3
2000	720-1,259	31.7-76.9	2,451-4,531	1,594-2,797	99-687	46.4-83.2	8.2-14.3
2001	1,053-1,883	47.0-113.5	3,346-6,110	3,299-6,016	839-1,985	47.4-85.0	3.8-6.9
2002	1,519-2,645	66.8-161.5	3,596-6,297	3,504-6,114	8-111	31.5-64.6	3.0-5.2
2003	1,457-2,403	62.6-150.3	3,093-5,128	3,062-5,056	1,161-2,700	27.5-58.7	4.1-6.7
2004	1,214-1,904	51.0-121.9	2,567-4,074	2,455-3,850	11-193	47.5-94.8	8.9-13.9
2005	969-1,506	40.4-96.8	2,098-3,327	2,057-3,237	1,936-4,495	45.9-90.2	11.2-17.7
2006	767-1,207	32.2-77.1	1,763-2,846	1,588-2,503	1,394-3,209	61.2-114.0	14.5-22.8
2007	592-974	25.3-60.9	1,441-2,417	1,350-2,255	6-88	60.5-116.5	12.9-21.6
2008	521-899	22.6-55.0	1,453-2,539	1,388-2,408	3,893-8,590	72.7-118.6	13.4-23.3
2009	475-865	21.1-51.9	1,277-2,346	1,008-1,825	751-2,415	56.8-103.0	9.8-17.8
2010	569-1,036	25.5-62.0	1,659-3,139	1,418-2,572	10,336-25,315	64.1-117.2	8.9-16.1
2011	562-1,036	25.2-61.5	2,072-4,076	1,363-2,513	162-915	62.7-118.5	11.4-21.1
2012	678-1,324	31.0-76.1	2,713-5,415	2,671-5,327	952-2,629	49.5-100.5	3.9-7.8
2013	1,248-2,409	56.8-139.1	3,127-6,072	3,032-5,867	128-759	46.4-89.8	4.9-9.4
2014	1,466-2,771	66.2-161.5	3,248-6,201	3,102-5,881	5,464-12,685	42.5-86.4	5.1-9.6
2015	1,078-2,017	48.1-118.1	2,566-4,893	2,164-4,047	8-107	29.3-68.6	4.8-9.0
2016	886-1,628	39.0-95.6	2,593-4,894	2,521-4,723	3,453-8,892	54.4-102.8	7.0-13.2
2017	1,184-2,251	52.6-130.9	2,813-5,507	2,475-4,709	770-2,700	57.0-117.0	9.4-17.8
2018	1,216-2,465	54.6-139.1	2,909-6,039	2,815-5,773	34-517	50.9-106.7	7.2-14.7
2019	964-2,055	43.7-115.7	2,269-4,932	2,260-4,889	37-685	58.1-112.1	8.4-18.2
2020	845-1,993	39.3-110.6	1,785-4,302	1,729-4,102	1,595-9,144	43.8-92.6	9.2-21.9
2021	629-1,706	30.5-92.5	1,516-4,447	1,257-3,399	2,890-19,307	43.7-96.6	9.6-26.0
2022	548-1,852	28.1-98.0	1,536-5,812	1,251-4,391	14-1,012	43.4-105.1	7.4-25.8
2023	560-2,548	29.9-132.6	1,455-6,787	1,428-6,715	474-1,850	35.5-99.6	3.9-18.5
2024	530-2,900	29.2-151.4	1,338-7,101	1,273-6,982	476-1,873	34.4-107.8	2.4-13.5
2025	521-3,028	28.9-157.3	1,189-6,433	1,120-6,302	476-1,881	–	–

Table 25. Select parameters, derived quantities, and reference point posterior median estimates for the (2025) base model compared to the previous assessment's (2024) base model. Dashes (–) in column for the previous assessment indicate quantities that were not available in that assessment

Parameter, Quantity, or Reference point	Base model	2024 Base model
Parameters		
Natural mortality (M)	0.233	0.235
Unfished recruitment (R_0, millions)	2,456	2,600
Steepness (h)	0.812	0.812
Additional biomass index SD	0.294	0.322
Catchability: biomass index (q_b)	0.894	0.838
Additional age-1 index SD	–	0.381
Catchability: age-1 index (q_1)	–	0.490
Dirichlet-multinomial fishery ($\log \theta_{\text{fish}}$)	-0.643	-0.663
Dirichlet-multinomial survey ($\log \theta_{\text{surv}}$)	2.729	2.770
Derived Quantities		
2010 recruitment (millions)	15,018	15,979
2014 recruitment (millions)	7,620	8,256
2016 recruitment (millions)	4,997	5,638
2021 recruitment (millions)	7,055	10,187
Unfished female spawning biomass (B_0, kt)	1,808	1,919
2024 relative spawning biomass	65.4%	98.7%
2025 relative spawning biomass	67.1%	–
2024 rel. fishing intensity: $(1 - \text{SPR})/(1 - \text{SPR}_{40\%})$	66.6%	–
Reference Points based on $F_{SPR=40\%}$		
Female spawning biomass at $F_{\text{SPR}=40\%}$ ($B_{\text{SPR}=40\%}$, kt)	642	681
SPR at $F_{\text{SPR}=40\%}$ (kt)	40.0%	40.0%
Exploitation fraction corresponding to SPR	19.1%	19.1%
Yield at $B_{\text{SPR}=40\%}$ (kt)	296	317
Negative log likelihoods		
Total	2,255.91	2,225.16
Survey index	-8.96	-4.40
Survey age compositions	306.19	305.08
Fishery age compositions	1,874.82	1,840.11
Recruitment	62.63	63.85
Parameter priors	1.10	1.13
Parameter deviations	20.13	19.38

Table 26. Summary of median and 95% credibility intervals of equilibrium conceptual reference points for the base assessment model. Equilibrium reference points were computed using 1975–2024 averages for mean weight-at-age and baseline selectivity-at-age (1966–1990; prior to time-varying deviations). Dashes (–) indicate values that are static at one value and do not have a credible interval associated with them.

Quantity	2.5%	Median	97.5%
Unfished female spawning biomass (B_0, kt)	1,173	1,808	3,038
Unfished recruitment (R_0, millions)	1,312	2,456	5,215
Reference points (equilibrium) based on $F_{SPR=40\%}$			
Female spawning biomass at $F_{\text{SPR}=40\%}$ ($B_{\text{SPR}=40\%}$, kt)	381	642	1,090
SPR at $F_{\text{SPR}=40\%}$	–	40%	–
Exploitation fraction corresponding to $F_{\text{SPR}=40\%}$	16.3%	19.1%	22.2%
Yield associated with $F_{\text{SPR}=40\%}$ (kt)	164	296	558
Reference points (equilibrium) based on $B_{40\%}$ (40% of B_0)			
Female spawning biomass ($B_{40\%}$, kt)	469	723	1,215
SPR at $B_{40\%}$	40.7%	43.5%	51.6%
Exploitation fraction resulting in $B_{40\%}$	12.5%	16.7%	20.3%
Yield at $B_{40\%}$ (kt)	163	288	545
Reference points (equilibrium) based on estimated MSY			
Female spawning biomass (B_{MSY}, kt)	281	459	859
SPR at MSY	23.1%	29.3%	46.4%
Exploitation fraction corresponding to SPR at MSY	15.1%	27.4%	36.8%
MSY (kt)	171	313	602

Table 27. Forecast quantiles of Pacific Hake relative spawning biomass at the beginning of the year. Catch alternatives are defined by letters a-o and are a constant value across all forecasted years unless otherwise defined in the first column. Acronyms are defined in the glossary (Appendix C).

Catch alternative			Biomass at	Relative spawning biomass		
	Catch year	Catch (t)	start of year	5%	50%	95%
			Start of 2025	0.33	0.67	1.36
a:	2025	0	Start of 2026	0.34	0.64	1.23
	2026	0	Start of 2027	0.34	0.60	1.09
	2027	0	Start of 2028	0.34	0.56	0.97
b:	2025	150,000	Start of 2026	0.30	0.60	1.19
	2026	150,000	Start of 2027	0.27	0.53	1.01
	2027	150,000	Start of 2028	0.25	0.46	0.86
c:	2025	200,000	Start of 2026	0.29	0.58	1.18
	2026	200,000	Start of 2027	0.25	0.50	0.99
	2027	200,000	Start of 2028	0.21	0.43	0.83
d:	2025	250,000	Start of 2026	0.28	0.57	1.16
	2026	250,000	Start of 2027	0.22	0.48	0.96
	2027	250,000	Start of 2028	0.17	0.40	0.79
e:	2025	300,000	Start of 2026	0.27	0.56	1.15
	2026	300,000	Start of 2027	0.20	0.45	0.94
	2027	300,000	Start of 2028	0.14	0.36	0.76
f:	2025	350,000	Start of 2026	0.25	0.54	1.13
	2026	350,000	Start of 2027	0.17	0.43	0.91
	2027	350,000	Start of 2028	0.11	0.33	0.73
g:	2025	400,000	Start of 2026	0.24	0.53	1.12
	2026	400,000	Start of 2027	0.15	0.41	0.89
	2027	400,000	Start of 2028	0.09	0.30	0.70
h:	2025	450,000	Start of 2026	0.23	0.52	1.11
	2026	450,000	Start of 2027	0.13	0.38	0.87
	2027	450,000	Start of 2028	0.09	0.27	0.67
i:	2025	500,000	Start of 2026	0.21	0.50	1.09
	2026	500,000	Start of 2027	0.12	0.36	0.84
	2027	500,000	Start of 2028	0.08	0.23	0.64
j:	2025	555,000	Start of 2026	0.20	0.49	1.08
2024 TAC	2026	555,000	Start of 2027	0.11	0.33	0.81
	2027	555,000	Start of 2028	0.08	0.20	0.60
k:	2025	560,742	Start of 2026	0.20	0.49	1.07
Default HR	2026	463,364	Start of 2027	0.12	0.35	0.84
($F_{\text{SPR}=40\%}$–40:10)	2027	406,150	Start of 2028	0.08	0.25	0.65

Table 28. Forecast quantiles of Pacific Hake relative fishing intensity (1 - SPR)/(1 - $\text{SPR}_{40\%}$), expressed as a proportion. Catch alternatives are defined by letters a-o and are a constant value across all forecasted years unless otherwise defined in the first column. Acronyms are defined in the glossary (Appendix C).

Catch alternative			Relative fishing intensity		
	Catch year	Catch (t)	5%	50%	95%
a:	2025	0	0.00	0.00	0.00
	2026	0	0.00	0.00	0.00
	2027	0	0.00	0.00	0.00
b:	2025	150,000	0.25	0.47	0.77
	2026	150,000	0.24	0.46	0.77
	2027	150,000	0.22	0.45	0.77
c:	2025	200,000	0.31	0.57	0.88
	2026	200,000	0.30	0.56	0.90
	2027	200,000	0.29	0.56	0.93
d:	2025	250,000	0.37	0.65	0.97
	2026	250,000	0.36	0.65	1.01
	2027	250,000	0.35	0.66	1.07
e:	2025	300,000	0.42	0.72	1.04
	2026	300,000	0.42	0.73	1.11
	2027	300,000	0.41	0.76	1.20
f:	2025	350,000	0.47	0.78	1.09
	2026	350,000	0.47	0.80	1.19
	2027	350,000	0.47	0.84	1.28
g:	2025	400,000	0.51	0.83	1.14
	2026	400,000	0.52	0.87	1.25
	2027	400,000	0.52	0.92	1.32
h:	2025	450,000	0.55	0.87	1.19
	2026	450,000	0.56	0.93	1.29
	2027	450,000	0.57	1.00	1.34
i:	2025	500,000	0.59	0.91	1.22
	2026	500,000	0.61	0.98	1.32
	2027	500,000	0.62	1.07	1.35
j: 2024 TAC	2025	555,000	0.63	0.96	1.26
	2026	555,000	0.65	1.03	1.34
	2027	555,000	0.67	1.15	1.36
k: Default HR ($F_{\text{SPR}=40\%}$–40:10)	2025	560,742	0.63	0.96	1.26
	2026	463,364	0.59	0.96	1.32
	2027	406,150	0.55	0.99	1.34

Table 29. Probabilities related to spawning biomass, relative fishing intensity, and the 2026 default harvest policy catch for alternative 2025 catch options (catch options explained in Table 27).

	Catch (t) in 2025	$B_{2026} < B_{2025}$	$B_{2026} < B_{40\%}$	$B_{2026} < B_{25\%}$	$B_{2026} < B_{10\%}$	2025 Fishing intensity > 100%	2026 Default HR catch < 2025 catch
a:	0	0.89	0.11	0.01	0.00	0.00	0.00
b:	150,000	1.00	0.17	0.02	0.00	0.00	0.01
c:	200,000	1.00	0.19	0.03	0.00	0.01	0.03
d:	250,000	1.00	0.21	0.03	0.00	0.03	0.08

Continued on next page ...

... Continued from previous page

	Catch (t) in 2025	$B_{2026} < B_{2025}$	$B_{2026} < B_{40\%}$	$B_{2026} < B_{25\%}$	$B_{2026} < B_{10\%}$	2025 Fishing intensity > 100%	2026 Default HR catch < 2025 catch
e:	300,000	1.00	0.23	0.04	0.00	0.07	0.15
f:	350,000	1.00	0.25	0.05	0.00	0.12	0.24
g:	400,000	1.00	0.27	0.06	0.00	0.18	0.34
h:	450,000	1.00	0.30	0.08	0.00	0.26	0.44
i:	500,000	1.00	0.32	0.09	0.00	0.33	0.53
j:	555,000	1.00	0.34	0.10	0.00	0.41	0.62
k:	560,742	1.00	0.34	0.11	0.00	0.42	0.63

Table 30. Probabilities related to spawning biomass, relative fishing intensity, and the 2027 default harvest policy catch for alternative 2026 catch options, given the 2025 catch level shown in Table 29 (catch options explained in Table 27).

	Catch (t) in 2026	$B_{2027} < B_{2026}$	$B_{2027} < B_{40\%}$	$B_{2027} < B_{25\%}$	$B_{2027} < B_{10\%}$	2026 Fishing intensity > 100%	2027 Default HR catch < 2026 catch
a:	0	0.93	0.12	0.01	0.00	0.00	0.00
b:	150,000	1.00	0.25	0.03	0.00	0.00	0.01
c:	200,000	1.00	0.30	0.05	0.00	0.02	0.03
d:	250,000	1.00	0.34	0.08	0.00	0.06	0.09
e:	300,000	1.00	0.39	0.11	0.00	0.12	0.17
f:	350,000	1.00	0.44	0.15	0.01	0.19	0.29
g:	400,000	1.00	0.49	0.19	0.01	0.28	0.40
h:	450,000	1.00	0.54	0.23	0.01	0.37	0.52
i:	500,000	1.00	0.58	0.28	0.02	0.46	0.61
j:	555,000	1.00	0.63	0.34	0.02	0.56	0.70
k:	463,364	1.00	0.59	0.29	0.02	0.44	0.58

Table 31. Posterior medians for select parameters, derived quantities, reference points, and negative log likelihoods for the base model and some sensitivity runs (described in Section 3.8). A dash (–) indicates that the parameter or derived quantity was not estimated in the model.

Parameter, Quantity, or Reference point	Base model	Steepness Mean Prior Low (0.5)	Steepness Fix 1.0	Sigma R 1.0	Sigma R 1.6	Natural Mortality (SD=0.2)	Natural Mortality (SD=0.3)	Natural Mortality (Hamel Cope prior)
Parameters								
Natural mortality (M)	0.233	0.237	0.232	0.229	0.235	0.286	0.307	0.309
Unfished recruitment (R_0, millions)	2,456	2,586	2,361	1,809	2,994	4,873	6,736	7,044
Steepness (h)	0.812	0.538	–	0.815	0.811	0.797	0.793	0.789
Additional biomass index SD	0.294	0.293	0.297	0.295	0.297	0.305	0.310	0.309
Catchability: biomass index (q_b)	0.894	0.875	0.894	0.894	0.889	0.638	0.537	0.525
Additional age-1 index SD	–	–	–	–	–	–	–	–
Catchability: age-1 index (q_1)	–	–	–	–	–	–	–	–
Dirichlet-multinomial fishery (log θ_{fish})	-0.643	-0.648	-0.641	-0.702	-0.627	-0.642	-0.643	-0.644
Dirichlet-multinomial survey (log θ_{surv})	2.729	2.726	2.697	2.729	2.709	2.741	2.736	2.742
Derived Quantities								
2010 recruitment (millions)	15,018	15,550	14,817	14,525	15,250	26,359	34,322	35,372
2014 recruitment (millions)	7,620	7,861	7,580	7,511	7,701	12,416	15,712	16,195
2016 recruitment (millions)	4,997	5,152	4,974	4,949	5,058	8,177	10,399	10,730
2021 recruitment (millions)	7,055	7,270	6,918	6,791	7,146	12,750	17,151	17,555
Unfished female spawning biomass (B_0, kt)	1,808	1,878	1,782	1,388	2,179	2,459	2,963	3,042
2024 relative spawning biomass	65.4%	65.1%	66.9%	86.3%	54.3%	74.5%	78.7%	78.7%
2025 relative spawning biomass	67.1%	66.5%	68.7%	90.2%	55.3%	75.2%	78.6%	78.8%
2024 rel. fishing intensity: (1 - SPR)/(1 - $\text{SPR}_{40\%}$)	66.6%	65.1%	66.5%	61.7%	68.2%	41.6%	32.3%	31.5%
Reference Points based on $F_{SPR=40\%}$								
Female spawning biomass at $F_{\text{SPR}=40\%}$ ($B_{\text{SPR}=40\%}$, kt)	642	421	713	495	773	856	1,023	1,050
SPR at $F_{\text{SPR}=40\%}$ (kt)	40.0%	40.0%	40.0%	40.0%	40.0%	40.0%	40.0%	40.0%
Exploitation fraction corresponding to SPR	19.1%	19.3%	18.9%	18.8%	19.2%	22.6%	24.0%	24.1%
Yield at $B_{\text{SPR}=40\%}$ (kt)	296	194	325	222	360	487	630	656

Table 32. Posterior medians for select parameters, derived quantities, reference points, and negative log likelihoods for the base model and further sensitivity runs (described in Section 3.8). A dash (–) indicates that the parameter or derived quantity was not estimated in the model.

Parameter, Quantity, or Reference point	**Base model**	**Add Age-1 Index**	**Down-weight Fishery Comps**	**eDNA Index**	**Earlier maturity**
Parameters					
Natural mortality (M)	0.233	0.237	0.233	0.226	0.233
Unfished recruitment (R_0, millions)	2,456	2,785	2,568	2,141	2,490
Steepness (h)	0.812	0.812	0.813	0.811	0.810
Additional biomass index SD	0.294	0.316	0.294	0.280	0.293
Catchability: biomass index (q_b)	0.894	0.832	0.929	0.988	0.884
Additional age-1 index SD	–	0.510	–	–	–
Catchability: age-1 index (q_1)	–	0.536	–	0.148	–
Dirichlet-multinomial fishery (log θ_{fish})	-0.643	-0.652	–	-0.643	-0.645
Dirichlet-multinomial survey (log θ_{surv})	2.729	2.747	–	2.662	2.724
Derived Quantities					
2010 recruitment (millions)	15,018	16,234	14,812	13,380	15,093
2014 recruitment (millions)	7,620	8,413	7,512	6,666	7,662
2016 recruitment (millions)	4,997	5,734	4,998	4,205	5,046
2021 recruitment (millions)	7,055	9,646	5,774	3,301	7,178
Unfished female spawning biomass (B_0, kt)	1,808	2,004	1,900	1,677	1,685
2024 relative spawning biomass	65.4%	81.6%	54.2%	35.5%	64.0%
2025 relative spawning biomass	67.1%	86.3%	55.3%	34.5%	75.2%
2024 rel. fishing intensity: $(1 - \text{SPR})/(1 - \text{SPR}_{40\%})$	66.6%	51.1%	68.7%	88.6%	62.5%
Reference Points based on $F_{SPR=40\%}$					
Female spawning biomass at $F_{\text{SPR=40\%}}$ ($B_{\text{SPR=40\%}}$, kt)	642	710	679	594	598
SPR at $F_{\text{SPR=40\%}}$ (kt)	40.0%	40.0%	40.0%	40.0%	40.0%
Exploitation fraction corresponding to SPR	19.1%	19.3%	19.1%	18.5%	16.4%
Yield at $B_{\text{SPR=40\%}}$ (kt)	296	332	312	265	285

Table 33. Posterior medians for select parameters, derived quantities, reference points, and negative log likelihoods for the base model and further sensitivity runs (described in Section 3.8). A dash (–) indicates that the parameter or derived quantity was not estimated in the model.

Parameter, Quantity, or Reference point	Base model	Phi t.v. selectivity (0.21)	Phi t.v. selectivity (0.70)	Phi t.v. selectivity (2.10)
Parameters				
Natural mortality (M)	0.233	0.219	0.230	0.237
Unfished recruitment (R_0, millions)	2,456	2,329	2,539	2,509
Steepness (h)	0.812	0.811	0.817	0.806
Additional biomass index SD	0.294	0.324	0.289	0.299
Catchability: biomass index (q_b)	0.894	0.902	0.928	0.865
Additional age-1 index SD	–	–	–	–
Catchability: age-1 index (q_1)	–	–	–	–
Dirichlet-multinomial fishery (log θ_{fish})	-0.643	-1.005	-0.714	-0.623
Dirichlet-multinomial survey (log θ_{surv})	2.729	2.771	2.631	2.761
Derived Quantities				
2010 recruitment (millions)	15,018	13,673	14,271	15,711
2014 recruitment (millions)	7,620	7,511	7,250	7,968
2016 recruitment (millions)	4,997	5,362	4,664	5,277
2021 recruitment (millions)	7,055	7,943	5,144	8,173
Unfished female spawning biomass (B_0, kt)	1,808	1,945	1,915	1,811
2024 relative spawning biomass	65.4%	77.5%	48.5%	72.5%
2025 relative spawning biomass	67.1%	83.0%	48.9%	75.2%
2024 rel. fishing intensity: (1 - SPR)/(1 - $\text{SPR}_{40\%}$)	66.6%	49.2%	71.0%	61.0%
Reference Points based on $F_{SPR=40\%}$				
Female spawning biomass at $F_{\text{SPR}=40\%}$ ($B_{\text{SPR}=40\%}$, kt)	642	688	684	643
SPR at $F_{\text{SPR}=40\%}$ (kt)	40.0%	40.0%	40.0%	40.0%
Exploitation fraction corresponding to SPR	19.1%	18.0%	18.8%	19.3%
Yield at $B_{\text{SPR}=40\%}$ (kt)	296	295	310	298

Table 34. Posterior medians from the base model for select parameters, derived quantities, reference point estimates, and negative log likelihoods for retrospective analyses. Some values are implied since they occur after the ending year of the respective retrospective analysis. A dash (–) indicates that the parameter or derived quantity was not output by the model.

Parameter, Quantity, or Reference point	Base model	-1 year	-2 years	-3 years	-4 years	-5 years
Parameters						
Natural mortality (M)	0.233	0.233	0.231	0.231	0.229	0.229
Unfished recruitment (R_0, millions)	2,456	2,414	2,408	2,367	2,285	2,267
Steepness (h)	0.812	0.809	0.810	0.812	0.810	0.808
Additional biomass index SD	0.294	0.298	0.288	0.289	0.313	0.311
Catchability: biomass index (q_b)	0.894	0.890	0.900	0.902	0.887	0.928
Additional age-1 index SD	–	–	–	–	–	–
Catchability: age-1 index (q_1)	–	–	–	–	–	–
Dirichlet-multinomial fishery ($\log \theta_{\text{fish}}$)	-0.643	-0.656	-0.641	-0.603	-0.599	-0.571
Dirichlet-multinomial survey ($\log \theta_{\text{surv}}$)	2.729	2.753	2.670	2.663	2.462	2.464
Derived Quantities						
2010 recruitment (millions)	15,018	14,987	15,440	15,434	15,735	14,858
2014 recruitment (millions)	7,620	7,606	8,090	8,141	9,010	9,326
2016 recruitment (millions)	4,997	5,020	5,548	5,450	4,930	4,475
2021 recruitment (millions)	7,055	7,781	877	855	828	824
Unfished female spawning biomass (B_0, kt)	1,808	1,786	1,822	1,795	1,758	1,742
2024 relative spawning biomass	65.4%	74.1%	108.0%	32.2%	33.7%	34.8%
2025 relative spawning biomass	67.1%	–	–	–	–	–
2024 rel. fishing intensity: $(1 - \text{SPR})/(1 - \text{SPR}_{40\%})$	66.6%	–	–	–	–	–
Reference Points based on $F_{SPR=40\%}$						
Female spawning biomass at $F_{\text{SPR}=40\%}$ ($B_{\text{SPR}=40\%}$, kt)	642	634	645	638	621	618
SPR at $F_{\text{SPR}=40\%}$ (kt)	40.0%	40.0%	40.0%	40.0%	40.0%	40.0%
Exploitation fraction corresponding to SPR	19.1%	19.0%	18.9%	18.9%	18.8%	18.8%
Yield at $B_{\text{SPR}=40\%}$ (kt)	296	291	294	289	280	278
Total	2,255.91	2,217.48	2,150.01	2,091.43	2,029.38	1,983.14
Survey index	-8.96	-8.86	-8.68	-8.70	-7.69	-7.56
Survey age compositions	306.19	305.19	287.87	288.20	269.85	269.46
Fishery age compositions	1,874.82	1,838.98	1,792.11	1,735.84	1,692.61	1,647.61
Recruitment	62.63	61.48	60.99	58.90	58.35	57.28
Parameter priors	1.10	1.14	1.01	1.00	0.84	0.85
Parameter deviations	20.13	19.55	16.70	16.19	15.42	15.49

---

7 FIGURES

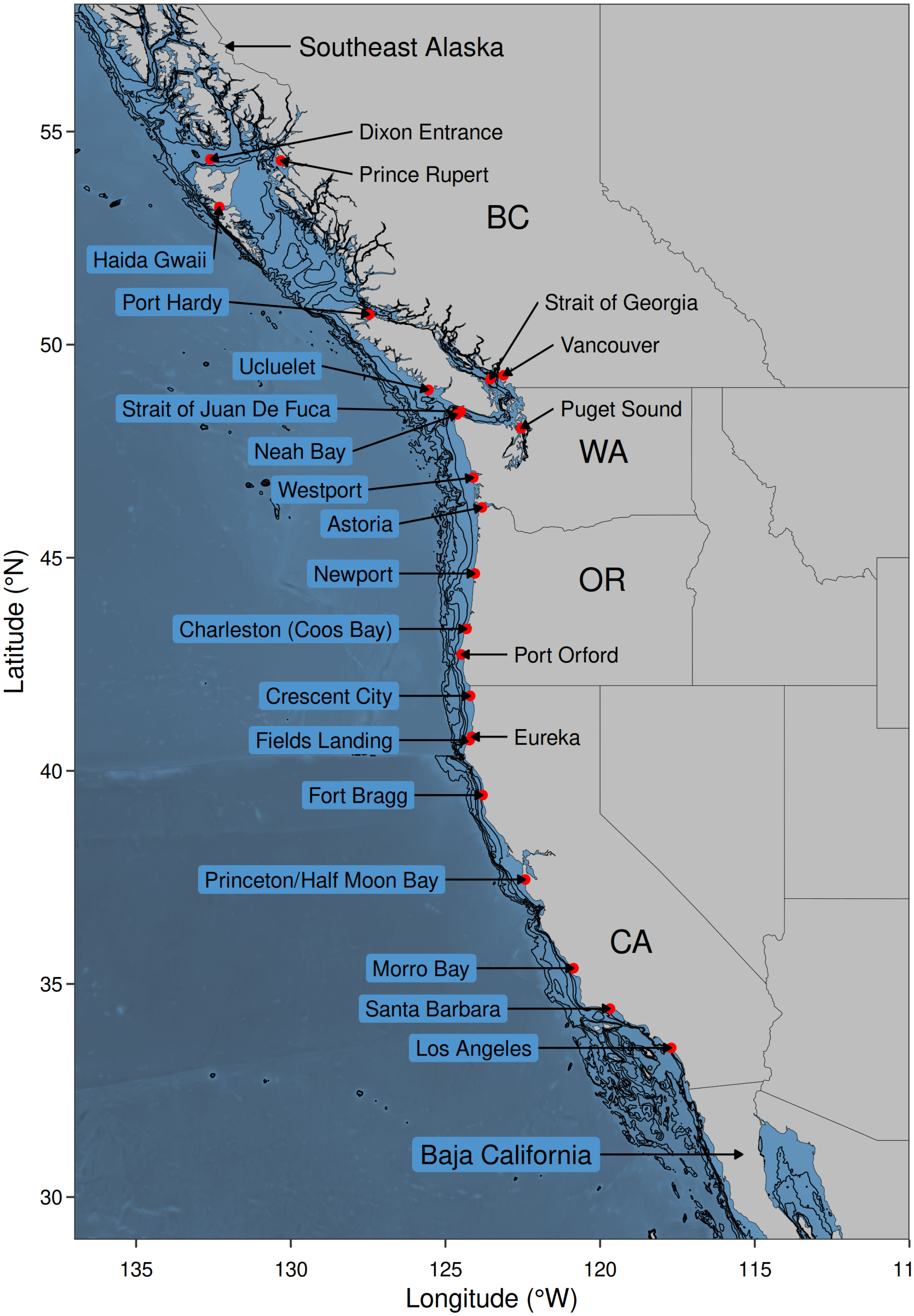

Figure 1. Overview map of the area in the Northeast Pacific Ocean occupied by Pacific Hake. Ports and areas of interest referred to in this document or past assessment documents are shown.

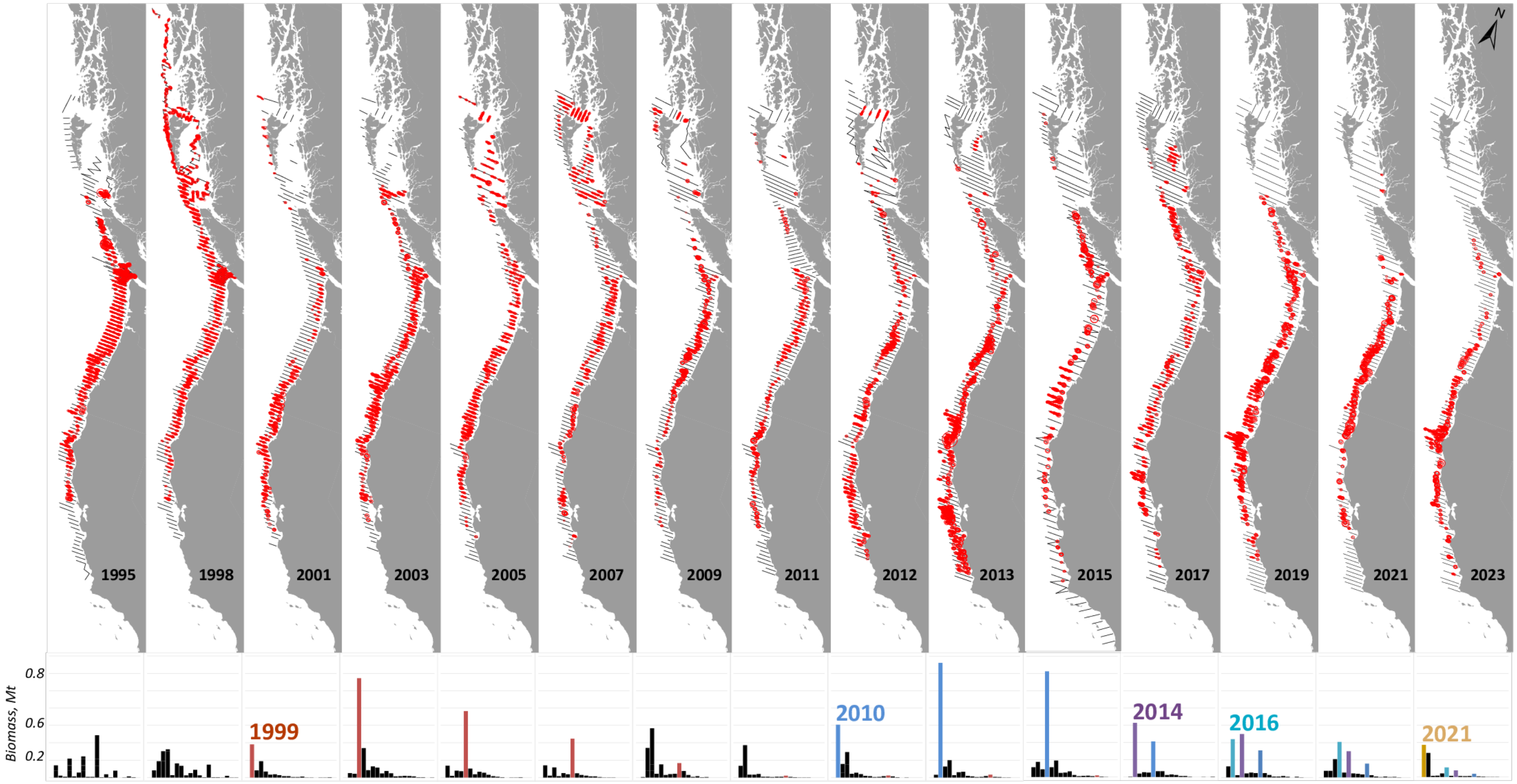

Figure 2. Spatial distribution of acoustic backscatter attributable to age-2 and older Pacific Hake from the Joint U.S. and Canadian Integrated Acoustic and Trawl Survey (1995–2023). Area of the circle is roughly proportional to observed backscatter. Bar plots show survey-estimated biomass for ages 2 to 20, with major cohorts highlighted in color. Figure produced by Julia Clemons (NOAA).

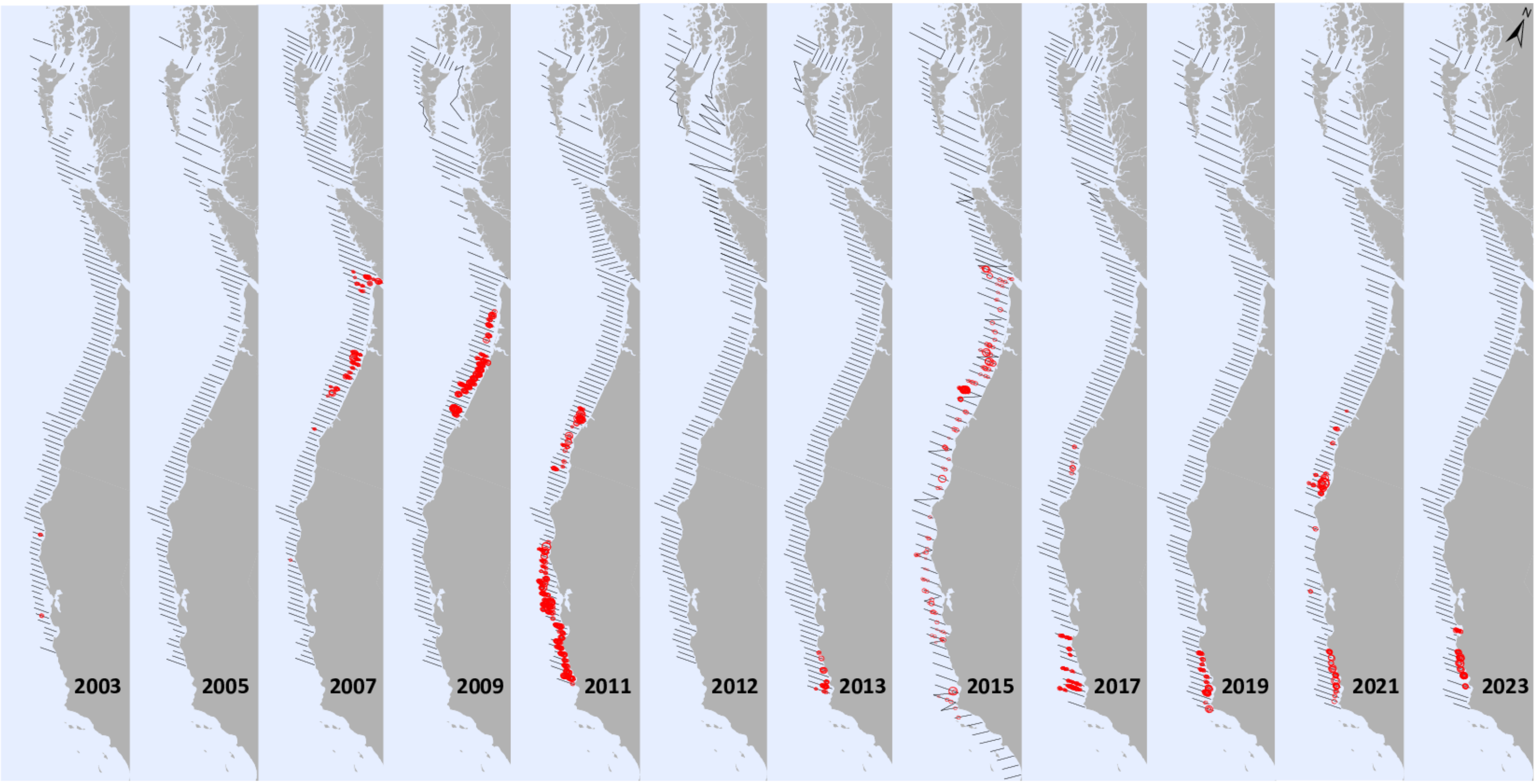

Figure 3. Spatial distribution of acoustic backscatter attributable to aggregations of age-1 Pacific Hake from the Joint U.S. and Canadian Integrated Acoustic and Trawl Survey 2003–2023 (spatial details are not available for survey years 1995, 1998, and 2001). Age-1 Pacific Hake are not fully sampled during the acoustic survey and were not explicitly considered during establishment of the survey sampling design. Additional backscatter from age-1 fish intermixed with older fish is not shown. Area of the circle is roughly proportional to observed backscatter. Figure produced by Julia Clemons (NOAA).

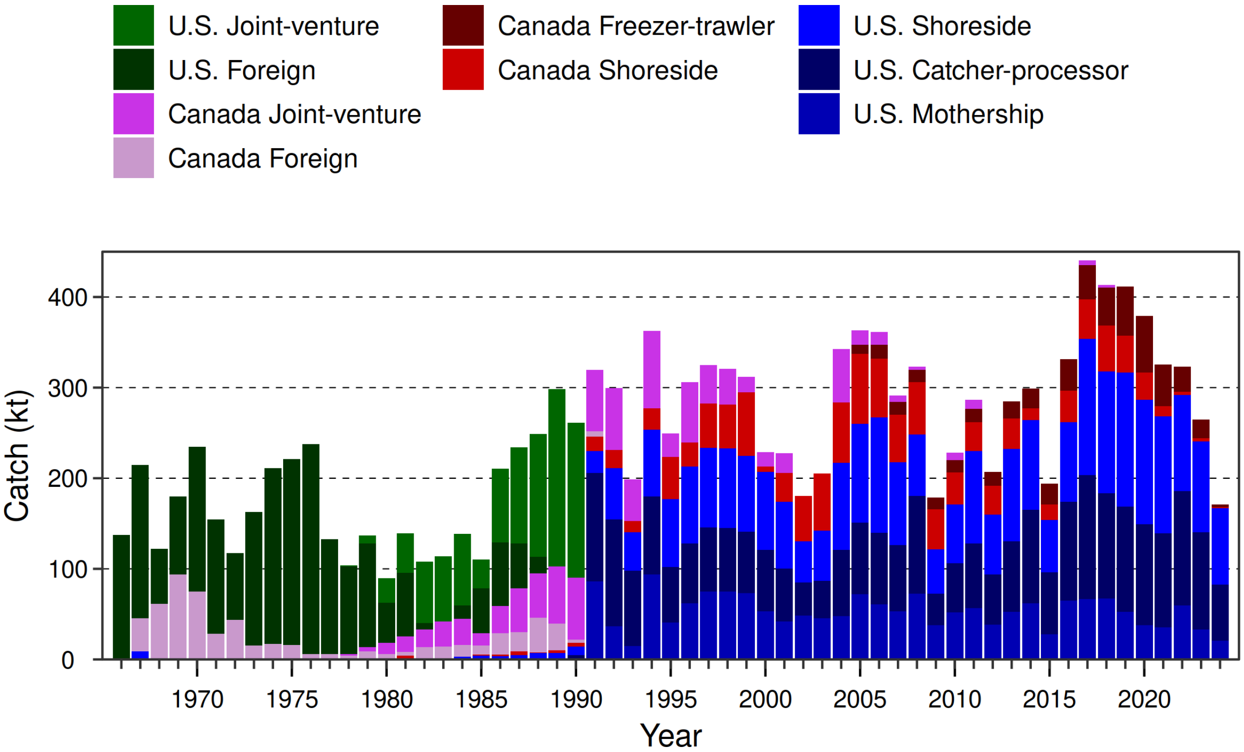

Figure 4. Total Pacific Hake catch used in the assessment by sector, 1966–2024. U.S. tribal catches are included in the sectors where they are represented.

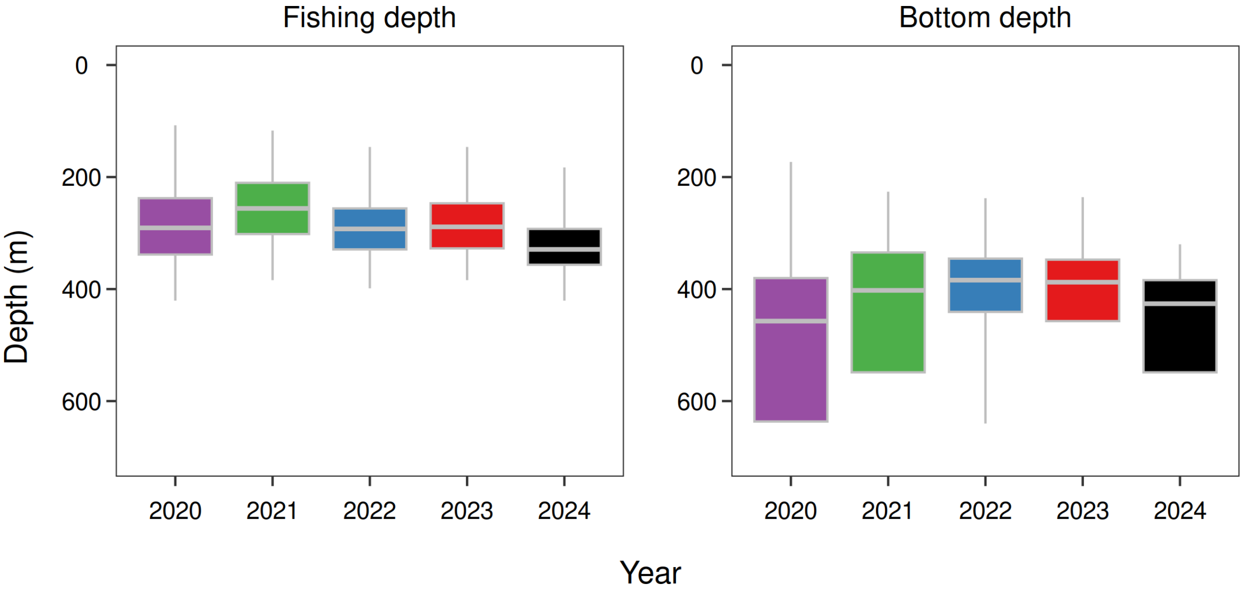

Figure 5. Distribution of fishing depths (left) and bottom depths (right), in meters, of hauls targeting Pacific Hake in the U.S. Catcher-Processor and Mothership sectors from 2020–2024. Horizontal lines in each box represent the median depth and boxes encompass the middle 50% of the data. Whiskers encompass the 95% quantiles.

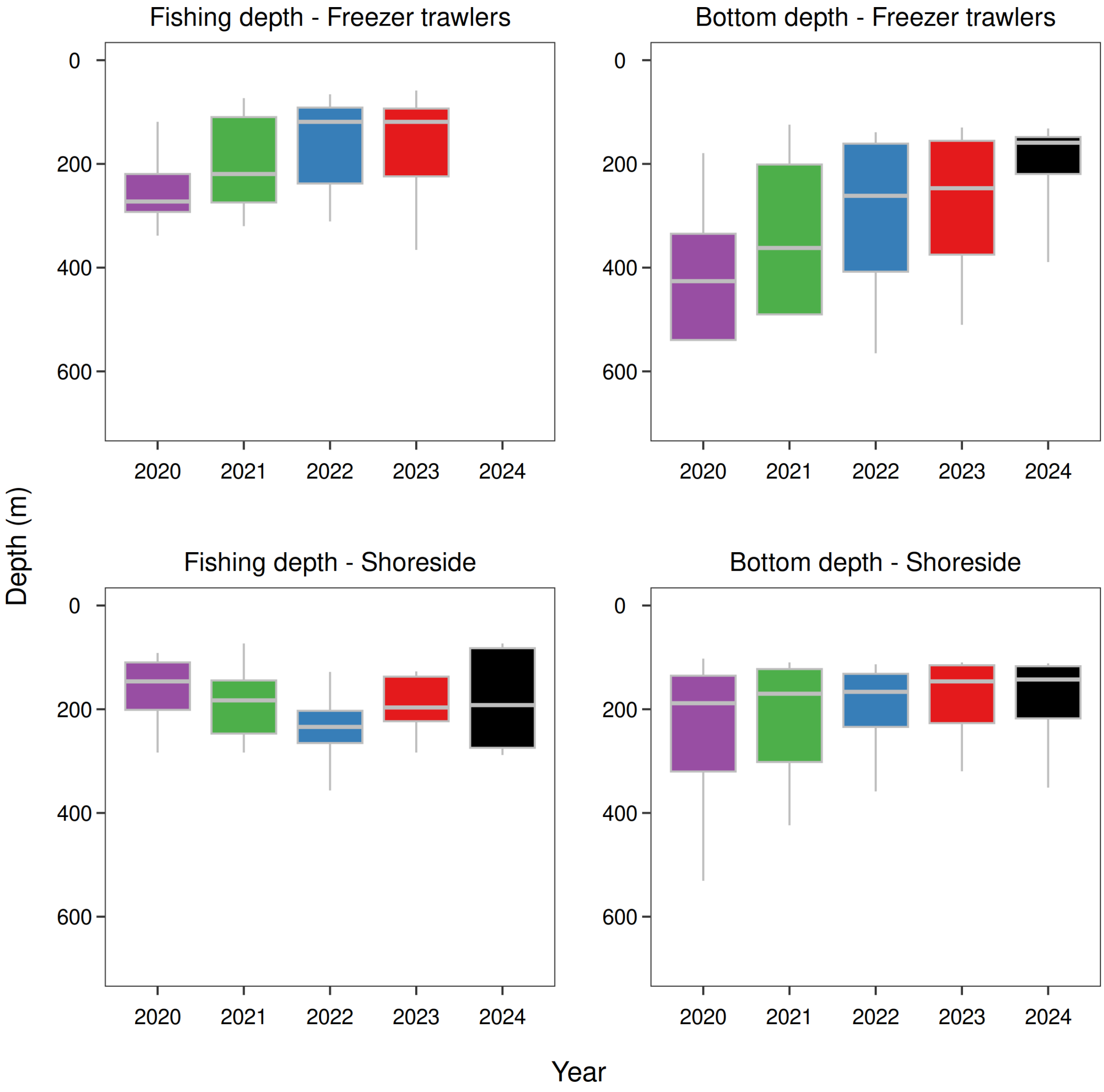

Figure 6. Distribution of fishing depths (left) and bottom depths (right), in meters, of hauls targeting Pacific Hake in the Canadian fleets from 2020–2024. Horizontal lines in each box represent the median depth and boxes encompass the middle 50% of the data. Whiskers encompass the 95% quantiles.

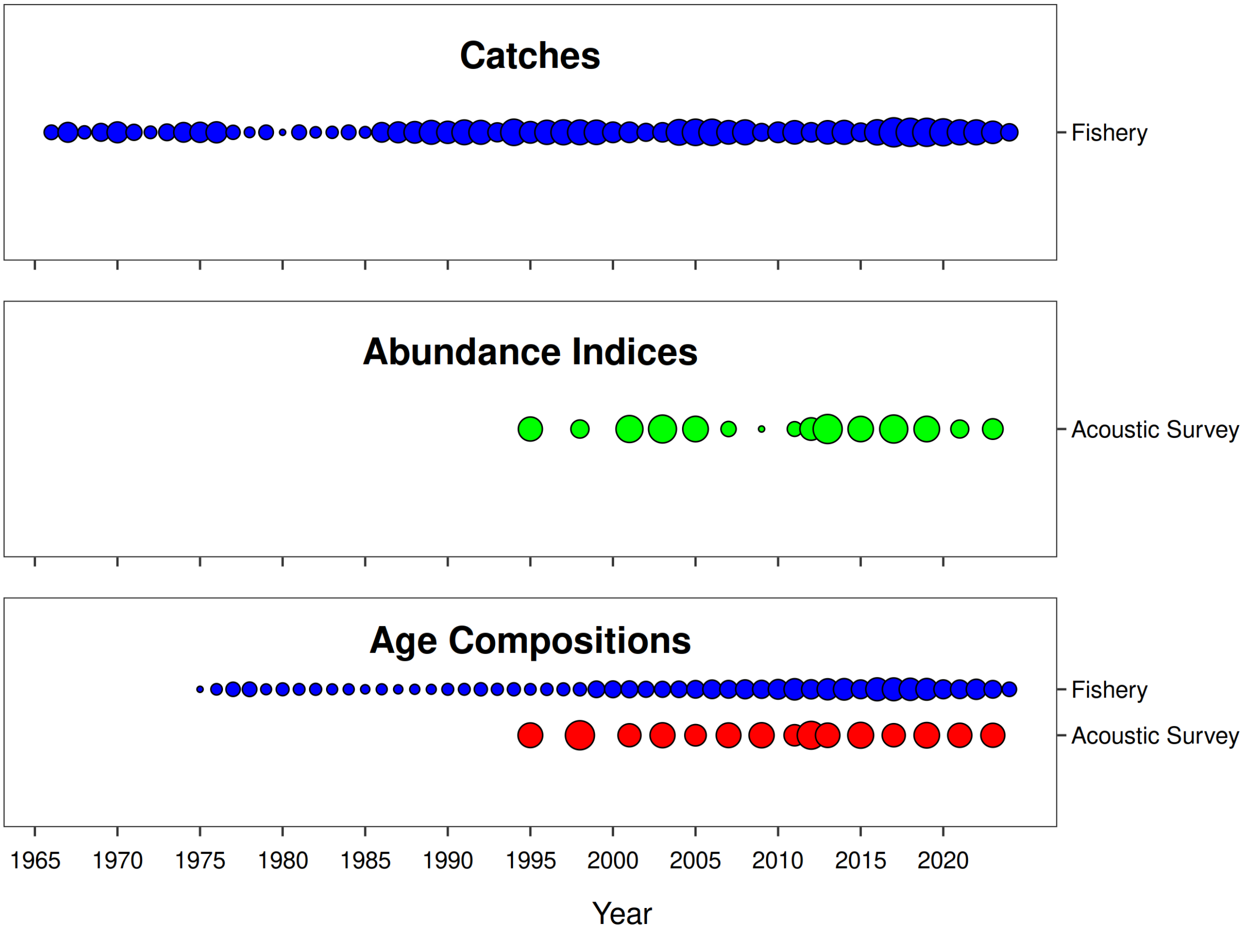

Figure 7. Overview of data used in this assessment. Circle areas are proportional to total catch for the fishery data, precision for the indices, and total sample size for the age compositions (and cannot be compared across data types). Additionally, weight-at-age data (1975–2024; not depicted here but see Figure 12 for sample sizes) are used to account for time-varying growth.

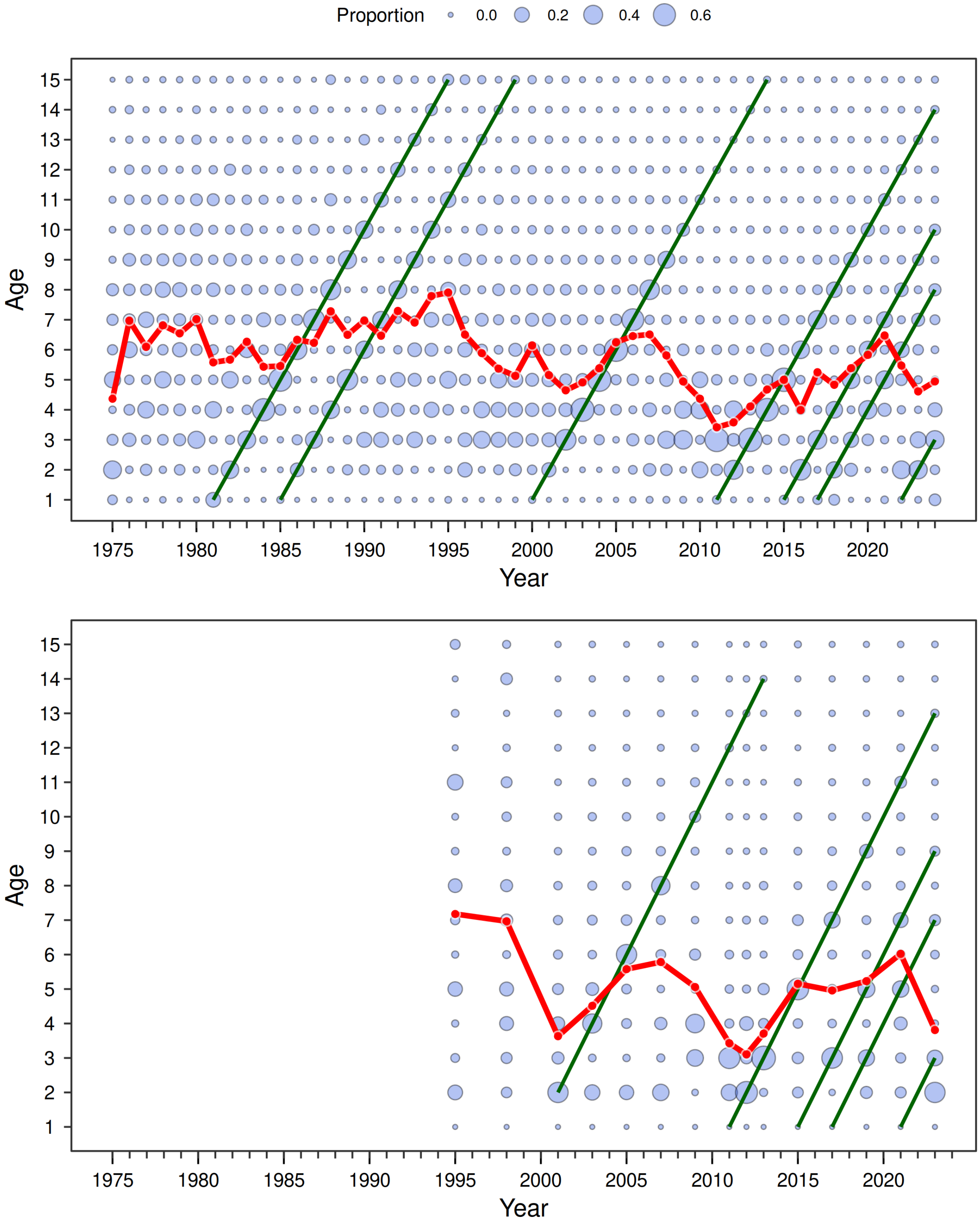

Figure 8. Age compositions for the aggregate fishery (top, all sectors combined) and acoustic survey (bottom) for the years 1975–2024. Proportions in each year sum to 1.0 and area of the bubbles are proportional to the proportion and consistent in both panels (see key at top). The largest bubble in the fishery data is 0.72 for age 3 in 2011 and in the survey data is 0.75 for age 3 in 2013. Green lines track large cohorts.

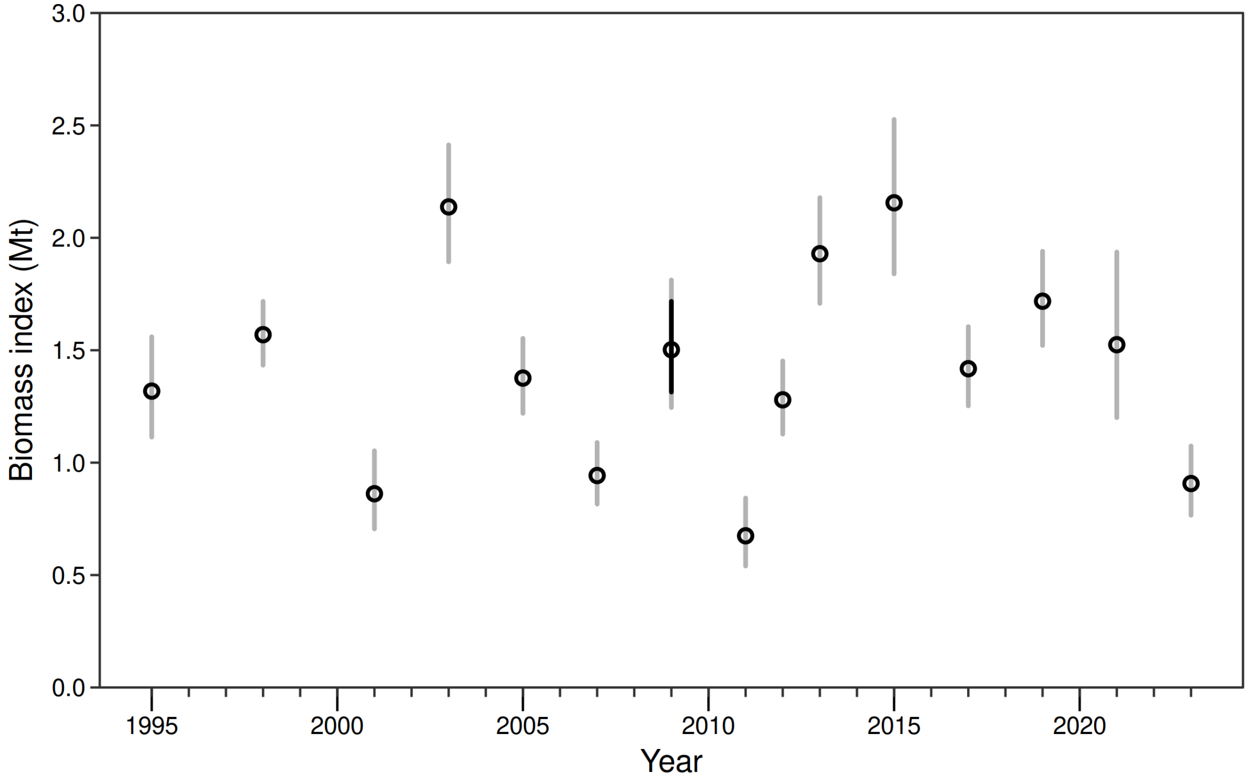

Figure 9. Acoustic survey biomass index of age-2+ fish (Mt, Table 12). Approximate 95% confidence intervals are based on sampling variability (intervals without the additional squid/Pacific Hake apportionment uncertainty included in 2009, black line).

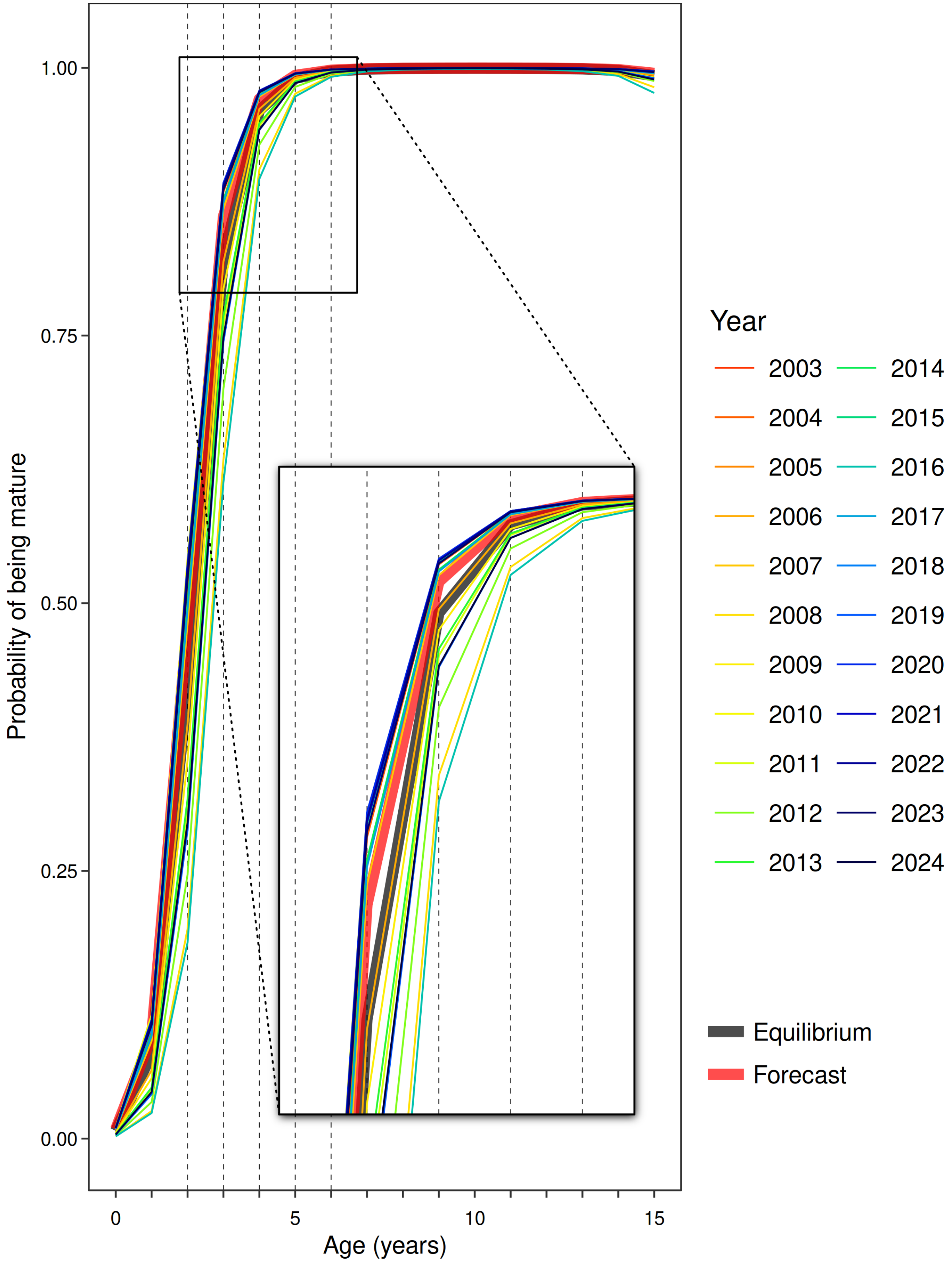

Figure 10. Maturity ogives by year used in the assessment. The thick black line shows the equilibrium ogive which is an average of all years; the thick red line shows the forecast ogive which is an average of the last five years (2020–2024). The colors of the year lines move from orange in 2009 through the spectrum to dark blue in 2024.

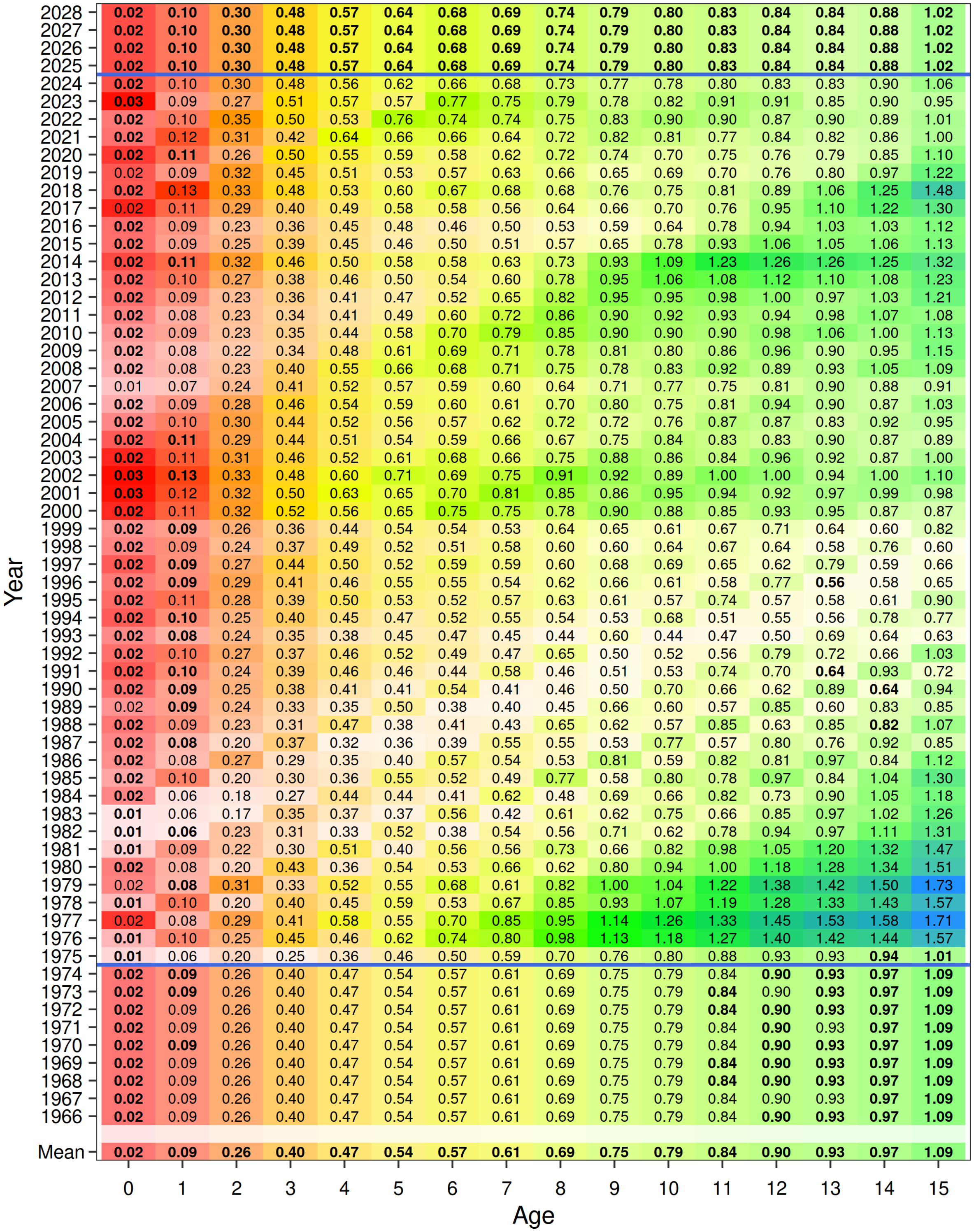

	Age															
Year	0	1	2	3	4	5	6	7	8	9	10	11	12	13	14	15
2028	**0.02**	**0.10**	**0.30**	**0.48**	**0.57**	**0.64**	**0.68**	**0.69**	**0.74**	**0.79**	**0.80**	**0.83**	**0.84**	**0.84**	**0.88**	**1.02**
2027	**0.02**	**0.10**	**0.30**	**0.48**	**0.57**	**0.64**	**0.68**	**0.69**	**0.74**	**0.79**	**0.80**	**0.83**	**0.84**	**0.84**	**0.88**	**1.02**
2026	**0.02**	**0.10**	**0.30**	**0.48**	**0.57**	**0.64**	**0.68**	**0.69**	**0.74**	**0.79**	**0.80**	**0.83**	**0.84**	**0.84**	**0.88**	**1.02**
2025	**0.02**	**0.10**	**0.30**	**0.48**	**0.57**	**0.64**	**0.68**	**0.69**	**0.74**	**0.79**	**0.80**	**0.83**	**0.84**	**0.84**	**0.88**	**1.02**
2024	**0.02**	0.10	0.30	0.48	0.56	0.62	0.66	0.68	0.73	0.77	0.78	0.80	0.83	0.83	0.90	1.06
2023	**0.03**	0.09	0.27	0.51	0.57	0.57	0.77	0.75	0.79	0.78	0.82	0.91	0.91	0.85	0.90	0.95
2022	**0.02**	0.10	0.35	0.50	0.53	0.76	0.74	0.74	0.75	0.83	0.90	0.90	0.87	0.90	0.89	1.01
2021	**0.02**	0.12	0.31	0.42	0.64	0.66	0.66	0.64	0.72	0.82	0.81	0.77	0.84	0.82	0.86	1.00
2020	**0.02**	**0.11**	0.26	0.50	0.55	0.59	0.58	0.62	0.72	0.74	0.70	0.75	0.76	0.79	0.85	1.10
2019	0.02	0.09	0.32	0.45	0.51	0.53	0.57	0.63	0.66	0.65	0.69	0.70	0.76	0.80	0.97	1.22
2018	**0.02**	0.13	0.33	0.48	0.53	0.60	0.67	0.68	0.68	0.76	0.75	0.81	0.89	1.06	1.25	1.48
2017	0.02	0.11	0.29	0.40	0.49	0.58	0.58	0.56	0.64	0.66	0.70	0.76	0.95	1.10	1.22	1.30
2016	**0.02**	0.09	0.23	0.36	0.45	0.48	0.46	0.50	0.53	0.59	0.64	0.78	0.94	1.03	1.03	1.12
2015	**0.02**	0.09	0.25	0.39	0.45	0.46	0.50	0.51	0.57	0.65	0.78	0.93	1.06	1.05	1.06	1.13
2014	**0.02**	**0.11**	0.32	0.46	0.50	0.58	0.58	0.63	0.73	0.93	1.09	1.23	1.26	1.26	1.25	1.32
2013	**0.02**	0.10	0.27	0.38	0.46	0.50	0.54	0.60	0.78	0.95	1.06	1.08	1.12	1.10	1.08	1.23
2012	**0.02**	0.09	0.23	0.36	0.41	0.47	0.52	0.65	0.82	0.95	0.95	0.98	1.00	0.97	1.03	1.21
2011	**0.02**	0.08	0.23	0.34	0.41	0.49	0.60	0.72	0.86	0.90	0.92	0.93	0.94	0.98	1.07	1.08
2010	**0.02**	0.09	0.23	0.35	0.44	0.58	0.70	0.79	0.85	0.90	0.90	0.90	0.98	1.06	1.00	1.13
2009	**0.02**	0.08	0.22	0.34	0.48	0.61	0.69	0.71	0.78	0.81	0.80	0.86	0.96	0.90	0.95	1.15
2008	**0.02**	0.08	0.23	0.40	0.55	0.66	0.68	0.71	0.75	0.78	0.83	0.92	0.89	0.93	1.05	1.09
2007	0.01	0.07	0.24	0.41	0.52	0.57	0.59	0.60	0.64	0.71	0.77	0.75	0.81	0.90	0.88	0.91
2006	**0.02**	0.09	0.28	0.46	0.54	0.59	0.60	0.61	0.70	0.80	0.75	0.81	0.94	0.90	0.87	1.03
2005	**0.02**	0.10	0.30	0.44	0.52	0.56	0.57	0.62	0.72	0.72	0.76	0.87	0.87	0.83	0.92	0.95
2004	**0.02**	**0.11**	0.29	0.44	0.51	0.54	0.59	0.66	0.67	0.75	0.84	0.83	0.83	0.90	0.87	0.89
2003	**0.02**	0.11	0.31	0.46	0.52	0.61	0.68	0.66	0.75	0.88	0.86	0.84	0.96	0.92	0.87	1.00
2002	**0.03**	**0.13**	0.33	0.48	0.60	0.71	0.69	0.75	0.91	0.92	0.89	1.00	1.00	0.94	1.00	1.10
2001	**0.03**	0.12	0.32	0.50	0.63	0.65	0.70	0.81	0.85	0.86	0.95	0.94	0.92	0.97	0.99	0.98
2000	**0.02**	0.11	0.32	0.52	0.56	0.65	0.75	0.75	0.78	0.90	0.88	0.85	0.93	0.95	0.87	0.87
1999	**0.02**	**0.09**	0.26	0.36	0.44	0.54	0.54	0.53	0.64	0.65	0.61	0.67	0.71	0.64	0.60	0.82
1998	**0.02**	0.09	0.24	0.37	0.49	0.52	0.51	0.58	0.60	0.60	0.64	0.67	0.64	0.58	0.76	0.60
1997	**0.02**	**0.09**	0.27	0.44	0.50	0.52	0.59	0.59	0.60	0.68	0.69	0.65	0.62	0.79	0.59	0.66
1996	**0.02**	**0.09**	0.29	0.41	0.46	0.55	0.55	0.54	0.62	0.66	0.61	0.58	0.77	**0.56**	0.58	0.65
1995	**0.02**	0.11	0.28	0.39	0.50	0.53	0.52	0.57	0.63	0.61	0.57	0.74	0.57	0.58	0.61	0.90
1994	**0.02**	**0.10**	0.25	0.40	0.45	0.47	0.52	0.55	0.54	0.53	0.68	0.51	0.55	0.56	0.78	0.77
1993	**0.02**	**0.08**	0.24	0.35	0.38	0.45	0.47	0.45	0.44	0.60	0.44	0.47	0.50	0.69	0.64	0.63
1992	**0.02**	0.10	0.27	0.37	0.46	0.52	0.49	0.47	0.65	0.50	0.52	0.56	0.79	0.72	0.66	1.03
1991	**0.02**	**0.10**	0.24	0.39	0.46	0.46	0.44	0.58	0.46	0.51	0.53	0.74	0.70	**0.64**	0.93	0.72
1990	**0.02**	**0.09**	0.25	0.38	0.41	0.41	0.54	0.41	0.46	0.50	0.70	0.66	0.62	0.89	**0.64**	0.94
1989	0.02	**0.09**	0.24	0.33	0.35	0.50	0.38	0.40	0.45	0.66	0.60	0.57	0.85	0.60	0.83	0.85
1988	**0.02**	0.09	0.23	0.31	0.47	0.38	0.41	0.43	0.65	0.62	0.57	0.85	0.63	0.85	**0.82**	1.07
1987	**0.02**	**0.08**	0.20	0.37	0.32	0.36	0.39	0.55	0.55	0.53	0.77	0.57	0.80	0.76	0.92	0.85
1986	**0.02**	0.08	0.27	0.29	0.35	0.40	0.57	0.54	0.53	0.81	0.59	0.82	0.81	0.97	0.84	1.12
1985	**0.02**	0.10	0.20	0.30	0.36	0.55	0.52	0.49	0.77	0.58	0.80	0.78	0.97	0.84	1.04	1.30
1984	**0.02**	0.06	0.18	0.27	0.44	0.44	0.41	0.62	0.48	0.69	0.66	0.82	0.73	0.90	1.05	1.18
1983	**0.01**	0.06	0.17	0.35	0.37	0.37	0.56	0.42	0.61	0.62	0.75	0.66	0.85	0.97	1.02	1.26
1982	**0.01**	**0.06**	0.23	0.31	0.33	0.52	0.38	0.54	0.56	0.71	0.62	0.78	0.94	0.97	1.11	1.31
1981	**0.01**	0.09	0.22	0.30	0.51	0.40	0.56	0.56	0.73	0.66	0.82	0.98	1.05	1.20	1.32	1.47
1980	**0.02**	0.08	0.20	0.43	0.36	0.54	0.53	0.66	0.62	0.80	0.94	1.00	1.18	1.28	1.34	1.51
1979	0.02	**0.08**	0.31	0.33	0.52	0.55	0.68	0.61	0.82	1.00	1.04	1.22	1.38	1.42	1.50	1.73
1978	**0.01**	0.10	0.20	0.40	0.45	0.59	0.53	0.67	0.85	0.93	1.07	1.19	1.28	1.33	1.43	1.57
1977	0.02	0.08	0.29	0.41	0.58	0.55	0.70	0.85	0.95	1.14	1.26	1.33	1.45	1.53	1.58	1.71
1976	**0.01**	0.10	0.25	0.45	0.46	0.62	0.74	0.80	0.98	1.13	1.18	1.27	1.40	1.42	1.44	1.57
1975	**0.01**	0.06	0.20	0.25	0.36	0.46	0.50	0.59	0.70	0.76	0.80	0.88	0.93	0.93	**0.94**	**1.01**
1974	**0.02**	**0.09**	0.26	0.40	0.47	0.54	0.57	0.61	0.69	0.75	0.79	0.84	**0.90**	**0.93**	**0.97**	**1.09**
1973	**0.02**	**0.09**	0.26	0.40	0.47	0.54	0.57	0.61	0.69	0.75	0.79	**0.84**	0.90	**0.93**	**0.97**	**1.09**
1972	**0.02**	0.09	0.26	0.40	0.47	0.54	0.57	0.61	0.69	0.75	0.79	**0.84**	**0.90**	**0.93**	**0.97**	**1.09**
1971	**0.02**	0.09	0.26	0.40	0.47	0.54	0.57	0.61	0.69	0.75	0.79	0.84	**0.90**	0.93	**0.97**	**1.09**
1970	**0.02**	**0.09**	0.26	0.40	0.47	0.54	0.57	0.61	0.69	0.75	0.79	0.84	**0.90**	**0.93**	**0.97**	**1.09**
1969	**0.02**	0.09	0.26	0.40	0.47	0.54	0.57	0.61	0.69	0.75	0.79	**0.84**	**0.90**	**0.93**	**0.97**	**1.09**
1968	**0.02**	0.09	0.26	0.40	0.47	0.54	0.57	0.61	0.69	0.75	0.79	**0.84**	**0.90**	**0.93**	**0.97**	**1.09**
1967	**0.02**	0.09	0.26	0.40	0.47	0.54	0.57	0.61	0.69	0.75	0.79	0.84	0.90	0.93	**0.97**	**1.09**
1966	**0.02**	0.09	0.26	0.40	0.47	0.54	0.57	0.61	0.69	0.75	0.79	0.84	**0.90**	**0.93**	**0.97**	**1.09**
Mean	**0.02**	**0.09**	**0.26**	**0.40**	**0.47**	**0.54**	**0.57**	**0.61**	**0.69**	**0.75**	**0.79**	**0.84**	**0.90**	**0.93**	**0.97**	**1.09**

Figure 11. Empirical weight-at-age (kg) values used for the base model as predicted from the time-varying model. Colors correspond to the values, with red being the lightest fish (across all years and ages) and blue being the heaviest fish. For each age, the most transparent cells indicate the lightest fish of that age. Data are only available from 1975–2024. Values based on assumptions for the pre-1975 and forecast years are shown outside the blue lines. Bold values between 1975–2024 represent unavailable data such that weights were predicted from the time-varying model. The bottom row (mean) is the mean weight-at-age over all years of data.

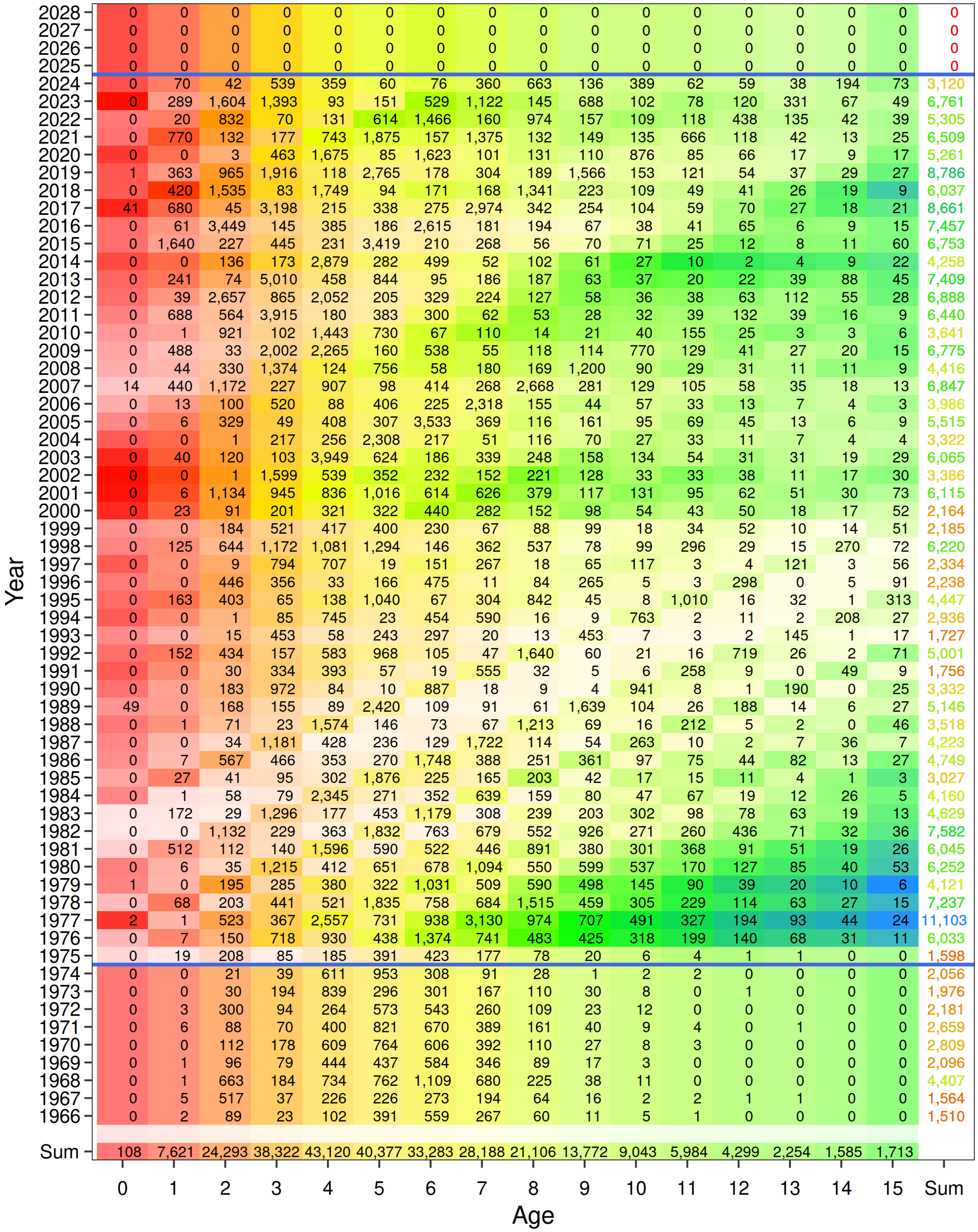

Year	0	1	2	3	4	5	6	7	8	9	10	11	12	13	14	15	Sum
2028	0	0	0	0	0	0	0	0	0	0	0	0	0	0	0	0	0
2027	0	0	0	0	0	0	0	0	0	0	0	0	0	0	0	0	0
2026	0	0	0	0	0	0	0	0	0	0	0	0	0	0	0	0	0
2025	0	0	0	0	0	0	0	0	0	0	0	0	0	0	0	0	0
2024	0	70	42	539	359	60	76	360	663	136	389	62	59	38	194	73	3,120
2023	0	289	1,604	1,393	93	151	529	1,122	145	688	102	78	120	331	67	49	6,761
2022	0	20	832	70	131	614	1,466	160	974	157	109	118	438	135	42	39	5,305
2021	0	770	132	177	743	1,875	157	1,375	132	149	135	666	118	42	13	25	6,509
2020	0	0	3	463	1,675	85	1,623	101	131	110	876	85	66	17	9	17	5,261
2019	1	363	965	1,916	118	2,765	178	304	189	1,566	153	121	54	37	29	27	8,786
2018	0	420	1,535	83	1,749	94	171	168	1,341	223	109	49	41	26	19	9	6,037
2017	41	680	45	3,198	215	338	275	2,974	342	254	104	59	70	27	18	21	8,661
2016	0	61	3,449	145	385	186	2,615	181	194	67	38	41	65	6	9	15	7,457
2015	0	1,640	227	445	231	3,419	210	268	56	70	71	25	12	8	11	60	6,753
2014	0	0	136	173	2,879	282	499	52	102	61	27	10	2	4	9	22	4,258
2013	0	241	74	5,010	458	844	95	186	187	63	37	20	22	39	88	45	7,409
2012	0	39	2,657	865	2,052	205	329	224	127	58	36	38	63	112	55	28	6,888
2011	0	688	564	3,915	180	383	300	62	53	28	32	39	132	39	16	9	6,440
2010	0	1	921	102	1,443	730	67	110	14	21	40	155	25	3	3	6	3,641
2009	0	488	33	2,002	2,265	160	538	55	118	114	770	129	41	27	20	15	6,775
2008	0	44	330	1,374	124	756	58	180	169	1,200	90	29	31	11	11	9	4,416
2007	14	440	1,172	227	907	98	414	268	2,668	281	129	105	58	35	18	13	6,847
2006	0	13	100	520	88	406	225	2,318	155	44	57	33	13	7	4	3	3,986
2005	0	6	329	49	408	307	3,533	369	116	161	95	69	45	13	6	9	5,515
2004	0	0	1	217	256	2,308	217	51	116	70	27	33	11	7	4	4	3,322
2003	0	40	120	103	3,949	624	186	339	248	158	134	54	31	31	19	29	6,065
2002	0	0	1	1,599	539	352	232	152	221	128	33	33	38	11	17	30	3,386
2001	0	6	1,134	945	836	1,016	614	626	379	117	131	95	62	51	30	73	6,115
2000	0	23	91	201	321	322	440	282	152	98	54	43	50	18	17	52	2,164
1999	0	0	184	521	417	400	230	67	88	99	18	34	52	10	14	51	2,185
1998	0	125	644	1,172	1,081	1,294	146	362	537	78	99	296	29	15	270	72	6,220
1997	0	0	9	794	707	19	151	267	18	65	117	3	4	121	3	56	2,334
1996	0	0	446	356	33	166	475	11	84	265	5	3	298	0	5	91	2,238
1995	0	163	403	65	138	1,040	67	304	842	45	8	1,010	16	32	1	313	4,447
1994	0	0	1	85	745	23	454	590	16	9	763	2	11	2	208	27	2,936
1993	0	0	15	453	58	243	297	20	13	453	7	3	2	145	1	17	1,727
1992	0	152	434	157	583	968	105	47	1,640	60	21	16	719	26	2	71	5,001
1991	0	0	30	334	393	57	19	555	32	5	6	258	9	0	49	9	1,756
1990	0	0	183	972	84	10	887	18	9	4	941	8	1	190	0	25	3,332
1989	49	0	168	155	89	2,420	109	91	61	1,639	104	26	188	14	6	27	5,146
1988	0	1	71	23	1,574	146	73	67	1,213	69	16	212	5	2	0	46	3,518
1987	0	0	34	1,181	428	236	129	1,722	114	54	263	10	2	7	36	7	4,223
1986	0	7	567	466	353	270	1,748	388	251	361	97	75	44	82	13	27	4,749
1985	0	27	41	95	302	1,876	225	165	203	42	17	15	11	4	1	3	3,027
1984	0	1	58	79	2,345	271	352	639	159	80	47	67	19	12	26	5	4,160
1983	0	172	29	1,296	177	453	1,179	308	239	203	302	98	78	63	19	13	4,629
1982	0	0	1,132	229	363	1,832	763	679	552	926	271	260	436	71	32	36	7,582
1981	0	512	112	140	1,596	590	522	446	891	380	301	368	91	51	19	26	6,045
1980	0	6	35	1,215	412	651	678	1,094	550	599	537	170	127	85	40	53	6,252
1979	1	0	195	285	380	322	1,031	509	590	498	145	90	39	20	10	6	4,121
1978	0	68	203	441	521	1,835	758	684	1,515	459	305	229	114	63	27	15	7,237
1977	2	1	523	367	2,557	731	938	3,130	974	707	491	327	194	93	44	24	11,103
1976	0	7	150	718	930	438	1,374	741	483	425	318	199	140	68	31	11	6,033
1975	0	19	208	85	185	391	423	177	78	20	6	4	1	1	0	0	1,598
1974	0	0	21	39	611	953	308	91	28	1	2	2	0	0	0	0	2,056
1973	0	0	30	194	839	296	301	167	110	30	8	0	1	0	0	0	1,976
1972	0	3	300	94	264	573	543	260	109	23	12	0	0	0	0	0	2,181
1971	0	6	88	70	400	821	670	389	161	40	9	4	0	1	0	0	2,659
1970	0	0	112	178	609	764	606	392	110	27	8	3	0	0	0	0	2,809
1969	0	1	96	79	444	437	584	346	89	17	3	0	0	0	0	0	2,096
1968	0	1	663	184	734	762	1,109	680	225	38	11	0	0	0	0	0	4,407
1967	0	5	517	37	226	226	273	194	64	16	2	2	1	1	0	0	1,564
1966	0	2	89	23	102	391	559	267	60	11	5	1	0	0	0	0	1,510
Sum	108	7,621	24,293	38,322	43,120	40,377	33,283	28,188	21,106	13,772	9,043	5,984	4,299	2,254	1,585	1,713	

Figure 12. Sample sizes of empirical weight-at-age measurements used to fit the time-varying model used to estimate mean weight-at-age that is used in the base model. Colors and transparency are identical to Figure 11. Sample sizes of zero highlight years for which data are not available, i.e., pre 1975 and post 2024. The total sample sizes for each age used in the model over all data years are shown at the bottom and year-specific sample sizes are shown to the right using the same color scale with red indicating small sample sizes and blue indicating the large sample sizes.

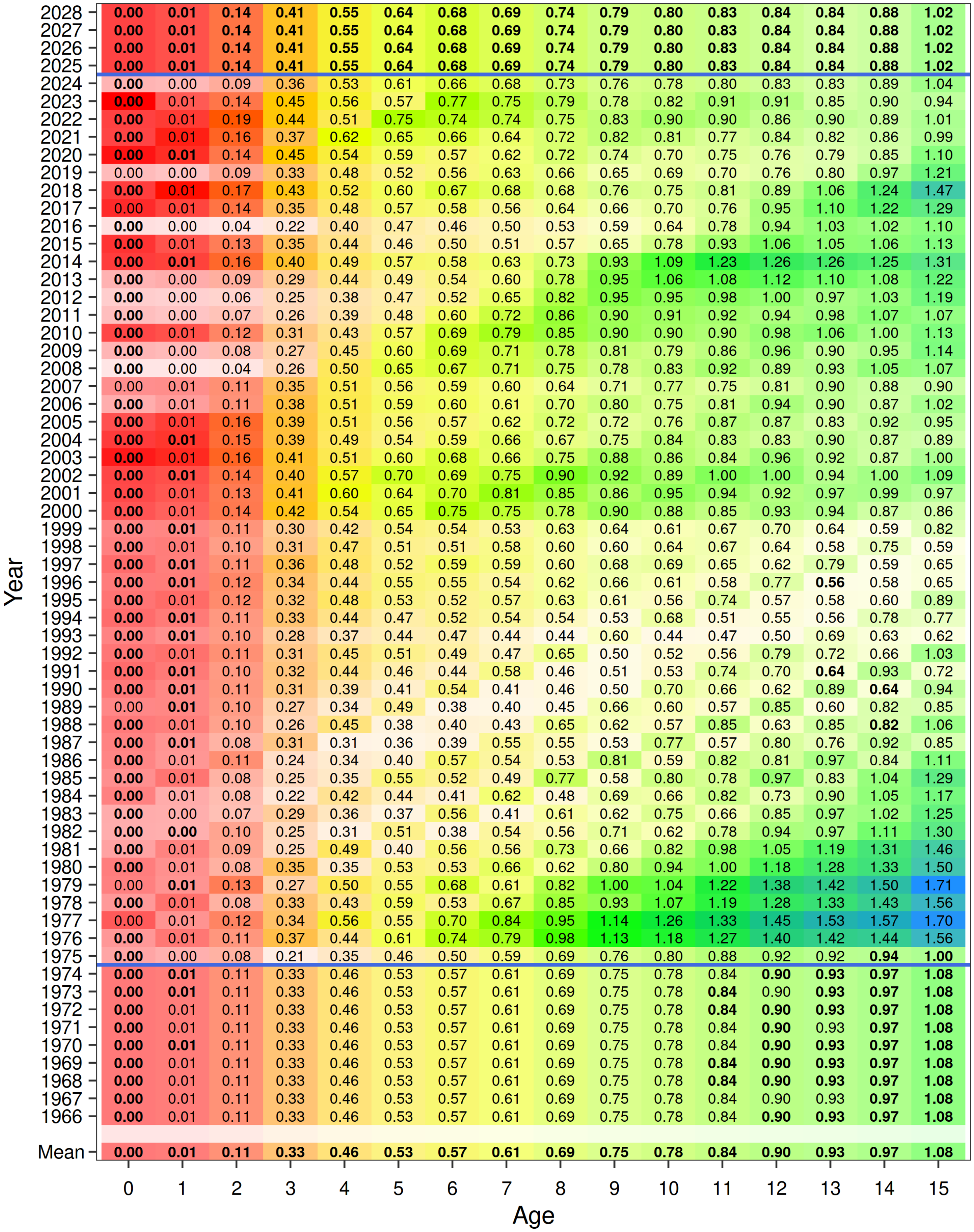

Year	0	1	2	3	4	5	6	7	8	9	10	11	12	13	14	15
2028	**0.00**	**0.01**	**0.14**	**0.41**	**0.55**	**0.64**	**0.68**	**0.69**	**0.74**	**0.79**	**0.80**	**0.83**	**0.84**	**0.84**	**0.88**	**1.02**
2027	**0.00**	**0.01**	**0.14**	**0.41**	**0.55**	**0.64**	**0.68**	**0.69**	**0.74**	**0.79**	**0.80**	**0.83**	**0.84**	**0.84**	**0.88**	**1.02**
2026	**0.00**	**0.01**	**0.14**	**0.41**	**0.55**	**0.64**	**0.68**	**0.69**	**0.74**	**0.79**	**0.80**	**0.83**	**0.84**	**0.84**	**0.88**	**1.02**
2025	**0.00**	**0.01**	**0.14**	**0.41**	**0.55**	**0.64**	**0.68**	**0.69**	**0.74**	**0.79**	**0.80**	**0.83**	**0.84**	**0.84**	**0.88**	**1.02**
2024	**0.00**	0.00	0.09	0.36	0.53	0.61	0.66	0.68	0.73	0.76	0.78	0.80	0.83	0.83	0.89	1.04
2023	**0.00**	0.01	0.14	0.45	0.56	0.57	0.77	0.75	0.79	0.78	0.82	0.91	0.91	0.85	0.90	0.94
2022	**0.00**	0.01	0.19	0.44	0.51	0.75	0.74	0.74	0.75	0.83	0.90	0.90	0.86	0.90	0.89	1.01
2021	**0.00**	0.01	0.16	0.37	0.62	0.65	0.66	0.64	0.72	0.82	0.81	0.77	0.84	0.82	0.86	0.99
2020	**0.00**	**0.01**	0.14	0.45	0.54	0.59	0.57	0.62	0.72	0.74	0.70	0.75	0.76	0.79	0.85	1.10
2019	0.00	0.00	0.09	0.33	0.48	0.52	0.56	0.63	0.66	0.65	0.69	0.70	0.76	0.80	0.97	1.21
2018	**0.00**	0.01	0.17	0.43	0.52	0.60	0.67	0.68	0.68	0.76	0.75	0.81	0.89	1.06	1.24	1.47
2017	0.00	0.01	0.14	0.35	0.48	0.57	0.58	0.56	0.64	0.66	0.70	0.76	0.95	1.10	1.22	1.29
2016	**0.00**	0.00	0.04	0.22	0.40	0.47	0.46	0.50	0.53	0.59	0.64	0.78	0.94	1.03	1.02	1.10
2015	**0.00**	0.01	0.13	0.35	0.44	0.46	0.50	0.51	0.57	0.65	0.78	0.93	1.06	1.05	1.06	1.13
2014	**0.00**	**0.01**	0.16	0.40	0.49	0.57	0.58	0.63	0.73	0.93	1.09	1.23	1.26	1.26	1.25	1.31
2013	**0.00**	0.00	0.09	0.29	0.44	0.49	0.54	0.60	0.78	0.95	1.06	1.08	1.12	1.10	1.08	1.22
2012	**0.00**	0.00	0.06	0.25	0.38	0.47	0.52	0.65	0.82	0.95	0.95	0.98	1.00	0.97	1.03	1.19
2011	**0.00**	0.00	0.07	0.26	0.39	0.48	0.60	0.72	0.86	0.90	0.91	0.92	0.94	0.98	1.07	1.07
2010	**0.00**	0.01	0.12	0.31	0.43	0.57	0.69	0.79	0.85	0.90	0.90	0.90	0.98	1.06	1.00	1.13
2009	**0.00**	0.00	0.08	0.27	0.45	0.60	0.69	0.71	0.78	0.81	0.79	0.86	0.96	0.90	0.95	1.14
2008	**0.00**	0.00	0.04	0.26	0.50	0.65	0.67	0.71	0.75	0.78	0.83	0.92	0.89	0.93	1.05	1.07
2007	0.00	0.01	0.11	0.35	0.51	0.56	0.59	0.60	0.64	0.71	0.77	0.75	0.81	0.90	0.88	0.90
2006	**0.00**	0.01	0.11	0.38	0.51	0.59	0.60	0.61	0.70	0.80	0.75	0.81	0.94	0.90	0.87	1.02
2005	**0.00**	0.01	0.16	0.39	0.51	0.56	0.57	0.62	0.72	0.72	0.76	0.87	0.87	0.83	0.92	0.95
2004	**0.00**	**0.01**	0.15	0.39	0.49	0.54	0.59	0.66	0.67	0.75	0.84	0.83	0.83	0.90	0.87	0.89
2003	**0.00**	0.01	0.16	0.41	0.51	0.60	0.68	0.66	0.75	0.88	0.86	0.84	0.96	0.92	0.87	1.00
2002	**0.00**	**0.01**	0.14	0.40	0.57	0.70	0.69	0.75	0.90	0.92	0.89	1.00	1.00	0.94	1.00	1.09
2001	**0.00**	0.01	0.13	0.41	0.60	0.64	0.70	0.81	0.85	0.86	0.95	0.94	0.92	0.97	0.99	0.97
2000	**0.00**	0.01	0.14	0.42	0.54	0.65	0.75	0.75	0.78	0.90	0.88	0.85	0.93	0.94	0.87	0.86
1999	**0.00**	**0.01**	0.11	0.30	0.42	0.54	0.54	0.53	0.63	0.64	0.61	0.67	0.70	0.64	0.59	0.82
1998	**0.00**	0.01	0.10	0.31	0.47	0.51	0.51	0.58	0.60	0.60	0.64	0.67	0.64	0.58	0.75	0.59
1997	**0.00**	**0.01**	0.11	0.36	0.48	0.52	0.59	0.59	0.60	0.68	0.69	0.65	0.62	0.79	0.59	0.65
1996	**0.00**	**0.01**	0.12	0.34	0.44	0.55	0.55	0.54	0.62	0.66	0.61	0.58	0.77	**0.56**	0.58	0.65
1995	**0.00**	0.01	0.12	0.32	0.48	0.53	0.52	0.57	0.63	0.61	0.56	0.74	0.57	0.58	0.60	0.89
1994	**0.00**	**0.01**	0.11	0.33	0.44	0.47	0.52	0.54	0.54	0.53	0.68	0.51	0.55	0.56	0.78	0.77
1993	**0.00**	**0.01**	0.10	0.28	0.37	0.44	0.47	0.44	0.44	0.60	0.44	0.47	0.50	0.69	0.63	0.62
1992	**0.00**	0.01	0.11	0.31	0.45	0.51	0.49	0.47	0.65	0.50	0.52	0.56	0.79	0.72	0.66	1.03
1991	**0.00**	**0.01**	0.10	0.32	0.44	0.46	0.44	0.58	0.46	0.51	0.53	0.74	0.70	**0.64**	0.93	0.72
1990	**0.00**	**0.01**	0.11	0.31	0.39	0.41	0.54	0.41	0.46	0.50	0.70	0.66	0.62	0.89	**0.64**	0.94
1989	0.00	**0.01**	0.10	0.27	0.34	0.49	0.38	0.40	0.45	0.66	0.60	0.57	0.85	0.60	0.82	0.85
1988	**0.00**	0.01	0.10	0.26	0.45	0.38	0.40	0.43	0.65	0.62	0.57	0.85	0.63	0.85	**0.82**	1.06
1987	**0.00**	**0.01**	0.08	0.31	0.31	0.36	0.39	0.55	0.55	0.53	0.77	0.57	0.80	0.76	0.92	0.85
1986	**0.00**	0.01	0.11	0.24	0.34	0.40	0.57	0.54	0.53	0.81	0.59	0.82	0.81	0.97	0.84	1.11
1985	**0.00**	0.01	0.08	0.25	0.35	0.55	0.52	0.49	0.77	0.58	0.80	0.78	0.97	0.83	1.04	1.29
1984	**0.00**	0.01	0.08	0.22	0.42	0.44	0.41	0.62	0.48	0.69	0.66	0.82	0.73	0.90	1.05	1.17
1983	**0.00**	0.00	0.07	0.29	0.36	0.37	0.56	0.41	0.61	0.62	0.75	0.66	0.85	0.97	1.02	1.25
1982	**0.00**	**0.00**	0.10	0.25	0.31	0.51	0.38	0.54	0.56	0.71	0.62	0.78	0.94	0.97	1.11	1.30
1981	**0.00**	0.01	0.09	0.25	0.49	0.40	0.56	0.56	0.73	0.66	0.82	0.98	1.05	1.19	1.31	1.46
1980	**0.00**	0.01	0.08	0.35	0.35	0.53	0.53	0.66	0.62	0.80	0.94	1.00	1.18	1.28	1.33	1.50
1979	0.00	**0.01**	0.13	0.27	0.50	0.55	0.68	0.61	0.82	1.00	1.04	1.22	1.38	1.42	1.50	1.71
1978	**0.00**	0.01	0.08	0.33	0.43	0.59	0.53	0.67	0.85	0.93	1.07	1.19	1.28	1.33	1.43	1.56
1977	0.00	0.01	0.12	0.34	0.56	0.55	0.70	0.84	0.95	1.14	1.26	1.33	1.45	1.53	1.57	1.70
1976	**0.00**	0.01	0.11	0.37	0.44	0.61	0.74	0.79	0.98	1.13	1.18	1.27	1.40	1.42	1.44	1.56
1975	**0.00**	0.00	0.08	0.21	0.35	0.46	0.50	0.59	0.69	0.76	0.80	0.88	0.92	0.92	**0.94**	**1.00**
1974	**0.00**	**0.01**	0.11	0.33	0.46	0.53	0.57	0.61	0.69	0.75	0.78	0.84	**0.90**	**0.93**	**0.97**	**1.08**
1973	**0.00**	**0.01**	0.11	0.33	0.46	0.53	0.57	0.61	0.69	0.75	0.78	**0.84**	0.90	**0.93**	**0.97**	**1.08**
1972	**0.00**	0.01	0.11	0.33	0.46	0.53	0.57	0.61	0.69	0.75	0.78	**0.84**	**0.90**	**0.93**	**0.97**	**1.08**
1971	**0.00**	0.01	0.11	0.33	0.46	0.53	0.57	0.61	0.69	0.75	0.78	0.84	**0.90**	0.93	**0.97**	**1.08**
1970	**0.00**	**0.01**	0.11	0.33	0.46	0.53	0.57	0.61	0.69	0.75	0.78	0.84	**0.90**	**0.93**	**0.97**	**1.08**
1969	**0.00**	0.01	0.11	0.33	0.46	0.53	0.57	0.61	0.69	0.75	0.78	**0.84**	**0.90**	**0.93**	**0.97**	**1.08**
1968	**0.00**	0.01	0.11	0.33	0.46	0.53	0.57	0.61	0.69	0.75	0.78	**0.84**	**0.90**	**0.93**	**0.97**	**1.08**
1967	**0.00**	0.01	0.11	0.33	0.46	0.53	0.57	0.61	0.69	0.75	0.78	0.84	0.90	0.93	**0.97**	**1.08**
1966	**0.00**	0.01	0.11	0.33	0.46	0.53	0.57	0.61	0.69	0.75	0.78	0.84	**0.90**	**0.93**	**0.97**	**1.08**
Mean	**0.00**	**0.01**	**0.11**	**0.33**	**0.46**	**0.53**	**0.57**	**0.61**	**0.69**	**0.75**	**0.78**	**0.84**	**0.90**	**0.93**	**0.97**	**1.08**

Figure 13. Fecundity-at-age values used for the base model. Colors correspond to the values, with red being the least fecund fish (across all years and ages) and blue being the most fecund fish. For each age, the most transparent cells indicate the least fecund fish of that age. Fecundity is the product of maturity and weight-at-age. Weight-at-age data are only available from 1975–2024. Values based on assumptions for the pre-data and forecast years are shown outside the blue lines. Bold values between 1975–2024 represent year/age combinations where weight-at-age data were unavailable to fit the model such that weights were predicted rather than estimated.

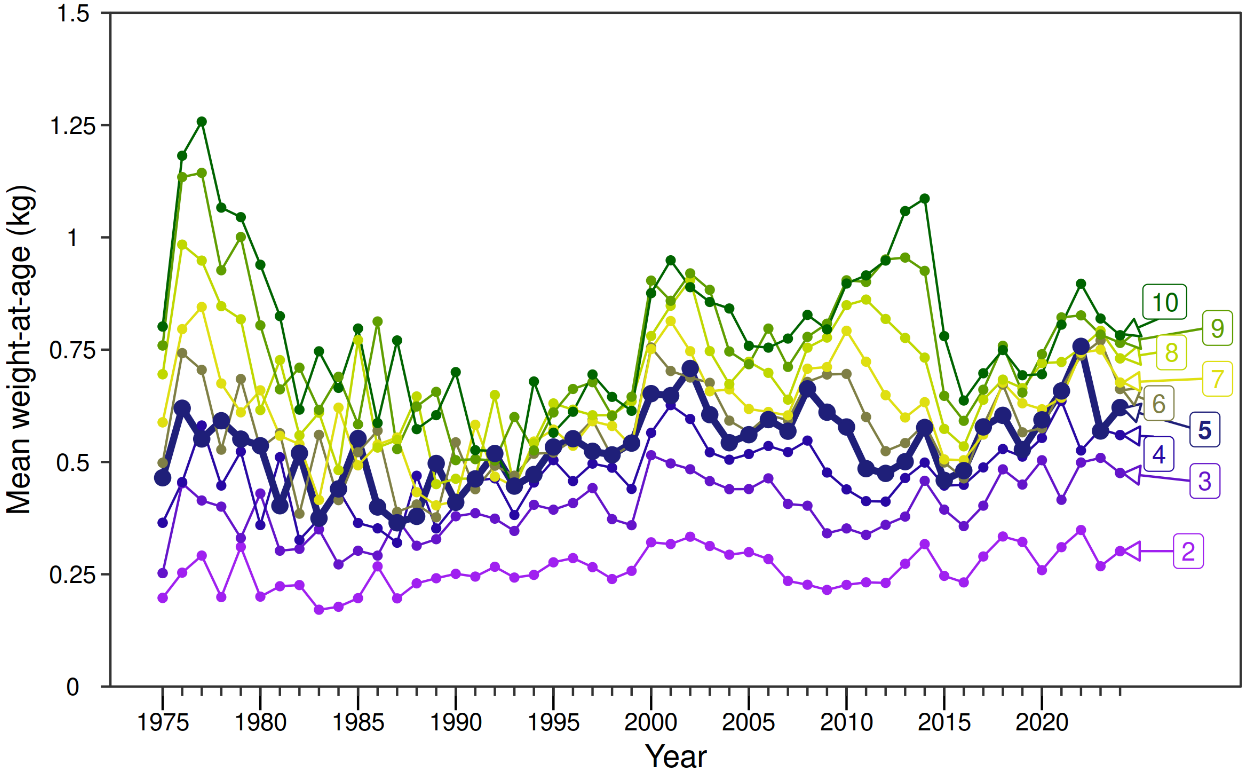

Figure 14. Empirical mean weight-at-age (kg) values for ages 2–10 used for the base model, as in Figure 11 but shown as time series. Purple lines are for the youngest ages and green lines are for the oldest ages shown, with age-5 having a thicker line and larger points as a visual aid.

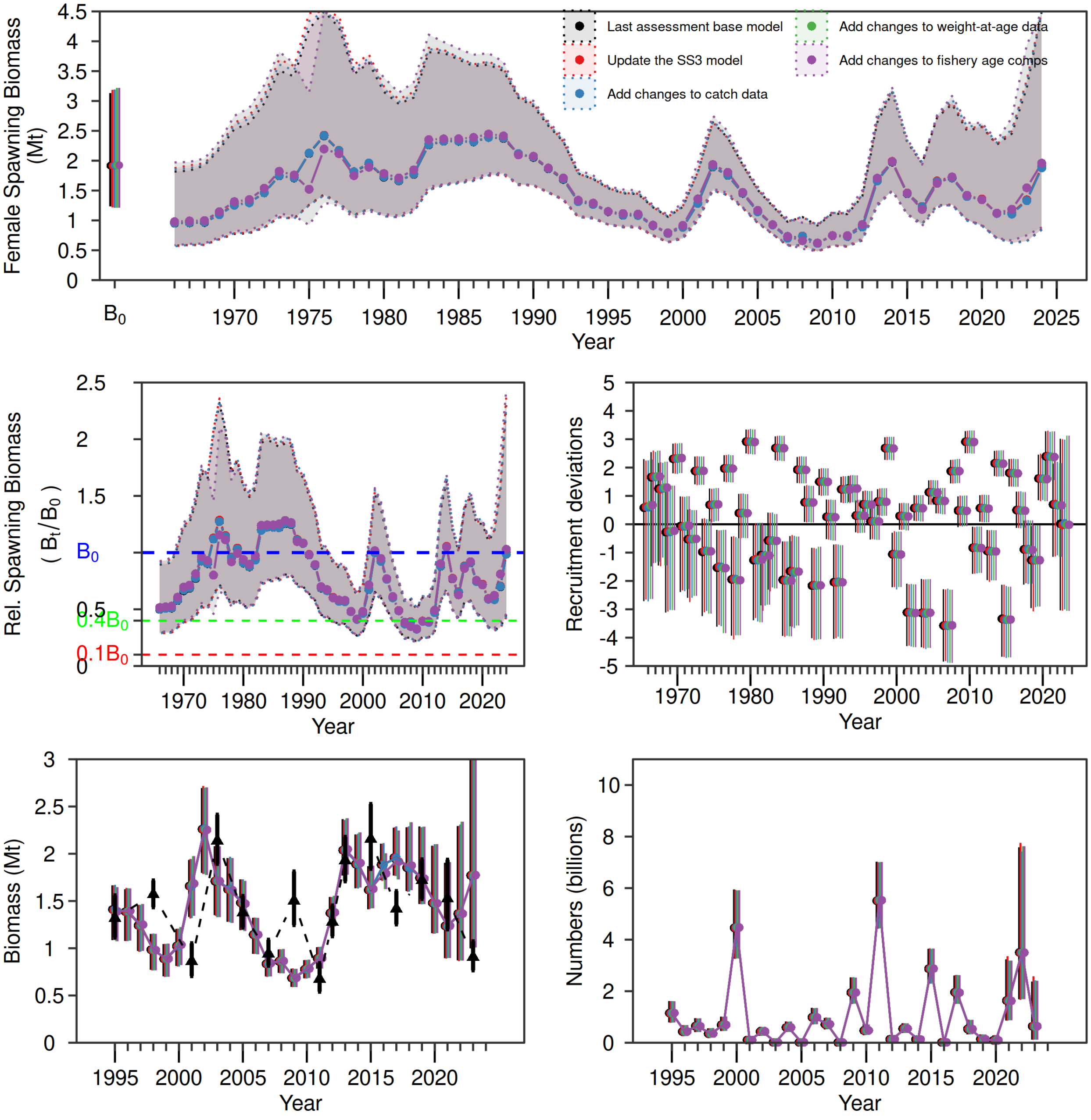

Figure 15. Bridging models showing some of the sequential steps made towards the 2025 base model from the 2024 base model. Models include shifting to the newest version of Stock Synthesis and amending older data sources. Panels are spawning biomass (upper panel); relative spawning biomass (spawning biomass in each year relative to the unfished equilibrium spawning biomass, middle left); recruitment deviations (middle right); and age-2+ survey biomass (lower left) and age-1 (lower right) indices, with triangles representing the observed survey indices.

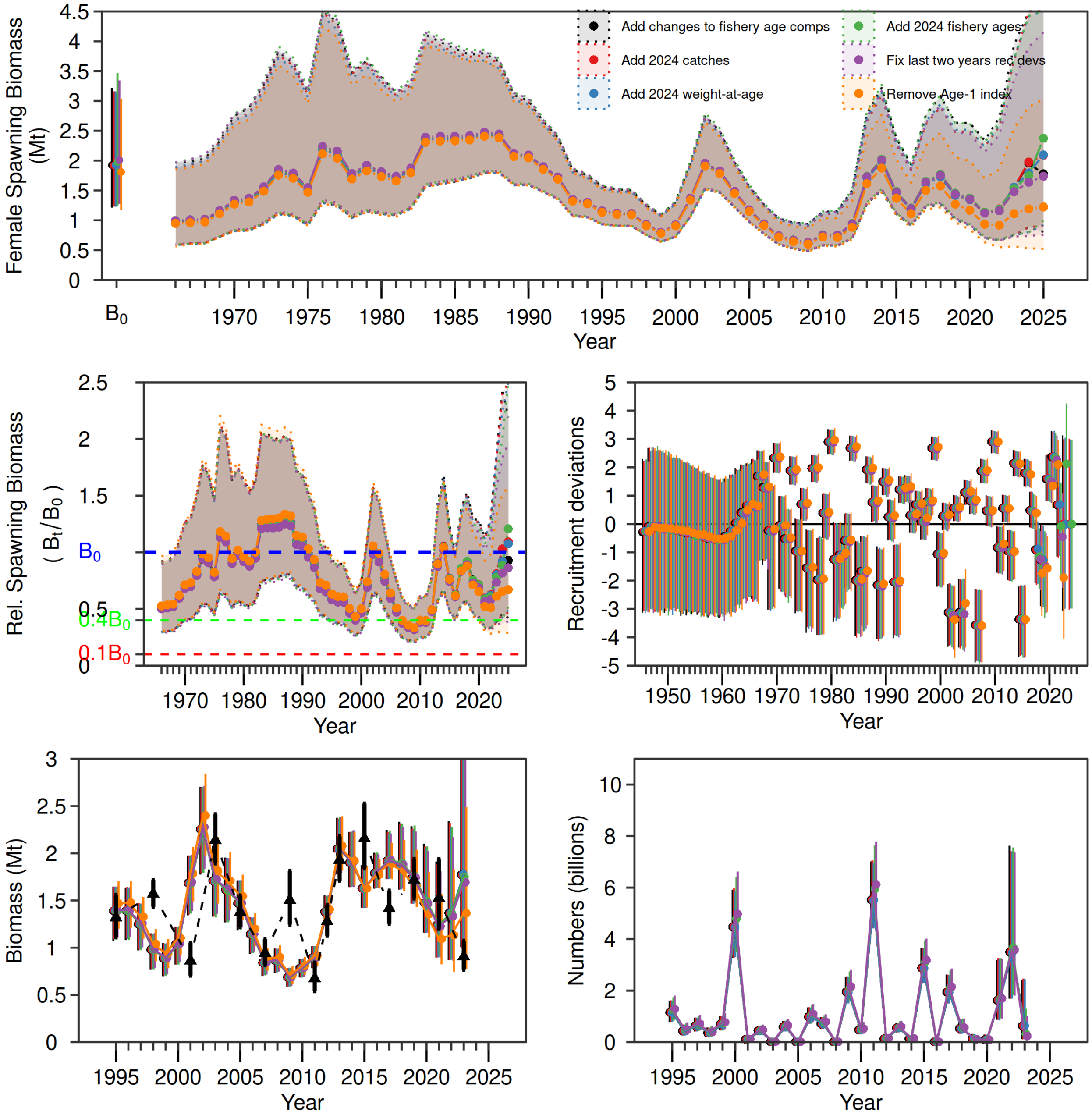

Figure 16. Bridging models showing some of the sequential steps made towards the 2025 base model from the 2024 base model. Models include the last step from the previous figure of updating older data, the addition of new data inputs for the current year, and structural changes to the model. Panels are spawning biomass (upper panel); relative spawning biomass (spawning biomass in each year relative to the unfished equilibrium spawning biomass, middle left); recruitment deviations (middle right); and age-2+ survey biomass (lower left) and age-1 (lower right) indices, with triangles representing the observed survey indices.

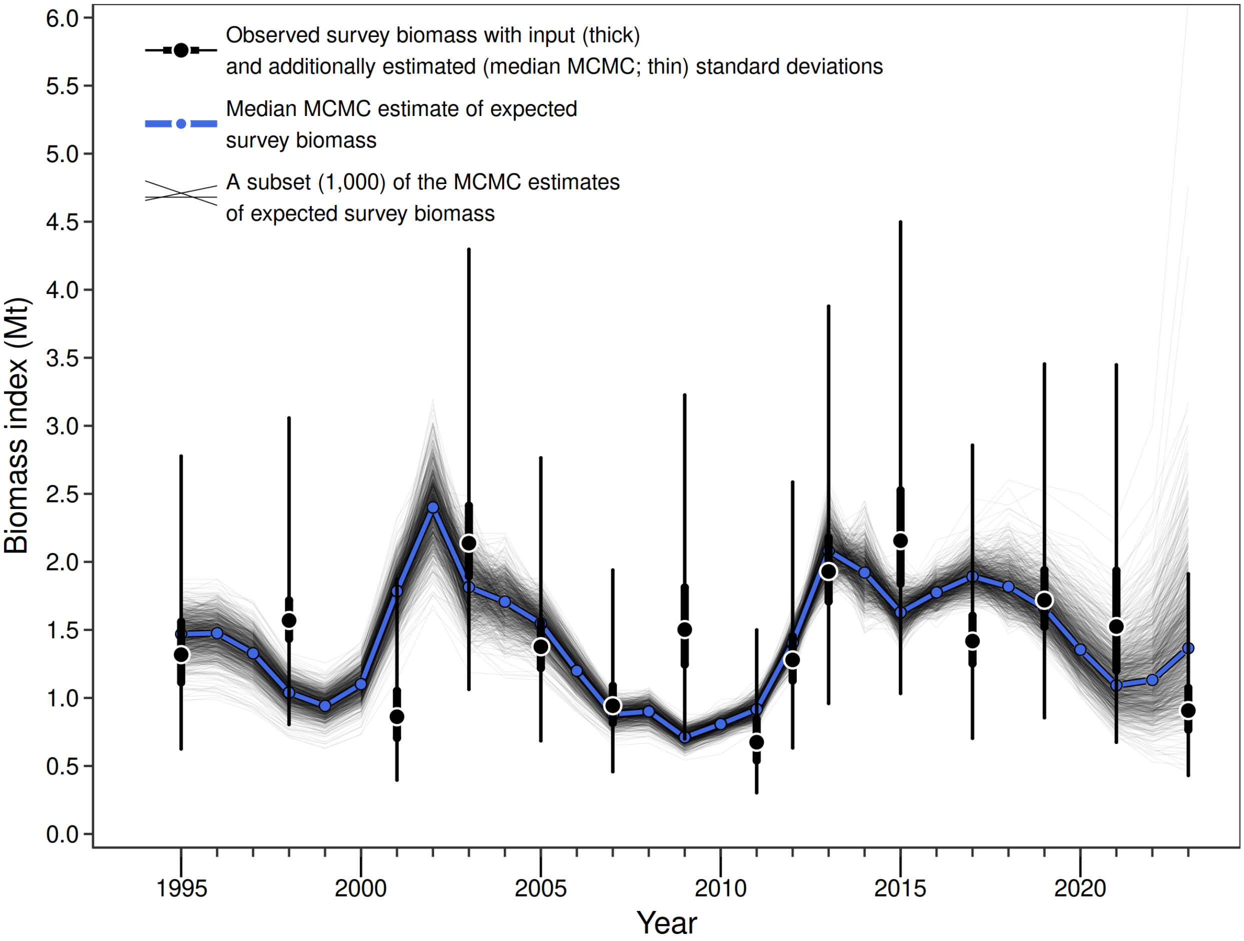

Figure 17. Fits (thin black lines) to the acoustic survey (points) with input 95% intervals around the observations. The thin black lines are the results of a random subset of individual Markov chain Monte Carlo (MCMC) samples. Thick, vertical black lines around observed survey points indicate 95% lognormal uncertainty intervals estimated by the kriging method and are used as input to the assessment model. Thin, vertical black lines indicate estimated 95% uncertainty intervals that account for the model estimate of additional uncertainty.

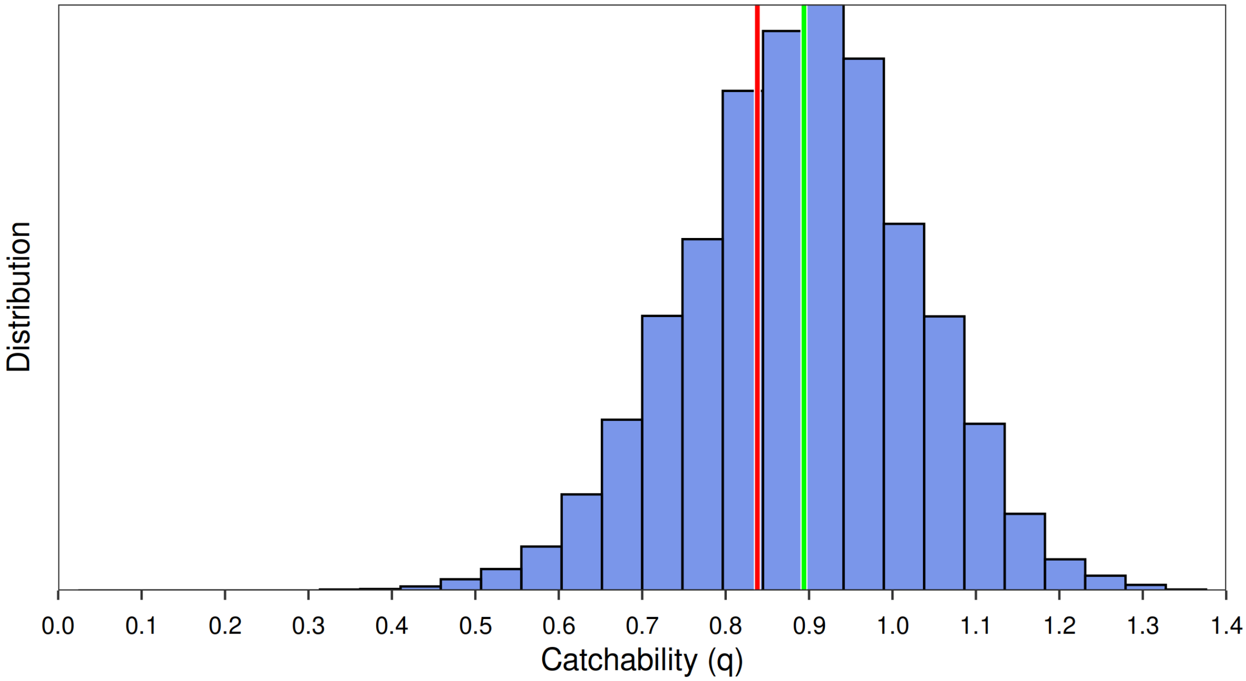

Figure 18. Density of the Catchability (q) parameter for the acoustic survey index. The green vertical line is the median of the posterior for 2025, which is 0.894; the red line is the median of the posterior for the last assessment year, 2024, which was 0.838.

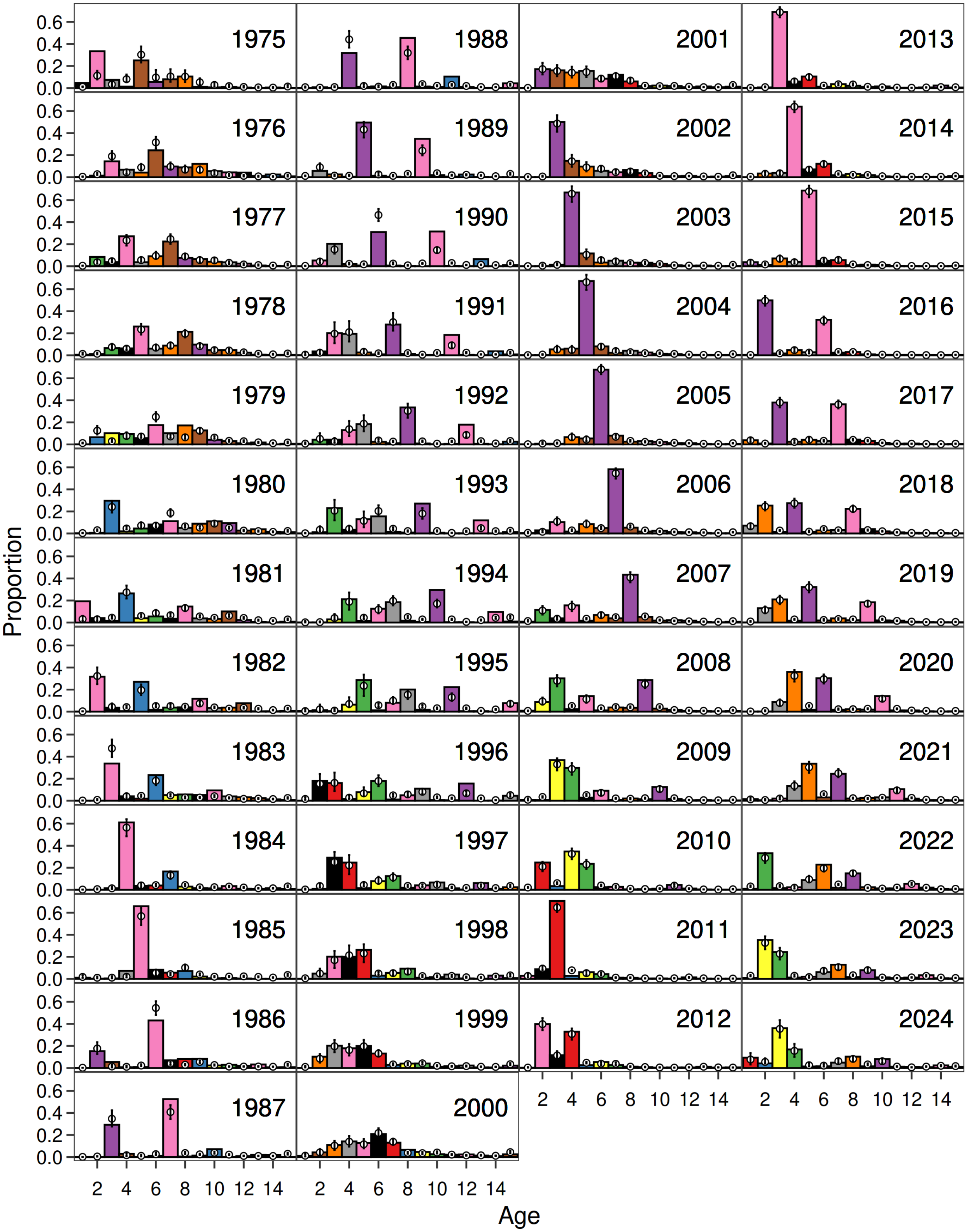

Figure 19. Base model fits to the fishery age-composition data. Colored bars show observed proportions with colors following each cohort across years. Points with intervals indicate median expected proportions and 95% credibility intervals from the Markov chain Monte Carlo calculations.

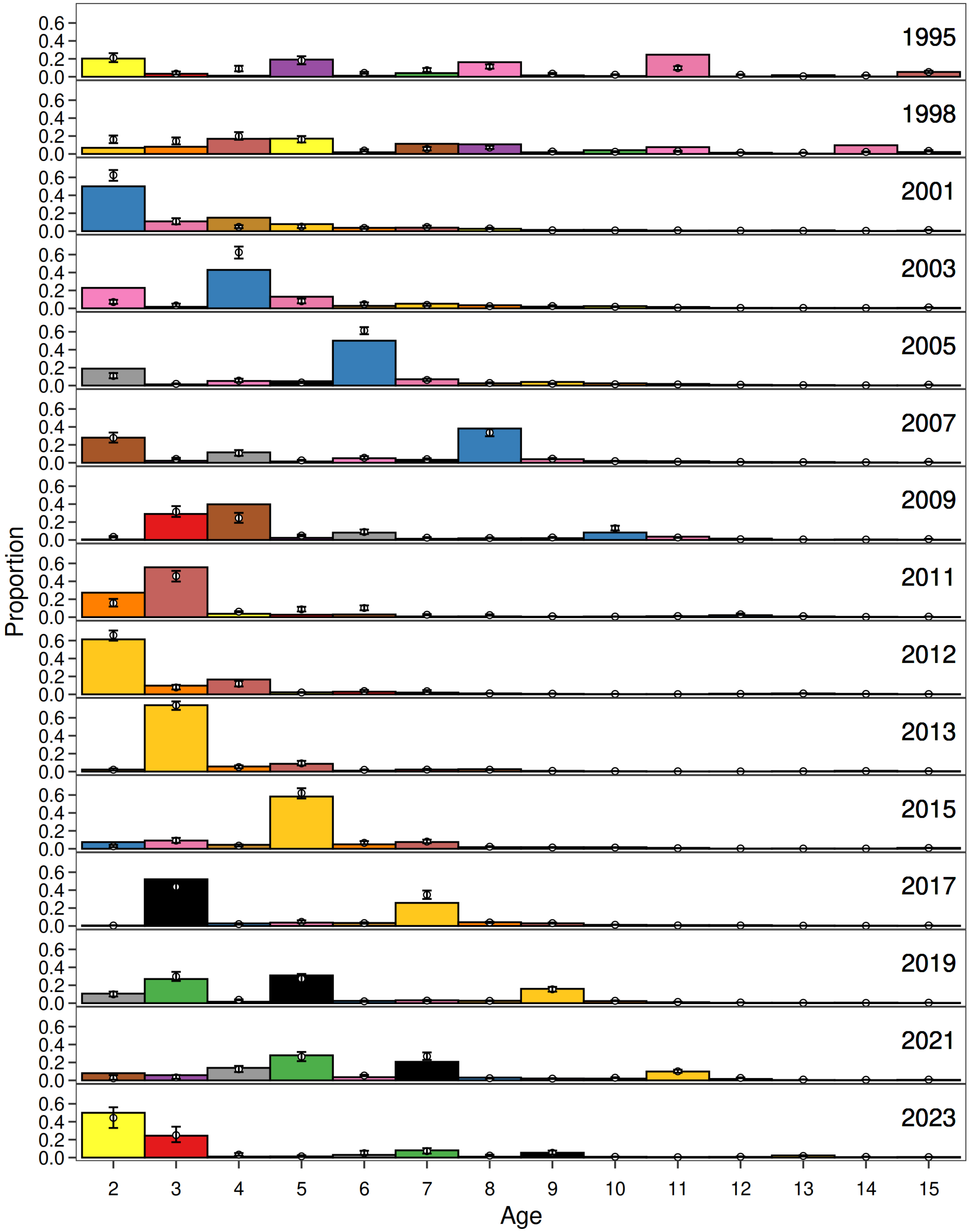

Figure 20. Base model fits to the acoustic survey age-composition data. Colored bars show observed proportions with colors following each cohort across years. Points with intervals indicate median expected proportions and 95% credibility intervals from the Markov chain Monte Carlo calculations.

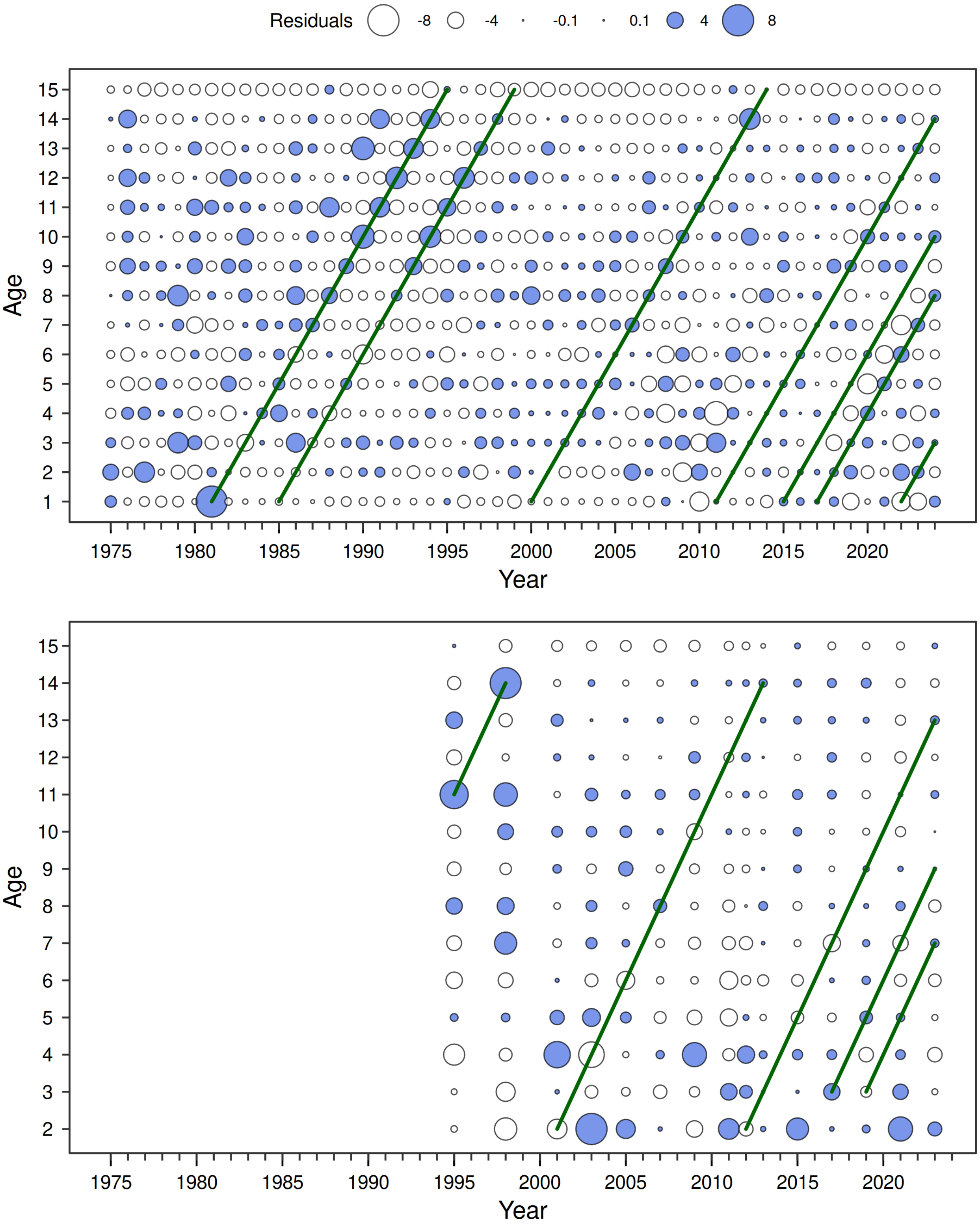

Figure 21. Pearson residuals for base model fits to the age-composition data for the medians of the Markov chain Monte Carlo posteriors for the fishery (top) and acoustic survey (bottom). Closed bubbles are positive residuals (observed > expected) and open bubbles are negative residuals (observed < expected). Green lines track cohorts from years of large recruitment events.

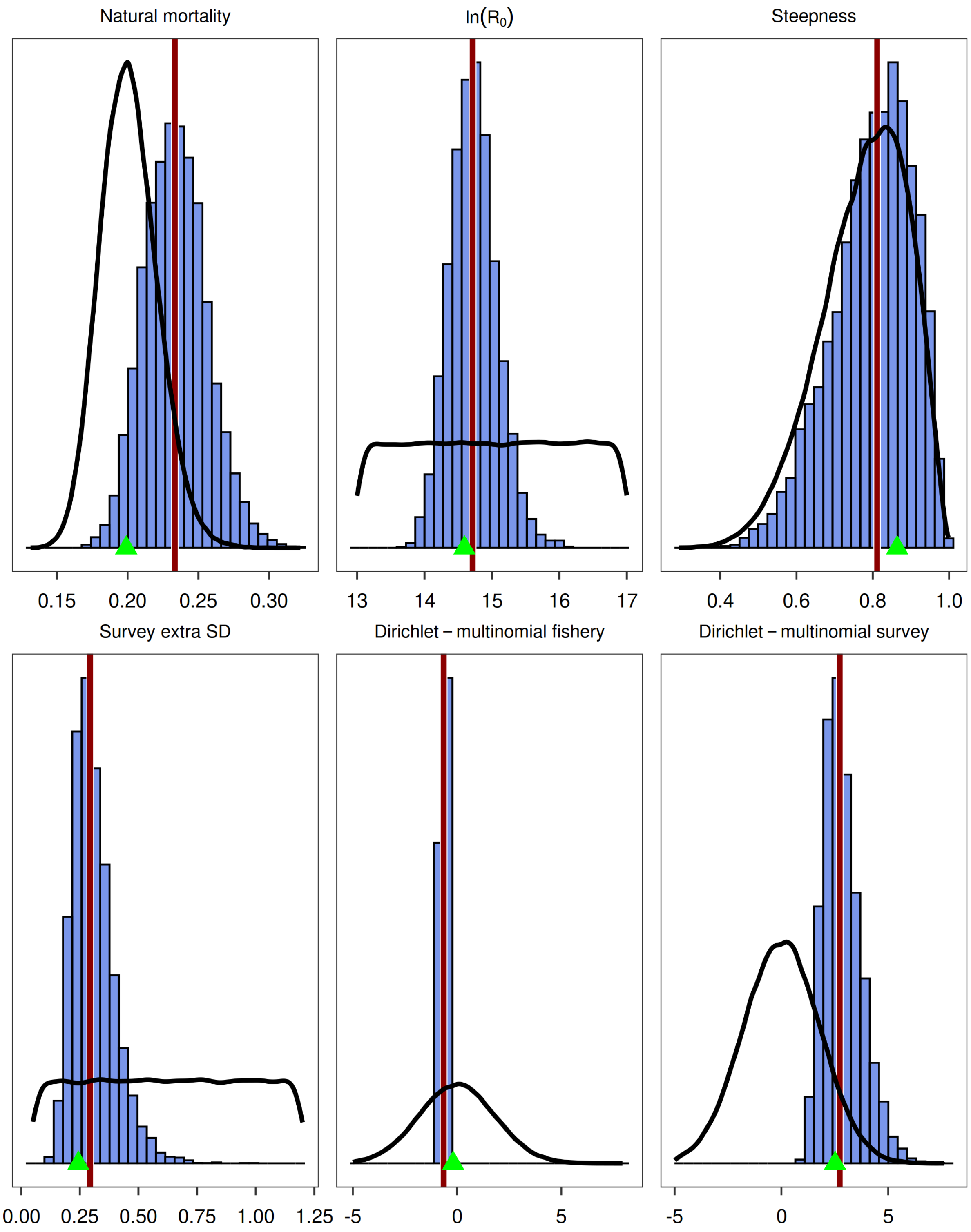

Figure 22. Prior (black lines) and posterior (blue histograms) distributions for natural mortality (M), equilibrium log recruitment ($\ln R_0$), steepness (h), the additional process-error standard deviation (SD) for the acoustic survey, and the Dirichlet-multinomial parameters for the fishery ($\log \theta_{\text{fish}}$) and the survey ($\log \theta_{\text{surv}}$). Green triangles signify the initial value for each parameter. Red vertical lines represent the median of the posterior. The small downturns at the ends of the uniform priors for $ln(R_0)$ and the acoustic survey extra SD parameters represent the hard limits (via the smoothed line) set for the priors in the Stock Synthesis control file.

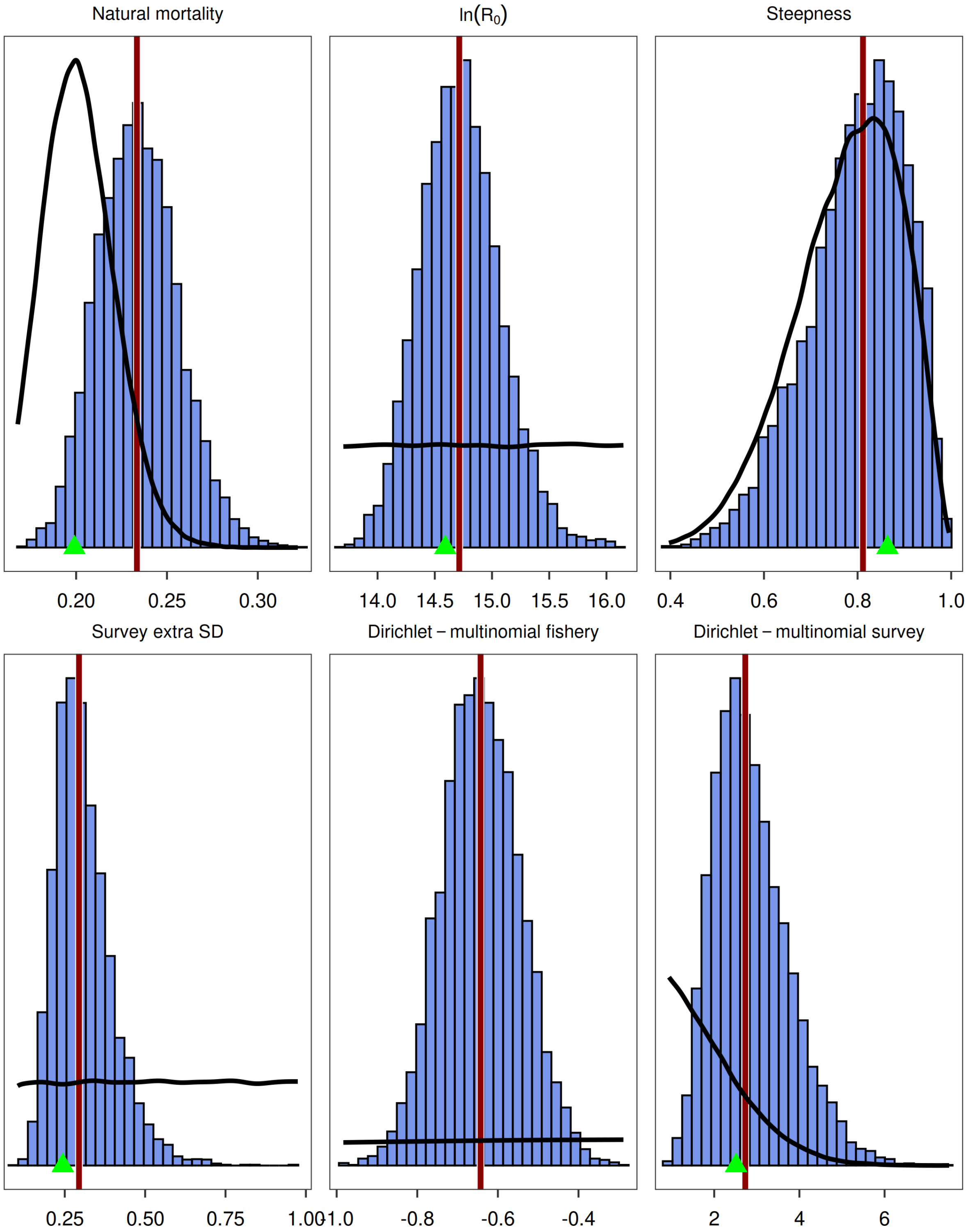

Figure 23. As for Figure 22 but the x axis of each panel is truncated to the range of the posterior distribution, and thus, there is the potential for the full range of the prior and the initial value to be missing from individual panels.

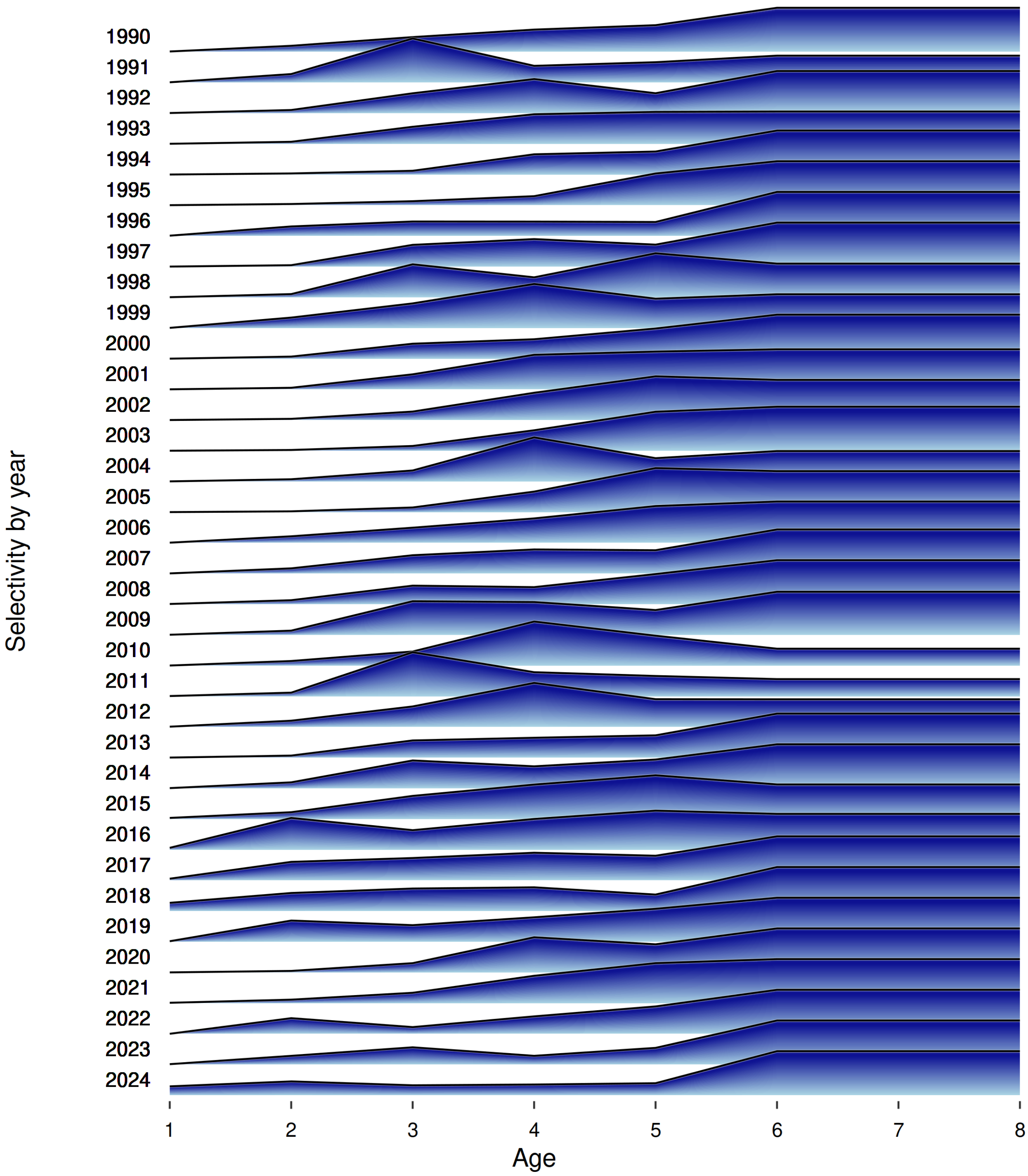

Figure 24. Mountains plot of median fishery selectivity in each year for the base model. The range of selectivity is scaled to be between 0 and 1 in each year.

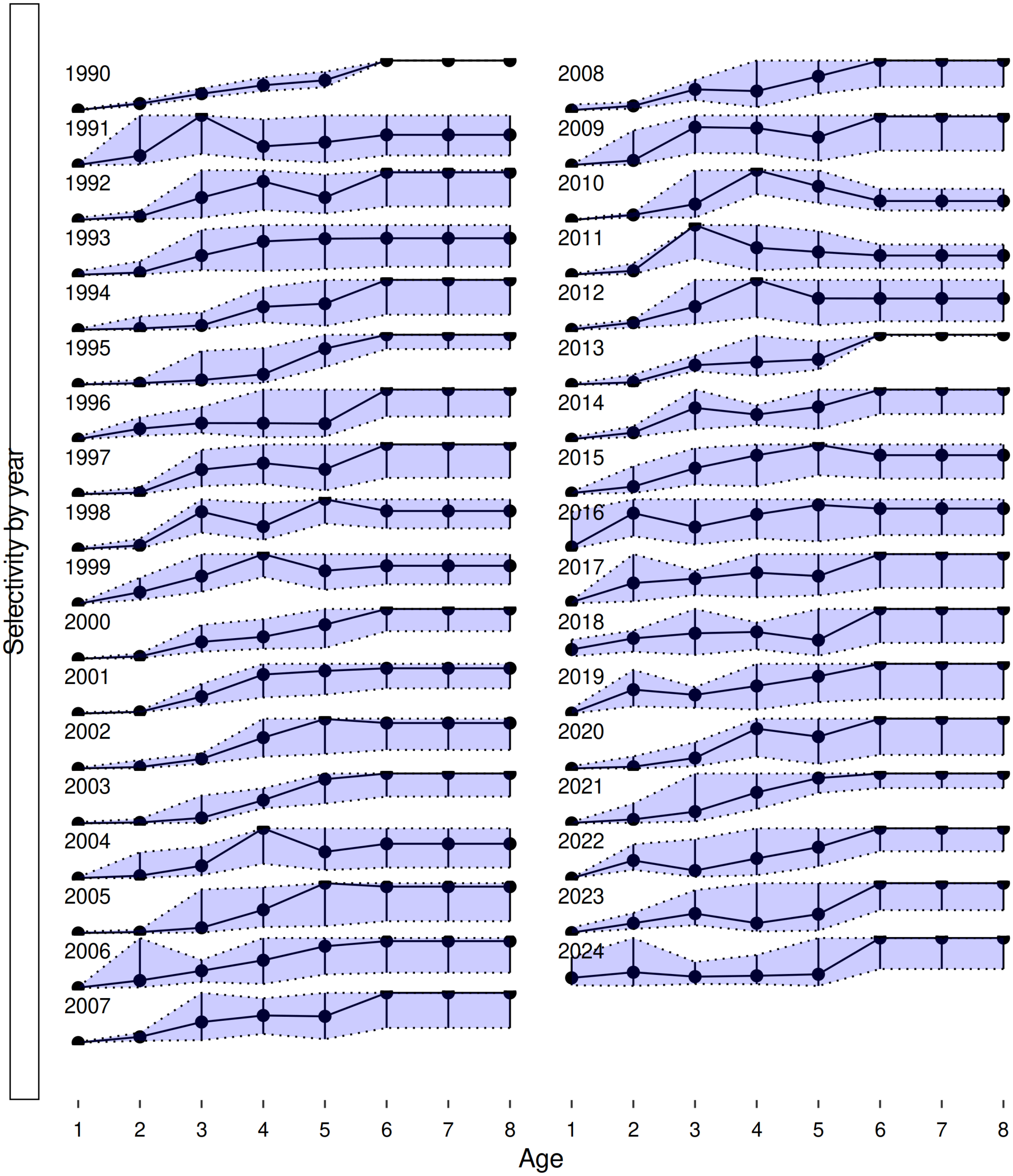

Figure 25. Fishery selectivity sampled from posterior probability distribution by year for the base model. Black dots and bars indicate the median and 95% credibility interval, respectively. The shaded polygon also shows the 95% credibility interval. The range of selectivity is scaled to be between 0 and 1 in each year. Selectivity for 1990 is shared for all years from 1966 to 1990.

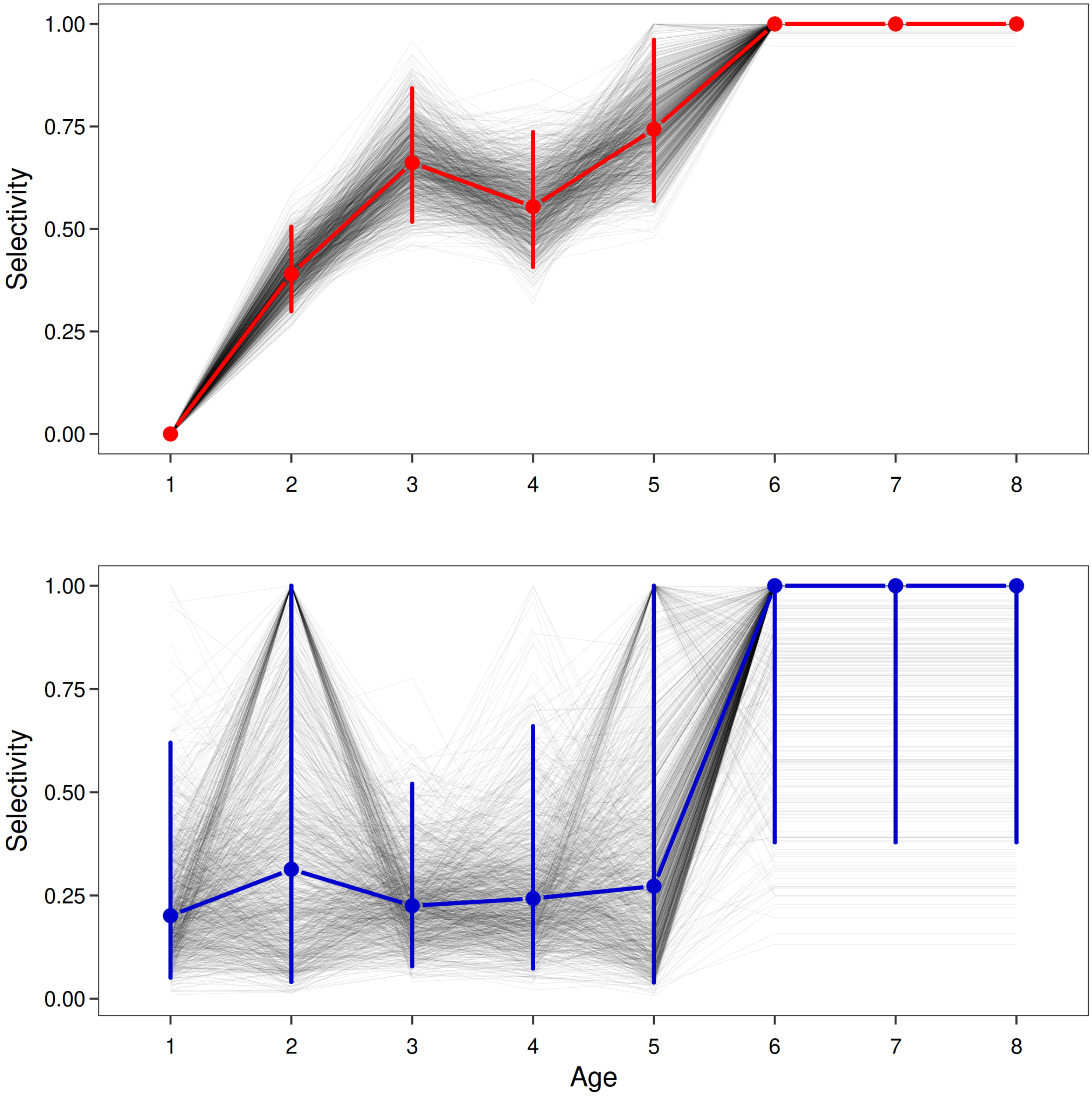

Figure 26. Estimated selectivities for the acoustic survey age-2+ biomass index (top, with selectivity of zero for age-1 fish) and fishery (bottom – shown for 2024 only, age-1 and older) from a subsample of 1,000 draws from the posterior distribution for the base model.

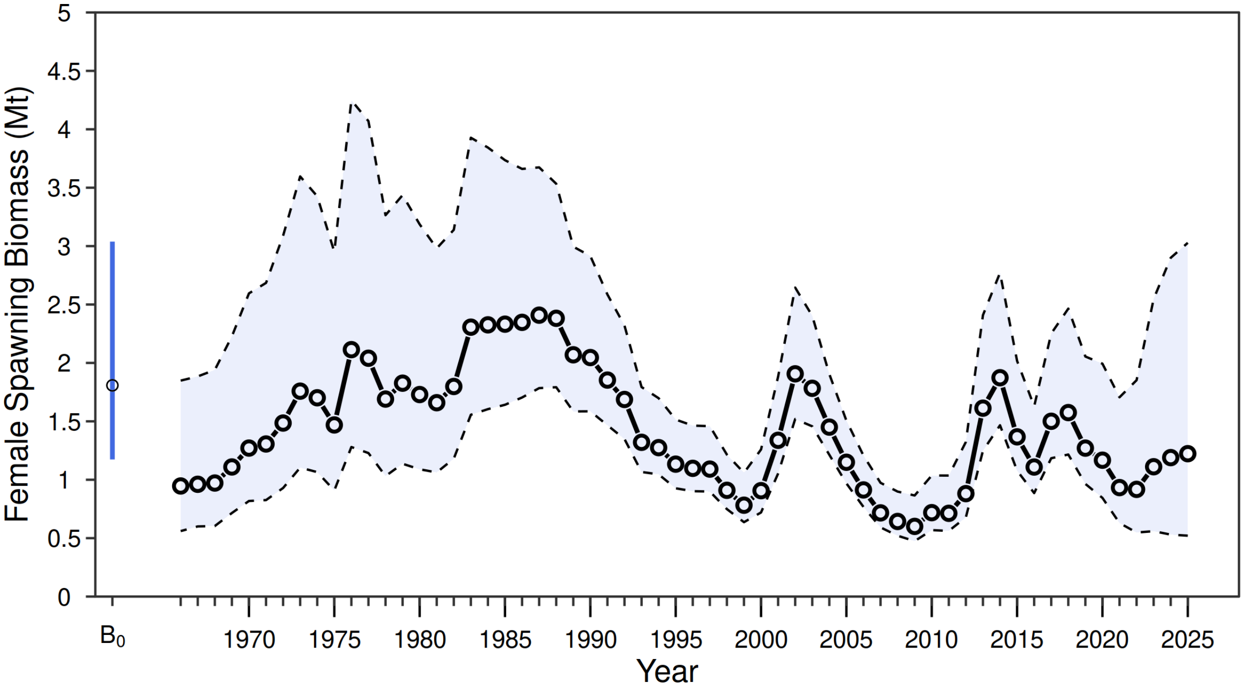

Figure 27. Median (solid line) of the posterior distribution for beginning of the year female spawning biomass (B_t in year t; Mt) through 2025 (solid line) with 95% posterior credibility intervals (shaded area). The left-most circle with a 95% posterior credibility interval is the estimated unfished equilibrium biomass, B_0.

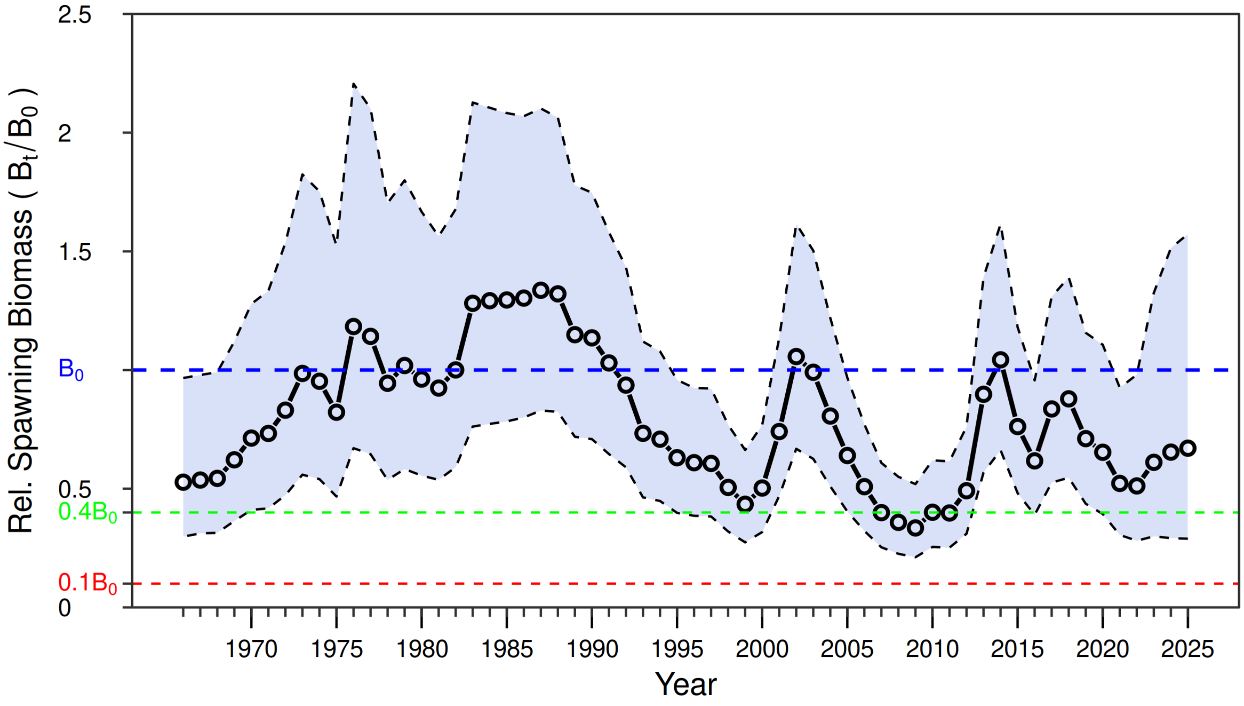

Figure 28. Median (solid line) of the posterior distribution for relative spawning biomass (B_t/B_0) through 2025 with 95% posterior credibility intervals (shaded area). Dashed horizontal lines show 10%, 40%, and 100% of the unfished equilibrium (B_0).

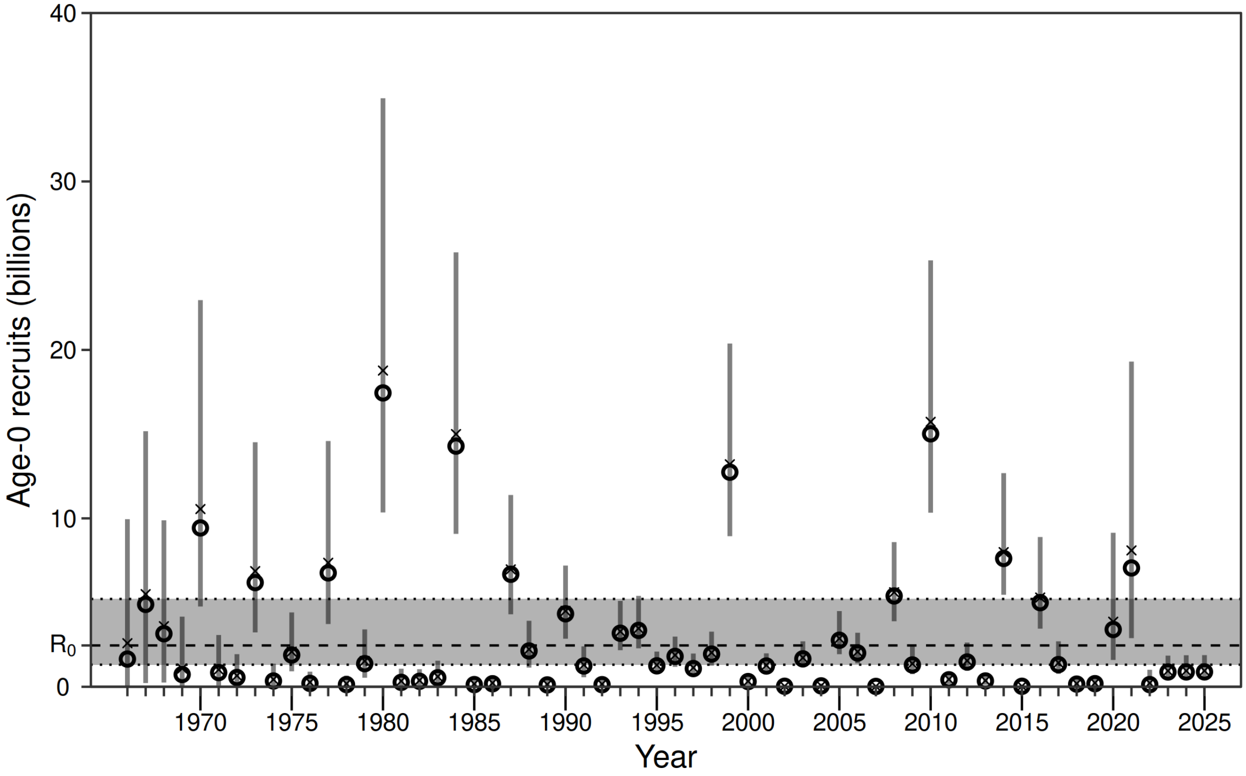

Figure 29. Medians (solid circles) and means (X) of the posterior distribution for recruitment (billions of age-0 fish) with 95% posterior credibility intervals (vertical lines). The median of the posterior distribution for mean unfished equilibrium recruitment (R_0) is shown as the horizontal dashed line with the 95% posterior credibility interval shaded between the dotted lines.

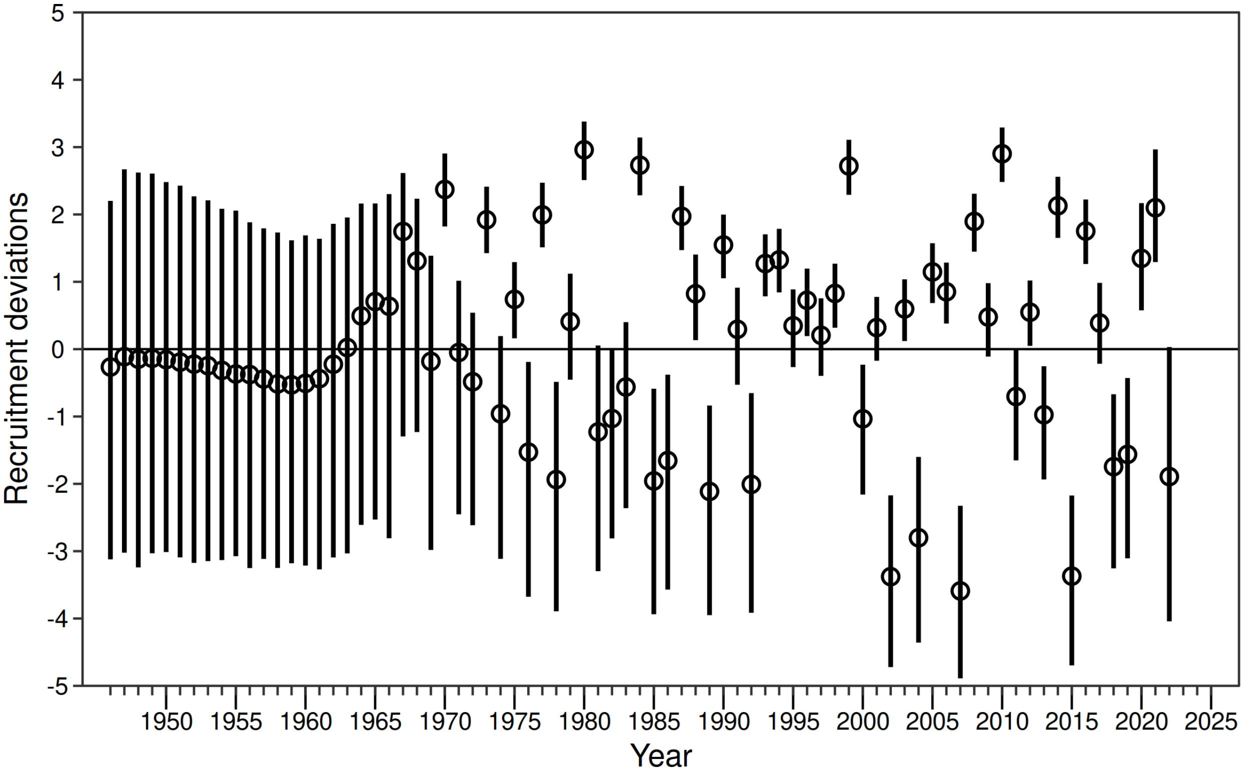

Figure 30. Medians (solid circles) of the posterior distribution for log-scale recruitment deviations with 95% posterior credibility intervals (vertical lines). Recruitment deviations for the years 1946–1965 are used to calculate the numbers at age in 1966, the initial year of the model. Those after 2022 were not estimated in the model.

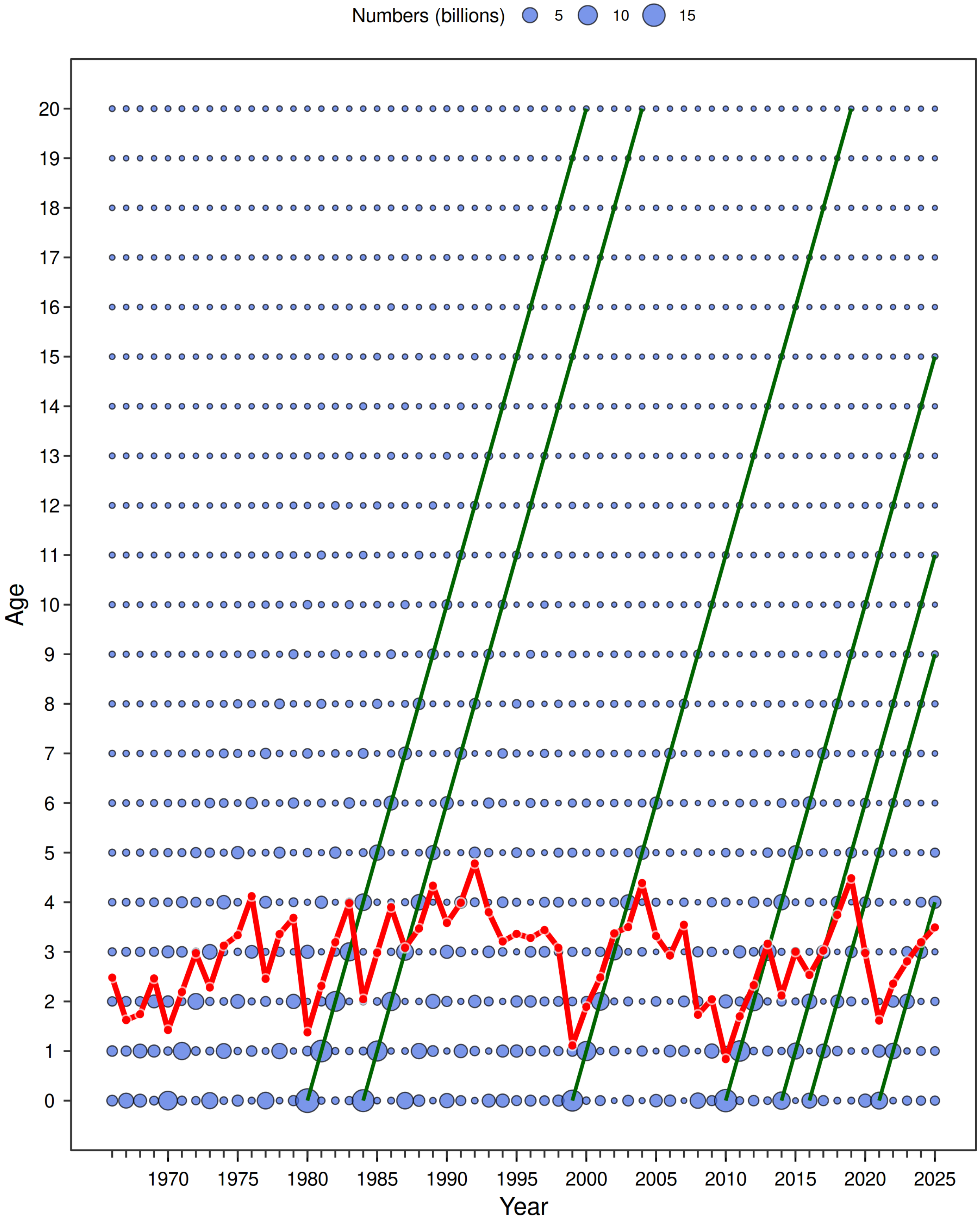

Figure 31. Bubble plot of the medians of the posterior distributions of population numbers at age at the beginning of each year, where green diagonal lines follow each larger-than-usual year-class through time. The red line represents the mean age. The scale of the bubbles is represented in the key where the units are billions of fish; the largest overall bubble represents the 17.4 billion age-0 recruits in 1980. See Table 17 for values.

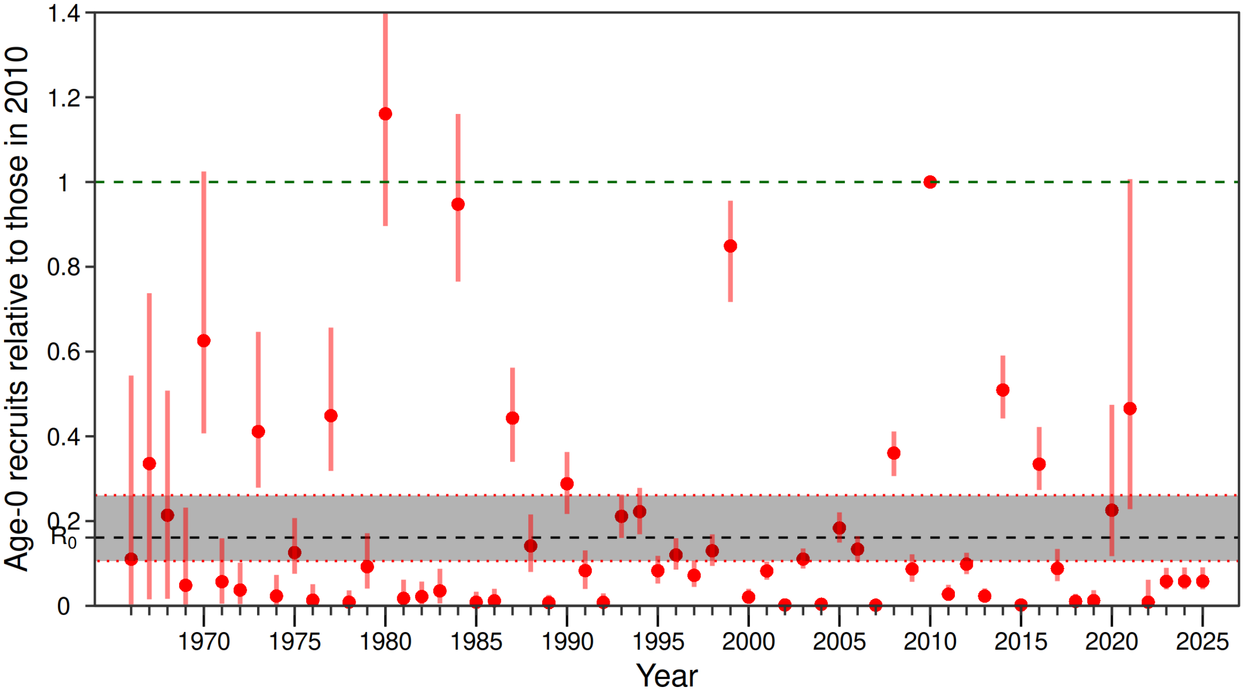

Figure 32. Medians (circles) of the posterior distribution of annual recruitment relative to recruitment in 2010 (recruitment divided by the 2010 recruitment for every MCMC sample), with 95% posterior credibility intervals (red lines). This procedure somewhat scales out the uncertainty due to uncertainty in mean unfished equilibrium recruitment (R_0), and better elicits comparisons of relative cohort sizes; for example, recruitment in 2014 is clearly smaller than in 2010 (horizontal green dashed line). The year 2010 was chosen as the basis for comparison due to its well recognized size and the stability of cohort strength estimates over time. The median of R_0/R_{2010} is shown as the horizontal dashed line with the 95% posterior credibility interval shaded between the dotted lines.

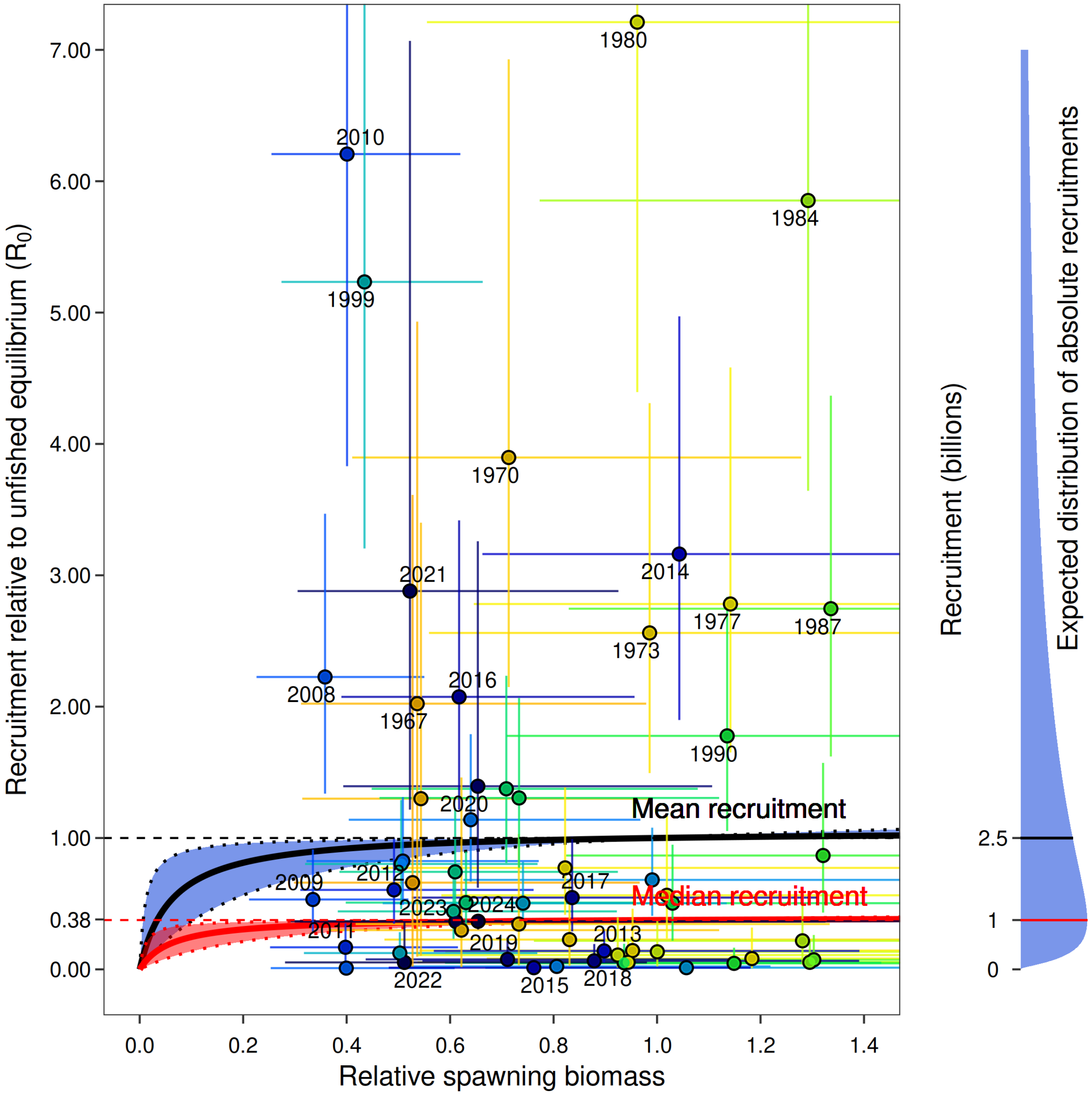

Figure 33. Estimated stock–recruitment relationship for the base model with median predicted recruitments and 95% posterior credibility intervals. Colors indicate time-period, with yellow colors in the early years and blue colors in the recent years. The thick solid black line indicates the central tendency (mean) and the red line indicates the central tendency after bias correcting for the lognormal distribution (median). Shading around the stock–recruitment relationship indicates uncertainty in shape associated with distribution of the steepness parameter (h). The blue polygon on the right indicates the expected distribution of absolute recruitments.

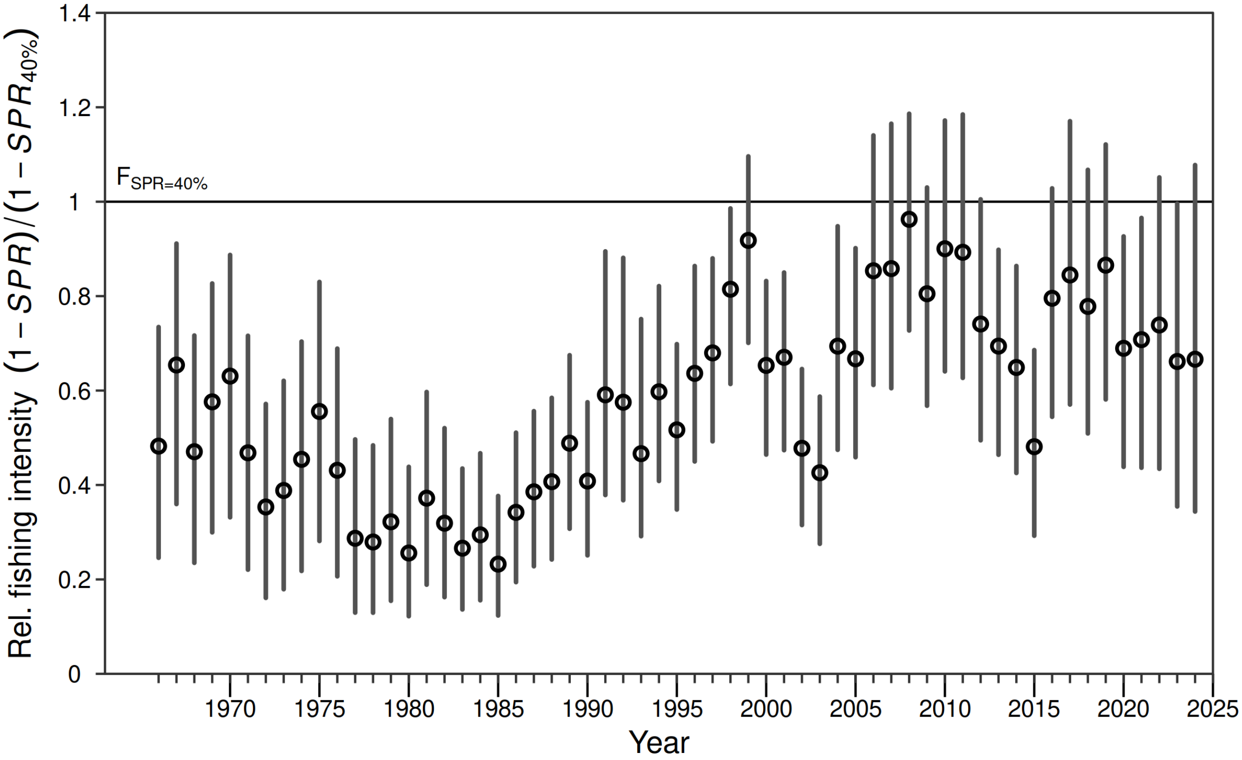

Figure 34. Trend in median relative fishing intensity (relative to the $F_{\text{SPR=40\%}}$ management level) through 2024 with 95% posterior credibility intervals. The $F_{\text{SPR=40\%}}$ management level defined in the Joint U.S.-Canada Agreement for Pacific Hake is shown as a horizontal line at 1.0.

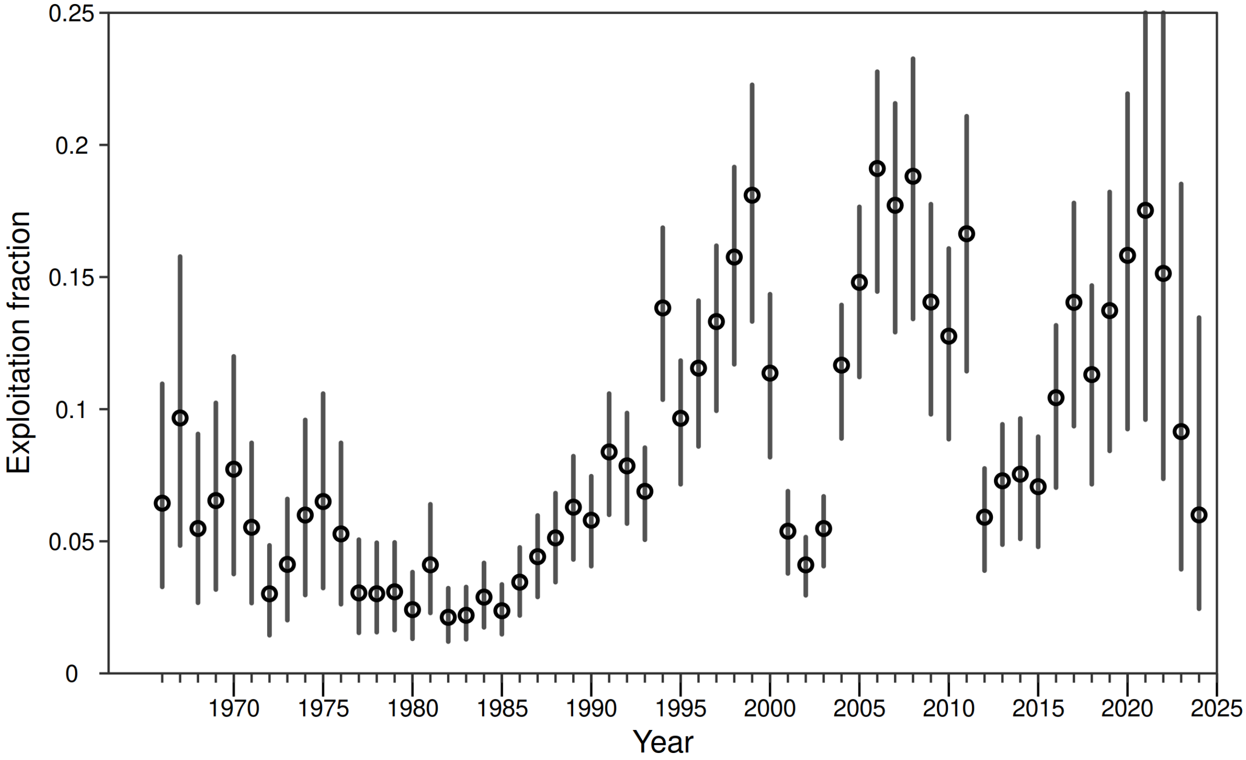

Figure 35. Trend in median exploitation fraction (catch divided by age-2+ biomass) through 2024 with 95% posterior credibility intervals.

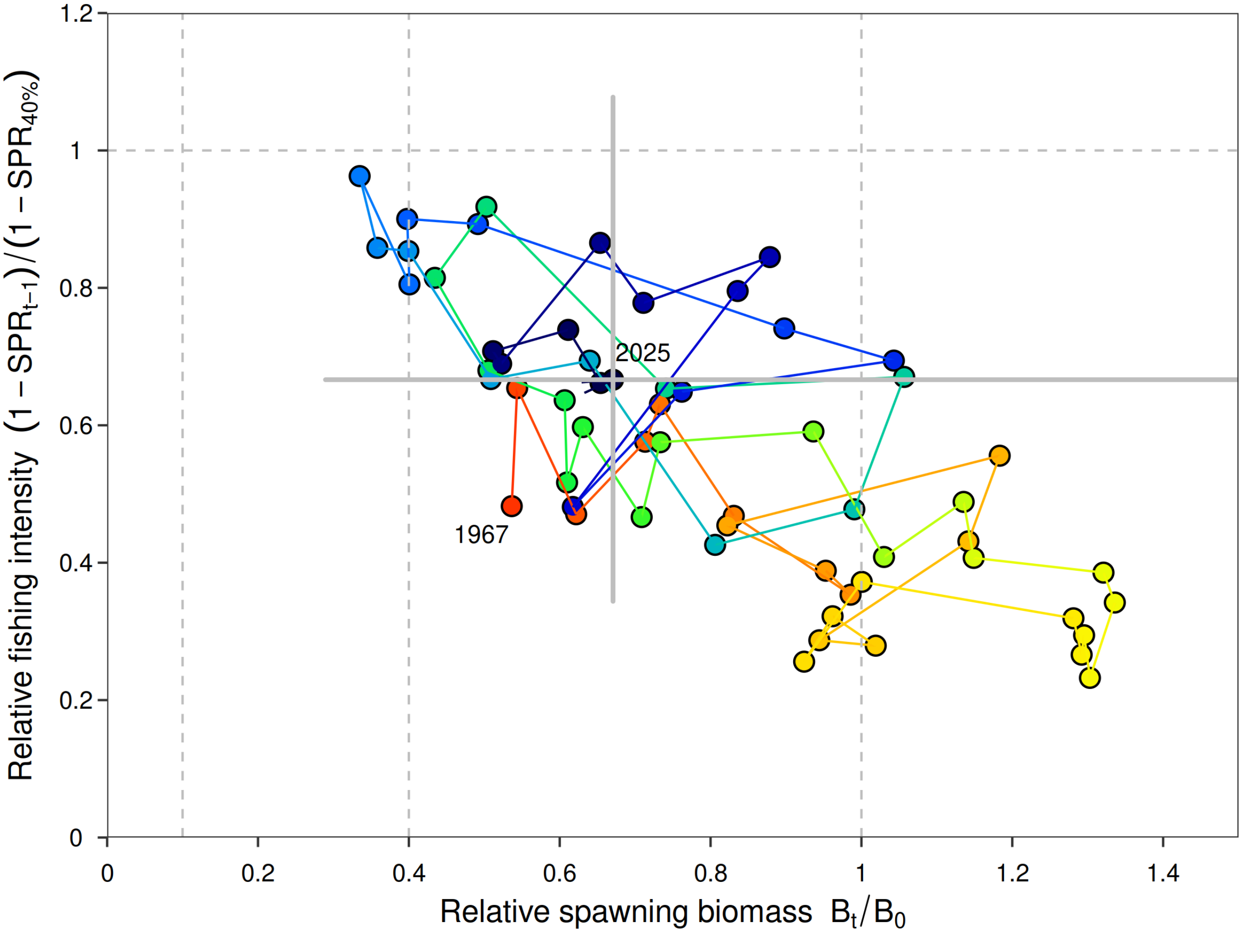

Figure 36. Estimated historical path of median relative spawning biomass at the beginning of year t and corresponding median relative fishing intensity in fishing year $t-1$ leading up to year t. Labels show the time series start and end years; labels correspond to year t (i.e., year of the relative spawning biomass). Gray bars span the 95% credibility intervals for 2025 relative spawning biomass (horizontal) and 2024 relative fishing intensity (vertical).

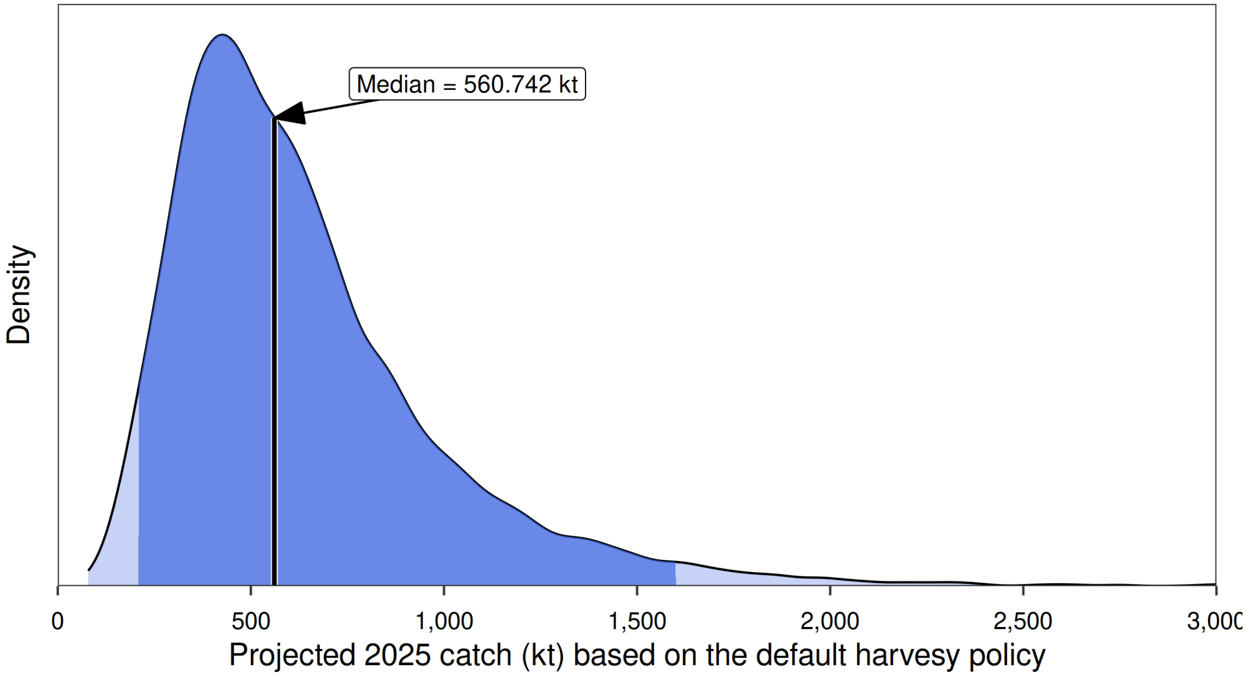

Figure 37. The posterior distribution of the default 2025 catch limit calculated using the default harvest policy ($F_{40\%}$–40:10). The median is 560,742 t (vertical line), with the dark shaded area ranging from the 2.5% quantile to the 97.5% quantile, covering the range 203,161–1,605,930 t.

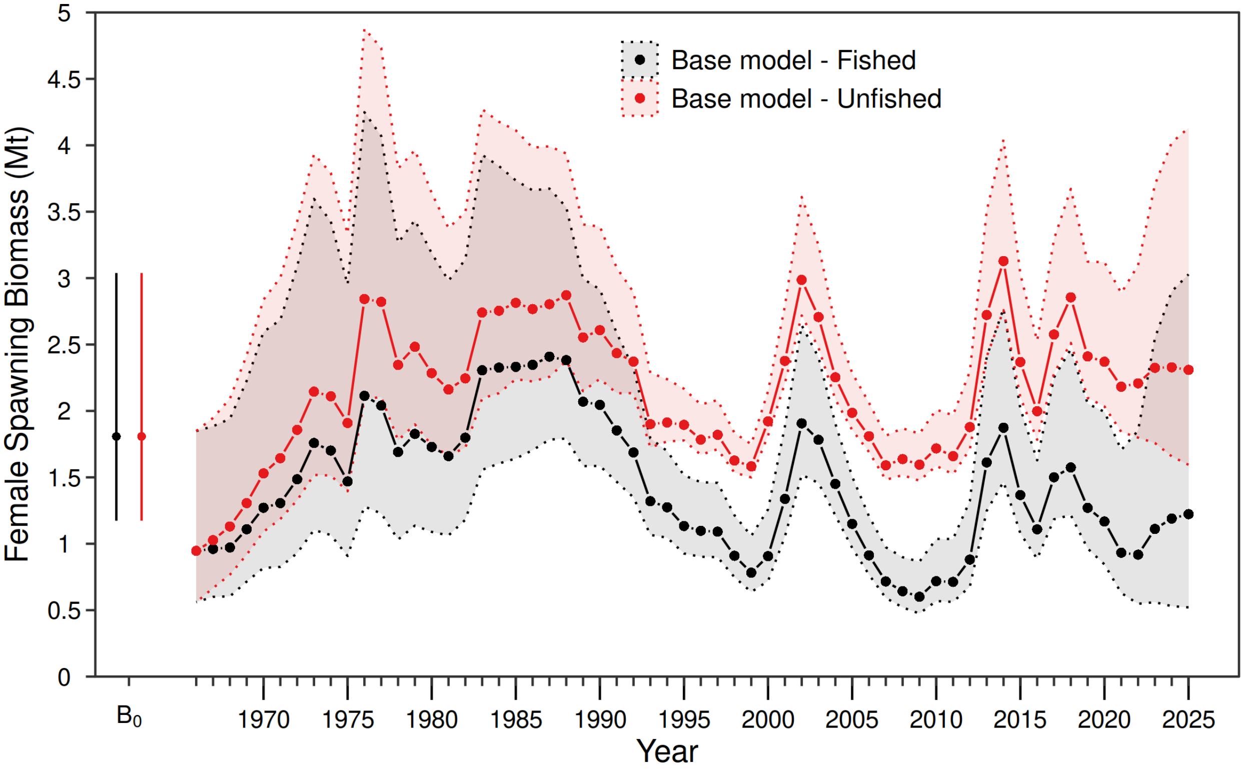

Figure 38. A comparison of female spawning stock biomass with fishing (black; as in Figure 27) and when the effects of fishing on the population are removed (red; unfished time series). Medians (solid lines) of the posterior distribution for beginning of the year female spawning biomass (B_t in year t; Mt) through 2025 (solid lines) with 95% posterior credibility intervals (shaded areas). The left-most circles with 95% posterior credibility intervals show the estimated unfished equilibrium biomass, B_0. The difference between the two lines shows the impact of removing fishing mortality from the population.

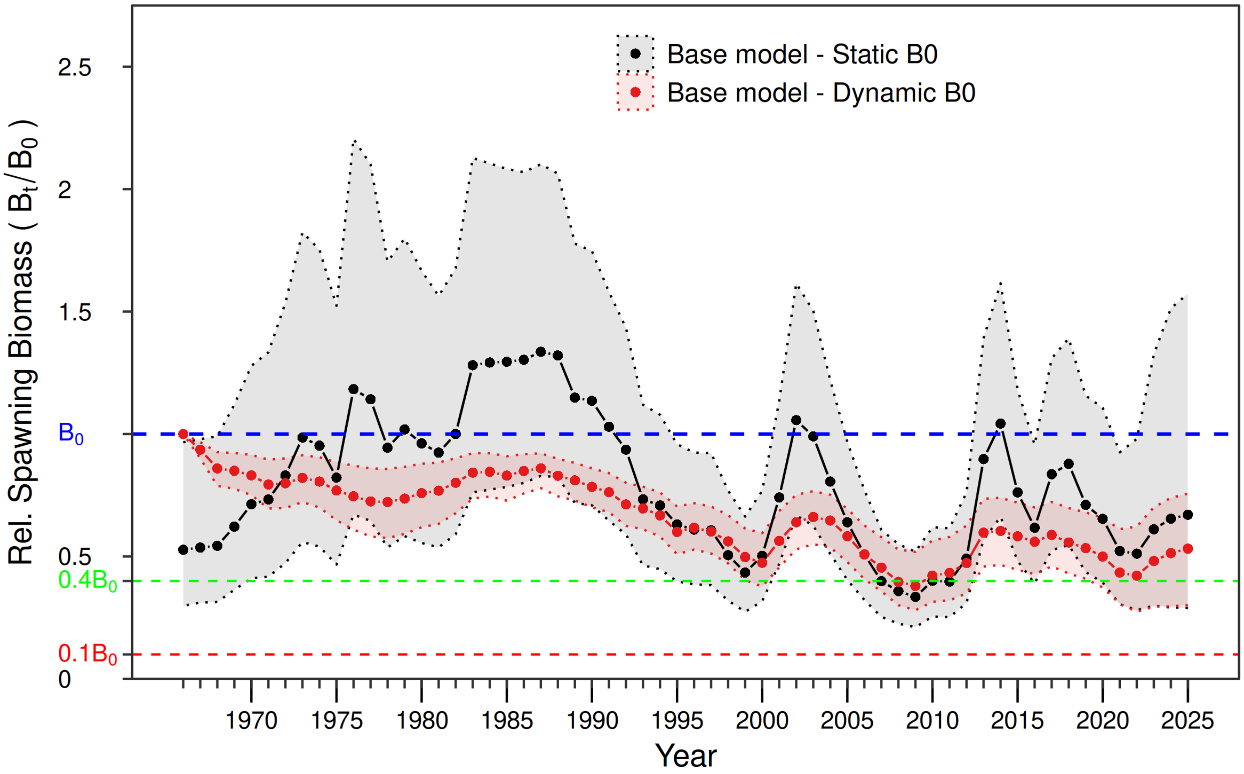

Figure 39. A comparison of relative spawning biomass when spawning biomass in year t is related to unfished equilibrium biomass, B_0 (static B_0, black; as in Figure 28) and when spawning biomass in year t is related to the unfished biomass time series in year t (dynamic B_0, red). Median (solid lines) of the posterior distribution for each calculation of relative spawning biomass through 2025 with 95% posterior credibility intervals (shaded areas). Dashed horizontal lines show 10%, 40%, and 100% of the unfished equilibrium (B_0). The default $F_{40\%}$–40:10 harvest policy uses relative spawning biomass based on a static B_0 determination of stock status.

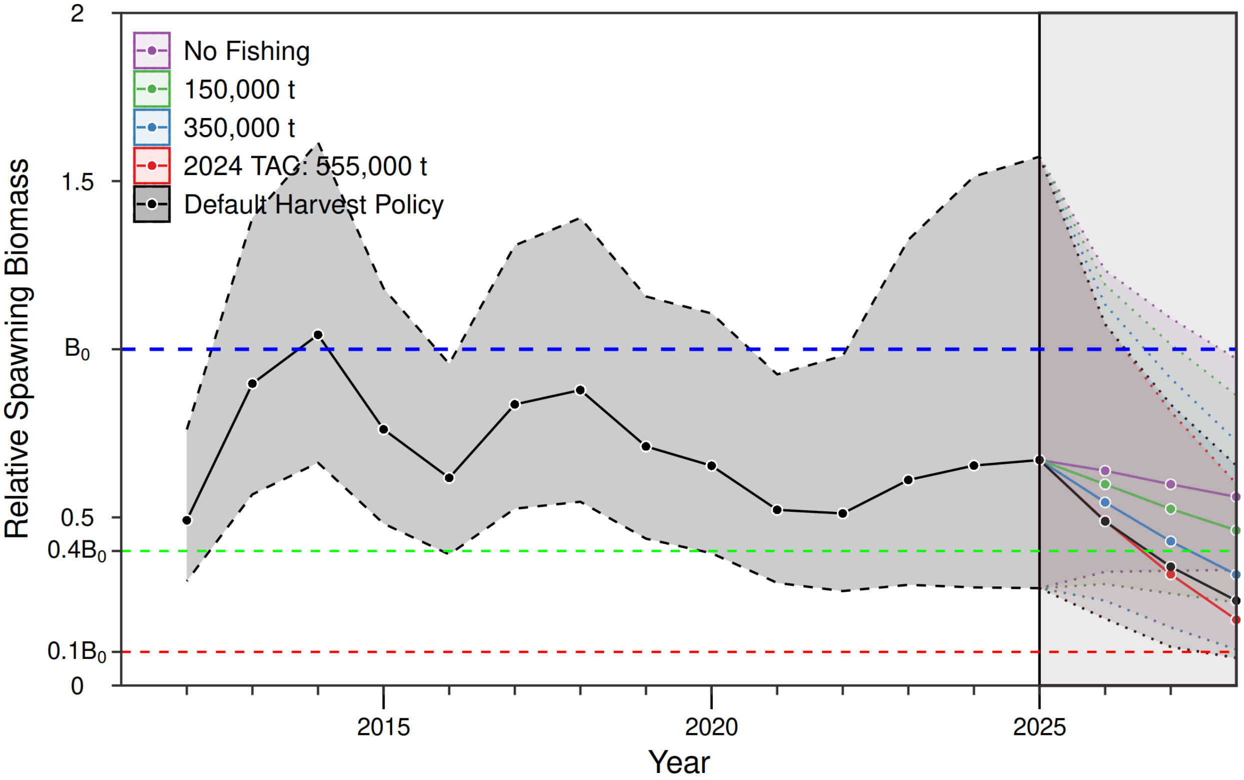

Figure 40. Median and 95% posterior credibility intervals of estimated relative spawning biomass to the start of 2025 from the base model and projections to the start of 2028 (vertical shaded rectangle) for several management actions, which are defined in the decision tables. The default harvest policy catches are 560,742 t in 2025, 463,364 t in 2026, and 406,150 t in 2027.

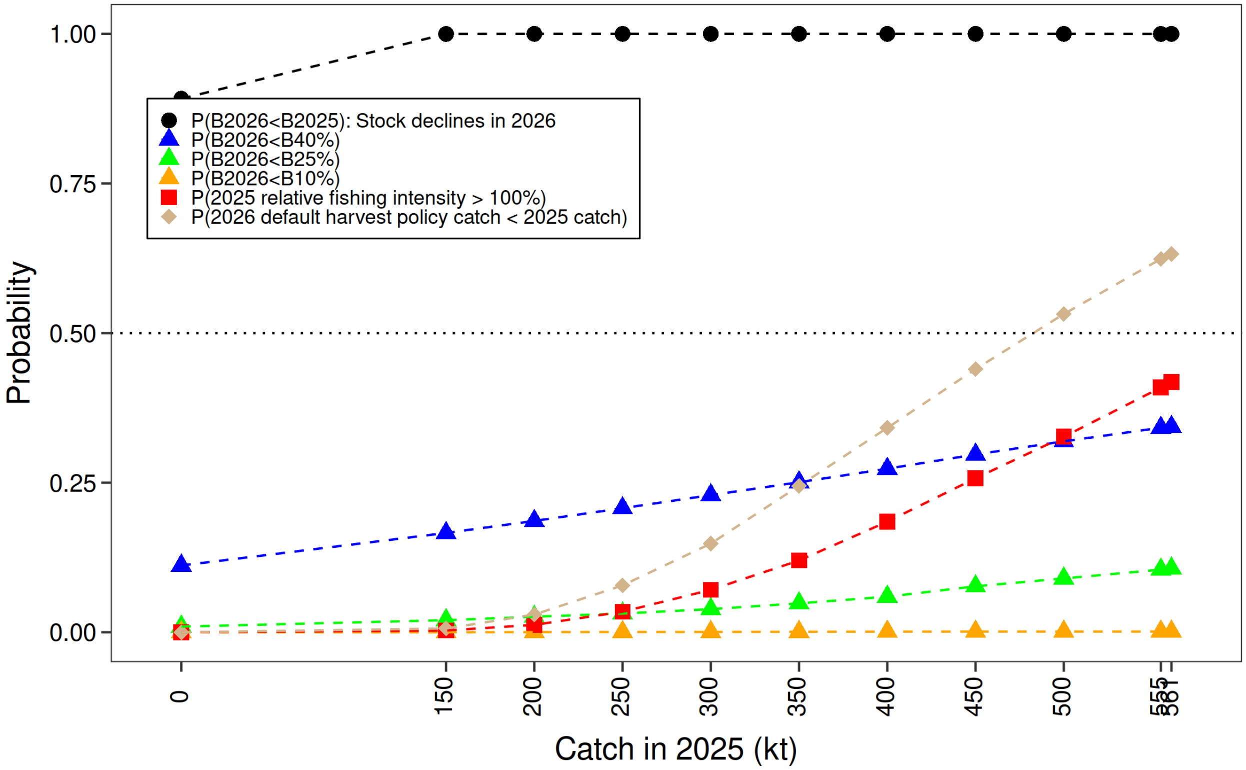

Figure 41. Graphical representation of the probabilities related to spawning biomass, relative fishing intensity, and the 2026 default harvest policy catch for alternative 2025 catch options (explained in Table 27) as listed in Table 29. The symbols indicate points that were computed directly from model output and lines interpolate between the points.

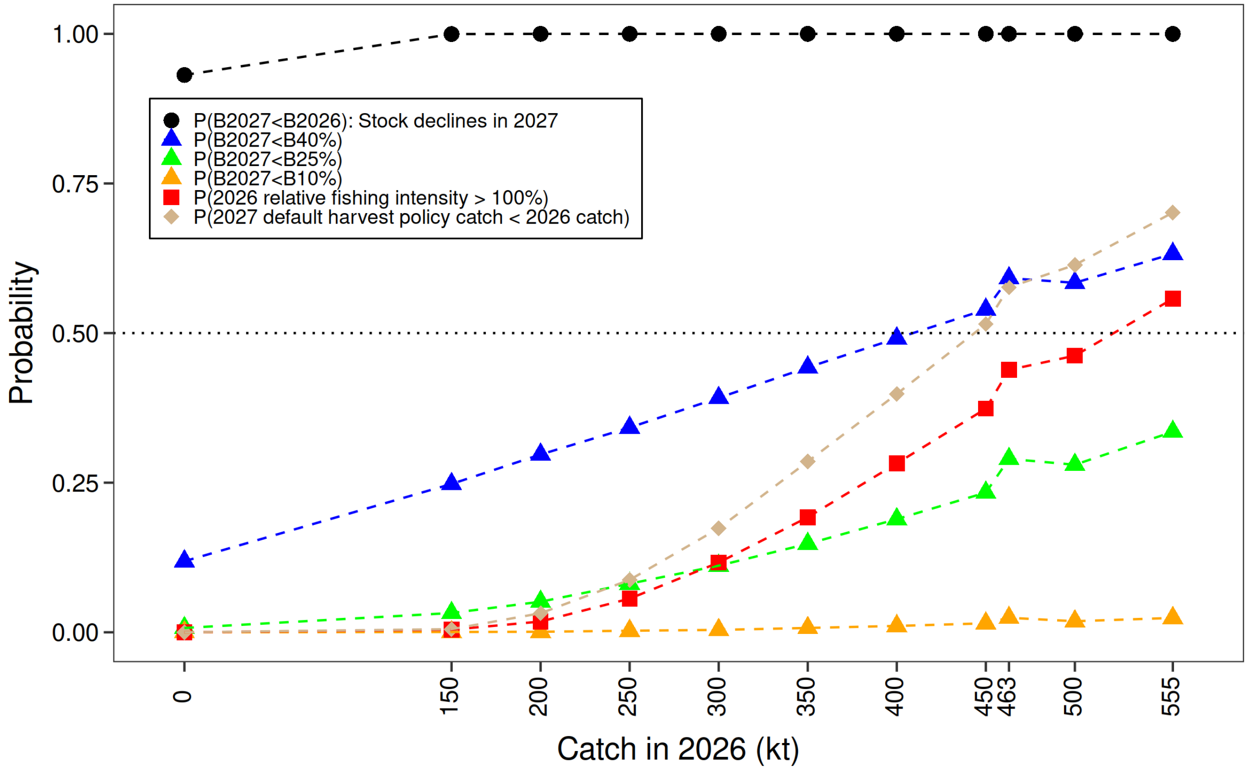

Figure 42. Graphical representation of the probabilities related to spawning biomass, relative fishing intensity, and the 2027 default harvest policy catch for alternative 2026 catch options (including associated 2025 catch; catch options explained in Table 27) as listed in Table 30. The symbols indicate points that were computed directly from model output and lines interpolate between the points.

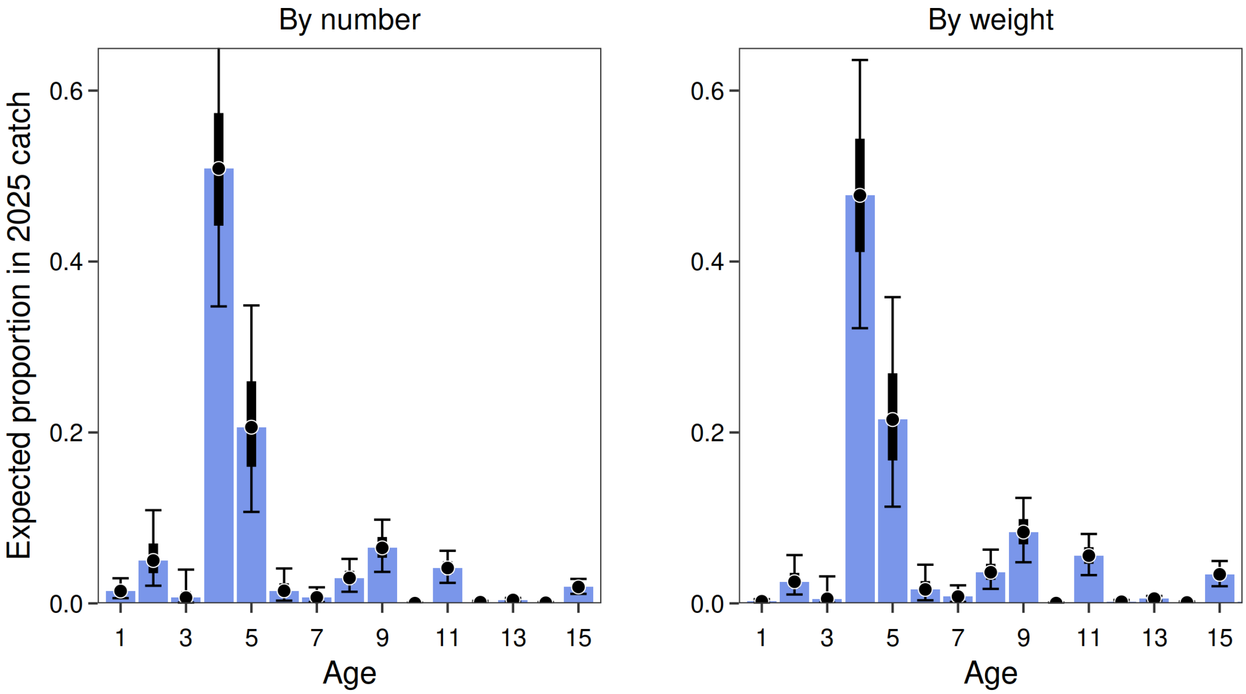

Figure 43. Forecast age compositions in numbers and in weight for the 2025 fishery catch (combined across all sectors in both countries). Light blue bars show median estimates. Thick black lines show 50% credibility intervals and thin black lines show 95% credibility intervals. These estimates are based on the posterior distribution for selectivity averaged across the most recent five years, weight-at-age data averaged across the most recent five years, and the distribution for expected numbers at age at the start of 2025 (see Table 17 for the Markov chain Monte Carlo medians of numbers-at-age for all years). The panel on the right is scaled based on the weight at each age averaged across the last five years.

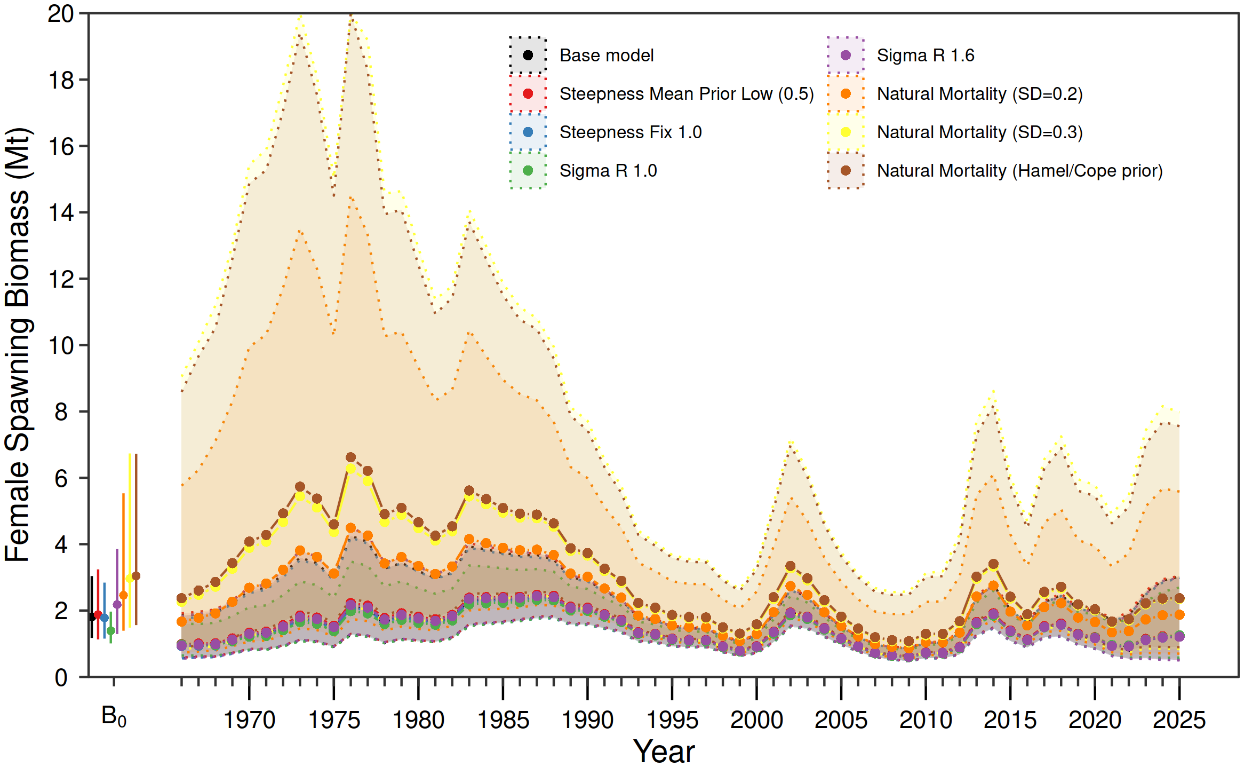

Figure 44. Markov chain Monte Carlo estimates of spawning biomass for the base model and alternative sensitivity runs representing changing the mean of the prior for steepness from 1.0 to 0.5, fixing steepness at 1.0, lower (1.0) and higher (1.6) levels of variation assumed about the stock–recruitment relationship (σ_r), changing the standard deviation of the prior for natural mortality, and using the Hamel/Cope prior distribution for natural mortality. Note that the results for the base model and first four sensitivities are very similar and somewhat hidden by the purple line.

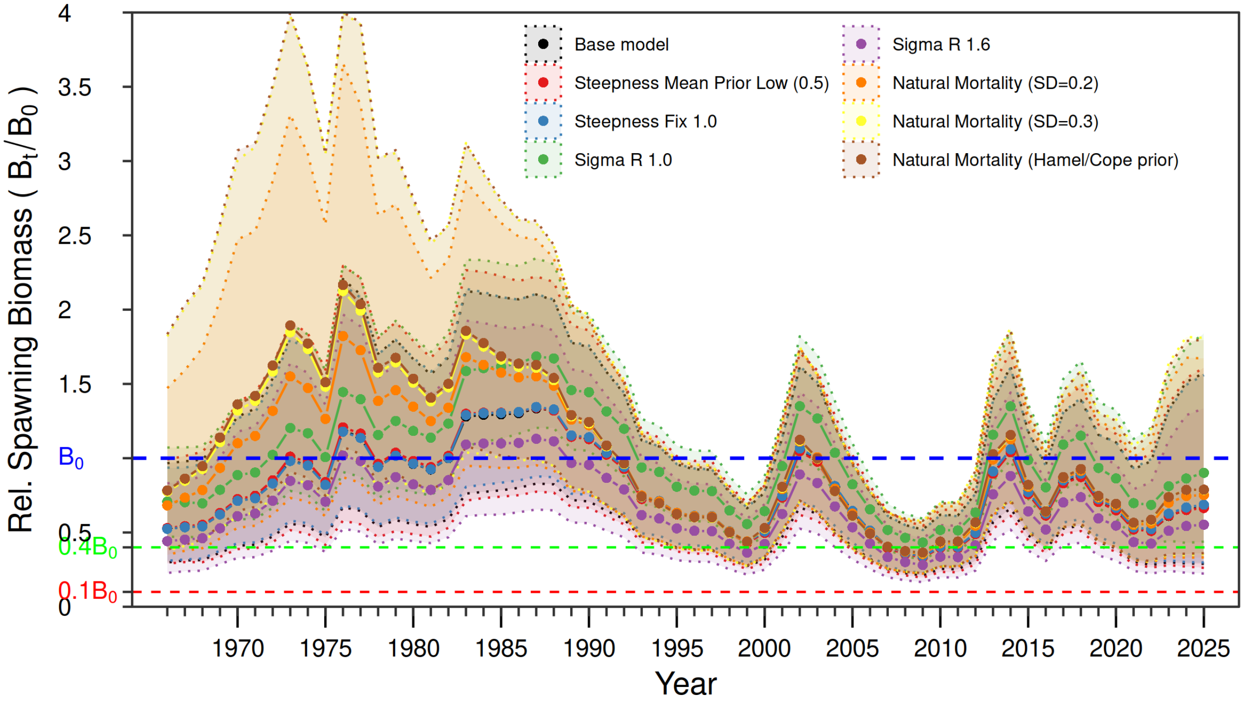

Figure 45. Markov chain Monte Carlo estimates of stock status (relative spawning biomass) for the base model and alternative sensitivity runs representing changing key parameters. See Figure 44 for sensitivity descriptions. Note that the results for the base model are very similar to the first two sensitivities and so are somewhat hidden by the blue and red lines.

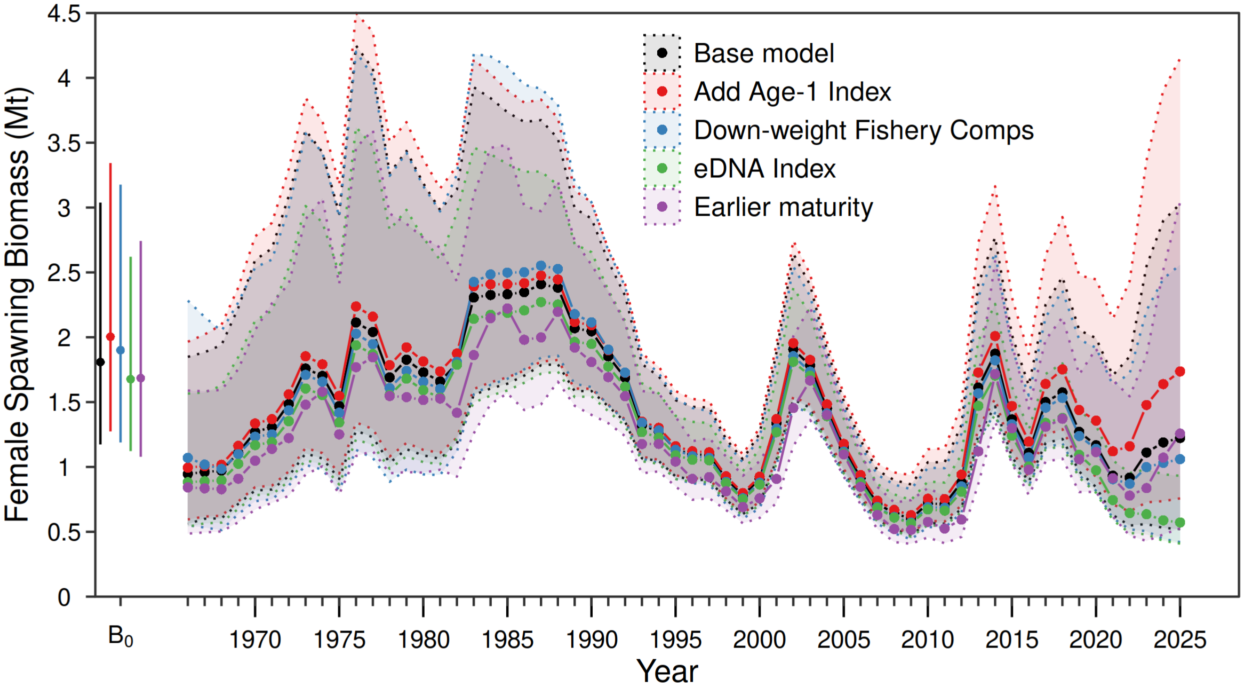

Figure 46. Markov chain Monte Carlo estimates of female spawning biomass for the base model and alternative sensitivity models that represent the following changes in data: removing the index of age-1 fish, down-weighting fishery composition data using the McAllister–Ianelli method, adding a relative index of abundance using environmental DNA, and using maturity estimates from mid-year rather than later in the year.

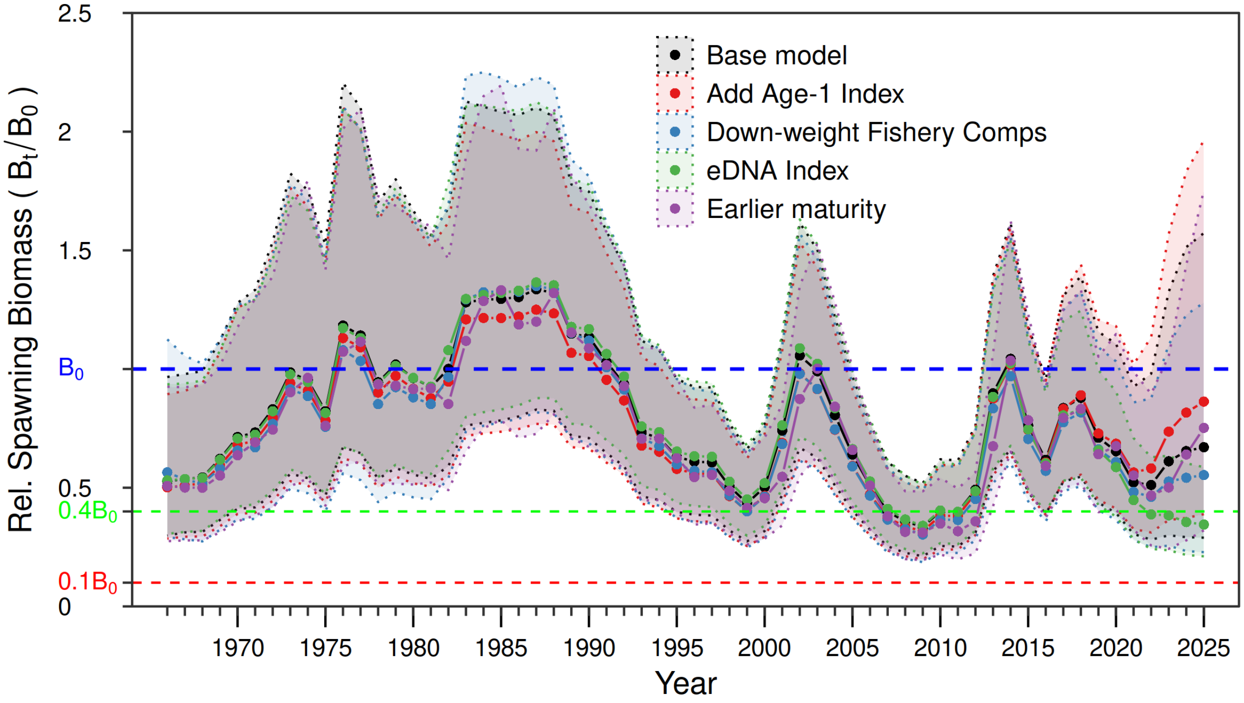

Figure 47. Markov chain Monte Carlo estimates of stock status (relative spawning biomass) for the base model and alternative sensitivity models that represent changes in data. See Figure 46 for sensitivity descriptions.

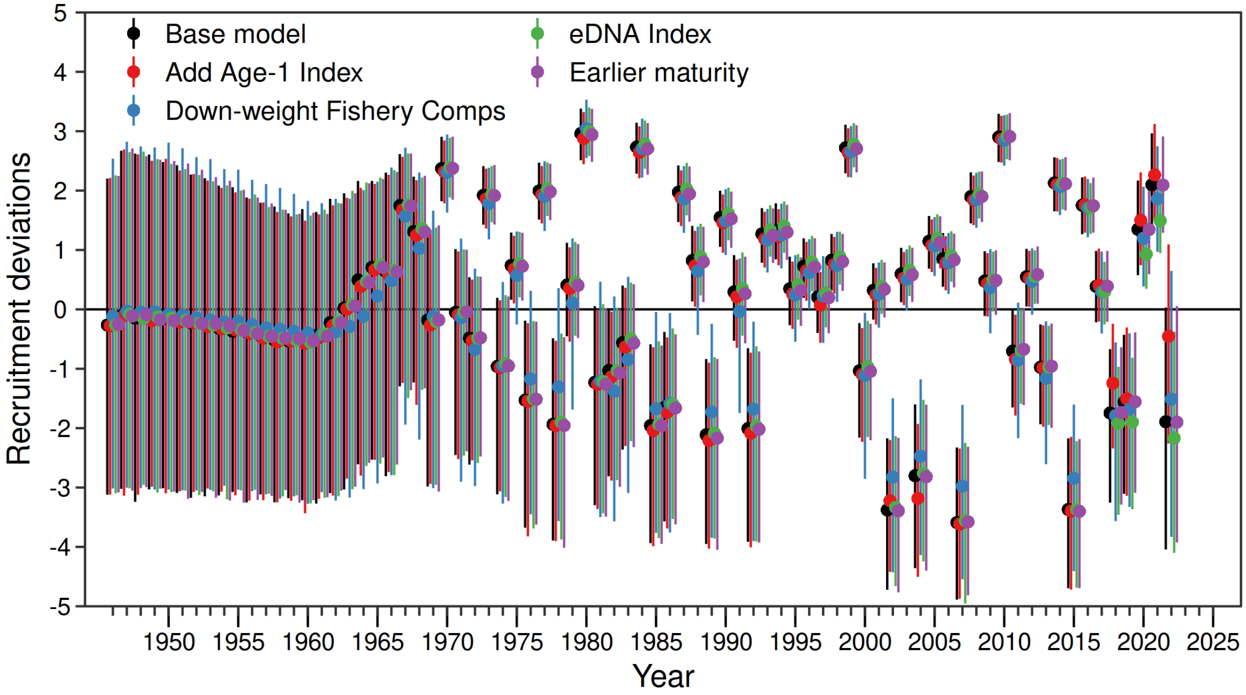

Figure 48. Markov chain Monte Carlo estimates of recruitment deviations for the base model and alternative sensitivity runs that represent changes in data. See Figure 46 for sensitivity descriptions.

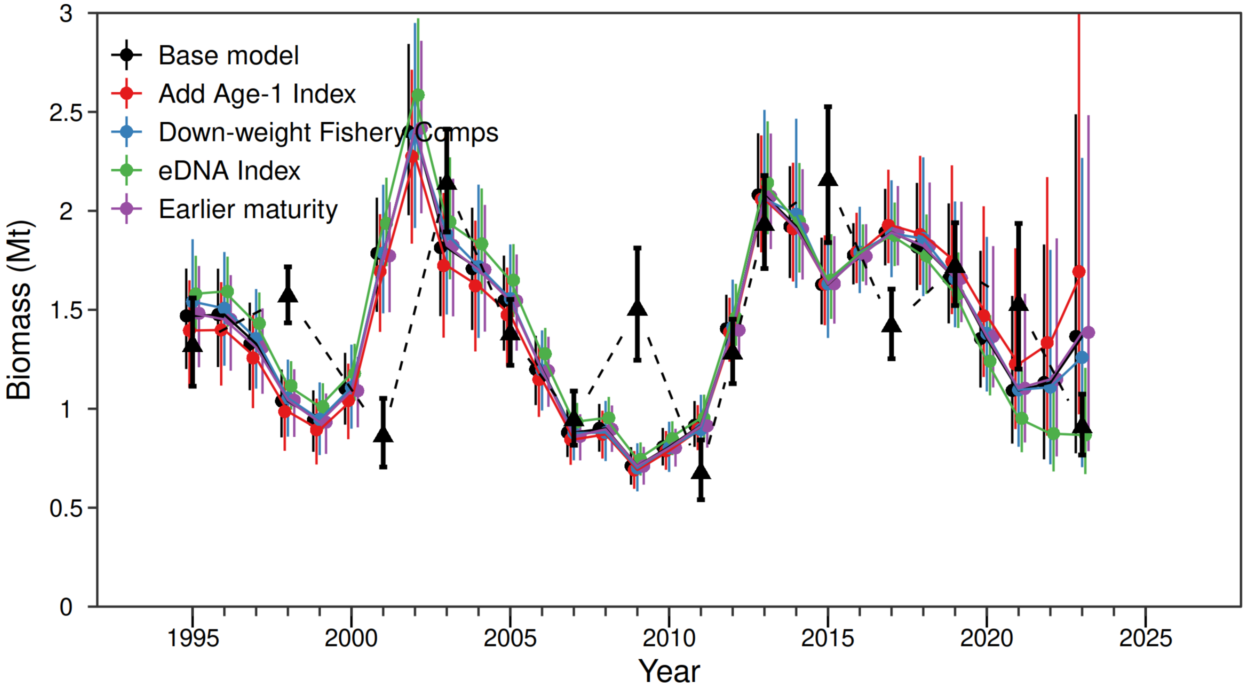

Figure 49. Markov chain Monte Carlo estimates of the fit to the acoustic survey biomass time series for the base model and alternative sensitivity runs that represent changes in data. The black triangles with error bars represent the input data points with associated uncertainty, and the blue dots are the estimated values for each year. See Figure 46 for sensitivity descriptions.

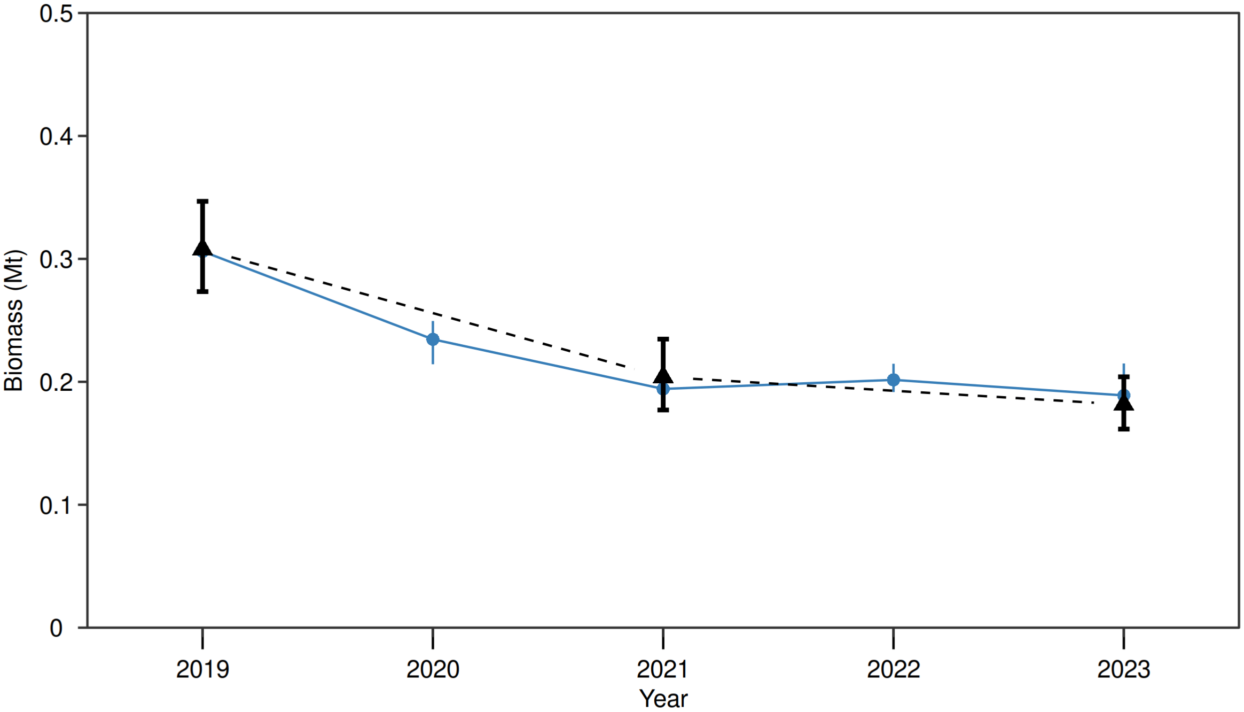

Figure 50. Markov chain Monte Carlo estimates of the fit to the eDNA survey biomass time series for the sensitivity model which includes the eDNA survey index. The black triangles with error bars represent the input data points with associated uncertainty, and the blue dots are the estimated values for each year.

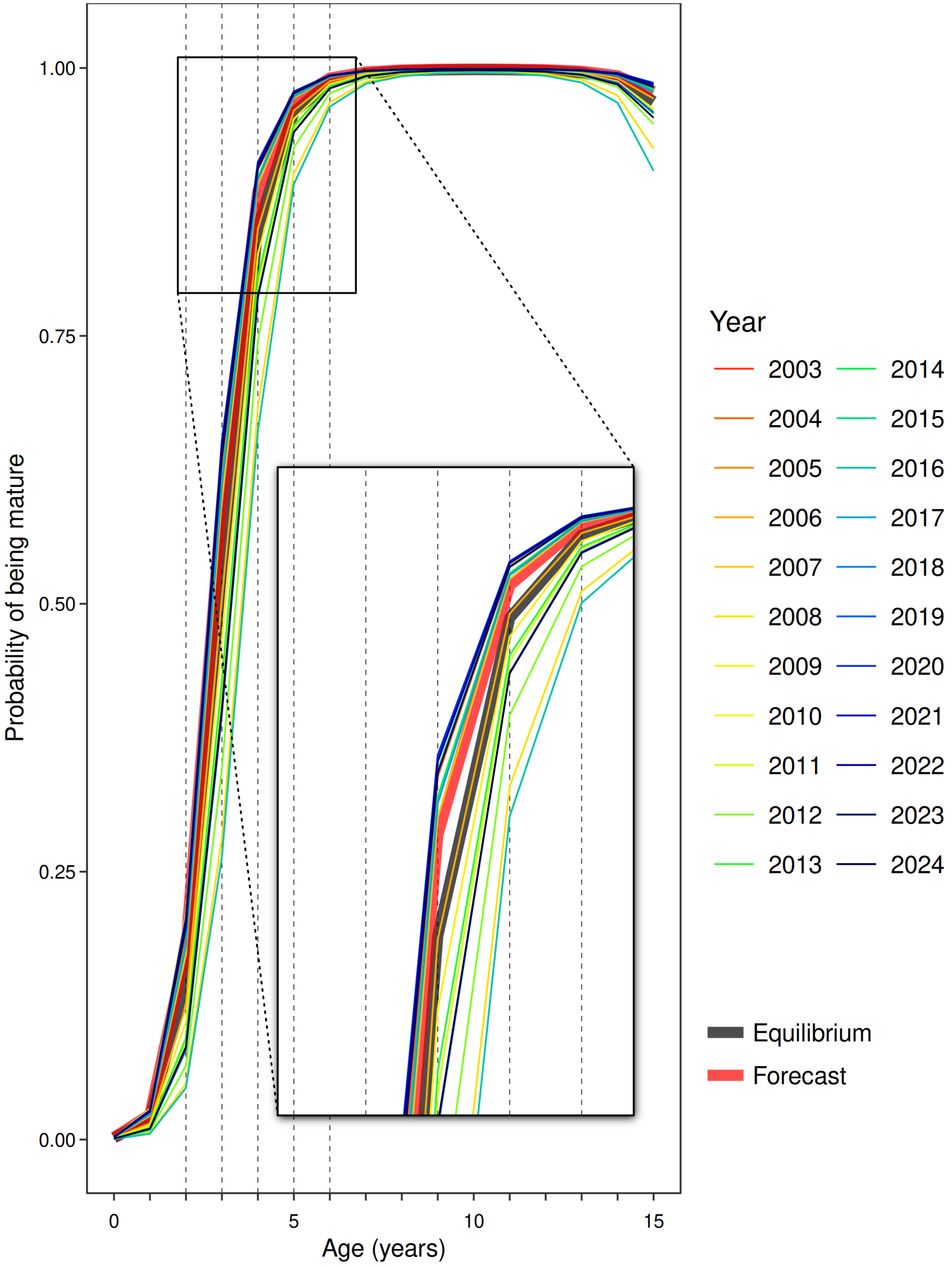

Figure 51. Maturity ogives by year used in the sensitivity to maturity being reached earlier in the year (July 1). The thick black line shows the equilibrium ogive which is an average of all years; the thick red line shows the forecast ogive which is an average of the last five years (2020–2024). The colors of the year lines move from orange in 2009 through the spectrum to dark blue in 2024.

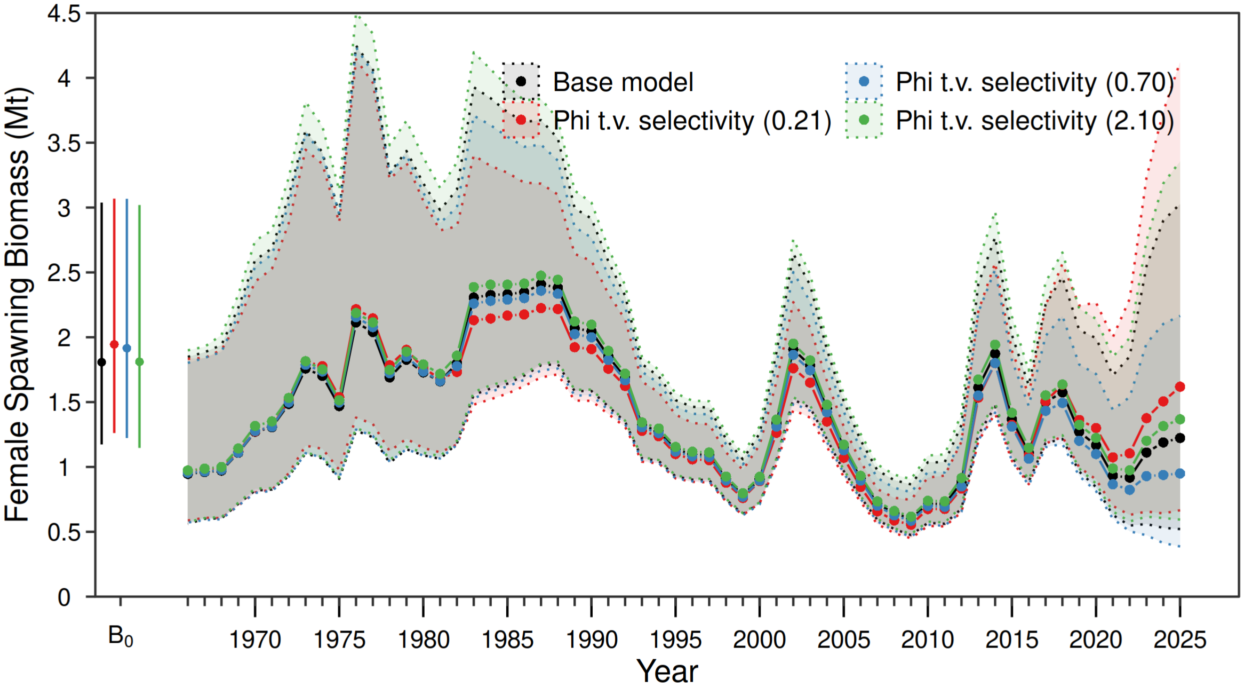

Figure 52. Markov chain Monte Carlo estimates of spawning biomass for the base model and alternative sensitivity runs representing different standard deviations (Φ) associated with time-varying selectivity. Standard deviations examined are below (0.21 and 0.70) and above (2.10) the base model value of 1.4.

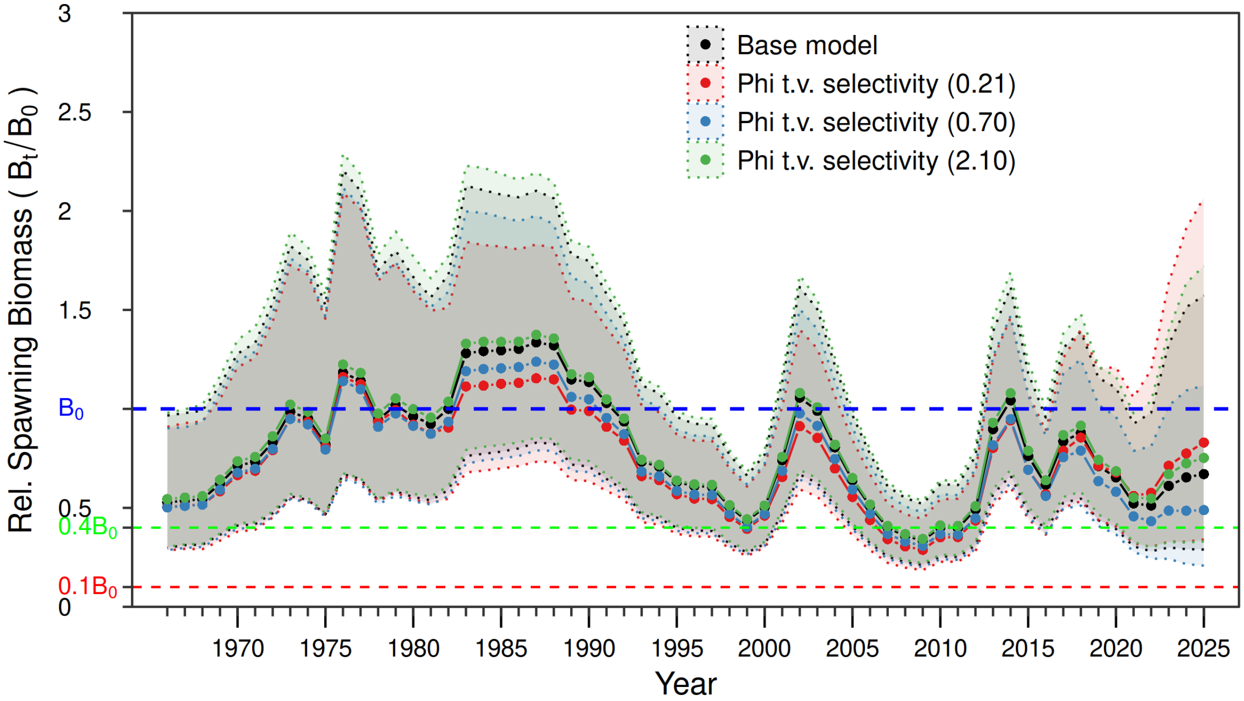

Figure 53. Markov chain Monte Carlo estimates of stock status (relative spawning biomass) for the base model and alternative sensitivity runs representing different standard deviations (Φ) associated with time-varying selectivity. See Figure 52 for sensitivity descriptions.

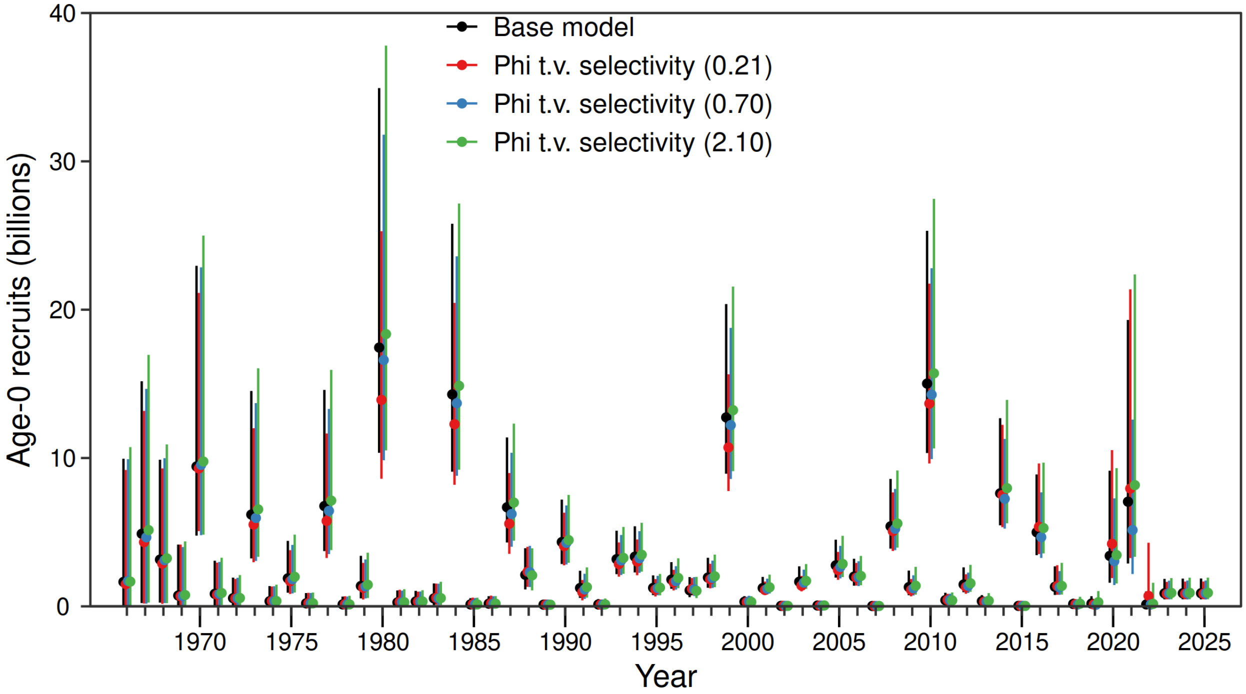

Figure 54. Markov chain Monte Carlo estimates of recruitment for the base model and alternative sensitivity runs representing different standard deviations (Φ) associated with time-varying selectivity. See Figure 52 for sensitivity descriptions.

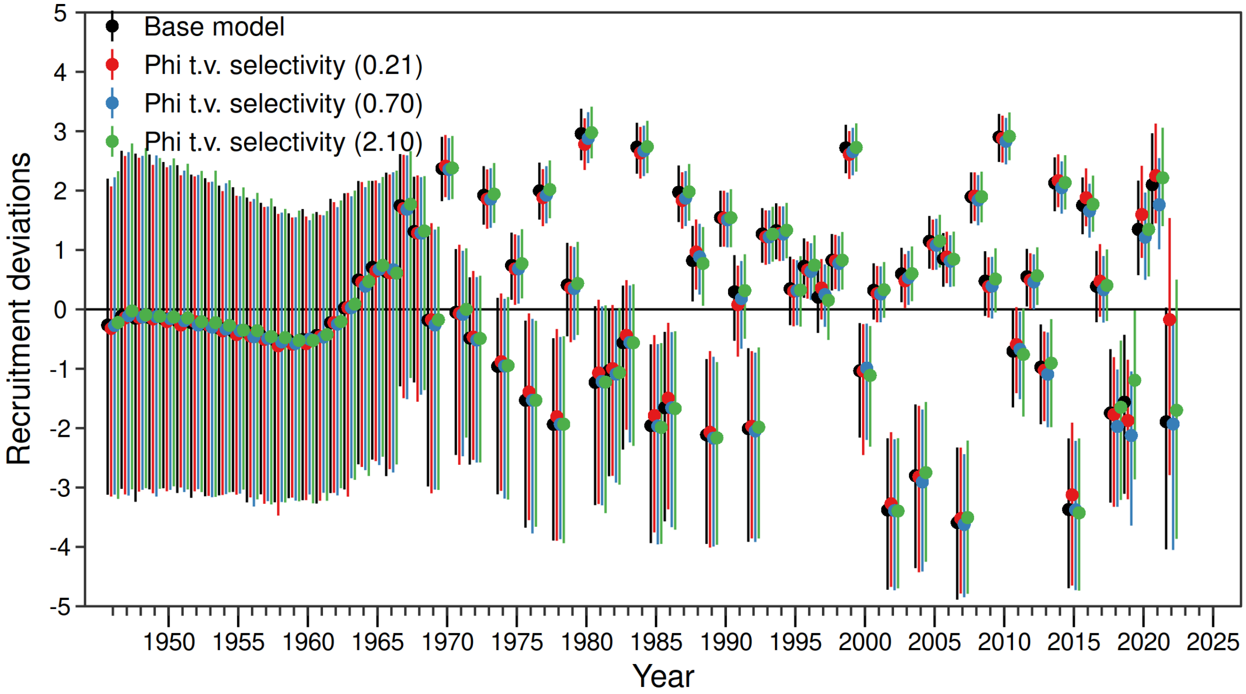

Figure 55. Markov chain Monte Carlo estimates of recruitment deviations for the base model and alternative sensitivity runs representing different standard deviations (Φ) associated with time-varying selectivity. See Figure 52 for sensitivity descriptions.

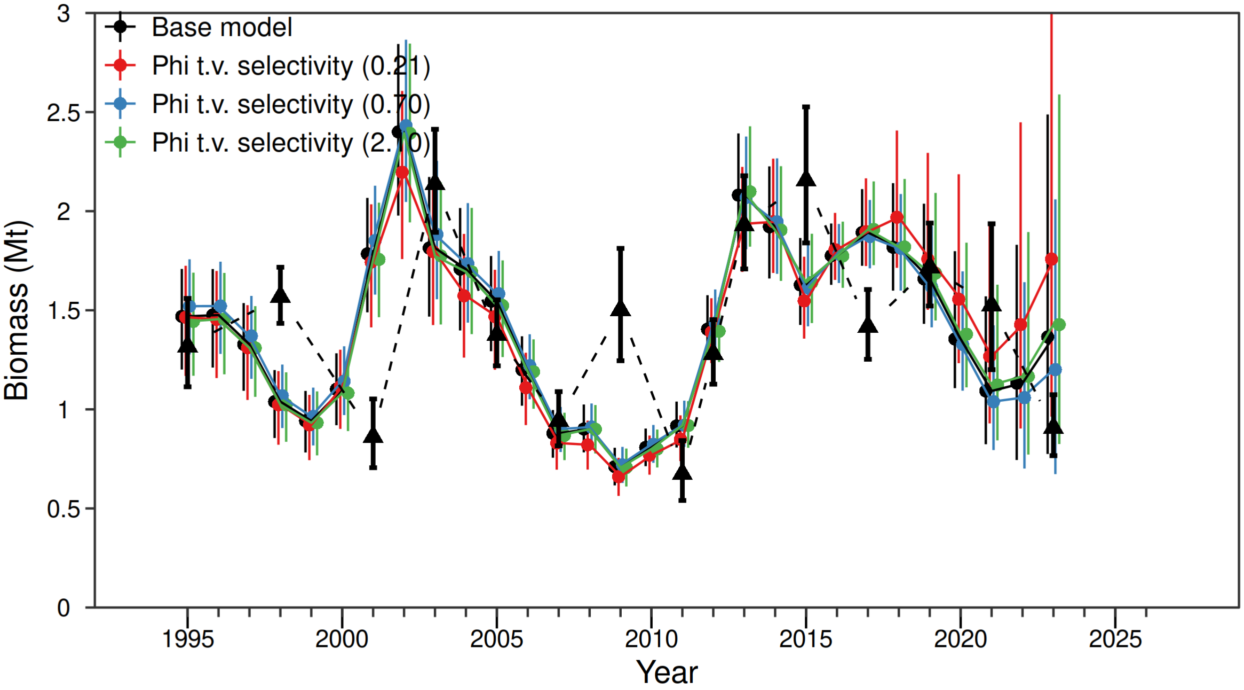

Figure 56. Markov chain Monte Carlo estimates of the fit to the survey index of age-2+ biomass for the base model and alternative sensitivity runs representing different standard deviations (Φ) associated with time-varying selectivity. See Figure 52 for sensitivity descriptions.

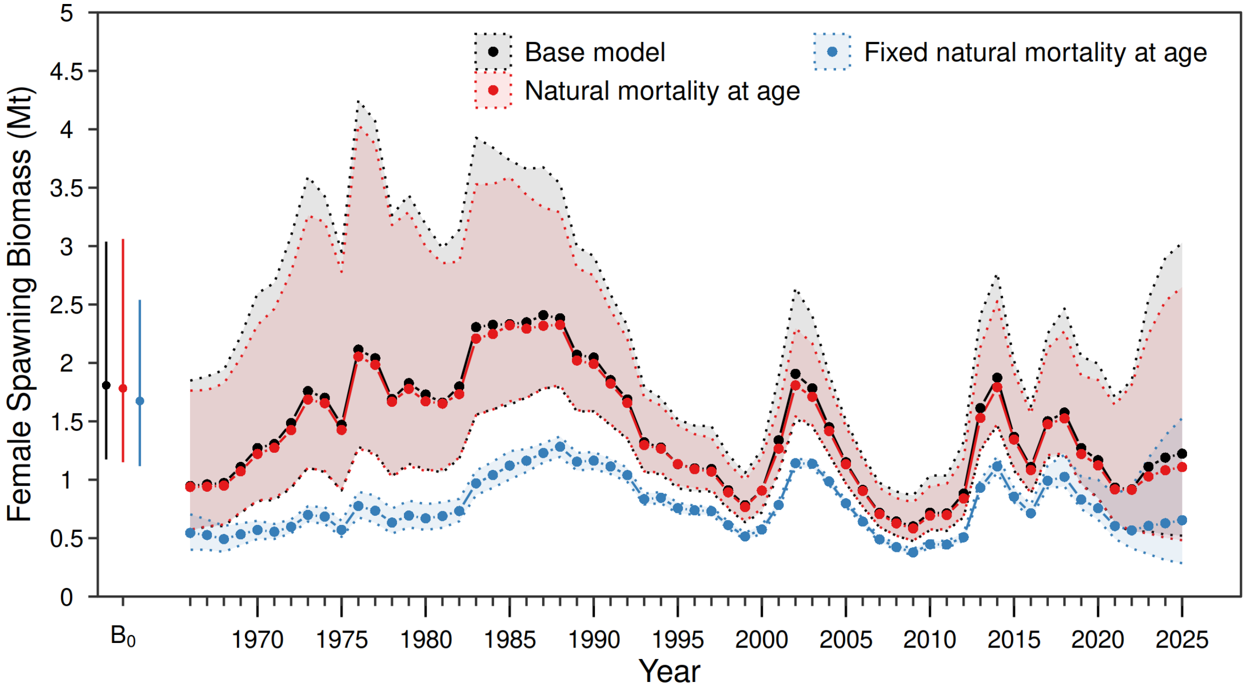

Figure 57. Markov chain Monte Carlo estimates of spawning biomass for the base model and alternative sensitivity runs representing different ways to parameterize natural mortality at age, where the baseline mortality is estimated (Natural mortality at age) or fixed (Fixed natural mortality at age). Year-specific deviations relating to cannibalistic mortality are added to the baseline mortality in both sensitivities. Natural mortality is assumed to be equal for all ages five and above.

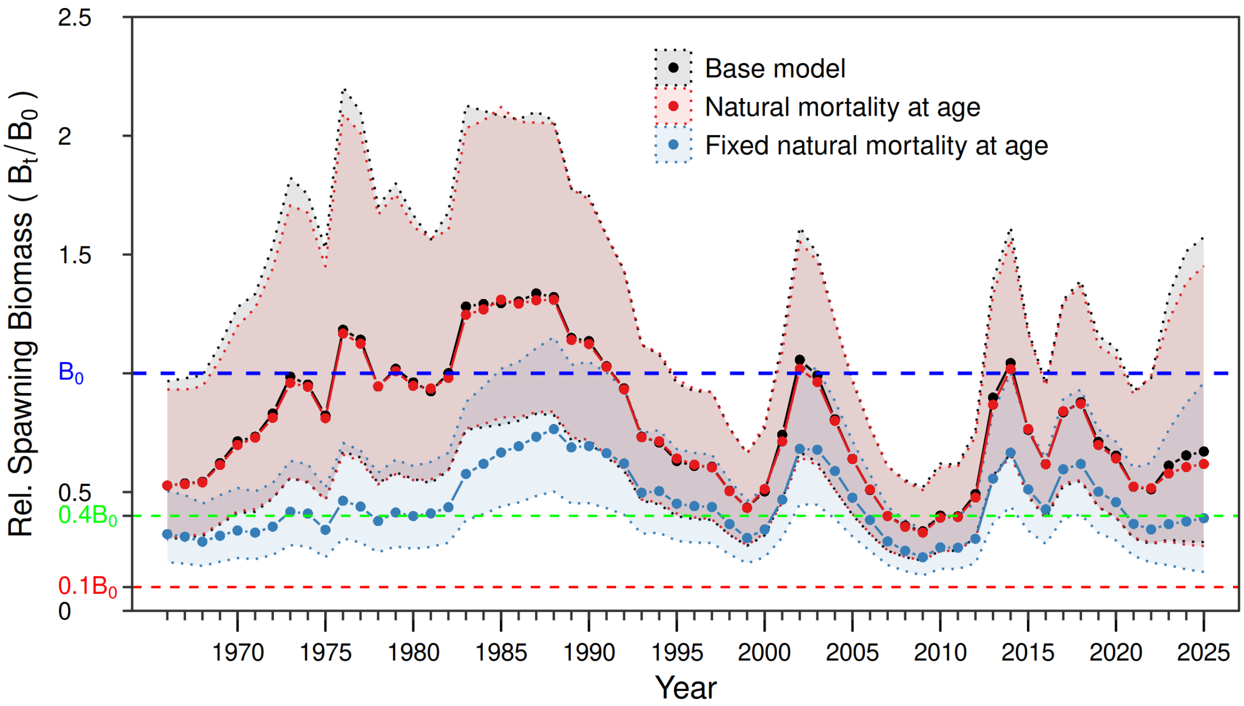

Figure 58. Markov chain Monte Carlo estimates of stock status (relative spawning biomass) for the base model and alternative sensitivity runs representing different ways to parameterize natural mortality at age. See Figure 57 for sensitivity descriptions.

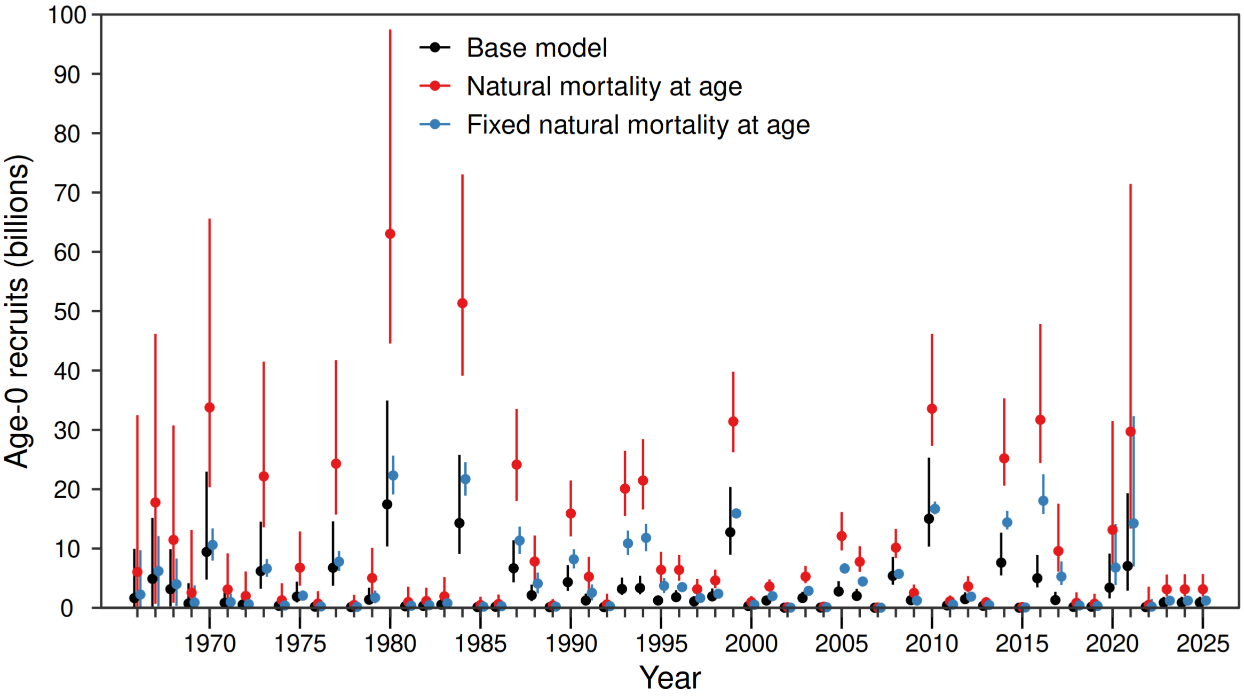

Figure 59. Markov chain Monte Carlo estimates of recruitment for the base model and alternative sensitivity runs representing different ways to parameterize natural mortality at age. See Figure 57 for sensitivity descriptions.

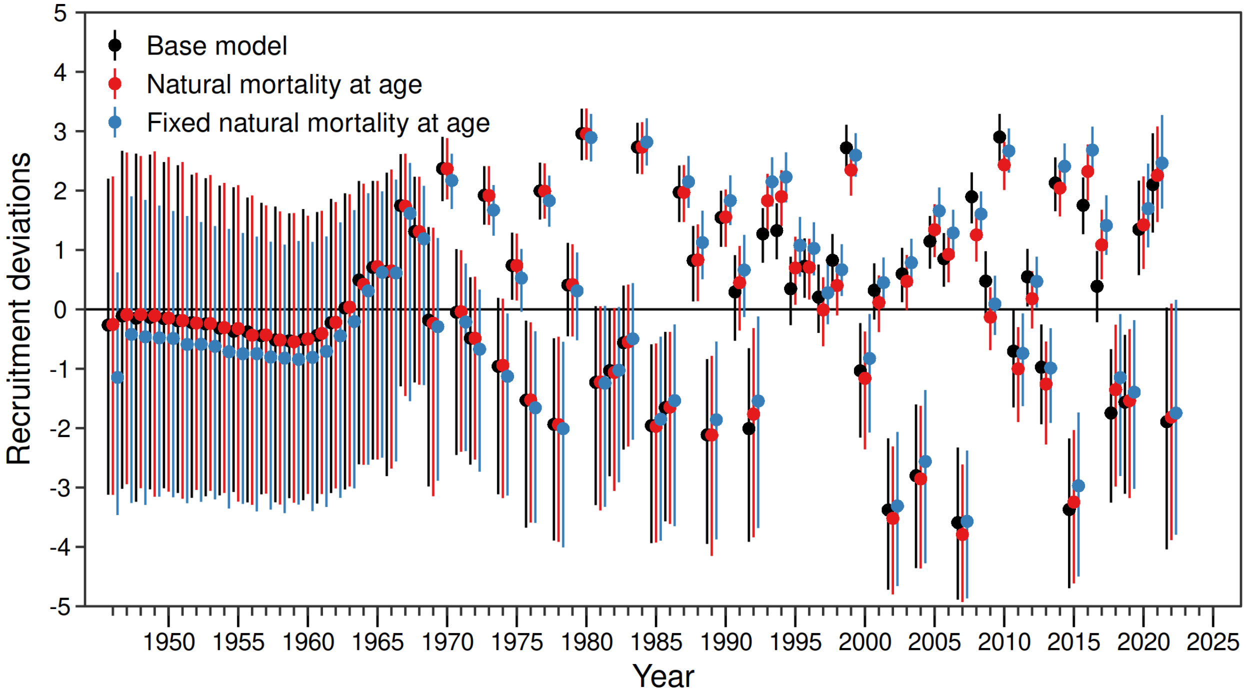

Figure 60. Markov chain Monte Carlo estimates of recruitment deviations for the base model and alternative sensitivity runs representing different ways to parameterize natural mortality at age. See Figure 57 for sensitivity descriptions.

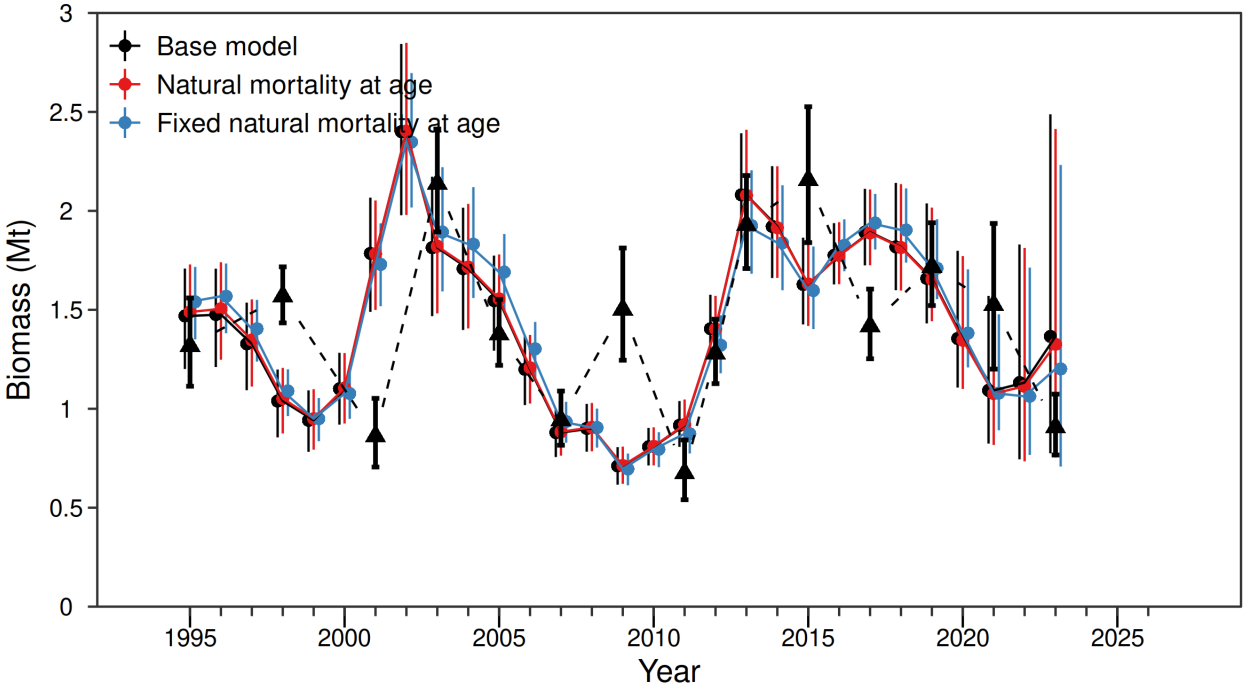

Figure 61. Markov chain Monte Carlo estimates of the fit to the survey index of age-2+ biomass for the base model and alternative sensitivity runs representing different ways to parameterize natural mortality at age. See Figure 57 for sensitivity descriptions.

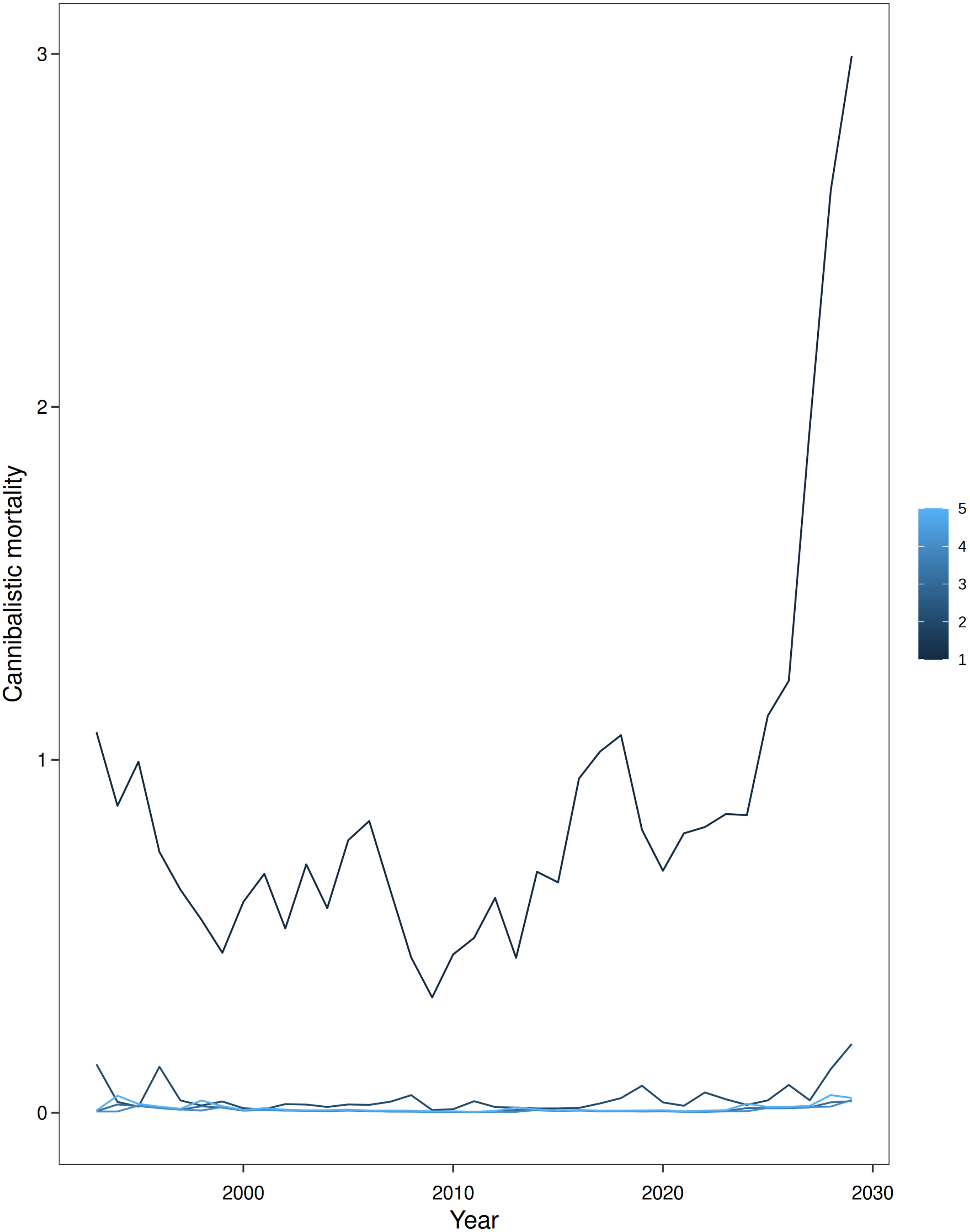

Figure 62. Mortality due to cannibalism for five age groups (darker colors for younger ages), where mortality is assumed to be equal for all ages five and above. Mortality is highest for younger ages and is increasing for all ages in the most recent years of projections from the Climate-Enhanced, Age-based model with Temperature-specific Trophic Linkages and Energetics (CEATTLE) model.

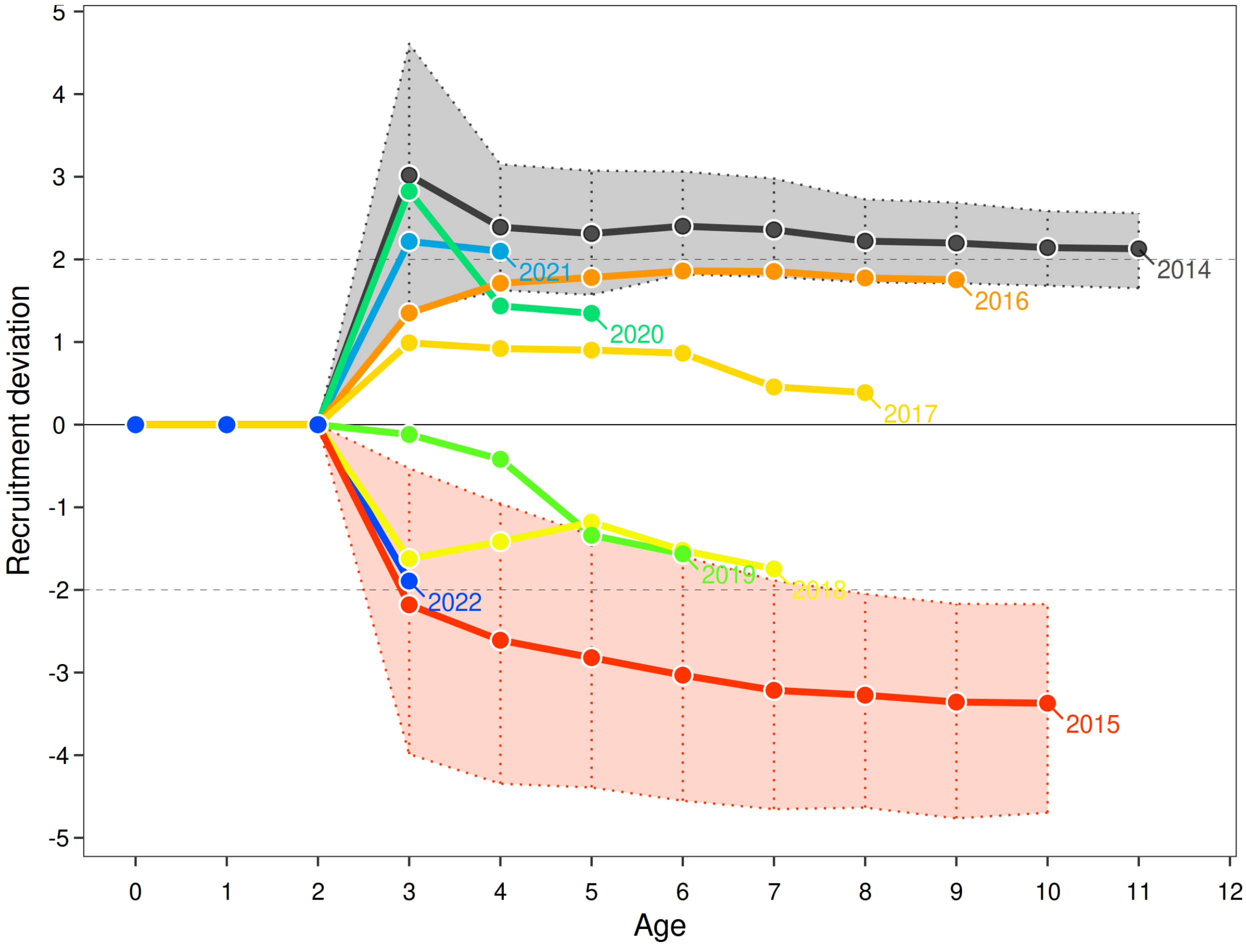

Figure 63. Retrospective analysis of recruitment deviations from Markov chain Monte Carlo models over the last 10 years. Recruitment deviations are the median log-scale differences between recruitment estimated by the model and expected recruitment from the stock-recruitment relationship (shading represents 95% posterior credibility intervals for a select low and high deviation). Age-0 recruitment deviations are non-zero because Markov chain Monte Carlo allows for sampling from the full lognormal distribution. Lines represent estimated recruitment deviations for cohorts born from 2014 to 2024, with cohort birth year marked at the right of each color-coded line. For example, the right-most point for the 2017 cohort shows the cohort at age-8 (i.e., at the start of 2025, which represents the base model and includes data through 2024). The next point to the left is the 2017 cohort at age-7, calculated by removing one year of data (so includes data up to 2023). Thus, models are fit to data available only up to the start of the year in which each cohort became a given age, such that the last year of data for a given point equals $cohort\ birth\ year + cohort\ age - 1$.

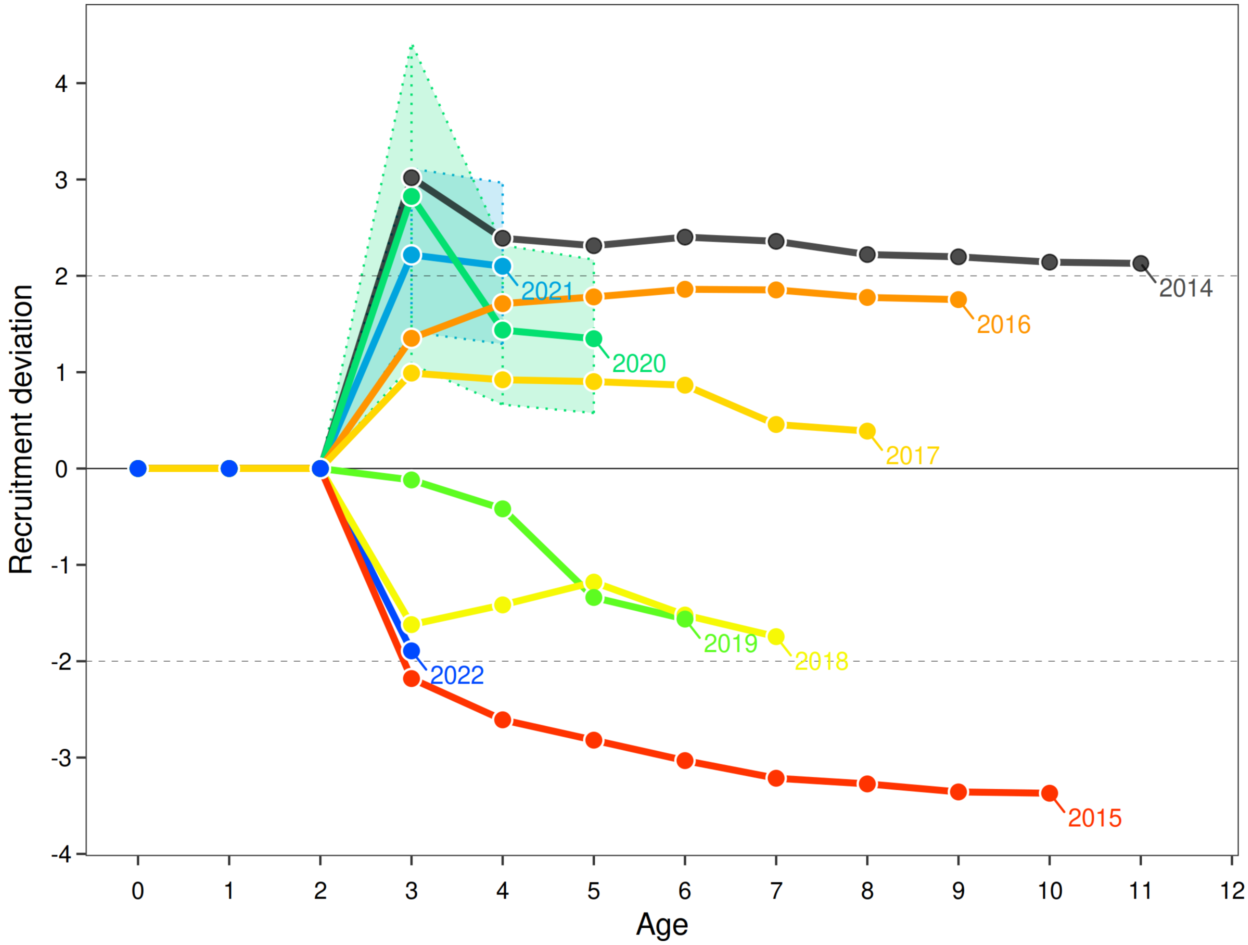

Figure 64. As for Figure 63 but with the credibility intervals shown for the 2020 and 2021 cohorts.

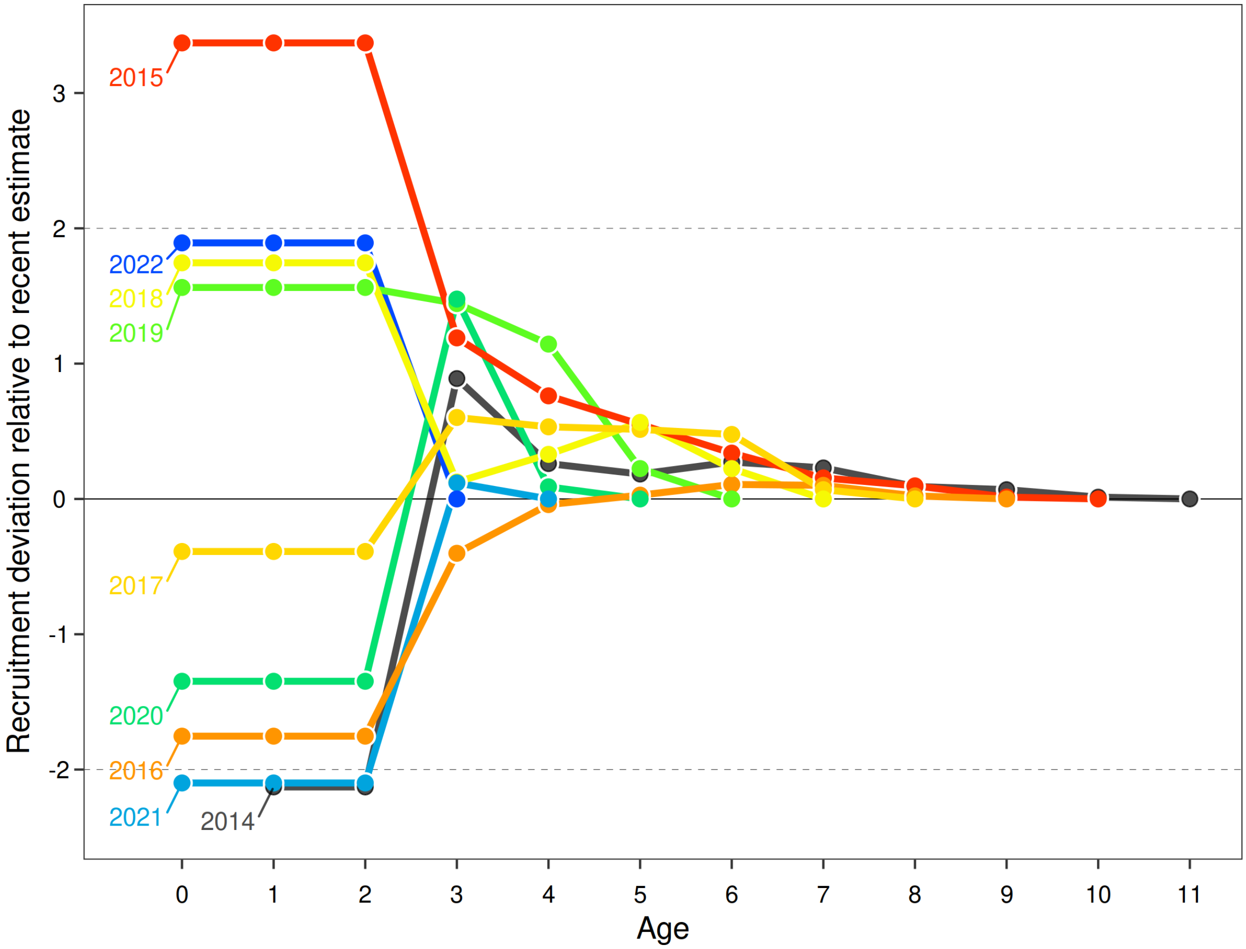

Figure 65. Retrospective recruitment estimates shown in Figure 63 scaled relative to the most recent estimate of the strength of each cohort.

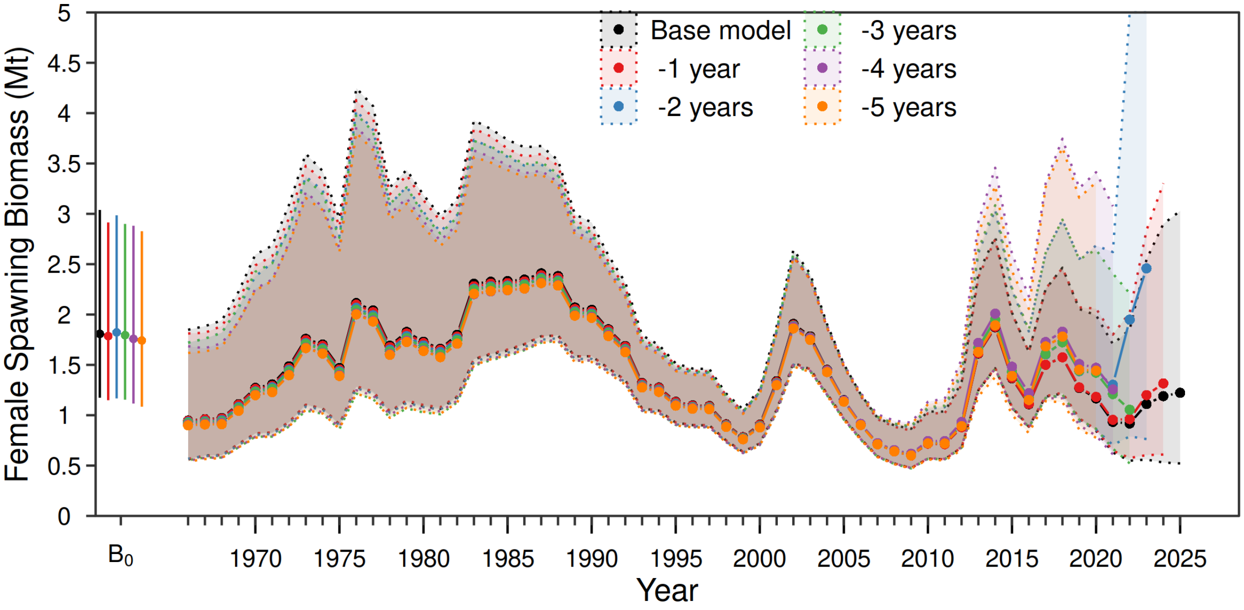

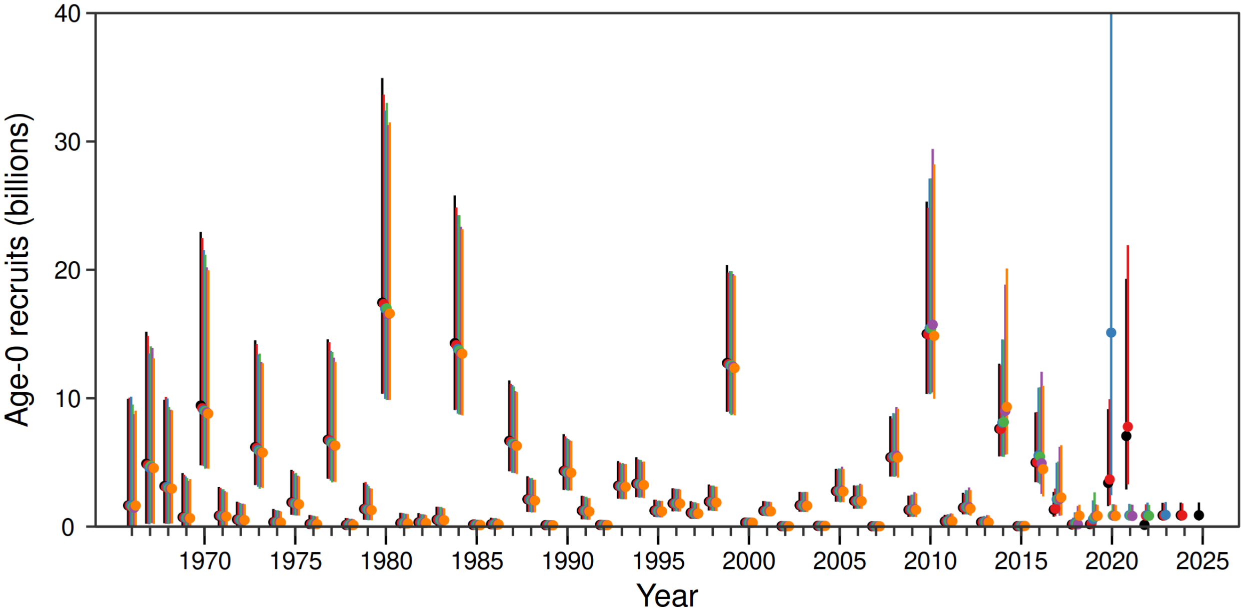

Figure 66. Markov chain Monte Carlo estimates of spawning biomass at the start of each year (top) and recruitment (bottom) for the base model and 5-year retrospective runs.

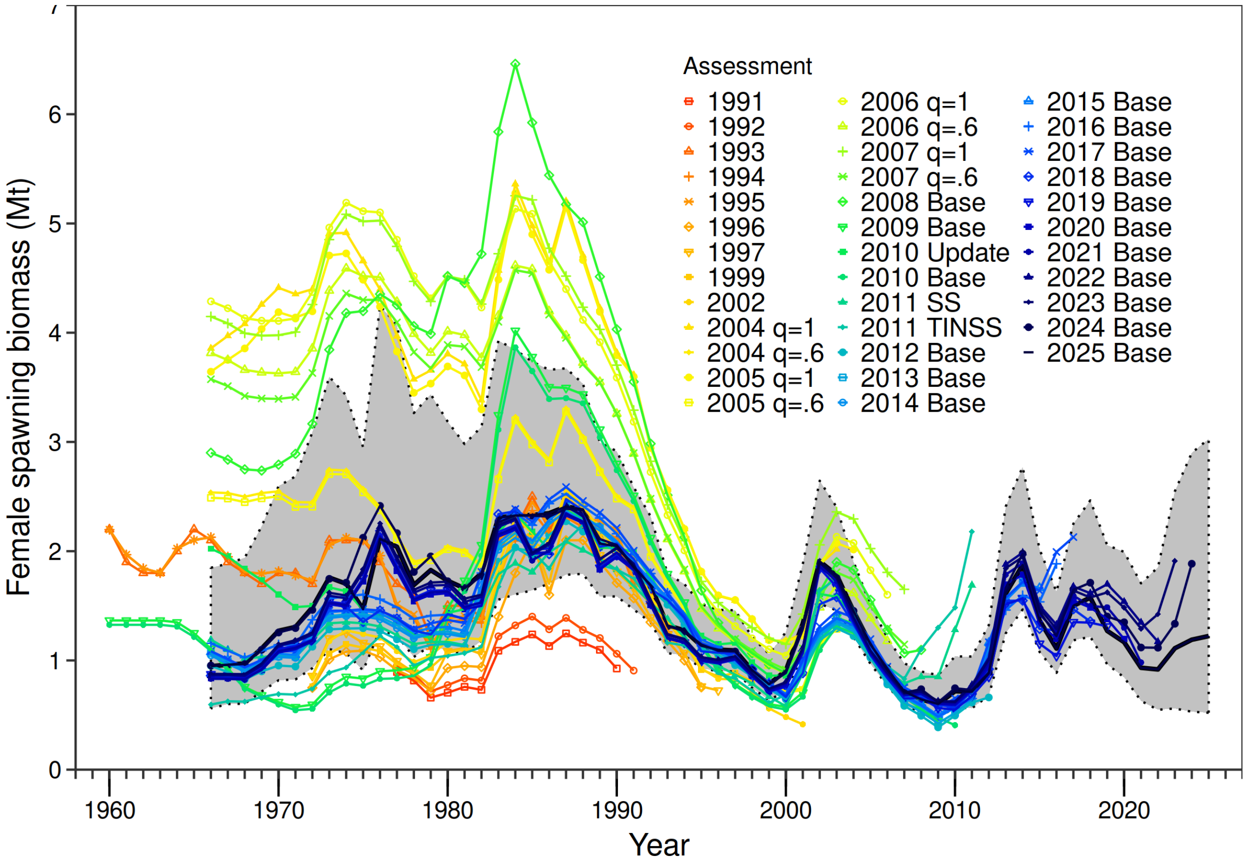

Figure 67. Summary of historical Pacific Hake assessment estimates of spawning biomass. Estimates are MLEs or Markov chain Monte Carlo medians depending on the model structure. Shading represents the 95% credible interval from the 2025 base model. Line colors are shades of orange for the oldest models, yellow shades for the 2000's, green shades for the 2010's and into blue shades from 2013 to present.

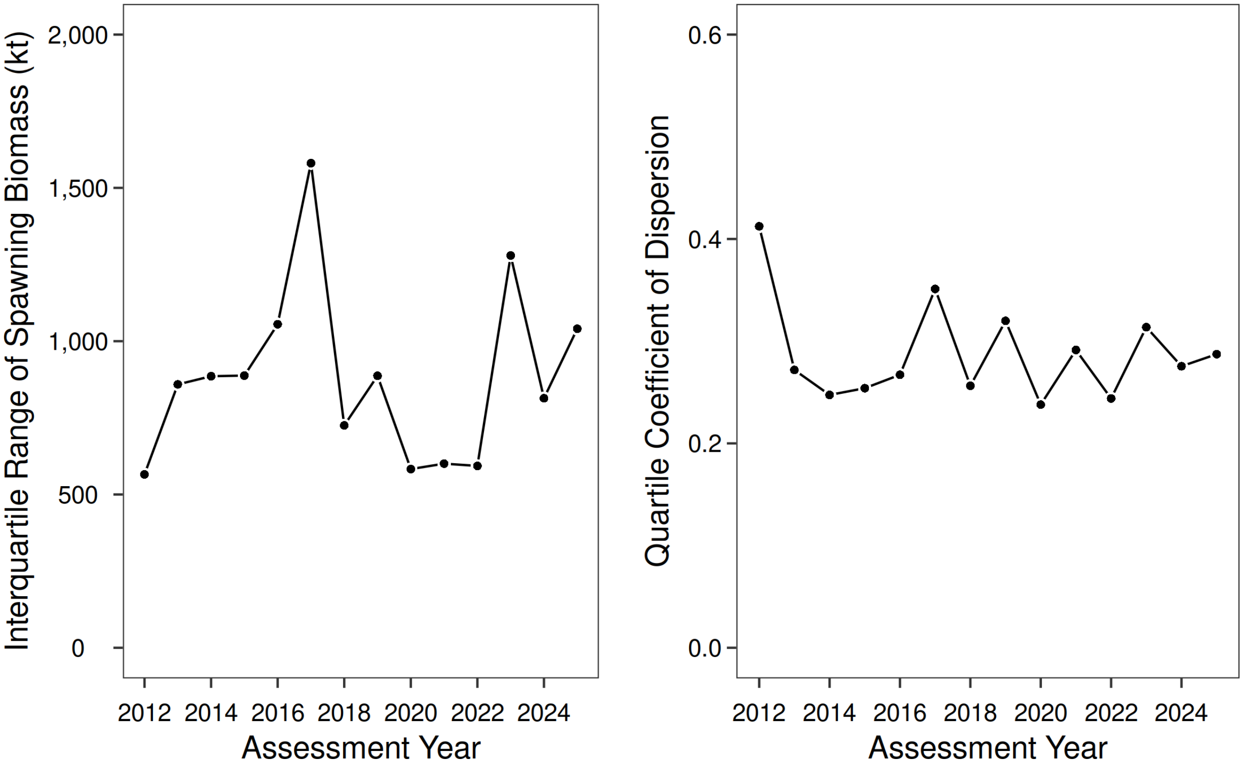

Figure 68. Comparison of absolute (left panel) and relative (right panel) variability associated with terminal year estimates of spawning biomass from Pacific Hake stock assessments dating back to 2012 (note: terminal year is the same as assessment year). The interquartile range specifies the width from quartile 1 (Q_1: 25th percentile) to quartile 3 (Q_3: 75th percentile) of terminal year spawning biomass from the posterior distribution and is a measure of absolute variability (similar to credible intervals). The quartile coefficient of dispersion is a relative measure of variability that can be compared across different data sets (similar to the coefficient of variation but less susceptible to outliers) and is calculated as $(Q_3 - Q_1)/(Q_1 + Q_3)$.

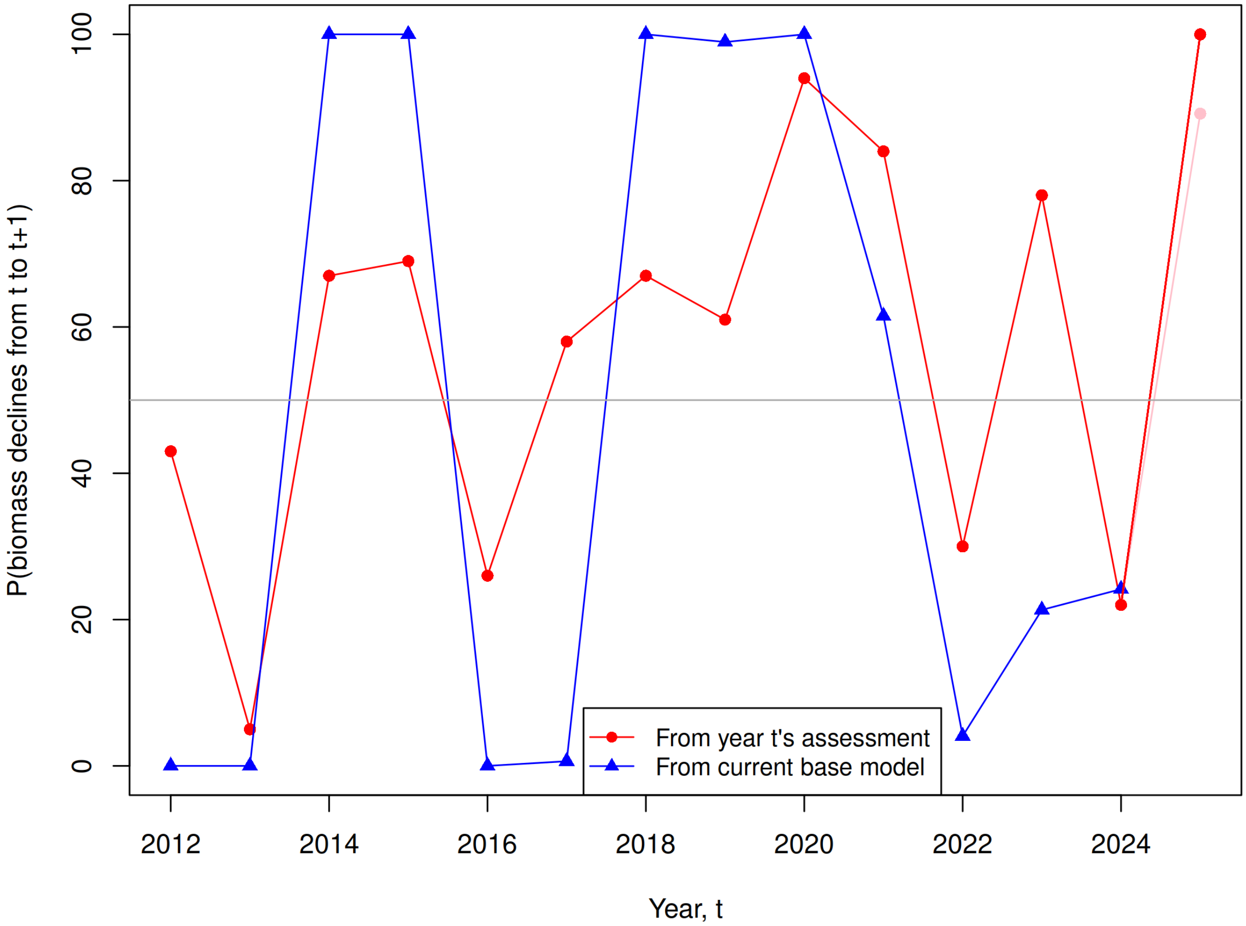

Figure 69. For each year t, $\mathrm{P}(B_{t+1} < B_t)$ is the probability that the spawning biomass at the start of $t+1$ is below that at the start of t. It is calculated in two ways. Red circles: the probability is taken from year t's stock assessment document, from the row in the decision table corresponding to the consequent catch in year t (with interpolation if necessary). Blue triangles: the probability is calculated using the current 2025 base model. The grey horizontal line is the 50% value. For each year except 2017, 2021, and 2023, both probabilities lie on the same side of the grey line, indicating that each year's assessment model has almost always 'correctly' estimated an increase or decrease in the subsequent year's biomass. For the 2025 assessment the probabilities are shown for all catch alternatives for 2025, as described in Table 27, with 0 t being the lowest probability, shown in pink (the others are all overlayed at 100%).

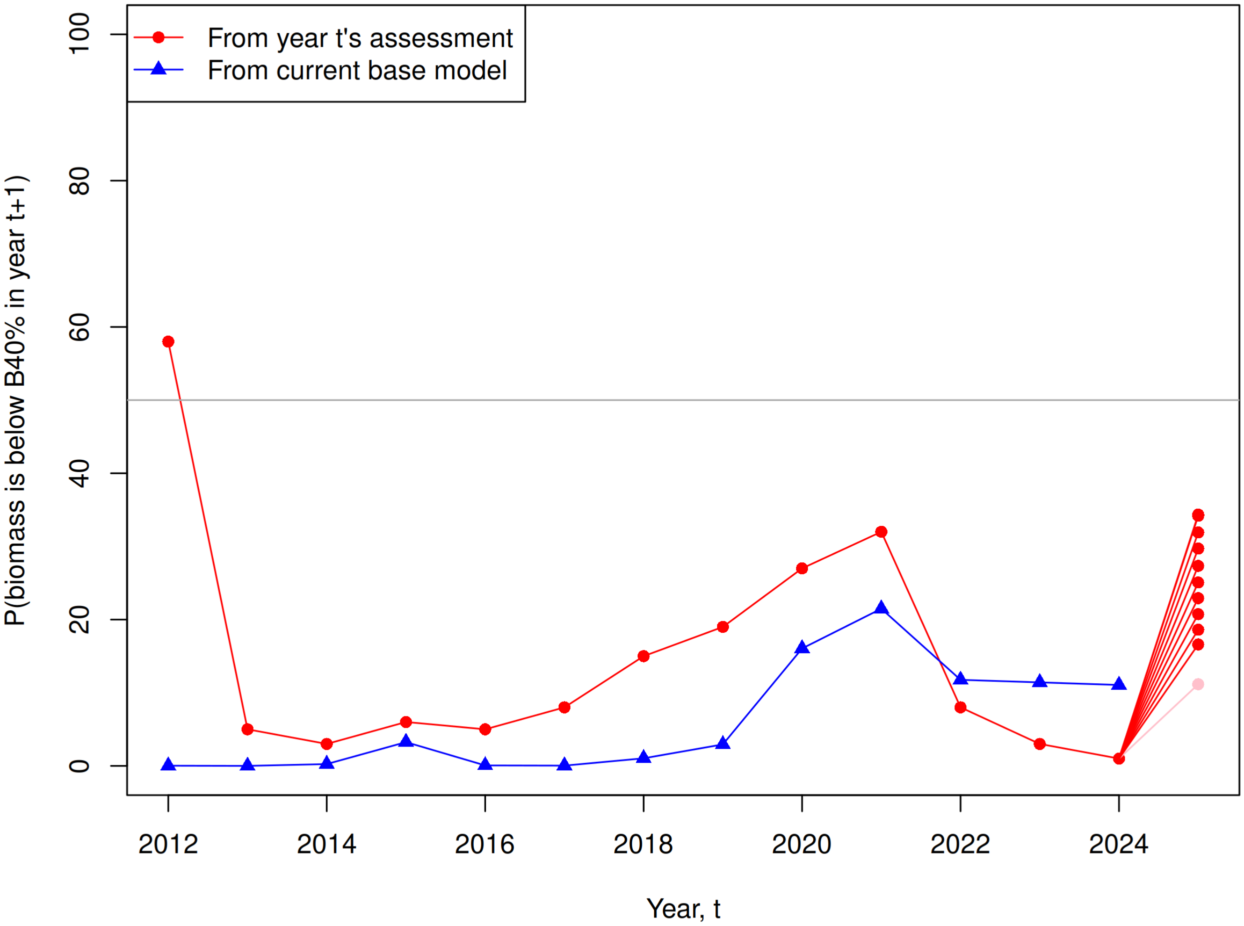

Figure 70. For each year t, $\mathrm{P}(B_{t+1} < B_{40\%})$ is the probability that the spawning biomass at the start of $t+1$ is below $B_{40\%}$. The red circles and blue triangles represent probabilities calculated analogously to Figure 69. The grey horizontal line is the 50% value. For each year except 2012, both probabilities lie on the same side of the grey line, indicating that each year's assessment model almost always correctly estimated that the subsequent year's biomass will not fall below $B_{40\%}$. For the 2025 assessment the probabilities are shown for all catch alternatives for 2025, as described in Table 27, with 0 t shown in pink.

A BASE MODEL MCMC DIAGNOSTICS

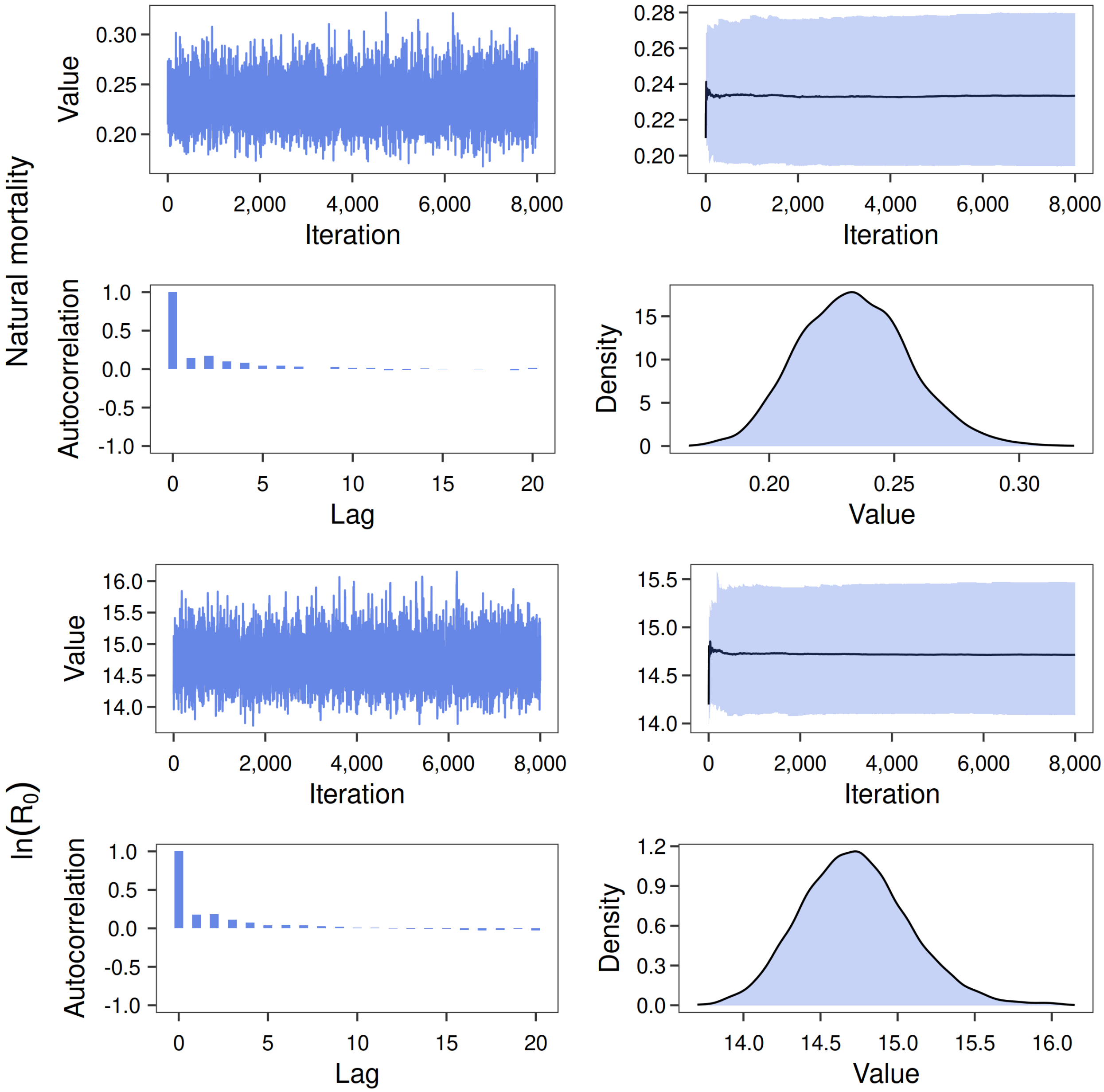

Figure A.1. Summary of Markov chain Monte Carlo diagnostics for natural mortality (upper 4 panels) and the natural log of mean unfished equilibrium recruitment ($\ln(R_0)$; lower 4 panels) in the base model. Top sub-panels show the trace of the sampled values across iterations (absolute values, top left; cumulative running median with 2.5th and 97.5th percentiles, top right). The lower left sub-panel indicate the autocorrelation present in the chain at different lag times (i.e., distance between samples in the chain), and the lower right sub-panel shows the distribution of the values in the chain (i.e., the marginal density from a smoothed histogram of values in the trace plot).

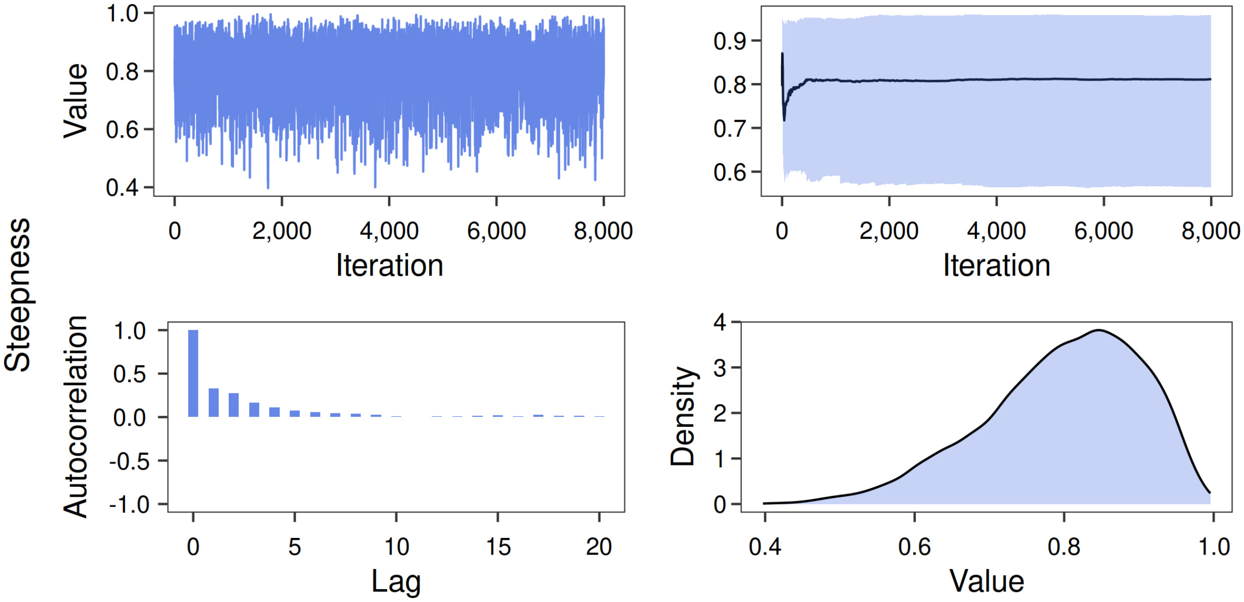

Figure A.2. Summary of Markov chain Monte Carlo diagnostics for steepness in the base model. Sub-panel descriptions as in Figure A.1.

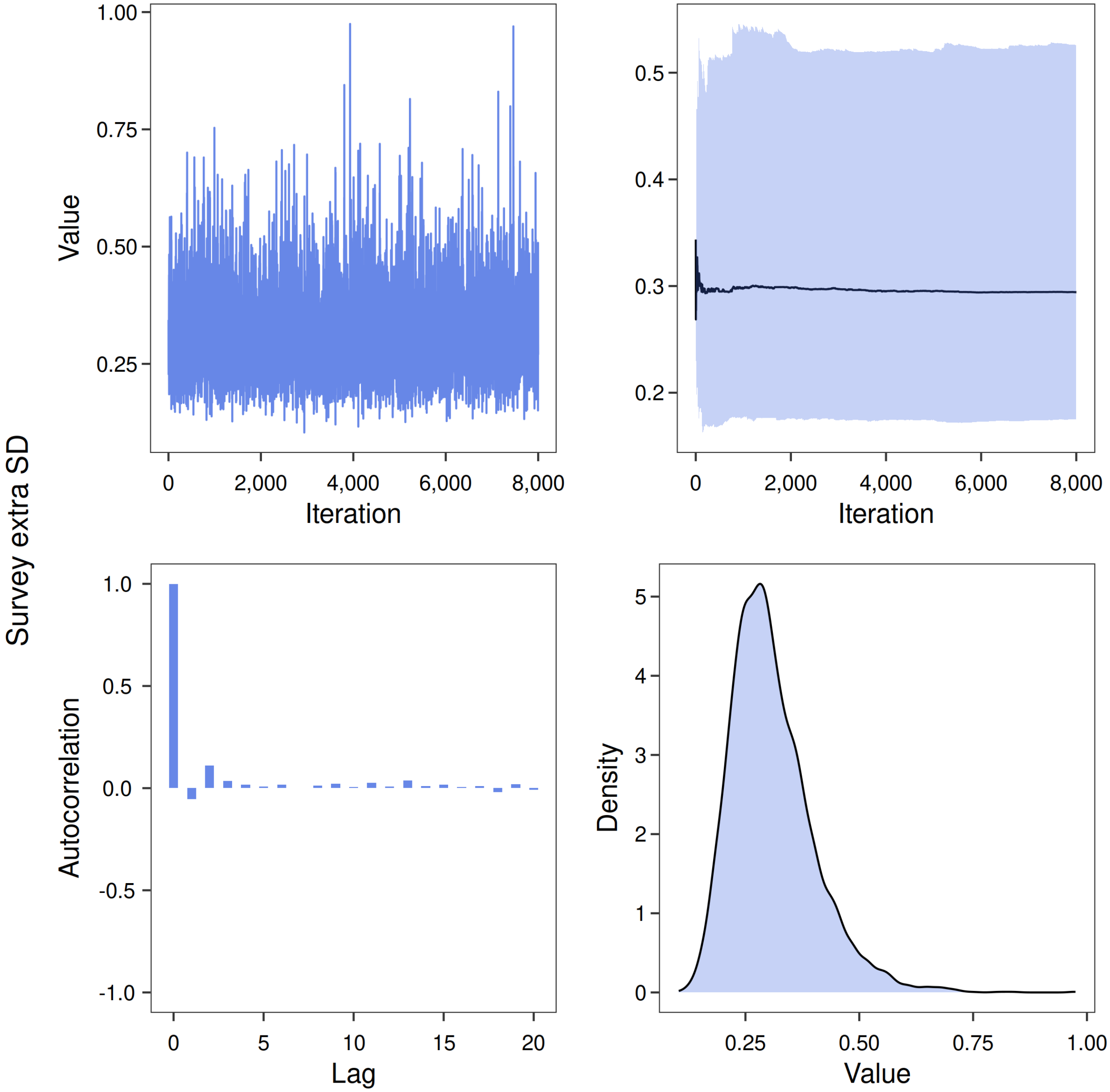

Figure A.3. Summary of Markov chain Monte Carlo diagnostics for the additional standard deviation (SD) in the biomass index. Sub-panel descriptions as in Figure A.1.

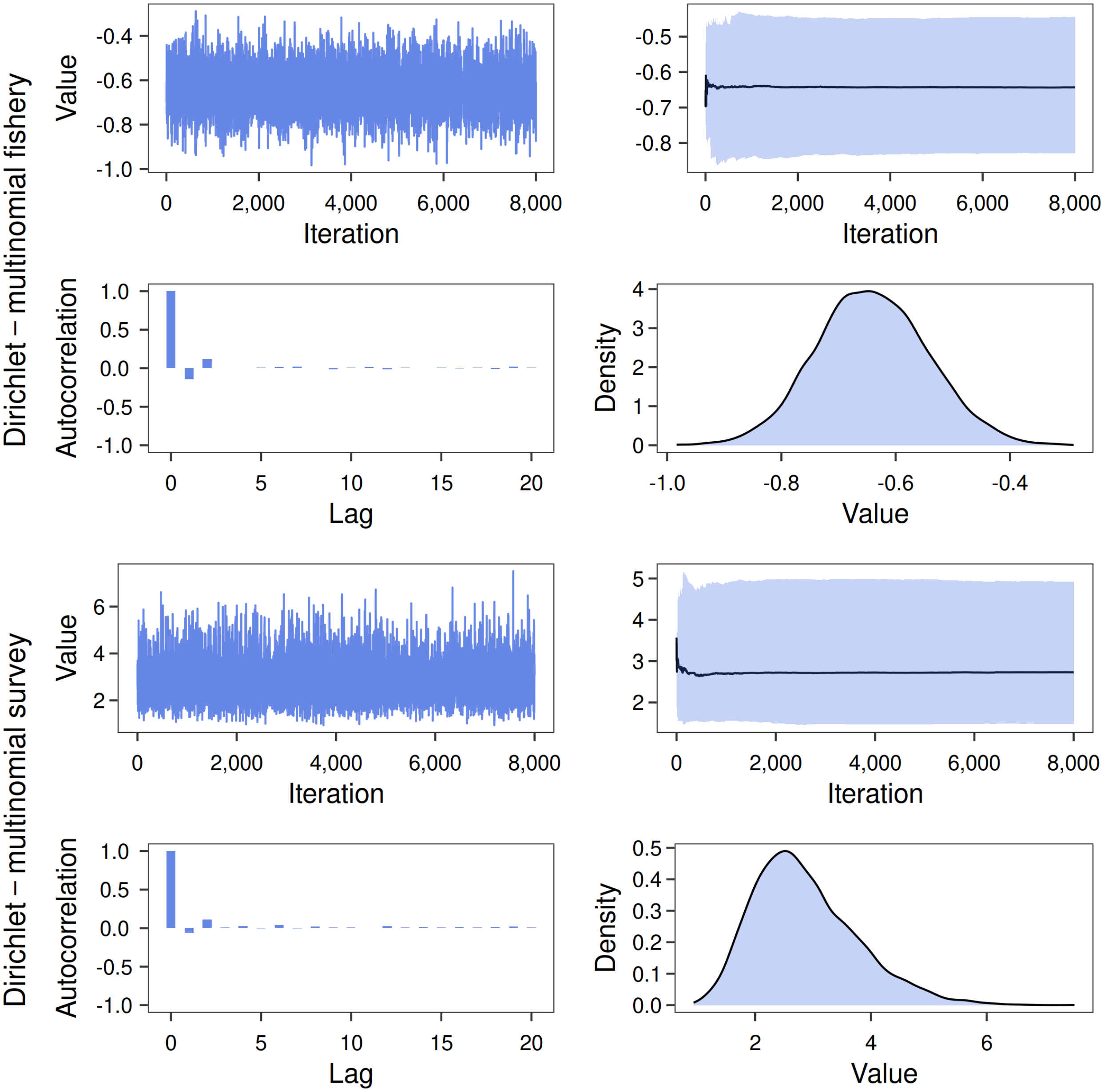

Figure A.4. Summary of Markov chain Monte Carlo diagnostics for the Dirichlet-multinomial age-composition parameters for the fishery (θ_{fish}, upper 4 panels) and the survey (θ_{surv}, lower 4 panels) in the base model. Sub-panel descriptions as in Figure A.1.

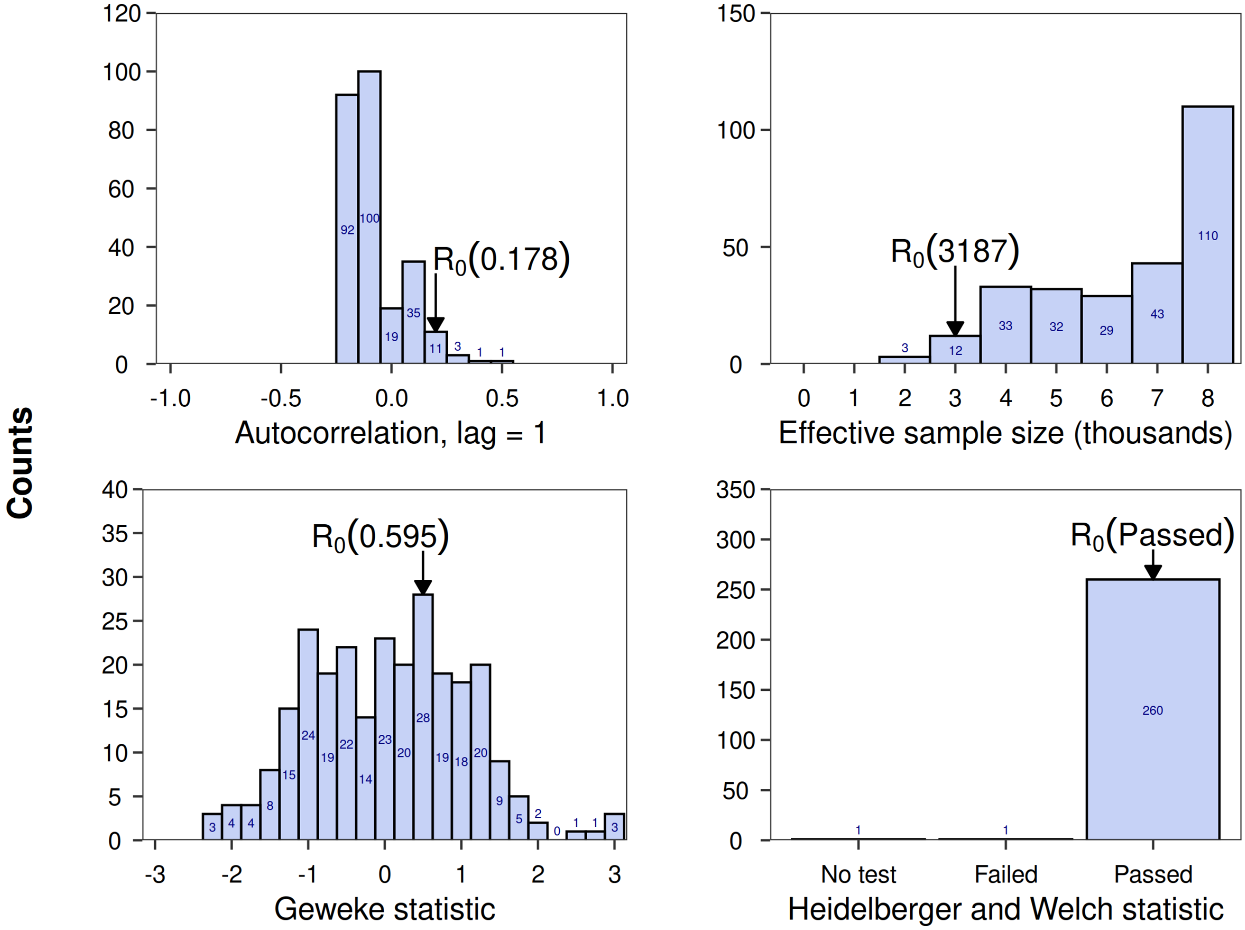

Figure A.5. Summary histograms of Markov chain Monte Carlo diagnostics for all base model parameters. The level of autocorrelation in the chain (distribution across lag times, i.e., distance between samples in the chain, shown in the top left panel) influences the effective sample size (top right panel) used to estimate posterior distributions. The Geweke statistic (lower left panel) tests for equality between means located in the first part of the chain against means in the last part of the chain. The Heidelberger and Welch statistic (lower right panel) tests if the sampled values come from a stationary distribution by comparing different sections of the chain. Values for the unfished equilibrium recruitment (R_0) are explicitly highlighted. Values inside the bars represent the number of parameters counted in that bin.

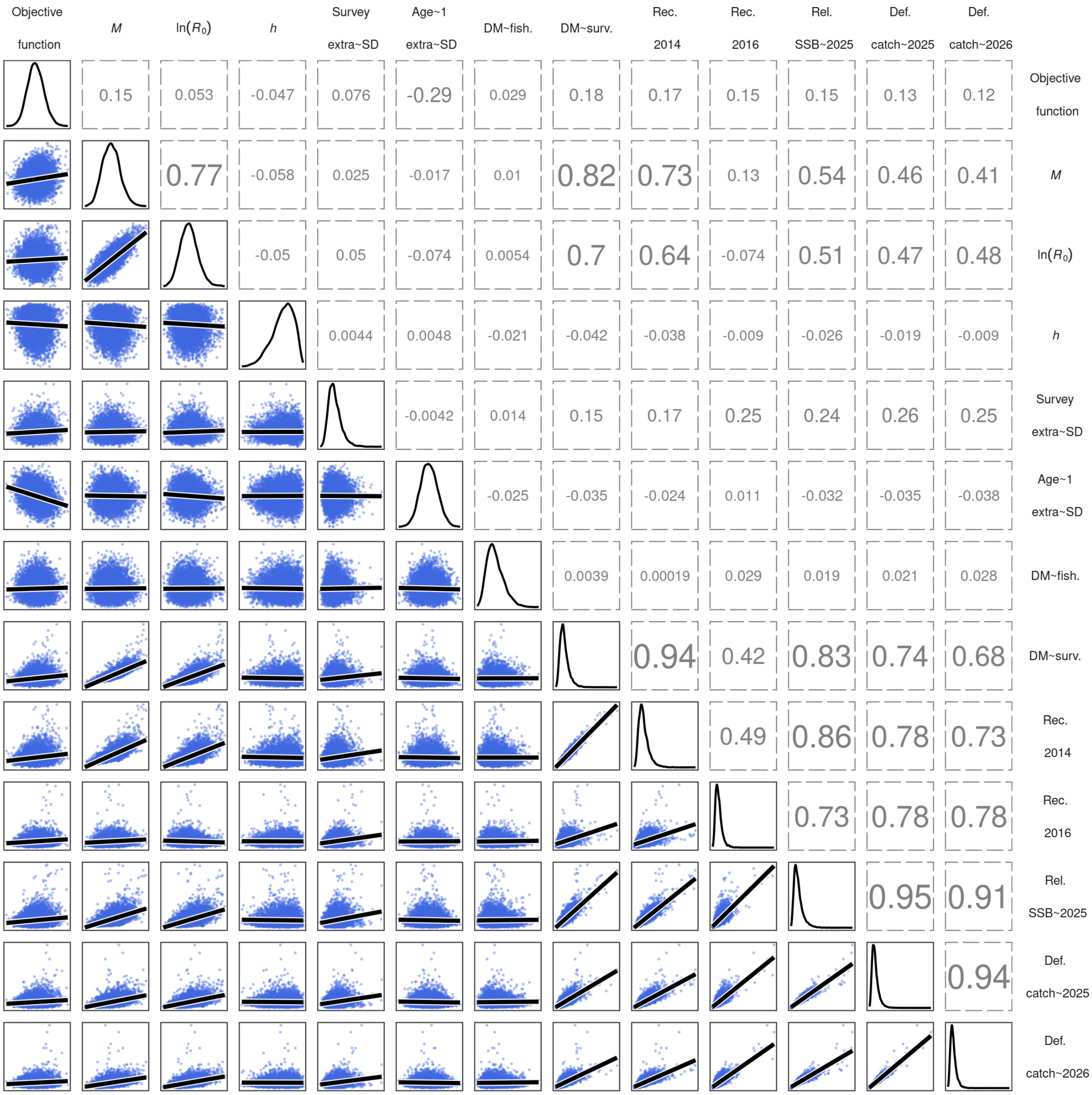

Figure A.6. Posterior correlations among the objective function which is minimized during model fitting, key base-model parameters, and derived quantities. Numbers refer to the absolute correlation coefficients, with font size proportional to the square root of the coefficient. Straight lines on the scatterplots are linear regressions.

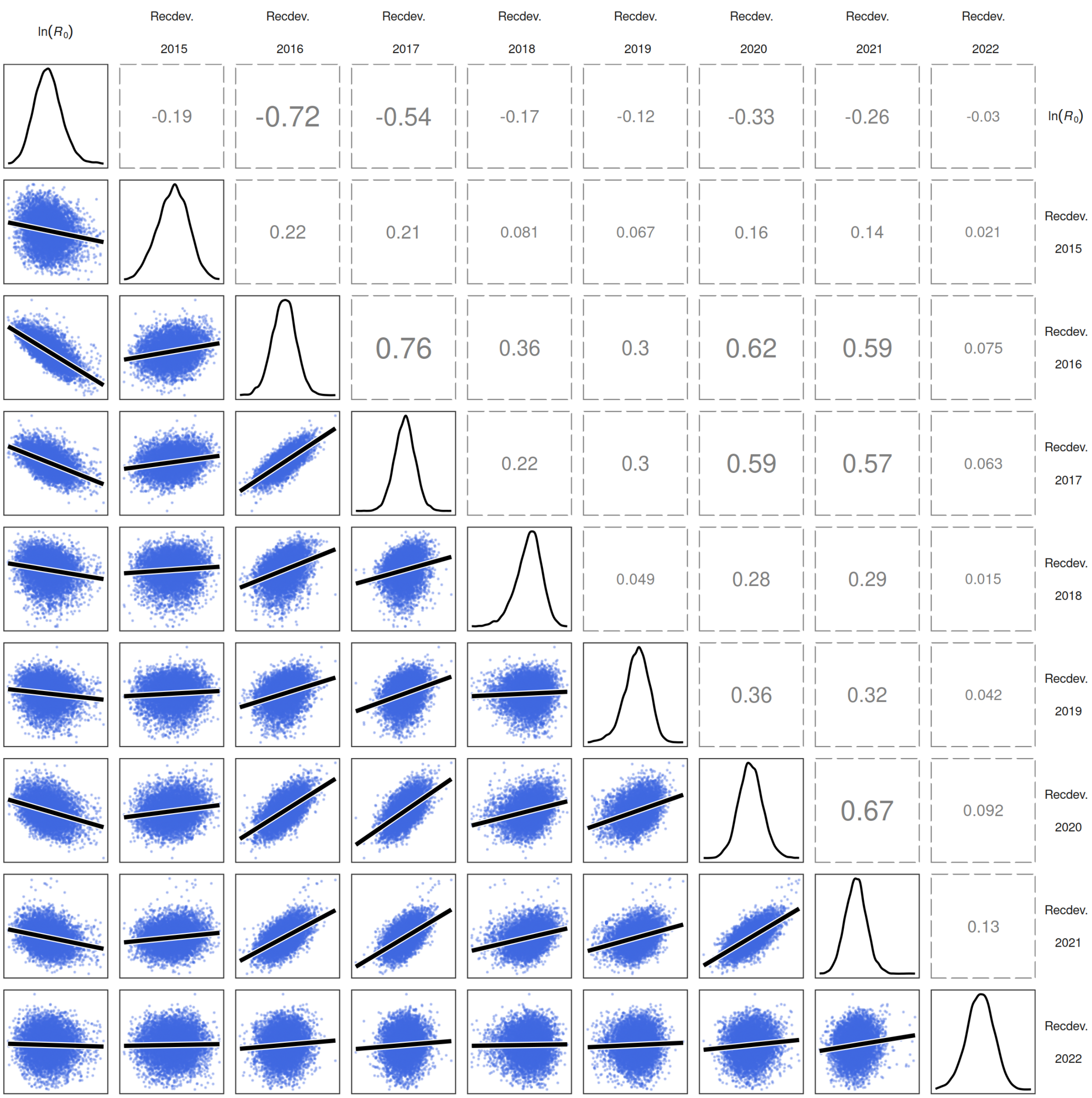

Figure A.7. Posterior correlations among recruitment deviations from recent years and mean unfished equilibrium recruitment. Numbers refer to the absolute correlation coefficients, with font size proportional to the square root of the coefficient. Straight lines on the scatterplots are linear regressions.

B SCIENTIFIC REVIEW GROUP (SRG) REQUESTS

This appendix summarizes results produced in response to Scientific Review Group requests made during the meeting held from February 10–13, 2025. Full presentations given at the meeting are available by request by contacting a Joint Technical Committee member (see the Treaty website for current members).

B.1 Day 1

Request 1

Conduct a 5-year retrospective for the sensitivity model that removes the age-1 index, with focus on the 2022 and 2020 year classes.

JTC Response

The generated squid plot (Figure 63) shows that the 2020 cohort has increased uncertainty at age 3 and the 2022 cohort is estimated to be smaller than the model that included the age-1 survey (not shown).

Request 2

Show the fit to survey index for the sensitivity model that removes the age-1 index (replicate plots from the assessment presentation on slides 16-20) and any other plots the JTC finds to be helpful.

JTC Response

All the requested plots were created and shared. After removing the age-1 index (new base model; Figure 17), the trajectory of the expected biomass was reduced, resulting in a poorer fit to the median in 2021 and an improved fit in 2023 (negligible change to the fit in 2019) when compared to the model with the age-1 index removed (Figure **??**). Plots of survey and fishery age composition fits showed a very small change in the survey age composition fit for age-3 fish in 2021. Otherwise, there were no substantial differences in the age composition fits (figures not shown).

Request 3

Provide plots of selectivity in 2024 as well as mountain plots for sensitivities to removing age-1 index, to the alternative values of phi (deviations for selectivity), and for adding in the eDNA index.

JTC Response

A series of figures were produced, including two that showed time-varying selectivity across all years and the posterior selectivity for the survey and fishery in 2024. The latter included 1000 draws from the posterior distribution. The set of figures based on the model that removes that age-1 index are included in the main document because it is now the base model. Shown are a representative subset of the requested figures for the other four models (Figures B.2–**??**).

Request 4

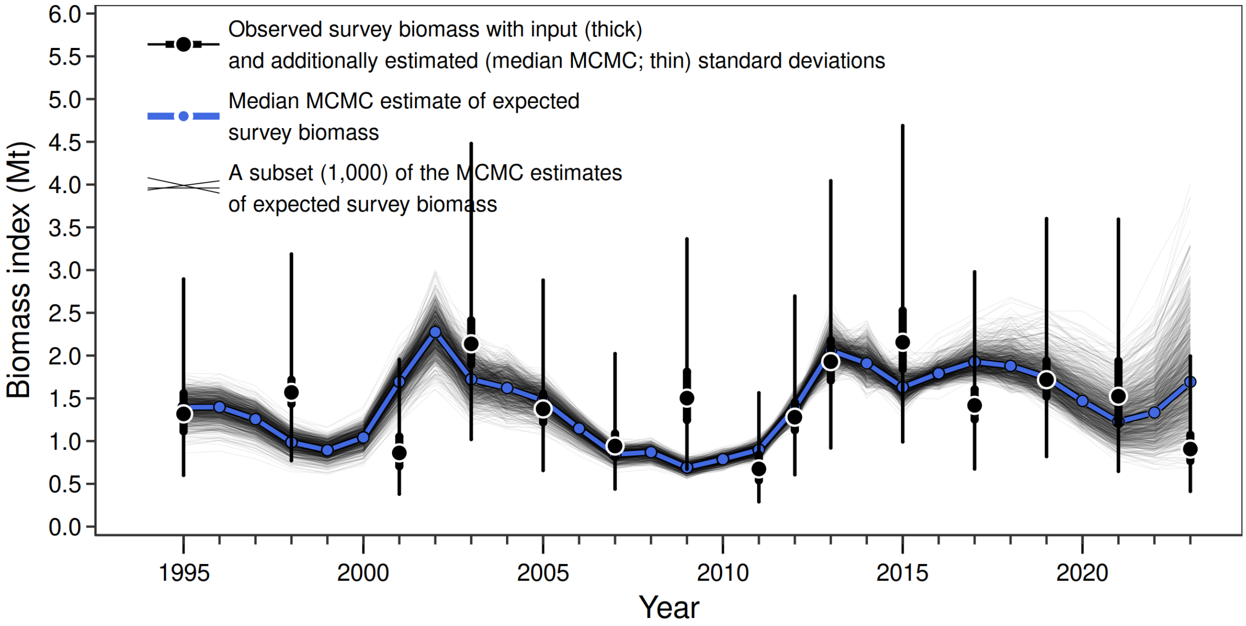

Figure B.1. Fit to the acoustic survey for the model that excludes the age-1 index (new base model).

As feasible, tomorrow or later in the week, show data on the spatial distribution of the stock over time (with a focus on the last two years), especially the proportion of the stock south of the main waters of the US fishery (e.g. 42 degrees N or what is available). For example from catch rates (CPUE), catches, fraction of groundfish trawl survey, eDNA from the hydroacoustic survey, and the hydroacoustic survey.

JTC Response

In collaboration with several researchers present at the meeting, figures were presented showing trends in an integrated (DFO and NOAA) bottom trawl index (Figure B.10) and the relative proportion by latitudinal sub-areas (Figure B.11), which provided some indication of increasing biomass in California over recent years. Additionally, the southern portion of the eDNA index covering years 2021 and 2023 showed a slight upward trend (Figure B.12). The distribution of At-Sea (Figure B.13) and Shoreside (Figure B.14) revenue over recent years indicated a tendency for the At-Sea fleet to catch fish closer to the southern extent of the fishing grounds in recent years. There was a more stable distribution for the Shoreside fleet. Additional information relevant to the request was shown in research presentations contributed by Owen Liu, Rebecca Thomas, Kristin Marshall, Mary Hunsicker, and Andy Edwards (not shown here).

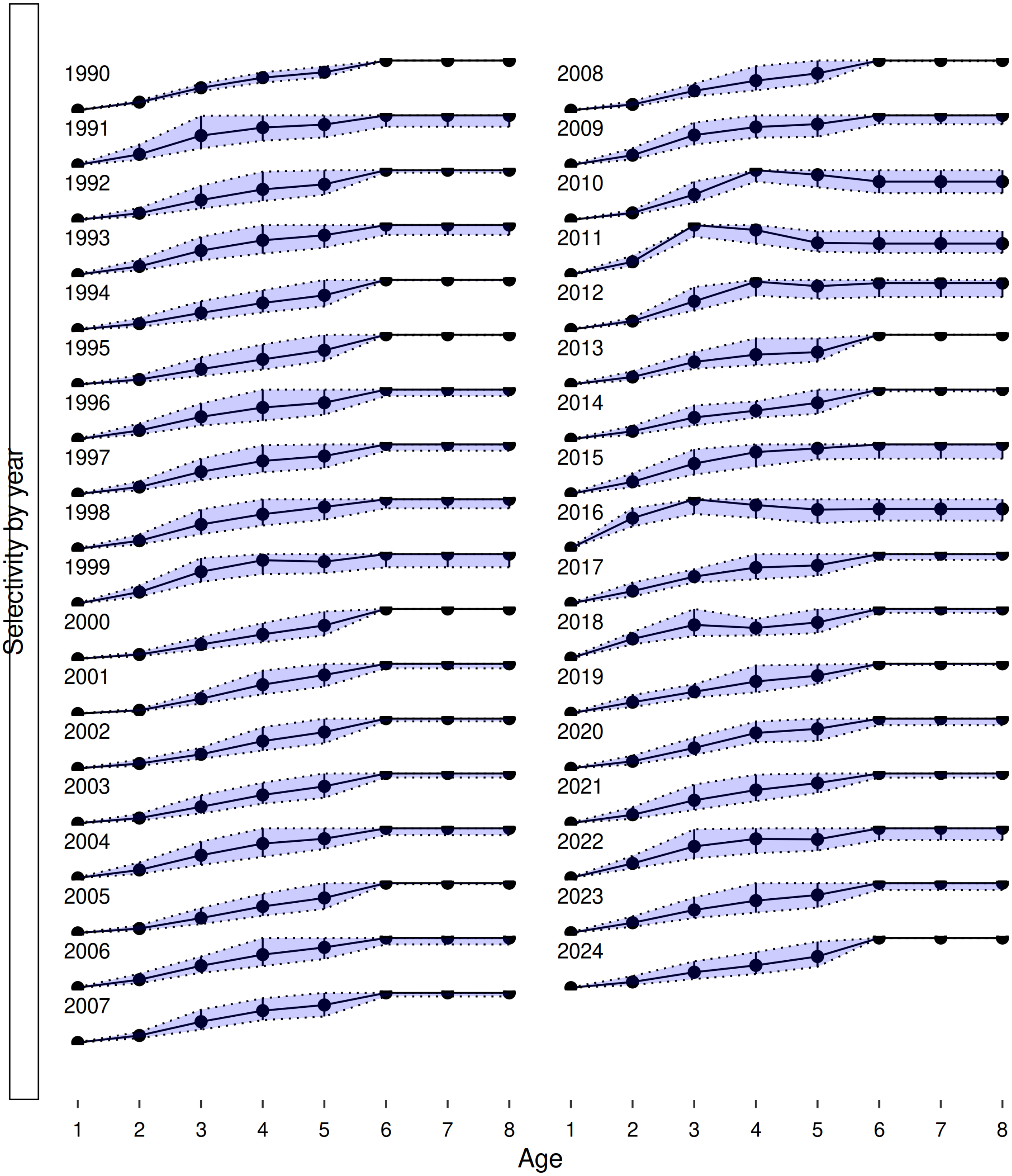

Figure B.2. Fishery selectivity sampled from posterior probability distribution by year for the sensitivity model with time-varying variance (phi) set to 0.21. See Figure 25 in the main text for further description.

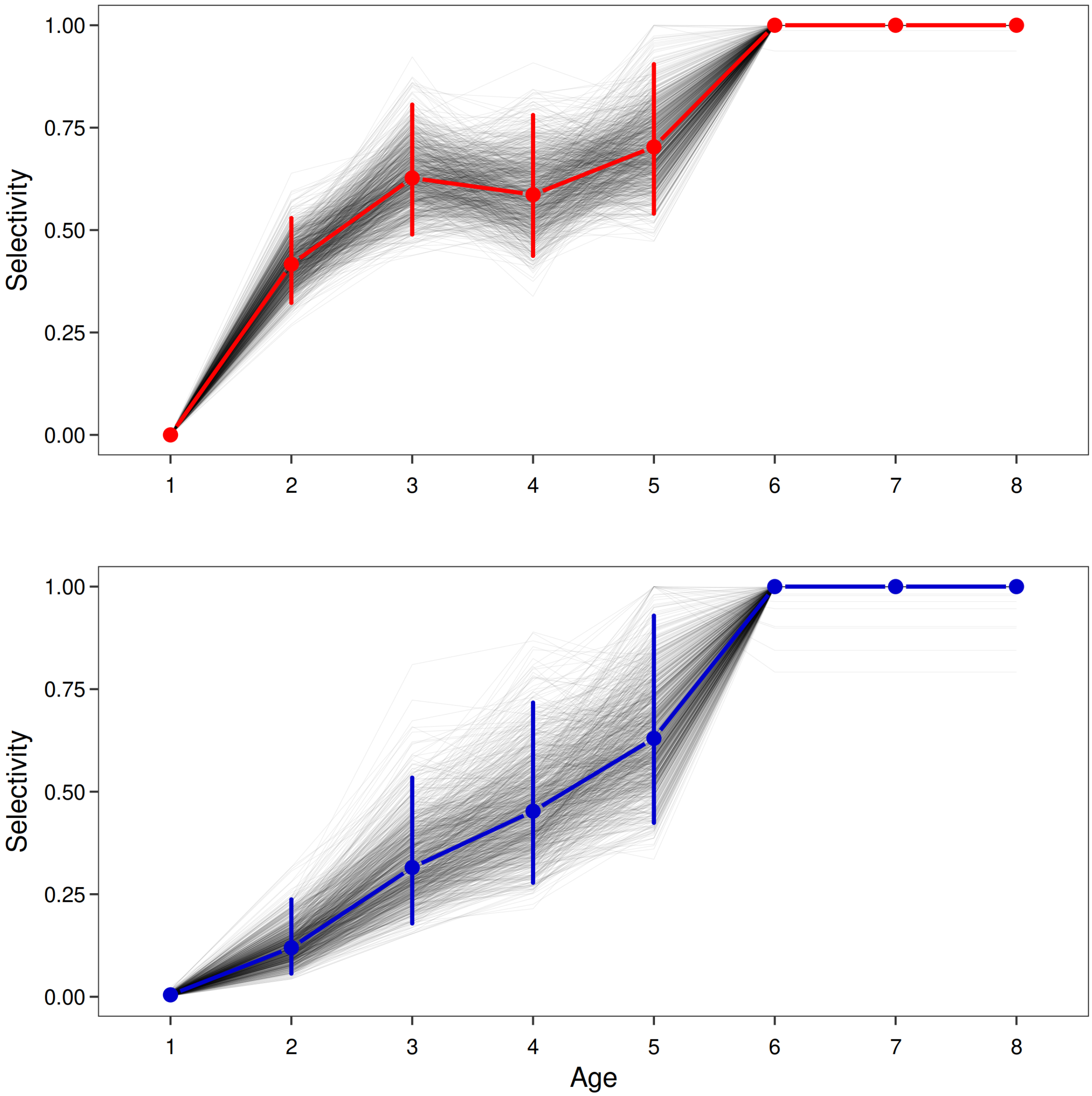

Figure B.3. Estimated selectivities for the acoustic survey age-2+ biomass index (top, with selectivity of zero for age-1 fish) and fishery (bottom – shown for 2024 only, age-1 and older) from a subsample of 1,000 draws from the posterior distribution for the sensitivity model with time-varying variance (phi) set to 0.21.

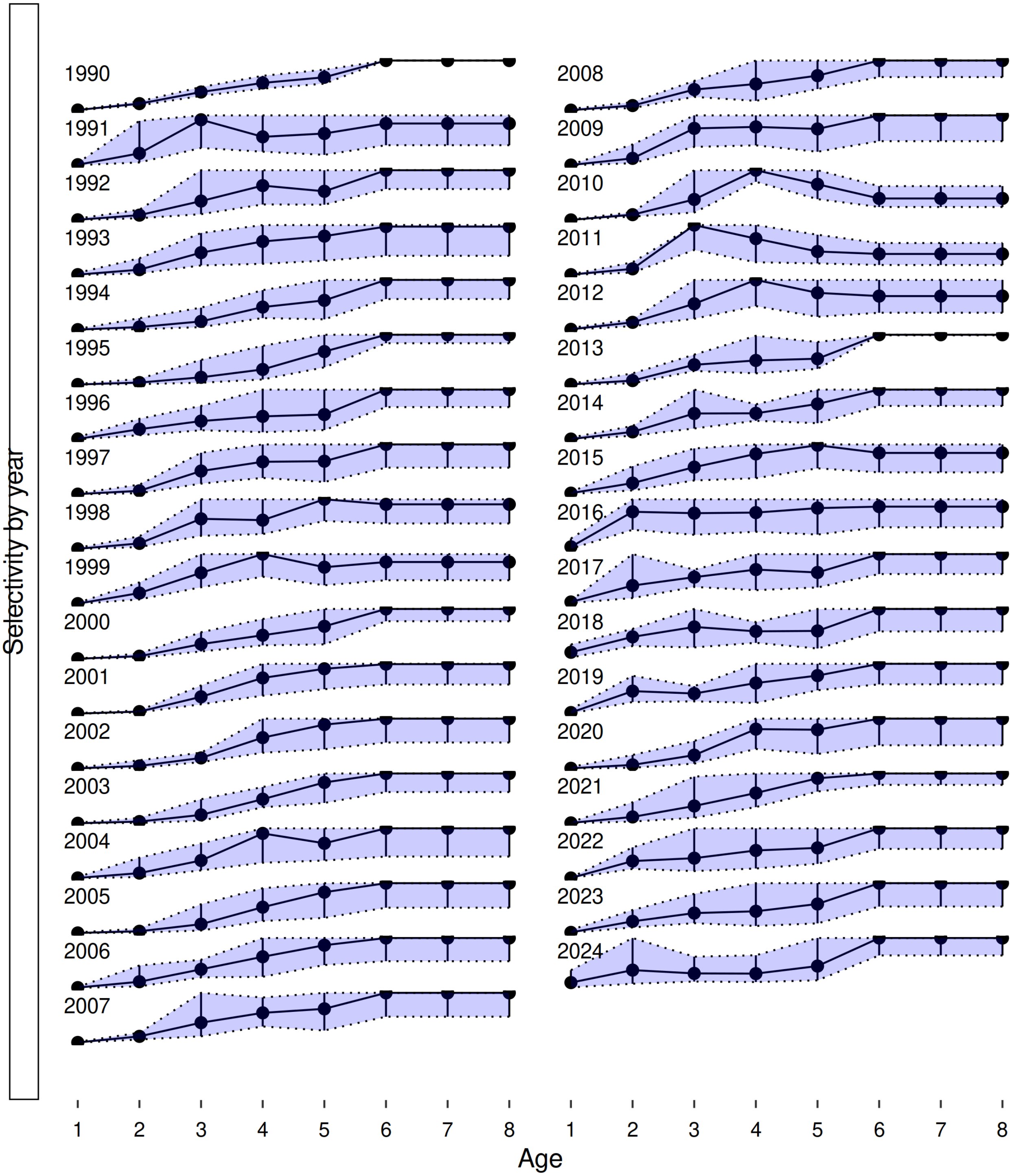

Figure B.4. Fishery selectivity sampled from posterior probability distribution by year for the sensitivity model with time-varying variance (phi) set to 0.70. See Figure 25 in the main text for futher description.

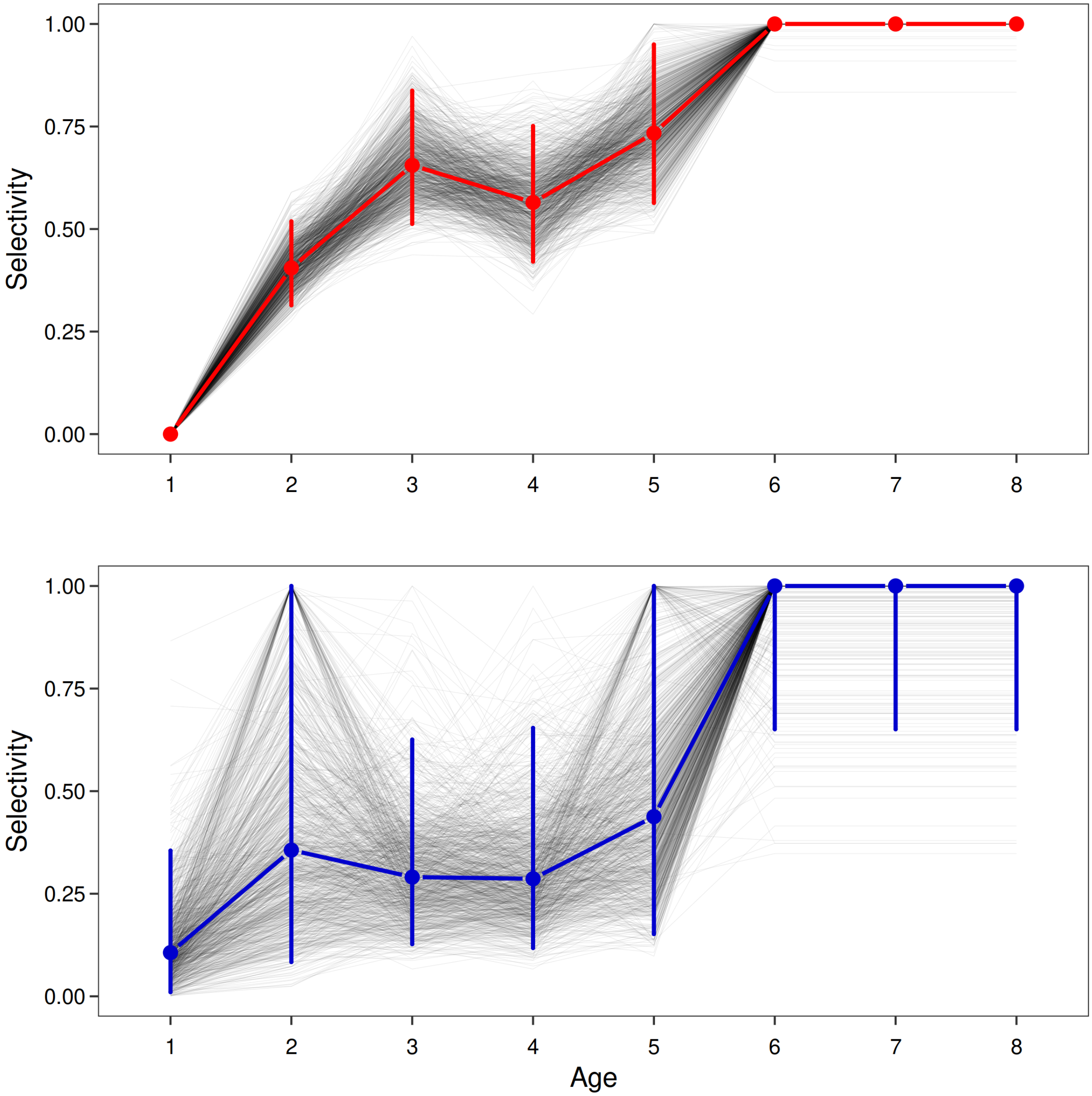

Figure B.5. Estimated selectivities for the acoustic survey age-2+ biomass index (top, with selectivity of zero for age-1 fish) and fishery (bottom – shown for 2024 only, age-1 and older) from a subsample of 1,000 draws from the posterior distribution for the sensitivity model with time-varying variance (phi) set to 0.70.

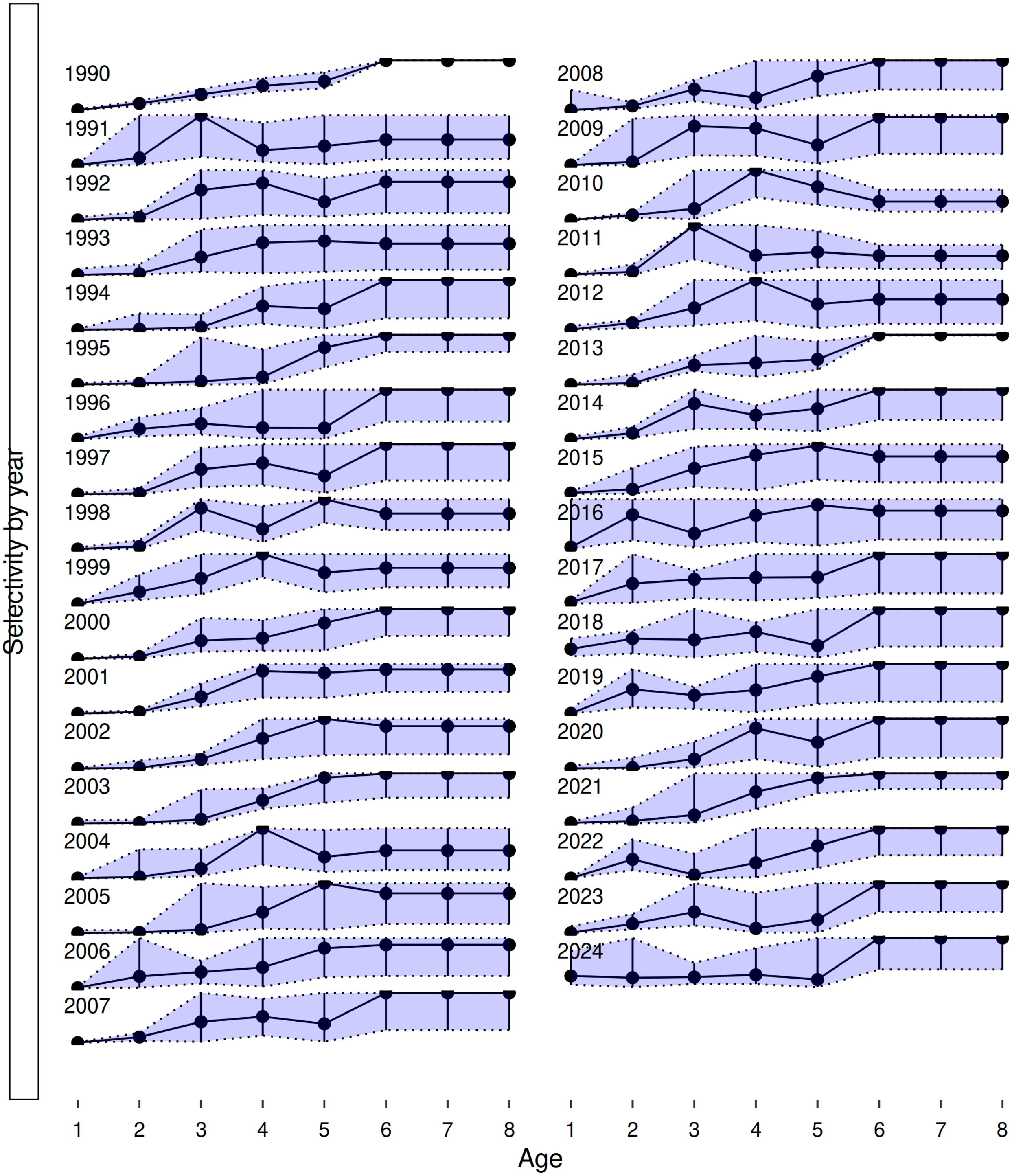

Figure B.6. Fishery selectivity sampled from posterior probability distribution by year for the sensitivity model with time-varying variance (phi) set to 2.10. See Figure 25 in the main text for futher description.

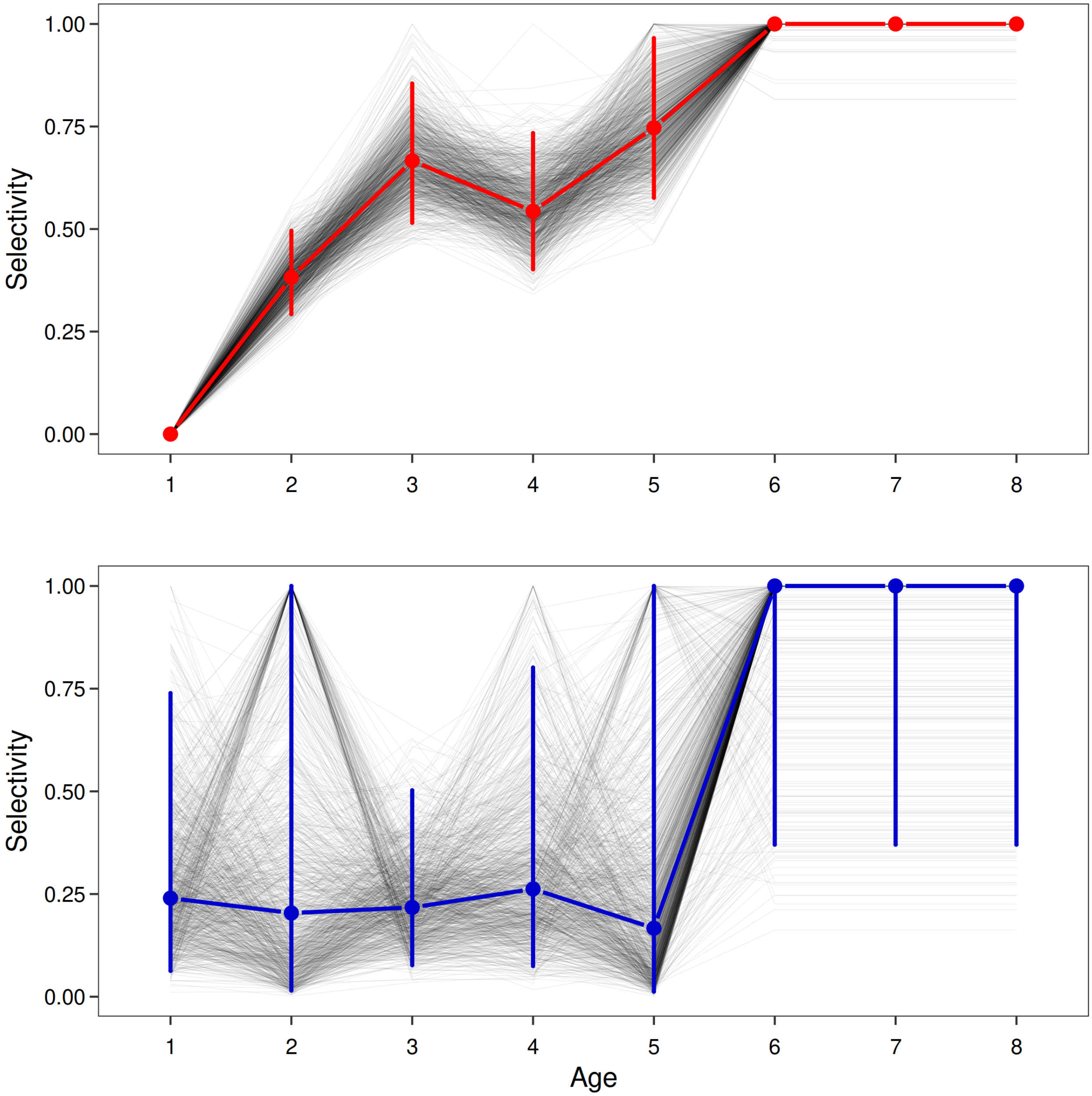

Figure B.7. Estimated selectivities for the acoustic survey age-2+ biomass index (top, with selectivity of zero for age-1 fish) and fishery (bottom – shown for 2024 only, age-1 and older) from a subsample of 1,000 draws from the posterior distribution for the sensitivity model with time-varying variance (phi) set to 2.10.

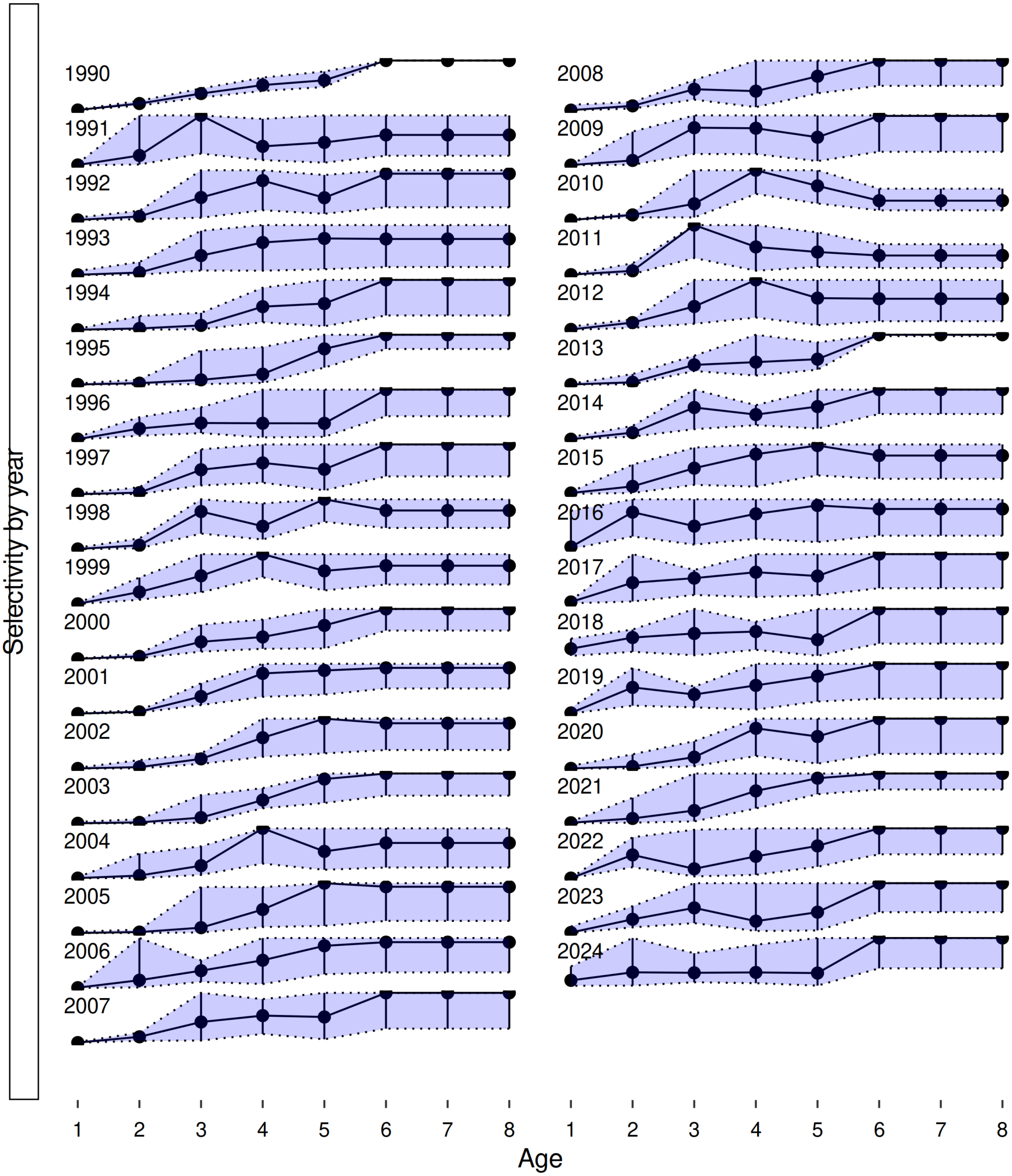

Figure B.8. Fishery selectivity sampled from posterior probability distribution by year for the sensitivity model that included the eDNA index. See Figure 25 in the main text for futher description.

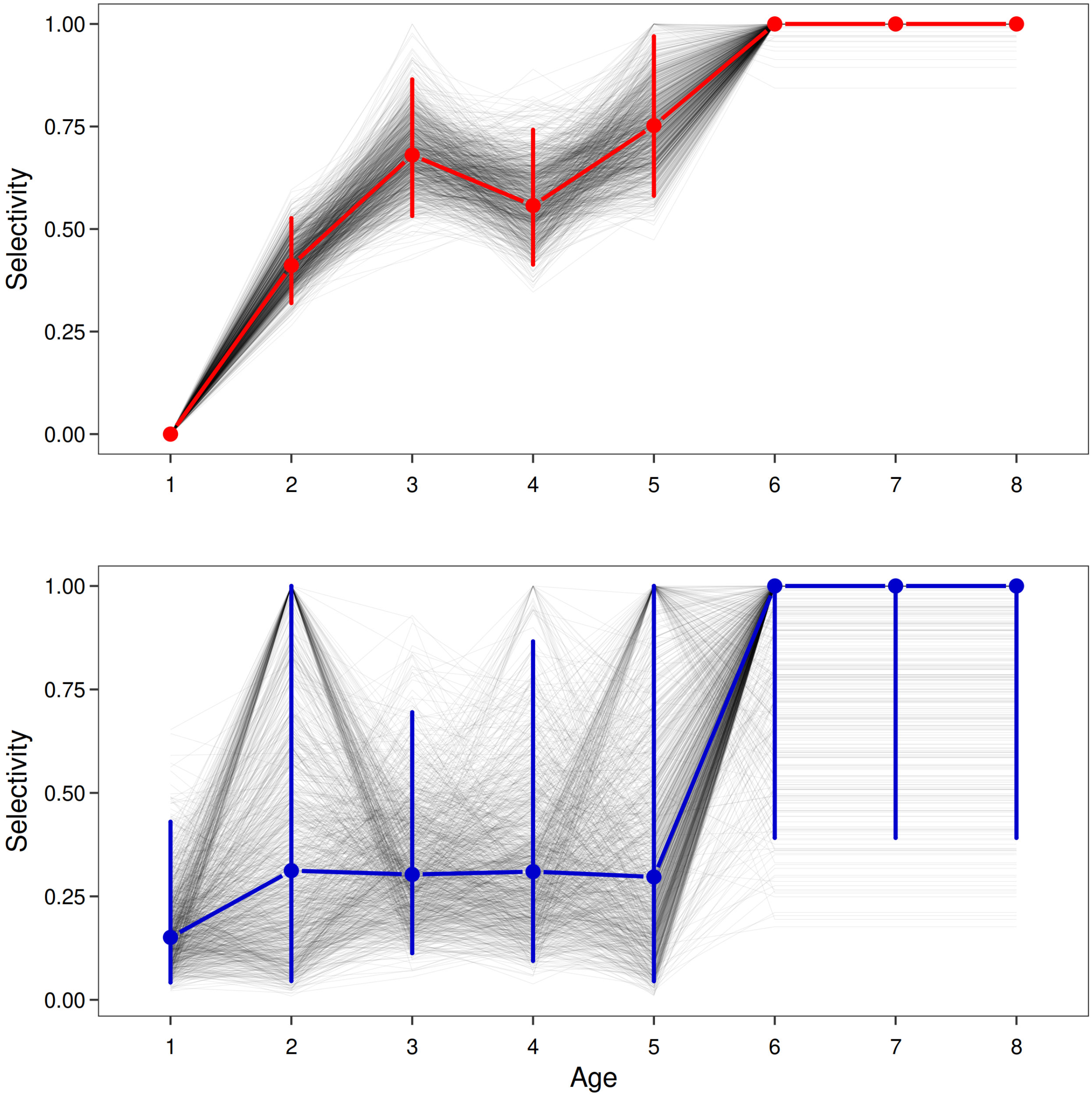

Figure B.9. Estimated selectivities for the acoustic survey age-2+ biomass index (top, with selectivity of zero for age-1 fish) and fishery (bottom – shown for 2024 only, age-1 and older) from a subsample of 1,000 draws from the posterior distribution for the sensitivity model that included the eDNA index.

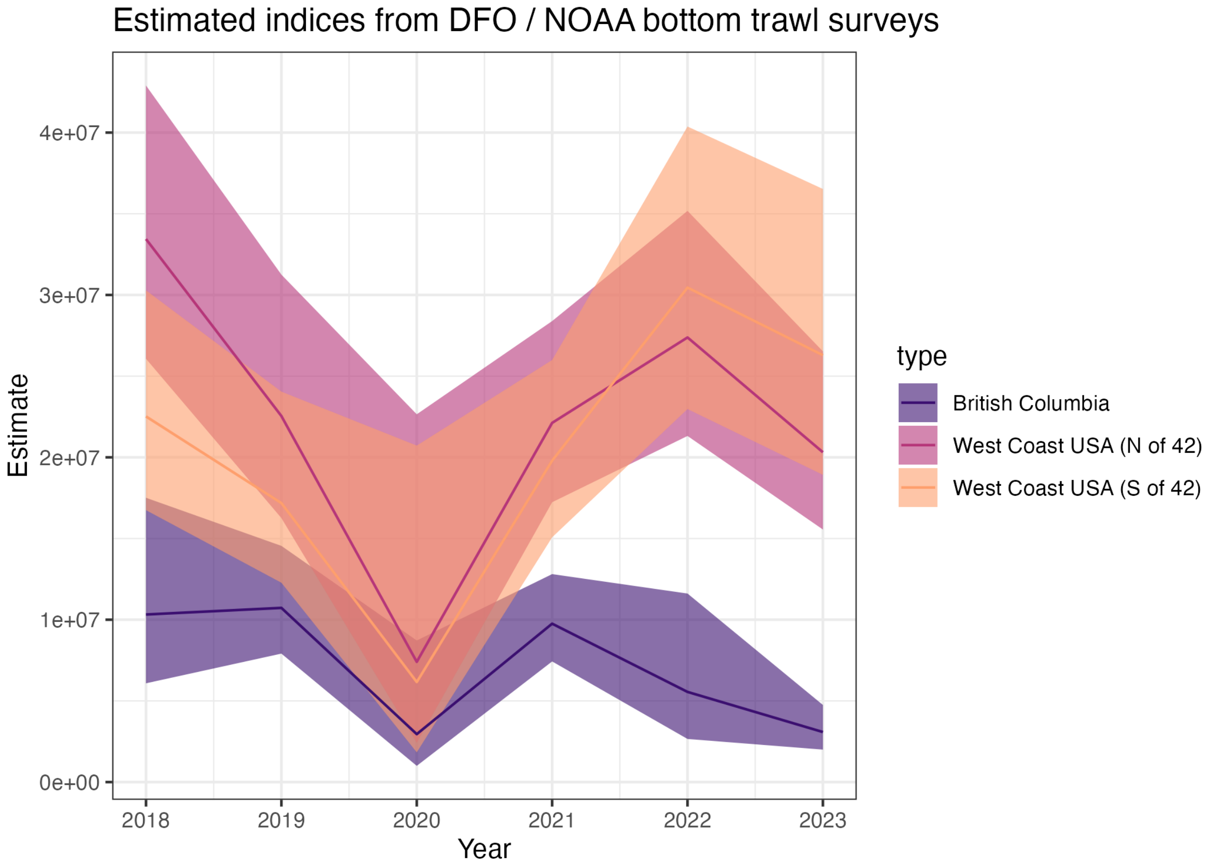

Figure B.10. Bottom trawl survey indices compiled by joining DFO and NWFSC data. Courtesy of Eric Ward.

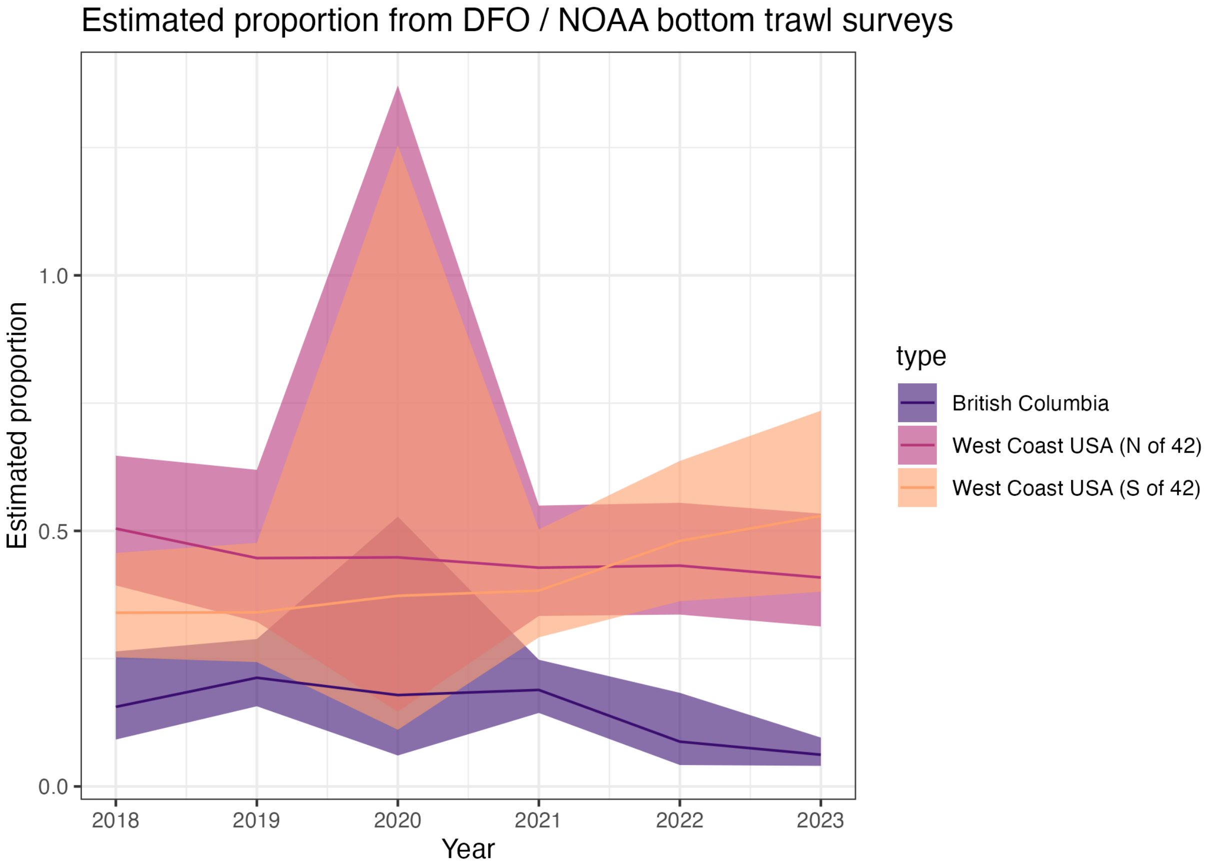

Figure B.11. Bottom trawl survey index proportions by area from the combined DFO and NWFSC data. Courtesy of Eric Ward.

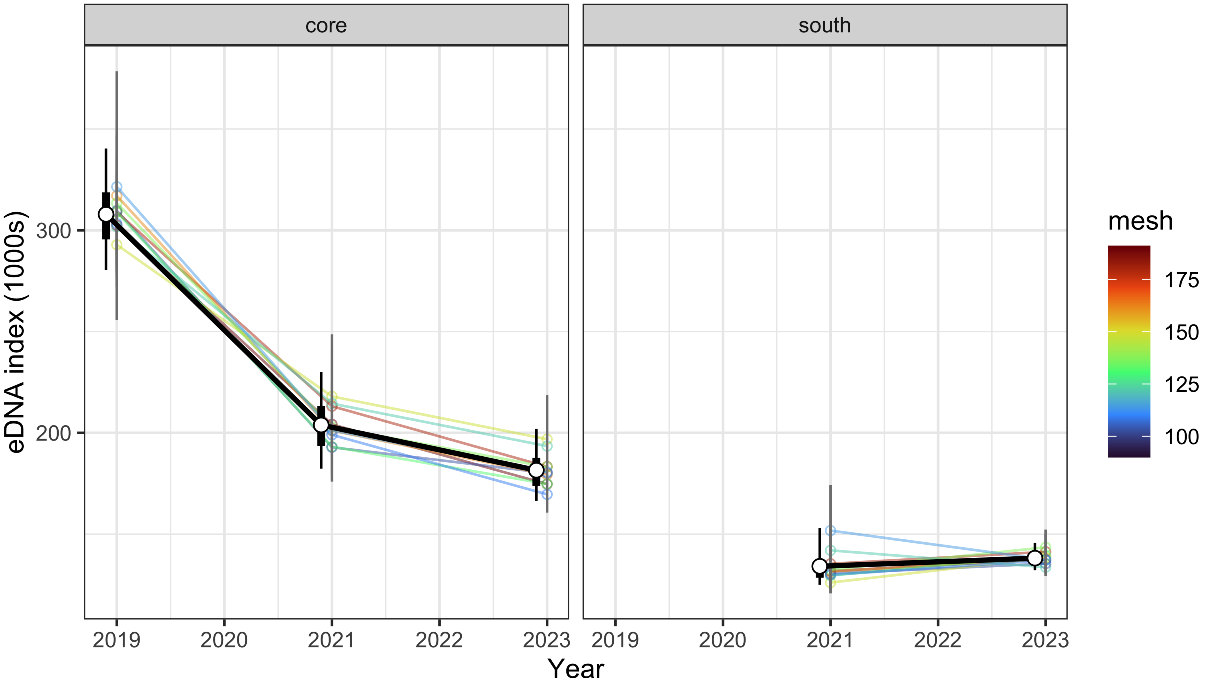

Figure B.12. eDNA indices by the core area (left) and the south area only (right). Courtesy of Ole Shelton.

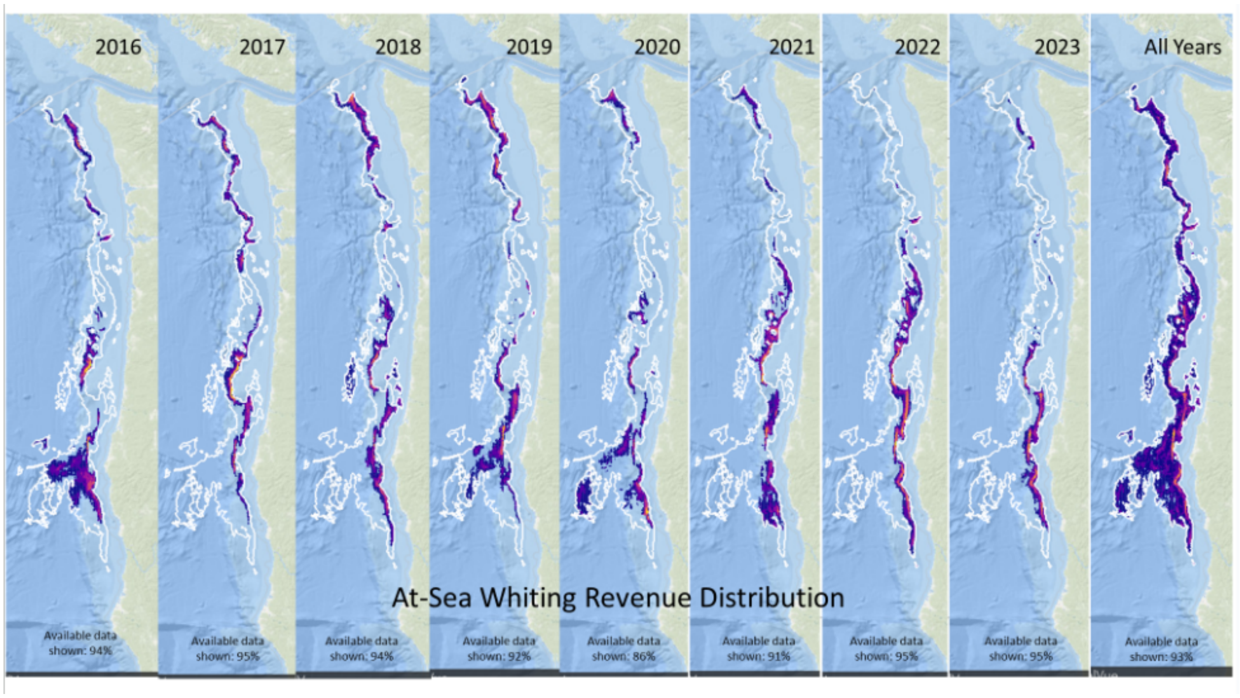

Figure B.13. Distribution of fishing revenue from 2016 to 2023 for the United States At-Sea fleet. Courtesy of Lisa Pfeiffer.

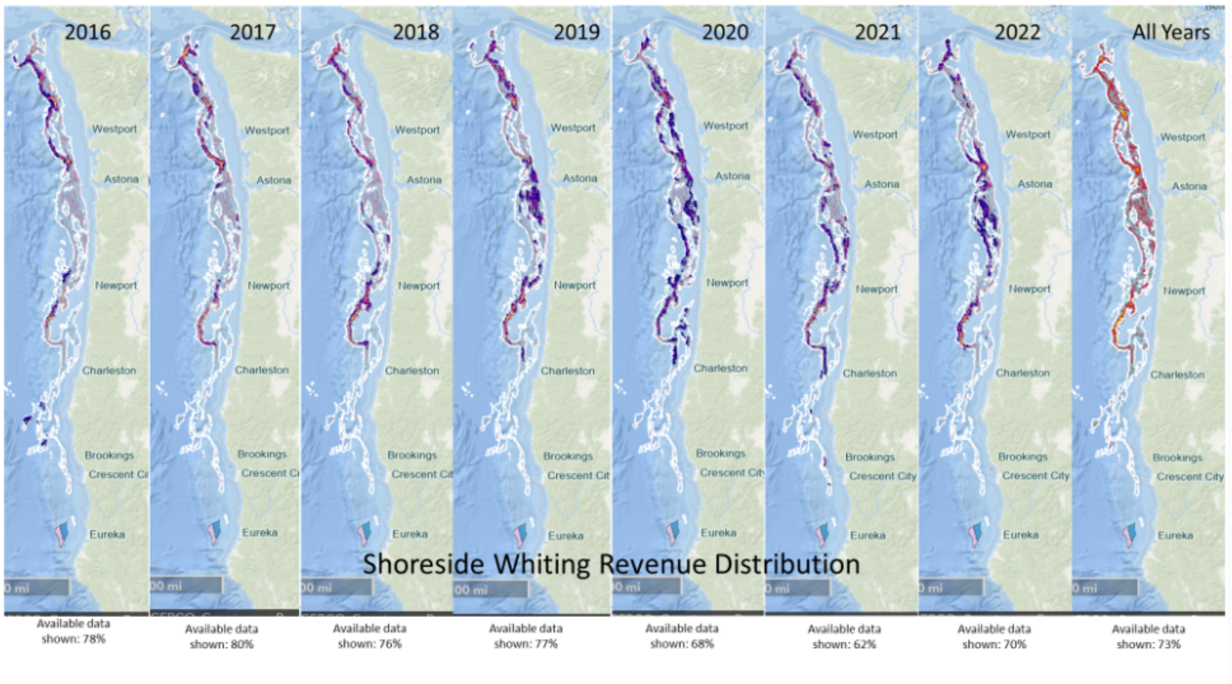

Figure B.14. Distribution of fishing revenue from 2016 to 2022 for the United States Shoreside. Courtesy of Lisa Pfeiffer.

B.2 Day 2

Request 1

The SRG requests reanalyzing the bottom trawl index such that uncertainty remains within the range of 0 and 1 given that these are proportions.

JTC Response

For completeness, the bottom trawl index was shown with the uncertainty fixed as requested (not shown here).

Request 2

The SRG requests that the bottom trawl index be analyzed with only US data incorporating 2024, and present the proportion of predicted biomass north and south of 42 degrees latitude.

JTC Response

Two bottom trawl survey figures were produced to show trends from both north and south of 42 latitude (Figures B.15 and B.16).

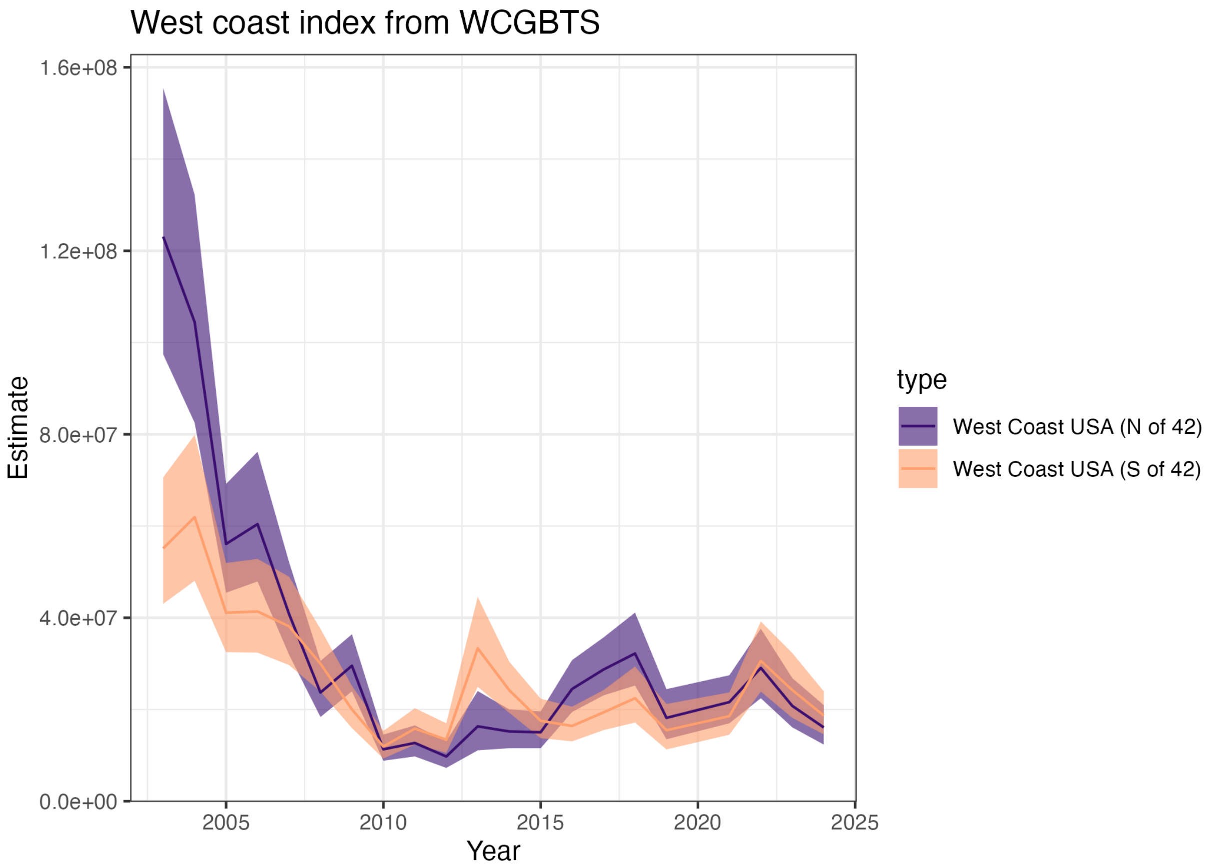

Figure B.15. Bottom trawl survey indices compiled by area in United States waters. Courtesy of Eric Ward.

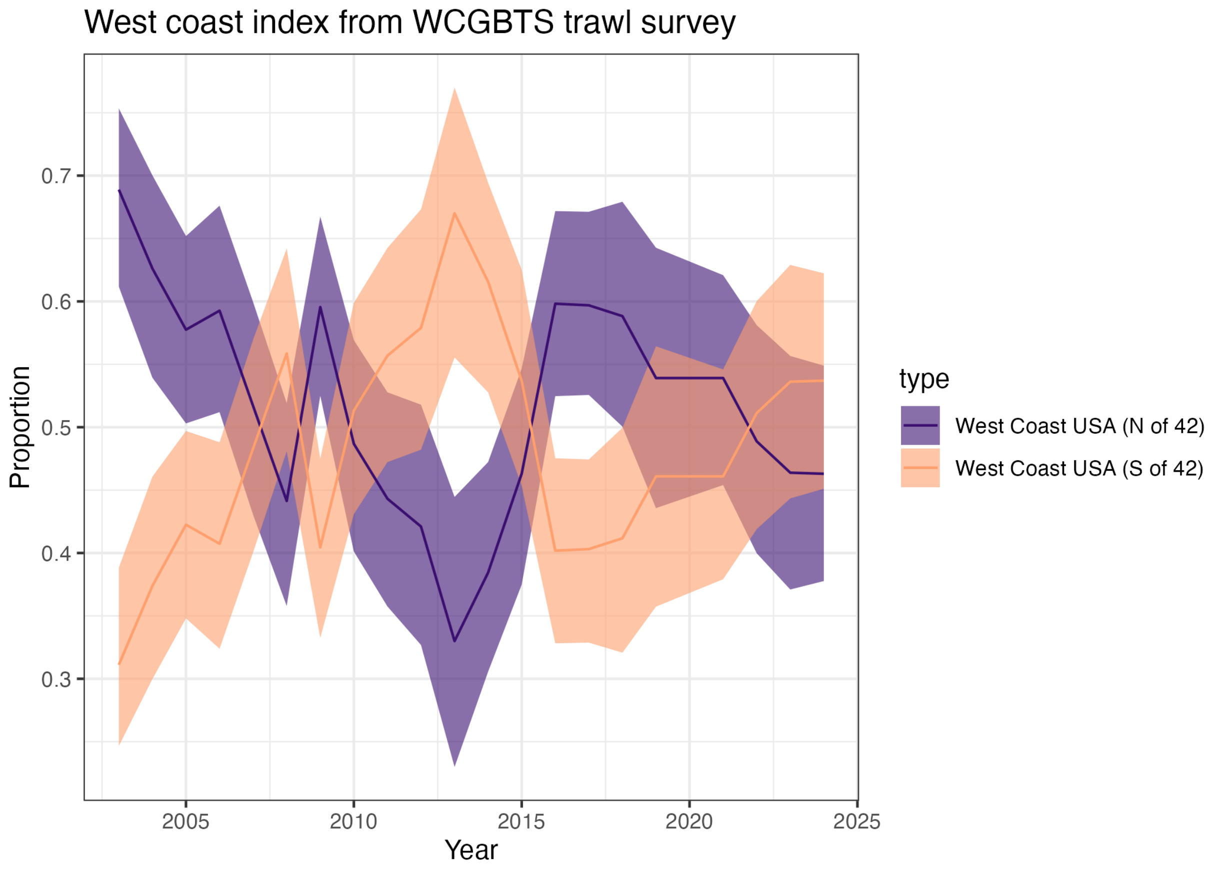

Figure B.16. Bottom trawl survey indices show as a proporiton of the total by area in United States waters. Courtesy of Eric Ward.

Request 3

The SRG requests sensitivities on fishery selectivity parameterization (in the base model) by increasing the maximum age beyond which selectivity is held constant to ages 8, 10, and 12. Present the resulting fishery selectivity (2024 with uncertainty and MCMC traces and individual years with uncertainty), spawning biomass trajectories, fits to the acoustic survey index, and recruitment deviation estimates.

JTC Response

The number of active parameters increases considerably when using a maximum age of 6 (base model; 262 parameters) for time-varying selectivity compared to a maximum of age of 8 (333 parameters), 10 (403 parameters), and 12 (473 parameters). A set of figures were produced to show some key results comparing the models that increase the age at maximum selectivity (see Figures B.17–B.28).

Request 4

The SRG requests running the base model with the age-1 index, keeping 2023 and beyond recruitment deterministic, and sequentially (backwards in time) removing the age-1 index from the data. Run the base model without the 2023 age-1 index, then without the 2023 and

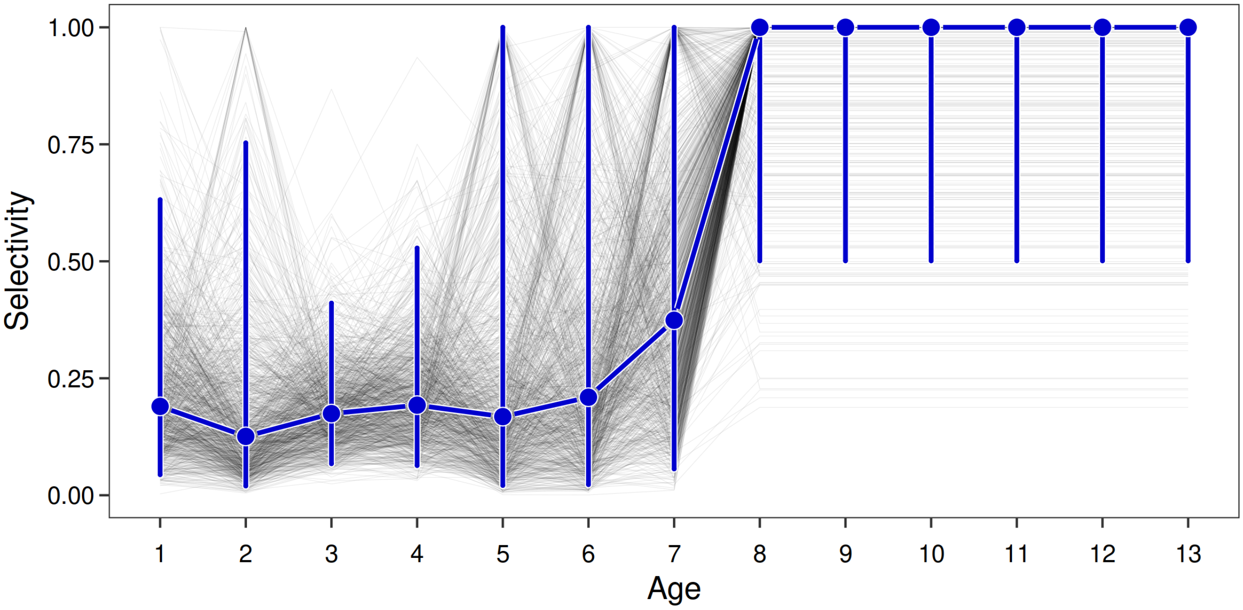

Figure B.17. Estimated selectivities for the fishery from a subsample of 1,000 draws from the posterior distribution for the model with a maximum age of 8 for selectivity.

2021 age-1 indices, then without the 2023, 2021, and 2019 age-1 indices, and then without the 2023, 2021, 2019, 2017, and 2015 age-1 indices. Present spawning biomass trajectories (with unfished equilibrium spawning biomass), recruitment deviation estimates, and fits to the acoustic survey index.

JTC Response

The figures requested include each of the four sequential age-1 index data point removal models (see Figures **??**–**??**). The base model shown in the figures is the pre-SRG base model (i.e., includes the age-1 index).

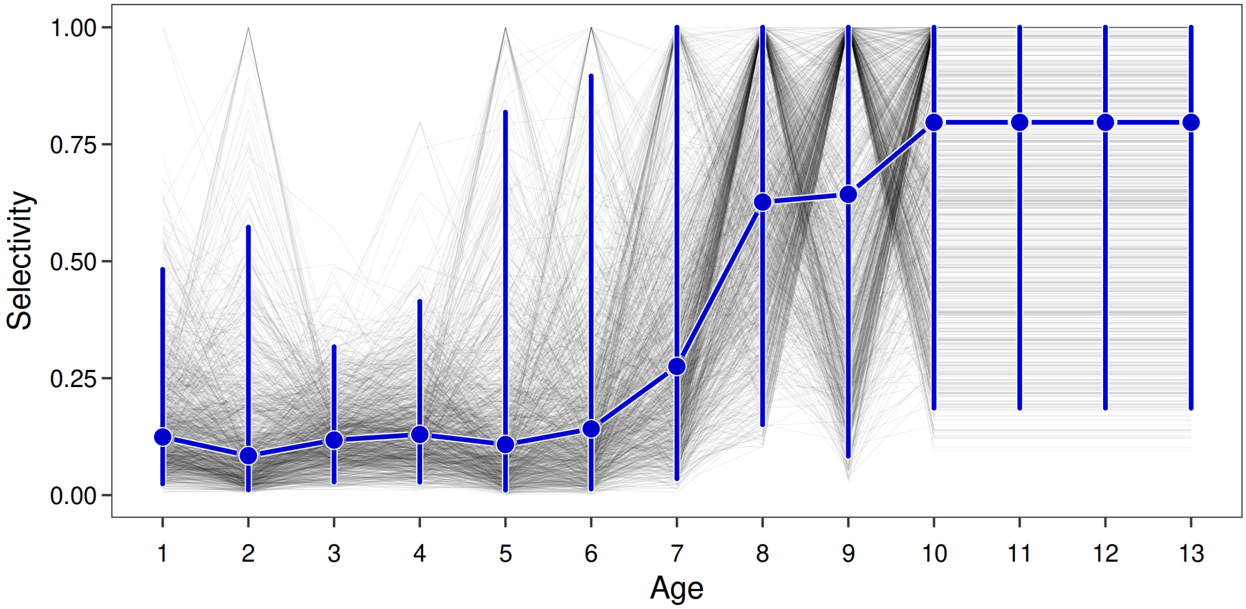

Figure B.18. Estimated selectivities for the fishery from a subsample of 1,000 draws from the posterior distribution for the model with a maximum age of 10 for selectivity.

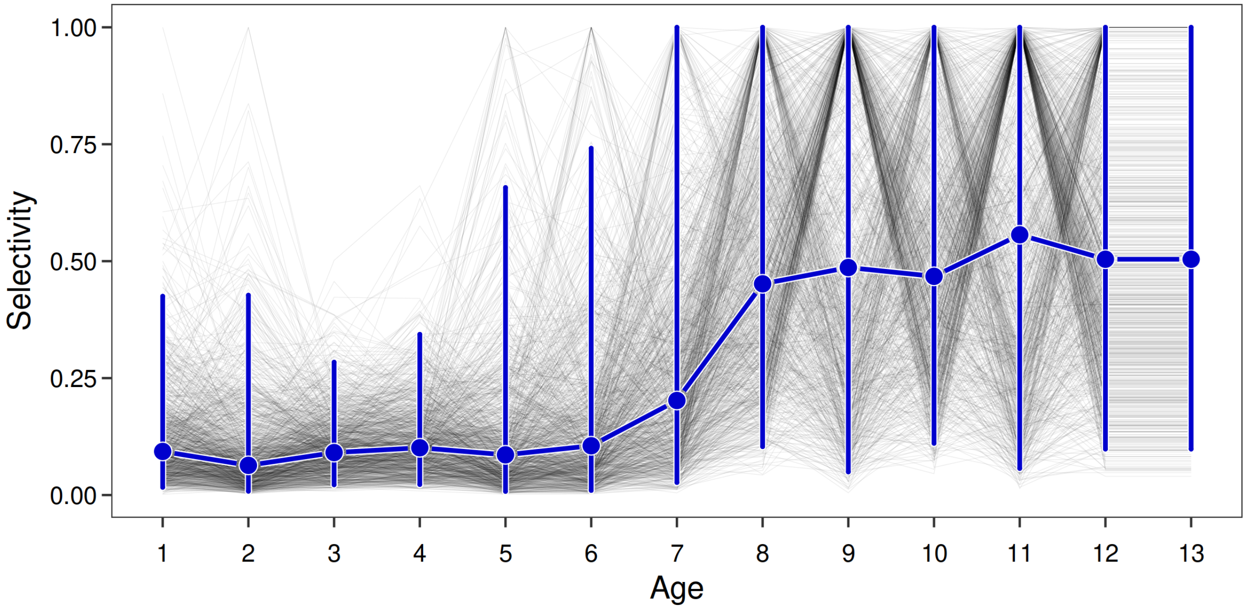

Figure B.19. Estimated selectivities for the fishery from a subsample of 1,000 draws from the posterior distribution for the model with a maximum age of 12 for selectivity.

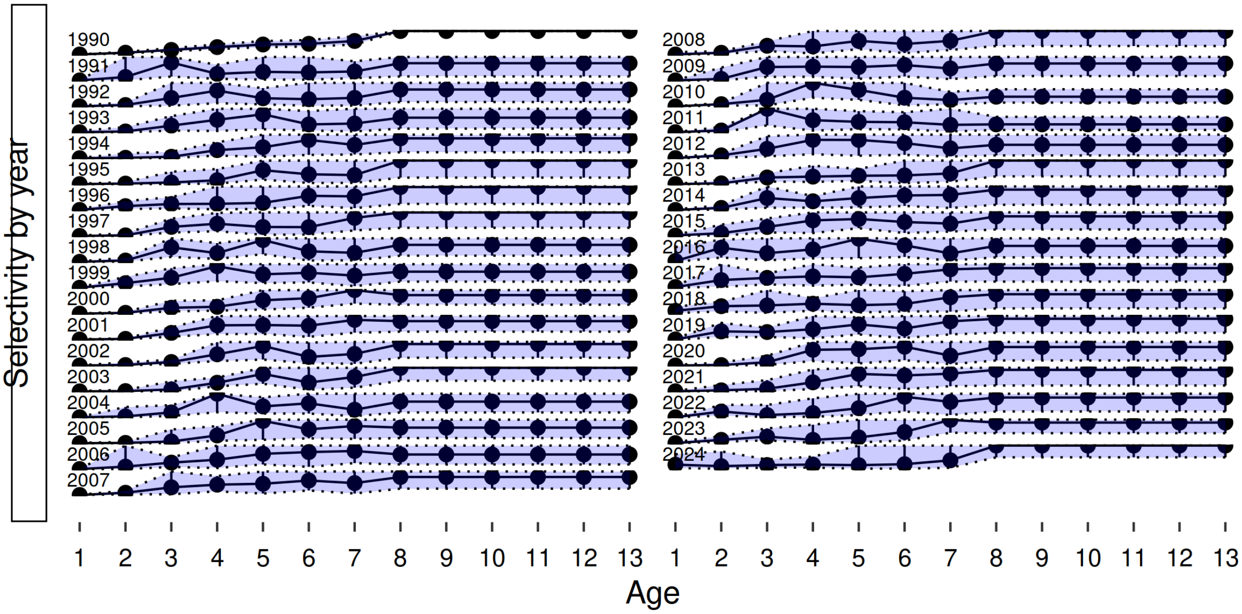

Figure B.20. Fishery selectivity sampled from posterior probability distribution by year for the sensitivity model with maximum age of 8 for selectivity. See Figure 25 in the main text for futher description.

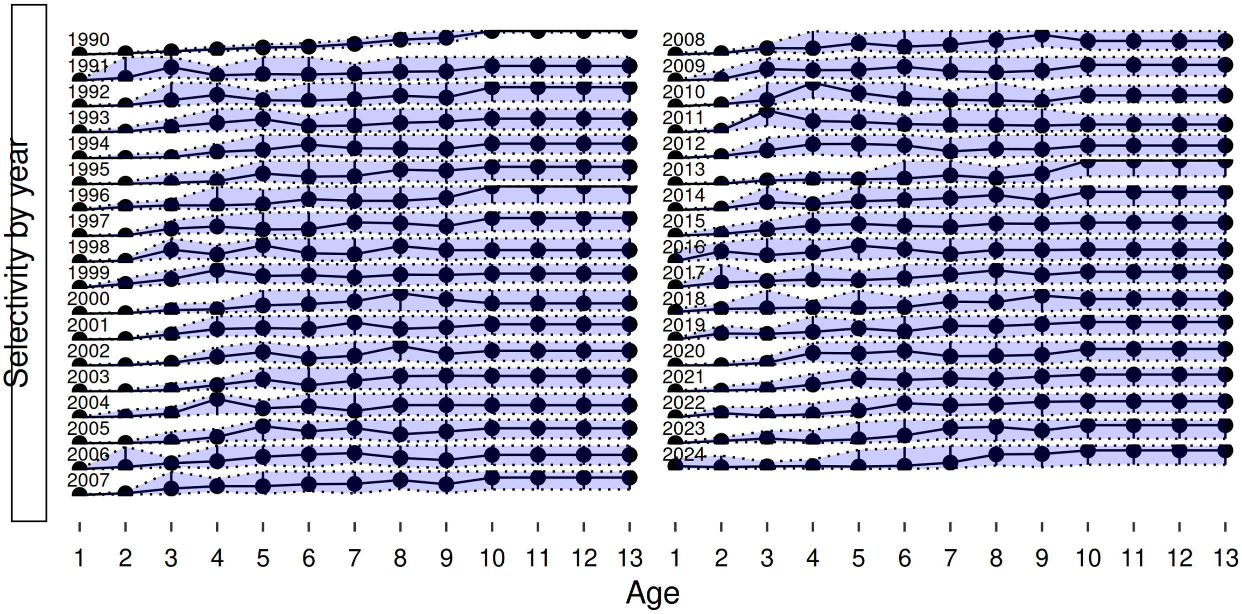

Figure B.21. Fishery selectivity sampled from posterior probability distribution by year for the sensitivity model with maximum age of 10 for selectivity. See Figure 25 in the main text for further description.

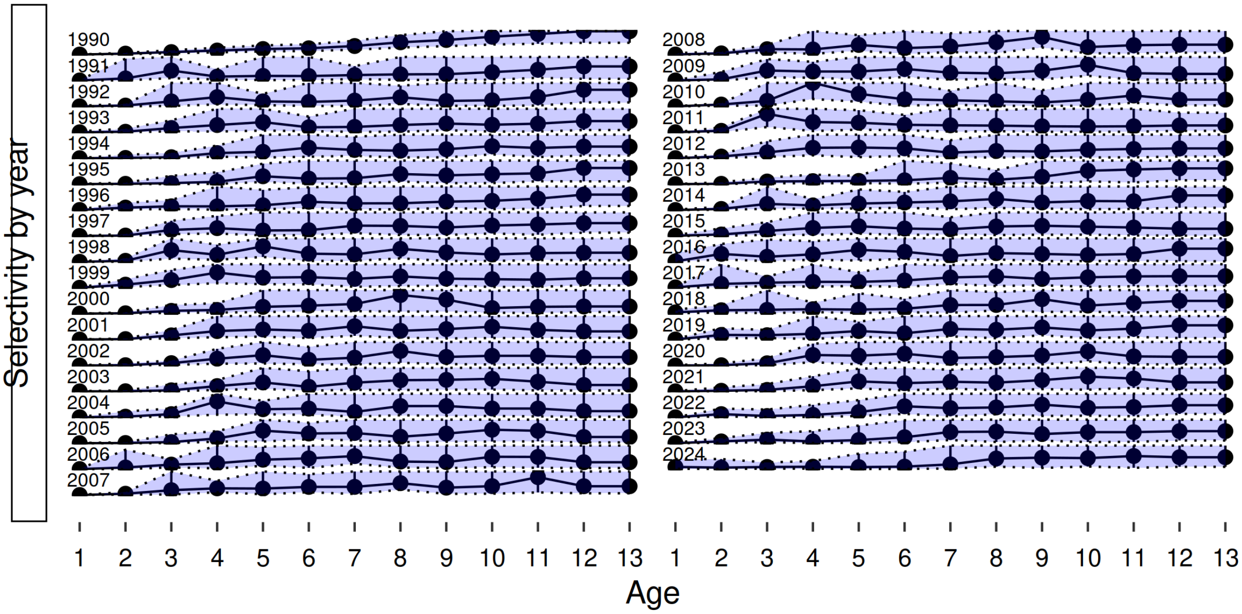

Figure B.22. Fishery selectivity sampled from posterior probability distribution by year for the sensitivity model with maximum age of 12 for selectivity. See Figure 25 in the main text for further description.

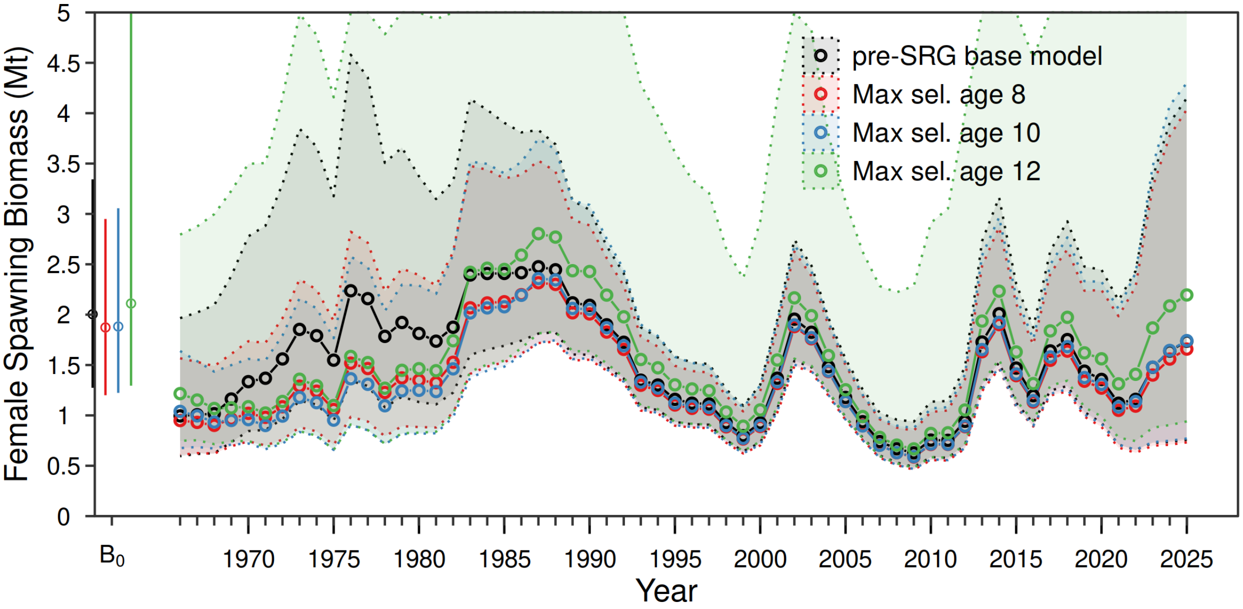

Figure B.23. Median (solid line) of the posterior distribution for beginning of the year female spawning biomass with 95% posterior credibility intervals (shaded area) for each maximum age sensitivity model. The base model in this figure represents the pre-SRG base model (i.e., includes the age-1 index).

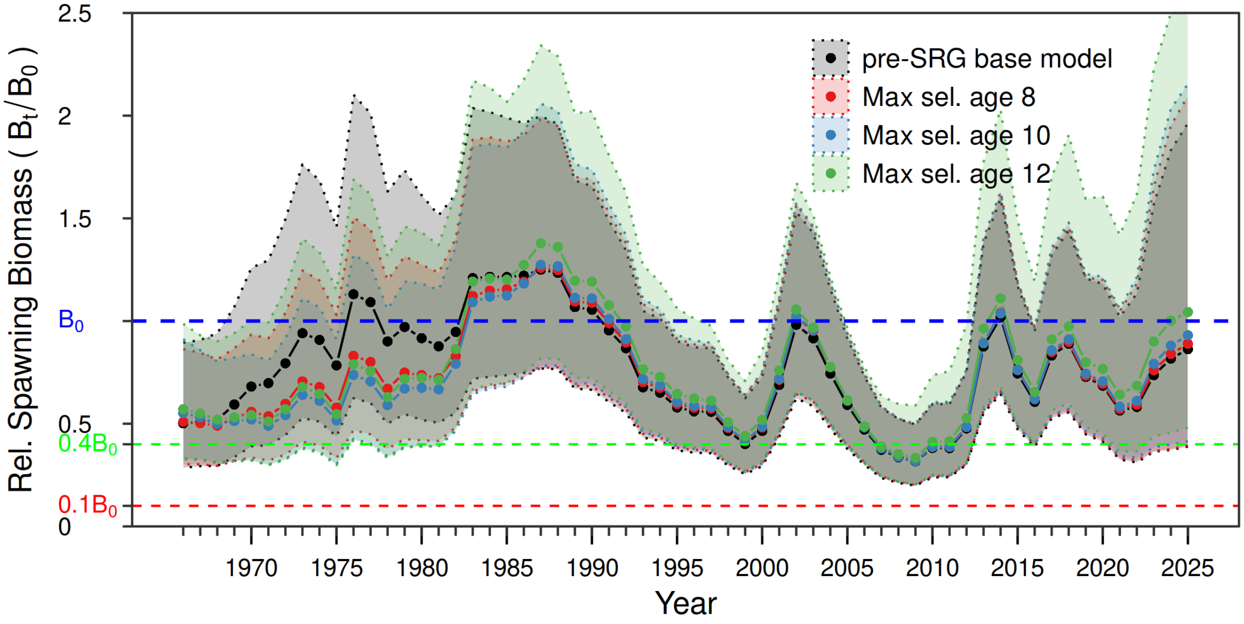

Figure B.24. Median (solid line) of the posterior distribution for relative female spawning biomass with 95% posterior credibility intervals (shaded area) for each maximum age sensitivity model. The base model in this figure represents the pre-SRG base model (i.e., includes the age-1 index).

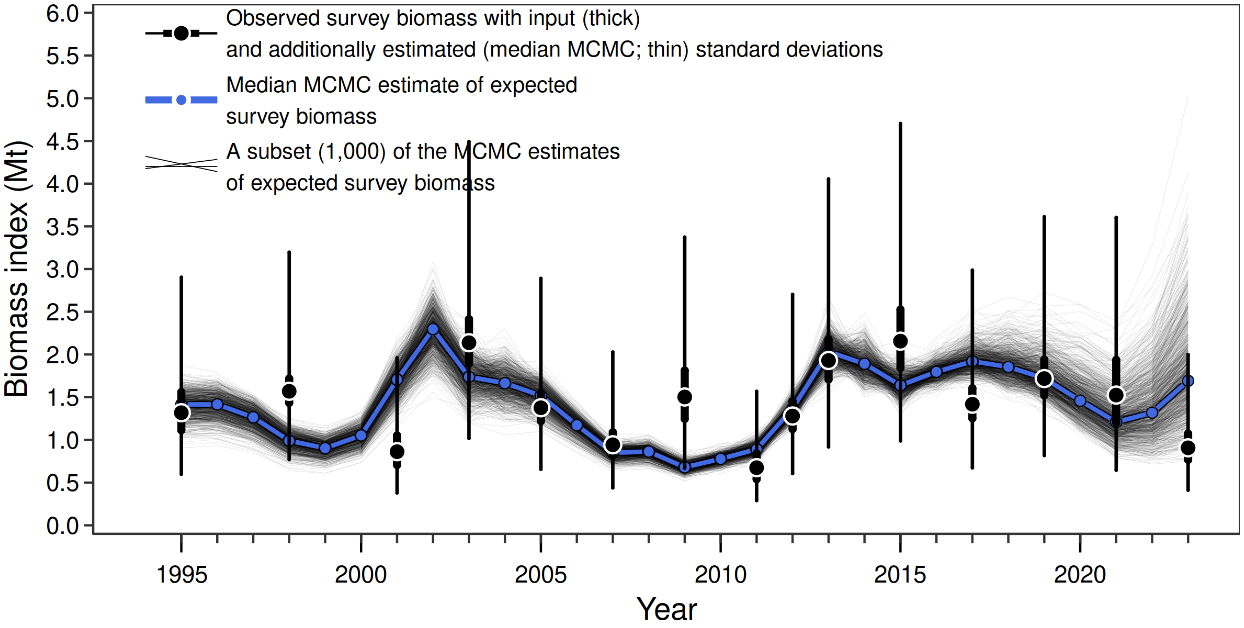

Figure B.25. Fit to the acoustic survey for the model that set the maximum age at 8 for selectivity.

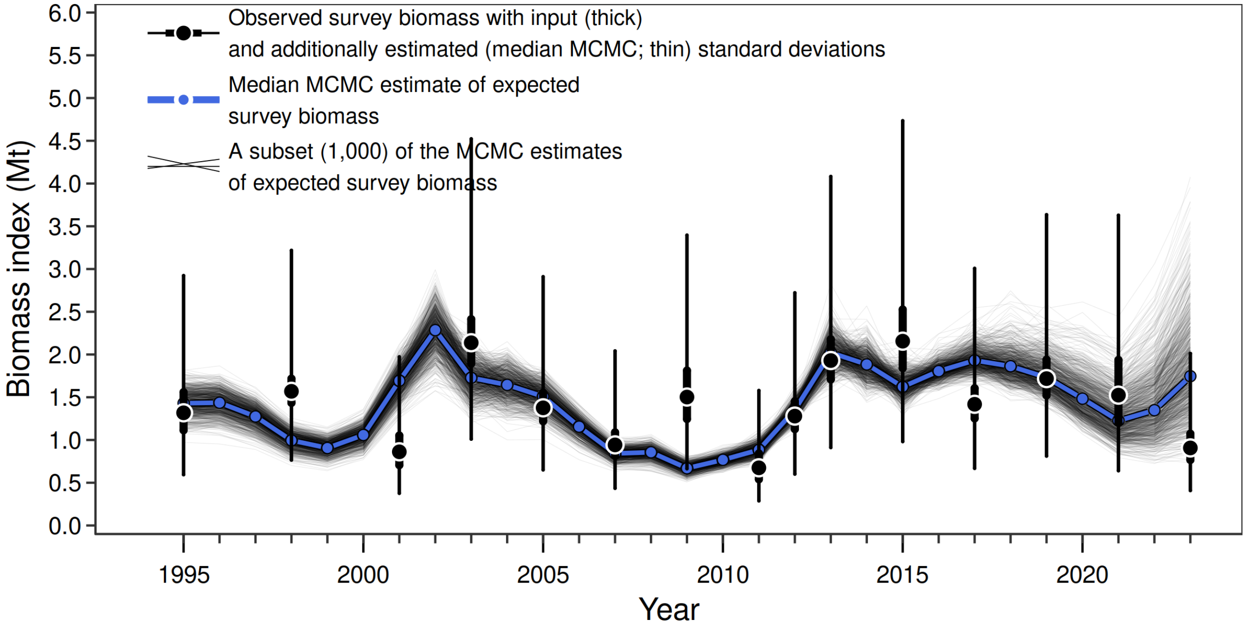

Figure B.26. Fit to the acoustic survey for the model that set the maximum age at 10 for selectivity.

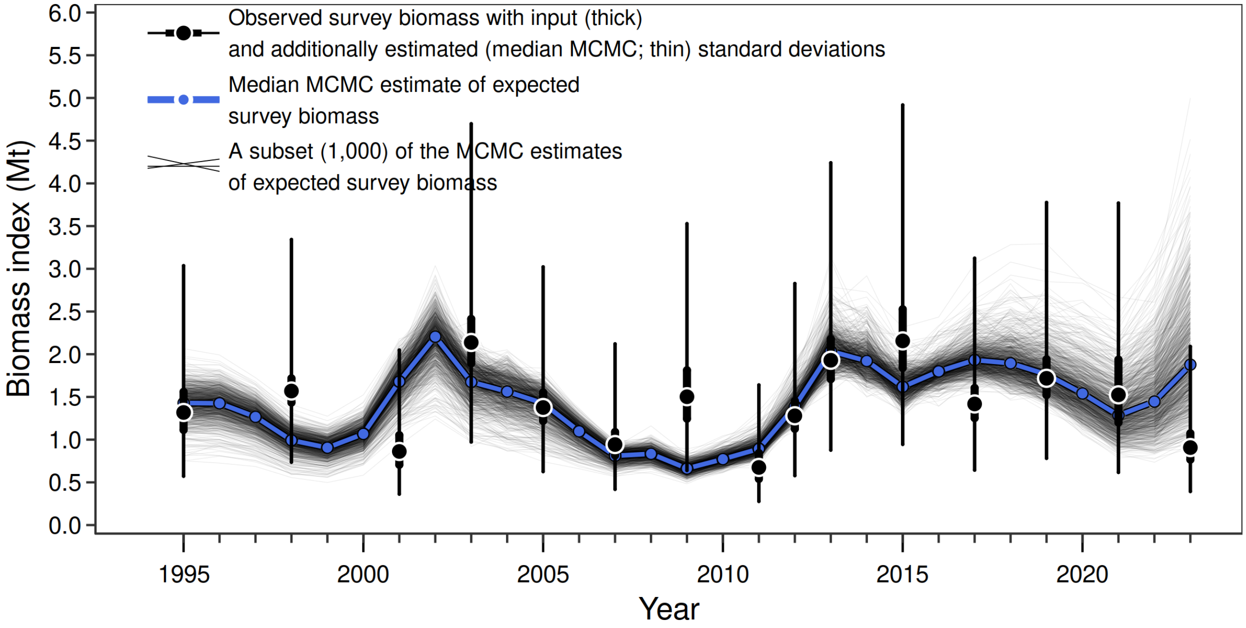

Figure B.27. Fit to the acoustic survey for the model that set the maximum age at 12 for selectivity.

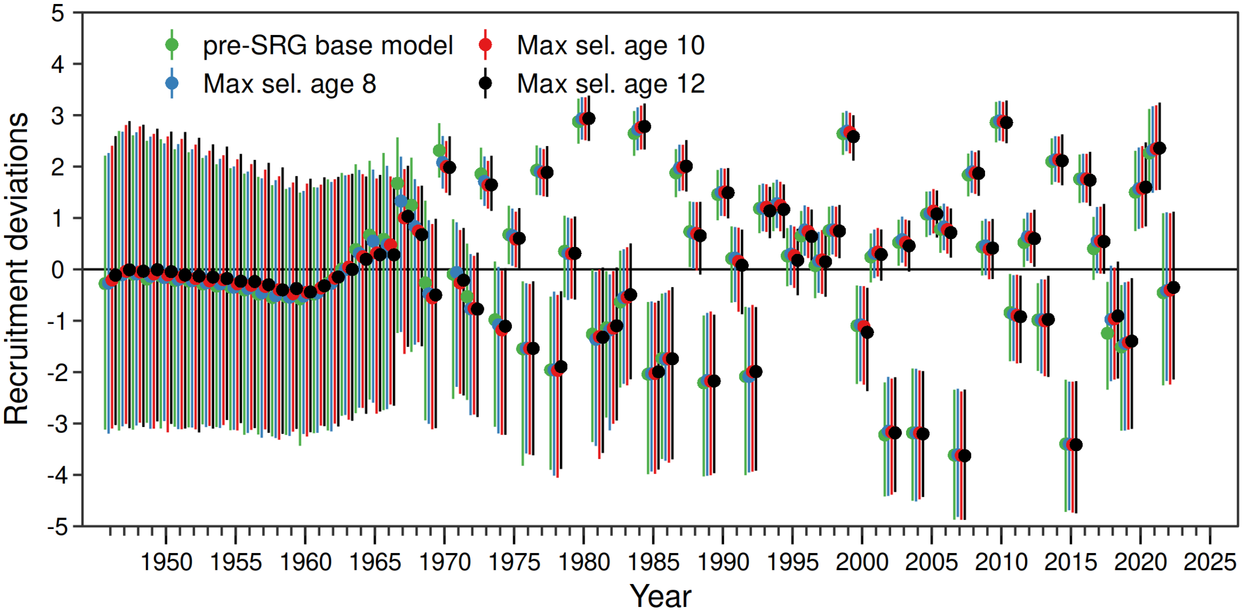

Figure B.28. Medians (solid circles) of the posterior distribution for log-scale recruitment deviations with 95% posterior credibility intervals (vertical lines) for alternative maximum age for selectivity models. The base model in this figure represents the pre-SRG base model (i.e., includes the age-1 index).

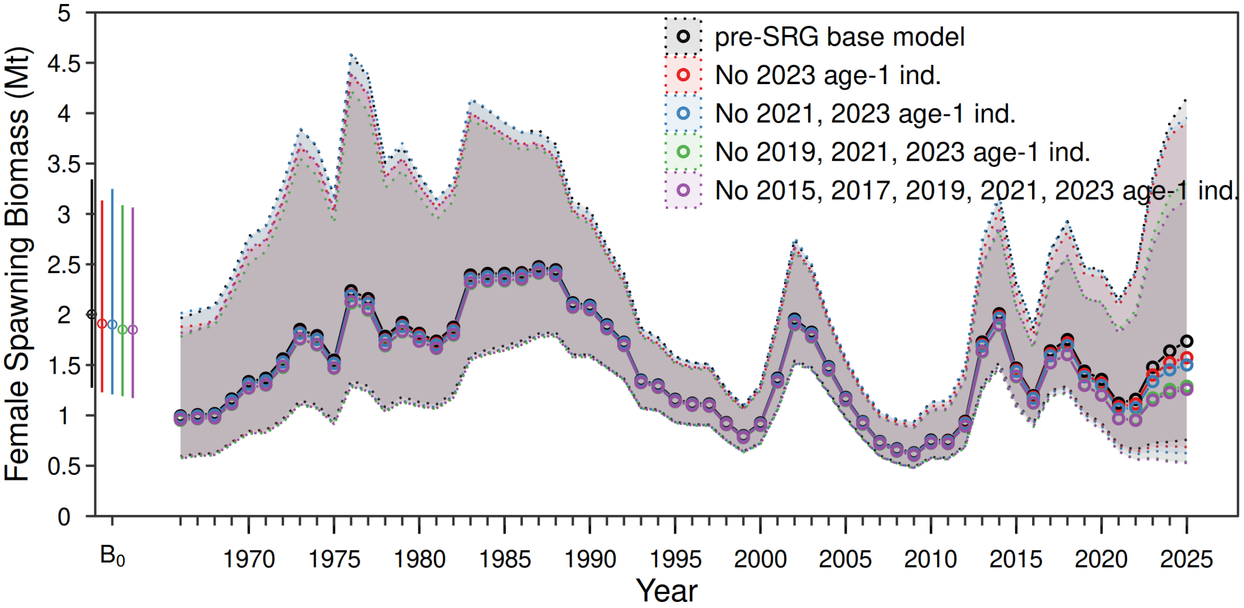

Figure B.29. Median (solid line) of the posterior distribution for beginning of the year female spawning biomass with 95% posterior credibility intervals (shaded area) for each age-1 data point removal model. The base model in this figure represents the pre-SRG base model (i.e., includes the age-1 index).

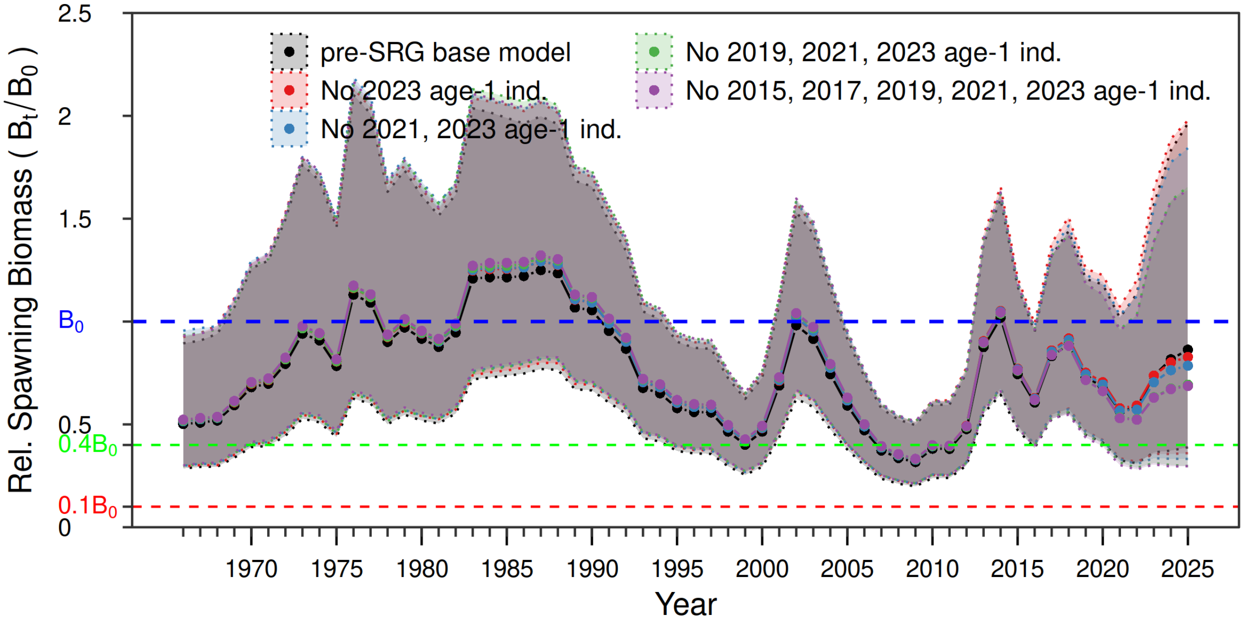

Figure B.30. Median (solid line) of the posterior distribution for relative female spawning biomass with 95% posterior credibility intervals (shaded area) for each age-1 data point removal model. The base model in this figure represents the pre-SRG base model (i.e., includes the age-1 index).

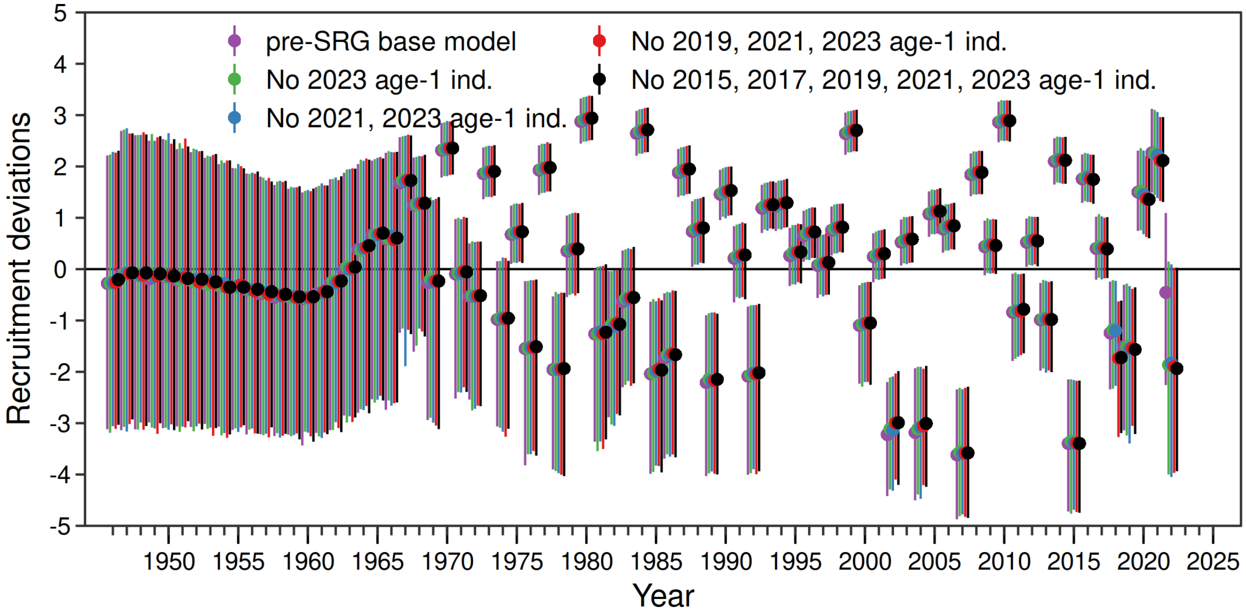

Figure B.31. Medians (solid circles) of the posterior distribution for log-scale recruitment deviations with 95% posterior credibility intervals (vertical lines) for each age-1 data point removal model. The base model in this figure represents the pre-SRG base model (i.e., includes the age-1 index).

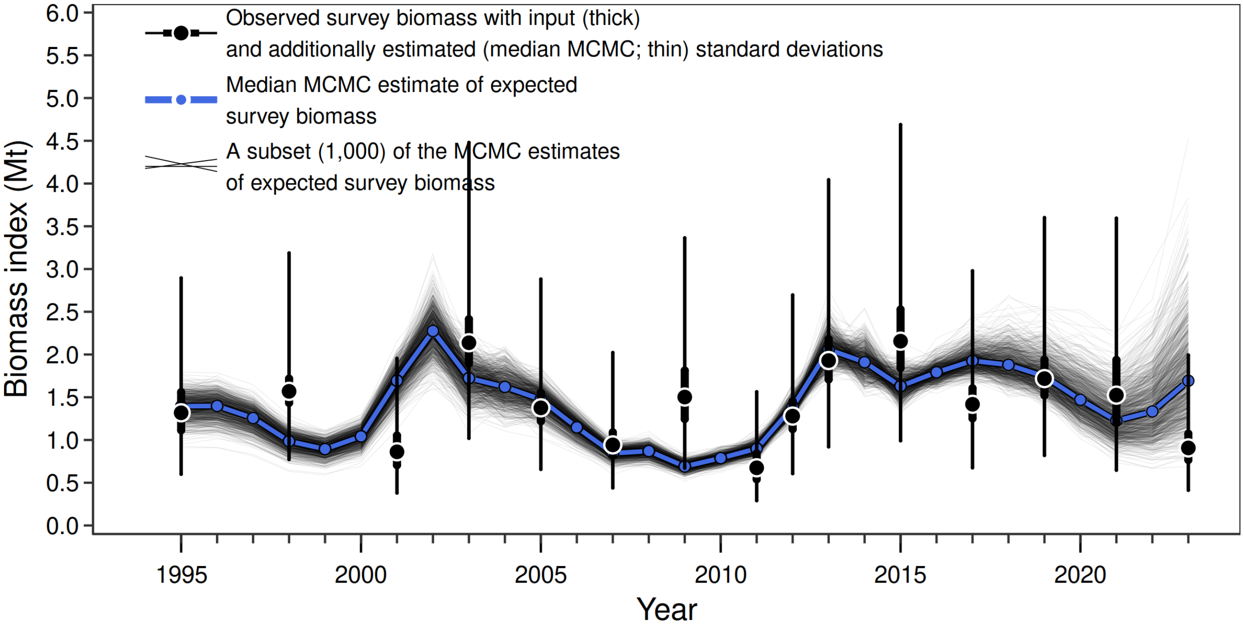

Figure B.32. Fit to the acoustic survey for the pre-SRG base model.

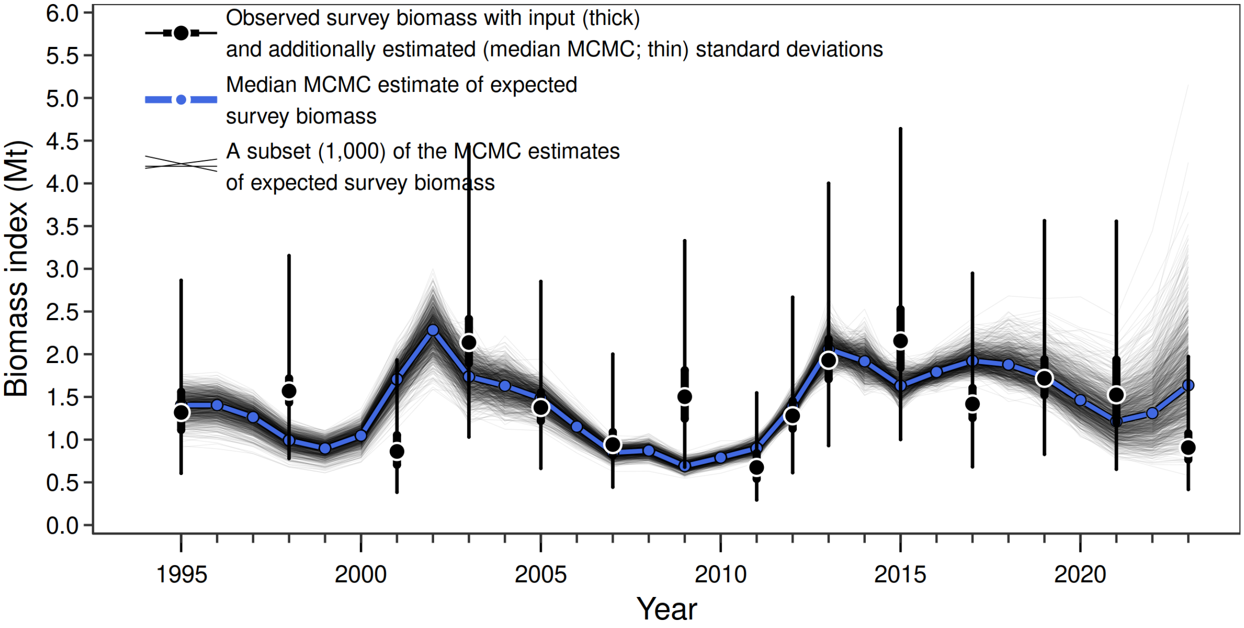

Figure B.33. Fit to the acoustic survey for the model that removes the 2023 age-1 index data point.

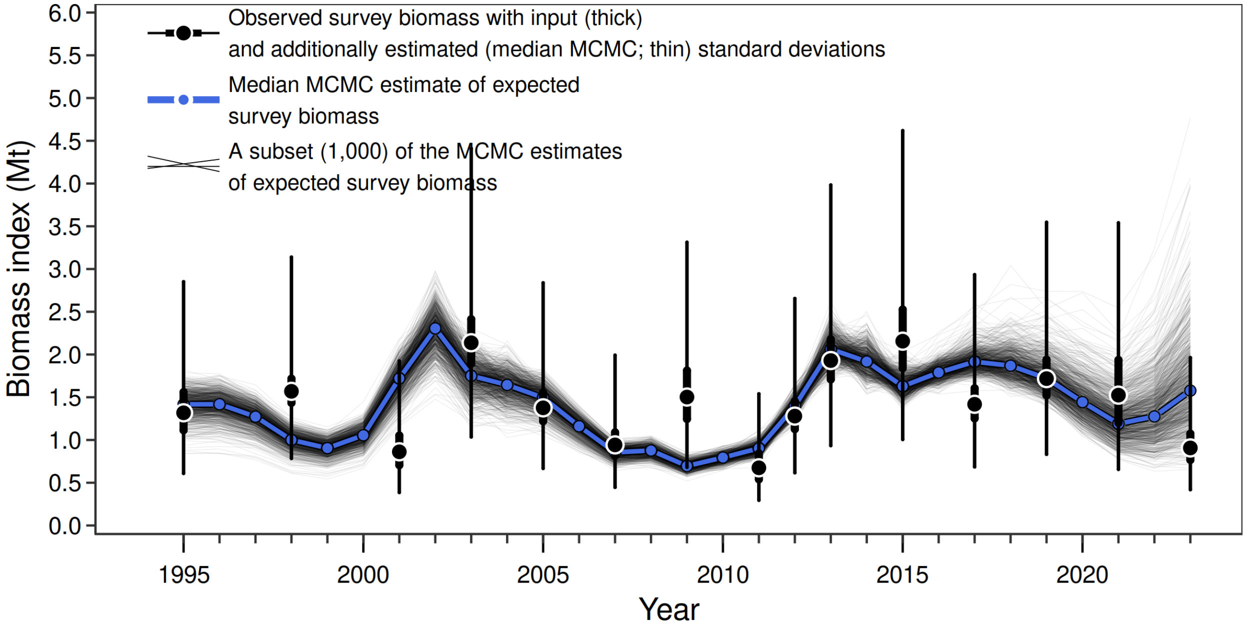

Figure B.34. Fit to the acoustic survey for the model that removes the 2023 and 2021 age-1 index data points.

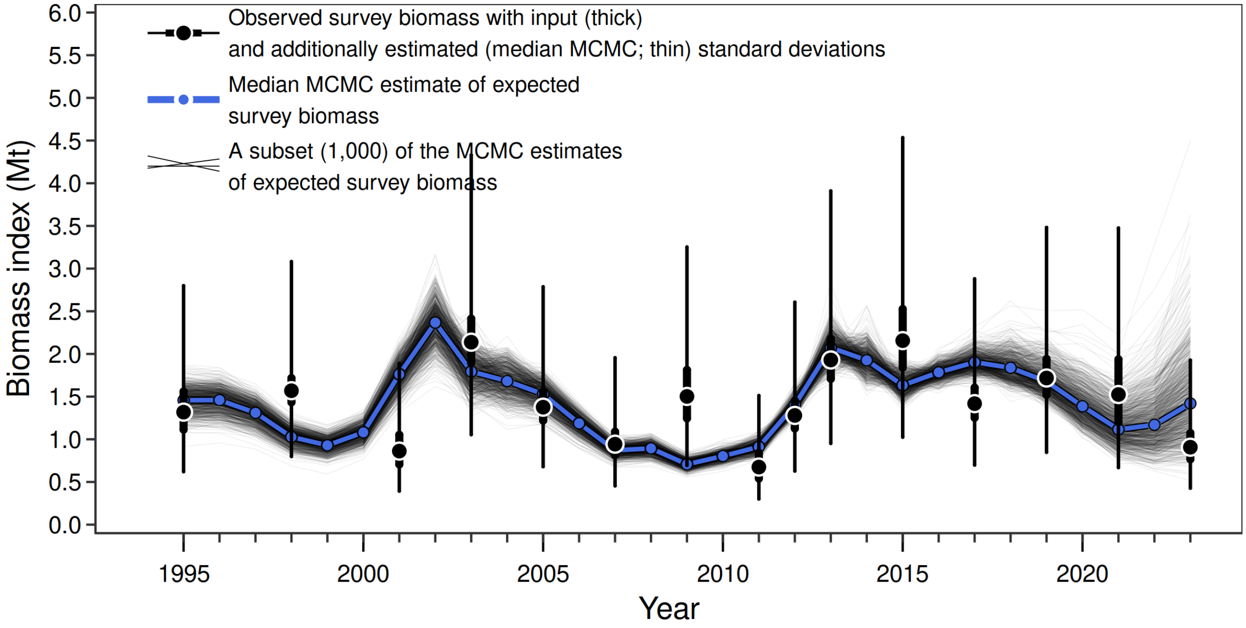

Figure B.35. Fit to the acoustic survey for the model that removes the 2023, 2021, and 2019 age-1 index data points.

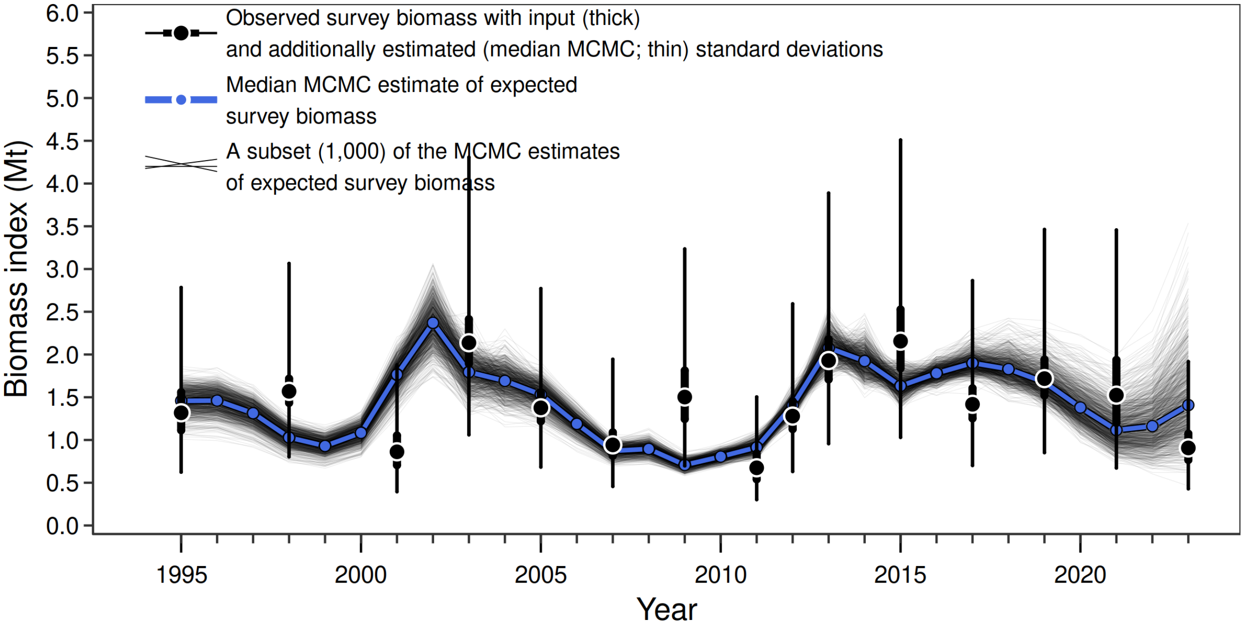

Figure B.36. Fit to the acoustic survey for the model that removes the 2023, 2021, 2019, 2017, and 2015 age-1 index data points.

B.3 Day 3

Request 1

The SRG requests a run without the age-1 index to be considered as the base model for producing management advice. Please produce the Executive Summary with this model for review on Day 4 of the 2025 SRG meeting.

JTC Response

An updated executive summary was provided for review.

Request 2

The SRG requests that decision tables and probability tables be produced with 2023 and onward recruitment estimated and incorporating uncertainty. This would be done on the model without the age-1 index.

JTC Response

Decision tables and probabilities were provided along with tables of recent spawning biomass and recruitment estimates.

C GLOSSARY OF TERMS USED IN THIS DOCUMENT

40:10 adjustment: A reduction in the overall total allowable catch that is triggered when the female spawning biomass falls below 40% of its unfished equilibrium level. This adjustment reduces the total allowable catch on a straight-line basis from the 40% level such that the total allowable catch would equal zero when the biomass is at 10% of its unfished equilibrium level. This is one component of the default harvest policy.

Acceptable biological catch (ABC): The acceptable biological catch is a scientific calculation of the sustainable harvest level of a fishery used historically to set the upper limit for fishery removals by the Pacific Fishery Management Council. It is calculated by applying the estimated (or proxy) harvest rate that produces the maximum sustainable yield from the estimated vulnerable biomass. For Pacific Hake, the calculation of the acceptable biological catch and application of the 40:10 adjustment is now replaced with the default harvest rate and the total allowable catch.

Adjusted: A term used to describe the total allowable catch or allocations that account for carryovers of uncaught catch from previous years.

Advisory Panel (AP): The Advisory Panel on Pacific Hake established by the Agreement.

Agreement ('Treaty'): The Agreement between the government of the United States and the government of Canada on Pacific Hake, signed in Seattle, Washington, on November 21, 2003 and entered into force June 25, 2008.

Alaska Fisheries Science Center (AFSC): One of six regional NOAA Fisheries Science Centers, primarily in Seattle, Washington but also present throughout Alaska.

B_0: Unfished equilibrium female spawning biomass.

$B_{10\%}$: The level of female spawning biomass corresponding to 10% of unfished equilibrium female spawning biomass, i.e., $B_{10\%} = 0.1B_0$. This is the level below which the calculated total allowable catch is set to 0, based on the 40:10 adjustment.

$B_{40\%}$: The level of female spawning biomass corresponding to 40% of unfished equilibrium female spawning biomass, i.e., $B_{40\%} = 0.4B_0$. This is the level below which the total allowable catch is decreased from the value associated with $F_{\text{SPR}=40\%}$, based on the 40:10 adjustment.

B_{MSY}: The estimated female spawning biomass which theoretically would produce the maximum sustainable yield under equilibrium fishing conditions (constant fishing and average recruitment in every year).

Backscatter: The scattering by a target back in the direction of an acoustic source. Specifically, the Nautical Area Scattering Coefficient (a measure of scattering per area) is frequently referred to as backscatter.

Benchmark spawning potential ratio ($B_{\text{SPR}=40\%}$): The spawning potential ratio of 40%, where 40% relates to the default harvest rate of $F_{\text{SPR}=40\%}$ specified in the Agreement. Even under equilibrium conditions, $F_{\text{SPR}=40\%}$ would not necessarily result in a female spawning biomass of $B_{40\%}$ because $F_{\text{SPR}=40\%}$ is defined in terms of the spawning potential ratio that depends on the female spawning biomass per recruit.

California Current Ecosystem: The waters of the continental shelf and slope off the west coast of North America, commonly referring to the area from Central California to Southern British Columbia.

Carryover: If at the end of the year, there are unharvested allocations, then there are provisions for some of these unharvested allocations to be carried over into the next year's allocation process. The Agreement states that "If, in any year, a Party's catch is less than its individual total allowable catch, an amount equal to the shortfall shall be added to its individual total allowable catch in the following year, unless otherwise recommended by the Joint Management Committee. Adjustments under this sub-paragraph shall in no case exceed 15 percent of a Party's unadjusted individual total allowable catch for the year in which the shortfall occurred."

Catchability (q): The parameter defining the proportionality between a relative index of abundance (often a fishery-independent survey) and the estimated abundance available to that survey (as modified by selectivity) in the assessment model.

Catch-per-unit-effort (CPUE): A raw or, frequently, standardized and model-based metric of fishing success based on the catch and relative effort expended to generate that catch. Catch-per-unit-effort is often used as an index of abundance in the absence of fishery-independent indices and/or where the two types of indices are believed to be proportional.

Catch target: A general term used to describe the catch value used for management. Depending on the context, this may be a limit rather than a target and may be equal to a total allowable catch, an acceptable biological catch, the median result of applying the default harvest policy, or some other number. The Joint Technical Committee welcomes input from the Joint Management Committee on the best terminology to use for these quantities.

Closed-loop simulation: A subset of a management strategy evaluation that iteratively simulates a population using an operating model, generates data from that population and passes it to an estimation method, uses the estimation method and a management strategy to provide management advice, which then feeds back into the operating model to simulate an additional fixed set of time before repeating this process.

Coefficient of variation (CV): A measure of uncertainty defined as the standard deviation divided by the mean.

Cohort: A group of fish born in the same year. Also see recruitment and year-class.

Constant catch: A catch scenario used for forecasting in which the same catch is used in successive years.

Default harvest policy (rate): The application of $F_{\text{SPR}=40\%}$ with the 40:10 adjustment. Having considered any advice provided by the Joint Technical Committee, Scientific Review Group, or Advisory Panel, the Joint Management Committee may recommend a different harvest rate if the scientific evidence demonstrates that a different rate is necessary to sustain the resource.

Department of Fisheries and Oceans (DFO) Canada: See Fisheries and Oceans Canada.

Depletion: Prior to the 2015 assessment, depletion was used instead of relative spawning biomass. 'Relative depletion' was also used.

El Niño: Abnormally warm ocean climate conditions in the California Current Ecosystem as a result of broad changes in the Eastern Pacific Ocean across the eastern coast of Latin America (centered on Peru) often around the end of the calendar year.

Exploitation fraction: A metric of fishing intensity that represents the total annual catch divided by the estimated population biomass over a range of ages assumed to be vulnerable to the fishery (set to ages 2+ in this assessment; note that in some previous assessments it was 3+). This value is not equivalent to the instantaneous rate of fishing mortality or the spawning potential ratio.

$F_{\text{SPR}=40\%}$: The rate of fishing mortality estimated to give a spawning potential ratio of 40%. Therefore, by definition this satisfies

$$0.4 = \frac{\text{spawning biomass per recruit with } F_{40\%}}{\text{spawning biomass per recruit with no fishing}}, \tag{C.1}$$

and SPR ($F_{40\%}$) = 40%. The 40% value is specified in the Agreement.

$F_{\text{SPR}=40\%}$–40:10 harvest policy: The default harvest policy.

Female spawning biomass: The biomass of mature female fish at the beginning of the year. Sometimes abbreviated to spawning biomass.

Fisheries and Oceans Canada (DFO): Federal organization that delivers programs and services to support sustainable use and development of Canada's waterways and aquatic resources. Was previously called Department of Fisheries and Oceans.

Fishing intensity: A measure of the magnitude of fishing, defined for a fishing rate (F) as:

$$\text{fishing intensity for } F = 1 - \text{SPR}(F), \tag{C.2}$$

where SPR(F) is the spawning potential ratio for the value of F accumulated over the entire year. It is often given as a percentage. Relative fishing intensity (Figures C.1 and C.2) is the fishing intensity relative to that at the SPR fishing rate $F_{\text{SPR}=40\%}$, where $F_{\text{SPR}=40\%}$ is the F that gives an SPR of 40% such that, by definition, $\mathrm{SPR}(F_{40\%}) = 40\%$ (the benchmark spawning ratio). Therefore

$$\text{relative fishing intensity for } F = \frac{1-\mathrm{SPR}(F)}{1-\mathrm{SPR}(F_{40\%})} \tag{C.3}$$

$$= \frac{1-\mathrm{SPR}(F)}{1-0.4} \tag{C.4}$$

$$= \frac{1-\mathrm{SPR}(F)}{0.6}. \tag{C.5}$$

For brevity we use $F_{\mathrm{SPR}=40\%} = \mathrm{SPR}(F_{40\%})$ in the text. Although this simply equals 40%, it can be helpful to explicitly write:

$$\text{relative fishing intensity for } F = \frac{1-\mathrm{SPR}(F)}{1-\mathrm{SPR}_{40\%}}. \tag{C.6}$$

Fishing mortality rate or instantaneous rate of fishing mortality (F): A metric of fishing intensity that is usually reported in relation to the most highly selected ages(s) or length(s), or occasionally as an average over an age range that is vulnerable to the fishery. Because it is an instantaneous rate operating simultaneously with natural mortality, it is not equivalent to exploitation fraction, percent annual removal, or the spawning potential ratio.

F_{MSY}: The rate of fishing mortality estimated to produce the maximum sustainable yield from the population.

Harvest strategy: A formal system for managing a fishery that includes the elements shown in Figure A.1 of Taylor et al. (2015).

Harvest control rule: A process for determining an acceptable biological catch from a stock assessment. Also see default harvest policy.

Joint Management Committee (JMC): The Joint Management Committee is established by the Agreement.

Joint Technical Committee (JTC): The Joint Technical Committee is established by the Agreement. The formal name is 'Joint Technical Committee of the Pacific Hake/Whiting Agreement Between the Governments of the United States and Canada'.

Kilotonne (kt). Metric abbreviation for 1,000 metric tonnes.

Logistic transformation: A mathematical transformation used to translate between numbers bounded within some range to numbers on the real line ($-\infty$ to $+\infty$).

Magnuson–Stevens Fishery Conservation and Management Act (MSFCMA): The MSFCMA, sometimes known as the 'Magnuson–Stevens Act', established the 200-mile fishery conservation zone, the regional fishery management council system, and other provisions of U.S. marine fishery law.

Management Strategy Evaluation (MSE): A formal process for evaluating harvest strategies.

Markov chain Monte Carlo (MCMC): A numerical method used to sample from the posterior distribution of parameters and derived quantities in a Bayesian analysis. It is more computationally intensive than computing the maximum likelihood estimate but provides a more accurate depiction of parameter uncertainty. See Stewart et al. (2013) for a discussion of issues related to differences between Markov chain Monte Carlo and maximum likelihood estimation.

Maximum sustainable yield (MSY): An estimate of the largest sustainable annual catch that can be continuously taken over a long period of time from a population under equilibrium ecological and environmental conditions.

Megatonne (Mt): Metric abbreviation for 1,000,000 metric tonnes.

Metric tonne (t): A unit of mass equal to 1,000 kilograms or 2,204.62 pounds. Some previous stock assessments used the abbreviation 'mt'.

National Marine Fisheries Service (NMFS): See NOAA Fisheries.

No-U-Turn Sampler (NUTS): An advanced Hamiltonian Bayesian Markov chain Monte Carlo sampling algorithm used to efficiently create posterior distributions and used in Pacific Hake Bayesian assessments beginning in 2021.

NOAA Fisheries: The division of the United States National Oceanic and Atmospheric Administration (NOAA) responsible for conservation and management of offshore fisheries (and inland salmon). This is also known as the National Marine Fisheries Service (NMFS), and both names are commonly used at this time.

North Pacific Groundfish and Halibut Observer Program Database (NORPAC): A database that stores data collected at sea by U.S. fishery observers.

Northwest Fisheries Science Center (NWFSC): One of six regional NOAA Fisheries Science Centers, primarily in Seattle, Washington but also in various locations in Oregon and Washington.

Not available (NA): Something that is not available, e.g., an entry in a table.

Operating model (OM): A model used to simulate data for use in the management strategy evaluation. The operating model includes components for the population and fishery dynamics, as well as the simulation of the data sampling process, potentially including observation error. Cases in the management strategy evaluation represent alternative configurations of the operating model.

Pacific Biological Station (PBS): The Pacific Biological Station of Fisheries and Oceans Canada located in Nanaimo, British Columbia.

Pacific Fisheries Information Network (PacFIN): A database that provides a central repository for commercial fishery information from Washington, Oregon, and California.

Pacific Fishery Management Council (PFMC): The U.S. organization under which historical stock assessments for Pacific Hake were conducted.

Pacific Hake: Common name for *Merluccius productus*, the species whose offshore population in the waters of the United States and Canada is subject of this assessment.

Pacific whiting: An alternative name for Pacific Hake commonly used in the United States.

Posterior distribution: The probability distribution for parameters or derived quantities from a Bayesian model representing the result of the prior probability distributions being updated by the observed data via the likelihood equation. For stock assessments, posterior distributions are approximated via numerical methods; one frequently employed method is Markov chain Monte Carlo sampling.

Prior distribution: A probability distribution for a parameter in a Bayesian analysis that represents the information available before evaluating the observed data via the likelihood equation. For some parameters, uninformative priors can be constructed that allow the data to dominate the posterior distribution. For other parameters, informative priors can be constructed based on auxiliary information and/or expert knowledge or opinions.

R_0: Estimated annual recruitment at unfished equilibrium.

Random walk Metropolis Hastings (rwMH): Bayesian Markov chain Monte Carlo sampling algorithm used to create posterior distributions used in Pacific Hake Bayesian stock assessment models prior to 2021.

Recruits/recruitment: the estimated number of new members in a fish population born in the same age. In this assessment, recruitment is reported at age 0. See cohort and year-class.

Recruitment deviation: The offset of the recruitment in a given year relative to the stock–recruitment relationship; values occur on a logarithmic scale and are relative to the expected recruitment at a given female spawning biomass.

Relative fishing intensity: See fishing intensity.

Relative spawning biomass: The ratio of the beginning-of-the-year female spawning biomass to the unfished equilibrium female spawning biomass (B_0). Thus, lower values are associated with fewer mature female fish. This term was introduced in the 2015 stock assessment as a replacement for 'depletion'.

Scientific Review Group (SRG): The Scientific Review Group established by the Agreement.

Scientific and Statistical Committee (SSC): The scientific advisory committee to the Pacific Fishery Management Council. The Magnuson–Stevens Fishery Conservation and Management Act requires that each council maintain a Scientific and Statistical Committee to assist in gathering and analyzing statistical, biological, ecological, economic, social, and other scientific information that is relevant to the management of the Council.

Simulation: A model evaluation under a particular state of nature, including combinations of parameters controlling stock productivity, stock status, and the time series of recruitment deviations. In this assessment, there are 8,000 simulations used to characterize alternative states of nature, each of which are based on a sample from the posterior distribution of the parameters, as calculated using Markov chain Monte Carlo, for a particular model (e.g., the base model).

Spawning biomass: Abbreviated term for female spawning biomass.

Spawning biomass per recruit: The expected lifetime contribution of an age-0 recruit, calculated as the sum across all ages of the product of spawning biomass at each age and the probability of surviving to that age. See Figure C.2 for a graphical demonstration of the calculation of this value, which is found in both numerator and denominator of the spawning potential ratio.

Spawning potential ratio (SPR): The ratio of the spawning biomass per recruit under a given level of fishing to the estimated spawning biomass per recruit in the absence of fishing. Often expressed as a percentage, it achieves a value of 100% in the absence of fishing and declines toward zero as fishing intensity increases (Figure C.2).

Standard deviation (sd): A measure of variability about the mean within a sample.

Steepness (h): A parameter of the stock–recruitment relationship representing the proportion of R_0 expected (on average) when the female spawning biomass is reduced to 20% of B_0 (i.e., when relative spawning biomass is equal to 20%).

Stock Synthesis (SS3): The age-structured stock assessment model applied in this stock assessment.

Target strength (TS): The amount of backscatter from an individual acoustic target.

Total allowable catch (TAC): The maximum fishery removal under the terms of the Agreement.

U.S./Canadian allocation: The division of the total allowable catch as 73.88% for the U.S. share and 26.12% for the Canadian share.

Vulnerable biomass: The demographic portion of the population available for harvest by the fishery.

Year-class: A group of fish born in the same year. See 'cohort' and 'recruitment'.

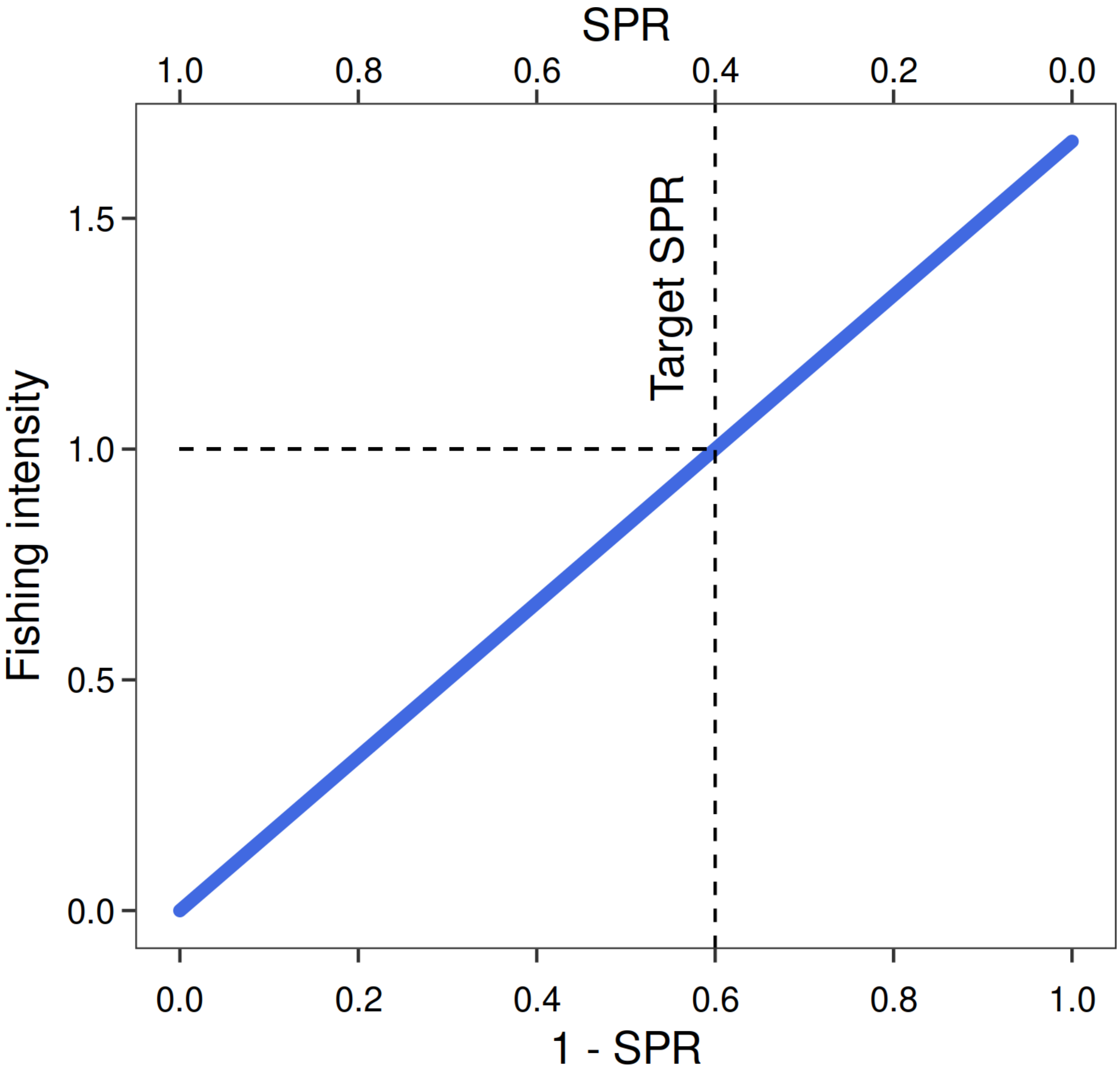

Figure C.1. Fishing intensity as a function of the spawning potential ratio (SPR; top axis) and 1-SPR (bottom axis); given the benchmark SPR of 40%, the solid blue line is simply 1/0.6, as shown in equation (C.3).

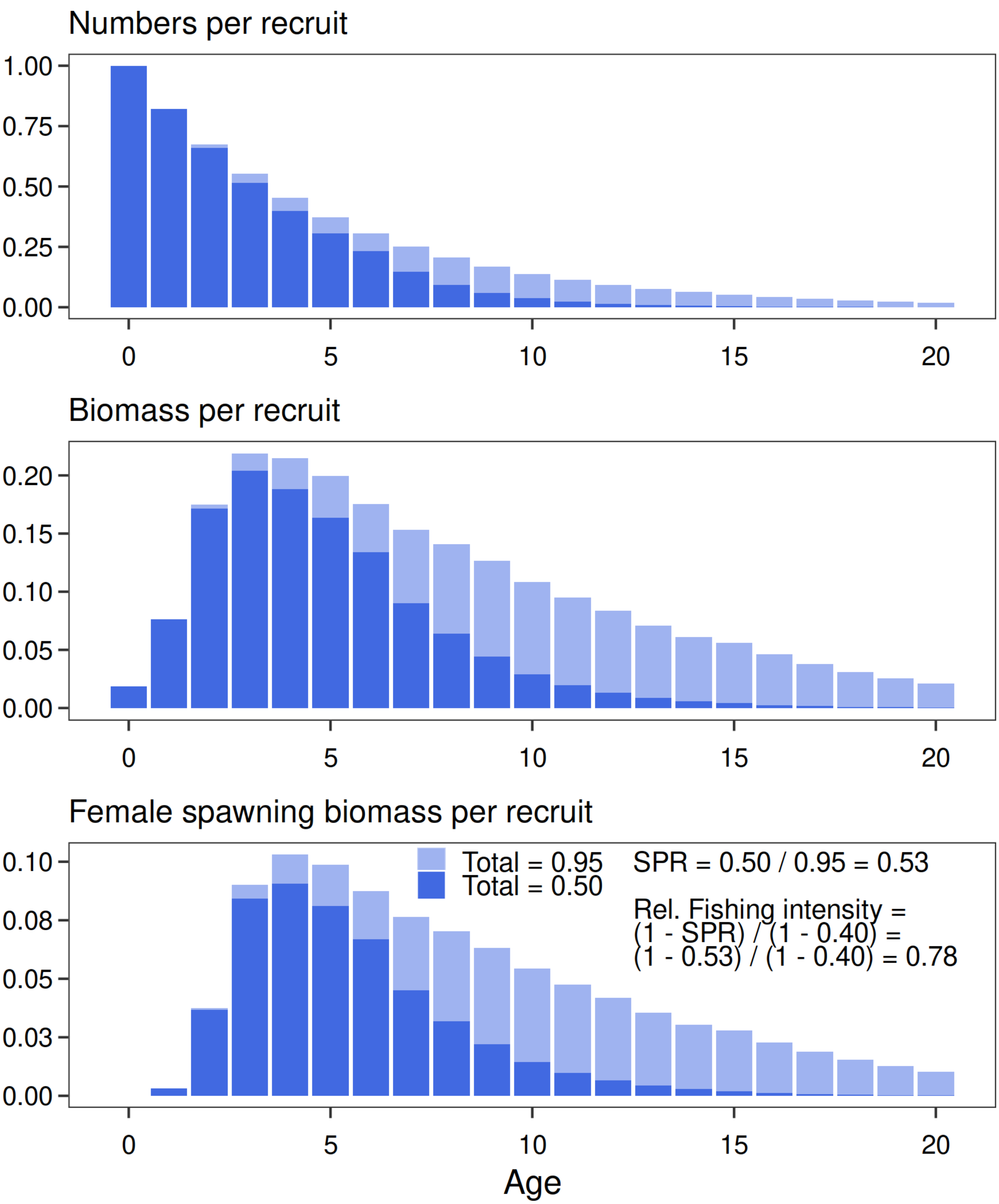

Figure C.2. Illustration of the spawning potential ratio (SPR) calculation based on the combination of maturity and fecundity used in the model, using the Markov chain Monte Carlo (MCMC) estimates of natural mortality, selectivity, and fishing mortality in the final year of the base model used in this year's assessment. The light blue bars represent unfished values, the dark blue bars represent fished values.

D REPORT OF THE 2024 PACIFIC HAKE FISHERY IN CANADA

Prepared by the Canadian Advisory Panel and submitted on January 21, 2025 for inclusion in this assessment document.

The Canadian Offshore Pacific Hake fishery catch was by far the lowest recorded since the fishery began in the late 1970s, with slightly more than 3,103 tonnes caught, or 3.3% of the 93,450 tonnes TAC set by the Canadian Industry. This was down from the 22,000 tonnes caught in 2023 when 21% of the 105,000 tonne TAC was harvested. The reports from the fishermen were consistent, fishing was very poor as evident in the extremely low catch. The fleet reported no body of Hake on the Canadian Zone that allowed for a fishery to take place. What little catch occurred was around Finger Bank and south into San Juan.

The Freezer Vessel Fleet searched the traditional area off Winter Harbour in shallow and off the edge, but no fish was found. The fish that were encountered were mostly larger older fish (greater than 1,000 grams). There were some small fish were seen by the Canadian Fleet. The bycatch was primarily pollock, and herring. The market for the Hake was strong again in 2024 but the catches were just not there to supply the plants or the Freezer Vessels. The Freezer Vessels accounted for 88% of the catch in 2024.

E REPORT OF THE 2024 PACIFIC HAKE FISHERY IN THE UNITED STATES

Prepared by the United States Advisory Panel on January 24, 2025 for inclusion in this assessment document.

Based on information provided by U.S. Advisory Panel members and data from the Pacific Fisheries Information Network (PacFIN), total U.S. harvest in the 2024 whiting fishery was **165,582 t** (see Table E.1), which is 40% of the U.S. allocation of 410,035 t. Compared to the 2023 season (240,189 t), total U.S. catch was down 31% in 2024.

Table E.1. 2024 U.S. whiting allocations and catch (tonnes, t). Tribal catch is estimated (SS sector), and MS catch was provided by the MS cooperative. Dashes represent unknown values.

U.S. Sector	Initial Allocation	Allocation After Reapportionment	Catch (t)	Utilization (%)
Tribal	71,756	26,756	1,541	6
Research	750	750	–	–
Shoreside (SS)	141,762	160,662	81,205	51
Mothership (MS)	81,007	91,807	20,927	23
Catcher-Processor (CP)	114,760	130,060	61,909	48
Total	**410,035**	**410,035**	**165,582**	**40**

Sources for Table E.1 are from the Federal register and PacFIN Whiting Report.

The lack of a Spring fishery for all sectors is one of the primary factors contributing to the low overall catch for the U.S. whiting fishery in 2024. It seems the hake were slow to show up (similar to 2023), and aggregation of fish observed in the Spring were located very far south, and, in many cases not feasible to pursue (due to cost/economics or regulation). The spring fishery was considered a failure for the catcher-processor (CP) sector, and boats in all sectors saw little to no fish north of 42 degrees through most of the spring. The mothership (MS) and shoreside (SS) vessels were able to get a few scratchy trips in June, but the fishery didn't start in earnest until July. Abnormally cold water temperatures were also reported in the Spring fishery, which did benefit fish quality compared to 2023.

Late summer into early fall (August – October) provided the best fishing of the season. The MS and SS fleets reported notably good, clean fishing in August and September. Fish aggregations moved northward from the CA/OR border north of Newport, OR. The fish were consistently 500-600 grams with good quality and recovery. By the end of September, catch began to slow, and fish size had dropped to the 300-400g range, on average. Most of the MS and SS effort was in mid to southern Oregon, with some catch in northern Oregon and Washington in October. Off northern OR and WA, fishing was spottier across the entire year. Some SS boats had success finding hake in the box off Northern Washington later in the year. Most fish caught of WA waters were larger fish, in the 700-900 gram range and larger.

The CP sector began participating in the Fall fishery in late August/early September, which is a typical timeframe. At no point in the fall season did the CP sector have a full complement of vessels participating at the same time. This is due to some vessels returning from the Alaska pollock fishery late, shipyard schedules, and poor fishing. Early in the fall season, strong aggregations of whiting were observed in California, however it did not appear that fish moved north across the OR/CA border. CP vessels generally encountered low CPUE in the Fall fishery and difficulty finding consistent aggregations of whiting resulting in significant efforts searching for whiting. Most CP harvest occurred in central and southern Oregon.

Bycatch was less of a problem than in most years, largely due to reduced catch and effort overall. Many MS and SS catcher boats use real time cameras and did report seeing very large numbers of small/juvenile hake in their cameras – Some fishermen reported seeing more 1 and 2 year-olds than they've seen in more than a decade. Boats in the pink shrimp fishery also reported seeing large numbers of juvenile hake.

Only two (2) out of six (6) mothership platforms participated in the U.S. whiting fishery in 2024. The shoreside sector continued to see reduced processing capacity with the loss of the Newport surimi plants for the 2024 season.

F ESTIMATED PARAMETERS IN THE BASE ASSESSMENT MODEL

Table F.1. Medians of estimated parameters for the base model.

Parameter	Posterior median
NatM_uniform_Fem_GP_1	0.2335
SR_LN(R0)	14.7140
SR_BH_steep	0.8115
Q_extraSD_Acoustic_Survey(2)	0.2943
ln(DM_theta)_Age_P1	-0.6430
ln(DM_theta)_Age_P2	2.7291
Early_InitAge_20	-0.2651
Early_InitAge_19	-0.1114
Early_InitAge_18	-0.1487
Early_InitAge_17	-0.1359
Early_InitAge_16	-0.1560
Early_InitAge_15	-0.1924
Early_InitAge_14	-0.2224
Early_InitAge_13	-0.2456
Early_InitAge_12	-0.3156
Early_InitAge_11	-0.3689
Early_InitAge_10	-0.3769
Early_InitAge_9	-0.4433
Early_InitAge_8	-0.5157
Early_InitAge_7	-0.5299
Early_InitAge_6	-0.5081
Early_InitAge_5	-0.4389
Early_InitAge_4	-0.2242
Early_InitAge_3	0.0238
Early_InitAge_2	0.4936
Early_InitAge_1	0.7070
Early_RecrDev_1966	0.6369
Early_RecrDev_1967	1.7476
Early_RecrDev_1968	1.3104
Early_RecrDev_1969	-0.1820
Main_RecrDev_1970	2.3710
Main_RecrDev_1971	-0.0493
Main_RecrDev_1972	-0.4842
Main_RecrDev_1973	1.9208
Main_RecrDev_1974	-0.9598
Main_RecrDev_1975	0.7395
Main_RecrDev_1976	-1.5292
Main_RecrDev_1977	1.9941
Main_RecrDev_1978	-1.9364
Main_RecrDev_1979	0.4093
Main_RecrDev_1980	2.9599

Continued on next page ...

... Continued from previous page

Parameter	Posterior median
Main_RecrDev_1981	-1.2292
Main_RecrDev_1982	-1.0303
Main_RecrDev_1983	-0.5622
Main_RecrDev_1984	2.7319
Main_RecrDev_1985	-1.9573
Main_RecrDev_1986	-1.6545
Main_RecrDev_1987	1.9726
Main_RecrDev_1988	0.8221
Main_RecrDev_1989	-2.1128
Main_RecrDev_1990	1.5468
Main_RecrDev_1991	0.2947
Main_RecrDev_1992	-2.0076
Main_RecrDev_1993	1.2706
Main_RecrDev_1994	1.3253
Main_RecrDev_1995	0.3471
Main_RecrDev_1996	0.7258
Main_RecrDev_1997	0.2058
Main_RecrDev_1998	0.8272
Main_RecrDev_1999	2.7198
Main_RecrDev_2000	-1.0346
Main_RecrDev_2001	0.3206
Main_RecrDev_2002	-3.3782
Main_RecrDev_2003	0.5973
Main_RecrDev_2004	-2.8006
Main_RecrDev_2005	1.1467
Main_RecrDev_2006	0.8517
Main_RecrDev_2007	-3.5900
Main_RecrDev_2008	1.8963
Main_RecrDev_2009	0.4763
Main_RecrDev_2010	2.9015
Main_RecrDev_2011	-0.7036
Main_RecrDev_2012	0.5486
Main_RecrDev_2013	-0.9740
Main_RecrDev_2014	2.1287
Main_RecrDev_2015	-3.3704
Main_RecrDev_2016	1.7532
Main_RecrDev_2017	0.3883
Main_RecrDev_2018	-1.7450
Main_RecrDev_2019	-1.5628
Main_RecrDev_2020	1.3475
Main_RecrDev_2021	2.0991
Main_RecrDev_2022	-1.8925
AgeSel_P3_Fishery(1)	2.8119

Continued on next page ...

... Continued from previous page

Parameter	**Posterior median**
AgeSel_P4_Fishery(1)	0.8946
AgeSel_P5_Fishery(1)	0.4129
AgeSel_P6_Fishery(1)	0.1753
AgeSel_P7_Fishery(1)	0.5031
AgeSel_P4_Acoustic_Survey(2)	0.5298
AgeSel_P5_Acoustic_Survey(2)	-0.1764
AgeSel_P6_Acoustic_Survey(2)	0.2953
AgeSel_P7_Acoustic_Survey(2)	0.2965
AgeSel_P3_Fishery(1)_DEVadd_1991	0.5738
AgeSel_P3_Fishery(1)_DEVadd_1992	-0.0140
AgeSel_P3_Fishery(1)_DEVadd_1993	0.0052
AgeSel_P3_Fishery(1)_DEVadd_1994	0.1171
AgeSel_P3_Fishery(1)_DEVadd_1995	-0.1822
AgeSel_P3_Fishery(1)_DEVadd_1996	0.4439
AgeSel_P3_Fishery(1)_DEVadd_1997	0.0969
AgeSel_P3_Fishery(1)_DEVadd_1998	0.2256
AgeSel_P3_Fishery(1)_DEVadd_1999	0.9934
AgeSel_P3_Fishery(1)_DEVadd_2000	0.5163
AgeSel_P3_Fishery(1)_DEVadd_2001	0.0330
AgeSel_P3_Fishery(1)_DEVadd_2002	0.1074
AgeSel_P3_Fishery(1)_DEVadd_2003	0.0041
AgeSel_P3_Fishery(1)_DEVadd_2004	0.3370
AgeSel_P3_Fishery(1)_DEVadd_2005	0.0050
AgeSel_P3_Fishery(1)_DEVadd_2006	0.6121
AgeSel_P3_Fishery(1)_DEVadd_2007	0.6007
AgeSel_P3_Fishery(1)_DEVadd_2008	-0.0367
AgeSel_P3_Fishery(1)_DEVadd_2009	0.4553
AgeSel_P3_Fishery(1)_DEVadd_2010	0.9486
AgeSel_P3_Fishery(1)_DEVadd_2011	-0.0688
AgeSel_P3_Fishery(1)_DEVadd_2012	0.1007
AgeSel_P3_Fishery(1)_DEVadd_2013	0.2320
AgeSel_P3_Fishery(1)_DEVadd_2014	0.3135
AgeSel_P3_Fishery(1)_DEVadd_2015	-0.7284
AgeSel_P3_Fishery(1)_DEVadd_2016	-0.0595
AgeSel_P3_Fishery(1)_DEVadd_2017	-0.3568
AgeSel_P3_Fishery(1)_DEVadd_2018	-1.4757
AgeSel_P3_Fishery(1)_DEVadd_2019	0.5553
AgeSel_P3_Fishery(1)_DEVadd_2020	0.0369
AgeSel_P3_Fishery(1)_DEVadd_2021	-0.3805
AgeSel_P3_Fishery(1)_DEVadd_2022	1.9036
AgeSel_P3_Fishery(1)_DEVadd_2023	0.2252
AgeSel_P3_Fishery(1)_DEVadd_2024	-1.7243
AgeSel_P4_Fishery(1)_DEVadd_1991	0.3831

Continued on next page ...

... Continued from previous page

Parameter	**Posterior median**
AgeSel_P4_Fishery(1)_DEVadd_1992	0.5983
AgeSel_P4_Fishery(1)_DEVadd_1993	0.8104
AgeSel_P4_Fishery(1)_DEVadd_1994	0.1998
AgeSel_P4_Fishery(1)_DEVadd_1995	0.2272
AgeSel_P4_Fishery(1)_DEVadd_1996	-0.3421
AgeSel_P4_Fishery(1)_DEVadd_1997	1.2639
AgeSel_P4_Fishery(1)_DEVadd_1998	0.9908
AgeSel_P4_Fishery(1)_DEVadd_1999	-0.0467
AgeSel_P4_Fishery(1)_DEVadd_2000	0.7627
AgeSel_P4_Fishery(1)_DEVadd_2001	0.9511
AgeSel_P4_Fishery(1)_DEVadd_2002	0.7098
AgeSel_P4_Fishery(1)_DEVadd_2003	0.6678
AgeSel_P4_Fishery(1)_DEVadd_2004	0.4401
AgeSel_P4_Fishery(1)_DEVadd_2005	0.6612
AgeSel_P4_Fishery(1)_DEVadd_2006	-0.0747
AgeSel_P4_Fishery(1)_DEVadd_2007	0.2441
AgeSel_P4_Fishery(1)_DEVadd_2008	0.4510
AgeSel_P4_Fishery(1)_DEVadd_2009	0.7826
AgeSel_P4_Fishery(1)_DEVadd_2010	0.1517
AgeSel_P4_Fishery(1)_DEVadd_2011	1.0677
AgeSel_P4_Fishery(1)_DEVadd_2012	0.2424
AgeSel_P4_Fishery(1)_DEVadd_2013	0.8809
AgeSel_P4_Fishery(1)_DEVadd_2014	0.4454
AgeSel_P4_Fishery(1)_DEVadd_2015	0.2086
AgeSel_P4_Fishery(1)_DEVadd_2016	-0.9488
AgeSel_P4_Fishery(1)_DEVadd_2017	-0.5080
AgeSel_P4_Fishery(1)_DEVadd_2018	-0.5146
AgeSel_P4_Fishery(1)_DEVadd_2019	-0.8328
AgeSel_P4_Fishery(1)_DEVadd_2020	0.5936
AgeSel_P4_Fishery(1)_DEVadd_2021	0.1198
AgeSel_P4_Fishery(1)_DEVadd_2022	-1.2362
AgeSel_P4_Fishery(1)_DEVadd_2023	-0.1505
AgeSel_P4_Fishery(1)_DEVadd_2024	-0.8500
AgeSel_P5_Fishery(1)_DEVadd_1991	-0.8466
AgeSel_P5_Fishery(1)_DEVadd_1992	0.0912
AgeSel_P5_Fishery(1)_DEVadd_1993	-0.0128
AgeSel_P5_Fishery(1)_DEVadd_1994	0.8885
AgeSel_P5_Fishery(1)_DEVadd_1995	0.2571
AgeSel_P5_Fishery(1)_DEVadd_1996	-0.3131
AgeSel_P5_Fishery(1)_DEVadd_1997	-0.1226
AgeSel_P5_Fishery(1)_DEVadd_1998	-0.6308
AgeSel_P5_Fishery(1)_DEVadd_1999	0.0870
AgeSel_P5_Fishery(1)_DEVadd_2000	-0.1174

Continued on next page ...

... Continued from previous page

Parameter	**Posterior median**
AgeSel_P5_Fishery(1)_DEVadd_2001	0.2548
AgeSel_P5_Fishery(1)_DEVadd_2002	0.5295
AgeSel_P5_Fishery(1)_DEVadd_2003	0.7475
AgeSel_P5_Fishery(1)_DEVadd_2004	0.6653
AgeSel_P5_Fishery(1)_DEVadd_2005	0.7131
AgeSel_P5_Fishery(1)_DEVadd_2006	-0.0142
AgeSel_P5_Fishery(1)_DEVadd_2007	-0.0870
AgeSel_P5_Fishery(1)_DEVadd_2008	-0.3785
AgeSel_P5_Fishery(1)_DEVadd_2009	-0.3072
AgeSel_P5_Fishery(1)_DEVadd_2010	0.5187
AgeSel_P5_Fishery(1)_DEVadd_2011	-0.7228
AgeSel_P5_Fishery(1)_DEVadd_2012	0.1593
AgeSel_P5_Fishery(1)_DEVadd_2013	-0.1921
AgeSel_P5_Fishery(1)_DEVadd_2014	-0.4382
AgeSel_P5_Fishery(1)_DEVadd_2015	-0.0791
AgeSel_P5_Fishery(1)_DEVadd_2016	-0.0054
AgeSel_P5_Fishery(1)_DEVadd_2017	-0.1429
AgeSel_P5_Fishery(1)_DEVadd_2018	-0.2253
AgeSel_P5_Fishery(1)_DEVadd_2019	-0.0677
AgeSel_P5_Fishery(1)_DEVadd_2020	0.6005
AgeSel_P5_Fishery(1)_DEVadd_2021	0.4001
AgeSel_P5_Fishery(1)_DEVadd_2022	0.3390
AgeSel_P5_Fishery(1)_DEVadd_2023	-0.7790
AgeSel_P5_Fishery(1)_DEVadd_2024	-0.2265
AgeSel_P6_Fishery(1)_DEVadd_1991	-0.0549
AgeSel_P6_Fishery(1)_DEVadd_1992	-0.4705
AgeSel_P6_Fishery(1)_DEVadd_1993	-0.0587
AgeSel_P6_Fishery(1)_DEVadd_1994	-0.0906
AgeSel_P6_Fishery(1)_DEVadd_1995	0.7507
AgeSel_P6_Fishery(1)_DEVadd_1996	-0.1341
AgeSel_P6_Fishery(1)_DEVadd_1997	-0.3314
AgeSel_P6_Fishery(1)_DEVadd_1998	0.3729
AgeSel_P6_Fishery(1)_DEVadd_1999	-0.3930
AgeSel_P6_Fishery(1)_DEVadd_2000	0.1510
AgeSel_P6_Fishery(1)_DEVadd_2001	-0.0778
AgeSel_P6_Fishery(1)_DEVadd_2002	0.1034
AgeSel_P6_Fishery(1)_DEVadd_2003	0.2717
AgeSel_P6_Fishery(1)_DEVadd_2004	-0.5621
AgeSel_P6_Fishery(1)_DEVadd_2005	0.2794
AgeSel_P6_Fishery(1)_DEVadd_2006	0.1806
AgeSel_P6_Fishery(1)_DEVadd_2007	-0.1805
AgeSel_P6_Fishery(1)_DEVadd_2008	0.3035
AgeSel_P6_Fishery(1)_DEVadd_2009	-0.3760

Continued on next page ...

... Continued from previous page

Parameter	**Posterior median**
AgeSel_P6_Fishery(1)_DEVadd_2010	-0.3838
AgeSel_P6_Fishery(1)_DEVadd_2011	-0.2028
AgeSel_P6_Fishery(1)_DEVadd_2012	-0.4461
AgeSel_P6_Fishery(1)_DEVadd_2013	-0.0464
AgeSel_P6_Fishery(1)_DEVadd_2014	0.0491
AgeSel_P6_Fishery(1)_DEVadd_2015	0.0275
AgeSel_P6_Fishery(1)_DEVadd_2016	-0.0355
AgeSel_P6_Fishery(1)_DEVadd_2017	-0.1930
AgeSel_P6_Fishery(1)_DEVadd_2018	-0.3514
AgeSel_P6_Fishery(1)_DEVadd_2019	0.1284
AgeSel_P6_Fishery(1)_DEVadd_2020	-0.3267
AgeSel_P6_Fishery(1)_DEVadd_2021	0.1307
AgeSel_P6_Fishery(1)_DEVadd_2022	0.1949
AgeSel_P6_Fishery(1)_DEVadd_2023	0.2913
AgeSel_P6_Fishery(1)_DEVadd_2024	-0.0796
AgeSel_P7_Fishery(1)_DEVadd_1991	-0.0998
AgeSel_P7_Fishery(1)_DEVadd_1992	0.0738
AgeSel_P7_Fishery(1)_DEVadd_1993	-0.3607
AgeSel_P7_Fishery(1)_DEVadd_1994	0.1001
AgeSel_P7_Fishery(1)_DEVadd_1995	-0.1259
AgeSel_P7_Fishery(1)_DEVadd_1996	0.4204
AgeSel_P7_Fishery(1)_DEVadd_1997	0.1179
AgeSel_P7_Fishery(1)_DEVadd_1998	-0.5025
AgeSel_P7_Fishery(1)_DEVadd_1999	-0.2613
AgeSel_P7_Fishery(1)_DEVadd_2000	-0.0925
AgeSel_P7_Fishery(1)_DEVadd_2001	-0.3092
AgeSel_P7_Fishery(1)_DEVadd_2002	-0.3722
AgeSel_P7_Fishery(1)_DEVadd_2003	-0.2752
AgeSel_P7_Fishery(1)_DEVadd_2004	-0.1776
AgeSel_P7_Fishery(1)_DEVadd_2005	-0.3843
AgeSel_P7_Fishery(1)_DEVadd_2006	-0.3081
AgeSel_P7_Fishery(1)_DEVadd_2007	0.0243
AgeSel_P7_Fishery(1)_DEVadd_2008	-0.1177
AgeSel_P7_Fishery(1)_DEVadd_2009	0.0113
AgeSel_P7_Fishery(1)_DEVadd_2010	-0.7652
AgeSel_P7_Fishery(1)_DEVadd_2011	-0.4968
AgeSel_P7_Fishery(1)_DEVadd_2012	-0.2975
AgeSel_P7_Fishery(1)_DEVadd_2013	0.1251
AgeSel_P7_Fishery(1)_DEVadd_2014	-0.0941
AgeSel_P7_Fishery(1)_DEVadd_2015	-0.4668
AgeSel_P7_Fishery(1)_DEVadd_2016	-0.3491
AgeSel_P7_Fishery(1)_DEVadd_2017	-0.0362
AgeSel_P7_Fishery(1)_DEVadd_2018	0.2543

Continued on next page ...

... Continued from previous page

Parameter	**Posterior median**
AgeSel_P7_Fishery(1)_DEVadd_2019	-0.1969
AgeSel_P7_Fishery(1)_DEVadd_2020	-0.0530
AgeSel_P7_Fishery(1)_DEVadd_2021	-0.3046
AgeSel_P7_Fishery(1)_DEVadd_2022	-0.0429
AgeSel_P7_Fishery(1)_DEVadd_2023	0.3257
AgeSel_P7_Fishery(1)_DEVadd_2024	0.5314

G DEVELOPING AN ABUNDANCE INDEX FOR PACIFIC HAKE USING ENVIRONMENTAL DNA

Contributed by Andrew O. Shelton, Krista Nichols, Kim M. Parsons, Madison Betts, Samantha Engster, Ana Ramón-Laca, Meghan Parsley, Megan Shaffer, Abigail Wells

G.1 Introduction

Environmental DNA (eDNA, residual genetic material sampled from water, soil, or air) is an increasingly common tool for non-invasively sampling marine and aquatic ecological communities, valuable for estimating species occurrence (Veilleux, et al. 2021), biodiversity (i.e., richness; Muenzel et al. 2024), and genetic structure (Andres et al. 2023). However, eDNA has not been widely used for quantitative abundance estimation (but see Shelton et al. 2022, Guri et al. 2024, Stoeckle et al. 2024). While the use of eDNA for quantification is supported both conceptually – where there is more of a species, more cells are shed into the environment, and thus there is more DNA – and empirically (e.g. there are strong linkages between single-species eDNA measures of in aquaria (Jo et al. 2019a, Ledger et al. 2024), rivers and streams (Pont 2024), estuaries and coastal oceans (DiBattista et al. 2022, Baetscher et al. 2024, Maes et al. 2023, Shelton et al. 2019), quantitative uses of eDNA observations have significantly lagged behind their use in occurrence and biodiversity applications.

Here we use environmental DNA samples from three years of the U.S.-Canada Integrated Ecosystem & Acoustic-Trawl Survey for Pacific Hake to develop an index of abundance for Pacific Hake. We incorporate samples collected over 13 degrees of latitude between the surface and 500m depth and spanning nearshore to the deep waters off the continental shelf. This effort is the largest and most extensive eDNA survey in the world and encompasses nearly 3000 sampling stations and nearly 6000 individual 2.5L water samples collected over the 3 survey years. In previous work, we showed that the distribution and abundance of hake DNA within a year (2019) largely mirrored the spatial distribution of hake biomass estimated from the acoustic trawl survey (Shelton et al. 2022). Here, we extend our analyses to use hake DNA to describe changes in the hake population through time. To our knowledge this is the first use of eDNA to develop an index of abundance for stock assessment purposes.

G.1.1 Connecting DNA and abundance metrics

Because this is the first use of an eDNA index in a stock assessment context, it is important to describe the logic and assumptions that connect observations of DNA from water samples to measures of fish biomass or abundance. The key difference between an eDNA survey and other traditional surveys is that traditional surveys depend on directly observing the organism of interest either through capture (e.g. via net sampling) or other means (e.g. via acoustic backscatter). eDNA, in contrast, detects traces left behind by organisms – cells derived from slime, scales, feces or other tissues – not the organism itself. A metaphor is that sampling eDNA is sampling the shadow of the organism. Therefore, the justification for using an eDNA index relies on understanding how such a shadow reflects the true population of interest. This relationship hinges on understanding two important processes: 1) the rate at which DNA is shed into the environment, and 2) the rate at which eDNA decays in aqueous environments. Recent reviews describe these processes in detail (e.g. Andruszkiewicz Allan et al. 2021, Lamb et al. 2022, Jo 2023) and we briefly describe some of the relevant literature here. Additional processes can affect eDNA (see e.g. Barnes and Turner 2016), but assumptions about shedding and decay predominate in this application.

Decay rates have been extensively studied in laboratory settings and show relatively rapid declines in eDNA with most eDNA decaying on the order of hours to a few days (Sassoubre et al. 2016; Andruszkiewicz Allan et al. 2021; Kirtane et al. 2021). While there are documented effects of environmental conditions (e.g. temperature, pH) on eDNA decay, within the range of conditions within our sampling domain, assuming an invariant rate of decay among the sampling depths and locations is reasonable. That is, we assume any differences in decay between, for example, the far north and south of the domain or between shallow and deep water samples are relatively trivial.

Shedding rates are far more difficult to study than decay rates and while there are estimates of shedding across a wide range of fish species under different conditions (e.g. Sassoubre et al. 2016, Thalinger et al. 2021, Jo et al. 2019b), estimates vary wildly both within and among species. In our application which is focused on a single species (Pacific Hake), the relevant question is whether shedding can be considered proportional to biomass. There is support from metabolic theory that shedding should scale in proportion to the surface area of individuals, not biomass (e.g. Yates et al. 2021). Furthermore, metabolic theory would suggest that different ontogenetic stages or different age fish may have different shedding rates (i.e. rapidly growing individuals may shed more DNA into the environment than slow growing individuals). To date, empirical evidence of differences among individuals of different ontogenetic stages or sizes is equivocal (Klymus et al. 2015, Ostberg and Chase 2022, Wilder et al. 2023) and remains an active area of research. We note that both laboratory studies of related species (gadids, Ledger et al. 2024) and previous work on hake (Shelton et al. 2022) support a proportionality between hake biomass and eDNA. Therefore we assume a proportionality between biomass and DNA concentration. Future work should challenge this assumption with an eye toward understanding how age or size structure may affect observed eDNA. In stock assessment terms, such work could inform developing an age- or size-dependent selectivity curve for an eDNA index. We do not pursue such approaches here.

G.2 Methods

G.2.1 Overview

The use of eDNA methods will be unfamiliar to many readers and so we provide a high level summary of the methods before providing technical details in the following sections. Many samples of water are collected during the U.S.-Canada Integrated Ecosystem & Acoustic-Trawl Survey for Pacific Hake. For each sample, 2.5 L of water is collected. Each sample is then filtered using vacuum filtration onto a filter paper and the filter is placed in a preservative and stored until it can be transported to the genetics laboratory at the end of the survey cruise. In the laboratory, samples are processed to extract and clean the DNA captured on the filter. The extracted DNA samples contain DNA from a wide variety of organisms (from bacteria to plankton to fish to whales). Each sample is assayed using quantitative polymerase chain reaction (qPCR) using a primer that amplifies a portion of the Pacific Hake mitochondrial genome. The qPCR assay provides a way of determining the concentration of hake mitochondrial DNA in each sample. From these qPCR observations we can construct a statistical model to describe the variation in hake DNA concentration across samples, space, depths, and among years. Finally, we can combine the estimates of hake concentration to generate an index based on DNA concentration for each year. This eDNA index, therefore, represents an estimate of overall DNA concentration in a given year which is related to the biomass of hake present in the environment (see Figure G.1).

In the sections that follow, we provided detailed information about the design and execution of water sampling and the creation of an eDNA index from the statistical model. We provide a brief overview of the spatio-temporal model and estimation procedure in the methods and a full description of the statistical model separately after the results. We largely omit the detailed protocols and laboratory analyses as they are described elsewhere (Ramón-Laca et al. 2021).

G.2.2 Field sampling and processing water samples for eDNA

We collected eDNA samples during the 2019, 2021, and 2023 U.S.-Canada Integrated Ecosystem & Acoustic-Trawl Survey for Pacific Hake aboard the NOAA Ship *Bell M. Shimada* (all years) and DFO Ship *Sir John Franklin* (2023) conducted between July and September (e.g. de Blois 2020).

We collected seawater from up to six depths (surface, 50, 100, 150, 300, and 500m in 2019; 200m samples replace the 100m depth in 2021 and 2023) where a Conductivity Temperature and Depth (CTD) rosette was deployed. We sampled water from at 186, 199, and 238 stations in 2019, 2021, and 2023, respectively. Two replicates of 2.5L of seawater were collected at each depth and station from independent Niskin bottles attached to a CTD rosette. Water samples from the surface were collected from the ship's salt water intake line but processed identically to Niskin samples. We refer to the depth of surface sampling at 0m, but in truth surface samples are collected at a depth of approximately 3m. Nearly all CTD casts and therefore water collection for eDNA occurred at night while acoustic sampling and trawl sampling took place during daylight hours. In addition to field samples, we collected a range of control water samples to test for laboratory contamination during water filtering, DNA extraction, and subsequent laboratory steps.

Sampling stations were spread across a spatial domain that varied slightly among years (Figure G.1) with water sampling occuring between San Francisco, CA and Cape Flattery, WA in 2019, expanding south in 2021 to include Pt. Conception, CA to Cape Flattery, WA, and including a slightly larger northern extent in 2023, spanning Pt. Conception, CA to west of Barkley Sound, BC (Figure G.1). This means that the spatial domain where water

Table G.1. Unique stations sampled for each sampling depth and year.

Depth (m)	2019	2021	2023
0	178	198	234
50	181	197	236
100	154	0	0
150	149	168	208
200	0	134	166
300	120	134	162
500	105	99	128
Total	**887**	**930**	**1,134**

samples are available varies among years. We discuss the implications of this varying sampling for developing indices of abundance below.

We assayed the DNA concentration of hake using qPCR in 1,752 (in 2019), 1,820 (2021), and 2,189 (2022) individual water samples. We analyzed each sample at least 3 times independently using qPCR. After DNA extraction and cleaning, a single water sample is 100 μL. Each qPCR reaction uses 2 μL and provides an estimate of the DNA concentration (units: DNA copies μL^{-1}) for each water sample. We analyzed control sample and qPCR standards of known DNA concentration alongside the field samples to calibrate the qPCR analysis. Across all samples and years, this represents more than 20,000 individual qPCR reactions.

G.2.3 Defining spatial areas for generating an index

The area sampled by the acoustic-trawl survey varies among years. In Figure G.1, we show the acoustic transect lines sampled during the hake survey and overlay the locations of CTD stations at which water was collected for eDNA sampling. Note that the east-west extent of both the acoustic transects and water sampling stations vary somewhat among years – transects in 2019 tend to cover more area than transects in 2021 and 2023, particularly in northern California near Cape Mendocino (40.4N).

To generate a spatial domain for each year, we used a 5km resolution gridded maps to project eDNA concentration. This vector-based grid was developed by Feist et al. (2021) and uses a custom coordinate reference system that conserves area and distance reasonably well across the west coast of the United States (see also Shelton et al. 2022). Each grid cell has an associated area-weighted mean bottom depth as well. To account for changes in survey area among years, we defined a polygon for each year by including the entirety of acoustic transects from that year and connecting adjacent transects along their eastern-most extent and their western-most extent. All 5km grid cells whose centroids fell within this polygon were included in the projection set. Because eDNA varies with depth as well as geospatially, we made prediction for each grid cell in 50m depth increments up to 500m or the bottom depth of each cell.

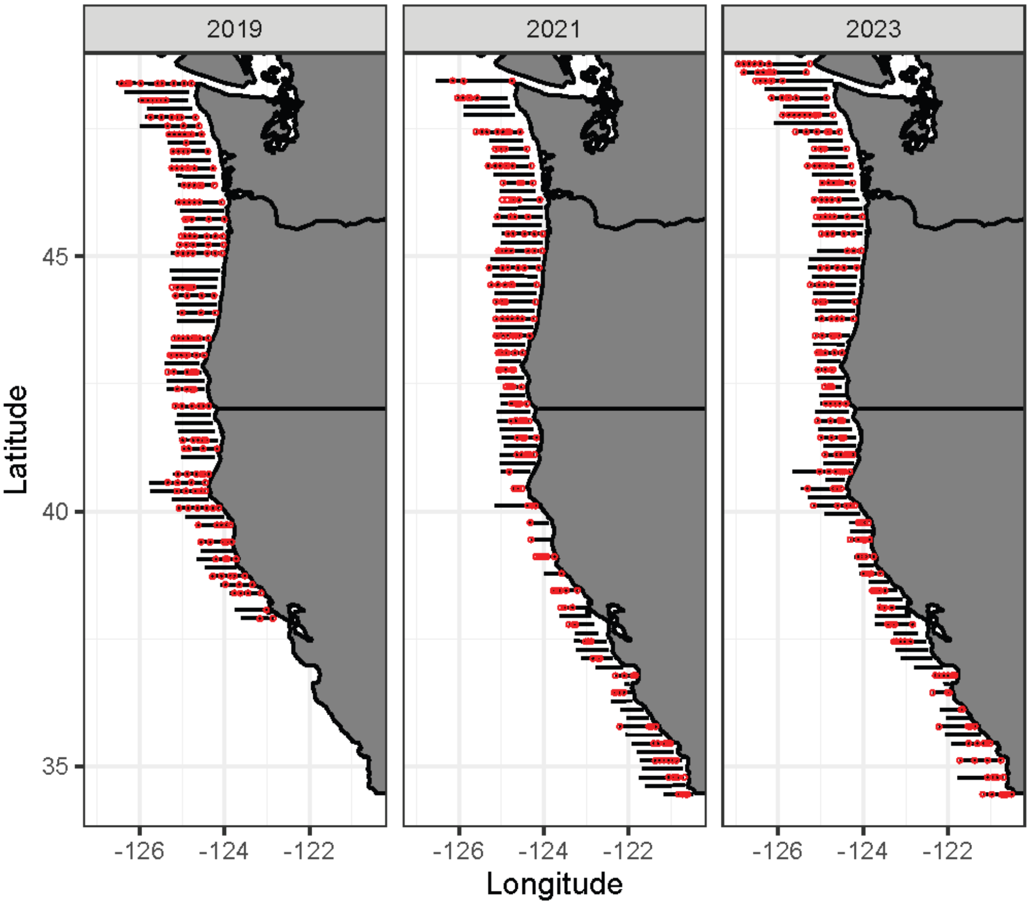

Figure G.1. Locations of acoustic transect and water samples collected from CTD stations in each year. Only transect lines within the range of water samples are shown.

Finally, we defined three areas based on latitude to enable the creation of abundance indices that are comparable across years. We created a core area between Cape Flattery, WA and San Francisco Bay, CA that is shared among all years. In addition, this region has historically contained the majority of hake biomass detected during the hake acoustic survey (hereafter "core area"; Figure G.2). We defined a second area from San Francisco Bay to Pt. Conception (hereafter "south area"), and a small area north of Cape Flattery, WA (hereafter "north area"). Observations of hake DNA are available for all years for the core area, for the south area in 2021 and 2023, and for the north area in 2023 (see Figure G.1), therefore we report summaries of hake DNA in each area for the appropriate years.

Therefore we made predictions for each grid cell on a regular grid at evenly spaced depths between the surface and 500m (or the bottom depth). To generate an eDNA index, we simply sum the predictions for each area-year combination and use the overall sum as the our hake eDNA index of abundance (units: DNA copies $\mu\mathrm{L}^{-1}$). Note that an index constructed in this way is sensitive to the density of prediction locations and depth – predicting to and summing over, say, a 2km grid would yield a larger value than predictions summed over a 5km grid – but as long as the density of predictions are equivalent among years and areas, the index will provide information about the relative abundance among areas and years.

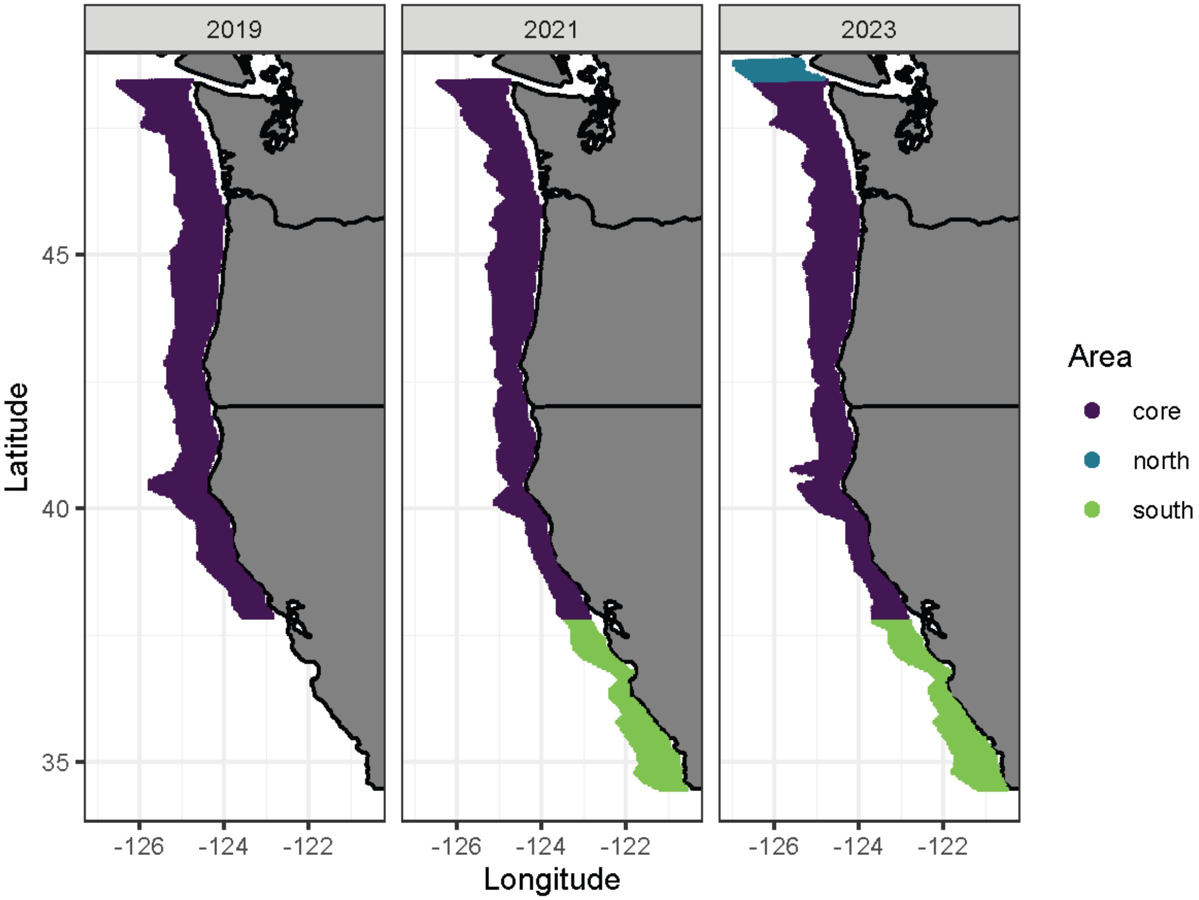

Figure G.2. Areas included in projections.

G.2.3.1 Summary of Statistical Model and Estimation

We developed a spatio-temporal model for modeling hake DNA concentration in the coastal ocean building and modifying the work of Shelton et al. (2022; see *Statistical model*). We model the concentration of hake DNA (log DNA copies μL^{-1}) present at spatial coordinates and sample depth in each year as a function of year-specific intercept parameters, a common smooth effect of bottom depth, and spatially smooth fields (Gaussian Markov Random Fields). The model includes observation models developed for use with qPCR data and is a hurdle-style model, including both an occurrence and conditional positive component.

This approach largely follows the statistical estimation procedure implemented in spatio-temporal model estimation software *sdmTMB* (Anderson et al. 2024) and *VAST* (Thorson et al. 2015a, 2019), but implemented in code to incorporate the unique details of the hake eDNA model. For spatial fields we use a Matern covariance function that allow for anisotropy and use have a single estimated a single range parameter shared among all fields

Table G.2. Number of 5km grid cells used in each year and area. Parentheses show the total number of prediction locations including depth (predictions at each grid cell at every 50m between the surface and bottom or 500m).

Year	Core	South	North
2019	3567 (27435)	–	–
2021	2993 (21121)	940 (8087)	–
2023	3165 (22969)	971 (8201)	215 (1191)

(see Figure G.4). Spatio-temporal models are well known for their computational burden. Our model requires estimating multiple spatial fields in each year. To implement the model we approximate the Gaussian Markov Random Fields using the SPDE approximation from Lindgren et al. (2011) and implemented in Template Model Builder (Kristensen et al. 2016) in the R statistical language (R Core Team 2024).

We checked for model convergence by examining the converged model for a positive definite Hessian matrix and also ran each model multiple times from randomly generated starting points. In the cases when identically configured models converged at different log-likelihoods, we retained the model with the lowest log-likelihood. We derive uncertainty bounds for parameter and unobserved states using bias-correction and the generalized delta-method which approximates the uncertainty around maximum likelihood estimates as following a multivariate normal distribution (Kristensen et al. 2016). This procedure provides a fast approximation of uncertainty bounds, but likely underestimates overall uncertainty in derived abundance indices.

In models using the SPDE approach, estimated spatial fields can be sensitive to the construction of the mesh used to approximate the smooth spatial field (see e.g. Dambly et al. 2023). Therefore, we estimated models with the same fixed and random effect configuration but that varied the density of the spatial mesh. We ran 15 models using an increasingly dense mesh ranging between 90 and 250 knots. We found that the 10 models using between 103 and 191 provided similar parameter estimates and predictions and, generally, quite similar total joint negative log-likelihood. To incorporate the variability among these multiple models into the estimated abundance index, we generated 2,000 simulations of the index in each area-year combination from each of the ten converged models using a multivariate normal approximation. We then equally weighted each of the ten spatio-temporal models to derive overall point estimates and uncertainty bounds across the 2,000 simulations.

G.3 Results

We first present visualizations and summaries of the eDNA observations under minimal manipulations, then present the overall index of abundance from eDNA, and finally present a range of model diagnostics and visualizations of model predictions. For diagnostics and spatial predictions, we present results for a single model that uses a 148 knot mesh.

G.3.1 Observations

Figure G.3 presents an overview of water sample level observations. While this figure is busy, we can see that the spatial distribution of observed eDNA concentration varies substantially among depths and years. Note in addition that there are clearly a few samples in each year that are notably higher concentration than the average.

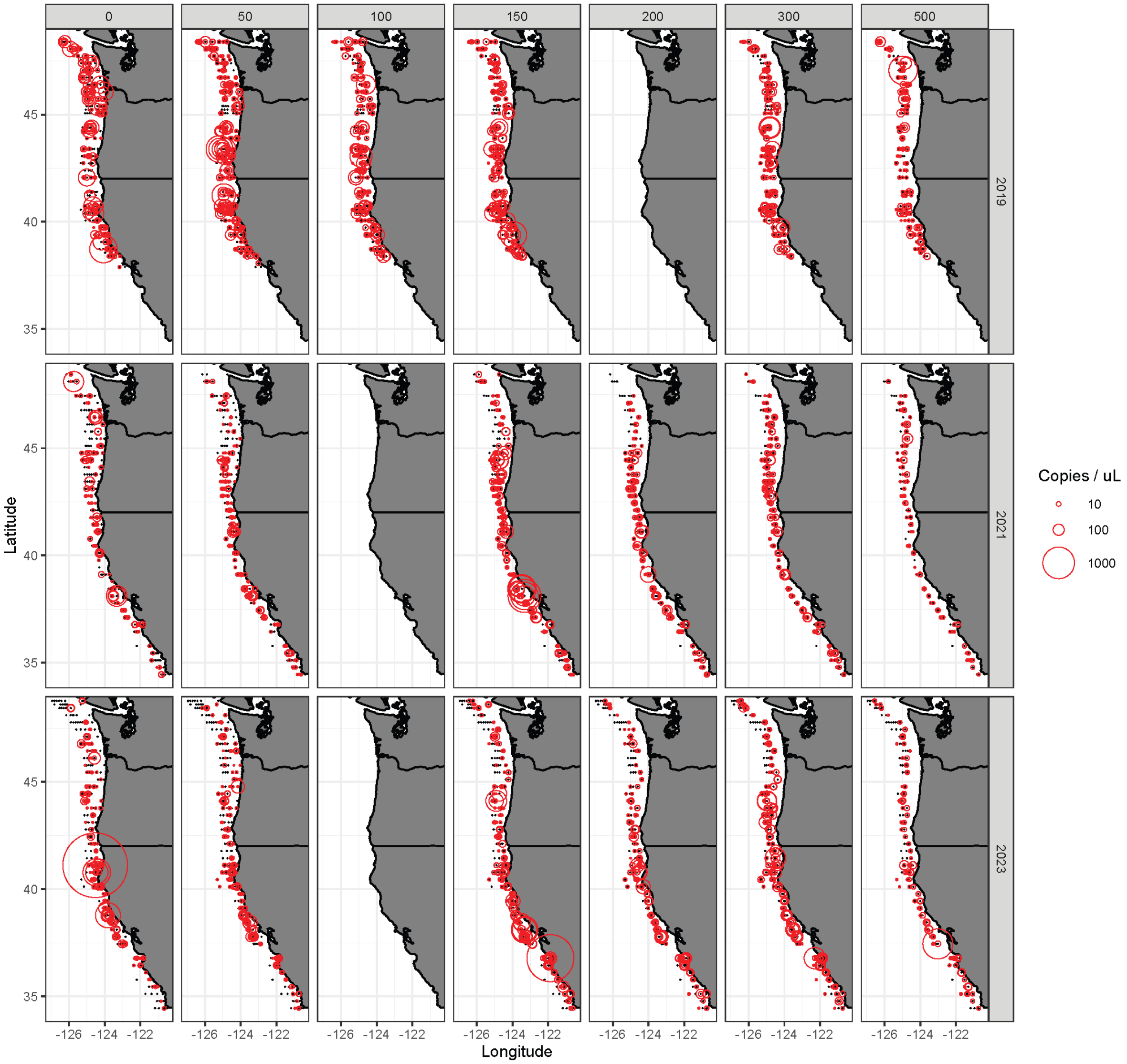

Figure G.3. Raw estimates of hake eDNA concentration by year (rows) and sampling depth (columns). Each circle represents estimated eDNA from a single water bottle. Black dots represent samples in which amplification was not detected. The sampling design by depth was changed after 2019 from a station at 100m to 200m, which is more representative of Pacific Hake habitat.

G.3.2 Model fit and spatial predictions

The model generated predictions that varied in space and time and was able to match qPCR observations. We present a few diagnostic plots including predicted-observed plots for both the occurrence and positive components in a section at the end of this document (see Figure G.4.1.1). We focus on the spatial predictions here as they are the most relevant component to generating an abundance index, but we also comment on the contribution of fixed, smooth, and random effects to model predictions.

First, we can provide a plot of the spatial predictions of hake DNA concentration (D, units: log copies μL^{-1}) to observed locations (Figure G.4). In truth, these figures are small and difficult to interpret, so we provide a second figure that shows the predictions for 50m and 150m depths (Figure G.5).

We can make predictions to the entire gridded 5km surface as well (Figure G.6). As with Figure G.4, this is too small to be particularly informative, so focus on 50m and 150m depths for this smooth prediction (Figure G.7). Hake DNA is generally most abundant in the 150m to 300m water depth range (see also Shelton et al. 2022).

Another way to look at the spatial patterns are along-transect perpendicular to the coastline. We show the same East-West slices across multiple years (Figures G.8 and G.9). Note the color scale is not identical among transect figures.

These predictions are the combination of a fixed effect of year intercept (Figure G.10) as well as the smooth as a function of bottom depth (Figure G.11). The year intercepts should not be interpreted as an estimate of overall abundance in each year because the sampling frame changes substantially among years. The depth smooth finds that peak hake abundance corresponds to bottom depths between approximately 100m and 200m (Figure G.11). This corresponds to the continental shelf break and agrees with existing information about hake distribution.

One important difference between eDNA and other traditional fisheries survey methods is that we have replicate water samples taken from a single location and time. We refer to these random effects as a bottle effect and they represent deviations of a single observed water sample from the mean log DNA concentration at a location (i.e. year-station-depth). We find that individual water bottles sampled from opposite sides of a CTD rosette can be quite large. We estimate the standard deviation among bottles declines with water depth (from about 1.48 at the surface to about 1.04 at 500m). These deviations are on the log-scale so a SD of 1.25 means that the on average, a bottle is $e^{1.25} = 3.49$ times the mean estimated DNA concentration. In concrete terms that means that for a mean concentration of 10 copies μL^{-1}, we could expect to often see observations between about 3 and 35 copies μL^{-1}.

Finally, we can look calculate the correlation of the spatial fields among water depths. This correlation derives from from the estimated factor weight matrix (see Figure G.4) and shows that there are strong estimated correlations among depths and but that generally, the surface samples are at best weakly correlated with depths below 150m where the majority of hake and hake DNA are found (Figure G.11).

We construct the eDNA index by generating predictions to each depth between the surface and 500m in 50m intervals and then summing. We can therefore sum across depths within each 5km grid cell to generate a depth-integrated map of DNA in each year (Figure G.14). Note that in these figures we make predictions to the entire spatial domain, even if there are no observations near some locations in particular year (e.g. south of San Francisco Bay in 2019). In general, the plots show higher DNA concentrations in 2019 relative to 2021 or 2023 particularly north of Cape Mendocino.

Differences among years become more obvious when we plot the index as a ratio between years to understand how hake DNA has changed in distribution between years (Figure G.15). Here bright colors indicate areas where estimated DNA concentration changed dramatically between years. For example, the predominance of blue in the panels "ratio_19_21" and "ratio_19_23" indicate areas that are substantially higher in 2019 relative to the other years.

G.3.2.1 Index Estimates

Following the estimation methods, we summed across the predictions to generate a coastwide index of abundances. We repeated this approach for 10 different spatial meshes to provide an estimate for an eDNA index for the core and south areas (Figure G.16). We show estimates for the individual model configurations and the consensus index (Figure G.16). Note that all model provide qualitatively the same pattern: a substantial ($\approx 35\%$) decline in DNA concentration between 2019 and 2021 and a further decline between 2021 and 2023. For 2021 and 2023 we can combine the core and south areas to provide an index covering Pt. Conception, CA to Cape Flattery, WA (Figure G.17). Our models suggest that the total DNA in 2023 in both the core and south areas was roughly equivalent to the DNA in the core area in 2019.

G.4 Statistical model

We developed a state-space framework for modeling hake DNA concentration in the coastal ocean building and modifying the work of Shelton et al. (2022). State-space models separate the true biological process from the methods used to observe the process. Let $D_t(x, y, d)$ be the true, but unobserved concentration of hake DNA (log DNA copies μL^{-1}) present at spatial coordinates $\{x, y\}$ (eastings and northings, respectively, in km) and sample depth d (meters) in year t. Let α_t be a year-specific intercept, $s(b)$ be a smooth that depends on bottom depth in meters at location $\{x, y\}$, b, and $\epsilon_t(x, y, d)$ be a random effect that allows for covariation among spatial locations, years, and water depth. We write these as additive on the log-scale,

$$D_t(x, y, d) = \alpha_t + s(b) + \epsilon_t(x, y, d), \qquad \text{(G.1)}$$

and so the hake DNA concentration of is a function of both fixed and random effects. Unlike many spatial datasets, the eDNA samples here are collected across depths at uneven spacing and at varying depths among years (in 2019 water was collected at the surface, 50, 100, 150, 300, and 500 meters while in 2021 and 2023, water was collect at the same depths except samples at 200m replace the 100m). The fixed effect of bottom depth $s(b)$ does not depend on year, reflecting a well documented bottom depth-association between hake and the shelf break (Malick et al. 2020), with the year-specific intercept terms allowing for region-wide shifts in hake DNA concentration.

Preliminary analyses showed clear correlations among depths at particular locations and so we developed a variant of factor analysis to efficiently estimate a spatial field for each depth in each year that allows correlation among the fields as a function of depth. We model $\epsilon_t(x,y,d)$ as a linear combination of Gaussian Markov Random Fields. Specifically, we let $\omega_{tf}(x,y)$ be a zero-centered spatial field for factor *f*,

$$\boldsymbol{\omega}_{tf}(x,y) \sim MVN(0, \boldsymbol{\Sigma}), \tag{G.2}$$

where covariance matrix $\boldsymbol{\Sigma}$ follows a Matern covariance function with marginal variance fixed at 1. We allow for anisotropy in the spatial correlation and estimate a single shared spatial range parameter (κ) for all spatial fields. We follow the parameterization and approach of *sdmTMB* (Anderson et al. 2024) for GMRFs.

We allow multiple independent factors, $f = 1,..,F$ in year t so $\omega_{tf}(x,y)$ are independent among years and factors. Then we estimate a weight coefficient for each factor that is a function of water depth so the realized spatial field in each depth is a linear combination of spatial fields and factor weights,

$$\epsilon_t(x,y,d) = \sum_{f=1}^{F} l_f(d)\omega_{tf}(x,y). \tag{G.3}$$

This can be expressed in matrix notation as

$$\boldsymbol{\epsilon}_t(x,y,d) = \mathbf{L}\boldsymbol{\Omega}_t \tag{G.4}$$

where $\mathbf{L}$ has F columns (one for each factor) and D rows (one for each projection depth) and $\boldsymbol{\Omega}_t$ has F rows and S (number of spatial locations) columns. Classic factor analysis estimates the factors $l_f(d)$ as independent parameters (e.g. to estimate spatial fields for multiple species that are correlated in space and provide among species correlations; Thorson et al 2016), but we are interested in maintaining the correlation structure across depths. Thus we introduce the potential for correlations among water depths by modeling the factor weights as a smooth function of water depth,

$$l_f(d) = s_f(d), \tag{G.5}$$

where $s_f(d)$ indicates a p-spline for factor *f*. In practice we have samples from at most six depths at any station, and so we limit the number of knots in the spline to four to avoid over-parameterization. To improve estimation and avoid identifiability and label-switching issues, we impose additional constraints on the factor smoothers. Specifically, we impose a penalty on the intercept term for each factor, such that the intercept associated with factor f has a prior distribution $a_{0f} \sim N(0, 3f^{-1})$. This has the practical impact of associating the first factor with the largest intercept, the second factor with a smaller intercept, etc. Using a smooth for the factor weights allows for model predictions to additional water depths that were unobserved during survey (e.g. 250m or 400m) using a relatively small number of parameters. Unlike most factor analyses, we are not expressly interested in the factors themselves or relating factors to environmental covariates and so we do not transform or further explore the factor loadings (e.g. varimax rotation). Note that we use a single smooth for each factor and do not estimate year-specific factor smoothers. Future work may justify relaxing this model form.

After experimenting with fits using a range of factors (1 and 4), we settled on using 2 factors in further analyses. Using 3 or more factors generally led to model convergence and identifiability problems, whereas using only one factor led to unsatisfactory model fits.

G.4.1 Observation models for DNA concentration

We are primarily interested in the DNA concentration over space, time, and depth, and thus the latent variable $D_t(x, y, d)$ is our focus. Unfortunately, qPCR does not allow us to directly measure this concentration. Instead qPCR measures the PCR cycle at which a $2\mu L^{-1}$ aliquot of extracted DNA was detected to fluoresce and compares that observation against the flourescence pattern of samples of known DNA concentration ("the standard curve"), to provide an estimate of DNA concentration for each unknown sample. Each water sample is analyzed using at least 3 independent qPCR replicates to account for laboratory and machine variability. In addition to qPCR variability among replicates, we also have to account for modifications that affect each water sample and occurred during water sampling and processing. First, we have three offsets that modify the true DNA concentration to affect what we observed in the qPCR: 1) V_i is the proportion of 2.5 L filtered from Niskin i (occasionally some seawater was spilled or not filtered; $V_i = 1$ for the vast majority of samples); 2) I_i is the known dilution used to on sample i to eliminate PCR inhibition. PCR inhibition is most commonly observed in surface samples and is vanishingly rare for samples collected below 100m; 3) $\mathbf{I}\zeta$ is an estimated offset for an ethanol wash error from 2019 (ζ is the estimated effect of the wash error and $\mathbf{I}$ is an indicator variable where $\mathbf{I} = 1$ for affected samples and $\mathbf{I} = 0$ otherwise; see Shelton et al. 2022 Supp S1 for additional description).

Finally, we add a random effect for the individual bottles sampled at each year-station-depth combination (for notational simplicity, let $\delta_i = \delta_t(x, y, d)$). This effect which describes the deviation of individual sampled bottles from the location mean, $\delta_i \sim N(0, \tau_d)$, with τ_d indicating a depth-specific standard deviation among bottles. We impose a smooth on τ_d so it is function of water depth. This reflects empirical observations of between water bottle variability that changes with depth (Shelton et al. 2022). Then, the log-concentration of DNA in a sample analyzed by qPCR, E_i (other subscripts suppressed for notational simplicity) is

$$E_i = D_t(x,y,d) + \log V_i + \log I_i + \mathbf{I}\zeta + \delta_i. \tag{G.6}$$

We connect the estimated concentrations to observations from qPCR using two likelihoods that are similar to a hurdle model. First we determine whether amplification was detected in each qPCR replicate r run on each plate j, $G_{ijr} \in \{0,1\}$ and if amplification was observed we model the PCR cycle at which amplification was detected C_{ijr}; C_{ijr} is observed as a continuous, positive value. DNA concentrations have a log-linear relationships with C_{ijr}; smaller values of C_{ijr} are associated with higher DNA concentrations (see Figure G.19).

Because we are modeling the discrete number of DNA molecules that are present in the assayed sample, we know that the Poisson distribution provides an appropriate observation distribution for the number of molecules present in a given qPCR reaction. Assuming a Poisson distribution, conditional on a true mean number of DNA copies in the sample X, the probability of having exactly zero DNA copies in a qPCR reaction is e^{-X} and the probability of having non-zero DNA copies is the complement, $1-e^{-X}$. If there are exactly zero molecules in a qPCR reaction, amplification, and therefore detection of amplification, will not occur. However, there are other factors that may reduce amplification further and therefore we expect the probability of amplification to be at most $1-e^{-X}$. As a result, we estimate an additional term, ϕ_j, representing the fractional reduction in amplification efficiency due to other factors on qPCR plate j $(0 < \phi_j < 1)$. Then we have pair of observation models for hake DNA, both of which are a function of DNA concentration:

$$G_{ijr} \sim \text{Bernoulli}\left(1-\exp(-2e^{E_{ij}}\phi_j)\right), \tag{G.7}$$

$$C_{ijr} \sim \text{Normal}(\beta_{0j} + \beta_{1j}E_{ij}, \sigma_C(E_{ij})) \qquad \text{if } G_{ijr} = 1. \tag{G.8}$$

The 2 is present in the first line of the equation because we use 2 μL of sample in each qPCR reaction and so the expected DNA copies in reaction is $2e^{E_{ij}}$. We allow $\sigma_C(E_ij)$ to vary as a log-linear function of DNA concentration to account for the fact that there is decreased variability in qPCR measures of C_t at higher DNA concentrations: $\sigma_C(E_{ij}) = \exp(\gamma_0 + \gamma_1 E_{ij})$.

By itself, the above model is unidentifiable because field samples do not provide information about the parameters that define relationship between the number of DNA copies and PCR cycle (β_{0j}, β_{1j}, and ϕ_j). Therefore, as is standard with qPCR analyses, we include standards of known concentration to estimate these parameters. Each qPCR plate has replicate samples with a known number of DNA copies. These standards span six orders of magnitude (1 to 100,000 copies μL^{-1}, each of 2μL) and determine the relationship between copy number and PCR cycle of detection. Let K_j be the log copy number in PCR plate j, then,

$$G_{jr} \sim \text{Bernoulli}\left(1 - \exp(-2e^{K_j}\phi_j)\right), \tag{G.9}$$
$$C_{jr} \sim \text{Normal}(\beta_{0j} + \beta_{1j}K_j, \sigma_C(K_j)) \quad \text{if } G_{jr} = 1. \tag{G.10}$$

Note that there are different intercept β_{0j}, slope β_{1j} and detectability ϕ_j parameters for each PCR plate to allow for among-plate variation in amplification. We model each calibration parameter $\beta_{0j}, \beta_{1j}, \phi_j$ hierarchically using a normal distribution, with among plate mean and variance; i.e. $\beta_{0j} \sim \text{N}(\mu_{\beta_0}, \sigma_{\beta_0})$.

For estimation, we fit the model for the standards first and treat them as fixed and known when we estimate the parameters for the field collected water samples.

G.4.1.1 Diagnostic Plots

Standards

We start by plotting the qPCR standards (qPCR analyses on DNA of a known concentration) for a single PCR plate individual, all of the plates run within a single year, and then all of the estimated relationships across all years. For presence-absence components see Figure G.18. Positive compnents are shown in Figures G.19 and G.20.

Unknown Samples

We provide a few plots of predictions and observations for pres-abs and positive components (each faceted by water depth) (Figures G.21 and G.22). We also present two figures of the relationship between DNA concentration (D) and the concentration within a given bottle (E; Figures G.23 and G.24) to illustrate the effect of the bottle random effects and offsets that affect each sampled water bottle.

G.5 Acknowledgements

Funding for this project was provided by the NMFS Genomic Strategic Initiative. We thank the crew and scientists of the NOAA ship *Bell M. Shimada* and DFO Ship *Sir John Franklin* for support during the shipboard collection effort. We thank E. Iwamoto and other members of the molecular genetics lab at the Northwest Fisheries Science Center supported laboratory work. We thank the many members of the FEAT team and the Northwest Fisheries Science Center including J. Clemmons, A. Billings, J. Pohl, D. Chu, E. Phillips, S. Parker-Stetter, R. Thomas, and S. deBlois. We thank A. Berger, O. Hamel, and D. Baetscher for discussions during the development of this project.

G.6 References

Anderson, Sean C., Eric J. Ward, Philina A. English, Lewis A. K. Barnett, and James T. Thorson. 2024. sdmTMB: An r Package for Fast, Flexible, and User-Friendly Generalized Linear Mixed Effects Models with Spatial and Spatiotemporal Random Fields. *bioRxiv* 2022.03.24.485545. https://doi.org/10.1101/2022.03.24.485545.

Andres, Kara J., David M. Lodge, Suresh A. Sethi, and Jose Andrés. 2023. Detecting and Analysing Intraspecific Genetic Variation with eDNA. Population Genetics to Species Abundance. *Molecular Ecology* 32 (15): 4118–32. https://doi.org/10.1111/mec.17031.

Andruszkiewicz Allan, Elizabeth, Weifeng Gordon Zhang, Andone C Lavery,and Annette F Govindarajan. 2021. Environmental DNA Shedding and Decay Rates from Diverse Animal Forms and Thermal Regimes. *Environmental DNA* 3 (2): 492–514.

Baetscher, Diana S., Meredith R. Pochardt, Patrick D. Barry, and Wes A. Larson. 2024. Tide Impacts the Dispersion of eDNA from Nearshore Net Pens in a Dynamic High-latitude Marine Environment. *Environmental DNA* 6 (2): e533. https://doi.org/10.1002/edn3.533.

Barnes, Matthew A, and Cameron R Turner. 2016. The Ecology of Environmental {DNA} and Implications for Conservation Genetics. *Conservation Genetics* 17 (1): 1–17.

Dambly, Lea I, Nick JB Isaac, Kate E Jones, Katherine L Boughey, and Robert B O'Hara. 2023. Integrated Species Distribution Models Fitted in INLA Are Sensitive to Mesh Parameterisation. *Ecography* 2023(7): e06391.

de Blois, Steven. 2020. The 2019 Joint U.S.–Canada Integrated Ecosystem and Pacific Hake Acoustic-Trawl Survey: Cruise Report SH-19-06. *U.S. Department of Commerce, NOAA Processed Report NMFS-NWFSC-PR-2020-03*.

DiBattista, Joseph D., Ashley M. Fowler, Indiana J. Riley, Sally Reader, Amanda Hay, Kerryn Parkinson, and Jean-Paul A. Hobbs. 2022. The Use of Environmental DNA to Monitor Impacted Coastal Estuaries. *Marine Pollution Bulletin* 181 (August): 113860. https://doi.org/10.1016/j.marpolbul.2022.113860.

Feist, Blake E, Jameal F Samhouri, Karin A Forney, and Lauren E Saez. 2021. Footprints of Fixed-Gear Fisheries in Relation to Rising Whale Entanglements on the US West Coast. *Fisheries Management and Ecology* 28 (3): 283–94.

Guri, Gledis, Andrew Olaf Shelton, Ryan P Kelly, Nigel Yoccoz, Torild Johansen, Kim Præbel, Tanja Hanebrekke, Jessica Louise Ray, Johanna Fall, and Jon-Ivar Westgaard. 2024. Predicting Trawl Catches Using Environmental DNA. Edited by W Stewart Grant. *ICES Journal of Marine Science*, August, fsae097. https://doi.org/10.1093/icesjms/fsae097.

Jo, Toshiaki S. 2023. Utilizing the State of Environmental DNA (eDNA) to Incorporate Time-Scale Information into eDNA Analysis. *Proceedings of the Royal Society B: Biological Sciences* 290 (1999): 20230979. https://doi.org/10.1098/rspb.2023.0979.

Jo, Toshiaki, Hiroaki Murakami, Satoshi Yamamoto, Reiji Masuda, and Toshifumi Minamoto. 2019. Effect of Water Temperature and Fish Biomass on Environmental DNA Shedding, Degradation, and Size Distribution. *Ecology and Evolution* 9 (3): 1135–46. https://doi.org/10.1002/ece3.4802.

Kirtane, Anish, Daniel Wieczorek, Thomas Noji, Liza Baskin, Claire Ober, Riley Plosica, Ashley Chenoweth, Katie Lynch, and Lauren Sassoubre. 2021. Quantification of Environmental DNA (eDNA) Shedding and Decay Rates for Three Commercially Harvested Fish Species and Comparison Between eDNA Detection and Trawl Catches. *Environmental DNA* 3(6): 1142–55. https://doi.org//url%7Bhttps://doi.org/10.1002/edn3.236}.

Klymus, Katy E., Catherine A. Richter, Duane C. Chapman, and Craig Paukert. 2015. Quantification of eDNA Shedding Rates from Invasive Bighead Carp Hypophthalmichthys Nobilis and Silver Carp Hypophthalmichthys Molitrix. *Biological Conservation* 183: 77–84. https://doi.org//url%7Bhttps://doi.org/10.1016/j.biocon.2014.11.020}.

Kristensen, Kasper, Anders Nielsen, Casper W. Berg, Hans Skaug, and Bradley M. Bell. 2016. TMB: Automatic Differentiation and Laplace Approximation. *Journal of Statistical Software* 70 (5): 1–21. https://doi.org/10.18637/jss.v070.i05.

Lamb, Philip D., Vera G. Fonseca, David L. Maxwell, and Chibuzor C. Nnanatu. 2022. Systematic Review and Meta-Analysis: Water Type and Temperature Affect Environmental DNA Decay. *Molecular Ecology Resources* 22 (7): 2494–2505. https://doi.org//url%7Bhttps://doi.org/10.1111/1755-0998.13627}.

Ledger, Kimberly J., Mary Beth Rew Hicks, Thomas P. Hurst, Wes Larson, and Diana S. Baetscher. 2024. Validation of Environmental DNA for Estimating Proportional and Absolute Biomass. *Environmental DNA* 6 (5): e70030. https://doi.org/10.1002/edn3.70030.

Lindgren, Finn, Håvard Rue, and Johan Lindström. 2011. An Explicit Link Between Gaussian Fields and Gaussian Markov Random Fields: The Stochastic Partial Differential Equation Approach. *Journal of the Royal Statistical Society: Series B (Statistical Methodology)* 73 (4): 423–98. https://doi.org//url%7Bhttps://doi.org/10.1111/j.1467-9868.2011.00777.x}.

Maes, Sarah M., Sam Desmet, Rein Brys, Klaas Sys, Tom Ruttink, Sara Maes, Kris Hostens, Lies Vansteenbrugge, and Sofie Derycke. 2023. Detection and Quantification of Two Commercial Flatfishes {{*Solea*}}{{ *Solea*}} and {{*Pleuronectes*}}{{*Platessa*}} in the North Sea Using Environmental DNA. *Environmental DNA*, April, edn3.426. https://doi.org/10.1002/edn3.426.

Malick, Michael J, Mary E Hunsicker, Melissa A Haltuch, Sandra L Parker-Stetter, Aaron M Berger, and Kristin N Marshall. 2020. Relationships Between Temperature and Pacific Hake Distribution Vary Across Latitude and Life-History Stage. *Marine Ecology Progress Series* 639: 185–97.

Muenzel, Dominic, Alessia Bani, Maarten De Brauwer, Eleanor Stewart, Cilun Djakiman, Halwi, Ray Purnama, et al. 2024. Combining Environmental DNA and Visual Surveys Can Inform Conservation Planning for Coral Reefs. *Proceedings of the National Academy of Sciences* 121 (17): e2307214121. https://doi.org/10.1073/pnas.2307214121.

Ostberg, Carl O., and Dorothy M. Chase. 2022. Ontogeny of eDNA Shedding During Early Development in Chinook Salmon (Oncorhynchus Tshawytscha). *Environmental DNA* 4 (2): 339–48. https://doi.org//url%7Bhttps://doi.org/10.1002/edn3.258}.

Pont, Didier. 2024. Predicting Downstream Transport Distance of Fish eDNA in Lotic Environments. *Molecular Ecology Resources* 24(4): e13934. https://doi.org/10.1111/1755-0998.13934.

R Core Team. 2024. *R: A Language and Environment for Statistical Computing*. Vienna, Austria: R Foundation for Statistical Computing. https://www.R-project.org/.

Ramón-Laca, Ana, Abigail Wells, and Linda Park. 2021. A Workflow for the Relative Quantification of Multiple Fish Species from Oceanic Water Samples Using Environmental DNA (eDNA) to Support Large-Scale 2021. *PLoS ONE* 16: e0257773. https://doi.org/10.1371/journal.pone.0257773.

Sassoubre, Lauren M, Kevan M Yamahara, Luke D Gardner, Barbara A Block, and Alexandria B Boehm. 2016. Quantification of Environmental {DNA} (e{DNA}) Shedding and Decay Rates for Three Marine Fish. *Environmental Science & Technology* 50 (19): 10456–64.

Shelton, Andrew Olaf, Ryan P Kelly, James L O'Donnell, Linda Park, Piper Schwenke, Correigh Greene, Richard A Henderson, and Eric M Beamer. 2019. Environmental DNA Provides Quantitative Estimates of a Threatened Salmon Species. *Biological Conservation* 237: 383–91.

Shelton, Andrew Olaf, Ana Ramón-Laca, Abigail Wells, Julia Clemons, Dezhang Chu, Blake E. Feist, Ryan P. Kelly, et al. 2022. Environmental DNA Provides Quantitative Estimates of Pacific Hake Abundance and Distribution in the Open Ocean. *Proceedings of the Royal Society B: Biological Sciences* 289 (1971): 20212613. https://doi.org/10.1098/rspb.2021.2613.

Stoeckle, Mark Y., Jesse H. Ausubel, Greg Hinks, and Stacy M. VanMorter. 2024. A Potential Tool for Marine Biogeography: eDNA–dominant Fish Species Differ Among Coastal Habitats and by Season Concordant with Gear-Based Assessments. Edited by Arga Chandrashekar Anil. *PLOS ONE* 19 (11): e0313170. https://doi.org/10.1371/journal.pone.0313170.

Thalinger, Bettina, Andreas Rieder, Anna Teuffenbach, Yannick Pütz, Thorsten Schwerte, Josef Wanzenböck, and Michael Traugott. 2021. The Effect of Activity, Energy Use, and Species Identity on Environmental DNA Shedding of Freshwater Fish. *Frontiers in Ecology and Evolution* 9. https://doi.org/10.3389/fevo.2021.623718.

Thorson, James T. 2019. Guidance for Decisions Using the Vector Autoregressive Spatio-Temporal (VAST) Package in Stock, Ecosystem, Habitat and Climate Assessments. *Fisheries Research* 210: 143–61. https://doi.org//url%7Bhttps://doi.org/10.1016/j.fishres.2018.10.013}.

Thorson, James T, Andrew O Shelton, Eric J Ward, and Hans J Skaug. 2015a. Geostatistical Delta-Generalized Linear Mixed Models Improve Precision for Estimated Abundance Indices for West Coast Groundfishes. *ICES Journal of Marine Science* 72 (5): 1297–1310.

Thorson, James T, Mark D Scheuerell, Andrew O Shelton, Kevin E See, Hans J Skaug, Kasper Kristensen. 2015b. Spatial factor analysis: a new tool for estimating joint species distributions and correlations in species range. *Methods in Ecology and Evolution* 6 (6):627–637.

Veilleux, Heather D., Melissa D. Misutka, and Chris N. Glover. 2021. Environmental DNA and Environmental RNA: Current and Prospective Applications for Biological Monitoring. *Science of The Total Environment* 782 (August): 146891. https://doi.org/10.1016/j.scitotenv.2021.146891.

Wilder, Maxwell L., John M. Farrell, and Hyatt C. Green. 2023. Estimating eDNA Shedding and Decay Rates for Muskellunge in Early Stages of Development. *Environmental DNA* 5 (2): 251–63. https://doi.org//url%7Bhttps://doi.org/10.1002/edn3.349}.

Yates, M. C., D. M. Glaser, J. R. Post, M. E. Cristescu, D. J. Fraser, and A. M. Derry. 2021. The Relationship Between eDNA Particle Concentration and Organism Abundance in Nature Is Strengthened by Allometric Scaling. *Molecular Ecology* 30 (13): 3068–82. https://doi.org//url%7Bhttps://doi.org/10.1111/mec.15543}.

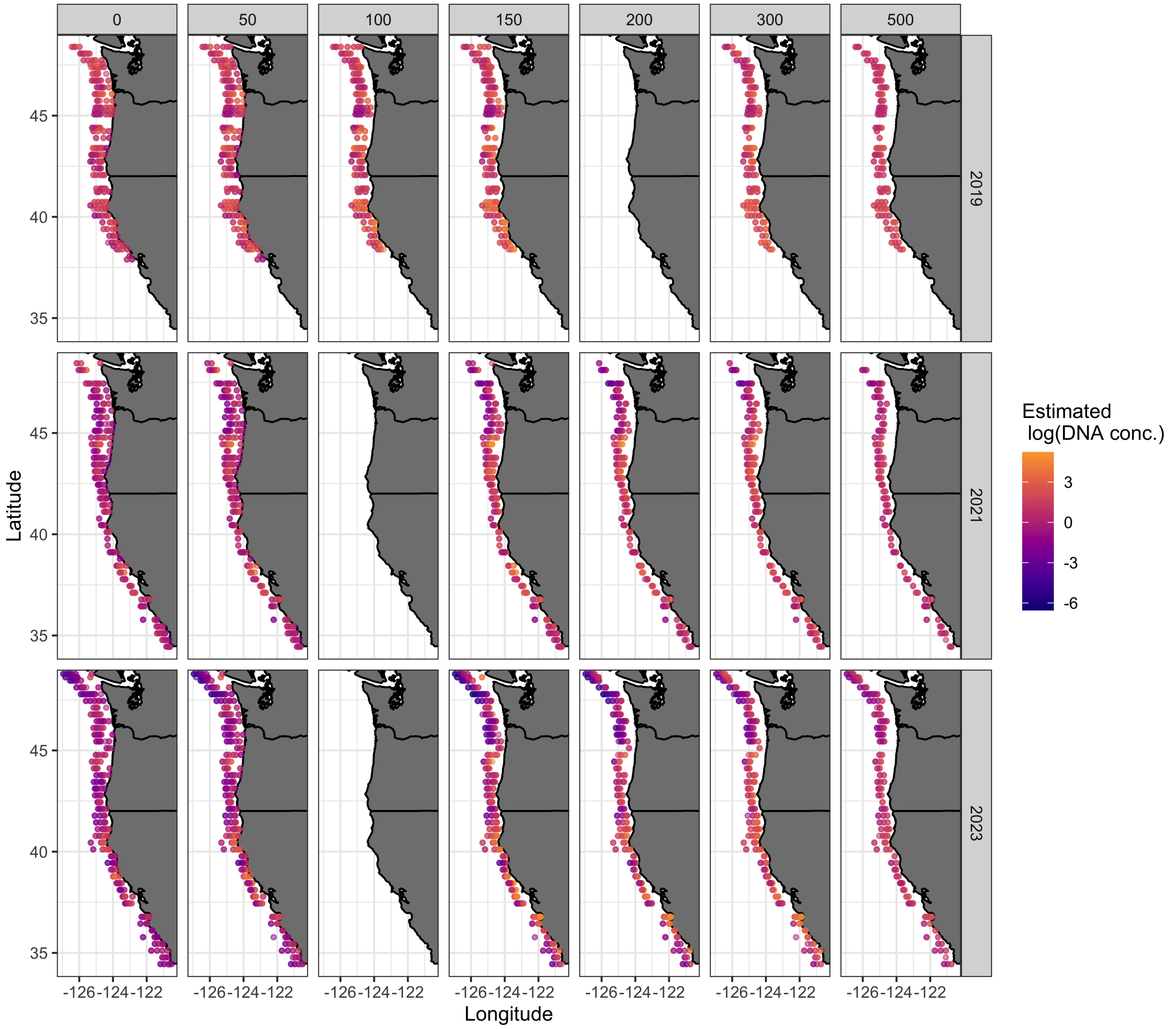

Figure G.4. Predictions of hake DNA concentration at sampled locations across years (rows) and sampled depths (columns).

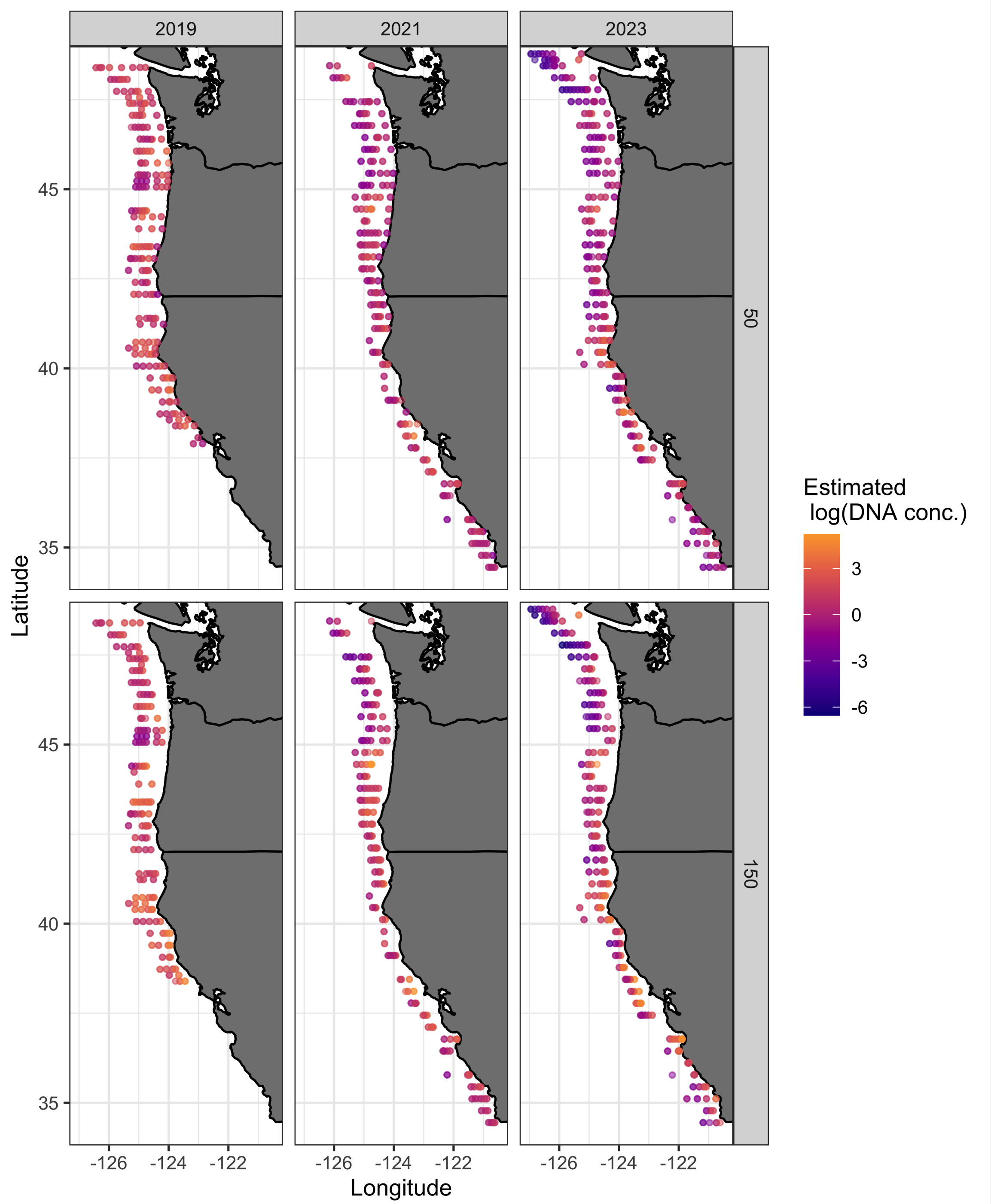

Figure G.5. Predictions of hake DNA concentration at sampled locations for two sampling depths (rows) across years (columns).

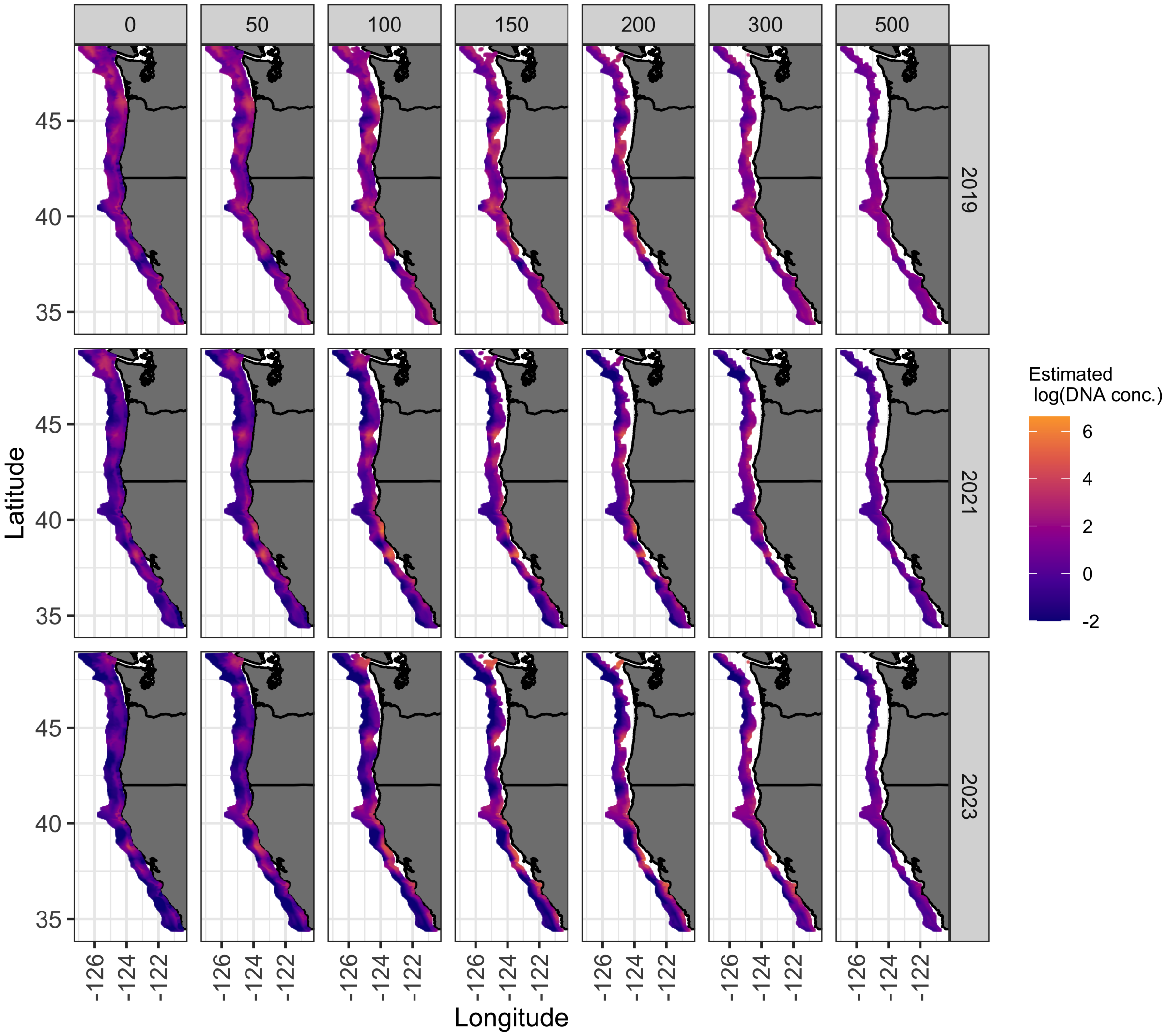

Figure G.6. Predictions of Hake DNA concentration from the spatio-temporal model across multiple years (rows) and depths (columns).

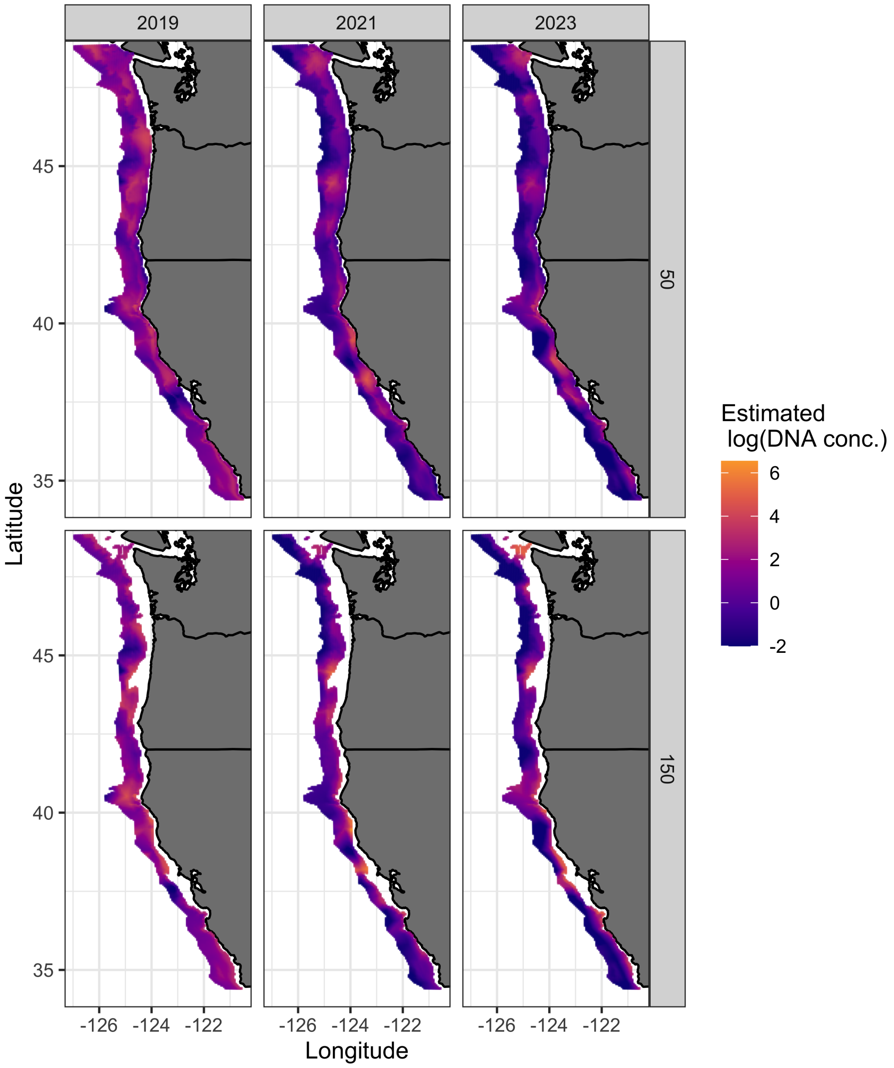

Figure G.7. Predictions of Hake DNA concentration from the spatio-temporal model for two depths (rows) among years. Note that predictions are made to locations included in any year, and may include spatial regions that do not have observations in a given year (e.g. south of San Francisco Bay in 2019).

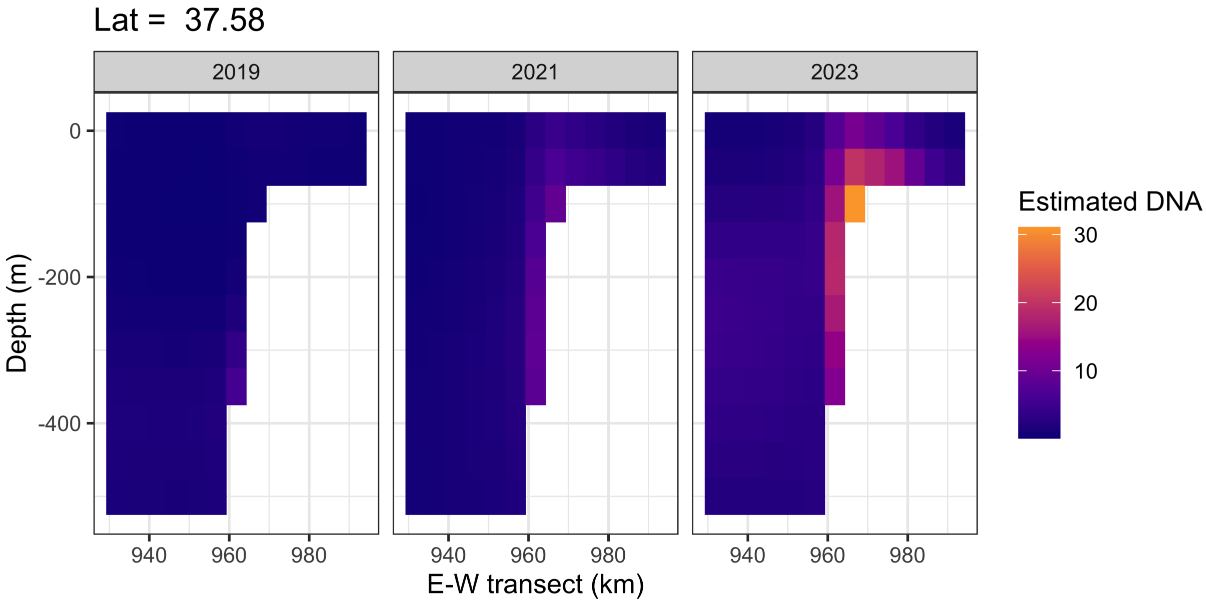

Figure G.8. Predicted hake DNA concentration (copies per uL) along E-W transect at 37.58 N. Projections are in 50m depth bins.

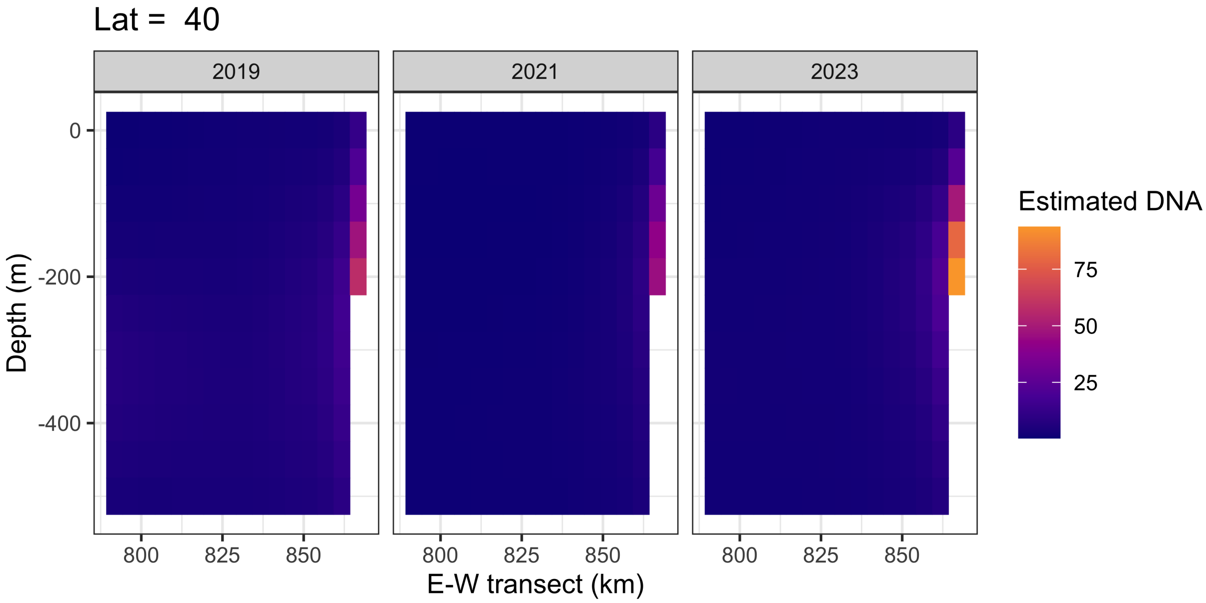

Figure G.9. Predicted hake DNA concentration (copies per uL) along E-W transect at 40 N. Projections are in 50m depth bins.

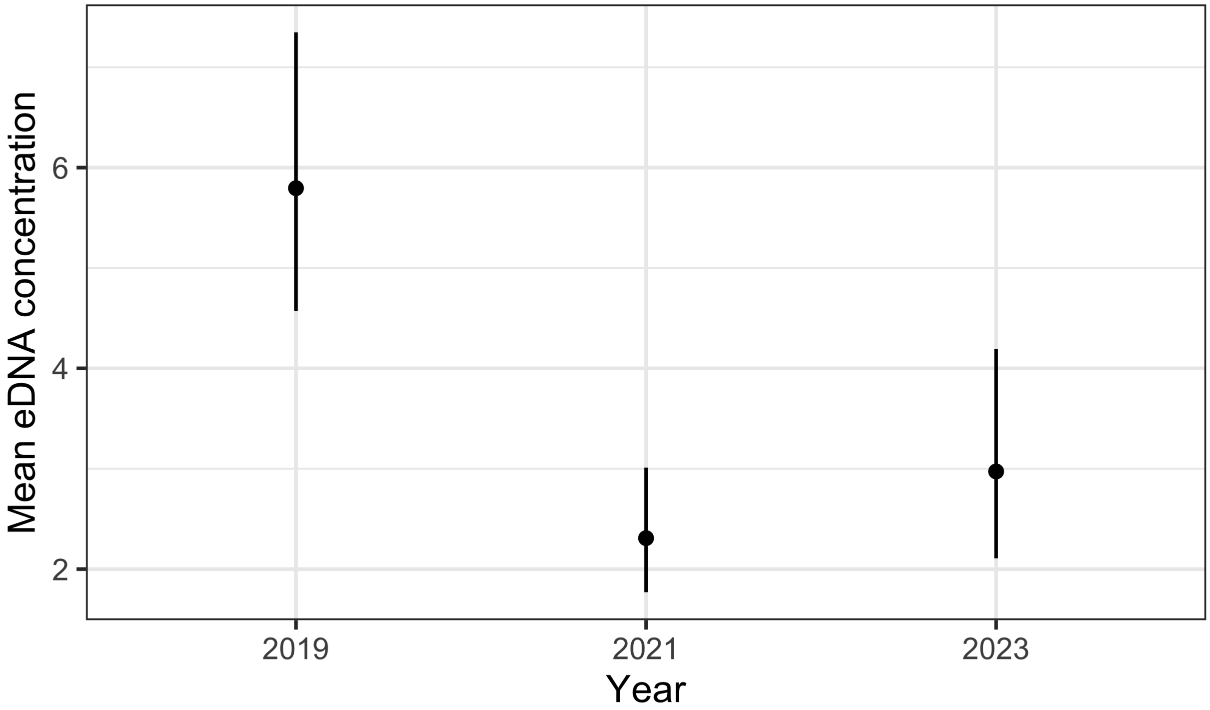

Figure G.10. Year intercepts and 95 percent intervals.

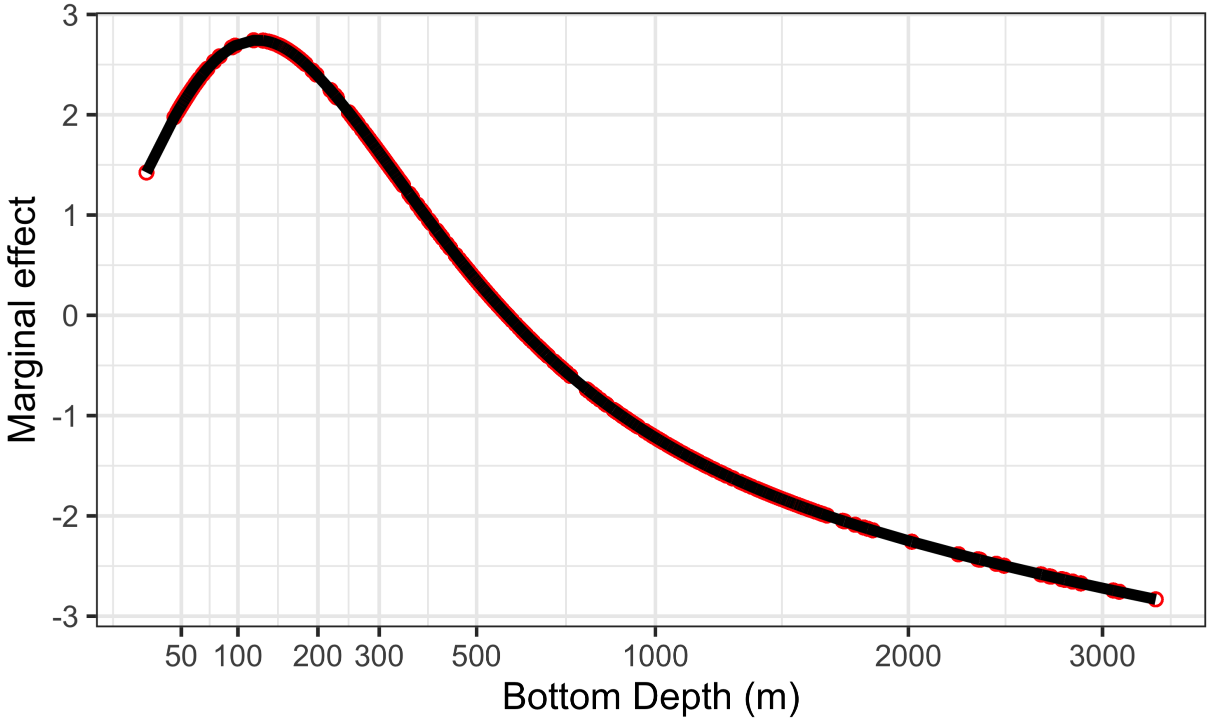

Figure G.11. Marginal effect of depth (p-spline smooth).

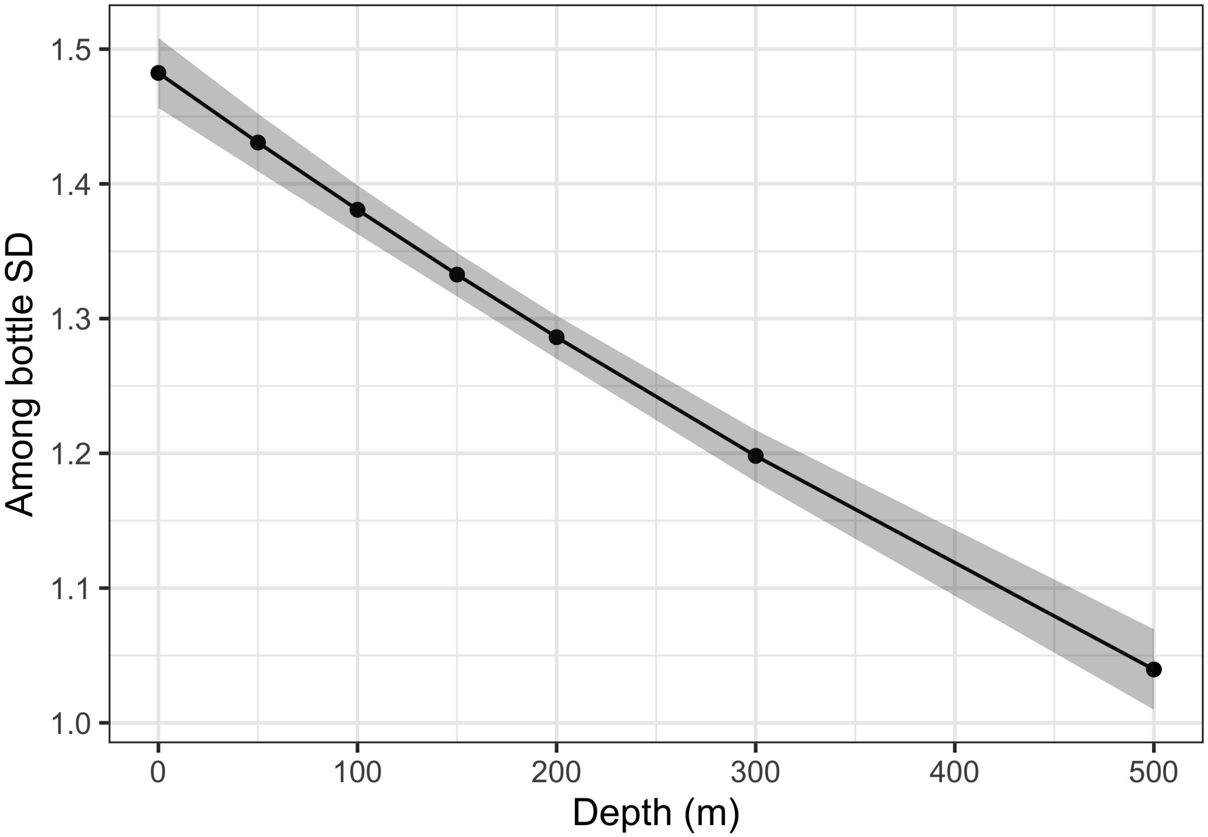

Figure G.12. Estimated among bottle standard deviation by depth.

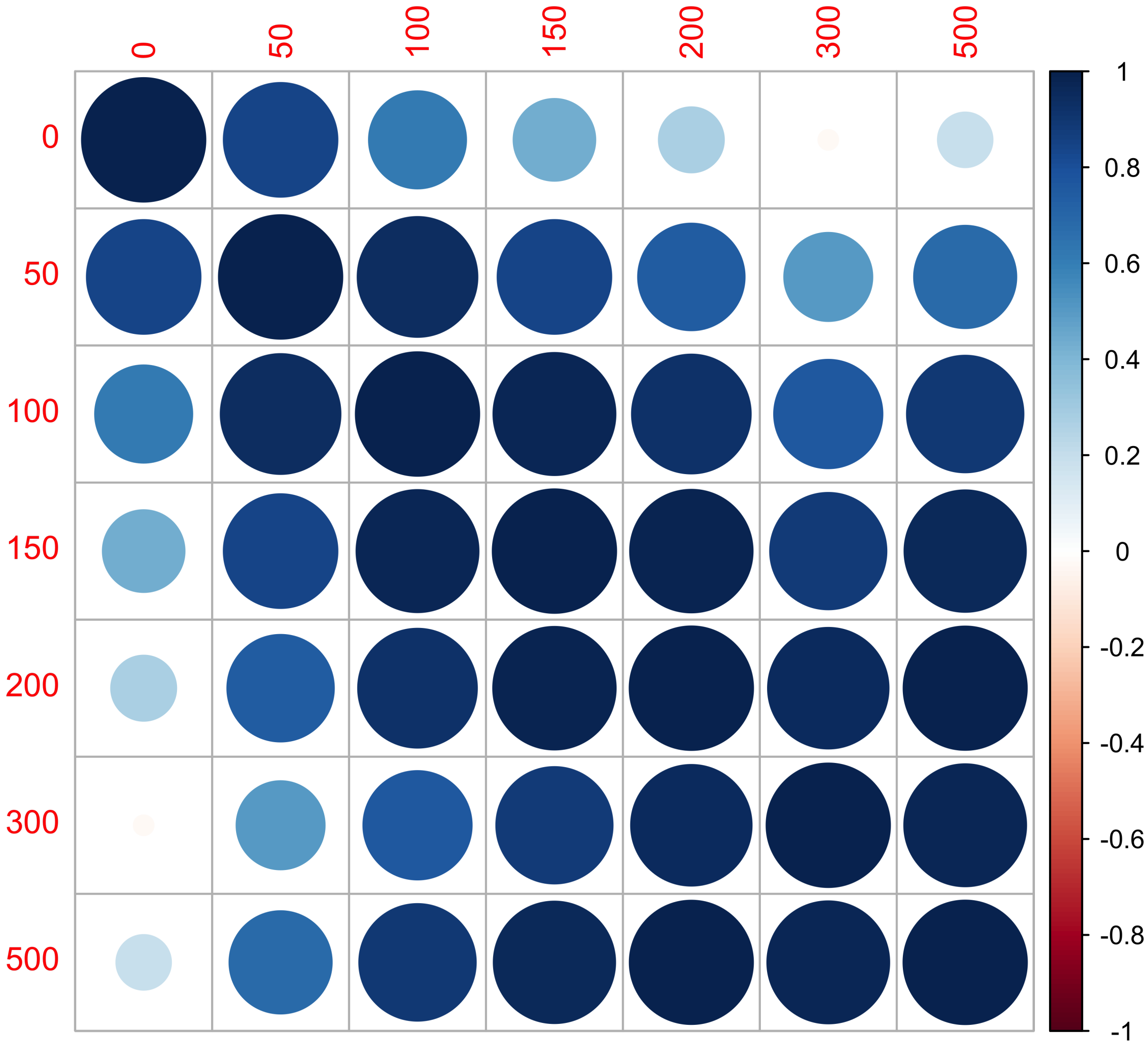

Figure G.13. Estimated correlation among depths for the spatial effect.

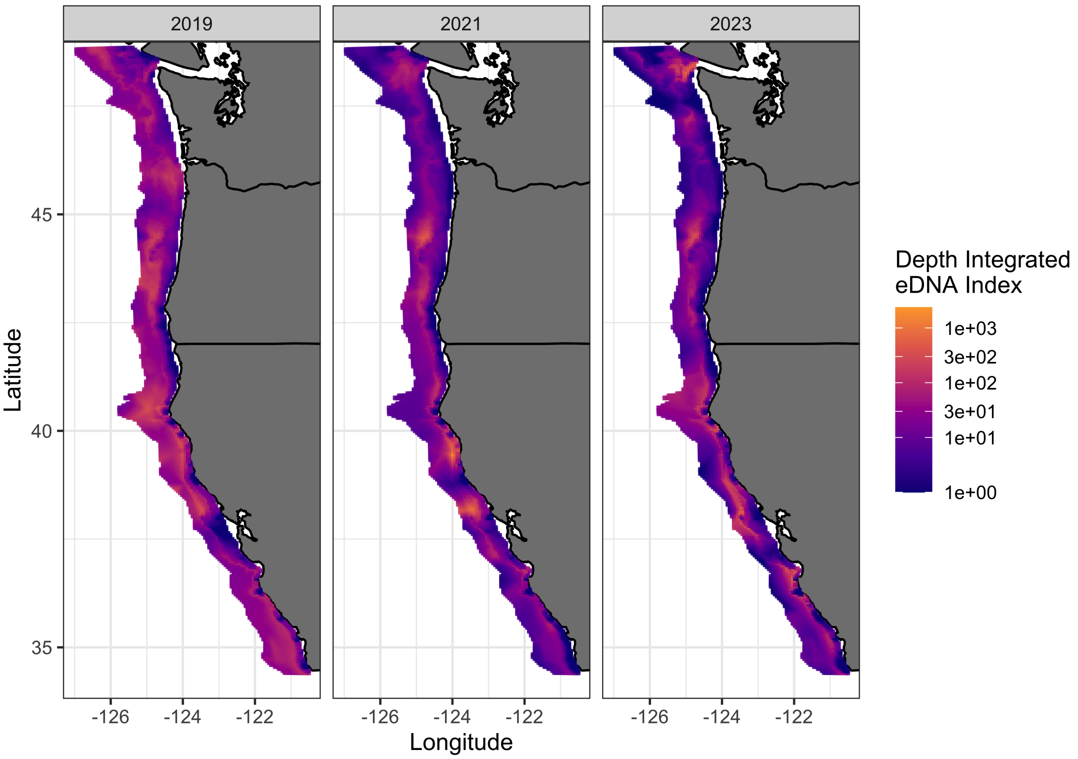

Figure G.14. Depth-integrated eDNA index for 5km grid cell in each year.

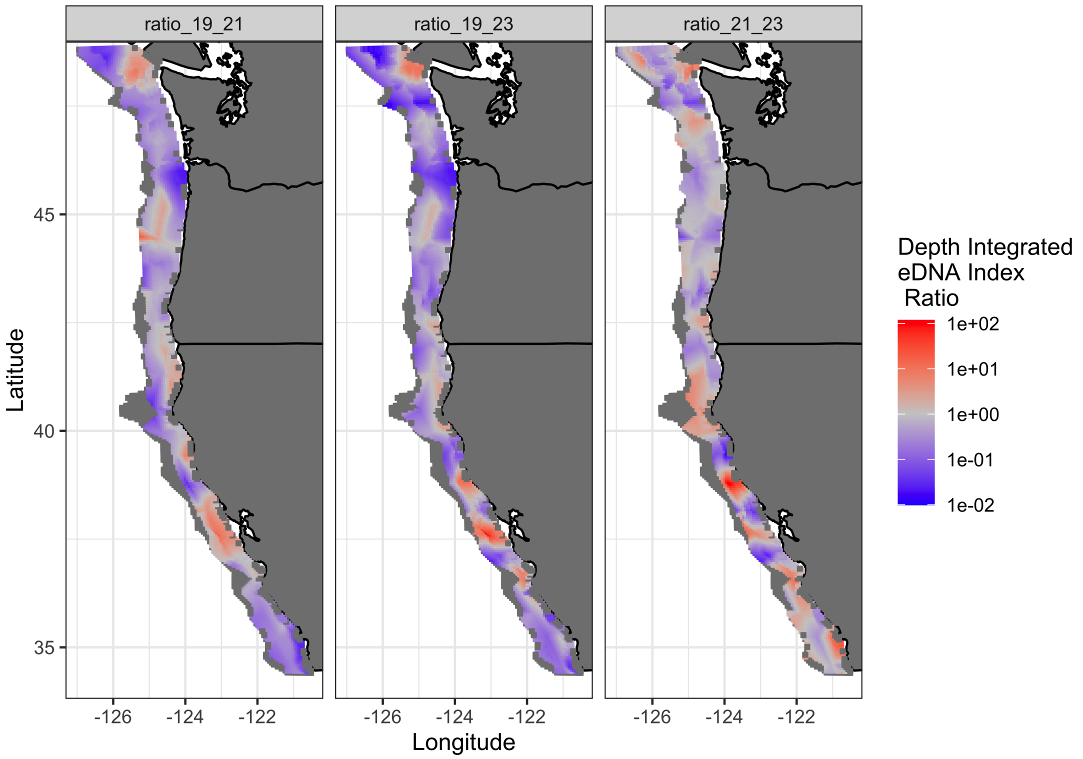

Figure G.15. The ratio of the depth-integrated eDNA index between all pairs of years for each year. This shows how areas have changed in their hake DNA among years. Each panel shows the relationship between two years. For example, ratio_19_21 is the predictions from 2021 divided by the predictions from 2019. This means blue cells are areas in which the predictions are larger in 2019 than 2021 (red areas indicate the converse). Grey areas indicate areas that are out of the survey area for one or both of the years.

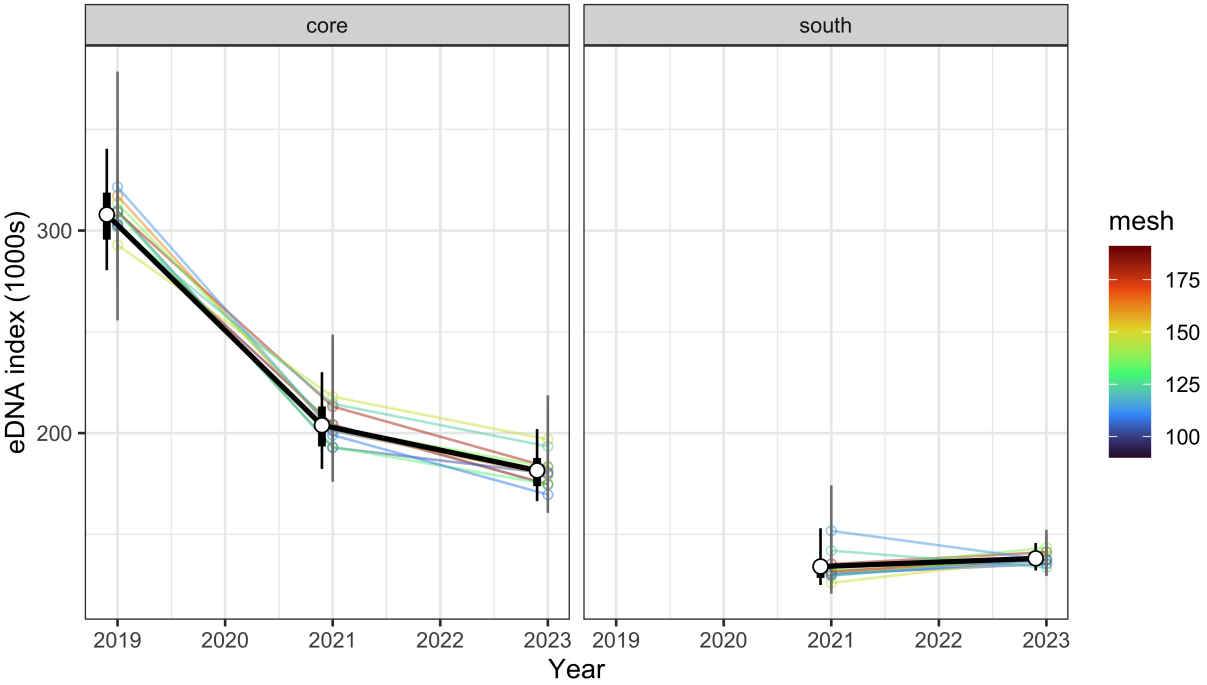

Figure G.16. The eDNA index calculated for appropriate years for the core and south areas (see also Figure G.2). Colored lines show estimates from individual spatio-temporal models and 95 percent interval. Black lines show the among model average, interquartile range and 90 percent intervals. Units of eDNA are DNA concentration (copies per uL).

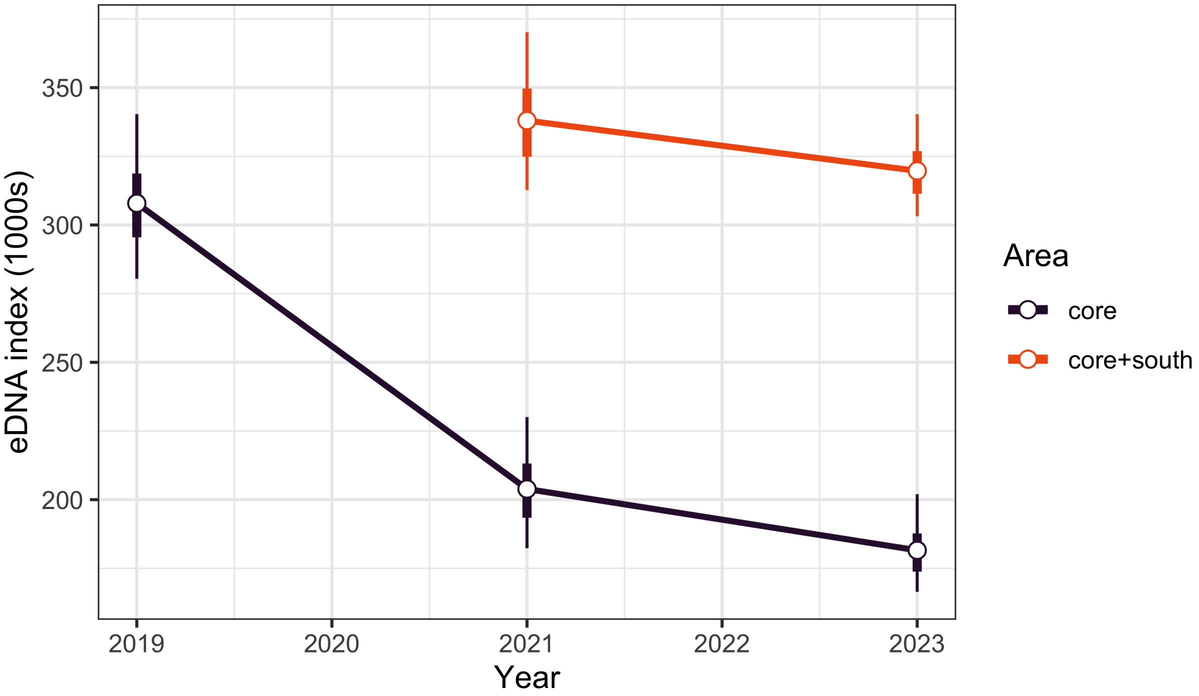

Figure G.17. The eDNA index calculated for appropriate years for the core and south areas (see also Figure G.2). Colored lines show estimates from individual spatio-temporal models and 95 percent interval. Points and error bars show the among model average, interquartile range and 90 percent intervals. Units of eDNA are DNA concentration (copies per uL).

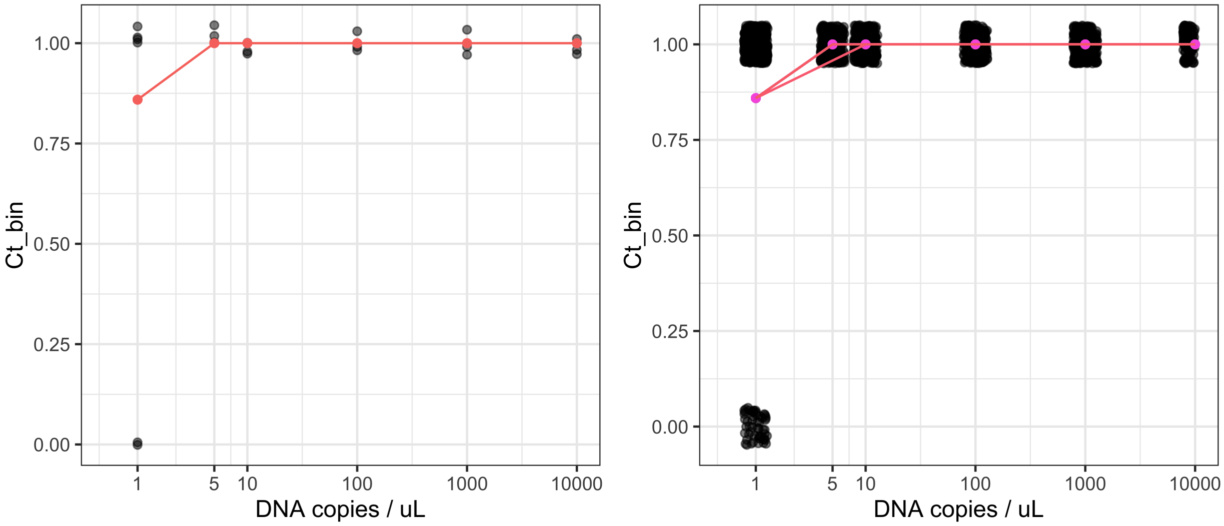

Figure G.18. Presence-absence plot for standards.

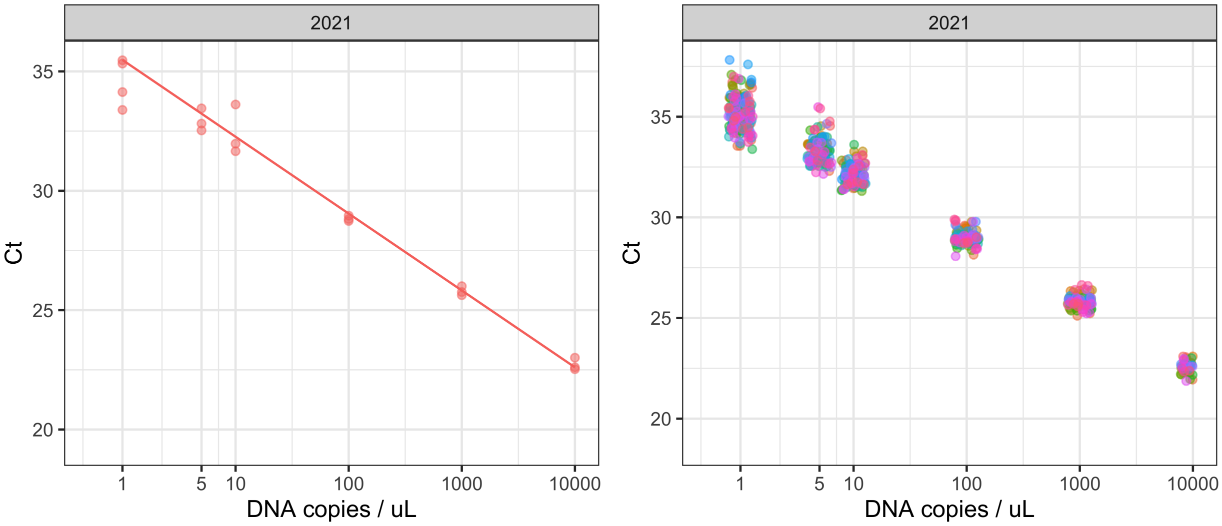

Figure G.19. Positive observations for standards. Left panel shows observations and fits from a single plate with known DNA concentrations, while the right panels shows the positive observations for all standard plates in a given year (points have been jittered to reduce overlap).

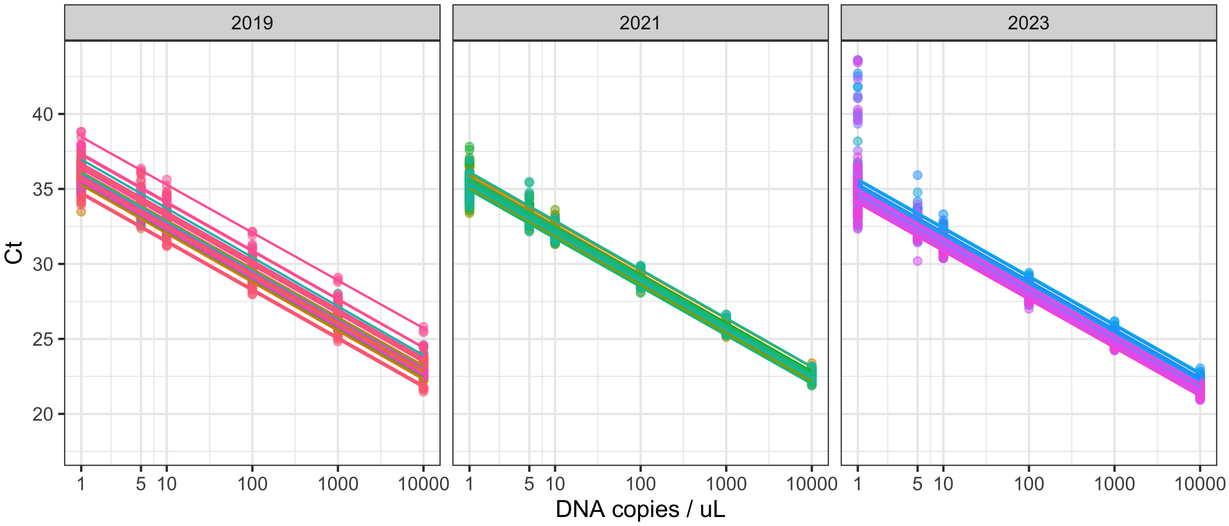

Figure G.20. Positives for standards, all years, all plates.

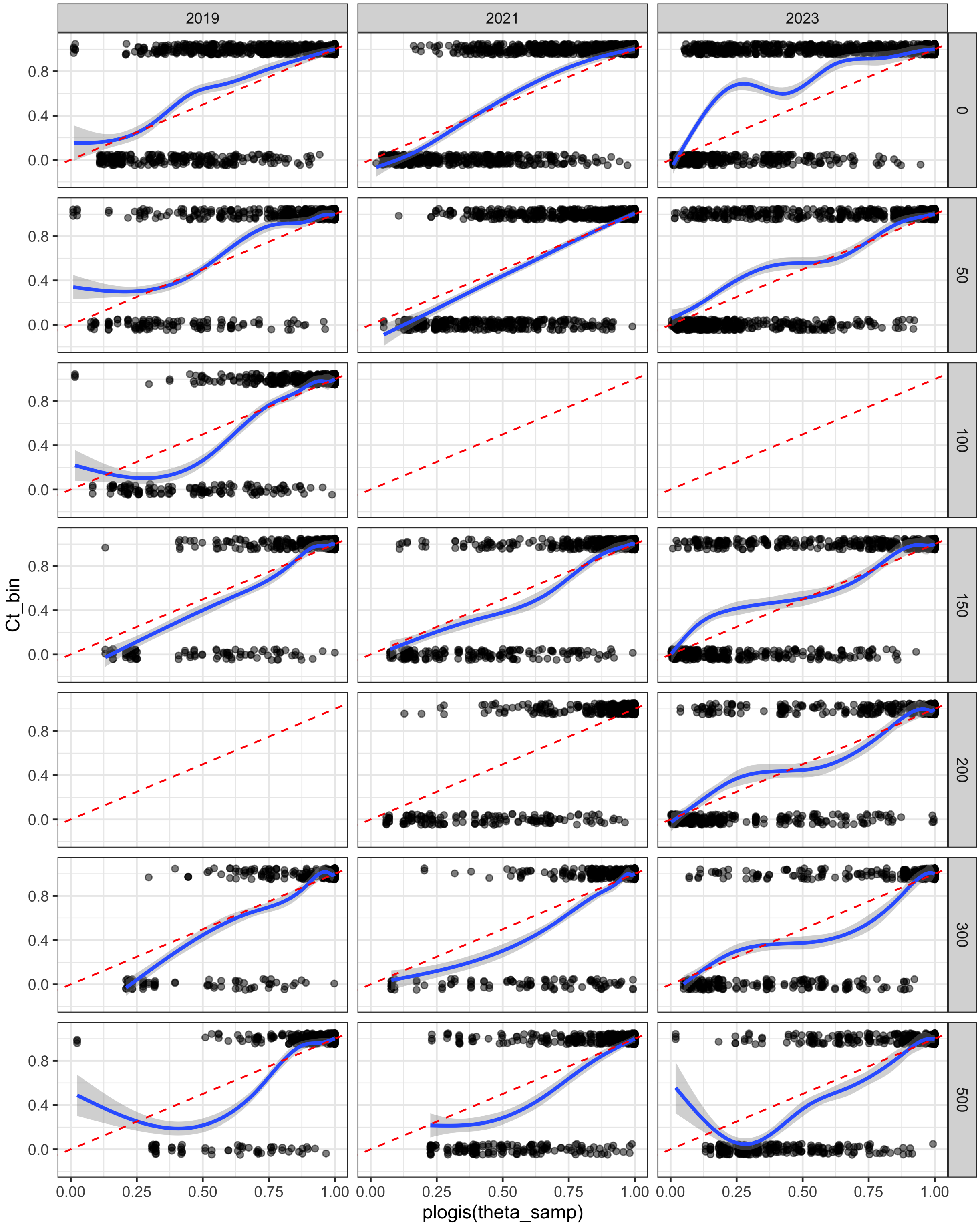

Figure G.21. Prediction vs. observed, presence-absence component.

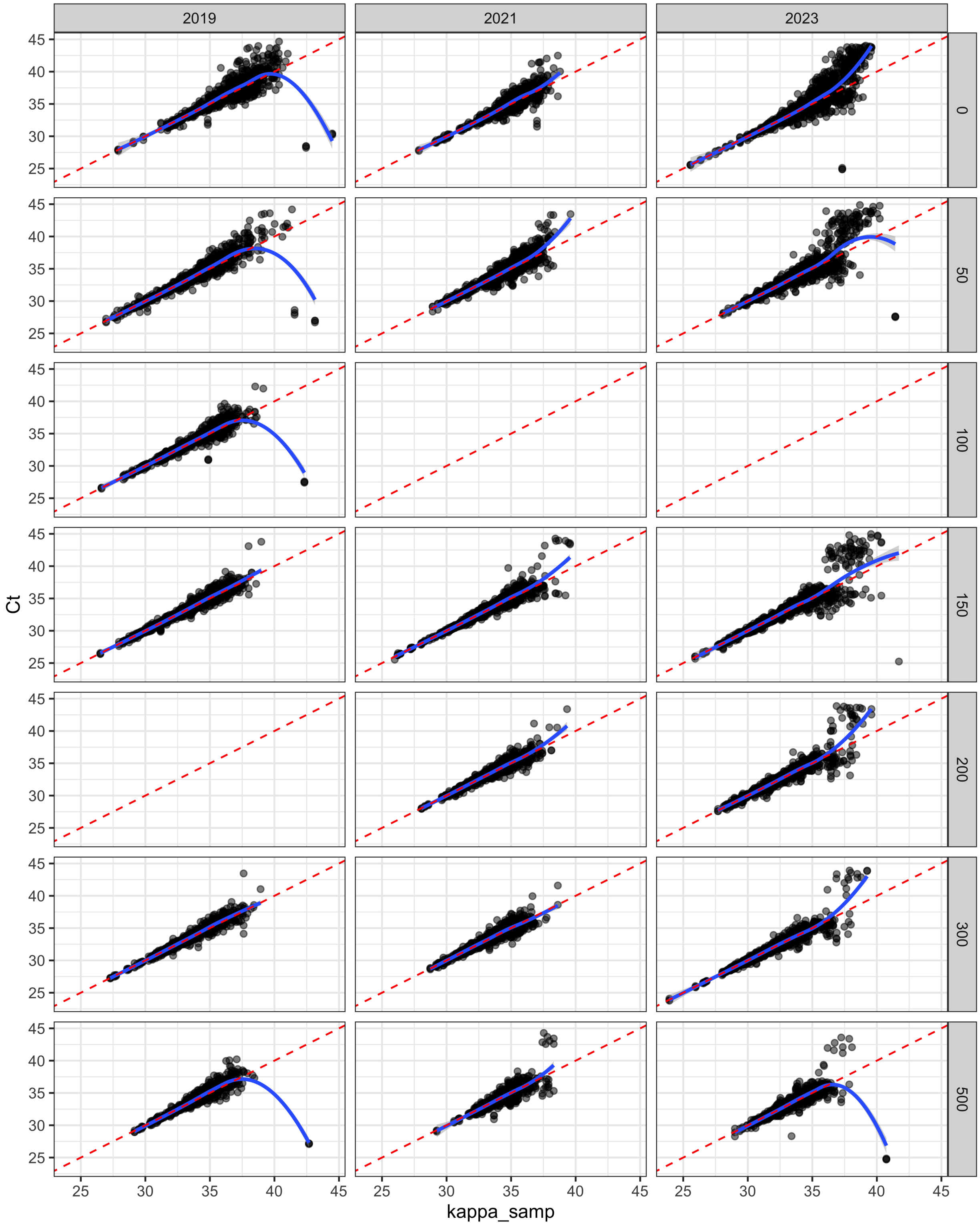

Figure G.22. Prediction vs. observed, positive component. Note the rare outliers; outliers are almost always one bottle of very high concentration that has a replicate bottle that has very low estimated concentration. Lines are loess smoothers.

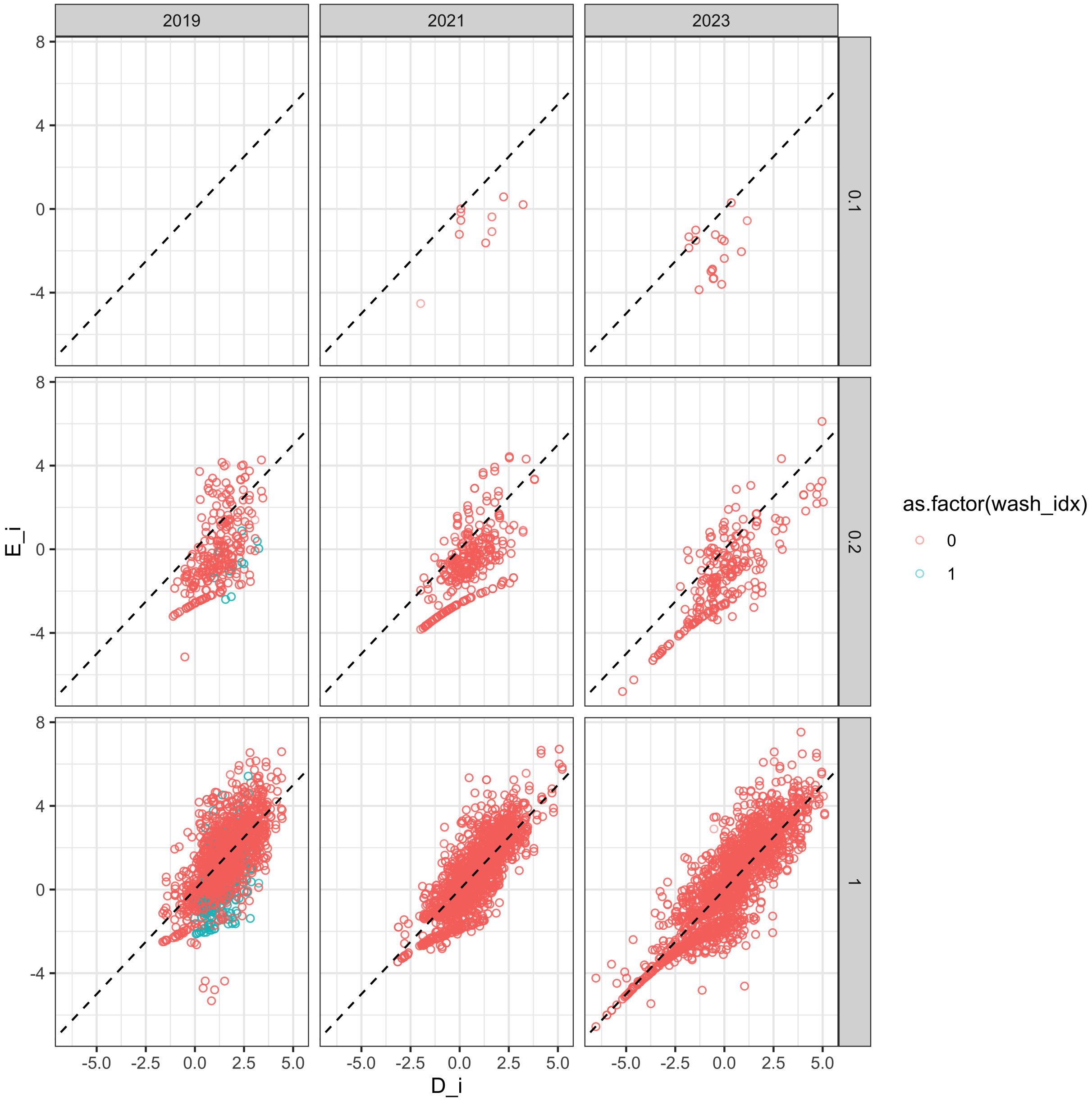

Figure G.23. Plot of the latent variable D vs. E (the concentration assayed by qPCR) faceted by year (columns) and dilution (rows). Note how the dilution shifts all points down relative to the 1:1 line.

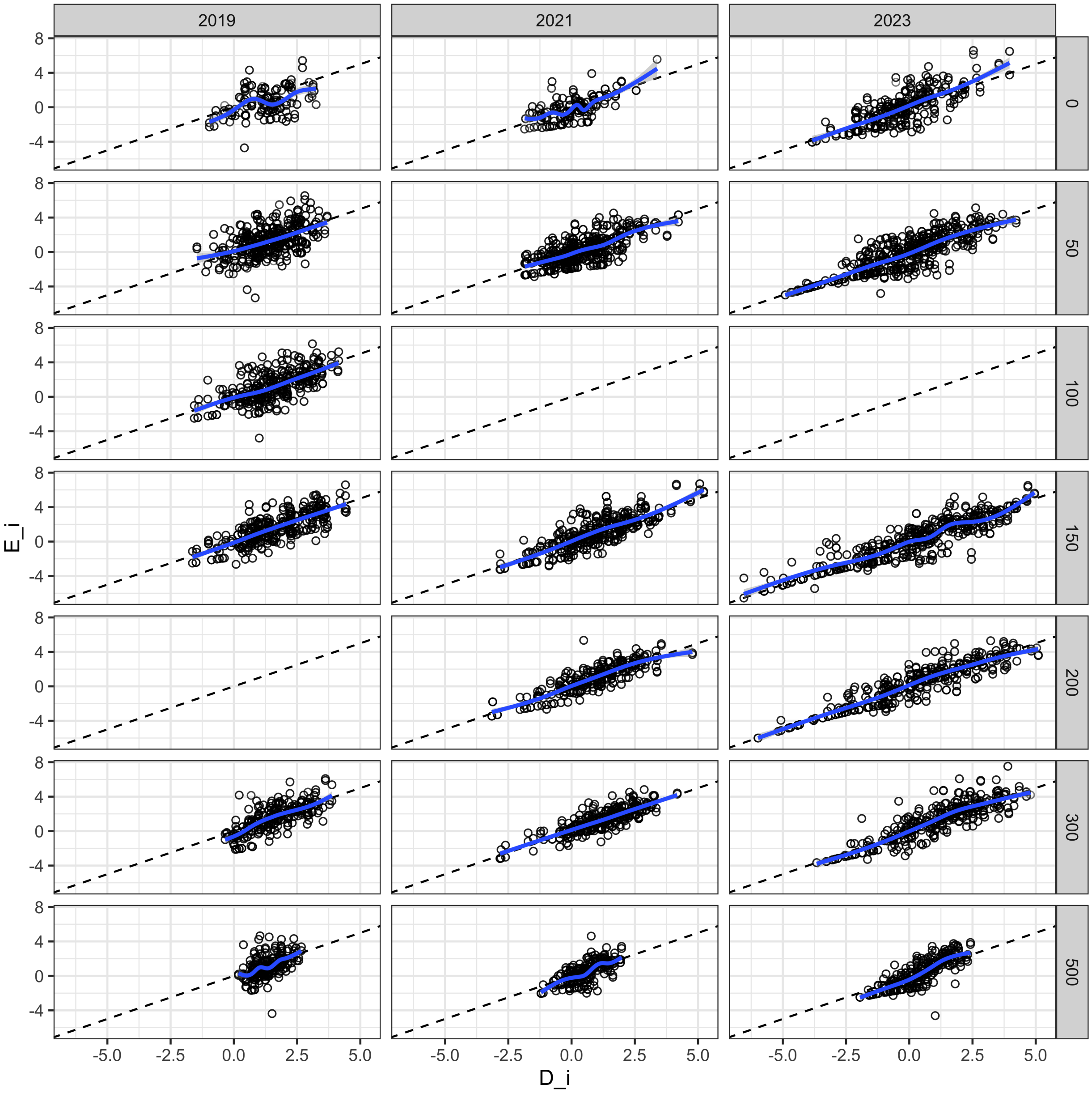

Figure G.24. Plot of the latent variable D vs. E for undiluted samples for years (columns) and water depths (rows).

H HAKE-SPECIFIC ECOSYSTEM SUMMARY

Contributed by Kristin N. Marshall, Mary E. Hunsicker, and Andrew M. Edwards

The base model for this stock assessment includes year-specific maturity-at-age that explicitly accounts for changes in temperature, and empirical weight-at-age data that may be due to ecosystem effects. As such, the assessment is consistent with an 'Ecosystem Approach to Fisheries Management'.

Section H.1 discusses relevant ecosystem information that has been previously found to influence Pacific Hake recruitment (Vestfals et al. 2023). We focus on easily-available and updatable information, and what is presented here is not exhaustive. As such it should be considered a first step in providing an operational summary (updatable and expanded upon every year) of relevant ecosystem information for Pacific Hake. Section H.2 then describes broader ecosystem and environmental conditions relevant to Pacific Hake. A risk table (Table H.2) summarizes conditions, uncertainty, and concerns related to Pacific Hake.

H.1 Ecosystem variables relevant for recruitment

We present some of the indicators that Vestfals et al. (2023) and subsequent analyses (Marshall et al., pers. comm.) found to correlate with higher Pacific Hake recruitment deviations (Table H.1). Vestfals et al. (2023) used estimated hake recruitment deviations from 1980 to 2010, based on results in the Grandin et al. (2020) hake assessment and ocean model variables from the University of California, Santa Cruz Regional Ocean Modeling System (ROMS) hindcast. We also conducted a preliminary update using a newer ocean modeling product (GLORYS, described below) that extends the analysis to a more recent time period (1993 to 2023), and used extended statistical methods that focus on within-sample and out-of-sample prediction for variable selection (K. Marshall, pers. comm.).

Overall, this resulted in 11 ecosystem indices described in Table H.1 that correlate with recruitment deviations of Pacific Hake. These include three of the five indices included in the best-fitting model of Vestfals et al. (2023) (see their Figure 7), and three of the further nine indices found in their top 16 candidate models (their Table 2). Time series for five indices are based on values amalgamated in the pacea R package (Edwards et al. 2024). The other six indices were calculated from outputs of the Global Ocean Physics Reanalysis (GLORYS12V1) product, which is a global ocean eddy-resolving oceanographic model covering 1993 onwards. Details of spatial, depth, and temporal ranges are given in Table H.1.

The following variables are taken from pacea. Pacific Herring (*Clupea pallasii*) spawning biomass index was calculated from latest results (DFO 2024) of the stock assessment, which is conducted using a statistical catch-at-age model (Cleary et al. 2019). The North Pacific Current Bifurcation Index (BI) was developed by Malick et al. (2017), who found that a northward-shifted bifurcation was associated with increased salmon productivity in British Columbia and Washington State waters. The index is updated annually (Michael Malick, pers. comm.). The Pacific Decadal Oscillation (PDO) is a monthly index which is

Table H.1. Descriptions of easily available ecosystem variables that were found to influence Pacific Hake recruitment either by Vestfals et al. (2023) or our updated analyses (unpublished). Variables are in order of life-history stage, following Table A1 of Vestfals et al. (2023); see that reference for full details. Shelf break is considered between 100 and 2,000 m isobaths, defining the longitudinal extent for several variables. The first subscripts refer to life-history stage ('pre' is preconditioning, while JA is Jan-Apr, in the egg to late larvae stage).

Abbreviation of variable	Definition	Effect on recruitment; expectation for an increase in variable
$\mathrm{PREY}_{\mathrm{pre,her}}$	Pacific Herring spawning biomass off the west coast of Vancouver Island	Increased competition with herring on summer feeding grounds leads to poorer feeding conditions and reduced adult condition; ↓ recruitment the following year
$\mathrm{BI}_{\mathrm{pre}}$	North Pacific Current Bifurcation Index	Northward-shifted bifurcation leads to increased advection of prey southwards, leading to poorer feeding conditions off British Columbia, Washington, and Oregon, and reduced adult condition; ↓ recruitment the following year
$\mathrm{PDO}_{\mathrm{pre}}$	Pacific Decadal Oscillation during preconditioning (Apr-Sep)	Indicator of basin-scale processes, negative phase linked to higher productivity and improved adult condition (Apr-Sep); ↓ recruitment the following year
$\mathrm{NPGO}_{\mathrm{pre}}$	North Pacific Gyre Oscillation during preconditioning (Apr-Sep)	Indicator of basin-scale processes, positive phase linked to higher nutrient concentrations and productivity, and improved adult condition; ↑ recruitment the following year
$\mathrm{TEMP}_{\mathrm{spawn}}$	Mean temperature during spawning (shelf break, Jan-Mar, 130-500 m depth, 31-36° N)	At higher temperatures, fish are less likely to spawn but growth rate of larvae increases; ∪-shaped relationship with recruitment that year
$\mathrm{AST}_{\mathrm{eggs}}$	Net along-shore transport (shelf break, Jan-Mar, 40-60 m depth, 31-36° N)	Increased northward advection away from juvenile nursery areas decreases recruitment; ↓ recruitment that year
$\mathrm{MLD}_{\mathrm{yolk}}$	Mean mixed layer depth (shelf break Jan-Apr, 31-36° N)	Larvae aggregate at base of mixed layer so mixed layer depth may limit how far they rise in the water column affecting later transport; ↓ recruitment that year
$\mathrm{SSH}_{\mathrm{JA.c}}$	Average sea-surface height off California as an indicator of basin-scale processes (from coast to 30 km offshore, Jan-Apr, 34.5-42.5° N)	Higher sea surface is indicative of higher productivity and better conditions for copepods; ↑ recruitment that year
$\mathrm{MLD}_{\mathrm{latelarv}}$	Mean mixed layer depth (shelf break Mar-Jun, 31-37° N)	Larvae aggregate at base of mixed layer so mixed layer depth may limit how far they rise in the water column affecting later transport, and possibly less competition and predation when mixed layer shallower; ↑ recruitment that year
$\mathrm{PU}_{\mathrm{latelarv}}$	Strength of poleward undercurrent (from coast to 275 m isobath, Mar-Jun, 75-275 m depth, 33.5-34.5° N)	Increased northward advection away from juvenile nursery areas decreases recruitment; ↓ recruitment that year
$\mathrm{PRED}_{\mathrm{age0.age1hake}}$	Biomass of age-1 Pacific Hake (from this stock assessment)	Age-1 hake predate on pelagic juveniles (roughly Apr-Sep); ↓ recruitment that year

a long-lived El Niño-like pattern of Pacific climate variability (Mantua et al. 1997). The North Pacific Gyre Oscillation (NPGO) is a climate pattern that is significantly correlated with fluctuations of salinity, nutrients, and chlorophyll-a in long-term observations in the California Current and Gulf of Alaska (Di Lorenzo et al. 2008). The estimates of age-1 Pacific Hake are taken from this current assessment model (and will be updated in pacea). The six further indices were calculated from GLORYS outputs by K. Marshall.

Estimates of Pacific Hake recruitment from this assessment are presented alongside the five indices calculated using outputs from pacea (Figure H.1) and the six indices calculated from GLORYS output (Figure H.2). All indices are standardised over the ranges of years shown (different for each figure), such that each index has a mean of zero and standard deviation of one. The x-axis corresponds to the year for which recruitment is expected to be influenced by the ecosystem variable represented by the index. For example, $\text{PREY}_{\text{pre,her}}$ is an index representing Pacific Herring spawning biomass off the west coast of Vancouver Island (Table H.1). Vestfals et al. (2023) found that increased herring biomass led to increased competition with hake on summer feeding grounds, leading to poorer feeding conditions and reduced adult condition. Pacific Hake recruitment would then be affected the following year. Thus, the $\text{PREY}_{\text{pre,her}}$ index for year 2020 in Figure H.1 represents the herring spawning biomass in 2019, because that is the biomass expected to influence hake recruitment in 2020. A similar shift is done for the other three variables that influence the adult preconditioning stage of hake.

The notation $\text{PREY}_{\text{pre,her}}$ represents herring being a prey item for adult hake in the preconditioning stage, although Vestfals et al. (2023) found a competition effect (not a predator-prey effect as originally hypothesised).

Some variables are plotted with a flipped y-axis, so that upwards in all plots consistently corresponds to conditions supposedly good for hake recruitment. For example, a lower herring biomass is expected to correspond to an increase in hake recruitment, and so the y-axis for the herring index in Figure H.1 is flipped, so that lower-than-average herring biomass is upwards on the plot. It is coloured blue to represent a negative herring biomass anomaly. Similarly, red represents a positive herring biomass anomaly but values point downwards to indicate a negative potential effect on hake recruitment. A similar flip is done for all variables for which a negative index was found to correspond to positive hake recruitment, to make it easier to visualise potential effects. A similar approach is taken for Figure H.2.

We have not conducted further analyses on these time series, but present them as a first attempt to compile varied ecosystem information into single figures that can stimulate thinking about ecosystem effects, and that can be updated and expanded upon for future assessments. Note that the strongest driver of hake recruitment found by Vestfals et al. (2023) was eddy kinetic energy between May and September (during the female spawning preconditioning stage) from point Conception to Cape Blanco, but an up-to-date index of this was not easily available.

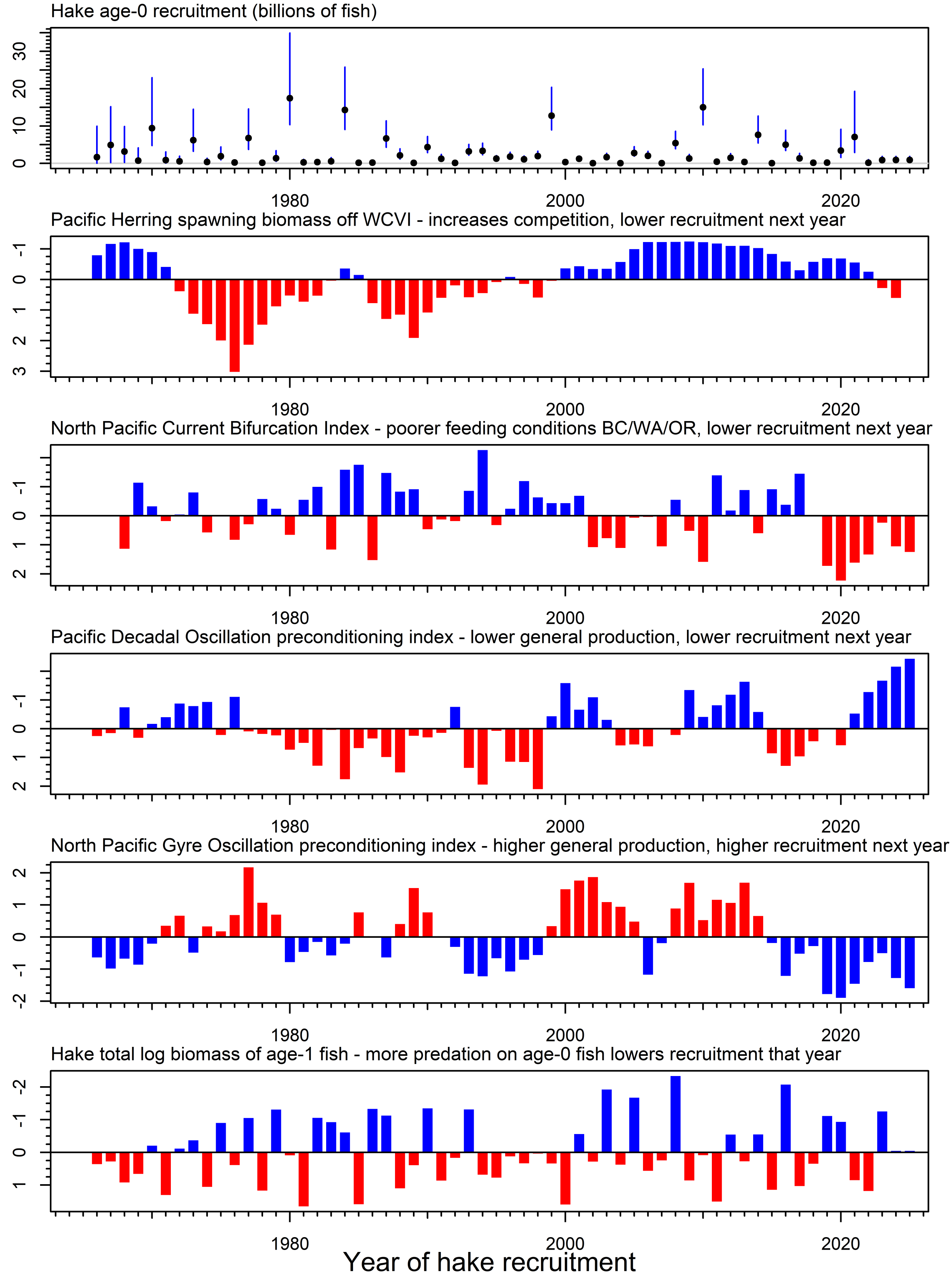

Figure H.1. Estimated hake recruitment from this assessment (top), plus five ecosystem indices based on the pacea R package. The x-axis corresponds to the expected influenced year of Pacific Hake recruitment (see text). Red (blue) bars represent a positive (negative) index, with the y-axis flipped for four indices so that upwards represents a positive expected influence on recruitment.

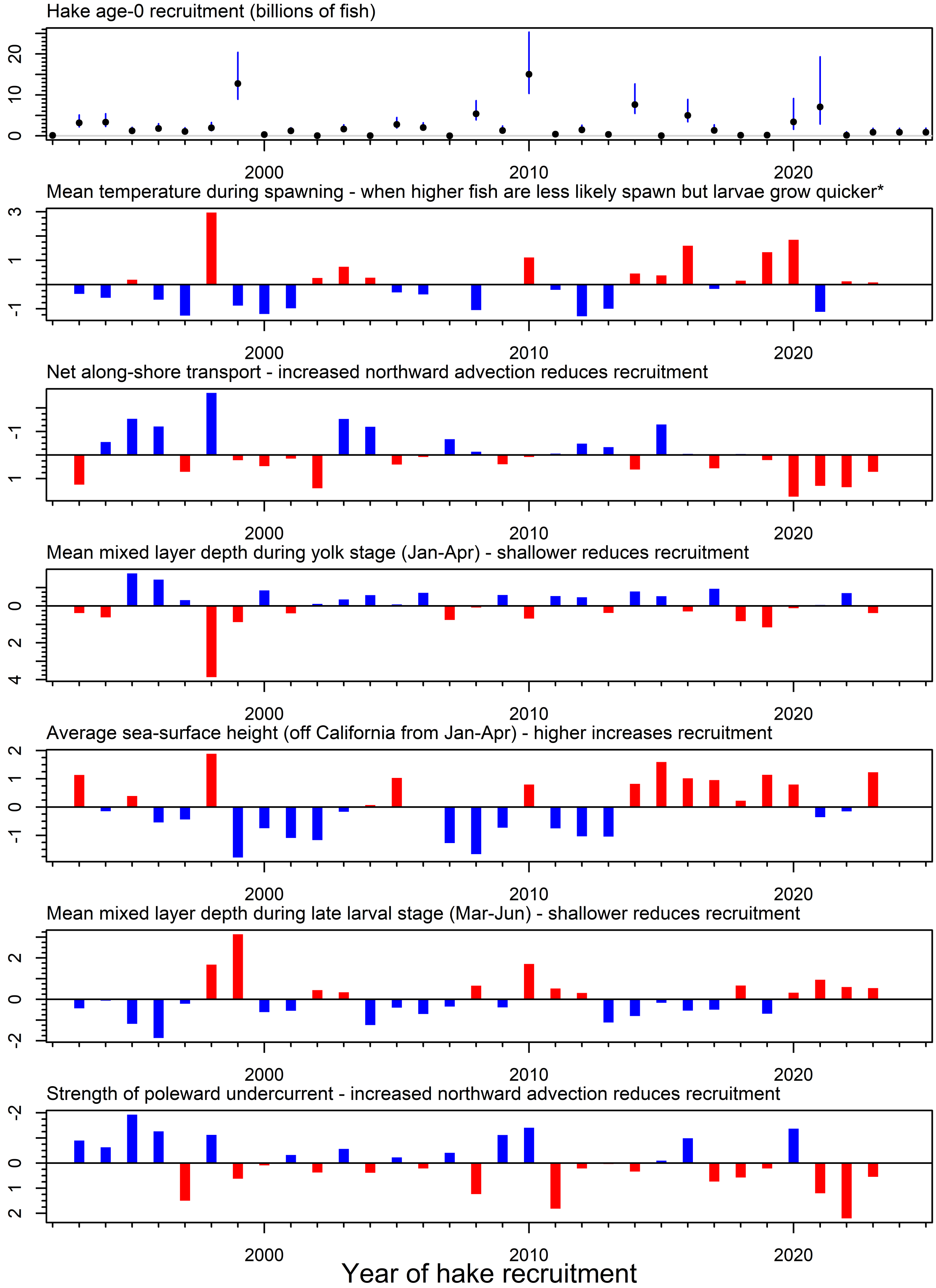

Figure H.2. Estimated Pacific Hake recruitment from the current assessment model (top), plus six ecosystem calculated from GLORYS output. Axes are defined as in Figure H.1 and in the text. *Recruitment has a ∪-shaped relationship with mean temperature during spawning and for simplicity we do not flip the axis.

Table H.2. 'Risk table' for Pacific Hake, to document ecosystem and climate factors potentially affecting stock productivity and uncertainty or other concerns arising from the stock assessment (see text). Level 1 is a favourable ranking, Level 2 neutral, and Level 3 is unfavourable. CVA is the Climate Variability Assessment approach (McClure et al., 2023).

Ecosystem and environmental conditions	Assessment data inputs	Assessment model fits and structural uncertainty
• Recruitment: 2021-2024 recruitment indicators neutral to favorable • Prey: favorable (krill, juvenile hake) • Predators: unfavorable (increasing) • CVA rank: low	• Very reliable catch reporting • Generally well-sampled fishery-dependent and -independent age compositions • Informative age-2+ fishery-independent survey biomass index every other year • Informative age-1 recruitment index every other year • Includes externally estimated time-varying weight-at-age (growth) and time-varying and temperature-dependent maturity (fecundity) as data inputs	• Fully Bayesian stock assessment, integrating over multiple sources of parametric uncertainty • High recruitment variability and no information on recent recruitment in assessment model from 2023 onwards, given no survey in 2024 • Key demographics estimated using priors (natural mortality and steepness) • Clear identity of large cohorts after at least age-3 • Model fits well to age compositions, though occasionally at the expense of the survey index of abundance • Uncertain how changes in the distribution of fishing relate to migration patterns and stock abundance
Level 2 (medium agreement, robust evidence)	Level 1	Level 2

H.2 Ecosystem and environmental conditions

To start the process of discussing the vulnerability of Pacific Hake to climate change, we evaluated recent trends in environmental drivers of hake recruitment and growth, predators, and prey, along with the climate vulnerability assessment (CVA) rank assigned to hake by McClure et al. (2023). We did not consider competitors, habitat, or non-fisheries human activities (such as offshore wind development) during this evaluation. Overall, we consider ecosystem and environmental conditions to be neutral (Level 2) for hake, with medium to high confidence, based on medium agreement among indicators and robust evidence. We use this, plus information related to this stock assessment, to fill out the 'risk table' in Table H.2, based on the framework outlined by the California Current Integrated Ecosystem Assessment (CCIEA) team.

Recruitment

A strong El Niño in 2023-24 caused warmer than average ocean temperatures in winter and spring. As expected during an El Niño, the biomass of lipid-rich northern copepods was generally lower during this period and indicators of krill abundance were below average. However, these conditions rapidly subsided in late spring. A delayed but strong spring upwelling ushered in cool and productive conditions, and the biomass of northern copepods and krill rebounded to near average levels for the remainder of the year. Overall, environmental conditions in winter and spring were likely less favorable for age-0 hake in 2024 (Vestfals et al. 2023, Table A.1) but conditions transitioned to those more favorable for hake productivity in summer and fall. Observations of larval hake off Southern California were above average during 2022-2024 and juvenile hake from Central California were at or above average 2021-2024.

In 2025, the ecosystem is transitioning back to La Niña conditions, however large areas of warmer than average temperatures are still prevalent. In addition, marine heatwaves are forecasted to occur in offshore waters with the possibility of moving into coastal regions in summer and fall. It's uncertain whether these conditions will negatively impact hake recruitment.

Hake distribution

Seasonal forecasts of hake distribution in the northern region of the California Current Ecosystem (Malick et al. 2020a) were not available at the time of writing this summary, however these temperature-driven forecasts will be presented at the 2025 SRG meeting. Given what we know about the influence of temperature on hake distribution and the role of temperature as a proxy for prey availability Phillips et al. (2022), we suspect that the delayed upwelling observed in 2024 may have delayed the extent of the northern migration of hake in the spring. Return to average conditions later in summer may have supported a later northern shift as feeding conditions for hake improved.

Predators and prey

Pacific Hake are common in many predator's diets (e.g., Bluefin Tuna, Swordfish, sharks, marine mammals, Sablefish, Arrowtooth Flounder, and adult hake). Recent trends (i.e. over the last five years) in many of these populations of hake predators are stable or increasing, suggesting mild concern about increased predation. For example, the consumption of hake by Bluefin Tuna and Swordfish has been well above average in recent years and the spawning biomass of these species has increased over this period as well (Leising et al., in prep). However, recent indices of prey abundance are favorable. Krill is a dominant diet item for juvenile and adult hake Bizzarro et al. (2023). The CCIEA krill indicator shows an increasing trend in the central CCE over the last five years.

Climate vulnerability assessment results

Hake are highly exposed with low sensitivity to climate change, with an overall rank of low (McClure et al. 2023). However, we note that the CVA work pre-dates recent studies on the relationships between hake distribution and recruitment and ocean conditions Vestfals et al. (2023).